

# Flood Management in a Complex River Basin with a Real-Time Decision Support System Based on Hydrological Forecasts

THÈSE N° 5093 (2011)

PRÉSENTÉE LE 23 SEPTEMBRE 2011

À LA FACULTÉ ENVIRONNEMENT NATUREL, ARCHITECTURAL ET CONSTRUIT  
LABORATOIRE DE CONSTRUCTIONS HYDRAULIQUES  
PROGRAMME DOCTORAL EN ENVIRONNEMENT

ÉCOLE POLYTECHNIQUE FÉDÉRALE DE LAUSANNE

POUR L'OBTENTION DU GRADE DE DOCTEUR ÈS SCIENCES

PAR

Javier GARCÍA HERNÁNDEZ

acceptée sur proposition du jury:

Prof. A. Rinaldo, président du jury  
Prof. A. Schleiss, Dr J.-L. Boillat, directeurs de thèse  
Prof. P. Burlando, rapporteur  
Dr D. Bérod, rapporteur  
Prof. J. Paredes Arquiola, rapporteur



ÉCOLE POLYTECHNIQUE  
FÉDÉRALE DE LAUSANNE

Suisse  
2011



# Abstract

## **Flood management in a complex river basin with a real-time decision support system based on hydrological forecasts**

Keywords: hydrological modelling, flood forecasting, decision support system, hydropower plants management, flood control.

During the last decades, the Upper Rhone River basin has been hit by several flood events causing significant damages in excess of 500 million Swiss Francs. From this situation, the 3rd Rhône river training project was planned in order to improve the flood protection in the Upper Rhone River basin in Vaud and Valais Cantons. In this framework, the MINERVE forecast system aims to contribute to a better flow control during flood events in this catchment area, taking advantage of the existing hydropower multi-reservoir network. This system also fits into the OWARNA national project of the Swiss Federal Office of Environment by establishing a national platform on natural hazards alarms.

The Upper Rhone River basin has a catchment area with high mountains and large glaciers. The surface of the basin is 5521 km<sup>2</sup> and its elevation varies between 400 and 4634 m a.s.l. Numerous hydropower schemes with large dams and reservoirs are located in the catchment area, influencing the hydrological regime. Their impact during floods can be significant as appropriate preventive operations can decrease the peak discharges in the Rhone River and its main tributaries, thus reducing the damages.

The MINERVE forecast system exploits flow measurements, data from reservoirs and hydropower plants as well as probabilistic (COSMO-LEPS) and deterministic (COSMO-2 and COSMO-7) numerical weather predictions from MeteoSwiss. The MINERVE hydrological model of the catchment area follows a semi-distributed approach. The basin is split into 239 sub-catchments which are further sub-divided into 500 m elevation bands, for a total of 1050 bands. For each elevation band, precipitation, temperature and potential

evapotranspiration are calculated. They are considered in order to describe the temperature-driven processes accurately, such as snow and glaciers melt.

The hydrological model was implemented in the Routing System software. The object oriented programming environment allows a user-friendly modelling of the hydrological, hydraulic and operating processes. Numerical meteorological data (observed or predicted) are introduced as input in the model. Over the calibration and validation periods of the model, only observed data (precipitation, temperature and flows) was used. For operational flood forecast, the observed measurements are used to update the initial conditions of the hydrological model and the weather forecasts for the hydrological simulations.

Routing System provides then hydrological predictions in the whole catchment area. Subsequently, a warning system was developed especially for the basin to provide a flood warning report. The warning system predicts the evolution of the hydrological situation at selected main check points in the catchment area. It displays three warning levels during a flood event depending on respective critical discharge thresholds.

Furthermore, the multi-reservoir system is managed in an optimal way in order to limit or avoid damages during floods. A decision support tool called MINDS (MINERVE Interactive Decision Support System) has been developed for real-time decision making based on the hydrological forecasts. This tool defines preventive operation measures for the hydropower plants such as turbine and bottom outlet releases able to provide an optimal water storage during the flood peak.

The overall goal of MINDS is then to retain the inflowing floods in reservoirs and to avoid spillway and turbine operations during the peak flow, taking into account all restrictions and current conditions of the network. Such a reservoir management system can therefore significantly decrease flood damages in the catchment area.

The reservoir management optimisation during floods is achieved with deterministic and probabilistic forecasts. The definition of the objective function to optimise is realised with a multi-attribute decision making approach. Then, the optimisation is performed with an iterative Greedy algorithm or a SCE-UA (Shuffled Complex Evolution – University of Arizona) algorithm. The developed decision support system combines the high-quality optimisation system with its user-friendly interface. The purpose is to help decision makers by being directly involve in main steps of the decision making process as well as by understanding the measures undertaken and their consequences.



# Résumé

## **Gestion des crues en temps réel sur un bassin versant complexe avec un système d'aide à la décision basé sur des prévisions hydrologiques**

Mots clés: modélisation hydrologique, prévision de crues, systèmes d'aide à la décision, gestion des aménagements hydroélectriques, contrôle des crues.

Durant les dernières décennies, le bassin versant supérieur du Rhône a été touché par des événements de crues qui ont causé d'importants dommages, dont les coûts ont dépassé les 500 millions de Francs Suisses. De cette situation est né le projet de la Troisième Correction du Rhône, dont l'objectif est d'améliorer la protection contre les crues du Rhône alpin dans les cantons de Vaud et du Valais. Dans ce contexte, le système MINERVE cherche à contrôler les débits pendant les événements de crues dans ce bassin versant, en tirant avantage du réseau d'aménagements hydroélectriques et des réservoirs existants. Ce système joue aussi un rôle dans le projet national OWARNA de l'Office Fédérale de l'Environnement dont le but est de mettre en place une plateforme nationale sur les niveaux d'alarme des dangers naturels.

La surface contributive du bassin versant supérieur du Rhône possède de hautes montagnes et de grands glaciers. Sa superficie est de 5521 km<sup>2</sup> et son altitude varie de 400 à 4634 m. s.m. Plusieurs aménagements hydroélectriques présentant de grands barrages et réservoirs sont situés sur ce bassin, influençant donc le régime hydrologique. Leur impact sur les crues peut ainsi être significatif. De la même façon, des opérations préventives appliquées sur ces installations sont capables de diminuer la pointe de débit dans le Rhône et ses affluents, réduisant ainsi les dommages.

Le système MINERVE s'appuie sur les débits observés, les caractéristiques des réservoirs et des aménagements hydroélectriques ainsi que sur les prévisions météorologiques d'ensemble COSMO-LEPS et les prévisions déterministes COSMO-7 et COSMO-2 fournies par l'Office Fédéral de Météorologie et de Climatologie, MétéoSuisse. Le modèle hydrologique suit un approche semi-distribué et contient 239 sous-bassins divisés en 1050 bandes d'altitude permettant de prendre en compte les processus liés à la température, tel que la fonte des

neiges ou des glaciers. Pour chaque bande d'altitude, la précipitation, la température et l'évapotranspiration potentielle sont calculés.

Le modèle hydrologique a été implémenté dans le logiciel Routing System dont la conception orientée objets permet la prise en compte et la modélisation aisée des processus hydrologiques, hydrauliques et opérationnels. Les données météorologiques (observées et prévues) sont introduites comme input dans le modèle. Durant les périodes de calage et de validation du modèle, seules des données observées (précipitation, température et débit) sont utilisées. Pour la prévision opérationnelle des crues, les observations sont utilisées pour la mise à jour des conditions initiales du modèle hydrologique, et les prévisions météorologiques pour les simulations hydrologiques.

Routing System fournit ensuite des prévisions hydrologiques sur tout le bassin versant. Ensuite, un système d'avertissements développé spécialement pour ce bassin fournit un rapport d'avertissements des crues. Celui-ci décrit l'évolution de la situation hydrologique aux principaux points de contrôle du bassin versant. Finalement, trois niveaux successifs d'avertissements sont affichés en fonction des seuils respectifs de débits critiques.

De plus, le système à multi-réservoirs est géré de manière optimale afin de limiter ou d'éviter les dommages pendant les crues. Un système d'aide à la décision appelé MINDS (MINERVE Interactive Decision Support System) a été développé pour la prise de décision en temps réel basé sur les prévisions hydrologiques. Cet outil propose des mesures préventives de turbinage ou de vidange des réservoirs aux opérateurs des aménagements hydroélectriques afin d'obtenir une capacité de stockage optimale. Le but est de retenir les débits entrants dans les réservoirs pendant les crues et de stopper la restitution pendant les pointes de crue, en prenant en compte toutes les restrictions et les conditions actuelles du réseau. Une telle gestion des réservoirs permet de limiter les dommages dans le bassin dus aux crues.

L'optimisation des réservoirs pour la gestion des crues est réalisée à l'aide de prévisions déterministes et probabilistes. La fonction objective pour l'optimisation est définie en suivant une méthodologie d'aide à la décision multi-attribut. Ensuite, l'optimisation est calculée soit avec un algorithme Greedy, soit avec un algorithme SCE-UA (Shuffled Complex Evolution – University of Arizona). Le système d'aide à la décision développé combine la grande qualité du système d'optimisation avec une interface conviviale. Le but est d'aider les décisionnaires à être impliqués directement dans les principales démarches à suivre dans la prise de décisions ainsi qu'à comprendre les mesures entreprises et leurs conséquences.

# Resumen

## **Gestión de crecidas en una cuenca compleja con un sistema de ayuda a la decisión en tiempo real basado en previsiones hidrológicas**

Palabras clave: modelización hidrológica, previsión de crecidas, sistemas de ayuda a la decisión, gestión de aprovechamientos hidroeléctricos, control de crecidas.

Durante las últimas décadas, la cuenca vertiente del río Ródano, aguas arriba del lago Lemán, ha sido sacudida por tres grandes crecidas que causaron importantes daños y superaron los 500 millones de Francos Suizos. De este entorno nació el proyecto de la 3<sup>ra</sup> corrección del río Ródano, cuyo objetivo es mejorar la protección contra las crecidas en la cuenca vertiente superior del Río Ródano, en los Cantones de Vaud y de Valais. En este marco, el sistema MINERVE busca contribuir a mejorar el control de caudales durante las crecidas en la cuenca, aprovechando la red de múltiples embalses existentes. Este sistema también está vinculado con el proyecto nacional OWARNA de la Oficina Federal Suiza de Medio Ambiente para establecer una plataforma nacional de niveles de alarma por riesgos naturales.

La Cuenca vertiente superior del río Ródano se sitúa en una zona con importantes montañas y grandes glaciares. La superficie de la cuenca es de 5521 km<sup>2</sup> y su elevación varía entre 400 y 4634 m s.n.m. Diversos aprovechamientos hidroeléctricos con grandes presas y embalses se encuentran localizados en esta zona, influenciando el régimen hidrológico. Su impacto durante los periodos de crecida puede ser significativo, de igual manera que las operaciones preventivas pueden disminuir los picos de caudal en el río Ródano y sus principales tributarios, reduciendo de esta manera los daños por posibles inundaciones.

El sistema MINERVE explota tanto observaciones de caudal, datos de embalses y aprovechamientos hidroeléctricos, como previsiones meteorológicas probabilistas (COSMO-LEPS) y deterministas (COSMO-2 y COSMO-7) de MeteoSwiss. El modelo hidrológico de la cuenca vertiente de estudio sigue un enfoque semi-distribuido. La cuenca se divide en 239 sub-cuencas, separadas en bandas de altitud de 500 m, para hacer un total de 1050. Para cada banda de altitud son calculadas la precipitación, la temperatura y la evapotranspiración

potencial. Estas bandas han sido consideradas para describir correctamente los procesos gobernados por la temperatura, tales como la fusión de nieve o de glaciares.

El modelo hidrológico ha sido implementado con el software Routing System. El entorno de programación orientada objeto permite una fácil modelización de los procesos hidrológicos, hidráulicos y operacionales. Los datos meteorológicos (observados y previstos) son introducidos como input en el modelo. Durante los periodos de calibración y validación del modelo, únicamente se utilizaron datos observados. Para las previsiones operacionales en crecidas, las observaciones se usaron para la actualización de las condiciones iniciales del modelo hidrológico y las previsiones meteorológicas para las simulaciones hidrológicas.

Posteriormente, Routing System proporciona previsiones hidrológicas en toda la cuenca vertiente. A continuación, un sistema de advertencias desarrollado especialmente para esta cuenca proporciona un informe de avisos por crecidas. Este informe suministra la evolución de la situación hidrológica en los principales puntos de control de la cuenca. Finalmente se muestran los tres niveles de advertencia durante una situación de crecida en función de los respectivos umbrales de caudales definidos para cada uno de ellos.

Además, el sistema de múltiples embalses es gestionado de manera óptima para limitar o evitar daños durante las crecidas. Un sistema de ayuda a la decisión llamado MINDS (MINERVE Interactive Decision Support System) ha sido desarrollado para la toma de decisiones en tiempo real basada en las previsiones hidrológicas. Esta herramienta propone operaciones preventivas como turbinajes y vaciados intermedios (o de fondo) en los aprovechamientos hidroeléctricos para obtener una capacidad de almacenamiento óptima. El objetivo es retener los caudales entrantes en los embalses durante las crecidas y parar las sueltas durante los caudales punta, teniendo en cuenta todas las restricciones y las condiciones actuales del sistema. Dicha gestión de los embalses ayuda a limitar los daños en el cuenca vertiente debido a las crecidas.

La gestión de presas para el control de crecidas se realiza con previsiones deterministas y probabilistas. La definición de la función objetivo para la optimización se hace por medio de la ayuda a la decisión multi-atributo. A continuación, la optimización se calcula con un algoritmo Greedy o con otro SCE-UA (Shuffled Complex Evolution – University of Arizona). El sistema de ayuda a la decisión desarrollado combina las grandes prestaciones del sistema de optimización con una interfaz de fácil manejo. El objetivo es ayudar a los responsables para que estén directamente implicados en los principales pasos a seguir durante un proceso de toma de decisiones y a comprender las medidas tomadas y sus consecuencias.

# Table of contents

Abstract	i
Résumé	iii
Resumen	v
1. Introduction	1
1.1 Preamble	2
1.2 Floods: today and tomorrow	3
1.3 Decision support systems for flood management	5
1.4 Framework of the project	5
1.5 The MINERVE project	7
1.5.1 First stage – MINERVE 2007	7
1.5.2 MINERVE 2011	8
1.6 Research objectives	10
1.7 Structure of the report	12
2. Review of hydro-meteorological forecasts	15
2.1 The forecast progress	16
2.2 Evolution of meteorological forecasts	18
2.2.1 First forecasts and evolution	18
2.2.2 Deterministic meteorological forecast	20
2.2.3 Ensemble Prediction System - EPS	23
2.2.4 Other models: analogue technique, radar and satellite	30
2.2.5 Reliability and utility of the meteorological forecasts	32
2.3 Hydrological models and forecast warning systems	32
2.3.1 General overview of hydrological models	32
2.3.2 Empirical models	33
2.3.3 Conceptual models	35
2.3.4 Physically-based models	36
	vii

2.3.5	Which is the best hydrological model?	37
2.3.6	Hydrological forecast systems	38
2.3.7	Flood alert systems	40
2.3.8	MINERVE hydro-meteorological system	41
<b>3.</b>	<b>State of the art of decision support systems for reservoirs management</b>	<b>45</b>
3.1	Operation of water storage systems	46
3.2	Hydropower plants operation	47
3.3	Decision support systems for water resources management	48
3.4	Optimisation methods for reservoir management and flood control	50
3.4.1	Introduction to optimisation methods for water resources management	50
3.4.2	Optimisation approaches of reservoirs without flood management	50
3.4.3	Optimisation approaches integrating flood management	52
3.4.4	Overview of the optimisation approaches	57
3.4.5	Optimisation inputs	59
3.5	Risk concept and multi-criteria decision making	60
3.5.1	The decision theory	60
3.5.2	Notion of risk	61
3.5.3	Multi-criteria decision making	62
3.6	User-friendly decision support systems	64
3.6.1	Case studies of user-friendly systems for water resources management	64
3.6.2	Required features for interactive flood management	66
3.7	Expert System of previous MINERVE project	66
3.7.1	Reservoir management objectives for flood control	66
3.7.2	Expert System objectives	67
3.7.3	Simplified methodology for a multi-reservoir system	68
3.7.4	Optimisation procedure	70
<b>4.</b>	<b>MINERVE hydrological modelling approach</b>	<b>73</b>
4.1	Meteorological observations and forecasts	74
4.1.1	An introduction to meteorology in the MINERVE framework	74
4.1.2	Meteorological data	75
4.1.3	Meteorological forecasts by MeteoSwiss	75
4.1.4	Historical floods	76
4.1.5	Analogue technique	76
4.2	Hydrological forecasts	78
4.2.1	An introduction to hydrology in the MINERVE framework	78
4.2.2	Hydrological data	78

---

4.2.3	Semi-distributed hydrological model	79
4.2.4	Flow routing	86
4.2.5	Catchment model	86
4.2.6	Routing System MINERVE	86
4.3	Warning system	88
4.3.1	Flood warnings overview	88
4.3.2	Warning levels	89
4.3.3	Flood management in the Upper Rhone River basin	90
4.3.4	Warning Report	93
5.	Hydro-meteorological forecasts in the Upper Rhone River basin	97
5.1	Performance evaluation of the forecasts	98
5.2	Analysis of meteorological performance	99
5.2.1	Meteorological indicators	99
5.2.2	Analysis of meteorological results	104
5.3	Hydrological simulations with Routing System MINERVE	108
5.3.1	Hydrological indicators	108
5.3.2	Hydrological results	114
5.3.3	Hydrological performance of studied events	127
5.4	Warning reports	128
5.5	Hydro-meteorological conclusions	131
5.5.1	Hydrological forecast system	131
5.5.2	Outlook of the hydrological forecasts	132
6.	MINERVE Interactive Decision Support System	133
6.1	Interactive decision support system for flood management	134
6.1.1	Hydraulic simulations	134
6.1.2	Optimisation approach	135
6.2	Hydraulic simulation model	136
6.2.1	Model description	136
6.2.2	Model equations	139
6.2.3	Turbining cycle with Business as Usual operations	141
6.3	Economical analysis of flood events	142
6.3.1	Expected damages	142
6.3.2	Costs of potential preventive operations	144
6.3.3	Global loss function	150
6.4	Multi-Criteria Optimisation	151
6.4.1	Perception of the objective function	151

6.4.2	Review of algorithms for Multi-Attribute Decision Making	153
6.4.3	Selected MADM methods for MINDS	157
6.5	Optimisation process of MINDS	163
6.5.1	System optimisation	163
6.5.2	Reference simulations of natural basin and equipped basin	164
6.5.3	Description of main model parameters	165
6.5.4	Preventive operation parameters	166
6.6	Iterative Ranking Greedy optimisation algorithm	168
6.6.1	Introduction to the Greedy approach	168
6.6.2	Model architecture of the Greedy approach	169
6.6.3	Groups ranking	171
6.6.4	Algorithm parameters of the IRGA approach	172
6.6.5	Objective function of the IRGA approach	172
6.7	SCE-UA optimisation algorithm	173
6.7.1	Introduction to the Shuffled Complex Evolution – University of Arizona approach	173
6.7.2	Model architecture of the SCE-UA approach	173
6.7.3	Algorithm parameters of the SCE-UA approach	178
6.7.4	Objective function of the SCE-UA approach	178
6.8	Hybrid optimisation algorithm	179
6.9	MINDS software	180
6.9.1	User interface	180
6.9.2	Results presentation	185
7.	Application of the MINERVE Interactive Decision Support System to the Upper Rhone River basin	191
7.1	Application to two historical reference flood events	192
7.2	Priority decisions and warnings	192
7.2.1	Introduction to decision making	192
7.2.2	Priority decisions for reservoir operations	193
7.2.3	Check points warnings	194
7.3	Parameters to optimise	195
7.4	Optimisation performance	196
7.4.1	Presented analysis	196
7.4.2	Optimisation of one group	197
7.4.3	Optimisation of two groups	205
7.4.4	Optimisation of the entire basin with all groups	212
7.4.5	Conclusions from the optimisation results	219
7.5	Real-time procedure and results	220



7.5.1	Real-time approach	220
7.5.2	Flood event of October 2000	222
7.5.3	Flood event of September 1993	230
7.6	Optimisation methods and results conclusions	238
7.6.1	Performance of the different methods	238
7.6.2	Computation time	239
7.6.3	Selected methods for real-time optimisations	240
8.	Conclusions and outlook	241
8.1	General overview	242
8.2	Hydro-meteorological forecasts and flood warnings	243
8.2.1	Meteorological forecasts	243
8.2.2	Hydrological model	243
8.2.3	Hydrological forecasts	244
8.2.4	MINERVE warning system	244
8.3	MINERVE Interactive Decision Support System - MINDS	245
8.3.1	Main goal of the MINERVE Interactive Decision Support System	245
8.3.2	Hydraulic simulation model	245
8.3.3	Optimisation methods for reservoir management	246
8.3.4	Decision Support System interface	247
8.3.5	Strengths of MINDS	248
8.4	Outlook	249
8.4.1	General perspectives of the MINERVE flood forecast and management system	249
8.4.2	Outlook for hydro-meteorological forecast systems	249
8.4.3	Outlook for the MINERVE Interactive Decision Support System - MINDS	251
9.	References	253
	Acknowledgments	285
	List of Figures	287
	List of Tables	295
	Notation	303
	Acronyms	309
	Appendices	313



“Floods are ‘acts of God’ but flood losses are largely acts of man”

(White, 1942)

## **1. Introduction**

## 1.1 Preamble

Predict the unpredictable, predict the floods. Each time the human knowledge grows, its dreams and aims go far away.

Two hundred years ago, fighting against floods meant taking all possible measures when possible and rebuilt the inevitable damage. Subsequently, first weather forecasts gave an option to anticipate the inevitable and be prepared for the consequences. However, these primitive systems have never been reliable enough. Inaccurate forecasts are related to uncertainty of the atmosphere behaviour. Meteorologists' primary intention was trying to fix the uncertainty, but they could not. Then, as James E. Watson once said (Kent, 1932): "if you can't beat them, join them", meteorologists did just this; their aim evolved from trying to be certain, to trying to predict the uncertainty.

From only single forecast in the 1980s, forecasts developed to an ensemble in the nineties. Starting from different initial conditions, they provided different possible scenarios or forecast members.

Currently, predicting floods goes hand in hand with probability. The scientific community knows more each day about this new "couple", particularly when coupling with decision support systems for real-time decision making.

Decision support systems have seen improved its performance thanks to computer development. In the eighties, these systems proposed one final result, difficult to validate, without the intervention of the decision maker and without an interface. The goal was basically to introduce all possible calculations in a code for obtaining a result faster than doing it manually.

Currently, decision support systems have undoubtedly evolved. Nobody conceives the idea of using a system without an interface or without having a minimum interaction with the problem to solve. Systems which are able of taking into account the opinion or position of decision makers are not any more only a plus value, but a requirement.

The development of decision support systems, combined with ensemble forecasts and optimisation methods is a new field which evolves very fast. Today is the present for these innovative coupled systems, but tomorrow will be just the past.

## 1.2 Floods: today and tomorrow

In the last and this centuries, floods have proven to be one of the severest natural disasters. Furthermore, there are strong scientific evidences that extreme flood events will become more frequent in the future, with an increase in precipitation during extreme events (Christensen and Christensen 2003). In fact, recent floods seem to be already more abundant and destructive in many regions of the globe (Kundzewicz and Schellnhuber, 2004) and are probably responsible for more damages than all other destructive natural events combined (Kron, 2005).

The increase of the floods intensity and its consequences can be basically explained by two reasons. First, global warming is producing bigger and more frequent flood events. Second, the intensification of the flood plain use by urbanisation increases the consequences of the events.

Numerous studies on extreme floods, their locations and their consequences have been recently realized (Hersch, 2002; Kundzewicz and Schellnhuber, 2004; Kron, 2005; Barredo, 2007, Gaume et al., 2009; Llasat et al, 2010). A literature review reveals numerous recent devastating floods. The Bangladesh flood in April 1991 caused 140'000 fatalities. Flood damages in China due to the 1998 summer flood exceeded thirty US-billion dollars damage (the number US-billion is equivalent to one thousand millions in Europe). Also the November 1999 flood caused by overflow of the Aude and Tarn Rivers, in France, produced thirty-three deaths and damage costs of five hundred US-million dollars. In 2001, a wind storm and flood event in Algeria caused more than six hundred casualties. The August 2002 flood in Germany produced damage on the order of sixteen US-billion dollars as well as forty-seven casualties. Also September of 2002, the Gard Department in France (Rhône River) had more than one US-billion dollars of damage and twenty three fatalities. In the UK, (Boscastle, Tintagel and Camelfor), the August 2004 flood damage totalled approximately one US-billion dollars. In Switzerland, the flood of August 2005 claimed six lives and caused material damage of three US-billion dollars. And the list could go on further.

According to Kron (2005), floods can be classified as three main types: storm surge, river flood and flash flood. Storms surges occur along the coasts of seas and big lakes. River floods results from intense and/or persistent rain during a certain time over a large area. Flash floods are associated with local events produced by intense rainfall over a small area, being sometimes the beginning of a river flood.

Focusing on river floods, which give the background to this research project, this flood type is the combination of different factors: weather conditions, soil saturation and soil properties as well as the current conditions and location of hydraulic structures. River floods can occur during the summer/autumn seasons, generally related with high rain falls and saturated soil. They also can happen during the winter/spring seasons, usually related with large-scale precipitations, sometimes connected to snow and ice melt (Barredo, 2007).

Table 1.1 shows examples of high flood damages in recent years, showing foremost that floods can take place in practically any region of the globe.

According to other sources from the previously presented literature, floods can be also classified in different ways, such as the weather characteristics or the type of flood. The idea to keep in mind is the magnitude of these events. Regarding economical values, at least a nine figure number seems usually linked to floods. Trying to reduce the enormous cost of floods becomes thus mandatory.

Table 1.1 High costs floods from 1990 to 2005 with original values, not adjusted for inflation (from Kron, 2005)

<b>Rank</b>	<b>Year</b>	<b>Country / Countries (mainly affected regions)</b>	<b>Economical losses US\$ billion</b>	<b>Insured (%)</b>
1	1998	China (Yangtze, Songhua)	31	3
2	1996	China (Yangtze)	24	2
3	1993	USA (Mississippi)	21	6
4	2002	Central Europe (Elbe, Danube)	19	16
5	1995	North Korea	15	0
6	1993	China (Yangtze, Huai)	11	0
7	1994	Italy (North)	9.3	<1
8	1993	Bangladesh, India, Nepal	8.5	0
9	2000	Italy (North), Switzerland (South)	8.5	6
10	1999	China (Yangtze)	8.0	0
11	1994	China (Southeast)	7.8	0
12	1995	China (Yangtze)	6.7	1
13	2001	USA (Texas)	6.0	58
14	1997	Czech Rep, Poland, Germany (Odra)	5.9	13

However, not all about the future includes bad prophecies. New concepts of flood risk management have been introduced. Hazard mapping is used more and more, especially in Europe with the aim of managing risk regions and implementing flood mitigation structures.

In addition, flood forecasts can help communities to be prepared for a storm surge or a river flood, which is still difficult for flash floods. Finally, but not least, flood management strategies are more and more developed and used. Pre-defined action plans to flood water diversion or reservoir management are often a very cost-efficient methods to reduce the event amplitude and have become new fields of research.

### **1.3 Decision support systems for flood management**

The risk of floods can never be completely removed. However, its impacts can be reduced thanks to early flood warnings and effective river basin management.

Decision Support Systems (DSS) are defined as tools for helping end users (usually called decision makers) to choose among a set of possible decisions or alternatives. In the domain of flood management, DSS are used for a lot of tasks and are becoming important as part of the decision making process.

Decision makers distinguish three phases of flood management: pre-flood, operational flood and post-flood management. Valuable flood DSS tools have to provide accurate flood forecast information for the first phase, and particular useful strategies for the second one.

They can be used for warning advertisements to population in general or to selected groups or services such as forest rangers, police forces, fire brigades, military forces or other intervention cells. The goal is to be prepared to fight against these natural disasters.

They can also be used, in a second step, to manage the tasks of the intervention groups, in order to have a better overview of the hazard situation, generally distributed in space and time.

Finally, they can be used also to direct actions for flood control, such as automatic opening of lateral weirs, automatic channel derivations or reservoir management.

### **1.4 Framework of the project**

During the last two decades, the Upper Rhone River basin has been hit by several flood events causing important damages. During September 1993, catastrophic inundations occurred in the “Haut-Valais” region, especially in the Brig city and in the Saas Valley, with a total cost of around 650 million CHF. In October 2000, “Bas-Valais” region was also affected as well as

the Gondo village, with a total cost of 670 million CHF. In September 2006, MeteoSwiss launched an alert after prediction of heavy precipitation in the Southeast region of the Valais Canton (Viège and Simplon), but rainfall did not cross the Alps barrier and remained intense on the Italian side. Similarly, during the May 2008 event, the surveillance system had been put into place. However, flooding was not produced because precipitations were less than expected.

These events were caused by heavy precipitation over a large part of the basin, combined on occasion with snowmelt (such as in October 2000), and can be considered as river floods. The soil capacity to store water was in these cases exceeded and runoff went quickly to the Rhone River, causing considerable water level raise with overtopping of the flood protection dykes in 1993 and 2000. After these floods, the Vaud and Valais Cantons decided to develop a real-time flood forecast system, able to manage such extreme events.

Following these severe floods, a project called “the Third Rhône Correction” was initiated. This ambitious project reconciled the need for flood prevention with the pressures of urban expansion and human activities in floodable zones as well as the improvement of the ecological condition of the river. The project is different from the preceding efforts because it is at first and foremost a global approach to the river that takes socio-economic, political and ecological elements into account. The project is based on collaboration and partnerships; the priority is to create sustainable development solutions which address also changes in the professional and leisure activities of the local populations.

In this framework, the MINERVE (Modelling of extreme events in the Rhone River and their effects) project was started with the purpose to contribute to the flood control in the Upper Rhone valley, taking advantage of the existing hydropower schemes with multi-reservoirs. The aim is to store inflows into reservoirs during the flood peak, imposing preventive operations before the flood peak when available storage volumes are not high enough.

Nevertheless, the flooding problem is also complex when using hydropower schemes for flood management because the possible loss of energy production must be avoided or compensated. Preventive operations for increasing storage capacity (during flood peaks) can lead to energy losses for operators and, consequently, to economical losses which should be considered in terms of producing a fully performing DSS.



## 1.5 The MINERVE project

### 1.5.1 First stage – MINERVE 2007

This first stage of the MINERVE project was developed during the period 2003-2007 at the Ecole Polytechnique Fédérale de Lausanne (EPFL) at the Hydraulic Constructions Laboratory (LCH) and at the Laboratory of Hydrology and Land Improvement (HYDRAM), with the main support of the Valais Canton, but also with the help of the Swiss Federal Office for the Environment (FOEN) and MeteoSwiss.

This scientific project was achieved with deterministic forecasts (Boillat, 2005; Jordan, 2007; Jordan et al., 2008) as presented in Figure 1.1, and allowed the development of:

- the semi-distributed hydrological model GSM-Socont,
- the hydrological and hydraulic simulation tool, Routing System II,
- the coupled hydro-meteorological deterministic system associated to COSMO-7 meteorological forecasts from MeteoSwiss and,
- the deterministic Expert System for preventive management of the hydropower plants during floods in the Upper Rhone River basin.

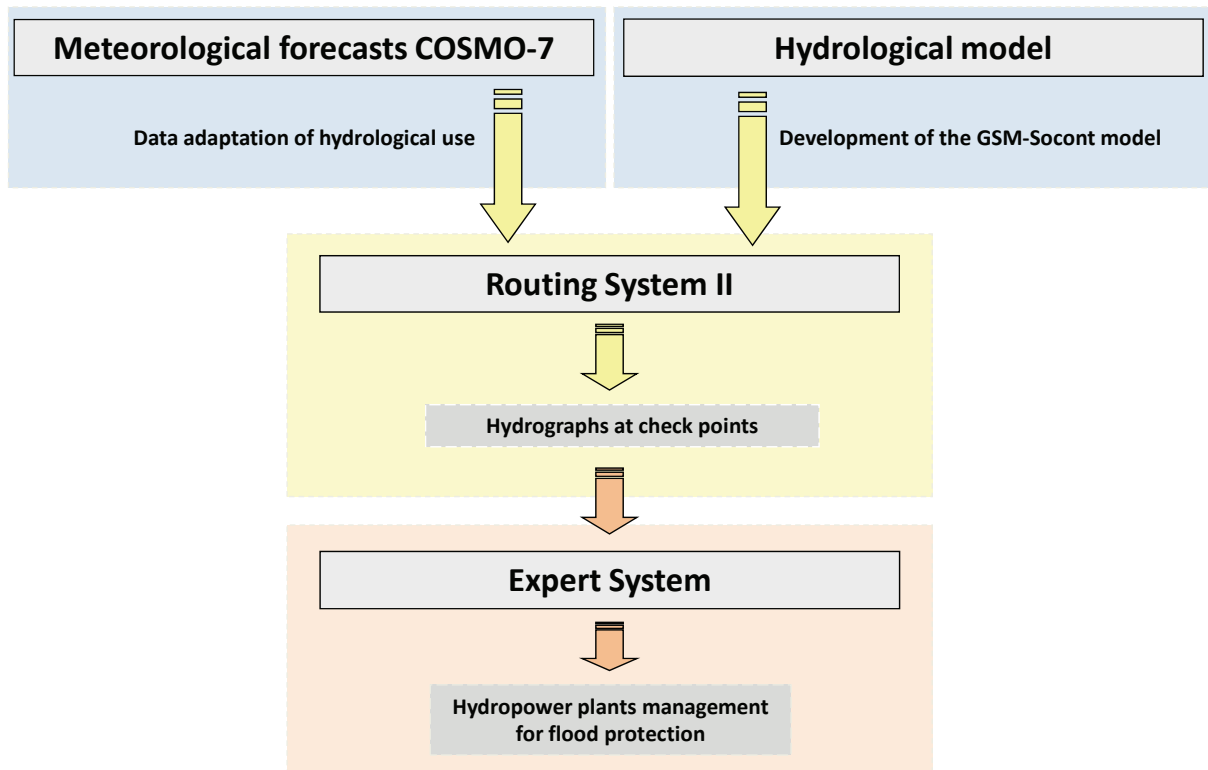


Figure 1.1 Scheme of the first stage of the project – MINERVE 2007

The goals of the project highlight two different modes of operation and use of the system. The first corresponds to normal continuous operation allowing to follow the evolution of the hydrological situation in the catchment area. The second responds to a crisis situation where the need is to inform and facilitate decision-making for the protection against floods.

In September 2006, the MINERVE system was operated in real-time for the first time in its history. Following a warning given by MeteoSwiss, a hydro-meteorological forecast was conducted for a time horizon of 72 hours. It helped to establish an assessment of the situation over the basin as well as of the reservoirs. Furthermore, the system facilitated the determination of the priority decisions to be taken, in terms of reservoir management, to strengthen the security of population and goods.

### **1.5.2 MINERVE 2011**

Although this manually operational system was convincing, it would be more efficient by using probabilistic meteorological forecasts since it can help decision makers to obtain a better assessment of the uncertainty and risk associated to a flood forecast (Boillat, 2009; García Hernández et al., 2009d). Furthermore, the analogue technique, which searches analogy between the current meteorological situation and past events, could also be helpful for increasing the robustness of the system (García Hernández et al., 2009e; Horton et al., 2011). Finally, the improvement of the hydrological model GSM-Socont could also provide an enhancement in the hydro-meteorological forecasts and remains a focus of interest (García Hernández et al., 2009e; Tobin et al., 2011a; Tobin et al., 2011b).

To obtain such a result, the collaboration of different research institutes is necessary. The MINERVE 2011 project has been developed in cooperation with two laboratories of EPFL, the Hydraulic Constructions Laboratory (LCH) and the Ecohydrology Laboratory (ECHO), as well as to the Institute of Geomatics and Analysis of Risk (IGAR) of the University of Lausanne (UNIL), as presented in Figure 1.2.

The MINERVE 2011 project is developed in partnership by the Swiss Federal Office for the Environment (FOEV), the Roads and Water courses Service and the Energy and Water Power Service of the Valais Canton as well as the Water, land and Sanitation Service of the Vaud Canton. The Swiss Weather Service (MeteoSwiss) provides the weather forecasts and hydroelectric companies communicate information concerning their hydropower plants.

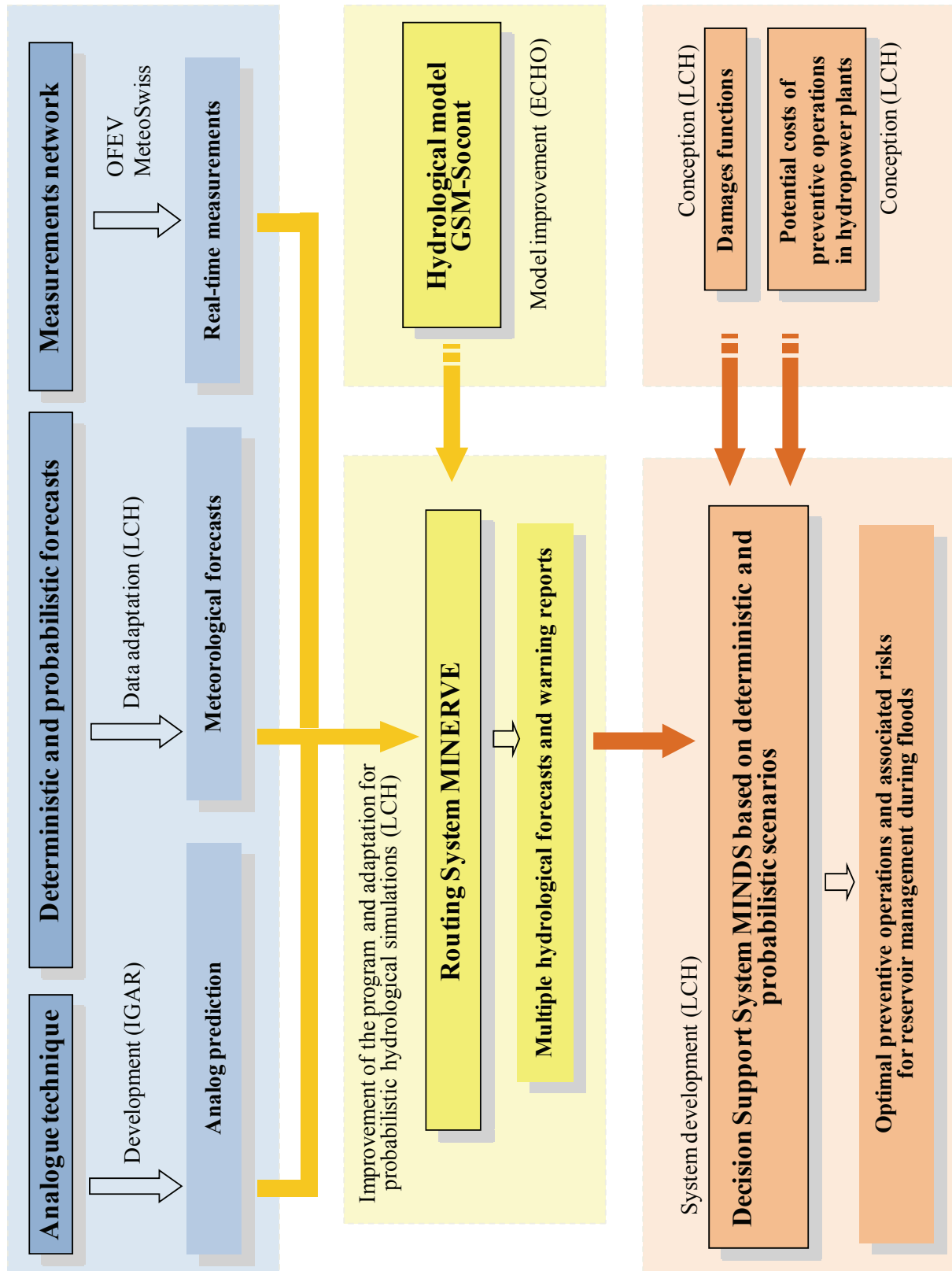


Figure 1.2 Scheme of the current stage of the project MINERVE 2011

## 1.6 Research objectives

The main objectives of the present research project are:

- to establish a system capable of providing hydrological ensemble forecasts,
- to propose a framework for flood warning advertisements,
- to develop a procedure and an optimisation methodology for hydropower plants management in case of expected flood,
- to implement an interactive user-friendly Decision Support System (DSS) for flood management to be used in real-time situations by decision makers, and
- to apply the developed system to the Upper Rhone River basin.

Figure 1.3 illustrates the main steps in order to reach the research objectives. Before creating a system for ensemble forecasts, a first study about the structure and the performance of the new ensemble meteorological forecasts was conducted. Then, the hydrological software was modified in order to be able to deal with different simulations at the same time.

Once working, deterministic and ensemble hydrological forecasts were simulated, and the system for flood prediction with COSMO-LEPS and COSMO-7 was assessed. Furthermore, a methodology for flood warning advertisements is proposed and a tool providing warning reports is developed and applied to the main check points of the Upper Rhone River basin.

Subsequently, a procedure for flood control based on reservoir management is also proposed. Different methodologies and algorithms for real-time solving are tested and its performance assessed.

Finally, algorithms are introduced in the developed DSS, with the aim of interactivity, user-friendliness and maximum performance. The application to the case study of the Upper Rhone River basin proves the practical relevance of this research project.

Besides mathematical developments, this research project is multidisciplinary. It encloses different disciplines as meteorology, hydrology, optimisation tools, decision support system,... as well as social sciences in terms of facing decision making tasks, sometimes neglected in such projects.

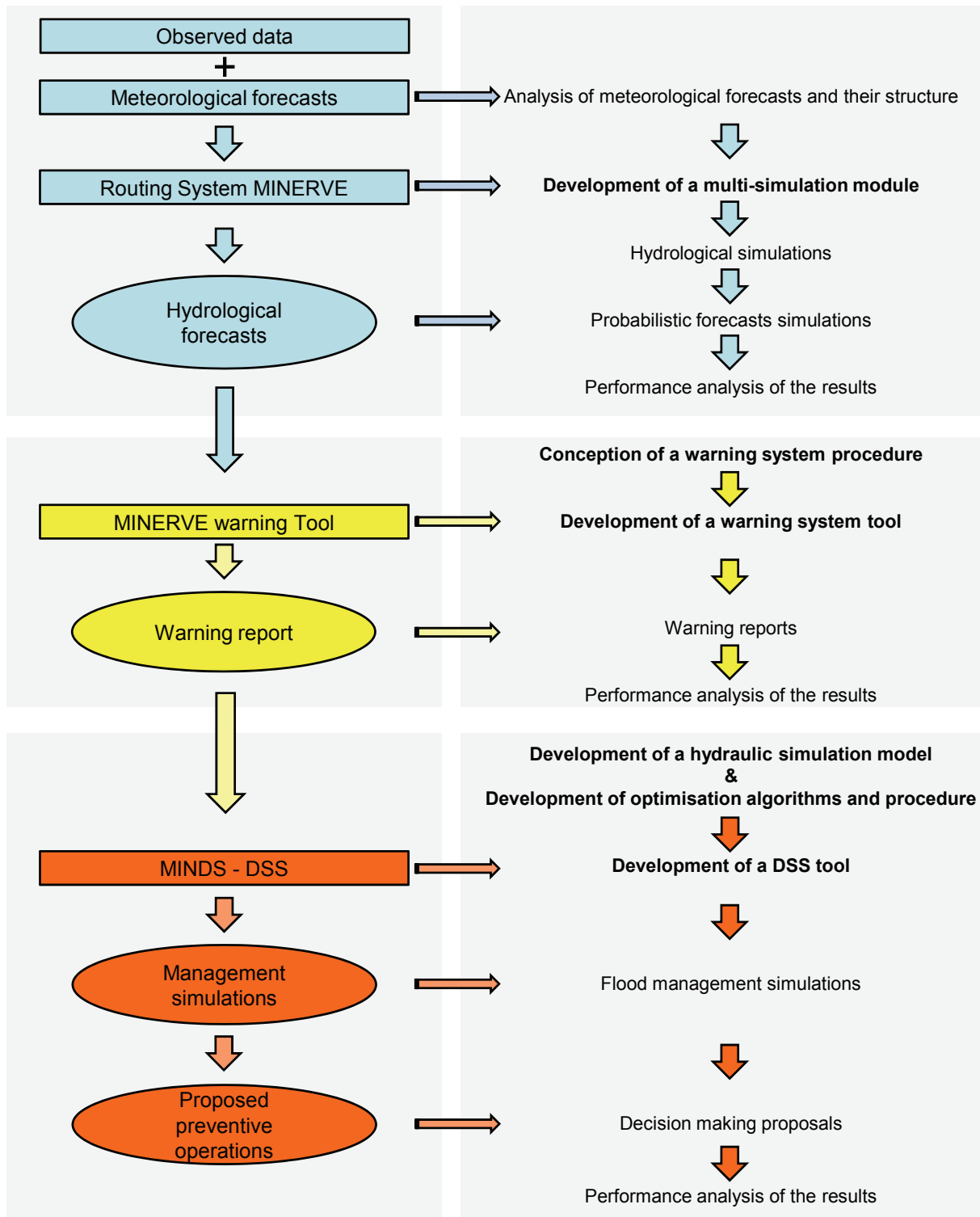


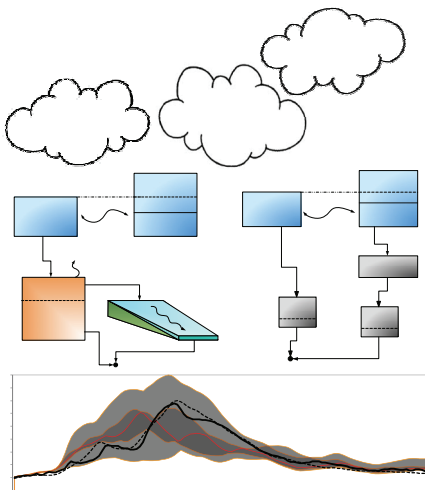
Figure 1.3 Scheme of the research project with the main objectives developed

## 1.7 Structure of the report

This report is divided in eight chapters. The first chapter introduces the framework of the MINERVE project. The second and third chapters summarise the literature review in the field of hydro-meteorology and decision support systems. Chapter four presents the data and the hydrological model used in this research project. Chapter five discusses the hydro-meteorological results with deterministic and probabilistic forecasts. In the sixth and seventh chapters, an optimisation algorithm for flood management is proposed and applied in the Upper Rhone valley with detailed discussion on the results. Finally, chapter eight concludes with an overview of the research project and the main results and perspectives.



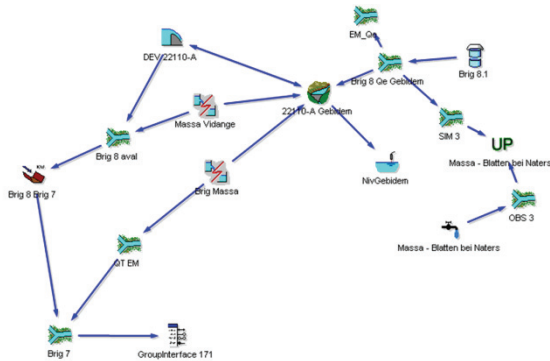
**Chapter 1** contains an introduction to the MINERVE project as well as a detailed overview of the most important objectives of the research project.



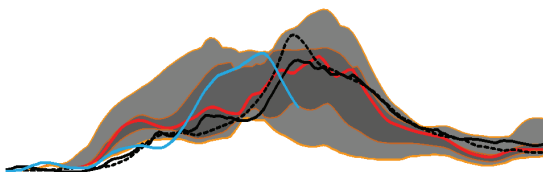
**Chapter 2** comprises a literature review on hydro-meteorological forecasts. Firstly, meteorological forecasts and their evolution to ensemble forecasts are presented. Secondly, a classification and a review of different hydrological models is discussed. Finally, hydro-meteorological forecasts and flood alert systems are presented.



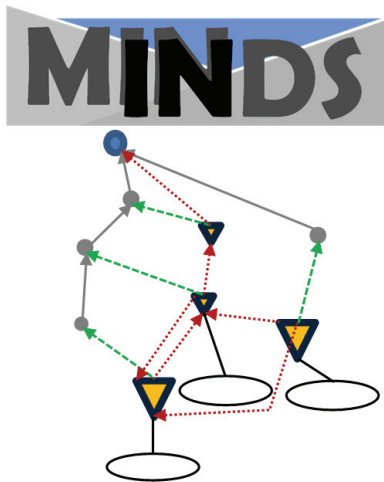
**Chapter 3** gives the state of the art in decision support systems with the focus on reservoir management and flood control using different scientific approaches. Special emphasis is given on multi-attribute decision making methods for flood management solutions based on probabilistic forecasts.



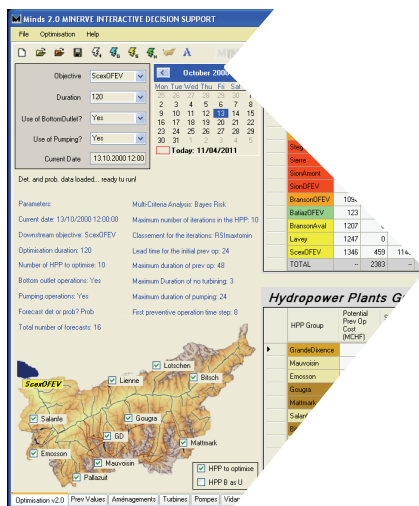
**Chapter 4** includes an overview of the hydrological model of the Alpine Rhone basin, the available data and the development of the warning report tool. The equations and the description of the hydrological model are thoroughly explained. The available meteorological forecasts for hydrological simulations are presented with their characteristics. Finally, a warning system is proposed and the required supplementary data presented.



**Chapter 5** is dedicated to simulation results and their performance. Different deterministic and probabilistic indicators are presented for the performance assessment, followed by the presentation of the warning reports and a discussion.



In **Chapter 6**, the basis of the MINERVE Interactive Decision Support System (MINDS) is presented. The hydraulic simulation model is explained with all existing elements. The Greedy and the Shuffled Complex Evolution optimisation algorithms for flood control are developed in detail, as well as the multi-attribute decision making methodology for dealing with probabilistic forecasts.



In **Chapter 7**, the decision support system MINDS is applied to the Alpine Rhone basin studying the performance of the system by resimulation of past events. The results are based on decreasing flood peaks and on analysis of theoretical damages reductions, taking into account the potential costs of preventive operations.



**Chapter 8** gives the general conclusions of the research project and highlights the main original contributions. Furthermore, some perspectives for the application of the project in the Vaud and Valais Cantons in Switzerland are presented as well as guidelines for future research.



“Remember that all models are wrong; the practical question is how wrong do they have to be  
to not be useful”

(Box and Draper, 1987)

## **2. Review of hydro-meteorological forecasts**

## **2.1 The forecast progress**

Weather is a chaotic system and small errors in the initial conditions of a forecast grow rapidly affecting the predictability. Furthermore, predictability is also limited by model errors linked to the approximate simulation of atmospheric processes. These two sources of uncertainty limit the skill of forecasts in an unpredictable way with random quality forecasts.

Weather forecasting systems have been improved thanks to advancement in the Numerical Weather Prediction (NWP). NWP uses the current weather situation as initial conditions for atmosphere mathematical models to provide a forecast. The performance of NWP models has been continuously improved thanks to progress in earth sciences and observation systems like meteorological and earth-observing satellite systems, information technologies and efficient telecommunication systems as well as better computer resources.

The forecasts have been traditionally expressed as single deterministic series. The aim is to reproduce the state of the atmosphere in a three dimensional grid and to solve the equations able to predict the future. These equations are clear nonlinear partial differential equations, with solutions obtained by approximation using numerical analysis. The models contain millions of grid points over a determined period and the time required for this computation is limited. Furthermore, small differences in the initial data can significantly affect the results. However, the estimate of the atmosphere current state is inaccurate and numerical models have inadequacies leading to forecast errors that tend to grow with the lead time and which depend on the atmosphere flow itself.

The Ensemble Prediction System (EPS) completes deterministic forecasts taking into account the existing uncertainty regarding the current state of the atmosphere. Ensemble forecasting helps to quantify this uncertainty and extend weather forecasting farther into the future than would otherwise be possible. Two main questions however remain, namely which is the best method for defining the initial ensemble of the prediction and which is the best way to use data assimilation.

New EPSs are also helpful information for hydrological predictions which are implemented nowadays in the hydrological systems. However, questions as how to use them in hydrological models and how to deal exactly with all this information are still not completely clarified.

Moreover, the simulation of the water cycle has become more complex than the first models proposed during last century. Amorocho and Hart (1964) proposed a partial system with two

parameters, one for the calculation of the rainfall infiltrated during a storm and the other one for the definition of the percentage of basin discharge coming from the runoff. Other researchers have developed different methodologies which have been criticized, improved and evolved (Brakensiek, 1967; Frind, 1969; Lee and Bray, 1969; Fleming, 1971; Klemes, 1983; Beven, 1989;...).

Hydrological modelling has been widely used in different fields of interest and the scale of applications ranges from small to global catchments. It is used in urban areas for flood prediction or pollution estimation and more generally for water resources management (irrigation, flood control, hydropower plants management,...). Its recent evolution comprises real-time operational forecast systems which improve user-friendly interfaces helping end users and facilitate decision making.

The adopted modelling approach depends on the type of catchment, on the system scale and on the desired detail of results-in space and time. At the simplest level, the requirements of such models are the simulation of catchment hydrological processes, and thus the relation between the rainfall input and the runoff. For that, studies about evaporation, soil moisture storage, ground water recharge and surface runoff are necessary to represent the dynamic modes of the catchment outcome. This is the basis of the unit hydrograph method, developed in the 1930s, which basically represents the stream response to individual storm events by a nonlinear loss function and linear transfer function. The simplicity of the method still provides a powerful tool for data analysis.

In any case, more complex and robust systems are coupling these hydrological models with meteorological forecasts for the new hydro-meteorological science.

At present, there is a major emphasis on the improvement of operational flood forecasting in Europe, with significant European Community spending on research and development of high-quality forecasting systems and flood risk management projects (Arduino et al., 2005). Coupling precipitation forecasts to hydrological models is the main task to achieve this objective accurately.

Additionally, Decision Support Systems (DSS) can provide valuable information which support decision-making activities. In hydrology, they are used to allow decisions in the case of flood event (flood alerts for the population, optimal management for the hydropower plants, different structural measures...) as well as in daily use for optimising hydropower plant operations. In this sense, EPSs (meteorological as well as hydrological) are becoming really valuable, being capable now of dealing with risk from forecast to decision-making.

## 2.2 Evolution of meteorological forecasts

### 2.2.1 First forecasts and evolution

There were a long time ago, and there are still different uses of weather forecasts. On an everyday basis, people use weather forecasts to determine what to wear on a given day. In agriculture, farmers can plan when to irrigate depending on temperature or predicted rainfall. Weather warnings are also important to protect life and property. Temperature forecasts can be used by electricity companies to estimate the energy demand over the following days. Forecasts are usually checked by individuals to plan outdoor activities and so on.

From centuries ago, people needed to know the weather and tried to forecast it for their activities or works. The Babylonians already predicted the weather 650 BC from cloud patterns as well as astrology. Aristotle described weather patterns in one of its manuscripts (Aristotle, around 350 B.C.E.). Later Theophrastus compiled a book (Theophrastus, around 350 B.C.E.) on weather forecasting, where he described how to predict the weather from common signs, such as a red sky at night or a ring around the moon.

In the twentieth century, weather predictions are largely based on historical or analogical schemes. Meteorologists studied reports of current weather conditions and drew up charts showing geographic patterns of barometric pressure, wind, temperature and precipitation. Then they looked for earlier events when similar patterns occurred and tried to make predictions about the future from what happened in the past.

#### *The first forecast*

Lewis Fry Richardson (1922) was a mathematician and meteorologist who made just a single weather forecast, some 90 years ago, with quite poor results. This might seem a dubious claim to fame, but Richardson was a key figure in the development of modern forecasting methods, and his ideas are still in use every day in weather offices around the world (Hayes, 2007).

Richardson's approach for weather calculation was unusual at that time. He built a mathematical model of the Earth's atmosphere, based on straightforward physical rules. First, he filled in initial conditions of pressure, wind velocity and so on, and then traced the model's evolution over time. The idea of the model was essentially based on the same principles as computer programs nowadays, but he worked with pencil and paper with the only help of a slide rule and a table of logarithms. His prediction was not for a real forecast, but for a reforecast (a past event, exactly from the May 20, 1910, at 7 a.m.). He tried to predict the

barometric pressure and the wind several hours in advance for two points in the middle of Europe. However, Richardson's forecast failed dramatically, predicting a huge 145 hectopascals rise in pressure over six hours when the pressure actually stayed more or less static.

Why was he wrong? Lynch (2006) did the same forecast than Richardson, but restored the gravitational balance, pre-processing the input data with a filtering method called initialization, which changed the observed parameters only slightly but in a coordinated way eliminating gravity waves. With this preliminary conditioning but no other changes, Richardson's basic model gave an essentially correct prediction for the weather on that morning in May 1910. Richardson came closer to the answer than he ever knew.

Later, Charney, Fj'rtoft and von Neuman (1950) computed a first weather forecast in 1948 using a barotropic filtered model. They incorporated the idea of performing arithmetic operations over different operands (loops!) without having to repeat the code. The equations and methods were close to those set out by Richardson and the results were quite encouraging. It served to introduce numerical weather forecasting in the United States, which became a practical possibility with the arrival of computers.

### ***Numerical Weather Prediction***

Operational computer meteorological forecasts were developed and performed in different weather centres, continuously improving the quality of the models and methods thanks to a better atmospheric knowledge, data assimilations techniques and the progress of computers.

Today, Numerical Weather Prediction (NWP) provides major guidance in daily weather forecast. The NWP is an initial/boundary value problem where an estimate of the present state of the atmosphere (initial conditions) and appropriate surface and lateral boundary conditions are given. The model simulates or forecasts the evolution of the atmosphere. The more accurate the model and the estimate of the initial conditions are, the higher is the quality of the forecasts. Operational NWP centres produce initial conditions through a statistical combination of observations and short-range forecasts. This approach is called data assimilation (Kalnay, E., 2002).

Forecasts had been deterministic in previous decades. However, in the following years, much impressive progress has been made in all aspects of NWP, including the success in model initialization and ensemble prediction systems. This success has become a major component of operational global weather prediction systems.

### **2.2.2 Deterministic meteorological forecast**

Different deterministic models are available and used around the world. The distance between grid points has been decreased in the last decade providing good results for a short-range forecast. Several of the most known deterministic models currently used are presented hereafter.

#### ***Mesoscale Model Generation 5 - MM5***

The MM5 forecast is a limited-area non-hydrostatic extension of the Pennsylvania State University - National Center for Atmospheric Research (PSU/NCAR) Mesoscale Model, Generation 5. It is an improvement of a mesoscale model used by Anthes in the early 70's that was later documented by Anthes and Warner (1978).

Since then, MM5 has undergone many changes designed to broaden its usage. It is one of the most used mesoscale models which can predict mesoscale atmospheric circulation. This forecast uses reference pressure as the basis for a terrain-following vertical coordinate and the fully compressible system of equations. In combination with the existing initialization techniques and physics of the current hydrostatic model, MM5 provides a model for real-data simulations on any scale, limited only by data resolution and by computer resources. The model is supported by several pre- and post-processing programs and its performance has been studied numerous times (Chandrasekar and al, 2004; Narapusetty and Mölders, 2005; Miao et al., 2008;...).

In addition, local numerical weather prediction were made possible by increased model resolution, improved model physics and fast computers. Now, local forecasts can be conducted by organizations with forecasts such as MM5, which is a free software provided and supported by the Mesoscale Prediction Group in the Mesoscale and Microscale Meteorology Division (NCAR). Initial conditions are obtained from global or synoptic forecasts provided by large weather forecasting organizations.

#### ***High Resolution Limited Area Model - HIRLAM***

The High Resolution Limited Area Model (HIRLAM) is an advanced short-range numerical weather forecasting tool (McDonald, 1994; Källén, 1996; Skalin and Bjorge, 1997). It was developed by eight European countries (Denmark, Finland, Iceland, Netherlands, Norway, Spain and Sweden) combining their knowledge in meteorology for generating the HIRLAM forecast, which is the basis for deterministic operational short-range forecasting in these

countries. The project started in 1985 and the first system was implemented in 1990. Since then, it has been updated and tuned according to scientific progress and available computer resources.

The forecast model is a hydrostatic simple equation grid-point model based on boundary conditions of the ECMWF. It includes a comprehensive package of physical processes. A semi-lagrangian advection scheme and a digital filtering initialization scheme are implemented today, working with a high-order turbulence scheme as well as with a condensation and convection scheme. The operational implementations of HIRLAM differ in horizontal and vertical resolution, but the typical resolution used is 20 km horizontal with about 30 vertical levels.

### ***Aire Limitée Adaptation dynamique Développement InterNational - ALADIN***

ALADIN International Project (Aire Limitée Adaptation dynamique Développement InterNational) was proposed by Meteo-France in 1990 to the Central and Eastern European countries for the common achievement of a Numerical Weather Forecast system which was used on limited geographical areas (relatively small but with a high resolution), requiring only a moderated calculation capacity (Radnoti et al., 1995; ALADIN International Team, 1997). The ALADIN partners are Algeria, Austria, Belgium, Bulgaria, Croatia, Czech Republic, France, Hungary, Morocco, Poland, Portugal, Romania, Slovakia, Slovenia, Tunisia and Turkey.

The horizontal resolution of ALADIN in MétéoFrance is approximately 9 km, with 60 levels vertically. It is applied every six hours (four times per day), obtaining the initial conditions by 4D-Var assimilation.

### ***COSMO***

The Consortium for Small-scale Modelling (COSMO) was set up in October 1998. Its general goal is to develop, improve and maintain a non-hydrostatic limited-area atmospheric model to be used both for operational and for research applications by the members of the consortium. Today, the consortium is constituted by national meteorological services from Germany, Switzerland, Italy, Greece, Poland and Russia.

For example, the meteorological MeteoSwiss Institute produces two deterministic forecast developed within the COSMO consortium and centred in Switzerland.

The regional COSMO-7 is driven by the global model of ECMWF and covers most of Western and Central Europe, computed on a grid spacing of about 6.6 km. It is calculated twice daily for 72 hours lead time. The local COSMO-2, driven by COSMO-7, covers the Alpine region with Switzerland at the center and is computed on a grid spacing of about 2.2 km. It is calculated 8 times per day for a 24 hours lead time. Both of them use the latest existing conditions and benefit of now-casting and short range forecasting.

### ***Still a future for deterministic forecasting?***

In the past, precipitation studies have been carried out in order to assess the performance of numerical models regarding the Quantitative Precipitation Forecasting (QPF) in complex mountain areas (Richard et al., 2007). Forecasting precipitation is a complex task because, in its genesis, the atmosphere behaviour results from interactions between many different types of processes at different scales (synoptic scale, mesoscale dynamics, boundary conditions, etc.). Furthermore, meteorological forecasts can highly depend on errors related to the atmosphere current state. In mountainous regions, the problem becomes still more complex because the topography significantly influences dynamics and precipitation microphysics.

If a decision has to be taken regarding flood warnings, flood management or emergency responses, a deterministic forecast can be not sufficient. Nevertheless, even with these deterministic forecasts, a set of different forecasts can be obtained by adding possible values of forecast error or simply a small random noise to the single deterministic forecast (Chen and Yu, 2007; Roulin, 2007).

In the field of hydro-meteorology, this approach has been followed, for example, by Montanari and Brath (2004), who presented a technique for assessing the reliability and uncertainty of rainfall-runoff simulations, using a meta-Gaussian approach in order to estimate the probability distribution of the model error conditioned by the simulated river flow. Tamea et al. (2005) also developed a nonlinear prediction, which was successfully applied to river flow deterministic forecasting. It allowed to estimate the probability distribution of the predicted discharge values and to quantify the total uncertainty related to the forecast, giving results that confirm the effectiveness and reliability of the proposed approach.

Deterministic forecasts from MeteoSwiss are one of the inputs of the MINERVE system. Due to their high resolution regarding the grid and time step calculations compared to the probabilistic forecasts from MeteoSwiss, as well as their small update time, their results are



promising for real-time optimisations. Furthermore, the multiple meteorological data available in the MINERVE system is a plus value in a real-time decision support system, since the process can be achieved even if one of the meteorological forecasts is missing.

In any case, the adoption of a set of forecasts from the deterministic forecast, using initial errors or random noise, is not realized in this research project. It is due to the availability of another probabilistic forecast. Nevertheless, it could be developed in the future.

### ***2.2.3 Ensemble Prediction System - EPS***

Ensemble prediction systems (EPS) appear as a fruitful methodology to enhance traditional deterministic forecasts with associated occurrence probabilities (Buizza et al., 2005). The existing uncertainty about the current state of the atmosphere is taken into account by calculating several different forecasts. In fact, forecasts obtained by EPS' for consecutive days have been reported to be more consistent than corresponding deterministic forecasts (Buizza, 2008). They constitute one of the most promising avenues in meteorological research, being developed by meteorologists to solve deterministic forecasting in the face of uncertainty (Demeritt et al., 2007).

#### ***Firsts Ensemble Prediction Systems***

Lorenz (1963, 1965) showed that the forecast skill of atmospheric models depends not only on the accuracy of the model and the initial conditions, but also on the instabilities of the flow itself. He demonstrated that any nonlinear dynamic system with instabilities (like the atmosphere) has a finite limit of predictability. The growth of errors due to instabilities implies that a small imperfection in the forecast model or a little error in the initial conditions, will inevitably lead to a loss of quality in the weather forecasts after a finite forecast length. He also pointed out that the predictability is strongly dependent on the evolution of the atmosphere itself. The study showed that NWP needs stochastic tools for understanding the atmosphere evolution.

One of the first forecasting methods to explicitly acknowledge the uncertainty of atmospheric model predictions was developed by Epstein (1969). He introduced the idea of the stochastic-dynamic approach in order to directly describe forecast error distributions (mean, variance and probability density function) in model equations.

EPS was also studied by Leith (1974), who was not mainly focused on producing an estimate of the forecast uncertainty but was trying to use the mean of the predicted ensemble as a

deterministic forecast. Leith examined the theoretical skill of Monte Carlo approximations to the stochastic dynamic forecasting technique proposed by Epstein. This skill was examined by means of an extension of earlier atmospheric predictability studies that used the test-field model of two-dimensional turbulence. He concluded that a Monte Carlo forecasting procedure represents a practical, computable approximation to the stochastic dynamic forecasts.

Many others studies focused on the uncertainty of atmospheric initial conditions and their evolution were the precursors of the ensemble forecasts known nowadays as EPS (among others: Tracton and Kalnay, 1993; Molteni et al., 1996; Atger, 1999; Buizza et al., 1999; Gneiting and Raftery, 2005; Marsigli et al., 2005; Leutbecher and Palmer, 2008).

EPSs were implemented operationally in the early 1990s at the National Centers for Environmental Prediction, NCEP, (Toth and Kalnay, 1993) and at the European Centre for Medium-Range Weather Forecasts, ECMWF (Molteni and Palmer, 1993). More recently, it has become operational in other meteorological centers, particularly at the Meteorological Service of Canada, MSC (Pellerin et al., 2003).

### ***National Center for Atmospheric Research - NCEP***

In the NCEP, each run of the system has an extension of 16 days, with a total of 12 ensemble members. Ten of the members are formed from perturbations added to the operationally produced analysis of initial conditions. Two control members, one at high resolution and the other at the same (lower) resolution as the perturbed members, are started from the unperturbed analysis. The NCEP system does not alter the physics within any of the member models. In order to conserve computing resources the resolution of the models is reduced at longer lead-times.

NCEP uses a spectral model as the basis of its ensemble system. Spectral models solve the equations of motion using spherical harmonics as opposed to using rate of change at fixed grid points. This is computationally more efficient than a regular grid-point model for global models at the current horizontal resolutions. Spectral model resolution is typically expressed as, e.g., T126L28, where 'T' is the spectral resolution or maximum number of waves resolved around the circumference of the earth, and 'L' is the number of model levels. There are a several ways of translating this to an effective horizontal resolution with half the smallest wavelength often being used. As computing power increases, the resolution of models generally becomes finer and improvements are made to their internal modelling of the physical world.

Since March 2004, the NCEP model is running four times a day (00, 06, 12, 18 UTC) and from 2005, a significant increase in model resolution and number of vertical levels occurred, together with slight changes to the way the initial perturbations are made.

Different reanalysis and improvements of the NCEP model are being constantly performed (Kalnay et al., 1996; Higgins et al., 1996; Saha et al., 2006; Whitaker et al., 2008; Higgins et al., 2010).

### ***Meteorological Service of Canada - MSC***

At the beginning of the nineties in the MSC, the ensemble included 17 members (1 control and 16 perturbations) which extend out of 10 days and the integration was conducted twice per day (00, 12 UTC). The control solution was obtained from the Spectral Finite Element model (Ritchie and Beaudoin, 1994; Buizza et al., 2005), as well as 8 of the perturbed members of the ensemble. The other 8 perturbations were produced from the same Global Environmental Multiscale (GEM) model (Côté et al., 1998) which generates the short- and medium-range deterministic forecasts disseminated by the Canadian Meteorological Centre. In 2001 the resolution of the spectral members was improved from TL95 to TL149 and that of the GEM members from 1.875 to 1.2 degrees (Pellerin et al., 2003; Buizza et al., 2005). In January 2005, the ensemble Kalman Filter method was incorporated into the assimilation cycle for the operational EPS. Starting in July 2007, four more members were added to produce a 20 members ensemble.

Finally, twice a day 20 "perturbed" 16-day weather forecasts are performed as well as an unperturbed 16-day control forecast. The 20 perturbed forecasts and the control forecast are performed with the GEM model. The 20 models have different physics parameterizations, data assimilation cycles and sets of perturbed observations.

### ***European Centre for Medium-Range Weather Forecasts - ECMWF***

The ECMWF general circulation model, TL799L91, consists of a dynamical component, a physical component and a coupled ocean wave component. The model formulation can be summarized by six basic physical equations, the way the numerical computations are carried out and the resolution in time and space. The ensemble consists of 50 perturbed forecasts and one unperturbed forecast solved for a 10 days lead time and with a time-step integration of 720 s. Ensemble forecasts are generated twice daily for 00 and 12 h UTC.

Regarding the horizontal resolution in the free atmosphere, a spectral method is used for the representation of upper-air fields and the computation of the horizontal derivatives. It is based on a spherical harmonic representation, triangularly truncated at total wave number 799. This roughly corresponds to a grid length of about 25 km.

In the vertical, the atmosphere is divided into 91 vertical layers up to 0.01 hPa (about 80 km) just over the mesopause, where the lowest temperatures of the atmosphere occur. The vertical resolution (measured in terms of geometrical height) is finer in the planetary boundary layer and coarser in the stratosphere and mesosphere. There are as many levels in the lowest 1.5 km of the model atmosphere as in the highest 45 km. There are also four layers near to the soil down to 1.9 meters.

COSMO-LEPS is one of the limited-area EPS developed within the COSMO consortium (Consortium for Small-scale Modelling) since November 2002. This system allows the combination of the benefits of the probabilistic approach with the high-resolution detail of the limited-area model integrations (Marsigli et al., 2005). The COSMO-LEPS system is therefore useful for the prediction of heavy precipitation with a probabilistic perspective, having been proven that the system is reliable in the prediction of intense rainfall events. It provides daily ensemble forecasts at a very high resolution (horizontal mesh-size of 7 km) based on a 16-member ensemble for central and Southern Europe with a forecast horizon of 132 h. Representative members of the global ECMWF ensemble are considered for initial boundary conditions.

The purpose of COSMO-LEPS to improve early and medium-range predictability (day 3-5) of extreme and localized weather events, particularly when orographic and mesoscale-related processes play a crucial role (Marsigli et al., 2007, 2008).

### ***Initial ensembles***

Several different techniques have been established for representing initial uncertainty in ensemble weather forecasting. This diversity arises from the limited quantitative knowledge about the relevant sources of uncertainty and the difficulty of conducting adequate comparisons of the different techniques using the same numerical model and real observational data.

The probability distributions for the various sources of errors are poorly known. In addition, the cost of explicitly integrate these distributions seems to be absolutely prohibitive for practical meteorological applications. This has led to the development of ensemble prediction.

In this type of prediction, the temporal evolution of the ensemble of model states is computed explicitly and the dispersion represents the uncertainty of the system.

Although the representation of initial uncertainty and model uncertainty can be realized separately, each has to be evaluated jointly because model uncertainty contributes to the initial condition uncertainty.

The best technique for representing initial uncertainty is not independent of the nature of the model error and the way it is represented in the EPS. Conceptually, two different techniques can be distinguished. The first aims at obtaining a sample from the probability distribution functions of initial states. The second selectively samples initial uncertainty only in those directions that are dynamically the most important for determining the ensemble dispersion.

At ECMWF, the elements of the initial ensemble are defined by adding perturbations to the current operational analysis. Those perturbations are linear combinations of the dominant singular vectors (SV) of the system. The SVs are the perturbations that grow most rapidly, over a finite time interval, in the dynamics linearized about a given solution of the forecast model (Descamps and Talagrand, 2006). They are defined over the last 48 hours period before the forecast and of ‘future’ singular vectors determined over the first 48 hours of the forecast period, being a mixture of past and future.

The SVs maximize perturbation growth over this time interval and identify those directions of initial uncertainty that are responsible for the largest forecast uncertainty at the end of the specified time interval. Due to this property, they provide a convenient way of generating an ensemble with sufficient dispersion in the most uncertain directions.

Regarding the NCEP, the initial ensemble is also defined by the addition of perturbations to the current analysis. Those perturbations are bred modes (BM) defined through a “breeding” process that is meant to simulate the analysis–forecast cycle. Bred modes result from integrations performed in parallel with the assimilation process and come entirely from the past.

MSC uses the ensemble Kalman filter (EnKF) which has been operational since January 2005. This forecast model explicitly evolves an ensemble over the assimilation period which is updated at successive observation times according to the equations of the standard Kalman filter. The ensemble obtained at the end of the assimilation can directly be used as the initial conditions for the ensemble prediction.

### **Data assimilation**

In order to define the initial state, it is not sufficient to perform spatial interpolation of observations into regular grids because there are not enough data available. Also, others sources of inaccuracy like observations errors can be the reason of an uncertainty which is, sometimes, difficult to determine and resolve.

Simple equations in a modern NWP have a number of degrees of freedom, typically 107 (Kalnay, 2002). However, for a time window of  $\pm 3$  hours, there are typically 104 to 105 conventional observations of the atmosphere, two orders of magnitude less than the number of freedom degrees of the model. Moreover, they are distributed non-uniformly in space and time. In addition, even if there are new types of data such as satellite and radar observations, these do not measure the variables used in the models and their distribution in space and time is very non-uniform.

Then, in addition to observations, it is necessary to use a first guess estimate of the atmosphere state at the grid points. For this additional information, the background field (also known as first guess or prior information) is the best estimate of the state of the atmosphere prior to the use of the observations. A short-range forecast is normally used as a background field in operational data assimilation systems. Most global operational systems uses intermittent data assimilation at the present-day, typically with a 6-h cycle performed four times a day. This forecast plays a very important role. Furthermore, the model is able to transport information from data-rich to data-poor areas. In the over data-rich regions, the analysis is dominated by the information contained in the observations. In data-poor regions, the forecast benefits from the information upstream.

To obtain the background or first guess “observations”, the model forecast is interpolated to the observation location. If the observed quantities are not the same as the model variables, the model variables are converted to observed variables. The difference between the observations and the background is called the observational increment or innovation.

The analysis, which is called “observation operator”, is obtained by adding the innovations to the background field with weights that are determined based on the estimated statistical error covariances of the forecast and the observations. Different analysis schemes like Successive Corrections Method (SCM), Optimal Interpolation (OI), three-dimensional variational assimilation (3D-Var) and Kalman Filtering (KF) are based on this procedure. They basically

differ by the approach taken to combine the background and the observations to produce the analysis.

Earlier methods such as the SCM use weights which are determined empirically. The weights are a function of the distance between the observation and the grid point, being the analysis iterated several times.

Thanks to the OI analysis technique, data is interpolated from random locations to a regular grid. OI has the advantage of using statistical estimates to determine appropriate relative weighting between noisy observations and a somewhat inaccurate first guess (usually a forecast model) to minimize the resulting error in the analysis.

Regarding the 3D-Var approach, a cost function proportional to the square of the distance between the analysis and both the background and the observations is defined. This function is minimized in order to obtain the analysis and it measures the distance of a field to the observations and the distance to the background. Lorenc (1986) showed that 3D-Var and OI approach can be equivalent with a specific kind of cost function.

Recently, the variational approach has been extended to four dimensions by including within the cost function the distance to observations over a time interval (assimilation window). The concept of combining current and past data in an explicit dynamical model such that the model's prognostic equations provide time continuity and dynamic coupling among the various fields has become really useful. This is called four-dimensional variational assimilation (4D-Var). It has been developed because, in the analysis cycle, the importance of the model cannot be overemphasized for the reason that it transports information from data-rich to data-poor regions. It provides a complete estimation of the four-dimensional state of the atmosphere.

The introduction of 4D-Var has resulted in marked improvements in the quality of medium-range forecasts. The use of 4D-Var is interesting for initialization (dynamic initialization) or as an analysis/research tool (dynamic analysis) in mesoscale models. This use is a logical extension of the traditional link between objective analysis methods and dynamic relationships.

### ***Ensemble Prediction System perspectives***

Although deterministic forecasts have been significantly improved, especially in the short-range, the quality is still not adequate for different applications like risk flood management.



For that reason, substantial improvements should still be carried out in order to improve the reliability of the system in medium/large range forecast.

The ensemble prediction systems solve this question providing an estimate of the probability density function thanks to the different forecasts. The performance of this EPS strongly depends on the quality of the data assimilation system used to create the unperturbed (best) initial condition and the numerical model used to generate the forecasts.

Linked to the EPSs, hydrological models provide probabilistic hydrographs which offer correlated uncertainty. They are useful for knowing the possible range of hydrographs and finding exceeded thresholds taking into account a given probability.

Most recent DSSs integrate information related to the last technological developments regarding weather forecasts as EPSs and their related products like the probabilistic hydrological forecast. The goal is the development of a more robust and reliable systems than the deterministic ones, integrating systematically the concept of uncertainty and probability from meteorology to decision.

The EPS from MeteoSwiss used in this research project has not been modified by a data assimilation process. However, it could be an interesting approach for the future, when having a bigger database. The aim would be to improve the hydrological forecasts, varying the initial data of the meteorological forecasts.

#### ***2.2.4 Other models: analogue technique, radar and satellite***

The use of latest radar, satellite and observational data allows a better analysis of the small scale features existing in the atmosphere and a more accurate forecast for the following few hours. The combination of these methods is largely used for improving the forecast at the Meteorological National Centers.

##### ***Analogue technique***

The statistical adaptation methods can be classified in different groups (Bárdossy, 2000; Xu, 1999). One of them is the analogue method, which searches an analogy between the meteorological situation to predict and similar passed situations (Obled et al., 2002 ; Ben Daoud et al., 2009). It examines past weather records to find ones that come close to duplicating current atmospheric conditions. The sensible weather variables linked to past situations is then used as forecast (Wetterhall, 2005).



This technique combines the approaches of the deterministic and statistic forecasts. It is based on the forecast of the general atmospheric circulation and creates a statistical relation between this circulation and the sensible weather variables (precipitation and temperature) measured at the meteorological stations (Wetterhall, 2005). The weather can be locally predicted from data generally considered as reliable (Bontron, 2004; Glahn and Lowry, 1972). This method is based on the hypothesis that a dominant relationship between the sensible weather variables and the global variables exists and subsists out of the period when it was established (Hewitson et Crane, 1996).

### ***Radar***

Nowcasting techniques are usually focused on analysis and extrapolation of the trend of a single variable (Golding, 1998), for instance the rain distribution observed by radar (Austin and Bellon, 1974). In contrast, numerical weather prediction (NWP) resolves the larger, slower evolving scales, while the local detail are filled in by parameterisation or statistics.

The need to establish the accuracy of radar forecasts was first requested by urban hydrologists confronted with the complex water-management problems of a combined stormwater and septic-sewer plant (Bellon and Austin, 1984). Since then, improvement of radar forecasting has been (and is being) improved considerably, usually combining radar and rain gages (Burlando et al., 1996; Kirstetter et al., 2009).

The predictability of hydrometeorological flood events has been also investigated through the combined use of radar nowcasting and distributed hydrologic modelling (Sun et al., 2000; Vivoni et al., 2006) or combining radars with other meteorological forecast methods (Llasat et al., 2009). It seems to be a good way of improving short range forecasts and it should be interesting to keep an eye on this technique for future developments of the MINERVE system. However, for current utilisation, this technique remains still a challenge in the Swiss Alps, where the three current radars installed in Switzerland do not accurately cover precipitation quantities in the Valais region (Tobin et al., 2011b).

### ***Satellite***

Weather forecasting relies heavily on information provided by polar and geostationary weather satellites. The primary importance of satellite information is to help to fill gaps in observational data, especially over the oceans. Weather satellites can generate several types of images that are used nowadays for rainfall estimates (Ebert and Manton, 1998) or combined

with NWP for the analysis and improvement of meteorological forecasts (Janowiak, 1992; Mo and al, 1995). They have the advantage of global coverage, but still have a lower accuracy and resolution.

### **2.2.5 Reliability and utility of the meteorological forecasts**

The improvement in the meteorological forecasts is a reality. Every day, more decision support systems are based on them for necessary information or decision making tasks. The variables of the meteorological forecasts have been improved and statistical analyses prove their reliability. The economical utility of weather forecasts has been studied in many occasions (Ogawara, 1955; Thompson and Brier, 1955; Katz and Murphy, 1997; Richardson, 2000; Wilks, 2001; Zhu et al., 2002) and their utility as well as their benefit are clear.

Nevertheless, it is worth to note that forecasting of precipitation has improved the least in the last decades. Therefore, the expert opinion of the meteorologists will always be a support to the forecasts themselves.

## **2.3 Hydrological models and forecast warning systems**

### **2.3.1 General overview of hydrological models**

Rainfall-runoff models play one of the main roles in flood forecasting systems. All these hydrological models are simplified representations of the natural system of the real world (Abbott and Refsgaard, 1996), i.e. a simplified representation of the hydrological cycle, which try to simulate all the existing processes: water storage in ice and snow, snowmelt, infiltration, runoff, freshwater storage, streamflow,... They are generally used for understanding hydrological processes and for hydrological forecasting.

Models can be either physical (e.g. laboratory scale models) or mathematical. Basing the research project in the mathematical part, three types of models can be distinguished (Abbott and Refsgaard, 1996; Grayson and Blöschl, 2000):

- Empirical models (or black box models): they are based on statistical and mathematical concepts to relate an input (such as the rainfall) to an output (such as the runoff discharge). They produce reasonably good results in a fast way thanks to different methods such as Regression models or Neural Networks. Nevertheless, there

is not a clear relation to the physical processes themselves and experience in the field is not an added value.

- Conceptual models (or grey box models, also called lumped, semi-lumped or semi-distributed): they are based on mathematical equation which describe the most important processes of the water cycle (snowmelt, runoff, base flow,...). They are normally simple models which estimated the processes in a simplified approach. The parameters are partially physical but have generally to be calibrated. Gauges stations are necessary in this kind of models to proceed to their calibration and validation.
- Physically-based models (or white box models, also called distributed models): they are based on a representation of hydrological processes such as snowmelt, runoff, percolation, subsurface flow, evapotranspiration and channel routing. The parameters of such models are directly measured in the field or assumed depending on experimental studies. They have in general a good performance, particularly for small scale problems. However, they need more computation effort and a large amount of input data. In addition, the implementation of complex hydraulic systems with reservoirs stays a complicated task when this type of model is used.

The models can also be classified as deterministic, i.e. one input data results in one output data, and stochastic, i.e. one input data results in some output data based on statistical deviation or on random variations of the parameters or data (Grayson and Blöschl, 2000; Karamouz et al., 2003).

### **2.3.2 Empirical models**

Empirical models use mathematical equations that are calibrated with observed measurements. Thus, they do not need physical considerations. Examples of this kind of models, among others, are Box-Jenkins, ARMAX, Geomorphological unit hydrographs and Neural Networks.

Autoregressive (AR) models such as Box and Jenkins (1970) and ARMAX (autoregressive moving average with exogenous inputs) may have constant parameters, parameters varying with time or a combination of both (Salas et al., 1980). They have been commonly applied to hydrology and water resources studies.

The Box-Jenkins methodology was explained by Hipel et al. (1977) with the theory and techniques to apply. Several applications were proposed as a continuation of the same work (McLeod et al., 1977), which have demonstrated an application of this method to the Saint

Lawrence River, with successful results. The Box and Jenkins method has been also used for other different hydrological studies such as for the modelling of the Euphrates River between Al-Qadissiya Dam and Abu-Ghraib stream (Hadi, 2006).

The classical approach of linear modelling ARMAX for rainfall-runoff forecasting (Karlsson and Yakowitz, 1987) has also proved its efficiency in different cases (e.g., Awwad and Valdés, 1992), especially when coupled to a Kalman filter (Ribeiro et al., 1998) or for comparison with other models (Hsu et al., 1995; Chibanga et al., 2003; Benkaci and Dechemi, 2004).

For the mathematical description of the unit hydrograph (UH), its original presentation was realized by Sherman (1932), being defined as the basin's response to a unit average effective rainfall. It was later generalized to the instantaneous unit hydrograph (IUH). Afterwards, Rodriguez-Iturbe and Valdés (1979) formulated the geomorphologic IUH (GIUH), interpreting the UH as the travel time probability density function to the basin outlet. Therefore, geomorphology based approach became a one of the most used modelling techniques for the computation of runoff hydrographs (Gupta et al., 1980; Rinaldo and Rodriguez-Iturbe, 1996; Rinaldo et al., 2006).

The Artificial Neural Network (ANN) was initially developed to mimic basic biological neural systems. It is generally composed of a number of interconnected simple processing elements called neurons or nodes, having attractive characteristics such as nonlinearity, parallelism, noise tolerance and learning and generalization capability. ANN is a data-driven, self-adaptive method in which just a few a priori assumptions about the models are necessary for problems resolution. It learns from examples and captures slight functional relationships among the data even if the underlying relationships are unknown or difficult to explain. Thus, ANN is well suited for problems whose solutions require knowledge that is difficult to specify and which have enough data or observations. In this sense, they can be treated as one of the multivariate nonlinear non-parametric statistical methods. Due to its high ability for modelling complex nonlinear systems, their application to hydrologic modelling has undergone many investigations in the last years (Zurada, 1992; Minns and Hall, 1996; Smith and Eli, 1995; Shamseldin, 1997; Zealand et al., 1999; Abrahart, 2003; Jeong and Kim, 2005; Pujol Reig et al., 2007; Ju et al., 2009; Chua and Wong, 2010; Wu et al., 2010).

### 2.3.3 Conceptual models

Conceptual models are important hydrological tools that can capture dominant catchment dynamics while remaining parsimonious and computationally efficient (Kavetski et al., 2006). Thus, they include a simplified description of the physical components and interaction of the surface- and ground-water systems. The purpose for constructing this kind of model is to simplify the problem, also according to the data available in the basin, for analyzing the system accurately.

A big number of conceptual models have been used all around the world: SACRAMENTO, MORDOR, HBV, SWAT, GSM-SOCONT,...

The Sacramento Soil Moisture Accounting, SAC-SMA (Bergström, 1976) is a conceptual model that simulates the runoff with precipitation and potential evapotranspiration inputs. It is made up of different water reservoirs located in the upper and lower zone and produces the main hydrological processes: runoff in impervious surface, runoff when the upper zone is saturated, evapotranspiration and several different baseflows.

The conceptual MORDOR model (Modèle à Réservoirs de Détermination Objective du Ruissellement), developed in France (Garçon, 1996), represents the snowpack accumulation/ablation processes and the rainfall - runoff transformation. The input parameters are the daily mean air temperature and the daily rainfall time series. The daily use of the MORDOR model in operational conditions and the tests on a large sample of watersheds have shown its reliability and robustness within a wide range of hydrological applications (Mathevet, 2005).

The hydrological model HBV (Hydrologiska Byråns Vattenbalansavdelning) has been widely used as a conceptual model in hydrology (Bergström, 1976; Lindström et al., 1997). The HBV original model was developed at the Swedish Meteorological and Hydrological Institute (SMHI) for runoff simulation and hydrological forecasting. Since then, the model has been modified several times, although the basic modelling philosophy has remained unchanged. A large literature about the HBV model and its applications can be easily found (Bergström et al., 1996; Renner et al., 2009; Abebe et al., 2010).

The SWAT (Soil and Water Assessment Tool) model is a dynamic rainfall-runoff model used for single event or continuous simulation which combines two methods for estimating surface runoff (Jeong et al., 2010): the SCS number method (SCS, 1972) and the Green and Ampt

Mein Larson excess rainfall method (Mein and Larson, 1973). This model has been applied in different basins (Santhi et al., 2006; Schuol et al., 2008).

The conceptual PREVAH (precipitation-runoff-evapotranspiration-hydrotope) model (Gurtz et al., 1999) was used for alpine tributaries modelling in the Rhine basin (Verbunt et al., 2006) as well as in other basins (Vitvar et al., 1999; Zappa et al., 2003).

The GSM-SOCONT (Schaepli et al., 2005) model has been used in different projects in Switzerland (LCH, 2006; Jordan, 2007; Jordan et al., 2007b, 2009; Cohen et al., 2009; Martinerie et al., 2009; Bieri et al., 2010) and abroad (Claude et al., 2010; LCH, 2010b). A precise description of the GSM-SOCONT, used in the MINERVE project, is given in given 4.2.2.

A comparison between lumped, semi-lumped and semi-distributed models was conducted for streamflow estimation in the Illinois River basin at Watts. According to Ajami et al. (2004), the difference between a semi-lumped and a semi-distributed model is that in the second case, the parameters can be defined differently in each sub-basin. The results show that moving from lumped to semi-distributed models creates more complexity in modelling and in the calibration procedure, therefore creating more uncertainty in the results. Research has proven that the increase in the complexity of the model does not always cause, systematically, an improvement of the results (Blöschl et al., 2008).

#### **2.3.4 Physically-based models**

These models describe the natural system using mathematical representations of the flows of mass, momentum and various forms of energy (Abbott and Refsgaard, 1996). They have been used since a first attempt by Freeze and Harlan (1969) and, due to the progress of the knowledge in physical process descriptions as well as the improvement in computer calculations, they are and they will continuously be improved.

As conceptual models, a big number of physically-based models exists according to the literature: SHE, MIKE SHE, TOPMODEL, PREVAH, WaSiM,...

The European Hydrological System - Système Hydrologique Européen SHE (Abbott et al., 1986a, 1986b) is a physically-based, distributed modelling system for constructing and running models of all or any part of the land phase of the hydrological cycle for any geographical area. The system has the aim to provide a strong European capability in hydrological modelling.

The MIKE-SHE distributed hydrologic simulation model, originally derived from the SHE model, has been used in different investigations, such as in the Hawaii Mountains (Sahoo et al., 2006) or in the Loess Plateau, China (Zhang et al., 2008). Feyen et al. (2000) also applied MIKE-SHE to a medium size catchment in Belgium.

The TOPMODEL (a TOPography based hydrological MODEL) original model was developed by Beven and Kirkby (1979). Since then, this quasi-physically based mathematical model (Holko and Lepistö, 1997) has been largely used in basins all around the world: U.K. (Beven et al., 1984), Czech Republic (Blazkova and Beven, 1997), Slovakia (Holko and Lepistö, 1997), USA (Peters et al., 2003). Beven (1997) discussed about the model and its performance.

Other distributed hydrological models, among others, are the Water balance Simulation Model (WaSiM-ETH), a fully distributed model with physical based algorithms for most of the process descriptions (Klok et al., 2001; Jasper et al., 2002), or the CDRMV3 (Kojima and Takara, 2003) which was used by Kim (2007) for developing a real-time algorithm for flood forecasting.

Other research compared performances between distributed and semi-distributed models. El-Nasr et al. (2005) modelled a catchment using a semi-distributed (SWAT) and a distributed model (MIKE SHE) in Belgium, remarking that both models were able to simulate the hydrology of the catchment in an acceptable way and the results were quite similar. Carpenter et al. (2006) compared a lumped versus a distributed hydrological model (in both cases with the Sacramento soil moisture accounting model) in the Illinois and Blue Rivers, concluding that distributed models offer clear performance advantages.

### ***2.3.5 Which is the best hydrological model?***

In general, there is not a clear answer to which is the best hydrological model. Each model fits with the available data in the concerned basin. The optimum model complexity is related with a certain availability of data (Grayson and Blösch, 2000), as schematically shown in Figure 2.1.

Hydrological models should not be over-parameterized. An excessive number of parameters can lead to non robust results after calibration periods. For example, a high resolution distributed model with distributed precipitation in a grid of 7 \* 7 km (with a homogeneous value in each cell of the grid) will logically not produce better results than a simpler model.



In any case, the study about the concerned basin and its characteristics as well as the preparation of a database with all available data seems to be the most important factors in deciding which kind of model will perform better. Increasing the complexity of the model does not always improve the performance of the model. Sometimes, even differences between models are questioned, which has generated a debate about whether so-called physically based distributed models are in reality lumped conceptual models operating at the grid scale (Smith, 2004).

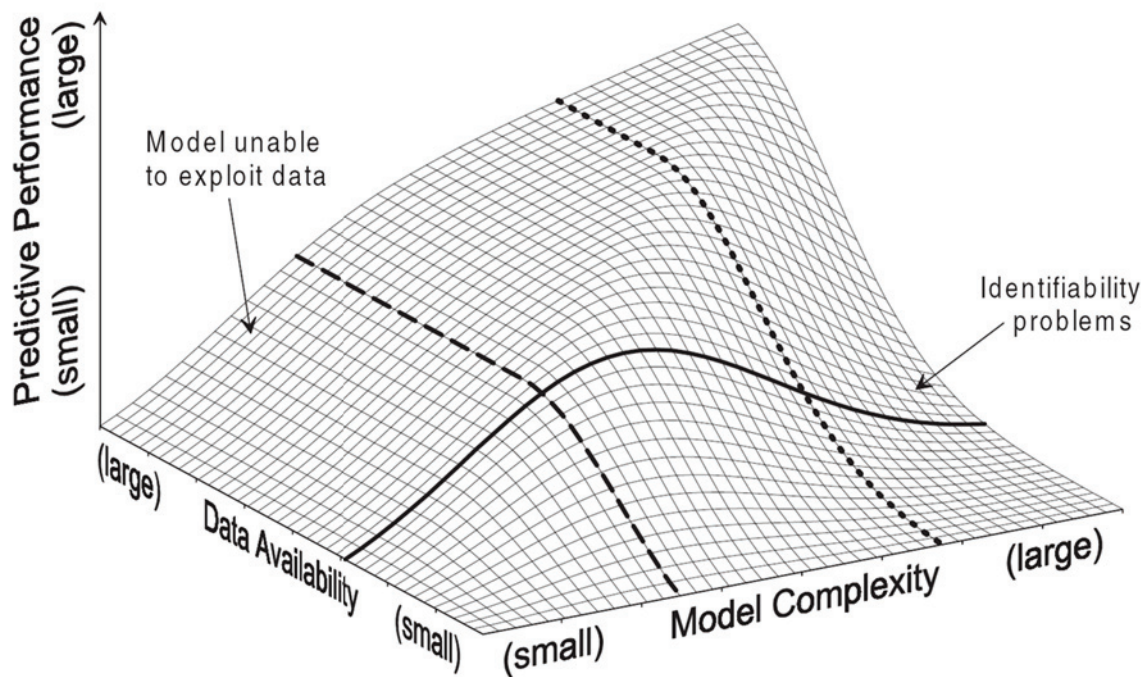


Figure 2.1 Schematic diagram of the relationship between model complexity, data availability and predictive performance (from Grayson and Blösch, 2000, p. 73).

It may be concluded that it is not easy to demonstrate the superiority of one approach or one model (Todini, 2007). Each case, located in a defined framework, needs a model adapted to the situation and the available data.

In the present research project, the hydrological model characterization is performed using (GSM-SOCONT) developed in the previous stage of the MINERVE project. In addition, an improvement of this model is developed in the framework of the MINERVE 2011 project, but it is not a part of the presented research work.

### 2.3.6 Hydrological forecast systems

Different deterministic hydrological systems are presented in the literature. Habets et al. (2004) proposed an operational precipitation forecast used for streamflow forecasts in the



whole Rhone River basin. The ARPEGE and ALADIN meteorological models were used as inputs to the one-way atmosphere-hydrology coupled model SAFRAN-ISBA-MODCOU. For the Piave basin in Italy, Alessi Celegon et al. (2007) coupled a meteorological precipitation forecast (ETA model) and a geomorphological model of the hydrologic response. They concluded that a final underestimation of the volumes precipitated was presented, but that there was a possibility to predict the main characters of the flood hydrograph several days before the flood peak.

These works, among others, were performed deterministically. However, this methodology may transmit an illusion of certainty to the user which can easily lead to suboptimal actions (Chen and Yu, 2007). Probabilistic forecasts mitigate this problem and, moreover, they present additional potential benefits (Krzysztofowicz, 2001). They express a degree of uncertainty and can be used for devising risk-based criteria regarding flood warnings, allowing risk to be explicitly taken into account.

A successful approach to the probabilistic hydrological forecasts is to use the meteorological ensemble predictions as input to the hydrological model, producing hydrological ensemble forecasts. In addition, deterministic hydrological forecasts (from the deterministic meteorological forecasts) can be obtained as a support to the probabilistic ones, especially for short range forecasting.

For example, De Roo et al. (2003) simulated a hydrological model forced with EPS meteorological data for their European Flood Forecasting System (EFFS), obtaining encouraging results about the potential utility of the system.

Roulin (2007) developed a hydrological ensemble prediction system based on the ECMWF EPS forecast system, testing the results on two Belgian catchments. Comparing the results with the deterministic forecast revealed that the hydrological ensemble predictions displayed greater skills.

Jaun et al. (2008) presented a case study of the extreme flood event of August 2005 in the Swiss part of the Rhine catchment, testing a hydrological-meteorological ensemble prediction system with COSMO-LEPS meteorological data and the semi-distributed hydrological model PREVAH. They showed that the hydro-meteorological ensemble prediction chain was quite effective and provided additional guidance for extreme event forecasting.

Finally, Olsson and Lindström (2008) also performed an evaluation and calibration of hydrological ensemble forecasts in Sweden using ECMWF and the HBV hydrological model.

Additional cases of flood forecasting using ensemble meteorological forecasts, as well as a detailed review on the subject can be found in Cloke and Pappenberger (2009).

It can be stated that the option of multi-model (several hydrological models) with ensemble forecasts generally outperform single model deterministic forecasts and often outperform ensemble forecasts from single models constructed by varying initial model conditions (Georgakakos et al., 2004). The results obtained give weight to each hydrological model or even combine them with a bayesian approach (Niggli and Musy, 2005).

The MINERVE 2011 system works with multiple meteorological forecasts (deterministic and probabilistic) which have been already implemented in this research project. However, the system still works with one single hydrological model with a fixed set of parameters. The adoption of different hydrological models or the inclusion of different sets of parameters for the current model (Tobin and al., 2011a) could be interesting in the future.

### **2.3.7 Flood alert systems**

At present, the performance of many flood forecasting systems in an operational framework is sub-optimal or below expectation. The source of this poor performance is quite often the weak connection in the chain linking the flood forecasting process with those charged with responding during a crises period (Arduino et al., 2005).

Nevertheless, a considerable effort is being completed by scientists and governments and flood systems are being improved day by day for their use in real-time. Different examples can be easily found in the literature: U.K. (Moore et al., 2005), China (Li et al., 2006), Sweden (Arheimer et al., 2010).

It is important to notice that operational medium range flood forecasting systems are increasingly moving towards the adoption of ensembles of NWP, known as EPS, to drive their predictions (Cloke and Pappenberger, 2009), but it does not mean that EPS represent the full uncertainty of the atmosphere state. Regardless, the results from literature give encouraging indications that such activity brings added value to medium-range flood forecasts, particularly in the ability to issue flood alerts of possible events earlier and with more confidence than ever before (Demeritt et al., 2007).

The European Flood Alert System (EFAS) is one of the most important and promising known systems. It has been producing probabilistic hydrological forecasts since 2005 (Thielen et al., 2009a; Bartholmes et al., 2009). The aim is to provide medium-range pre-alerts for the trans-

national river basins in Europe, and could thus raise preparedness prior to a possible upcoming flood event.

Another important and powerful system found in the literature is the Flood Early Warning System (FEWS), which is a real time software infrastructure for operational water management and forecasting. It has been applied in several operational forecasting systems used by national authorities in, for example, England, Wales, Germany, Switzerland, Taiwan and Netherlands. In Switzerland, FEWS is related to the OWARNA (Optimization of Early Warning and Alerting) project, which aims to establish a national platform on natural hazards alarms (Hess, 2010).

The results in this kind of systems are not the only issue. Representation of such results takes a central importance and new approaches which easily represents the warnings are necessary (e.g. by Thielen et al. (2009b)). The communication and how probabilistic flood forecasts should be presented is another non negligible aspect of flood warnings (Nobert et al., 2010). The objective is to identify useful information for real-time flood forecasting applications and to clearly visualize that information (Leedal et al., 2010).

### **2.3.8 MINERVE hydro-meteorological system**

#### ***Hydrological model MINERVE***

The semi-distributed hydrological model includes 239 sub-catchments and covers the entire 5520 km<sup>2</sup> catchment area (Figure 2.2). If a glacier part exists, the sub-catchment is divided into glacier and non-glacier elevation bands. Otherwise, it is just divided into non-glacier elevation bands. Every band is supplied by a virtual meteorological station, which provides hourly precipitation and temperature series, and a model of snow composed of a double reservoir (snow and liquid water contained in the snow layer). It uses the hydrological simulation to follow the temporal evolution of the height and saturation degree of the snow. The snow melt is calculated according to a degree-day formula and produces an equivalent precipitation starting from a rate of saturation threshold.

In addition, all the hydraulic structures of the basin, such as hydropower plants, reservoirs, turbines, spillways, etc. are also modelled in order to achieve an analogous behaviour to the current state of the basin.

The results obtained with this model are then compared with the observed discharge at several check points. When the differences between observed and simulated discharges are important,

the model is automatically updated according to a data assimilation procedure (Jordan et al., 2007a). After updating the hydrological model, the meteorological forecast of the COSMO-7 model is used as input of the hydrological model for the flood forecast of the next 72 h.

Furthermore, not only the hydrological model for the current situation of the basin has been achieved. The model of the theoretical natural basin, before hydropower development, has also been built. This model does not include the hydraulic structures and its hydrological results are used as reference for comparison.

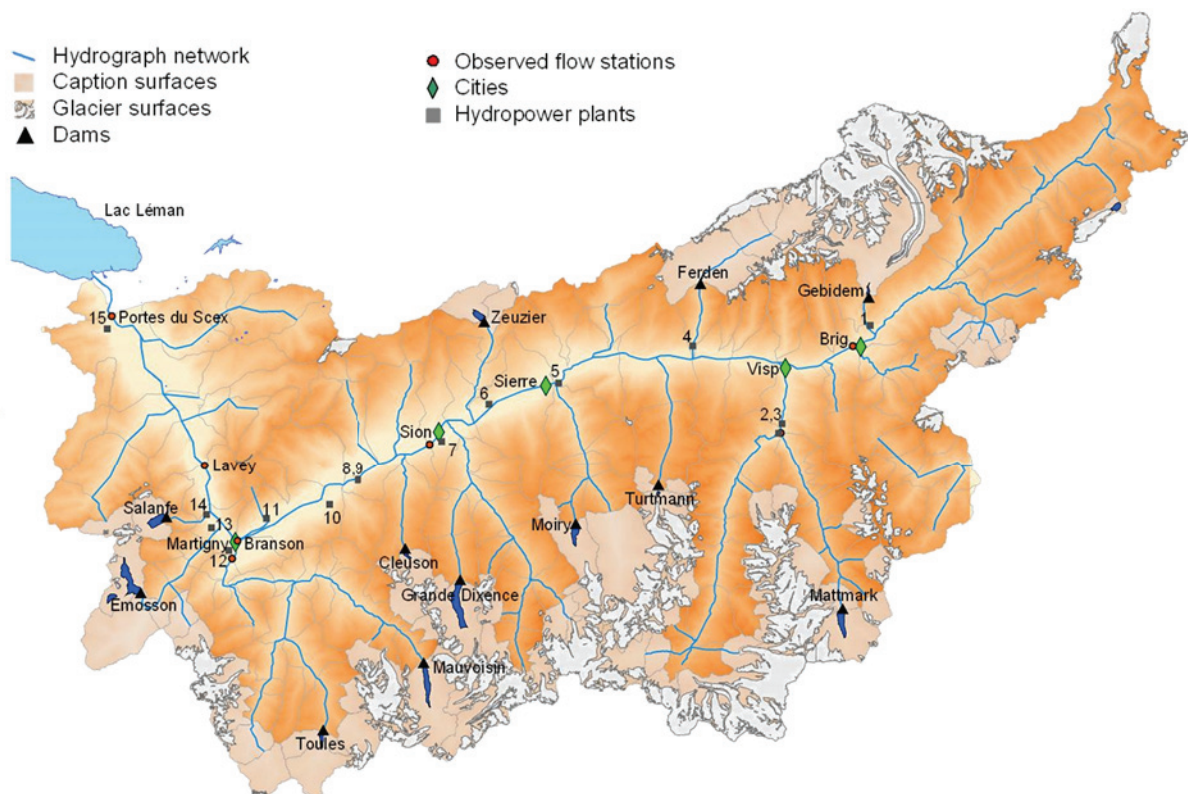


Figure 2.2 The Rhone River basin in Switzerland upstream from the Lake of Geneva

### Previous system – MINERVE 2007

The MINERVE system, at the initial state, achieved a 72 h lead time flood forecast over the entire catchment area. The hydrological simulation was computed with a semi-distributed model, including the snow-melt and glacier-melt processes, as well as soil infiltration and runoff (Schäfli et al., 2005).

For the computation of flood prediction, the numerical meteorological forecasts provided by MeteoSwiss were assimilated. The precipitation and temperature data were available at an hourly rate every 12 hours, for a 72 hour lead time. The spatial resolution comprised a grid of

7 x 7 km<sup>2</sup> (6.6 x 6.6 km<sup>2</sup> since 2007) and the vertical resolution was about 100 m depending on the topography.

This hydro-meteorological model has proven its efficiency since 2006 (Jordan, 2007; Jordan et al., 2008). At that time, only deterministic meteorological forecasts were used in the model. However, the use of probabilistic forecasts such as ensembles was already foreseen as a further development of the MINERVE system (Jordan et al., 2007a).

### ***Current system – MINERVE 2011***

The MINERVE 2011 system exploits deterministic (COSMO-7 and COSMO-2) and ensemble (COSMO-LEPS) meteorological forecasts from MeteoSwiss, coupled with the same semi-distributed hydrological model (GSM-Socont, section 4.2.2). In addition, new incorporations to the meteorological inputs as well as improvements in the hydrological semi-distributed model are planned (García Hernández et al., 2009e).

Furthermore, a new tool providing flood warnings has been developed (García Hernández et al., 2011b). It gives a prediction of the risk situation at check points along the catchment area. A three levels warning report is drawn up during flood situations (notice, alert and alarm) depending on critical discharge thresholds and on the occurrence probability when the probabilistic forecast is considered (García Hernández et al., 2010).



“The most useful science is that the fruit of which is most communicable”

Leonardo Da Vinci (1452-1519)

### **3. State of the art of decision support systems for reservoirs management**

### **3.1 Operation of water storage systems**

From the XIX century, improvements in hydraulic and reservoir constructions, with optimal conception of the structures for economical gain, were introduced. McElroy was the first engineer in designing a water supply system for Brooklyn city using reservoirs (Judd, 2004). He also mentioned that, if the engine in a hydropower scheme was properly designed and managed, the annual cost of pumping could be considerably decreased (McElroy, 1862). This search of optimality is logically used day by day in new constructions since the performance of the systems influences directly the possible benefits (economical or not).

Furthermore, possible reductions in flood peaks thanks to the reservoirs were already recognized long time ago. Haupt (1908) discovered that “the establishment of reservoirs for irrigation or for power will incidentally restrict the storm flow, as do the great Alpine lakes in Switzerland, and discharge the clarified effluent for navigation or for domestic or manufacturing purposes”. Around six months later, Taylor (1908) also commented that reservoirs were a possible way to decrease flood damages. One hundred years later, they are effectively used for reducing the peak flow in an active way.

Even more, regarding energy issues, energy peaks demand was studied for designing hydropower plants long ago (Perrine, 1906). The coordination of a hydropower plant to serve a distant demand through the agency of a transmission was secured for the first time in the world in Oregon in 1889. The hydropower plant at Oregon city transmitted single-phase power at 4 kV, over a distance of thirteen miles to Portland (Markwart, 1927). Once more, hydroelectricity is, at the present time, the most successful renewable energy.

Mason (1914) already mentioned that the advantages of water storage were numerous and the disadvantages a few. He probably thought about multiple water resources uses. The first reservoirs were planned for water consumption and distribution. Currently, complex schemes are generally designed and managed as multipurpose reservoirs (Valadares Tavares, 1984; Piccardi and Soncini-Sessa, 1989; Vedula and Mohan, 1990; Boillat et al., 2002; Tilmant et al, 2002; Bakis, 2007; Heller, 2007; Wei and Hsu, 2009). They are used to store water, generate hydropower, provide flood retention, enable irrigation, improve river ecology and offer recreational services. But it is not a new issue. The Hoover Dam in the United States is one of the first cases of multipurpose reservoir. The act of Congress of the United States of America in 1928 (United States Congress, 1928) lists the purposes of the Boulder Canyon Project (or Hoover Dam) as “flood control; improvement of navigation and regulation of the



Colorado River; storage and delivery of Colorado River waters for reclamation of public lands and other beneficial uses exclusively within the United States; and hydroelectric power production.”

Consequently, it is justifiable to say that the management of hydropower plants for increasing global performance has been one of the main tasks of engineers and operators since the first water and energy supply systems. This management still remains as an important task in the water resources management for improving the benefit of the system and the community.

### 3.2 Hydropower plants operation

Hydroelectricity is a major application of water in many reservoir systems (Karamouz and al, 2003). It refers to electricity generated by hydropower plants through the use of the gravitational force of falling or flowing water. Major terms in hydroelectricity and hydropower plants are power and energy. Power is the rate at which electrical energy is transferred by the system in a given time unit, and is defined as follows:

$$P_{HPP} = \rho \cdot g \cdot Q \cdot H_{HPP} \cdot \eta_{HPP} \quad 3.1$$

with  $\rho$ : density of water [1000 kg/m<sup>3</sup>];  $g$ : gravity [9.81 m/s<sup>2</sup>];  $Q$ : turbined discharge [m<sup>3</sup>/s];  $H$ : net hydraulic head [m],  $\eta$ : efficiency of the hydropower plant.

The energy production of a hydropower plant is obtained according to Eq. 3. 2:

$$E_{HPP} = \int_{t=t_a}^{t=t_b} \frac{P_{HPP}}{1000} dt \quad 3.2$$

with  $E$ : electric energy output of the hydropower plant for the period between  $t_a$  and  $t_b$  [kWh];  $P$ : hydropower capacity for a given turbined discharge, also depending on the efficiency and the water level at the reservoir [W].

In hydropower schemes, the basic elements are the reservoir, the intake structure, the headrace waterway system and the power plant (Mays, 1996). The reservoir creates the necessary head that provides the power required for the turbines. The intake structure guides water from the reservoir into the headrace waterway system. Gates or valves are used to control the water discharge. Finally, in the powerhouse, energy is produced by the help of turbines, generators and transformers.

The efficiency of the power plant depends on the performance of the electro-mechanical equipment, the type of turbine, the discharge flowing through the turbine and on the head losses in the pressure system. In addition, high head storage power plants provide energy by small discharges but relatively high heads, which allows the adaptation of the production to peak load hours.

These two requirements (high head and energy production at peak hours) are sometimes in conflict with flood control, since a certain storage capacity has to be available during the flood peak. Consequently, preventive emptying has to be ordered to hydropower plants' operators in order to create a supplementary retention volume. This means that energy has to be sold at base load hours for low prices.

As a result, DSS for flood control has to deal not only with expected damages due to flooding, but also with the planned hydroelectric production, its variation and its consequences.

### **3.3 Decision support systems for water resources management**

A Decision Support System (DSS) is defined as a system for helping decision makers to choose between alternatives depending on rules, observations, defined thresholds and estimated economic values. It could be classified in the area of the information systems discipline which focuses on supporting and improving decision-making tasks (Arnott and Pervan, 2008). DSS has as main objectives to increase both the efficiency and effectiveness of the system (Power, 2002). It is especially useful for risk management.

DSS has been used in many environmental and civil engineering problems in general (Rizzoli et al., 1998; Toll and Barr, 2001; Farinha et al., 2005; Yang, 2008; Yehia et al., 2008) and in hydraulic engineering in particular. An overview of DSS in water resources management was performed by Bruen (2006). It gives several examples of specific applications in drought management, groundwater protection strategies, emergency management, channel navigation, dam and reservoir operation, agriculture and irrigation management as well as in environmental issues.

The management of hydrological disasters has become a high priority in the field of water resources management. The availability of information concerning the meteorology and the hydrological characteristics of the concerned basin is essential for performing such a task. The methods of risk and reliability analysis have taken more importance during last years in

engineering decisions (Faber and Stewart, 2003). They allow the decision makers to know the rationality of their decisions. It is especially important in flood forecasting with very high uncertainty. Therefore, the risk estimation is considered as a necessary aspect in flood forecasting (Arduino, G. et al., 2005).

Regarding the flood management, a lot of works have been undertaken and different DSSs developed (Chang and Moore, 1997; Manos and al, 2004, Ahmad and Simonovic, 2000, 2001, 2006; Jordan, 2007; Wang, 2007; Kort and Booij, 2007; Harvey et al., 2008). In these works, the issues concerning reservoir operations and water control during floods are different from others like structural calculations or machine performance. It is not essential to find the global optimal solution from all alternatives (Cheng, 1999) but only a feasible alternative near to global optimum, easy to understand and possible to carry out in real-time. In addition, it is not either realistic to apply complicated measures in case of flood management when the decision makers have both technical and non-technical backgrounds (Akter and Simonovic, 2005). Accordingly, easy, clear and convivial systems turn out to be necessary, and a DSS is almost mandatory.

DSSs have become thus unavoidable for the optimisation of complex networks with numerous objectives like hydropower generation, water supply or flood control. In addition, flood management is always associated with an uncertainty degree coming from meteorology, hydrology or even from a lack of knowledge. These uncertainties have to be appropriately addressed by a robust decision support tool effective for flood control or management. Many works approaches exist for multi-objective decision-making, but a suitable methodology for real flood management should be still developed (Akter and Simonovic, 2005).

Guariso et al. (1984) analysed the effectiveness of information in real-time operation of multipurpose reservoirs. They tested the method for Lake Como (Italy) confirming that considerable benefits could be achieved when operating a multipurpose reservoir by using real-time information in the catchment. However, they concluded that a revision of the inflow-forecasting philosophy was probably necessary for having useful tools for reservoir management.

New Ensemble Prediction System (EPS) at high-resolution scale could be called a new philosophy. The EPS is a potential improvement coming from meteorological inputs. Many projects are introducing and implementing the EPS approach for their systems. It opens a big change which requires deep modifications in the DSS concept. However, this change will

provide a better estimation of the future and therefore better decisions because of the integration of uncertainty and probability.

Furthermore, the European Commission proposed in 2007 a directive on the assessment and management of floods (The European Parliament and the Council of the European Union, 2007) where preliminary flood risk assessment, flood risk maps and flood risk management plans are considered as necessary and fundamental. Moreover, it is said that *“It is feasible and desirable to reduce the risk of adverse consequences, especially for human health and life, the environment, cultural heritage, economic activity and infrastructure associated with floods. However, measures to reduce these risks should, as far as possible, be coordinated throughout a river basin if they are to be effective.”*

### **3.4 Optimisation methods for reservoir management and flood control**

#### ***3.4.1 Introduction to optimisation methods for water resources management***

Water resources management usually refers to water demand, water quality, hydropower or flood control. These objectives can create conflicts, especially when dealing with floods. Furthermore, efficient operations of reservoir systems still remain a dynamic research field when combining multipurpose water uses (Castelletti et al., 2008).

For solving these conflicts in reservoir management, different mathematical methodologies are used in DSS. The most known are Linear Programming (LP), Non-Linear Programming (NLP), Dynamic Programming (DP), Artificial Neuronal Network (ANN), Genetic Algorithm (GA) and Expert Systems (ES). Heuristic approaches and hybrid algorithms, among others, are also largely used in DSS.

The significance of multi-criteria decision making methods (e.g. Fuzzy Sets theory, FS) is increasing for solving multi-objective or multi-attribute function criteria and is also part of new developments of DSSs.

#### ***3.4.2 Optimisation approaches of reservoirs without flood management***

Without considering flood control, optimisation can be mostly reduced to economical issues. Therefore, the aim of the optimisation simply becomes the maximization of the benefit. The notion of risk (e. g. for potential damages) is thus not necessarily included.

Ali et al. (2003) proposed an optimal water management for a reservoir in Malaysia aiming to minimize the deficit of the irrigation demand and to optimise the reservoir releases. They used deterministic data and a Linear Programming (LP) model, convenient for multipurpose allocation of scarce resources. They concluded that the optimised results with the selected methodology were satisfactory.

Sharma (2004) proposed an approach based on two-phase neural network (TPNN) for the optimal operation of multi-reservoir control problems and applied the technique to a ten theoretical reservoir network. The interaction among all water release variables of the problem were taken into account and the results demonstrated the efficiency of the method. Only one objective, namely the minimization of the difference between energy demand and energy generation, was taken into account for the definition of the utility function.

Artificial Neural Network (ANN) was applied by Chandramouli and Deka (2005) for optimal operation of the Aliyar reservoir in South India with deterministic data, combining Expert System and ANN models for the optimal use of available water resources.

Reis et al. (2005) used a hybrid Genetic Algorithm (GA) and Linear Programming (LP) approach for the optimisation of a four theoretical reservoirs system. The objective function was expressed in terms of optimal reservoir storage and releases to obtain rule curves. The proposed algorithm was a stochastic approximation to the system operation problem, with advantages such as simple implementation and the possibility of extracting useful parameters for future operational decisions.

Ganji et al. (2007) developed a management reservoir methodology dealing with conflicts due to limited water and applied it to the Zayandeh-Rud River basin in Iran. They used a Stochastic Dynamic Nash Game method and an Annealing Approach. The Stochastic Dynamic Nash Game method is used for the preferences of the decision makers and calculation of expected utilities, being similar to the multi-criteria decision making method. The Annealing Approach is a stochastic search procedure aiming to minimize a numerical function. The results revealed that this approach performed better than the Bayesian Stochastic Dynamic Programming, sequential Genetic Algorithm (GA) and classical Dynamic Programming (DP) regression.

Cheng et al. (2007) developed a hybrid algorithm, using GA and Chaos algorithms, for optimizing hydropower reservoir operations. This algorithm was applied to the Chaishitan reservoir, upstream of Nanpan River in the Yunnan province of China. They concluded that the hybrid proposed methodology combining the advantages of powerful global searching

capability of GA and the powerful local searching capability of Chaos optimisation algorithm performed better than classical GA.

A heuristic approach to obtain rule curves was also developed for multi-reservoir systems by Paredes Arquiola et al. (2008). This approach is based on searching the minimum volume for a given system and inflows for maintaining a chosen degree of reliability for one or several demands. This approach was applied to the Mijares River basin, a water resources system located in Eastern Spain. This basin is characterized by severe droughts, a water rights system very deeply rooted amongst users, and the possibility of a joint use of surface- and groundwater resources.

In all these presented cases, the objectivity of the utility function of the system is usually manifest. Conflicts among end users' preferences are not common and better options reveal their advantages. Compromise coefficient are not generally used and the point of view of the end users takes a reduced importance.

### ***3.4.3 Optimisation approaches integrating flood management***

On the contrary to the cases presented in previous section, dealing with flood control problems is usually included in decision support tools. Flood control by reservoirs is not a new approach. Levin (1969) already explained closely the problematic: *“Inflow into the reservoir is of a stochastic nature and varies seasonally throughout the year. During some of the winter months, considerable amounts of water are expected to enter the reservoir over short periods, and unless the water level is sufficiently low at the beginning of the flood, there is danger of an overflow and serious damage. The most effective means for preventing such a situation is deliberate spilling of some of the stored water in advance and the object of control is to minimize water losses due to such spills, while keeping the level of risk of an overflow below a certain probability.”*

In fact, the floods in Europe are more common in spring and autumn, but the optimisation problem remains the same.

Although the following overview is far from exhaustive, it reflects the importance and most significant characteristics of the main approaches currently used, presenting the different algorithms and procedures applied in such projects.

### ***Case studies of single reservoir management***

Unver and Mays (1990) developed a Non-Linear Programming (NLP) methodology with a flood-routing simulation model for the real-time optimal flood operation of river-reservoir systems and applied it to the Lake Travis on the Lower Colorado River in Texas (United States). They encouraged the real-time optimisation methodologies for flood control, but noted that there was still a lack of available methodologies and software to use in conjunction with real-time data for having good floods estimates and to optimally operate reservoir systems for flood damage minimization.

Karbowski (1991) established a program for reservoir management during floods, designed as a real-time DSS where operators could analyse the consequences of a decision before applying it. The program was used to simulate the operation of the Roznów reservoir located in Southern Poland. The proposed methodology, with two-stage stochastic control scheme, improved the traditional results. It was then implemented in experimental and training use until fully implementation.

An evolution of the Dynamic Programming (DP), called Stochastic Dynamic Programming (SDP), is sometimes used for modelling optimisation problems that involve uncertainty and is considered as a useful tool for decision-making. Faber and Stedinger (2001) implemented a variation of the SDP, called Sampling SDP (SSDP), in the Williams Fork reservoir in Colorado (United States) with ensemble streamflow prediction (ESP) forecasts, affirming that frequently updated ESP forecasts provided more efficient operating decisions than a more sophisticated model employing historical time series coupled with snowmelt volume forecasts.

Other methodologies like a Bayesian approach was proposed to solve a stochastic flood control approach (Andrade et al., 2001). It was tested in the Chavantes hydropower plant in Southeast Brazil for a nine years daily inflow period, obtaining valuable results.

A hybrid analytic/rule-based approach has been also proposed for a one reservoir system management during floods (Karbowski et al., 2005). The objective was the minimization of damages due to high flow downstream the reservoir. The procedure was applied once again to the Roznów reservoir, located on the Dunajec River in Poland.

Another variation from the SDP, called Neuro-dynamic programming (NDP), was applied by Castelletti et al. (2007) in the Piave reservoir network in Italy. They combined Artificial Neural Network (ANN) with SDP to reduce the problem of “curse of dimensionality” of



dynamic programming systems. This technique considerably reduced the computation time, but there was still potential to optimise the methodology. For dealing with different objectives, they reduced the problem to the weighted sum of costs associated to the number of  $k$  objectives of the system.

Bagis and Karaboga (2007) used an evolutionary algorithm (EA) based on a fuzzy controller to reservoir management with the purpose of spillway gates operating during any flood of any magnitude. They applied it to the Adana Catalan Dam in Turkey. The idea of EA comes from mixing Evolutionary Programming (EP) and Genetic Algorithms (GA), using a finite population which evolves over generations to produce better solutions to the problem. The objective was the real-time spillway operation during floods. The results presented an accurate and reliable method to manage the reservoir.

A probabilistic model to support reservoir operation decisions during flash flood was developed by Mediero et al. (2007), based on Bayesian networks and Monte Carlo simulations. The methodology was applied to the Conde de Guadalhorce reservoir in the Turón River in the Southeast of Spain. The flood control objective was defined in terms of the risk of dam overtopping and downstream damage that could be accepted. The objective was fixed by maximum probability of occurrence of an outflow discharge and/or a water level which could be accepted due to their associated damages.

The Genetic Algorithm (GA) approach was also applied by Chang (2008) to the Shihmen reservoir in North Taiwan for finding rational release and required storage volumes. GA with penalty strategies for parameters was used to guide the GA in the solutions searching process. Because the study case was deterministic, the objective function was reduced to a minimum of releases depending on inflow and water level.

Karaboga et al (2008) presented an operation method based on Fuzzy Logic (FL) control for the operation of spillway gates of the Adana Catalan Dam in Turkey during floods. They also used a Tabu Search (TS) algorithm as optimisation technique to overcome local optimality in the solution process, with the aim to minimize the objective function of the system, considering hydrographs, peak values and different fuzzy rules. They concluded that this method provided more desirable and reliable control actions than human-based (manual) control methods.

Wang et al. (2010) developed an integrated modelling system for improved multi-objective reservoir operation, applying it to the Hoa Binh reservoir in Vietnam. The purpose of this work was to deal with the trade-off between flood control and reservoir hydropower



generation. Different weighted objectives were combined for optimisation of the final aggregated objective function. The previous objectives were thus transformed into a single scalar objective function or utility function. The Shuffle Complex Evolution algorithm developed at the University of Arizona (SCE-UA) was used in this system as the global optimisation method. It is based on an ensemble of four concepts: combination of deterministic and probabilistic approaches, systematic evolution of a set of points in the direction of the global improvement, competitive evolution as well as complex shuffling. The integrated modelling system demonstrated the ability to achieve the optimal operation rule for the Hoa Binh Reservoir.

### ***Case studies of multi-reservoir management***

Windsor (1973) developed a recursive Linear Programming (LP) technique for the analysis of multi-reservoir flood control systems. By dividing the flood period into shorter operational periods, the system policies could be adjusted to incorporate latest forecast information and maximize the flexibility under current operational conditions. It was applied to a theoretical reservoir network, concluding that even with not entirely realistic assumptions the methodology was enough flexible to provide great computational advantages over existing operating procedures.

Expert System (ES) methodology is based on IF-THEN rules which need previous knowledge. It was applied by Chang and Moore (1997) for the water management of four flood-control reservoirs located in the Scioto River basin in Ohio (United States), in case of drought. The goal was the minimization of the total water releases of the four reservoirs, demonstrating the flexibility of incorporating expert opinions within an optimisation model.

The Stochastic Dynamic Programming (SDP) methodology in the classical way was studied by Cervellera (2006) with stochastic inflows in a theoretical ten reservoirs network for the minimization of costs. For solving such a high-dimensional problem, they used efficient discretization of the solutions space and approximations of the value functions over the continuous solution space.

Kim et al. (2007) also used the SSDP (Sampling Stochastic DP) with ensemble streamflow prediction, this time for a multi-reservoir system located on the Geum River in Korea. They found out that the combination of the system objective weights for a final single objective was not always successful. Some tradeoffs between multiple objectives were not applicable in real

operations. Consequently, further studies are needed to incorporate this aspect into the algorithm.

A flood-control operation strategy using a Balanced Water Level Index was developed by Wei and Hsu (2008) for a multipurpose multi-reservoir system. The method was applied to the reservoir system located in the Tanshui River basin in Northern Taiwan with deterministic inflows. Three main goals were summed and weighted to define one single objective function before applying the optimisation method.

### ***Case studies of multipurpose optimisation***

Ambrosino et al. (1979) proposed a multi-goal formulation approach with pareto-optimal alternatives for water resources management and lake regulation with the aim to maximize the water sale return and to minimize potential floods damage. They applied it to the Lake Maggiore, in Italy and Switzerland and concluded that it was necessary to assume a compromise rule and that the obtained solution had a certain degree of arbitrariness.

Piccardi and Soncini-Sessa (1989) proposed a software for multipurpose water reservoir, with the general aim of satisfying water demand avoiding at the same time flood damages. They applied it to the management of “El Carrizal” reservoir near to Mendoza in Argentina. The simulation time step was generally one day, but it was reduced to two hours when a flood risk appeared. Different multi-criteria decision making methodologies could be applied by users, depending on the “risk-aversion” of decision makers.

A multi-objective optimisation approach to define operations of Lake Kariba by its hydropower scheme in Zimbabwe and Zambia was also proposed by Gandolfi and Salewicz (1991). It was based on two main goals: maximization of hydropower production and minimization of flood peak releases. Operation rules combined with a random search algorithm were applied in this case.

Fuzzy set theory was used for the optimal modelling of the basin of the upper and middle reaches of the Yangtze River in China (Cheng, 1999). The objective was to use it in multi-reservoir operation and to establish comprehensive schemes which could be effectively applied for real-time flood operations. He combined fuzzy logic and Dynamic Programming (DP) for multi-objective function calculation, concluding that this method was quickly adjusted to actual flood situations and easy understandable by operators.

The heuristic approach using ES was also applied by Ahmad (2001) for the selection of flood damage reduction measures for Ste. Agathe city in Manitoba (Canada). It was integrated with

analytical tools to support multi-objective decision making, implementing the model to identify appropriate flood damage reduction options, such as levees and/or dikes, floodwalls, diversions, retention basins, etc.

Akter and Simonovic (2005) used Fuzzy Expected Value to flood management in the Red River Basin in Manitoba (Canada). They considered that it was necessary to develop a tool able to consider multiple stakeholders with multiple objectives to deal with the complexity of flood management decisions. This procedure by itself is valuable for multi-criteria decision making, but needs to be connected with another algorithm when dealing with a large number of possible alternatives and many calculations have to be performed.

Fu (2008) proposed a fuzzy optimisation method based on the concept of ideal and anti-ideal points to solve multi-criteria decision making problems. It was performed for the flood operation in the Sanmenxia reservoir in the middle reach of the Yellow River (China). Once again, this methodology was used as a single optimisation when only a limited number of already known alternatives are tested. In these cases, all alternatives are simulated and then, evaluated by this selected multi-criteria decision making method for ranking them.

A multi-objective reservoir operation optimisation model using multi-criteria analysis was also developed and applied to the Dez and Bakhtiari reservoirs on the Dez River in Southwest Iran (Malekmohammadi et al., 2011). For this purpose, they implemented a Non-dominated Sorting Genetic Algorithm (NSGA) as well as an evolution of the multi-criteria decision making method ELECTRE, called ELECTRE-TRI, for the selection of alternatives considering the preferences of decision maker. Two main goals of optimisation were the minimization of probable flood damages and the maximization of water demand supply. The results directly depended on the weight factors taken into account for each goal.

#### **3.4.4 Overview of the optimisation approaches**

When the system is nonlinear, the information is uncertain and mathematical models are badly defined, the conventional control techniques for solving the objective function may be insufficient to provide an optimal solution (Karaboga et al., 2008). Nonetheless, it is assumed that no algorithm can guarantee the global optimum (Andreu, 1993).

Dynamic Programming has the cited “curse of dimensionality” problem: computational operations increase exponentially with the dimension of the problem and the problem quickly becomes insolvable. In addition, even if relaxation rules can reduce the dimensionality

problem, they make global optimisation difficult. The resolution of the problem can then not be achieved with the needed certainty.

Genetic Algorithm (GA) gives interesting results but it is difficult to apply for solving complex catchments. Local solutions or the need of too many convergences to obtain the global optimal solution are the reason. Another key factor in real-time calculations is time and therefore, GA is not always applicable.

Artificial Neural Network (ANN) is an adaptive system that changes its structure based on information achieved in training process. In the present research, not enough data is available for the training. Moreover, ANN realisation is not easy to apply for large and complex catchments.

Fuzzy logic approach allows multi-objective optimisation and is an effective technique to control real, complex and unpredictable processes in a system with nonlinear and non-stationary conditions (Bagis, A., 2007). However, this technique dealing with different objectives at the same time is not developed for solving system optimisation problems.

#### ***Selected approach for the development of the decision support system MINDS***

Finally, two different possibilities have been developed in the present research project in order to compare their optimal solutions. The first of them corresponds to a heuristic approach, called greedy algorithm, which solves the optimisation problem making a locally optimal choice at each stage of the calculation, expecting the global optimum. In the cases on which the greedy algorithm demonstrates to achieve the global optimum for a given problem, it typically becomes the method of choice because it is faster than other optimisation methods. In this research project, each stage is related to groups of reservoirs physically connected. Their hydropower plants are then optimised assuming the other hydropower plants operations (of the other groups) as known. It can be assumed that each stage corresponds to a local optimisation. This methodology is similar to the Expert System developed by Jordan (2007) for deterministic inputs.

The second method corresponds to a powerful algorithm for nonlinear optimisations: the Shuffled Complex Evolution - University of Arizona (SCE-UA). This algorithm is a general global optimisation method developed by Duan et al. (1992, 1993), being very effective to handle nonlinear problems with high-parameter dimensionality and having similar performance comparing to GA for water resource systems (Celeste et al., 2004). In addition,

this method is also efficient concerning computation time compared once again to GA (Ndiritu, 2005).

### **3.4.5 Optimisation inputs**

Philbrick et al.(1999) compared deterministic and probabilistic inputs for optimisation purposes. They affirmed that deterministic optimisation could produce suboptimal reservoir-control policies by failing to incorporate adequately the impact of low-probability events. They also demonstrated that optimisation of probabilistic inflows performed better for reservoir operations. Other studies corroborate that probabilistic forecasts are generally more useful than deterministic ones for flood forecasts and assessment (Krzysztofowicz, 2001; De Roo et al., 2003; Verbunt et al., 2007; Buizza, 2008; Di Baldassarre et al., 2010).

One of the goals of the developed DSS was to perform probabilistic as well as deterministic optimisations in order to compare and to use the two approaches depending on the results and on the available forecasts.

Both reservoir management and flood control depend on the risk the decision maker can accept, which is strongly associated with probabilistic forecasts. If the marginal risk of flooding has to be as low as possible, corresponding to significant preventive operations, reservoir will probably not be full at the ending of the period, resulting in energy production losses. On the contrary, flood higher risk acceptance would ask for smaller preventive operations and, consequently, full reservoir at the end of the period and smaller energy production losses.

In other terms, the questions to be solved by decision makers are:

- Which probabilistic forecast do you more believe in?
- Do you want to reduce flood risk to a minimum?
- Do you accept a high risk or do you prefer to base your decisions on an expected mean risk?

This choice is not only mathematically-based and depends on subjective criteria. Several possibilities are implemented in the decision support system developed in this research project, allowing the decision maker's selection.

Thus, a multi-criteria decision making approach has been used for defining the global utility function (or objective function) of the system depending on probabilistic forecasts.

## **3.5 Risk concept and multi-criteria decision making**

### ***3.5.1 The decision theory***

In statistics, the decision theory is based on different methods for reaching optimal decisions. Analytical techniques are designed to help the decision makers to choose among a set of alternatives depending on their consequences. The decision theory (French, 1986) can be applied to conditions of certainty, risk, or uncertainty. For a series of alternatives and a set of consequences (or just one for a deterministic evaluation) linked to each alternative, the decision theory gives conceptually simple procedures for optimal final choice, i.e. for the definition of the global utility function.

#### ***Decision under certainty***

Decision under certainty involves the biunivocal relation between an alternative and its consequence. Then, the choice among alternatives is equivalent to the choice among consequences. Thus, the decision maker's preferences are simulated by a single value function introducing an order in the set of consequences and ranking directly the alternatives.

An example could be given by a deterministic flood forecast. Different alternatives to manage the flood could be proposed. Then, the global loss function value for calculating damages would be obtained and the alternative with most damage reduction could be selected.

#### ***Decision under risk***

Decision under risk links one alternative to several possible consequences, each one with a known occurrence probability. The choice is made among a set of consequences and probability distributions, not any more comparing between single final function values. The decisions are usually based on the utility concept (measure of consequences, i.e. expected damages in the flood protection case). The preferences of the decision maker are described by a function calculating the expected utility of each alternative. The alternative with the highest utility (e.g. smallest flood consequences) is considered as the most preferable.

As example, a probabilistic forecast with a known occurrence probability can be mentioned. The objective function could be defined as the minimization of the expected mean loss function (utility function). The best alternative would be the one which offers the highest expected utility (the lowest mean losses function value).

### ***Decision under uncertainty***

Decision under uncertainty is performed when the occurrence probabilities are unknown. Then, two main approaches can be applied. The first is based on certain values of the set of consequences, such as selecting the best option according to the highest value of the loss function without taking into account the occurrence probability. The second method consists in eliminating the uncertainty using subjective probabilities based on expert knowledge or on a statistical-theoretical approach.

An example of decision under uncertainty could be also performed with a set of forecasts, but without an associated occurrence probability. The selected alternative could be, for example, the one that reduces the worst consequence, i.e. which minimizes the maximum expected loss function value.

In the present research project, the ensemble hydrological forecast is assumed as certain, with known probabilities of occurrence for each member of the forecast. The decision theory is thus assumed under risk. Nevertheless, methods of decision under uncertainty have been also considered due to their high efficiency under certain circumstances.

To obtain rational decisions for reservoir management, two steps are necessary for finding an optimal solution with the decision theory. First, a utility function has to be defined in accordance with the decision maker. Secondly, the expected value of the utility function has to be optimised (maximization or minimization) for guiding the decision maker to the optimal solution.

According then to the decision theory and in order to take rational decisions for reservoir management, two steps are necessary for finding an optimal solution. The first is the definition of a utility function in accordance with the decision maker. The second consists in the optimisation (maximization or minimization) of the expected value of the utility function, guiding the decision maker to the optimal solution.

#### ***3.5.2 Notion of risk***

The number of research studies about risk has increased over the last decades. They deal with the general concept (Aven and Pörn, 1998; Hansson, 2007), the civil engineering approach (Faber and Steward, 2003) as well as applied to the water resources management (Haimes, 1984) and flood risk assessment (Jonkman et al., 2003; Pistrika and Tsakiris, 2007; Hall and Solomatine, 2008; Egorova et al., 2008; Apel et al., 2008).



The definition of risk for a given situation (Faber and Steward, 2003; Manen and Brinkhuis, 2005; Pistrika and Tsakiris, 2007) can be assumed as the product of vulnerability (costs, as economical value) and hazard (or occurrence probability), as defined in Eq. 3. 3:

$$r_i = C(s_i) \cdot P(s_i) \quad 3.3$$

with  $r_i$ : risk for the event assuming a scenario called  $s_i$  is produced [economical value];  $C(s_i)$ : costs of consequences assuming scenario  $s_i$  is produced [economical value];  $P(s_i)$ : occurrence probability of scenario  $s_i$ .

When dealing with probabilistic inputs and, thus, with a set of possible scenarios, the expected mean risk can be obtained by:

$$r = \frac{1}{n} \cdot \sum_{i=1}^{i=n} (C(s_i) \cdot P(s_i)) \quad 3.4$$

with  $r$ : mean risk for the event [economical value];  $n$ : total number of scenarios.

Sometimes, the assessment of the expected mean risk (assumed as the global utility function of the system) is not sufficient, even inadequate (Haimes and Li, 1991), especially when considering flood events. The notion of risk, or the utility function definition, has to take into account more possibilities than just the expected mean value. All values of possible damages have also to be analysed. Thus, it would be more appropriate to define this approach as a multi-criteria decision making analysis rather than risk analysis, which is normally associated with mean values. Then, the expected mean risk, as defined in Eq. 3.4, would be one of the potential utility functions to optimise. Additionally, as example, another definition of the utility function could be taken into account, such as the one given by the consequences of the worst scenario of the flood event. It has to be noted that the occurrence probability in this case would not be used and the definition of risk would so be imprecise or would not exist. Consequently, as explained previously, the multi-criteria decision making is the correct term for the methodology defining the global utility function.

### 3.5.3 Multi-criteria decision making

Multi-Criteria Decision Making (MCDM) methods refer to decisions among multiple conflicting criteria. In literature, there are two main approaches (Hwang and Yoon, 1981): Multi-Objective Decision Making (MODM) with decision variable values to be determined in



a continuous or discrete domain of infinite or large number of choices; and Multi-Attribute Decision Making (MADM) with a limited number of alternatives.

In MODM problems, the number of alternatives is infinite and the decision alternatives are thus not given. The set of decision alternatives is not explicitly defined by a finite list (Stewart, 1992) and it is not even clear if it can be pre-defined at the beginning of the analysis. MODM provides a framework for designing a set of decision alternatives which are assessed in order to know if they satisfy the objective or multiple objectives.

In MADM problems, the alternatives are limited and require inter and intra-attribute comparisons, involving implicit or explicit tradeoffs (Zanakis et al., 1998). First examination on multi-attribute decision making methods was carried out by MacCrimmon (1968, 1973). Since then, many methods were developed by researchers in various disciplines as statistics, economics, management or decision making. There, MADM methodology is used for selecting alternatives among a finite number of decision criteria (Poh, 1998; Ma et al., 1999; Devi et al., 2009).

Since the solutions space is assumed in this research project as discrete and depending on a parameter which affects the solution discretization, the alternatives of preventive operations are considered as limited possibilities known beforehand and the term MADM is preferred.

### ***Multi-attribute decision making - MADM***

MADM methods are not included in a DSS for defining the optimal result. Their goal is rather to assist the end users to define the global utility function of the system and to learn more about the problem and solutions in order to reach the ultimate decision (Zanakis et al., 1998), as proposed in MINDS (see Chapter 6).

The numerous MADM methods found in literature can be compared to the utility functions defined in the decision theory and are: Expected Mean Value or Simple Additive Weighting Method, Dominance Method, Maximin Method, Maximax Method, Hurwicz Criterion, Conjunctive Method, Disjunctive Method, Lexicographical Method, Elimination by Aspect Permutation Method, Linear Assignment Method, Analytical Hierarchy Process (AHP), Elimination et Choice Translation Reality (ELECTRE), Technique for Order Preference by Similarity to Ideal Solution (TOPSIS). An overview of most of these methods was given by Kahraman (2008).

All these methods have the goal to define a final analytical utility function, combining attributes (forecasts in this research project) and weights. Both linear and nonlinear utility

functions can be defined. The principal methods are briefly described in section 6.4.1. The final selected methods, according to the aim of optimisation proposed for this research project, are presented in detail in section 6.4.2.

## **3.6 User-friendly decision support systems**

### ***3.6.1 Case studies of user-friendly systems for water resources management***

Flood management by the help of reservoir operations involves a large number of potential intervention measures. Thus, a Decision Support Systems (DSS) is required for assessing the flood impact as well as to propose choices to decision makers.

Flood emergency DSS have been used by emergency managers for a long time (Mirfenderesk, 2009) and recent advances in computer sciences and decision making theory are making such approaches even more useful. Exchange and collaboration between the DSS developers and end users (or decision makers) during the entire building, testing, evaluation and implementation process is needed (Loucks, 1995).

According to the requirements of the decision makers, DSS have to give reliable results as well as to be able to provide easy-to-use propositions (hiding the complex procedures, models and algorithms) and to present consequences in a reliable and transparent manner.

The DSS “WaterWare” was developed in a research programme with the goal to have a comprehensive, easy-to-use DSS for river-basin planning (Jamieson and Fedra, 1996a, 1996b; Fedra and Jamieson, 1996). It was designed to support government agencies and river-basin commissions in decision-making tasks for efficient water resources management. The quality of decision-making in this increasingly complex field is improved by combining geographical information systems, database technology, modelling techniques, optimisation procedures and expert systems.

Another concept of DSS was proposed by Simonovic and Bender (1996). They focused on a collaborative planning-support system integrating available computer technologies with modelling and analysis tools in a user-friendly environment. Areas of common understanding are identified by the DSS, encouraging the users to explore compromise solutions and reach a consensus. Using the concept of ‘grounded theory’ from social sciences, the proposed DSS is used as a tool for developing evaluation criteria. The use of the concept is illustrated by an

example from Northern Manitoba in Canada which focused on fish habitat issues relating to a hydropower development project.

Makropoulos et al. (2003) developed a DSS for urban water management to assist decision makers in implementation of optimal planning strategies. Once possible strategies are defined, DSS explores and produces spatial results and maps, allowing the decision maker's recommendations as a final outcome. The last stage consists in a water optimisation under user investment constraints. The results show the utility of the DSS based on approximate reasoning and user's advices to complement engineering expertise for urban water management applications.

A DSS for water monitoring and sustainable management based on ground stations and satellite images was developed in the framework of the Copernicus project (Manos et al., 2004) for the monitoring and management of the Strymon River in Southern Balkans. The specific DSS allows the decision makers to monitor the Strymon region, to control and forecast the quality and quantity of the river water as well as to make objective decisions based on data provided by radio computers, gauging stations and satellite images.

A pilot DSS for flood control was developed and applied to the Red River basin in Vietnam and China (Kort and Booij, 2007). A methodology allowing the ranking of measures while taking into account uncertainty was proposed with the purpose of evaluating different flood control measures. The total flood damage is used as decision variable. Potential flood reduction measures are dike heightening, reforestation and construction of a retention basin. The methodology consists of a Monte Carlo uncertainty analysis using Latin Hypercube Sampling and a ranking procedure based on the significance of the difference between output distributions for the different measures.

Harvey et al. (2008) developed a tool for dealing with flood risk analysis. The system consists in a user-friendly interface and automatic diagrams of calculations, enhancing transparency and helping communication and interaction. This software is used in a theoretical but realistic flood analysis, working satisfyingly. Its efficiency is also tested by uncertainty analysis in a risk model of the Thames Estuary in United Kingdom for selecting robust alternatives to flood risk management.

Ito et al. (2001) also proposed a DSS for hydrologic modelling and risk evaluation of the surface water management alternatives in a river basin. Water management policies are evaluated with the goal of facilitating the integration of user-selected scenarios into planning strategies in the Chikugo River basin in Japan, a multipurpose multi-reservoir system. The

DSS uses object-oriented programming techniques and different numerical models are available through a user interface, facilitating communications between end users and models. It is shown that the use of DSS may significantly improve the speed and quality of decision making and increase flexibility by analysing different scenarios.

### ***3.6.2 Required features for interactive flood management***

An efficient DSS has to incorporate both theory and knowledge in different fields such as computer programming, DSS theory, hydrology, hydraulics, mathematics, statistics, etc.

A DSS should allow to choose the main methods and parameters of the decision making process, editing, changing or selecting them from a user-friendly interface. It should be thus possible to answer to “what if” questions and to investigate alternative scenarios. Furthermore, DSS has to assist decision makers in evaluation and decision tasks.

Finally, the decision maker should be able to visualize the main results of the simulations and/or scenarios conveniently and rapidly in order to fully understand the decisions undertaken and their consequences or costs. A graphical user-friendly interface helps understanding and gives an overview on the critical aspects in the intervention area.

## **3.7 Expert System of previous MINERVE project**

### ***3.7.1 Reservoir management objectives for flood control***

Strategies for hydropower plant reservoir operation during flood events usually focused on dam safety and flood routing in the reservoir. Water level should not exceed a maximum safety level during the flood peak. This can be ensured by four main operations: stop pumping water into the reservoir, close the intakes of water transfer tunnels, start full turbining and release water through outlet structures as spillways or bottom outlets. However, the effect of reservoir routing can be reduced or the peak discharge in the downstream river reaches even increased due to these operations. This strategy might be appropriate under the aspect of dam safety, but is obviously not optimal regarding flood protection downstream of the dam.

In order to increase the flood safety in the valley downstream, the maximization of the reservoir routing effect in the whole catchment area is required. For this purpose, the intakes of the water transfer tunnels into the reservoirs should stay completely open and the pumps should operate at maximum capacity. Additionally, no water should be released from the dam

during the flood peak. According to this strategy, a sufficiently high storage volume before the flood peak is needed. If it is not available, the required volume has to be created by preventive emptying before the flood peak (Jordan et al., 2006; Jordan et al, 2008). Limited discharge capacity in the river network downstream of the dam has also to be considered. Furthermore turbine and/or bottom outlet operations have to be stopped at the right time, before reaching critical discharge values.

This subchapter presents a briefly description of the initially developed deterministic expert system developed for the Rhone River basin (Jordan, 2007).

### **3.7.2 Expert System objectives**

Two objectives have to be satisfied by the operation of the numerous hydropower plants in a catchment area during floods. The first objective is the reduction of damage along the river downstream due to limited flow capacity of critical river sections. The second objective is the minimization of economical losses due to the preventive water release. Therefore, preventive turbinning at a low price, bottom outlet operation for lowering the water level in the reservoir, no turbine operation during the flood peak or pumping at high energy prices should be avoided. Despite this large number of optimisation objectives, it is possible to compare different alternatives of preventive operations assuming all the consequences in monetary values.

Flood damage depends on the difference between peak discharge and on the river reach capacity. Preventive turbinning sequences and bottom outlet releases try to minimize the flood damages and their economical costs depend on the released volumes.

The major costs in the optimisation model are due to flood damages which are computed at check points in the catchment area. Relatively minor costs are caused by economical losses due to preventive turbine operations or restrictions during floods. As a consequence, the optimisation focuses principally to limit maximum discharge at check points.

A full simulation model is normally unsuitable in the real-time optimisation of complex reservoir systems due to an excessive computation time. Therefore a simplified method was developed by Jordan (2007), which provides a fast estimation of the near-optimal hydraulic solution. Nevertheless, the optimal solution is then validated by a full simulation at the end of the optimisation procedure.

### 3.7.3 Simplified methodology for a multi-reservoir system

Preventive operations at hydropower plants and dams are defined by using three types of input data: inflow forecasts, initial reservoir storage volume and predicted hydrographs at critical river locations (check points). Since the goal of the preventive operations is to maximize the reservoir routing effect within the catchment, a routing efficiency  $E_i$  related to the catchment outlet was introduced (Eq. 3.5). The routing efficiency calculates the rate between the stored volume and the total predicted flow volume at the catchment outlet during a certain period of time (typically 72 hours, corresponding to the lead time of deterministic forecast COSMO-7) as follows (Jordan et al., 2005):

$$E_i = \frac{\int_{t_0}^{t_f} Q_i(t) \cdot dt}{\int_{t_0}^{t_f} Q_{tot}(t) \cdot dt} = \frac{V_i}{V_{tot}} \quad 3.5$$

with  $V_i$  and  $V_{tot}$ : predicted flow volumes at location  $i$ , respectively at the catchment outlet;  $Q_i(t)$  and  $Q_{tot}(t)$ : predicted discharge at time  $t$  at location  $i$ , respectively at the catchment outlet;  $t_0$  and  $t_f$ : start, respectively end of the studied period.

The supply efficiency of reservoir  $j$ ,  $E_{sup,j}$ , represents the inflows during the flood. It is obtained using the predicted reservoir inflow in Eq. 3.5, which depends on the meteorological, hydrological and geographical situation of the catchment, on the installed capacity of the water intakes and transfer tunnels and on the pumps capacity transferring water into the reservoir. The maximum reservoir routing effect is obtained by maximizing  $E_{sup,j}$  considering the initial storage efficiency  $E_{stock,j}$  of the reservoir  $j$ , as presented in Eq. 3.6:

$$E_{stock,j} = \frac{V_{av,j}}{V_{tot}} \quad 3.6$$

with  $V_{av,j}$ : available volume in the reservoir  $j$  at the beginning of the studied period.

The optimisation problem, i.e. the objective function, can then be expressed as follows:

$$Max (E_{sup,j}) \quad 3.7$$

considering:

$$\begin{aligned}
 E_{\text{sup},j} &\leq E_{\text{sup,max},j} \\
 E_{\text{sup},j} &\leq E_{\text{stock},j} \\
 E_{\text{stock},j} &= E_{\text{av},j} + E_{\text{PO},j}
 \end{aligned}
 \tag{3.8}$$

with  $E_{\text{sup,max},j}$ : maximum theoretical value of the supply efficiency,  $E_{\text{PO},j}$ : efficiency of preventive operation.

The predicted hydrographs without the effect of the existing hydropower plants and reservoirs are obtained at every check point in the catchment area by a numerical simulation. The predicted inflow hydrographs at the reservoir  $j$  result from the numerical simulations considering the maximum supply efficiency  $E_{\text{sup,max},j}$ . The effective reservoir routing can be determined by taking into account the preventive emptying operation ( $E_{\text{PO},j}$ ), which finally gives the outflow of the reservoir. Therefore, the mass balance equation of the reservoir  $j$  has been defined as:

$$\frac{\partial V_j}{\partial t} = Q_{\text{in},j}(t) - Q_{\text{out},j}(t) - Q_{\text{PO},j}(t)
 \tag{3.9}$$

with  $V_j$ : stored volume in reservoir  $j$ ,  $Q_{\text{in},j}(t)$ : inflow into reservoir  $j$ ,  $Q_{\text{out},j}(t)$ : released discharge through surface spillway,  $Q_{\text{PO},j}(t)$ : released discharge by turbines and gates.

The resulting discharge  $Q_k(t)$  at river location  $k$  depends on the predicted discharge without the effect of the hydropower plant  $Q_{\text{nat},k}(t)$  and on the sum of the predicted inflow discharges  $Q_{\text{in},j}(t)$  in all the  $n$  reservoirs located upstream of  $k$  as well as on the sum of the turbine discharges  $Q_{\text{PO},j}(t)$  of all  $n$  hydropower plants (when located upstream of  $k$ ), considering the transfer period  $t_{t,\text{PO},jk}$  between the discharge release of  $j$  and the check point  $k$ .  $Q_{\text{nat},k}(t)$  is also influenced by the sum of the released discharges at  $n$  spillways  $Q_{\text{out},j}(t)$  (when located upstream of  $k$ ) considering the transfer period  $t_{t,\text{out},jk}$  between the spillway  $j$  and the location  $k$ .

The released discharges of all reservoirs are obtained after an evaluation of the mass balance of the reservoir and the rating curve of the spillway. For  $n$  considered hydropower plants, the resulting discharge at location  $k$  can be computed as follows:

$$Q_k(t) = Q_{\text{nat},k}(t) - \sum_{j=1}^{j=n} [Q_{\text{in},j}(t - t_{t,\text{in},jk}) - Q_{\text{PO},j}(t - t_{t,\text{PO},jk}) - Q_{\text{out},j}(t - t_{t,\text{out},jk})]
 \tag{3.10}$$

### **3.7.4 Optimisation procedure**

The optimisation problem described above is highly nonlinear. The effect of the reservoirs on the downstream hydrograph depends on flood routing, considering the transit time between the reservoir and the check point. The water released by turbines or gated spillways can reach to different locations. Therefore, various transit times may be considered for a reservoir.

The decision variables for each hydropower plant are the starting and ending times of the turbine and bottom outlet operations. Since the turbine operation has to start as soon as possible in order to create a sufficient high storage volume in the reservoir, the starting time of the turbine operation is fixed at zero. Three variables have to be optimised for each considered hydropower plant, which represent a multidimensional solution space. Moreover, every solution has to be evaluated at various check points along the river. Therefore, a rule-based deterministic optimisation is applied, which provides acceptable solutions for flood protection. The two main steps of the optimisation procedure are explained in the following.

#### ***Hydropower plant operation***

The operation of each hydropower plant is individually determined without considering the downstream constraints. The maximum preventive release operation for each hydropower plant  $j$  is determined by solving Eq. 3.5 to 3.8. As mentioned, the solver takes into account the layout and functionality of the hydropower plant, such as the hydrological characteristics of the upstream sub-catchments, the design discharge of the water intakes, pumps, transfer tunnels, turbines and spillways as well as the reservoir filling curves and spillways rating curves. The result is obtained by applying four basic rules with the purpose of maximizing the quantity of water stored in the reservoir during the flood peak:

- a) use all water transfer intakes under operation during the flood peak
- b) if pumps and turbines are installed on the same headrace system, operate the turbines before the flood peak and operate the pumps during the flood peak
- c) use the following storage priorities within a reservoir: water from the own catchment area; water from transfer tunnels fed by intakes in neighbouring catchment areas; water pumped from intakes into tunnels and reservoirs during the flood peak
- d) use the following water release priorities: turbines; gated spillways and bottom outlets; and non-gated free surface spillways.



**Global optimisation**

The optimal preventive operation of the hydropower plant  $j$  is obtained by pre-emptive goal programming (in this research project, an analogous methodology is named Greedy algorithm). The hydropower plants are ranked at first regarding their supply efficiency. The variables of hydropower plant with the highest supply efficiency are optimised first.

The objective function for the global optimisation is defined as presented in Eq. 3. 11 (Jordan, 2007). It consists in the minimization of flood damages and economical costs due to emptying operations.

$$\min \left( \sum_{k=1}^K [loss(k)] + \sum_{j=1}^J [loss(j)] \right) \quad 3.11$$

with  $K$ : total number of check points in the studied basin;  $J$ : total number of hydropower plants in the studied basin;  $loss(k)$ : damage (monetary value) linked with the check point  $k$ ;  $loss(j)$ : costs (monetary value) linked with the hydropower plant  $j$ .

The optimisation procedure described above was compared to an evolutionary algorithm (Jordan, 2007). The results obtained were quite similar. A lower limit of the hydrograph at every check point for a given hydrological situation was also calculated. For this purpose, a sufficient storage volume was assumed in every considered reservoir. This means that all the water inflows to reservoirs can be stored without any preventive turbine or gate operation. If the optimal solution produces a peak flow similar to the one of the lower limit hydrograph, it corresponds to the global optimum of the problem.



“Errors using inadequate data are much less than using no data at all”

(Charles Babbage, 1792-1871)

#### **4. MINERVE hydrological modelling approach**

## 4.1 Meteorological observations and forecasts

### 4.1.1 *An introduction to meteorology in the MINERVE framework*

Since 1881, the Federal Office of Meteorology and Climatology MeteoSwiss has provided detailed weather forecasts as well as warnings to the authorities and the population due to bad weather or storms. For this purpose, MeteoSwiss operates a full-scale meteorological network and gathers and analyses climate data with its over 800 meteorological stations and four regional centres, as well as its monitored system, a prerequisite for high forecasts quality.

Scientists at MeteoSwiss are also involved in national and international projects for the understanding of weather and climate in Alpine regions. In addition, with the latest generation of weather stations, MeteoSwiss continuously provides (and improves) high-quality data on a wide range of forecasts.

The meteorological forecasts of the MINERVE system are provided by MeteoSwiss. It operates and further develops the high-precision numerical weather prediction system COSMO in order to automatically generate regional and local forecasts in complex topography. A detailed image of the future state of the atmosphere is computed, from the low stratosphere to the surface, including the evolution of the snow cover, the lake temperature and the soil characteristics. Meteorological forecasts are available up to three or five days in advance on a domain covering central Europe (COSMO-7 and COSMO-LEPS respectively). More detailed forecasts are available up to 24 hours in advance on a domain including the Alpine arc (COSMO-2). These data provide a quantitative guidance for the daily forecasts and decision maker tasks. Furthermore, MeteoSwiss contributes to the security of the Swiss population by the generation of warnings, e.g. in case of high-impact weather or floods. These warnings complement the OWARNA (Optimization of Early Warning and Alerting) project, aiming to provide a Swiss alarm platform for natural hazards.

As an alternative to the weather forecasts provided by MeteoSwiss and in order to ensure additional information to decision makers, it is planned to develop in parallel an adaptation of weather forecasting model based on the analogue type methodology (Horton et al., 2011). The model uses the fields at the synoptic scale, regarding different atmospheric variables better predicted by the meteorological models than the surface variables (like precipitations and temperature). This method is similar to that developed by Obled et al. (2002) and is used for the identification of precipitation scenarios.

### 4.1.2 Meteorological data

The selected meteorological data correspond to the years with observed flood events. Databases start at the same time than the previous hydrological year (1st October), with the aim of simulating from correct initial conditions, as well as for having the capacity of adapting during a warm-up time before floods.

The data covers precipitation and temperature at different meteorological stations distributed on the Upper Rhone River basin and the surrounding area.

### 4.1.3 Meteorological forecasts by MeteoSwiss

MINERVE system makes use of the deterministic meteorological forecast COSMO-7, which is driven by the global model ECMWF (European Centre for Medium-Range Weather Forecasts) and covers most of Western and Central Europe. Deterministic COSMO-2 forecast is also used. It is driven by COSMO-7 (for the initial and boundary conditions) and covers, with a finer resolution, the Alpine region with Switzerland at the center. Both of them offer the benefit of nowcasting and short range forecasting.

Furthermore, the probabilistic forecast COSMO-LEPS (Limited-area Ensemble Prediction System) is also used. It supplies 16 ensembles with high resolution for central and Southern Europe. Initial boundary conditions are representative members of the ECMWF ensemble. The purpose of COSMO-LEPS is to improve the early and medium-range predictability of extreme and localized weather events, particularly when orographic and mesoscale-related processes play a crucial role.

The characteristics of the MeteoSwiss meteorological forecasts are presented in Table 4.1.

Table 4.1 Characteristics of the different COSMO models of MeteoSwiss

	<b>COSMO-LEPS</b>	<b>COSMO-7</b>	<b>COSMO-2</b>
Forecast type	Probabilistic (16 members)	Deterministic	Deterministic
Boundary conditions	ECMWF	ECMWF	COSMO-7
Spatial resolution	7 x7 km	6.6 x6.6 km	2.2 x2.2 km
Vertical levels	40	60	60
Lead time	132 h	72 h	24 h
Temporal resolution	3 h	1 h	1 h
Update	24 h	12 h	3 h

COSMO-7 is operational for the MINERVE project since 2006, COSMO-LEPS since 2008 and COSMO-2 since 2009.

Deterministic forecasts COSMO-7 and COSMO-2 are complementary to COSMO-LEPS. With the purpose to combine both deterministic and probabilistic forecasts, all are used in the MINERVE system. The complementarity is thus exploited rather than promoting the replacement of the deterministic by the probabilistic forecasts as proposed by Gouwelleuw et al. (2005).

#### 4.1.4 Historical floods

Reforecasts were provided by MeteoSwiss for COSMO-LEPS and COSMO-7 for the October 2000 and September 1993 floods in order to analyse the performance of the forecast for documented events (Table 4.2).

Table 4.2 Recent events in the Upper Rhone River basin and available forecasts COSMO-LEPS (C-L), COSMO-7 (C-7) and COSMO-2 (C-2). Start and end time are only proposed for guidance.

Start	End	Peak Flow (m <sup>3</sup> /s)	C-7	C-L	C-2
08.24.1987 12h -	08.26.1987 12h	992	✓	-	-
09.23.1993 12h -	09.26.1993 12h	1081	✓	✓	-
09.24.1994 00h -	09.26.1994 00h	707	✓	-	-
14.10.2000 00h -	18.10.2000 00h	1358	✓	✓	-
27.05.2008 12h -	01.06.2008 12h	815	✓	✓	-

Since no data is available during floods for COSMO-2 forecasts, the system for flood prediction is assessed for COSMO-LEPS and COSMO-7.

#### 4.1.5 Analogue technique

The aim of analogue techniques, developed by the IGAR Institute of the University of Lausanne (UNIL) in the MINERVE 2011 project (Horton et al., 2011), is to avoid difficulties of physical processes simulation generating precipitations. The detail level of forecasts is still poor for precisely estimating the location of extreme events. This difficulty is linked to the fact that precipitations are of a stochastic nature and created by complex physical processes, which are difficult to reproduce by numerical models (Deidda, 1999). This produces large uncertainties, particularly in a complex environment such as the alpine basins.

The alpine basin of the Rhone River is very sensitive to certain meteorological situations. It is known that the Binn-Simplon region is particularly exposed to extreme precipitations when humid air masses come up from the South attached with current jet at high altitude. The existence of a link between the general circulation and the studied weather parameters

(precipitation and temperature) is underlined in Figure 4.1, which illustrates the inverse air masses trajectories at 500 hPa (around 5500 m a.s.l.) for rainy days with more than 100 mm at the Binn station.



Figure 4.1 Inverse air masses trajectories at 500 hPa, corresponding to rain days with more than 100 mm at Binn station (from García Hernández et al., 2009e)

Figure 4.2 gives an overview of the analogue technique procedure and the steps for achieving final results and their occurrence probabilities. Such approach, coupled with classical Numerical Weather Predictions (COSMO forecasts in the MINERVE system), will allow confirming or refuting the forecasts of the meteorological numerical models, increasing the confidence in the general forecast system (Horton et al., 2011).

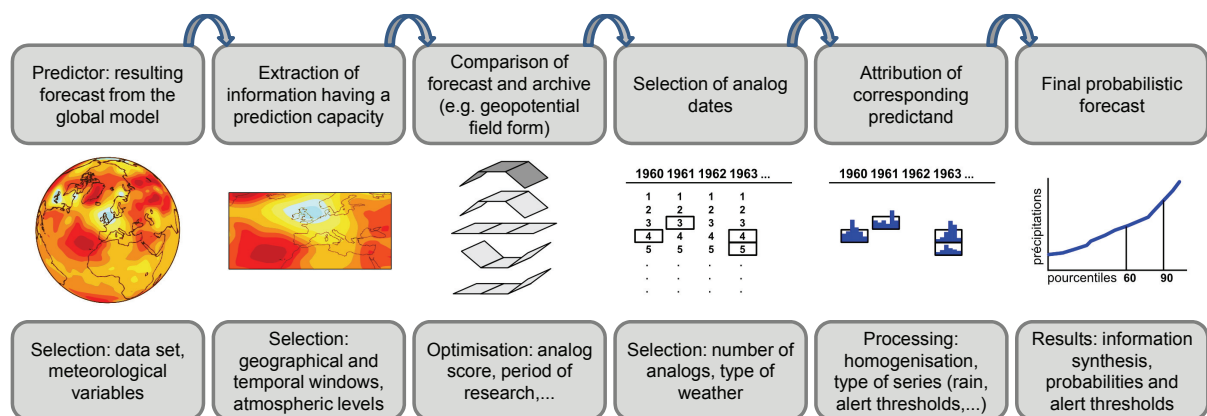


Figure 4.2 Illustration of successive stages of the analogue technique (from García Hernández et al., 2009e)

## 4.2 Hydrological forecasts

### 4.2.1 *An introduction to hydrology in the MINERVE framework*

Hydraulic schemes, especially hydropower plants and flood protection devices, become more and more complex due to the actual demand regarding optimal operational issues and their environmental integration into landscape. Appropriate tools are required for the planning and optimal management of such hydraulic systems. These tools required a good performance to provide a broad and comprehensive vision while analysing the interactions between the different elements of the hydraulic network.

The model GSM-Socont (Schäfli & al., 2005; Jordan, 2007) was selected for the hydrological production and transfer of the MINERVE system. It is a semi-distributed hydrological model, developed in the first stage of the MINERVE project, which computes snow accumulation and snow- and ice melt per altitude bands, taking into account time series of precipitation, temperature and evapotranspiration. It interpolates these values according to the gravity center of the band and its altitude.

The computer program Routing System II (Dubois and Boillat, 2000; García Hernández et al., 2007a) has been developed at the Laboratory of Hydraulic Constructions (LCH) at the Ecole Polytechnique Fédérale de Lausanne (EPFL). The program simulates the formation of free surface run-off flow and its propagation. The tool allows for hydrological and hydraulic modelling according to a semi-distributed conceptual scheme. In addition to hydrologic processes such as snowmelt, glacier melt, surface and underground flow due to infiltration, also hydraulic control elements, for example gates, spillways, diversions, junctions, turbines and pumps are implemented.

### 4.2.2 *Hydrological data*

The data used for calibration and validation of hydrological simulations cover the same periods than shown in Table 4.2 for the meteorological data.

The data is mainly available from gauging stations operated by the Federal Office for the Environment (FOEN) at different locations along the Rhone River and its main tributaries: Gletsch, Reckingen, Massa, Goneri, Saltina, Brig, Visp, Lonza, Sion, Branson, Châble, Martigny and Léman.



Turbine discharge from the hydropower plants as well as reservoirs levels are also available. Nevertheless, these data are more heterogeneous, sometimes provided with daily time step, sometimes with hourly time step, with lacks of data over some periods.

### **4.2.3 Semi-distributed hydrological model**

In catchment areas with a rather complex morphology, a large number of different hydrological processes can occur. In mountain regions the presence of snow and glaciers has a considerable influence on the hydrological response of the catchment area. Hence, apart from snowmelt and glacier melt, infiltration and surface run-off processes have to be considered as well. Moreover, the reservoirs, spillways, turbine and pump operations, channel routing, diversions and junctions have to be linked among each other to allow the correct flux of information.

All hydraulic structures are described by their hydraulic function by the help of six basic functions (generation, routing, storage, diversion, aggregation and regulation).

The hydrological models (Snow, Glacier, GR3, SWMM and GSM-Socont) have been developed within the framework of different research projects, namely CRUEX (Bérod, 1994), SWURVE (Schäfli & al., 2005), CONSECRU (Hingray et al., 2006) and MINERVE (Hamdi et al., 2003, 2005a, 2005b, Jordan et al., 2008).

In the modelling concept everything is related to functions. The catchment areas have a production function, diversions serve for flow distribution, channels are routing functions, lakes and reservoirs are storage functions, junctions are used for aggregation,...

### **GSM-Socont hydrological model**

The modelled basin is divided in several subcatchments. Then, each subcatchment can be divided further in different altitude bands for taking into account the temperature driven processes. The altitude bands are composed of a glacier or non glacier part.

The non-glacier part is modelled by: snowmelt, infiltration and run-off (Figure 4.3). The snow model simulates the transient evolution of the snow pack (melt and accumulation) as a function of the temperature ( $T$ ) and precipitation ( $P$ ), thus providing an equivalent precipitation ( $P_{eq}$ ) that is used as input by the SOCONT model. This one also takes into account the potential evapotranspiration ( $ETP$ ). The outflow discharge  $Q_s$  is transferred to the outlet of the sub-catchment.

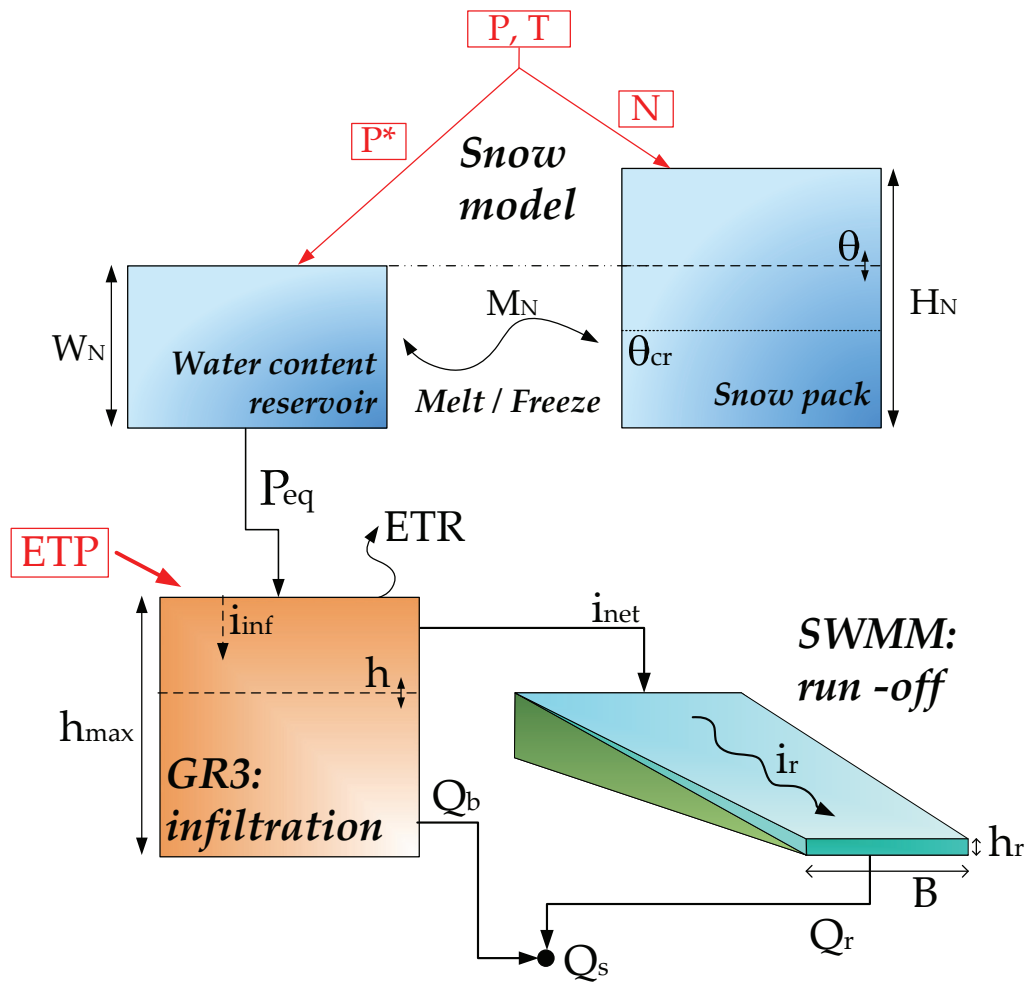


Figure 4.3 Model of non glacier altitude band

The glacier part, illustrated in Figure 4.4, is modelled by: snowmelt and glacier (still divided in 3 sub-models). The snow model produces an equivalent precipitation ( $P_{eq}$ ) which is transferred to the glacier model. It takes into account the height of the snow ( $H_N$ ) and the temperature ( $T$ ). In the glacier model the equivalent precipitation is transferred to the linear snow reservoir ( $R_N$ ) and finally to the outlet of the sub-catchment ( $Q_{NGL}$ ). In addition, the sub-model of the glacier melt produces a flow only when the height of snow is zero ( $H_N=0$ ). This glacier flow ( $P_{eqGL}$ ) is transferred to the linear glacier reservoir ( $R_{GL}$ ) and the resulting flow ( $Q_{GL}$ ) to the outlet of the sub-catchment.

The final flow produced by the sub-catchment ( $Q_{tot}$ ) is the sum of both flows.

### Snow Model

The snow model (Figure 4.3 and Figure 4.4, upper part in both figures) is composed of two sub-models which simulate the transient evolution of the snow pack (accumulation and melt)

as function of the temperature ( $T$ ) and precipitation ( $P$ ), producing an equivalent precipitation ( $P_{eq}$ ) which can be used as an input variable by the infiltration or the glacier model.

In a first step, the precipitation is divided into a solid precipitation ( $N$ ) and into a liquid precipitation ( $P^*$ ) depending on the temperature (Eq. 4.1 to Eq. 4.3):

$$P^* = \alpha \cdot P \quad 4.1$$

$$N = (1 - \alpha) \cdot P \quad 4.2$$

$$\begin{aligned} \alpha &= 0 & \text{si } T < T_{cp1} \\ \alpha &= (T - T_{cp1}) / (T_{cp2} - T_{cp1}) & \text{si } T_{cp1} < T < T_{cp2} \\ \alpha &= 1 & \text{si } T > T_{cp2} \end{aligned} \quad 4.3$$

with  $P^*$ : liquid precipitation [m/s];  $\alpha$ : separation factor;  $P$ : precipitation [m/s];  $N$ : solid precipitation [m/s];  $T$ : temperature [°C];  $T_{cp1}$ : minimum critical temperature for liquid precipitation [°C];  $T_{cp2}$ : maximum critical temperature for solid precipitation [°C].

If the observed temperature is lower than  $T_{cp1}$ , only solid precipitation is produced. If the temperature is higher than  $T_{cp2}$ , only liquid precipitation is produced. If the temperature observed lies between these two critical values, liquid and solid precipitations are produced. The solid precipitation ( $N$ ) is used as input for the snow pack, varying its content depending on the melting or freezing. The snowmelt calculation is performed as described in Eqs. 4.4 and 4.5:

$$\begin{aligned} M_N &= A_n \cdot (1 + b_p \cdot P^*) \cdot (T - T_{cr}) & \text{if } T > T_{cr} \\ M_N &= A_n \cdot (T - T_{cr}) & \text{if } T \leq T_{cr} \end{aligned} \quad 4.4$$

$$\begin{aligned} dH_N / dt &= N - M_N \\ M_N &\leq N + H_N / dt \\ M_N &\geq -W_N / dt \end{aligned} \quad 4.5$$

with  $M_N$ : snowmelt or freezing [m/s];  $A_n$ : degree-day coefficient [m/s/°C];  $b_p$ : precipitation coefficient due to melt [s/m];  $T_{cr}$ : critical snowmelt temperature [°C];  $H_N$ : height of snow [m];  $W_N$ : water content [m];  $dt$ : time step [s].

The differential equation 4.5 is solved according to Euler (first order) by the following scheme:

$$H_{N,t+1} = H_{N,t} + (N_t - M_{N,t}) \cdot \Delta t \quad 4.6$$

with index  $t$  and  $t+1$  representing time;  $\Delta t$ : time step [s].

The equivalent precipitation ( $P_{eq}$ ) is produced by the water content of the snow (Eq. 4. 7 to 4.9):

$$\theta = W_N / H_N \quad 4.7$$

$$\begin{aligned} P_{eq} &= P^* + W_N / dt && \text{if } H_N = 0 \\ P_{eq} &= 0 && \text{if } H_N > 0 \text{ et } \theta \leq \theta_{cr} \end{aligned} \quad 4.8$$

$$\begin{aligned} P_{eq} &= (\theta - \theta_{cr}) \cdot H_N / dt && \text{if } H_N > 0 \text{ et } \theta > \theta_{cr} \\ dW_N / dt &= P^* + M_N - P_{eq} \end{aligned} \quad 4.9$$

with  $\theta$ : relative water content in the snow pack [-];  $\theta_{cr}$ : critical relative water content in the snow pack, from which water is produced [-].

The differential equation 4.9 is solved as before by the same scheme than 4.5 (Euler, first order):

$$W_{N,t+1} = W_{N,t} + (P^*_t + M_{N,t} - P_{eq,t}) \cdot \Delta t \quad 4.10$$

The variables for the initial situation associated to this model are  $\theta$  and  $H_N$ . The parameter to adjust is  $A_n$ . The remaining parameters ( $b_p = 0.0125$ ,  $\theta_{cr} = 0.1$ ,  $T_{cp1} = 0$  °C,  $T_{cp2} = 6$  °C,  $T_{cr} = 0$  °C) are supposed to be constant.

The input variables of the model are precipitation and temperature, the output value is the equivalent precipitation.

### **GR3 Infiltration model**

The gross intensity (or equivalent precipitation  $P_{eq}$  coming from the snow model) and potential evapotranspiration ( $PET$ ) are introduced in the GR3 model (Edijatno and Michel, 1989; Consuegra et al., 1998).

The infiltration reservoir GR3 (Figure 4.3, down left) is defined according to Eq. 4.11 to 4.15:

$$\begin{aligned} i_{inf} &= P_{eq} \cdot (1 - (h_{inf} / h_{max})^2) && \text{if } h_{inf} \leq h_{max} \\ i_{inf} &= 0 && \text{if } h_{inf} > h_{max} \end{aligned} \quad 4.11$$

$$\begin{aligned} ETR &= ETP \cdot \sqrt{h_{inf} / h_{max}} && \text{if } h_{inf} \leq h_{max} \\ ETR &= ETP && \text{if } h_{inf} > h_{max} \end{aligned} \quad 4.12$$

$$i_{net} = P_{eq} - i_{inf} \quad 4.13$$

$$\begin{aligned} Q_{base\ inf} &= k \cdot h_{inf} \cdot S && \text{if } h_{inf} \leq h_{max} \\ Q_{base\ inf} &= k \cdot h_{max} \cdot S && \text{if } h_{inf} > h_{max} \end{aligned} \quad 4.14$$

$$dh_{inf} / dt = i_{inf} - ETR - Q_{base} / S \quad 4.15$$

with  $PET$ : potential evapotranspiration [m/s];  $i_{inf}$ : infiltration intensity [m/s];  $h_{inf}$ : level in infiltration reservoir [m];  $h_{max}$ : capacity of infiltration reservoir [m];  $RET$ : real evapotranspiration [m/s];  $Q_{base\ inf}$ : infiltration base discharge [m<sup>3</sup>/s];  $k$ : release coefficient of infiltration reservoir [1/s];  $S$ : surface [m<sup>2</sup>];  $i_{net}$ : net intensity [m/s].

The solution of the differential Eq. 4.15 is performed once again according to the Euler method (first order):

$$h_{inf,t+1} = h_{inf,t} + (i_{inf,t} - ETR_t - Q_{base,t} / S) \cdot \Delta t \quad 4.16$$

The variable for the initial state associated to this model is  $h_{inf}$ . The parameters to adjust are  $k$  and  $h_{max}$ . The parameter  $S$  is assumed to be constant.

The input variables of the model are the equivalent precipitation (or gross intensity) and the potential evapotranspiration ( $PET$ ). As a result the net intensity, the base discharge and the real evapotranspiration are obtained.

### ***SWMM: run-off model***

The transfer of the net intensity to an impermeable surface is carried out by the help of a non-linear transfer reservoir (Figure 4.3) depending on equations 4.17 to 4.19:

$$\begin{aligned} dh_r / dt &= 2 \cdot (i_{net} - i_r) \\ h_r &> 0 \end{aligned} \quad 4.17$$

$$i_r = K_s \cdot \sqrt{J_o} \cdot h_r^{5/3} \cdot B_r / S \quad 4.18$$

$$Q_r = i_r \cdot S \quad 4.19$$

with  $h_r$ : runoff water level downstream of the surface [m];  $i_r$ : outflow runoff intensity [m/s];  $K_s$ : Strickler coefficient [m<sup>1/3</sup>/s];  $J_o$ : average slope of the plane [-];  $B_r$ : width of the plane [m].

As for the infiltration model GR3, it is necessary to solve the differential equation with the first order Euler method.

The variable for the initial condition associated to the model is  $h_r$ . the parameter to adjust is  $K_s$ . The other parameters ( $J_o$ ,  $B_r$ ,  $S$ ) are supposed to be constant.

The SWMM model (Metcalf et al.,1971), supplied by a hyetograph of net rainfall, provides a hydrograph downstream of the considered surface.

### **Glacier model**

The glacier melt (Figure 4.4, downer part) depends on the temperature and the presence of snow on the glacier. The total discharge of the glacier also depends on the transfer processes within the linear snow and glacier reservoirs  $R_N$  and  $R_{GL}$ .

A gross precipitation (or equivalent precipitation  $P_{eq}$  of the snow model) is transferred to the linear snow reservoir ( $R_N$ ) according to Equation 4.20:

$$dH_{NGL}/dt = P_{eq} - K_N \cdot H_{NGL} \quad 4.20$$

with  $H_{NGL}$ : level in linear snow reservoir [m];  $K_N$ : release coefficient of linear snow reservoir [1/s].

The outflow of the linear snow reservoir  $Q_{NGL}$  is (Eq. 4.21):

$$Q_{NGL} = K_N \cdot H_{NGL} \cdot S_{GL} \quad 4.21$$

with  $Q_{NGL}$ : outflow of linear snow reservoir [ $m^3/s$ ];  $S_{GL}$ : glacier surface [ $m^2$ ].

The glacier melt sub-model only provides a discharge when the snow level is zero ( $H_N=0$ ). Then, the discharge produced by the glacier melt ( $P_{eqGL}$ ) is transferred to the linear glacier reservoir ( $R_{GL}$ ) and the resulting discharge ( $Q_{GL}$ ) at the outlet of the sub-catchment.

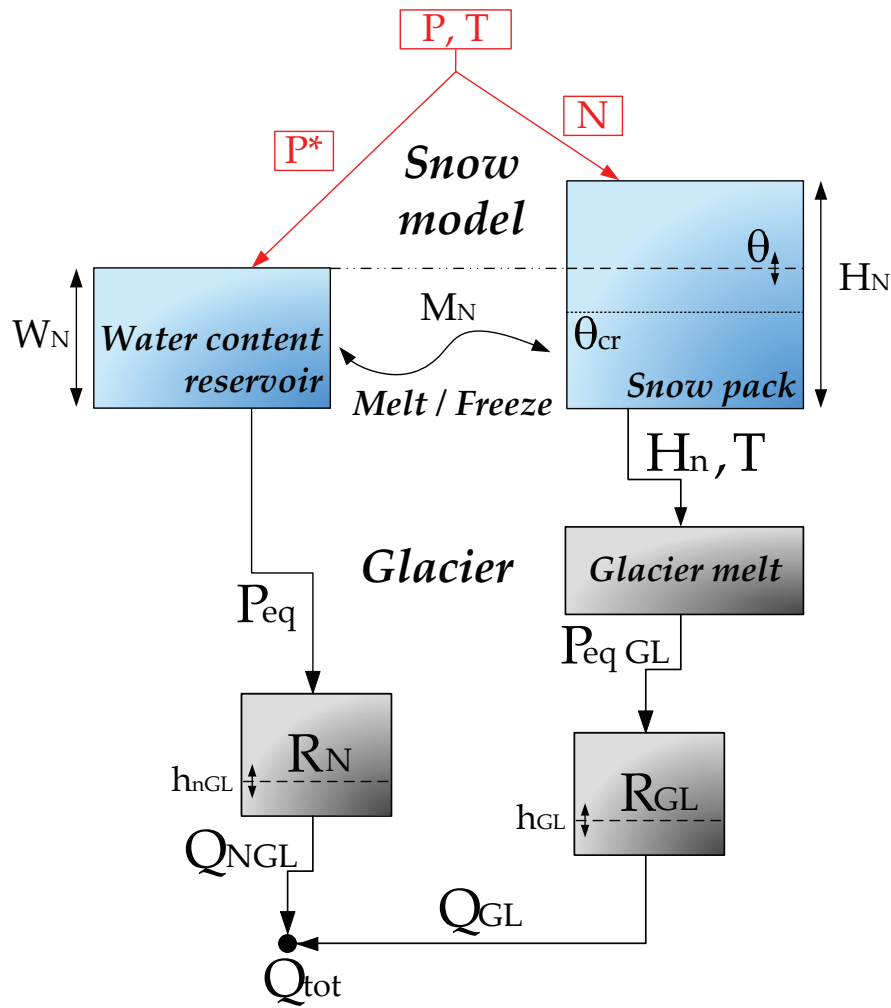


Figure 4.4 Model of glacier altitude band

The glacier melt  $Q_{GL}$  is defined according to equations 4.22 to 4.24:

$$\begin{aligned}
 P_{eqGL} &= 0 & \text{if } T \leq T_{cr} \text{ or } H_N > 0 \\
 P_{eqGL} &= A_{GL} \cdot (T - T_{cr}) & \text{if } T > T_{cr} \text{ and } H_N = 0
 \end{aligned}
 \tag{4.22}$$

$$\frac{dH_{GL}}{dt} = P_{eqGL} - K_{GL} \cdot H_{GL}
 \tag{4.23}$$

$$Q_{GL} = K_{GL} \cdot H_{GL} \cdot S_{GL}
 \tag{4.24}$$

with  $P_{eqGL}$ : glacier melt [m/s];  $A_{GL}$ : degree-day glacier melt coefficient [m/s/°C];  $H_{GL}$ : level of glacier melt reservoir [m];  $K_{GL}$ : coefficient of linear glacier reservoir [1/s];  $Q_{GL}$ : outflow of linear glacier reservoir [m<sup>3</sup>/s].

The variables of this model are  $H_N$ ,  $\theta$ ,  $H_{RN}$ , and  $H_{RGL}$ . The parameters to adjust are  $A_{GL}$ ,  $K_{GL}$  and  $K_N$ . The parameter  $S_{GL}$  is assumed to be constant after its calculation.

Model inputs are snow level, temperature and gross precipitation (or equivalent precipitation of snow model). The output is the total discharge at the model outlet.

This conceptual glacier model has been improved (García Hernández et al., 2009c) by considering the mass balance and snow transfer describing the glacier evolution. This approach was applied to the Rhone glacier to examine its evolution, after a previous calibration and validation using annual changes of glacier surface and monthly runoff measurements. The results showed a continuous and significant reduction of the area of the Rhone glacier while the hydrological cycle was strongly affected.

#### **4.2.4 Flow routing**

Channel routing can be solved by St. Venant, Muskingum-Cunge and Kinematic Wave. These resolutions are presented in Appendix 3.

#### **4.2.5 Catchment model**

Finally, two different hydrological models were created. The first does not include the hydraulic schemes and is therefore the hydrological model of the “natural basin”. The second model is the one of the equipped basin with hydraulic structures, directly named “equipped basin”.

##### ***Natural basin***

The simulation with the first model, the natural basin, provides the results for the basin without any hydraulic structures (no reservoirs or hydropower plants) and is used as reference. Furthermore, it is also used as initial condition for calculating the final hydrographs at check points for the equipped basin.

##### ***Equipped basin***

The equipped basin represents the current state of the basin. The simulations take into account all reservoirs and hydropower plants as well as appurtenant hydraulic structures of the basin. Final hydrographs of the model are calculated using reference hydrographs at check points from the natural model as well as inflows and outflows of the reservoirs.

#### **4.2.6 Routing System MINERVE**

The models described in the above chapter have been implemented in the software Routing System II (García Hernández et al., 2007a). Routing System II is a program using object-oriented programming. It has been developed for the simulation of flood events in complex



systems constituted of several sub-catchments, diversions, junctions, reservoirs, turbines and hydraulic and hydrological elements with free surface flow.

The objects are described by their hydraulic function. The description of the network is basically carried out by the help of six basic functions, namely: generation of flow, flow transport in a channel, storage, diversion, additional inflow and flow regulation. These functions, each represented by an icon, can be freely assembled on the graphic interface. The data flux between the different functions is carried out by linking the icons among each other using the mouse.

This kind of approach allows the modelling of systems with a complex typology as well as the analysis at different scale levels by the aggregation of sub-catchments. An enhanced version of Routing System II, called Routing System MINERVE, is used for this purpose. Simulations with all kind of COSMO forecasts (deterministic and probabilistic) can be realised by the help of the imported hydrological model of the Upper Rhone River catchment as well as the meteorological database.

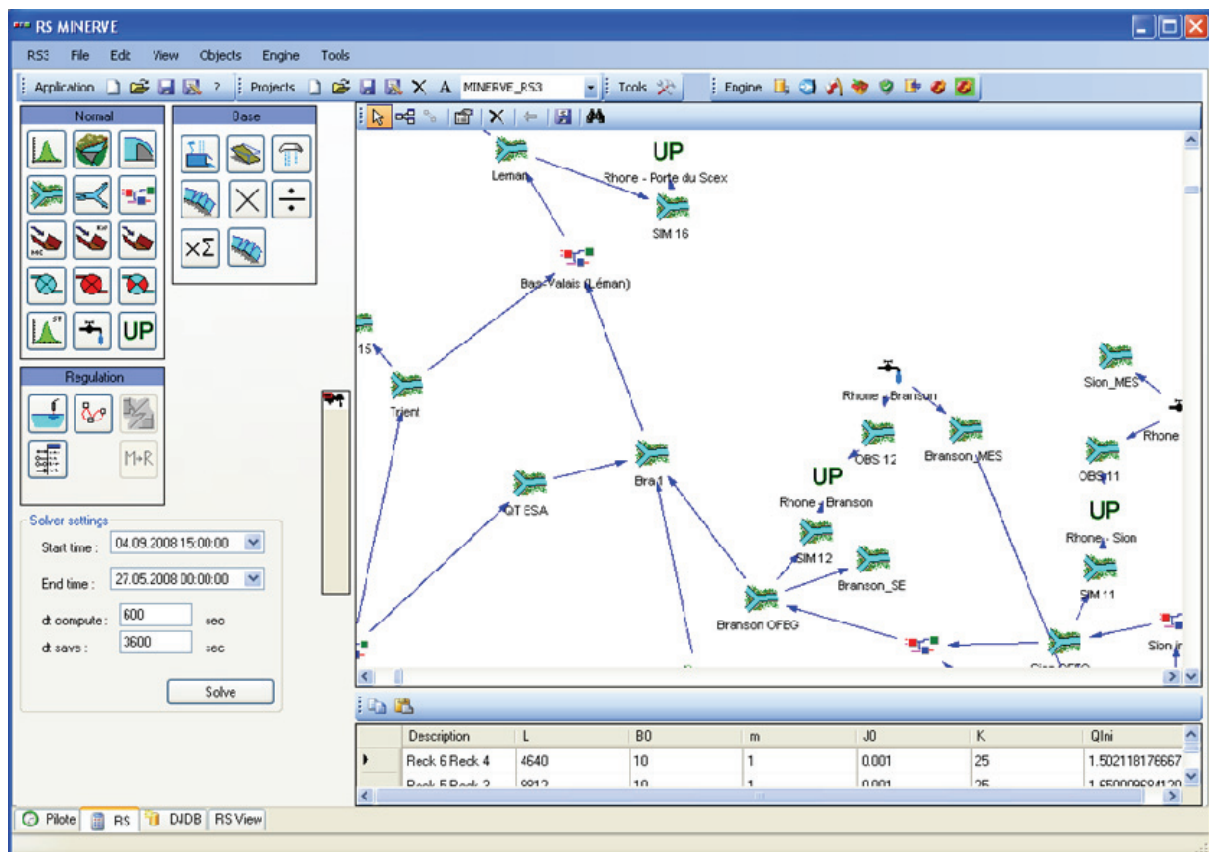


Figure 4.5 Routing System MINERVE main window

Employed as a standard executable program, Routing System MINERVE has a convenient up-to-date graphic interface. The interface allows the creation of a hydrological model and its

numerical simulation. Special attention has been given on an appealing graphic visualization of all data and results which constitutes an essential functionality for the verification of model computations and the analysis of results.

### Multiple simulations

Multiple simulations can be performed at the same time by running probabilistic forecasts. When a deterministic forecast is selected, only one hydrological forecast is obtained. When a probabilistic forecast is applied, a probabilistic hydrological forecast is generated by multiple simulations of all independent forecast members (i.e. no combination of forecast members) is thus carried out.

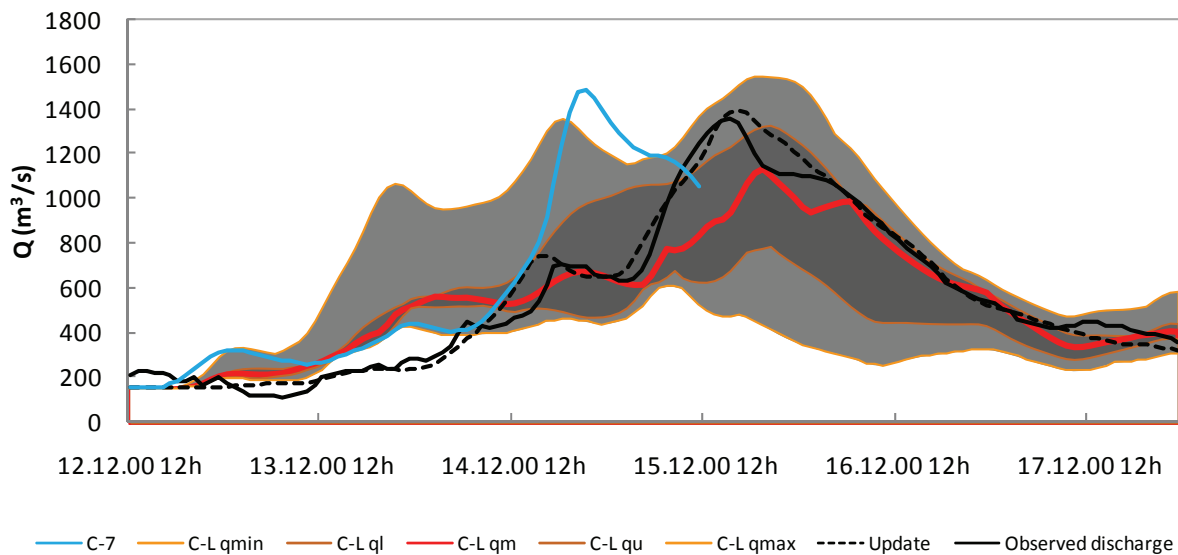


Figure 4.6 Hydrographs obtained by deterministic and probabilistic hydrographs. C-7 represents COSMO-7 and C-L COSMO-LEPS represented by the median  $q_m$ , the upper  $q_u$  and lower quartile  $q_l$  as well as by the minimum  $q_{min}$  and maximum discharge  $q_{max}$ . Update symbolises the simulations with meteorological observations and the update of the initial conditions of the hydrological model.

## 4.3 Warning system

### 4.3.1 Flood warnings overview

Hydrological forecasts and flood warning systems are coming together towards different facets of the same core task thanks to the strengthening union between scientists, end users and the general population for purpose of dealing with flood events. Several studies have been performed regarding flood risk in long-term planning (Hutter and Schanze, 2008), flood risk

from a social point of view (November et al., 2009), flood forecast operational services (Jal et al., 2009) or real-time flood forecast systems (Thielen et al., 2009a; Hess, 2010).

A similar procedure as the developed in this research project was implemented in the Cantabria North basin in Spain (LCH, 2010b). A warning system with the deterministic HIRLAM forecast and two hydrological models (PRESKO and GSM-Socont) was successfully applied and is operational since 2010.

Although a big number of flood forecasting techniques is presently available in the literature, most operational flood forecasting schemes currently implemented are rudimentary (Werner et al., 2005). A reason for this is that the gap between models used in research projects and flood forecasting for operational purposes. Furthermore, when developing new flood forecasting schemes, the difficulties faced are more often institutional than technical.

The wide collaboration between authorities and research groups in the framework of the MINERVE project allowed designers and researchers to go unusually far in developing a flood forecast system, integrating the operational tools and the institutional procedures for coping with flood events and, at the same time, obtaining feedbacks from all partners involved.

The warning system developed in the present research project for the MINERVE project improves the data presentation concerning critical situations. It gives an overview of last forecasts as well as the alert thresholds at main check points located in the basin.

### **4.3.2 Warning levels**

The MINERVE system is part of the flood management procedure in the Upper Rhone valley (Figure 4.7). It has the purpose to establish, plan and coordinate floods in real-time situations of the basin (Rhone and tributaries as well as hydropower plants and reservoirs) based on hydrological forecasts. The decisional-making organism (flood task force) decides on the intervention level and initiates adequate preventive measures.

As soon as a critical flood situation is identified, the MINERVE decision support system suggests intervention strategies for the preventive management of hydropower plants and reservoirs. The goal is to prevent or reduce of floods in the basin, in agreement with the pre-established objectives and taking into account existing constraints.

In order to assess the performance of the system, several meteorological resimulations of past events were conducted at MeteoSwiss.

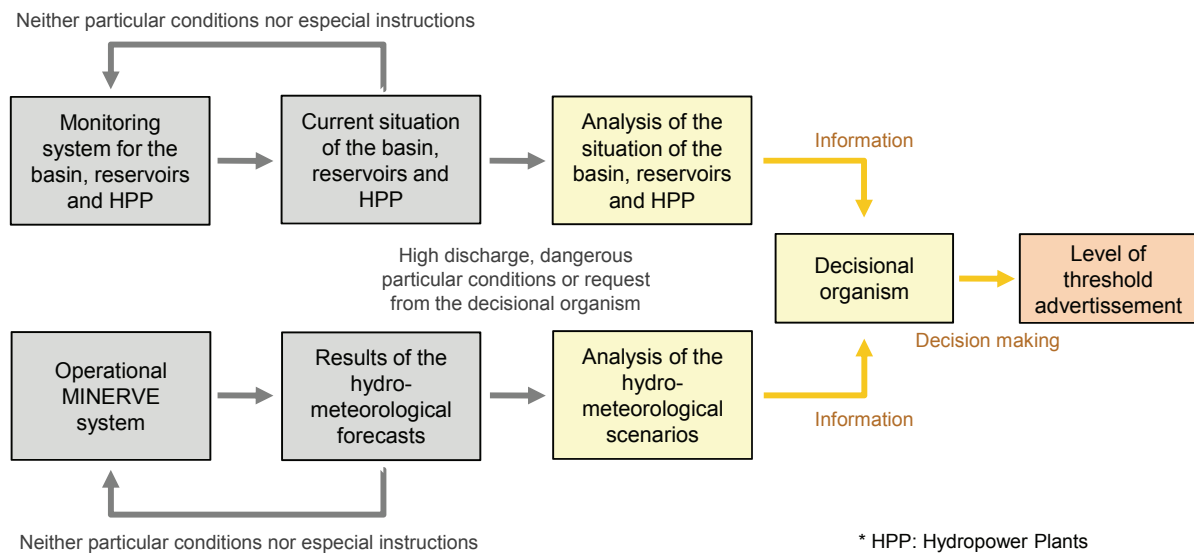


Figure 4.7 Operational scheme of flood management in the Upper Rhone valley.

Before activating the decision support system, the MINERVE warning report gives in a synthetic way the evolution of the hydrological situation at different check points of the basin. Warning (notice, alert or alarm) messages are given depending on the different flow exceedance thresholds (Table 4.3) and probability of the ensemble forecasts. The selected check points are distributed throughout the basin in the Rhône River (Reckingen, Brig, Sion, Branson, Lavey and Porte-du-Scex) and its two main tributaries (Vispa and Dranse) and have been set in accordance with a hydraulic study of flooding at the vicinity of each check point.

Table 4.3 Critical discharge ( $m^3/s$ ) for different threshold warnings at check points (indicative, under validation by the Valais Canton).

Check Point	NOTICE threshold	ALERT threshold	ALARM threshold
Rhône – Reckingen	75	95	115
Rhône – Brig	245	340	410
Rhône – Sion OFEV	450	530	640
Rhône – Branson OFEV	475	550	650
Rhône – Lavey	650	800	1000
Rhône – Porte-du-Scex	700	1000	1200
Vispa – Visp OFEV	370	450	550
Dranse – Martigny	70	82	95

### 4.3.3 Flood management in the Upper Rhone River basin

When an exceptional storm is expected, the procedure for the flood management in the Upper Rhone River basin is triggered in the cantons of Valais (VS) and Vaud (VD) (Service de la

sécurité civil et militaire, 2009). Flows at the check points, levels in reservoirs and hydro-meteorological forecasts provide basic information to decision makers to apply the crisis procedure. The decisions and the associated steps depend on the following elements (Figure 4.8):

- observed flows at check points (higher or lower than the discharge thresholds),
- precipitation forecasts (increasing, constant or decreasing),
- MINERVE hydrological forecasts (favourable, stable or unfavourable) and
- Potential of flood retention in reservoirs (full, partial or insufficient capacity).

Based on the predicted situation, a warning threshold can be reached at certain check points, as defined by the Roads and Water courses Service (SRCE) in the Canton of Valais, in coordination with the Water, land and Sanitation Service (SESA) of the Vaud Canton and the Civil and Military Security Service (SSCM) of the Vaud Canton. The first two threshold levels (notice and alert AQUA) are triggered by the Cantonal Police of Valais, the third one (alarm ALTO) by the cantonal authorities.

### ***Notice warning***

The notice warning is defined for frequent events and provides general information. A light monitoring of the event is also started. The CERISE crisis cell (flood task force) and MINERVE operators begin to monitor the situation.

The procedures and resources are then verified and the information is transmitted to the other partners (Weather Group-VD). SRCE-VS informs also SESA-VD and the Water Field (Department of the territory) of Geneva (DomEAU-GE).

### ***Alert AQUA***

The alert AQUA is activated for a no-frequent event with a return period between 20 and 50 years. In this case, specialists are on site, the surveillance is increased and the intervention systems are set up.

The Weather Group-VD and the CERISE crisis cell continuously monitor the evolution of the event and regularly exchange information. Experts (Cell of Reinforced Intervention, CIR) are called on site. Regular contacts are established between decision-makers. AQUA warnings are given to the VS villages and to the Intervention Cells of VD (reinforced monitoring of dikes, preparations for population evacuation, local interventions). Recommendations adapted to the situation and coordinated by the cantonal police VD and/or VS are provided to the population.

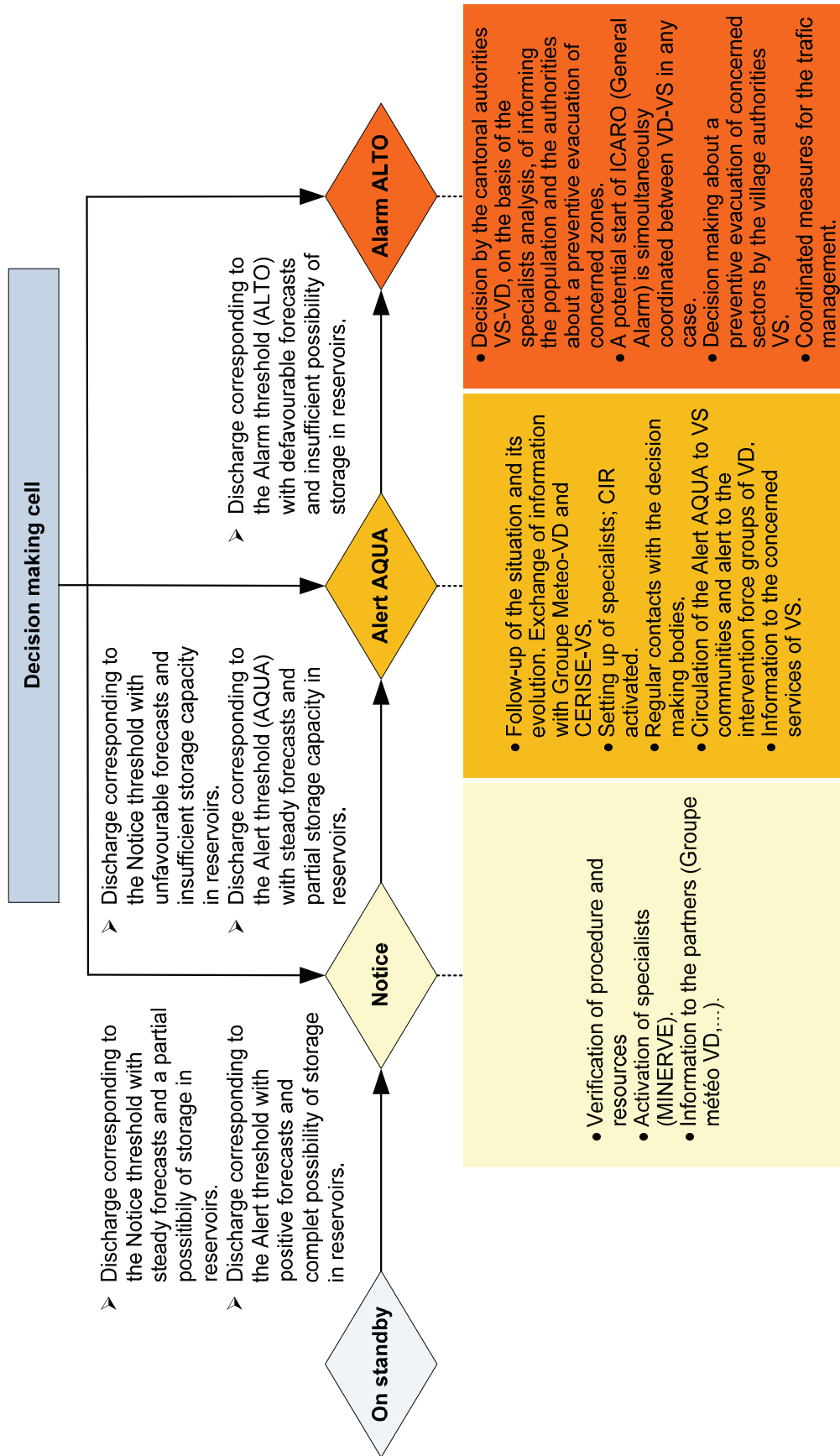


Figure 4.8 Operational scheme of the procedure in case of flood in the Vaud and Valais Cantons (from Service de la Sécurité Civil et Militaire, 2009)

### ***Alarm ALTO***

Finally, the alarm ALTO is launched for rare events (about 100 year return period). The alarm and the evacuation plans of the potentially affected population are activated.

A preventive evacuation of the endangered areas may be decided by the cantonal authorities of VS-VD on the basis of the analysis provided by specialists. A possible simultaneous triggering of ICARO (General alarm) between VS-VD must be coordinated in all cases. The VS authorities decide preventive evacuations of the endangered sectors under their responsibility.

#### ***4.3.4 Warning Report***

##### ***Creation of the warning report***

Once the weather forecast available, it is translated into hydrological forecasts at the check points of the basin. The goal of the warning report is that results are easily interpretable by the security concerned authorities of the cantons of Vaud and Valais, which will be responsible for reducing the potential risks for the population and infrastructures.

For an overview of the situation at check points, a new warning report tool was created, allowing a prior judgement of the situation over the basin before the usage of the decision support system for flood management. This tool is intended to provide a good tractability of results and, at the same time, a view of the uncertainty associated to the forecasts. The provided information aims to be understandable not only for specialized hydrologists, but also for the wider variety of all possible users. Its main purpose is to provide warning in face of potential dangerous situations. To this goal, on the basis of a simple visual interpretation, the user must be able to decide:

- If the situation is critical,
- if it is necessary to provide some warning (notice, alert or alarm) and
- if the decision support system MINDS has to be run.

Hydrological forecasts and discharge thresholds are necessary for operating the warning report tool. Routing System MINERVE provides the hydrological forecasts when the three types of COSMO forecasts are available. For the existing forecasts, the values of flows are calculated for all points of the model and recorded in a database. After this step, hydrographs at main check points of the basin can be acquired and compared to the discharge thresholds for the three types of warnings.







The warning report allows the visualisation of the hydrographs corresponding to the last COSMO forecasts available. The hydrograph of the deterministic forecast is represented by a single curve for each forecast while the COSMO-LEPS ensemble forecasts are represented by the minimum, maximum, median hydrographs and those of the upper and lower quartiles. The different warning thresholds are also indicated by a straight line.

**Representation and activation of the warnings**

For the representation of the forecast results, a gradation of colours is used according to the severity of the hydrological situation at check points. This coding system (Table 4.4) shows the results in a simplified manner and highlights the persistence of the hydrological situation.

Table 4.4 Code of colours, threshold and associated warning

Colour	Threshold	Description
	No risk	Water level steady or slightly high but without risk of overflowing
	Medium risk	Frequent event. High water levels but without risk of overflowing
	High risk	Non-frequent event. Situation near to the overflowing and with the possibility of inundations.
	Critical risk	Rare event. High possibilities of overflowing and inundations, potentially dangerous






The activation of warnings is done for a fixed percentage of probabilistic forecasts exceeding the threshold value or when the deterministic forecast exceeds this value. The three thresholds of exceedance (notice, alert and alarm) are presented in Table 4.5. This value may still be modified or even differentiated for each level of warning, according to future performance of the forecasts.

**Visualization of the warnings**

The MINERVE warning report is structured in the hydrographs of the last available forecasts and the warning table, as shown in Figure 4.9. The graphic with the hydrographs at a selected check point shows the predicted discharge evolution for the three types of COSMO forecasts. The graphic starts one day before the current date, presenting the last observed discharges, and shows a predicted horizon of 132 h, corresponding to the lead time of COSMO-LEPS (higher than COSMO-7 or COSMO-2, which provides a forecast with a lead time of 72 and 24 respectively). The out-dated forecast intervals are shown with the same code of colours, but with a lighter tonality.



Table 4.5 Code of colours for the different warnings and associated forecasts to

Colour	COSMO-LEPS	COSMO-7 & COSMO-2
	Data not available	Data not available
	50% of the forecast members do not exceed the threshold of the Notice Warning	Forecast does not exceed the threshold of the Notice warning
	50% of the forecast members exceed the threshold of the Notice Warning	Forecast exceeds the threshold of the Notice Warning
	50% of the forecast members exceed the threshold of the Alert Warning	Forecast exceeds the threshold of the Alert Warning
	50% of the forecast members exceed the threshold of the Alarm Warning	Forecast exceeds the threshold of the Alarm Warning

In the table of the warning report, forecasts are placed linewise from the starting time of each forecast. The table presents all forecasts containing a prediction for the next days. As shown in the example of the Figure 4.9, the table contains six lines for the COSMO-LEPS forecasts (one line for the last forecast and five for previous forecasts). The same number of lines is shown for COSMO-7.

In order to greatly simplify the interpretation of the results, and to work on an appropriate temporal scale, the results are grouped in three hourly intervals, taking into account the highest discharge value within the three hours period. Each cell of the table represents the evaluation of this lapse of time. If forecasts exceed one of the thresholds during the considered three hours, the warning is activated on the report.

The presented COSMO forecasts have different updates. The warning report can be updated every three hours, which is the update time of the smallest of the three forecasts (corresponding to COSMO-2). If COSMO-7 or COSMO-LEPS forecasts are not available at the selected time, the most recent forecast available is used to draw its hydrograph.

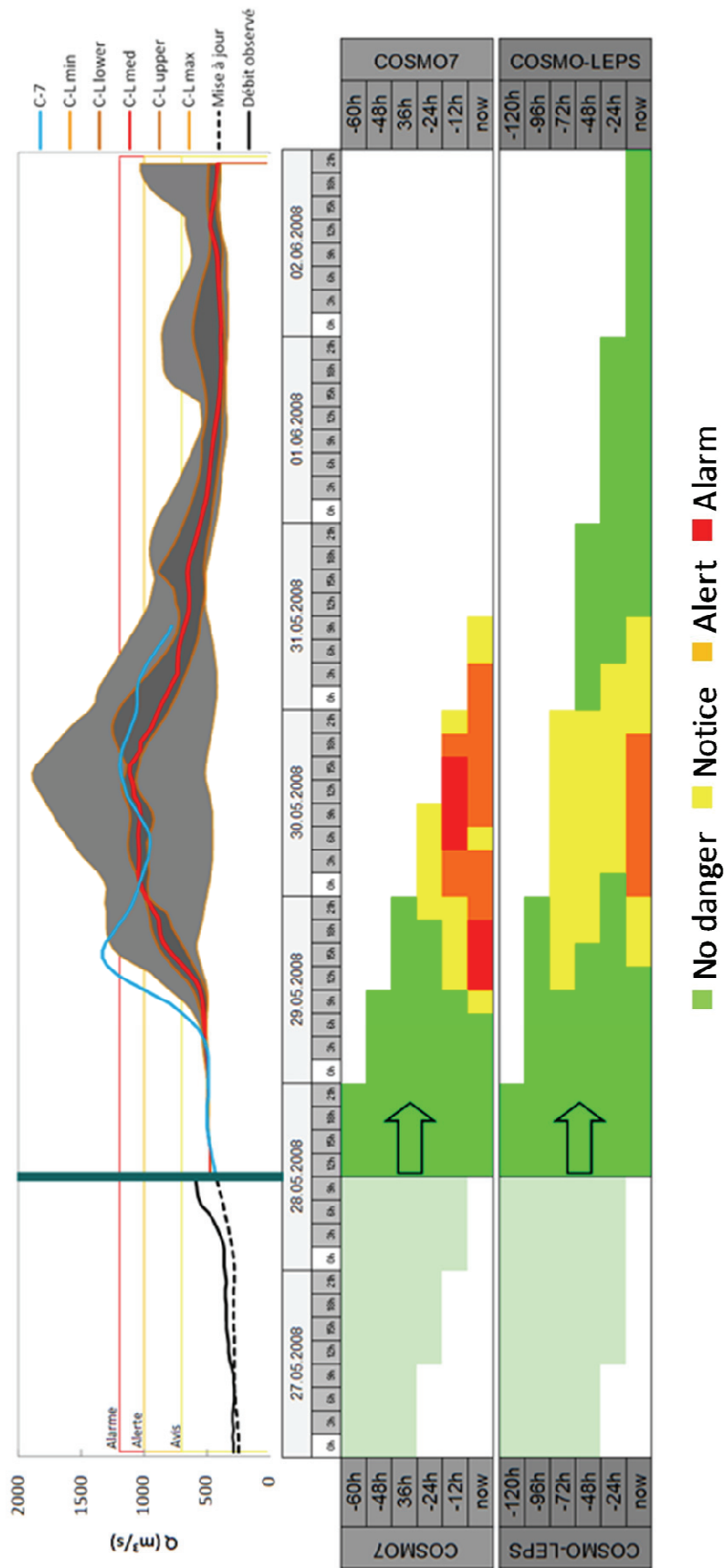


Figure 4.9 Example of a warning report

“Prediction is very difficult, especially about the future”

Niels Bohr (1885-1962)

## **5. Hydro-meteorological forecasts in the Upper Rhone River basin**

## 5.1 Performance evaluation of the forecasts

Hydrological flood systems have to include an analysis of the available data and results (Krzysztofowicz et al., 1994; Krause, 2005; Roulin, 2007). Even if the available data is not sufficient for evaluating the reliability of the system, it helps to develop a consistent system and to learn about the decision making tasks.

The main goal of this chapter is the assessment of the MINERVE system for flood forecast carried out from COSMO-LEPS and COSMO-7 meteorological predictions (LCH, 2009; LCH, 2010a). As COSMO-2 forecasts are available only since 2009, their analysis is not discussed. The two meteorological forecasts (COSMO-LEPS and COSMO-7) are compared in order to understand the specificities of their applicability (horizon of use, error, uncertainty,...) and how to present their results to final users adequately.

The flood events forecasted by COSMO-LEPS and COSMO-7 are taken into account for performance evaluation as presented in Table 5.1.

Table 5.1 Evaluated flood events

Start		Fin	Peak Flow	C-7	C-L
09.23.1993 12h	-	09.26.1993 12h	1081	✓	✓
14.10.2000 00h	-	18.10.2000 00h	1358	✓	✓
27.05.2008 12h	-	01.06.2009 12h	815	✓	✓

The meteorological forecasts as well as the hydrological forecast have been evaluated. Performance of the meteorological or hydrological deterministic forecasts can be evaluated with different methods like the Normalised Peak Error (NPE), Peak Timing Error (PTE), Root Mean Square Error (RMSE), Volume Ratio and Nash coefficient (Ajami et al., 2004; Gabellani et al., 2007; Jordan, 2007; Pujol Reig et al., 2007; Sun et al., 2000).

For the performance of the probabilistic forecasts, indices normally used in meteorology are the Brier Score (BS), the Brier Skill Score (BSS) and the Relative Operating Characteristic (ROC) (Stefanova and Krishnamurti, 2002; Buizza et al., 2005; Marsigli et al., 2005). These indicators are also commonly used in hydrology (Georgakakos et al., 2004; Roulin, 2007; Jaun et al., 2008).

The BS is similar to the RMSE, measuring the difference between a forecast probability of an event and its occurrence. The value of the BS is dependent on three factors: reliability, resolution and uncertainty. The BSS is normally defined as the relative probability score

compared to the probability score of a reference forecast. Finally, the ROC curve measures the ability of forecast to discriminate between situations predicting the occurrence and the non-occurrence of an event.

## 5.2 Analysis of meteorological performance

### 5.2.1 Meteorological indicators

In order to evaluate the performance of the deterministic and probabilistic meteorological forecasts, the predicted precipitation intensities and temperatures have been compared with the observed values at different measurement stations (Table 5.2).

Table 5.2 Meteorological stations located in the Upper Rhone River basin

Measurement Station	Coordinates [m]		Altitude a.s.l. [m]
	X	Y	
<b>Adelboden</b>	609'400	148'975	1'320
<b>Aigle</b>	560'120	130'630	381
<b>Evolene</b>	605'415	106'740	1'825
<b>GSB</b>	579'200	79'720	2'472
<b>Moleson</b>	567'740	155'175	1'972
<b>Montana</b>	603'600	129'160	1'508
<b>Sion</b>	592'200	118'625	482
<b>Ulrichen</b>	666'740	150'760	1'345
<b>Visp</b>	631'150	128'020	640
<b>Zermatt</b>	624'300	97'575	1'638

“Deterministic indexes” are defined as indicators which can assess a unique forecast, while “probabilistic indexes” are defined as indicators able to evaluate an entire ensemble of forecasts (composed by one or more members). Deterministic indexes are included in the comparison, such as the intensity or temperature bias and volume or average temperature bias for different time periods. Probabilistic indexes such as the Brier Score (BS) and the Relative Operating Characteristic (ROC) are also considered, which compare the skill of the entire ensemble with that of the deterministic forecast.

**Precipitation intensity bias ( $b_i$ ) and temperature bias ( $b_T$ )**

These indicators measure the average hourly error of the forecast through Eqs. 5.1 and 5.2:

$$b_i = \frac{\sum_{t=t_i}^{t_f} |i_{sim,t} - i_{obs,t}|}{t_f - t_i} \quad 5.1$$

$$b_T = \frac{\sum_{t=t_i}^{t_f} |T_{sim,t} - T_{obs,t}|}{t_f - t_i} \quad 5.2$$

with  $b_i$ : average hourly precipitation intensity bias in absolute value for the considered period [mm/h];  $i_{sim,t}$ : simulated intensity at time step  $t$  [mm];  $i_{obs,t}$ : observed intensity at time step  $t$  [mm];  $b_T$ : average hourly temperature bias in absolute value for the considered period [°C];  $T_{sim,t}$ : simulated temperature at time step  $t$  [mm];  $T_{obs,t}$ : observed temperature at time step  $t$  [mm];  $t_i$ : initial time step [h];  $t_f$ : final time step [h].

**Relative volume bias ( $Rb_{Vol}$ ), cumulated volume ratio ( $r_{CVol}$ ) and average temperature bias ( $b_{aT}$ )**

These indicators are defined by Eqs. 5.3 to 5.5. They are assessed for 24 hour consecutive periods from the start of the forecast.

$$Rb_{Vol} = \frac{\sum_{t=t_i}^{t_f} i_{sim,t} - \sum_{t=t_i}^{t_f} i_{obs,t}}{\sum_{t=t_i}^{t_f} i_{obs,t}} \quad 5.3$$

$$r_{CVol} = \frac{\sum_{t=t_i}^{t_f} i_{sim,t}}{\sum_{t=t_i}^{t_f} i_{obs,t}} \quad 5.4$$

$$b_{aT} = \frac{\sum_{t=t_i}^{t_f} T_{sim,t}}{t_f - t_i} - \frac{\sum_{t=t_i}^{t_f} T_{obs,t}}{t_f - t_i} \quad 5.5$$

with  $R_{bvol}$ : relative volume bias between the forecast and the observation for the selected period [-];  $r_{CVol}$ : cumulated volume ratio between the forecast and the observation for the selected period [-];  $b_{aT}$ : temperature bias between the average temperature forecasted and observed for the selected period [°C].

### **Brier Score (BS)**

The BS allows the comparison of the forecast probability of an event and its occurrence (Brier, 1950; Buizza et al. 2005). The event is assumed to occur when a determinate fixed threshold is exceeded. The BS depends on three main factors: reliability, resolution and uncertainty and is defined by Eq. 5.6.

$$BS = \frac{1}{m} \cdot \sum_{k=1}^m (f_k - o_k)^2 \quad 5.6$$

with BS: Brier Score [-];  $f_k$ : occurrence probability of the event  $k$  according to the forecast [-];  $o_k$ : occurrence of the event  $k$ , one if the event occurs and zero otherwise [-];  $m$ : number of given forecasts [-].

For BS=0, the forecast is perfect. The worst forecast is given by BS=1.0.

### **Relative Operating Characteristic**

The ROC curve defines the ability of a probabilistic or categorical forecasting system to distinguish between situations predicting the occurrence and the non-occurrence of an event. (Mason and Graham, 1999; Marsigli et al., 2008). It is insensitive to bias and does not provide direct information on reliability. A biased forecast can still have good results and produce a good ROC curve, although it may still be improved through calibration.

For obtaining the ROC curve, a threshold is first selected. Each observation in the set is taken as “yes” or “no”  $\{Y, N\}$  set according to if it exceeds the threshold or not. The denominations  $\{y, n\}$  are used for the forecasts with the same methodology. Following this approach, four events are possible. If the observation as well as the forecast exceeds the threshold ( $Y$  and  $y$ ), a *Hit* is registered; if only the observation exceeds the threshold ( $Y$  and  $n$ ), a *Miss* is registered; if neither the observation nor the forecast exceed the threshold ( $N$  and  $n$ ), a *Correct*

*Rejection* is recorded; and finally, when only the forecast exceeds the threshold ( $N$  and  $y$ ), a *False Alarm* is considered.

A two by two matrix can be created by placing each forecast in the appropriate place (Table 5.3), an approach valid either for a deterministic forecast or for each member of a probabilistic forecast.

Table 5.3 Set matrix for the creation of the ROC index

		Observations (Event occurrence)	
		Yes ( $Y$ )	No ( $N$ )
Forecasts	yes ( $y$ )	<b><i>Hit</i></b>	<b><i>False Alarm</i></b>
	no ( $n$ )	<b><i>Miss</i></b>	<b><i>Correct Rejection</i></b>

After assembling the matrix, Hit Rate (HR, Eq. 5.7) and False Alarm Rate (FAR, Eq. 5.8) indices are calculated, also for a deterministic forecast and probabilistic forecast members alike. HR is the fraction of the events classified as true compared with all the forecasted positive events and FAR is the fraction of predicted false negatives compared with all the negative forecasts.

$$HR = \frac{Hit}{Hit + Miss} \tag{5.7}$$

$$FAR = \frac{False Alarm}{False Alarm + Correct rejection} \tag{5.8}$$

According to these two indicators, a graphic can be plotted for each chosen threshold. For the deterministic forecasts, the result is a point FAR-HR. For the probabilistic ones, a curve with the points corresponding to each member is drawn as shown in the example of Figure 5.1. Each of these points represents an average threshold of occurrence probability.

The ROC curve allows the quantification of the number of hits forecasted in comparison with the number of false alarms and defines a probability decision threshold for an event.



The likelihood ratio (HR/FAR) is an indicator of the performance of the forecast. If HR/FAR is higher than one, the performance is positive. If it is equal to one, the performance is null and if it is lower, the performance is negative.

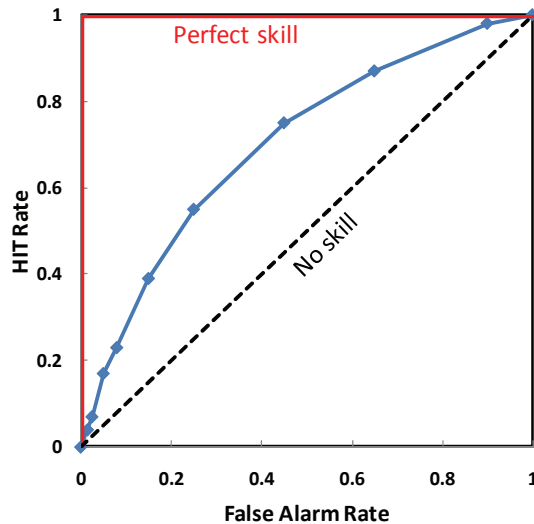


Figure 5.1 Example of a ROC curve showing the performance of a perfect forecast (solid black line), a forecast with skills (solid grey line with markers), and a forecast with no skills (dotted line).

The surface between the curve and the x-axis ( $A_{ROC}$ ) is often interpreted as the score of the ROC: the larger surface is, the better the performance of the forecast is. A forecast without any performance follows the diagonal ( $A_{ROC}=0.5$ , assuming the total area is equal to one). A perfect forecast follows the y-axis up to the point (1,0), then until (1,1), obtaining a maximum surface ( $A_{ROC}=1$ ).

### **Fuzzy logic**

Previous traditional methods often result in poor scores due to the difficulty of predicting with exactitude the observations at high resolutions. Grid point-based error measures are appropriate for the verification of fields dominated by synoptic-scale structures, but they are considered as problematic when evaluating forecasts for parameters like precipitation or temperature, which are typically characterized by complex structures on scales smaller than 100 km. The classical example to illustrate the limitations of gridpoint-based error measures is the “double penalty problem”: a prediction of a precipitation structure that is correct in terms of amplitude, size and timing but incorrect concerning its position is very poorly rated by categorical scores.

Novel approaches to QPF verification try to avoid the double penalty problem and aim to provide useful information about the characteristics and scales of the identified prediction

error (Wernli and Paulat, 2008). They can be categorized into fuzzy scores, techniques focusing on spatial scales and object-based approaches.

Applied to forecasts performance evaluation, fuzzy verification rewards closeness by relaxing the requirement for exact matches between forecasts and observations. The key to the fuzzy approach is the use of a spatial window or neighbourhood surrounding the forecast and/or observed points. Different fuzzy techniques have been proposed in the literature (Casati et al., 2004; Theis et al., 2005; Roberts and Lean, 2008; Ebert, 2008).

In a complex basin divided into sub-basins, however, the double penalty occurs even if novel evaluation approaches are used. Each precipitation forecasted for a sub-basin other than the target of the prediction may effectively reproduce the double penalty effect, even though they may be geographically close. That is why the fuzzy methodology is not either completely exact and categorical statistics are preferred still today.

### **5.2.2 Analysis of meteorological results**

#### ***Introduction to the meteorological analysis***

The analysis of results obtained from the ensemble meteorological forecasts (COSMO-LEPS) and comparison with the deterministic one (COSMO-7) is conducted in order to evaluate the performance of the predictions, their range of variability and other significant characteristics.

The proposed indexes allow the comparison over different time periods. Forecasts were divided in periods of 24 h (where “day 1” represents the 0-24 h period, “day 2” the 24-48 h period, etc) in order to examine the performance depending on the horizon time. Only the forecasts for days coinciding with the flood period were taken into account. In practice, this means that several forecasts were used, but not all of them for full three/five days periods, as several days fall out of the flood event.

Ensemble forecasts were characterized by representative hyetographs like those of the median ( $i_m$ ), the upper ( $i_u$ ) and lower quartile ( $i_l$ ) as well as by the minimum ( $i_{min}$ ) and maximum precipitation ( $i_{max}$ ) for an easier understanding of the forecast behaviour.

#### ***Results of deterministic indexes***

The relative volume bias indicator,  $R_{bVol}$ , reveals a high dispersion for both ensemble and deterministic forecasts (Table 5.4 left and Figure 5.2). Comparing the hyetograph  $i_m$  of COSMO-LEPS with COSMO-7, the results are similar. According to the cumulated volume

ratio  $r_{CVol}$  (Table 5.4 right and Figure 5.3), the hyetograph  $i_m$  of the ensemble forecast provides better results than COSMO-7 and less overestimation.

A first look Table 5.4 (left) seems to reveal that  $i_{min}$  and  $i_l$  provides the better results for the forecasts, knowing that zero represents the best performance for the relative volume bias indicator. However, as shown in the same table (right), best results are given for the hyetograph  $i_m$ , with values near to one, representing the best performance for the cumulated volume ratio. Good  $R_{bVol}$  for  $i_{min}$  and  $i_l$  are the result of simulations providing smaller values than observations. Errors are smaller than one in any case, promoting some skewness in the results. However, for simulated values higher than observations,  $R_{bVol}$  provides values higher than one (e.g., a nine times lower precipitation than the observation provides a  $R_{bVol}$  value around 0.1; a nine times higher, a value of 9).

Table 5.4 Precipitation performance for COSMO-7 (C-7) and for the ensemble forecasts COSMO-LEPS which is represented by the median  $i_m$ , the upper  $i_u$  and lower quartile  $i_l$  as well as by the minimum  $i_{min}$  and maximum precipitation  $i_{max}$ . Left: relative volume bias ( $R_{bVol}$ ). Right: cumulated volume ratio ( $R_{CVol}$ ).

$R_{bVol}$ [-]	COSMO-LEPS					C-7
	$i_{min}$	$i_l$	$i_m$	$i_u$	$i_{max}$	
<b>day 1</b>	0.35	0.68	1.01	1.99	5.57	1.52
<b>day 2</b>	0.40	1.18	2.85	6.88	18.83	3.34
<b>day 3</b>	0.29	0.50	2.93	8.37	19.59	2.40
<b>day 4</b>	0.33	0.38	0.82	7.01	22.72	
<b>day 5</b>	0.11	0.10	0.42	1.33	15.56	

$r_{CVol}$ [-]	COSMO-LEPS					C-7
	$i_{min}$	$i_l$	$i_m$	$i_u$	$i_{max}$	
<b>day 1</b>	0.34	0.74	0.99	1.37	2.37	1.14
<b>day 2</b>	0.34	0.86	1.31	2.01	3.23	1.61
<b>day 3</b>	0.21	0.81	1.30	2.03	3.40	1.38
<b>day 4</b>	0.08	0.42	0.98	2.06	4.01	
<b>day 5</b>	0.08	0.41	1.09	2.39	5.87	

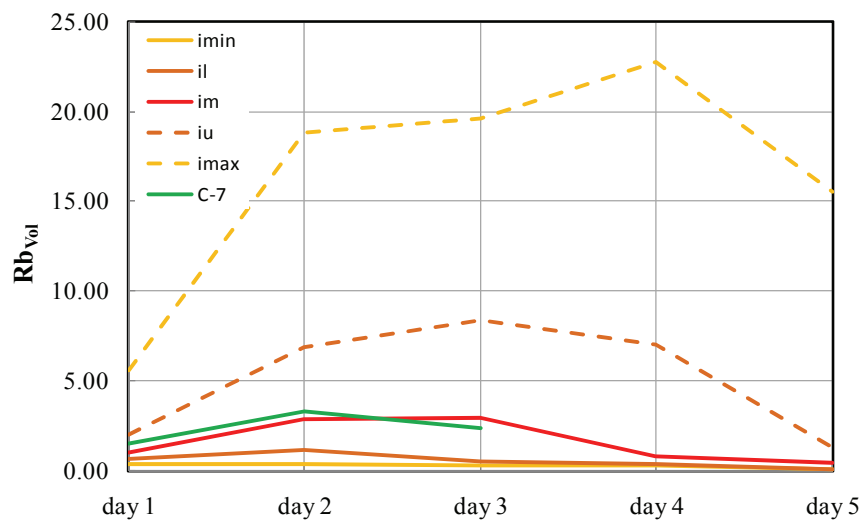


Figure 5.2 Relative volume bias ( $R_{bVol}$ ) depending on the day for COSMO-7 and for the representative hyetographs of COSMO-LEPS: the median  $i_m$ , the upper  $i_u$  and lower quartile  $i_l$  as well as by the minimum  $i_{min}$  and maximum precipitation  $i_{max}$ .

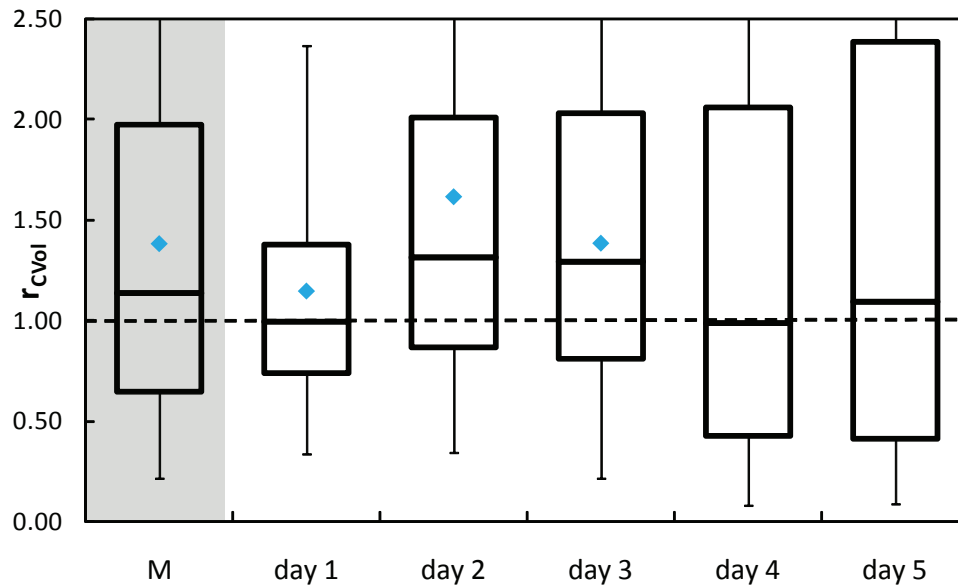


Figure 5.3 Cumulated volume ratio depending on the day as well as in average for COSMO-7 (diamond point) and for the representative hyetographs of COSMO-LEPS. M represents the average of the results.

Temperature is better predicted than precipitation volumes (results are shown in Table 5.5). An interesting outcome of the analysis is that any representative series of temperature of COSMO-LEPS provides generally better results than COSMO-7. Furthermore, the forecast does not seem to deteriorate noticeably depending on the horizon of the comparison.

Table 5.5 Average temperature bias ( $b_{aT}$ ) for COSMO-7 (C-7) and for the ensemble forecasts COSMO-LEPS which is represented by the median  $i_m$ , the upper  $i_u$  and lower quartile  $i_l$  as well as by the minimum  $i_{min}$  and maximum precipitation  $i_{max}$ .

$b_{aT}$ [°C]	COSMO-LEPS					C-7
	$i_{min}$	$i_l$	$i_m$	$i_u$	$i_{max}$	
<b>day 1</b>	1.52	1.49	1.35	1.46	1.52	1.84
<b>day 2</b>	1.63	1.58	1.46	1.43	1.50	1.69
<b>day 3</b>	1.66	1.72	1.52	1.63	1.74	1.31
<b>day 4</b>	1.91	1.76	1.89	1.77	1.82	
<b>day 5</b>	2.31	1.91	1.94	1.88	1.82	

### Results of probabilistic indexes

The results for the Brier Score indicator (BS) are shown in Figure 4. The values remain smaller than 0.5 for all studied forecasts and smaller than 0.2 for the probabilistic ones considering different thresholds (only 30 and 50 mm/day threshold are shown in Figure 5.4). Also, a higher quality is always displayed for the COSMO-LEPS forecasts.

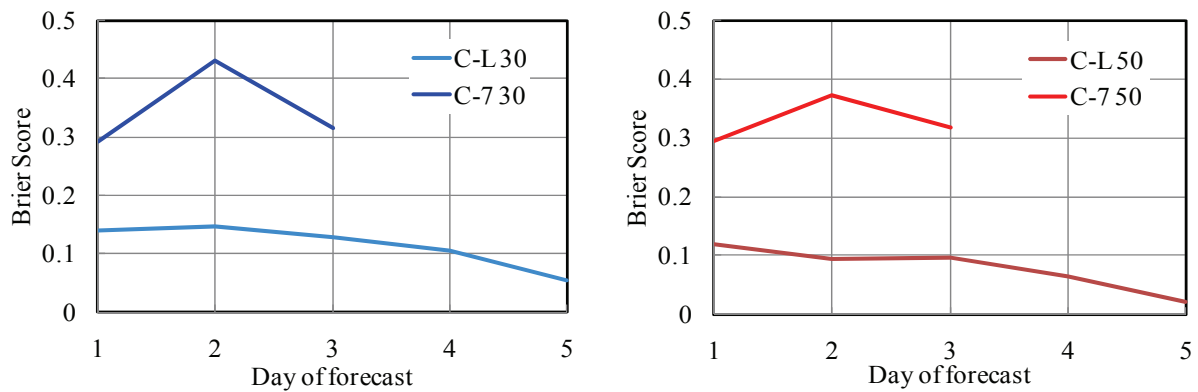


Figure 5.4 Brier Score performance depending on the day for COSMO-7 (C-7) and COSMO-LEPS (C-L). Left: 30 mm/day threshold (C-L 30 and C-7 30). Right: 50 mm/day threshold (C-L 50 and C-7 50).

The ROC analysis shows similar results, also considering thresholds of 30 and 50 mm/day (Figure 5.5). Observing the figures, it can be noted that the quality of forecasts does not decrease appreciably on the horizon time.

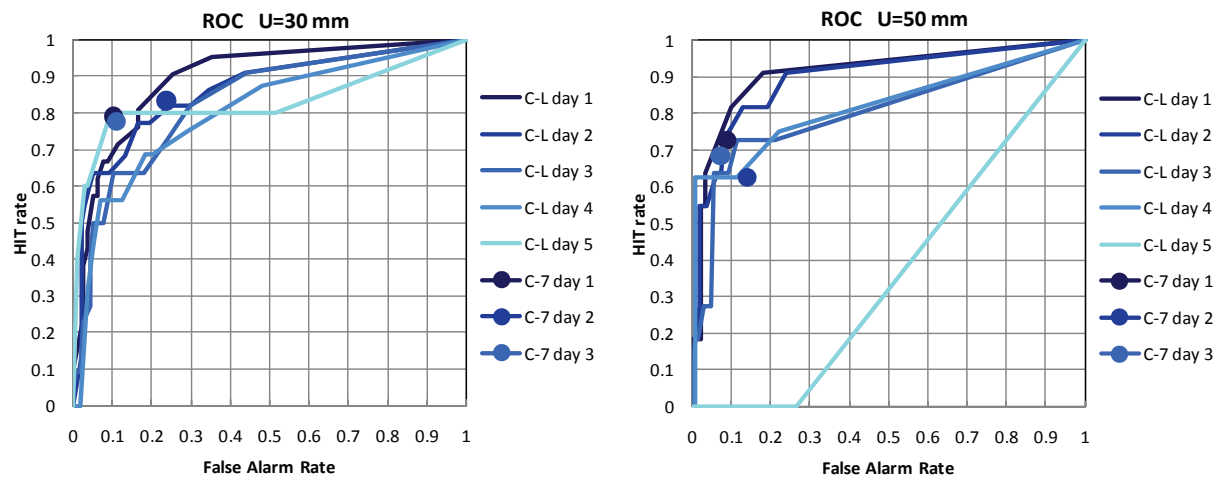


Figure 5.5 ROC curves for different days of COSMO-7 (C-7) and COSMO-LEPS (C-L). Left: 30 mm/day threshold. Right: 50 mm/day threshold

Table 5.6 shows the values for a 30 mm/day threshold, where better results are obtained by COSMO-LEPS (analogous results are given for the threshold  $i=50$  mm/day).

Table 5.6 Probabilistic indexes BS (Brier Score) and ROC (Relative Operating Characteristic) for COSMO-LEPS (C-L) and COSMO-7 (C-7) for the threshold  $i=30$  mm/day.

Flood	1993		2000		2008		All events	
	<u>C-7</u>	<u>C-L</u>	<u>C-7</u>	<u>C-L</u>	<u>C-7</u>	<u>C-L</u>	<u>C-7</u>	<u>C-L</u>
<b>BS</b>	0.34	0.11	0.33	0.14	0.38	0.09	0.35	0.12
<b>ROC</b>	0.74	0.69	0.80	0.92	0.76	0.81	0.77	0.81

Other studied indicators as  $b_i$  and  $b_T$  are not discussed in-depth due to their non representative results. They provide poor comparisons because the models do not achieve good performances considering an hourly time step. Furthermore, they provide a large range of values and basing the analysis in average results may not yield significant conclusions.

### 5.3 Hydrological simulations with Routing System MINERVE

In the following, the Routing System MINERVE program is used for the hydrological numerical computation (García Hernández et al., 2007a). Simulations with the COSMO meteorological forecasts can be performed by importing the meteorological database and running the hydrological model of the Upper Rhone River catchment. Once the parameters are chosen (initial and final time for the simulation and time step computation), the simulation can be launched.

#### 5.3.1 Hydrological indicators

As for meteorological forecasts, the hydrological forecasts are divided in daily periods and, in the case of COSMO-LEPS, characterized by their representative hydrographs  $q_{min}$ ,  $q_l$ ,  $q_m$ ,  $q_u$  and  $q_{max}$ . The performance is evaluated depending on time and on the representative hydrographs for the ensemble forecast, with several deterministic and probabilistic indexes presented hereafter.

#### *Relative Volume bias ( $Rb_{Vol}$ )*

The relative volume bias corresponds in this case to the relative error between the simulated and the observed volumes during the studied period (Ajami and al, 2004; Schaefli and al, 2005) according to Eq. 5.9:

$$Rb_{Vol} = \frac{\sum_{t=t_i}^{t_f} (Q_{sim,t} - Q_{obs,t})}{\sum_{t=t_i}^{t_f} (Q_{obs,t})} \quad 5.9$$

with  $Rb_{Vol}$ : relative volume bias between forecast and observation for the considered period [-];  $Q_{sim,t}$ : simulated discharge at time  $t$  [ $m^3/s$ ];  $Q_{obs,t}$ : observed discharge at time  $t$  [ $m^3/s$ ].

The  $Rb_{Vol}$  varies from -1 to  $+\infty$ . An index near to zero indicates a good performance of the simulation.

**Root Mean Square Error (RMSE) and Relative RMSE (RRMSE)**

The RMSE measures the differences between simulated and observed values of discharge, giving a major importance to the differences between high values (Ajami and al, 2004; Georgakakos and, 2004; Habets and al, 2004; Sun and al, 2000). It is defined as follows (Eq. 5.10):

$$RMSE = \sqrt{\frac{\sum_{t=t_i}^{t_f} (Q_{sim,t} - Q_{obs,t})^2}{n}} \quad 5.10$$

with RMSE: square root of the mean square error [ $m^3/s$ ];  $n$  : total number of observations [-].

Because it is difficult to compare the errors of a model when a wide range of observed discharges are produced, the relative RMSE is also used. It is defined as the RMSE normalized to the mean of the observed values (Feyen et al., 2000; El-Nasr et al., 2005; Heppner et al., 2006) and is presented in Eq. 5.11.

$$RRMSE = \frac{\sqrt{\frac{\sum_{t=t_i}^{t_f} (Q_{sim,t} - Q_{obs,t})^2}{n}}}{\bar{Q}_{obs}} \quad 5.11$$

with RRMSE: relative RMSE [-];  $\bar{Q}_{obs}$ : average observed discharge for the considered period [ $m^3/s$ ].

It varies from 0 to  $+\infty$ . The smaller RRMSE, the better the model performance is.

**Cumulated volume ratio ( $r_{CVol}$ )**

This ratio reflects the tendency of the forecast for over or sub-estimations of the run-off discharge and is defined as (Eq. 5.12):

$$r_{CVol} = \frac{\sum_{i=t_i}^{t_f} (Q_{sim,t})}{\sum_{i=t_i}^{t_f} (Q_{obs,t})} \quad 5.12$$

with  $r_{CVol}$ : cumulated volume ratio between the forecast and the observation for the studied period [-].

It varies from 0 to  $+\infty$ . An index near to one represents the best performance of the simulated values, less than one a sub-estimation and more than one indicates an over-estimation.

### **Index of agreement (IA)**

The index of agreement represents the ratio of the mean square error and the potential error (Willmott, 1981; Krause et al., 2005; Harmel et al., 2007) as presented in Eq. 5.13:

$$IA = 1 - \frac{\sum_{t=t_i}^{t_f} (Q_{sim,t} - Q_{obs,t})^2}{\sum_{t=t_i}^{t_f} (|Q_{sim,t} - \bar{Q}_{obs}| + |Q_{obs,t} - \bar{Q}_{obs}|)^2} \quad 5.13$$

with IA: Index of agreement [-].

The IA varies from zero to one, one being the optimal performance.

### **Index of resemblance (IR)**

Sometimes, it is difficult to assess the performance of different evaluations when one or only a few points present a high dispersion compared to the rest. For such cases, the RMSE as well as the relative RMSE, provide little insight. As such, a complementary and dimensionless index for flood assessment is proposed (Eq. 5.14):

$$IR = \frac{1}{1 + \sqrt{\frac{\sum_{t=t_i}^{t_f} (Q_{sim,t} - Q_{obs,t})^2}{\sum_{t=t_i}^{t_f} (Q_{obs,t})^2}}} \quad 5.14$$

with IR: Index of resemblance [-].

The IR varies from zero to one, where one represents the optimal performance.

### **Normalised peak error (NPE)**

The NPE measures the relative error between the simulated and the observed flow peaks (Masmoudi and Habaieb, 1993; Sun and al, 2000; Ajami and al, 2004; Gabellani and al, 2007). It is computed according to Eqs. 5.15 to 5.17.



$$NPE = \frac{S_{\max} - O_{\max}}{O_{\max}} \quad 5.15$$

$$S_{\max} = \bigvee_{t=t_i}^{t_f} Q_{sim,t} \quad 5.16$$

$$O_{\max} = \bigvee_{t=t_i}^{t_f} Q_{obs,t} \quad 5.17$$

with NPE: relative error between simulated and observed peak discharge [-];  $S_{\max}$  : maximum simulated discharge for the studied period [ $m^3/s$ ];  $O_{\max}$  : maximum observed discharge for the studied period [ $m^3/s$ ].

The NPE varies from -1 to  $+\infty$ . Negative values are returned when simulated peak discharge is below the observed one, while positive values mean the opposite. Values near to zero indicate a good performance of simulated peaks regarding observed ones.

#### **Peak timing error (PTE)**

The PTE defines the time difference between the simulated and the observed peak flows (Masmoudi and Habaieb, 1993; Sun and al, 2000; Li and Zhang, 2008) according to Eq. 5.18.

$$PTE = t_{S_{\max}} - t_{O_{\max}} \quad 5.18$$

with PTE: time-lag between observed and simulated peak discharge [h];  $t_{S_{\max}}$ : date with maximum simulated discharge during the studied period [date];  $t_{O_{\max}}$ : date with maximum observed discharge during the studied period [date].

The indicator takes any value from  $-\infty$  to  $+\infty$  but normal differences are given in hours.

#### **Nash-Sutcliffe model efficiency coefficient**

The Nash-Sutcliffe measure is used to assess the predictive power of hydrological models (Ajami et al., 2004; Schaefli and al, 2005; Jordan, 2007). It is defined as presented in Eq. 5.19.

$$Nash = 1 - \frac{\sum_{t=t_i}^{t_f} (Q_{sim,t} - Q_{obs,t})^2}{\sum_{i=1}^n (Q_{obs,t} - \bar{Q}_{obs})^2} \quad 5.19$$

with Nash: Nash-Sutcliffe model efficiency coefficient [-].

It varies from  $-\infty$  to 1, with one representing the best performance of the model and zero the same performance than assuming the average of all the observations at each time step.

**Brier Score (BS) and Brier Skill Score (BSS)**

The BS is also used in meteorology as presented in Eq. 5.6. The BSS (Eq. 5.20) is conventionally defined as the relative probability score compared with the probability score of a reference forecast (Georgakakos and al, 2004; Roulin, 2007; Jaun et al., 2008), typically given by the climatology.

$$BSS = \frac{BS - BS_{ref}}{-BS_{ref}} \quad 5.20$$

with BSS: Brier Skill Score [-];  $BS_{ref}$ : Reference Brier Score [-].

Skill scores of the BSS take a range of  $-\infty$  to 1. Negative values indicate that the forecast is less accurate than the reference forecast. Values higher than zero reflect forecasting skills.

**Relative Operating Characteristic (ROC)**

The ROC curve, introduced for meteorology (see section 5.2.1), is also used in hydrology (Krzysztofowicz et al., 1994; Georgakakos and al, 2004; Norbiato et al., 2008; He et al., 2009).

Besides the *ROC*, the Correct-Alarm Ratio (*CAR*) and the Miss Ratio, (*MR*), defined by Eqs. 5.21 and 5.22 (Mason and Graham, 1999), are used. The *CAR* represents the correct number of alarms compared with all the alarms given and the *MR* represents the number of Missed events compared with all the non-predicted events

$$CAR = \frac{HIT}{HIT + False\ alarm} \quad 5.21$$

$$MR = \frac{Miss}{Miss + Correct\ rejection} \quad 5.22$$

with *CAR*: Correct-Alarm Ratio [-]; *MR*: Miss Ratio [-].

The range of the *CAR* goes from zero to one, being one the perfect forecast. The *MR* has the same range as the *CAR*, but a perfect forecast is given by a value of zero.

**Relative Economic Value (REV)**

The benefit of a hydrological forecast depends on its performance, as well as on the consequences of the discharge magnitude on the basin (damages and preventive operations). The Relative Economic Value (REV) takes into account these distinct components to accomplish the forecast evaluation (Wilks, 1995; Richardson and al, 2000; Wilks, 2001; Zhu and al, 2002; Roulin, 2007).

In a similar way to the ROC and for a given flood event, four possibilities can occur in the REV reasoning (Table 5.7). If the flood event takes place and a (preventive or mitigating) action of cost  $C$  was taken, total losses will be equal to the cost  $C$  of the action plus the unavoidable cost,  $L_u$ . If no preventive action was taken, the losses will be comprised of the unavoidable cost  $L_u$  and the avoidable cost  $L_a$ . Other total losses, equalling  $C$  could occur when an action is taken and no flood arrives. The last combination, naturally, has no costs and takes place when neither an action nor a flood event occurs.

Table 5.7 Set matrix for the Relative Economic Value (REV)

		<b>Observations</b> (Event occurrence)	
		Yes	No
<b>Forecasts (Action)</b>	yes	<b>Hit (h)</b> <i>Reduced loss</i> ( $C + L_u$ )	<b>False alarm (f)</b> <i>Cost</i> ( $C$ )
	no	<b>Miss (m)</b> <i>Loss</i> ( $L_a + L_u$ )	<b>Correct rejection (c)</b> <i>Neither loss nor cost</i> (0)

For an optimal strategy, a comparison with the climatology is performed. The data required is the frequency of occurrence of the event and the decision to be taken would be to carry out the preventive or mitigating action always or never, depending on its total cost, regarding Eq. 5.23. If a perfect forecast would be taken into account, the total cost would be as presented in the Eq. 5.24. Finally, the cost of the studied forecast depends on his performance as presented in the Eq. 5.25.

$$E_{\text{clim}} = \min\{\bar{o} \cdot (L_p + L_u); C^* + \bar{o} \cdot L_u\} \quad 5.23$$

$$E_{\text{perfect}} = \bar{o} \cdot (C^* + L_u) \quad 5.24$$

$$E_{\text{forecast}} = h \cdot (C^* + L_u) + f \cdot C^* + m \cdot (L_p + L_u) \quad 5.25$$

with  $E_{\text{clim}}$ : costs obtained from the climatology;  $E_{\text{perfect}}$ : costs obtained from the perfect forecast;  $E_{\text{forecast}}$ : costs obtained from the studied forecast;  $h+f+m+c=1$  ( $h$ ,  $f$ ,  $m$  and  $c$  are explained in Table 5.7).

The Relative Economic Value compares the expenses reduction achievable with a given forecasts tool with the reduction which would be accomplish by a perfect forecast through the ratio of Eq. 5.26. If a cost-loss ratio  $\psi$  (with  $\psi=C/L_u$ ) is included in this equation, it results into Eq. 5.27.

$$V = \frac{E_{\text{clim}} - E_{\text{forecast}}}{E_{\text{clim}} - E_{\text{perfect}}} \quad 5.26$$

$$V = \frac{\min(\bar{o}; \psi) - (h + f) \cdot \psi - m}{\min(\bar{o}; \psi) - \bar{o} \cdot \psi} \quad 5.27$$

with  $V$ : Relative economic value [-];  $\bar{o}$ : occurrence probability of the event [-].

The range of this index goes from  $-\infty$  to 1, one representing a perfect forecast, zero a forecast having the same performance as the climatology and negative values a bad forecast which does not provide any information.

### 5.3.2 Hydrological results

#### Visual flood analysis

In spite of all the proposed indexes, a first visual analysis of the three studied floods remains useful. The September 1993 flood was in general underestimated and predicted too early by COSMO-LEPS. The maximum discharge was predicted by hydrograph  $q_{\text{max}}$  up to two days before the observed peak flow occurred (Figure 5.6). One day later, the forecast improved, predicting the peak discharge at the correct moment for the forecasts between  $q_u$  and  $q_{\text{max}}$  (Figure 5.7). In the case of COSMO-7, forecasts were at first also biased, predicting the flood

peak too soon. Later, at the last two days, they forecasted quite well the event, both for discharge and for peak time (Figure 5.7).

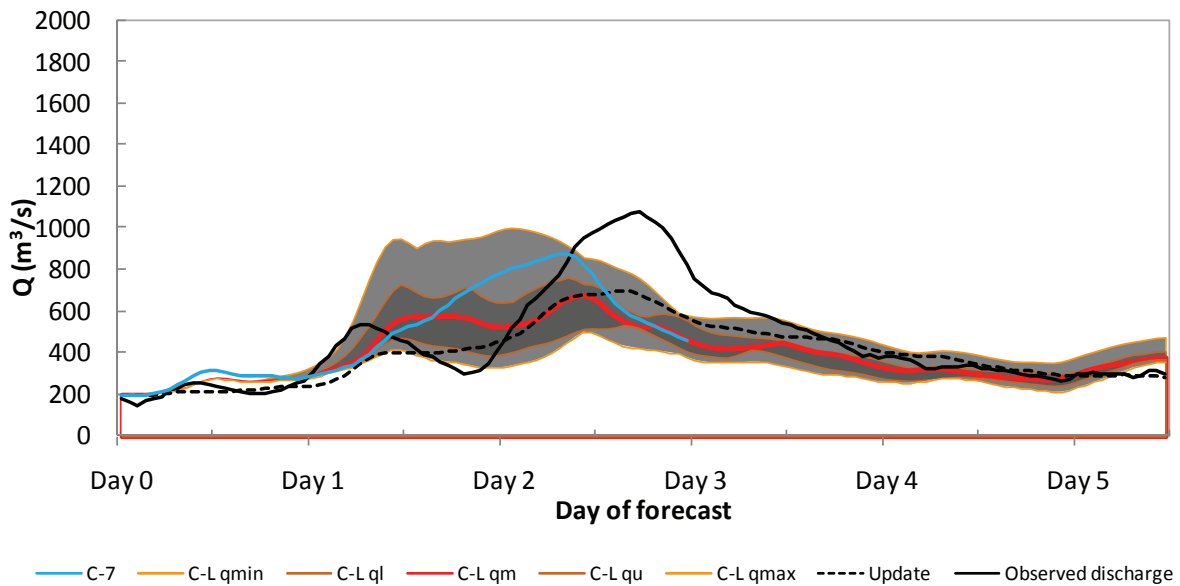


Figure 5.6 Hydrological forecasts starting the 22.09.1993 12h00 C-7 represents the simulation with COSMO-7 forecast and C-L the simulation with COSMO-LEPS, represented by the median  $q_m$ , the upper  $q_u$  and lower quartile  $q_l$  as well as by the minimum  $q_{min}$  and maximum discharge  $q_{max}$ . Update symbolises the simulations with meteorological observations and the update of the initial conditions of the hydrological model.

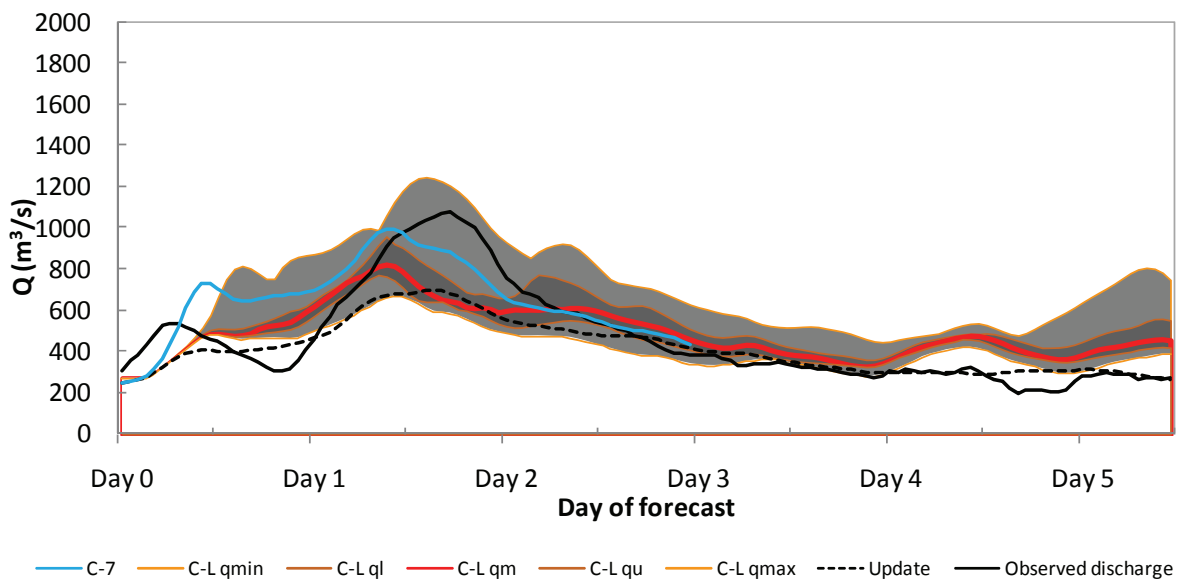


Figure 5.7 Hydrological forecasts starting the 23.09.1993 12h00.

The October 2000 flood is predicted rather well by COSMO-LEPS three days before the peak flow occurred, although with a large variability on the discharge (Figure 5.8) depending on the representative hydrograph and with the best results for the upper quartile hydrograph  $q_u$ . COSMO-7 was more unstable in this case, predicting the peak in advance for first forecasts, three days before the peak flow. Then, COSMO-7 delays the peak during the next forecasts, two days before the peak flow (Figure 5.9).

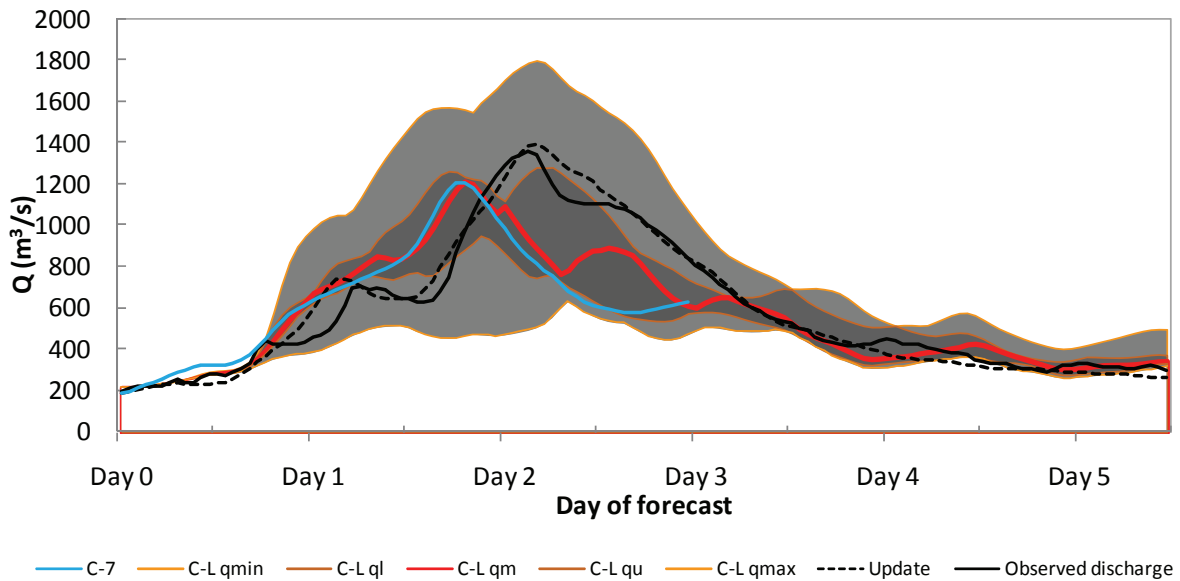


Figure 5.8 Hydrological forecasts starting the 13.10.2000 12h00. C-7 represents the simulation with COSMO-7 forecast and C-L the simulation with COSMO-LEPS, represented by the median  $q_m$ , the upper  $q_u$  and lower quartile  $q_l$  as well as by the minimum  $q_{min}$  and maximum discharge  $q_{max}$ . Update symbolises the simulations with meteorological observations and the update of the initial conditions of the hydrological model.

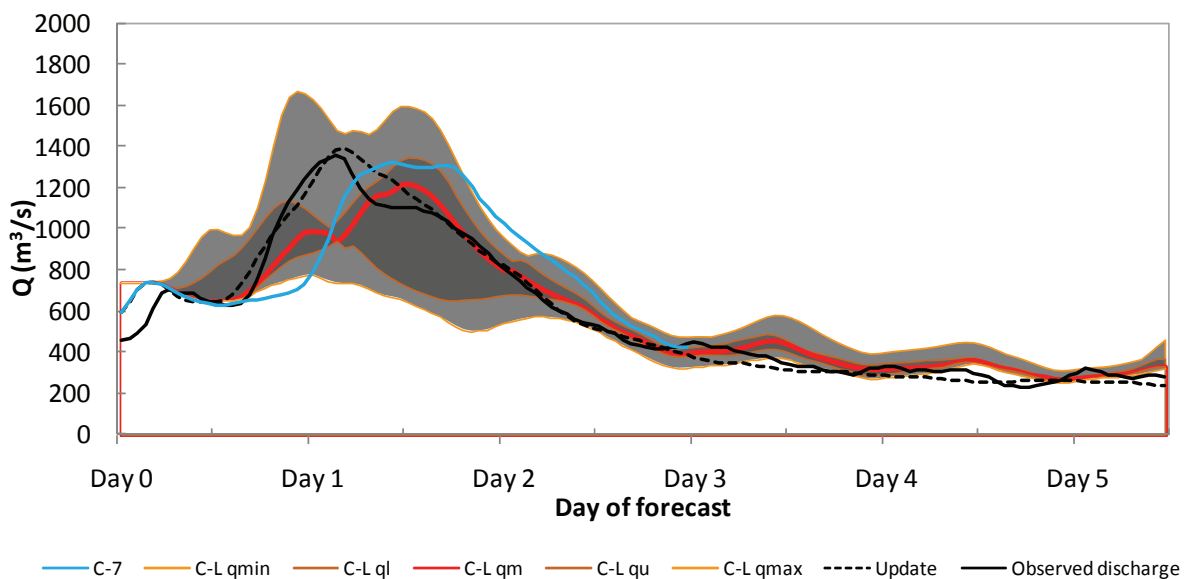


Figure 5.9 Hydrological forecasts starting the 14.10.2000 12h00.

The May 2008 flood is overpredicted by COSMO-LEPS regarding hydrographs  $q_u$  and  $q_{max}$  (Figure 5.10). Better results are obtained this time by hydrographs  $q_l$  and  $q_m$ . COSMO-7 also overestimated the peak flow three and two days before its arrival. The results improved only one day before the peak time. Three and two days before the peak flow, COSMO wrongly forecasted a high discharge, whereas only a medium increase took place (Figure 5.11).

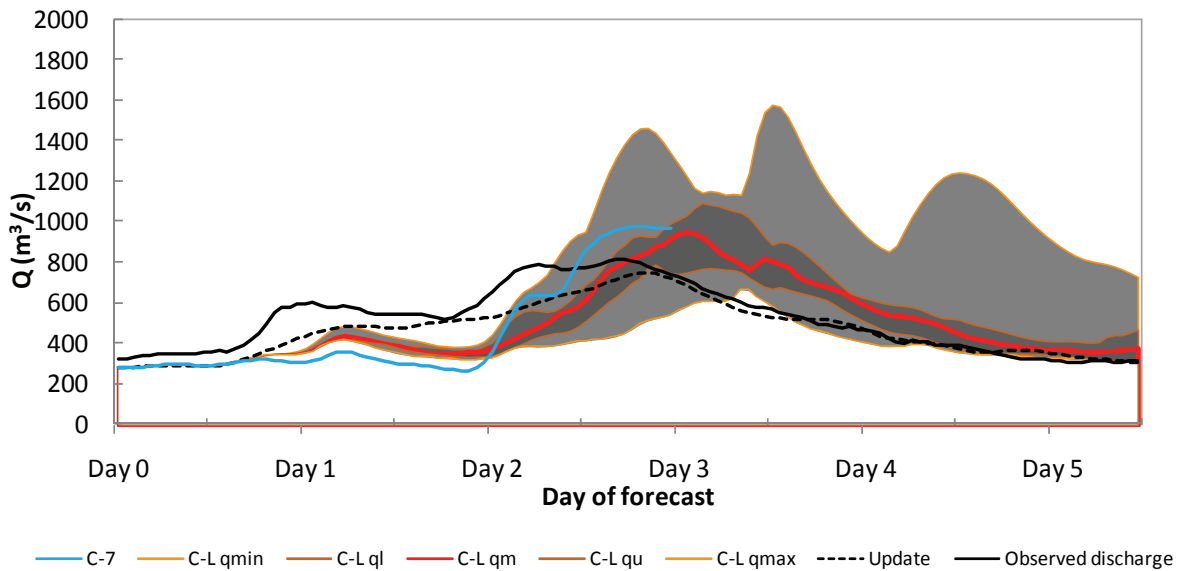


Figure 5.10 Hydrological forecasts starting the 27.05.2008 12h00. C-7 represents the simulation with COSMO-7 forecast and C-L the simulation with COSMO-LEPS, represented by the median  $q_m$ , the upper  $q_u$  and lower quartile  $q_l$  as well as by the minimum  $q_{min}$  and maximum discharge  $q_{max}$ . Update symbolises the simulations with meteorological observations and the update of the initial conditions of the hydrological model.

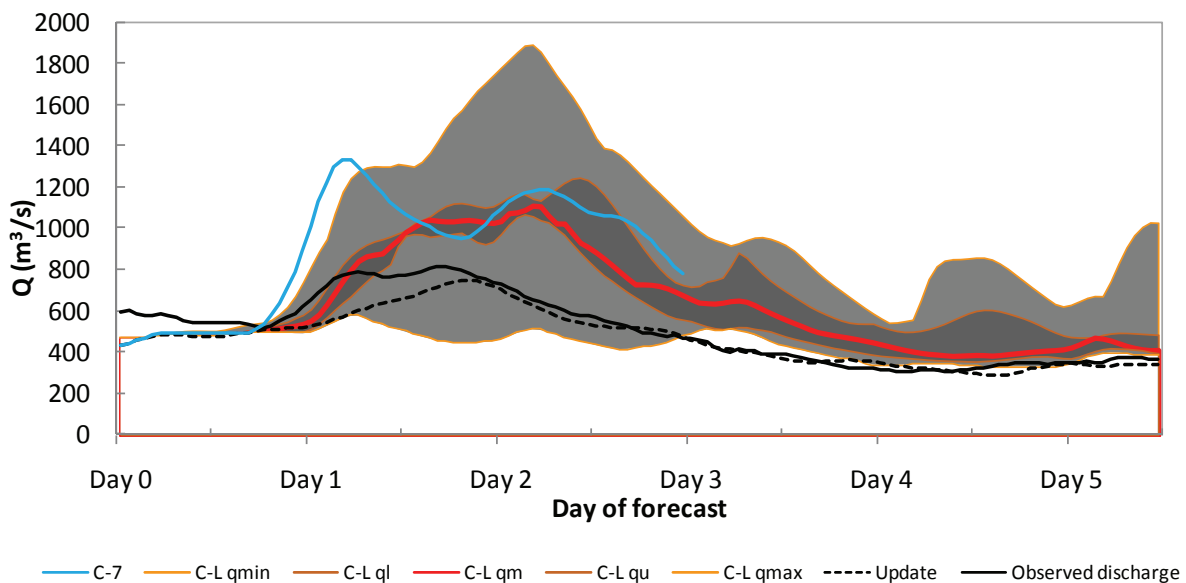


Figure 5.11 Hydrological forecasts starting the 28.05.2008 12h00.

**Results of deterministic indexes**

Even though graphs show various complete forecasts, the series used for computing the hydrological indexes, as was the case in the meteorological analysis, are those falling into the period of different events (Table 5.1).

The relative volume bias and the RMSE results reveal some degree of degradation in COSMO-LEPS discharge forecasts with time horizon, especially for  $q_{max}$ . Other hydrographs,  $q_{min}$ ,  $q_l$ ,  $q_m$  and  $q_u$ , provide similar skills for first three days of the forecast (Figure 5.12 and Figure 5.13). COSMO-7 appears to be degraded in the same way as  $q_{max}$ . This means that it is preferable to use any representative hydrograph of the ensemble (except  $q_{max}$ ) instead of COSMO-7.

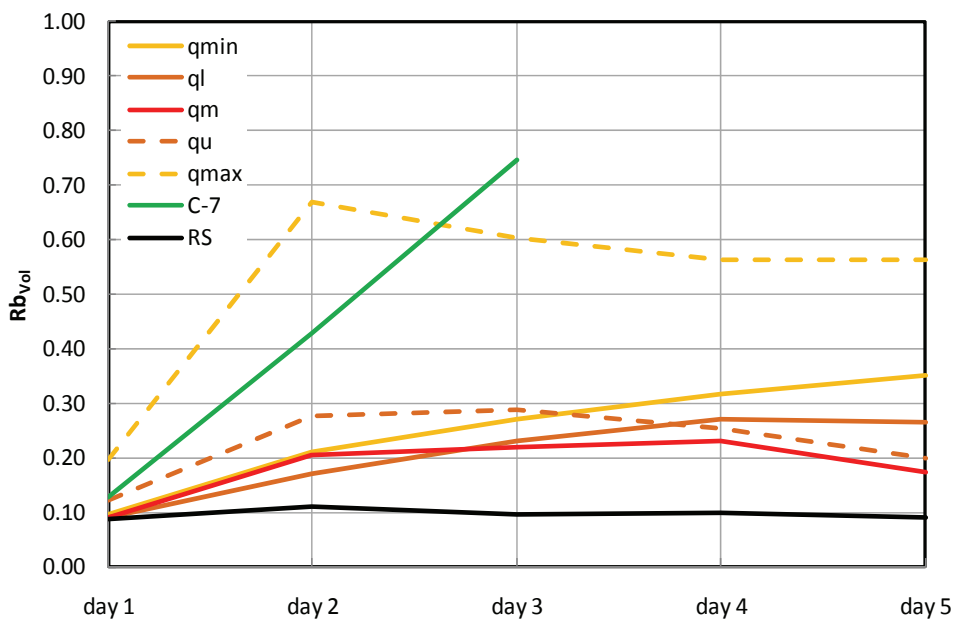


Figure 5.12 Results at Porte-du-Scex for the studied events depending on the day for Relative volume bias ( $R_{bVol}$ ) for COSMO-7 (C-7) and for the ensemble forecasts COSMO-LEPS which is represented by the median  $q_m$ , the upper  $q_u$  and lower quartile  $q_l$  as well as by the minimum  $q_{min}$  and maximum volume  $q_{max}$ . RS represents the results of the simulation with a perfect forecast (meteorological observations)



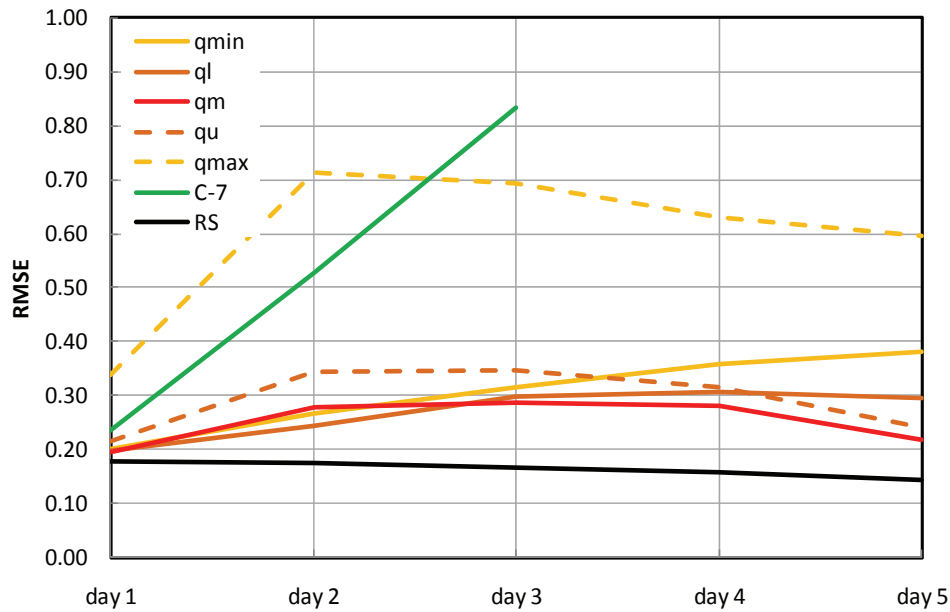


Figure 5.13 Results at Porte-du-Scex for the studied events depending on the day for Root Mean Square Error (RMSE) for COSMO-7 (C-7) and for the ensemble forecasts COSMO-LEPS which is represented by the median  $q_m$ , the upper  $q_u$  and lower quartile  $q_l$  as well as by the minimum  $q_{min}$  and maximum volume  $q_{max}$ . RS represents the results of the simulation with a perfect forecast (meteorological observations).

In Figure 5.14, the cumulated volume ratio is shown for a simulation with a perfect forecast (hydrological simulation with observed meteorological data), with COSMO-LEPS and with COSMO-7. The results are given for different thresholds  $T_1$ ,  $T_2$  and  $T_3$  (700, 1000 and 1200  $m^3/s$  respectively) as well as for different days of the forecast. The average  $\bar{a}$  of the global results is also shown for comparison.

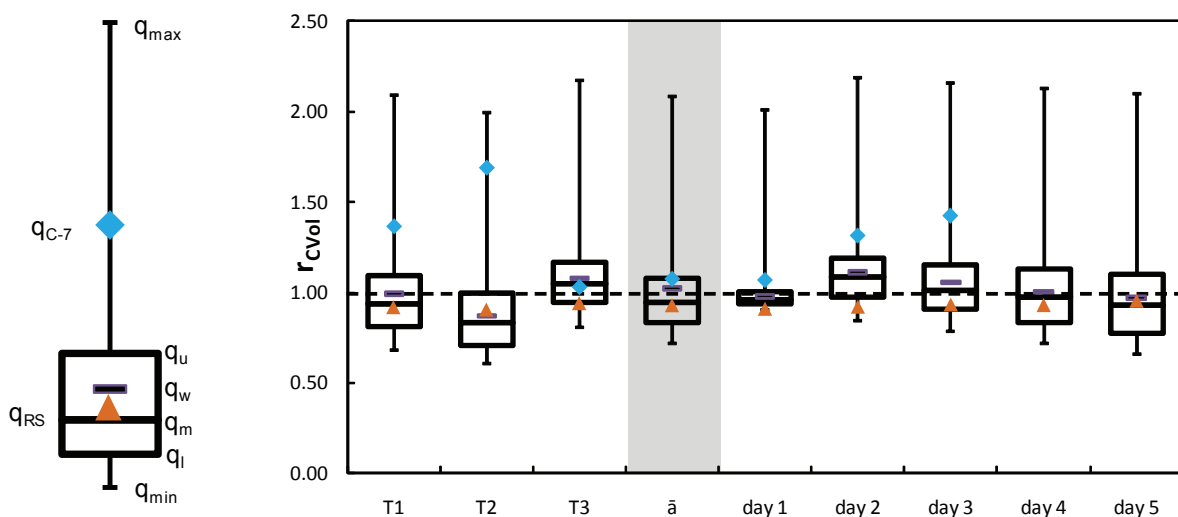


Figure 5.14 Cumulated volume ratio ( $r_{CVol}$ ) for COSMO-7 ( $q_{C-7}$ ) and COSMO-LEPS depending on different days or thresholds and in average ( $\bar{a}$ ), Porte-du-Scex. COSMO-LEPS is represented by the weighted value  $q_w$ , the median  $q_m$ , the upper  $q_u$  and lower quartile  $q_l$  as well as by the minimum  $q_{min}$  and maximum volume  $q_{max}$ .  $q_{RS}$  represents the results of the simulation with a perfect forecast (meteorological observations).

The hydrological simulation with meteorological observations ( $q_{RS}$ ) gives generally good results with a volume ratio near to one in all cases.

COSMO-LEPS (assumed as the hydrological simulations done with COSMO-LEPS meteorological forecasts) does not lead to a bias for the median  $q_m$  (in average for all the studied forecasts). The average hydrograph seems not to depend substantially on the forecasts horizon either. Nonetheless, the range between quartiles  $q_l$  and  $q_u$  increases with the time horizon. It should be also emphasized that the weighted average hydrograph  $q_w$  always displays more volume than the median  $q_m$ , which happens because several members of the ensemble provide (in general) high values of discharge, as is the case for the hydrograph  $q_{max}$  with values twice higher than the observed one in all cases. Regarding the three thresholds results, the hydrograph  $q_m$  of the ensemble provides values smaller than one for the first two thresholds,  $T_1$  and  $T_2$ , and slightly over one for the third,  $T_3$ . The hydrograph  $q_l$  always led to results smaller than one. For the hydrograph  $q_u$ , on the contrary, results higher than one are obtained.

In general, COSMO-7 provided substantially overestimated values for the first two thresholds (400 and 800 m<sup>3</sup>/s). The quality of the forecast visibly degrades with the horizon time. In addition, the most values given by COSMO-7 are higher than even the hydrograph  $q_u$  of COSMO-LEPS.

Comparing Figure 5.14 with the analogue Figure 5.3 (Cumulated volume ratio for the rainfall), similar values are shown, even though differences are smaller in the hydrological forecasts, due to the inertia of the basin and the effect of the hydropower plants.

The Index of Agreement and the Index of Resemblance are shown in Figure 5.15 and Figure 5.16, where the value of one represents the best performance and zero the worst. The conclusions are similar as the conclusions obtained for the relative volume bias and the RMSE. Since the inertia of the system is important due to initial conditions of the hydrological model, results for the first day are similar in all cases.

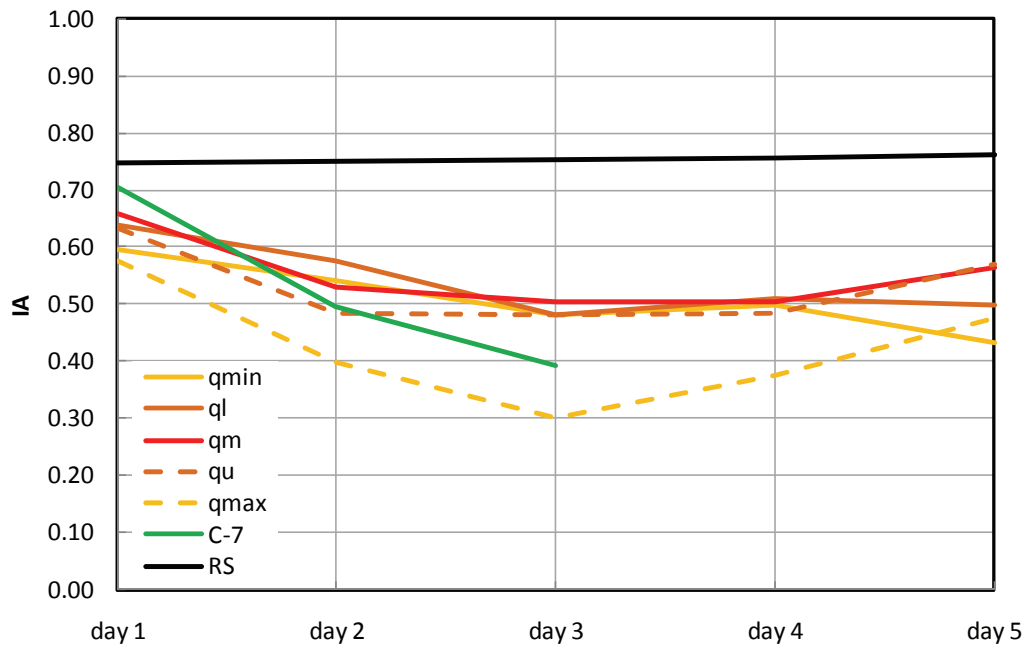


Figure 5.15 Results at Porte-du-Scex for the studied events for the Index of agreement (IA) for COSMO-7 (C-7) and for COSMO-LEPS which is represented by the median  $q_m$ , the upper  $q_u$  and lower quartile  $q_l$  as well as by the minimum  $q_{min}$  and maximum volume  $q_{max}$ . RS represents the results of the simulation with a perfect forecast (meteorological observations).

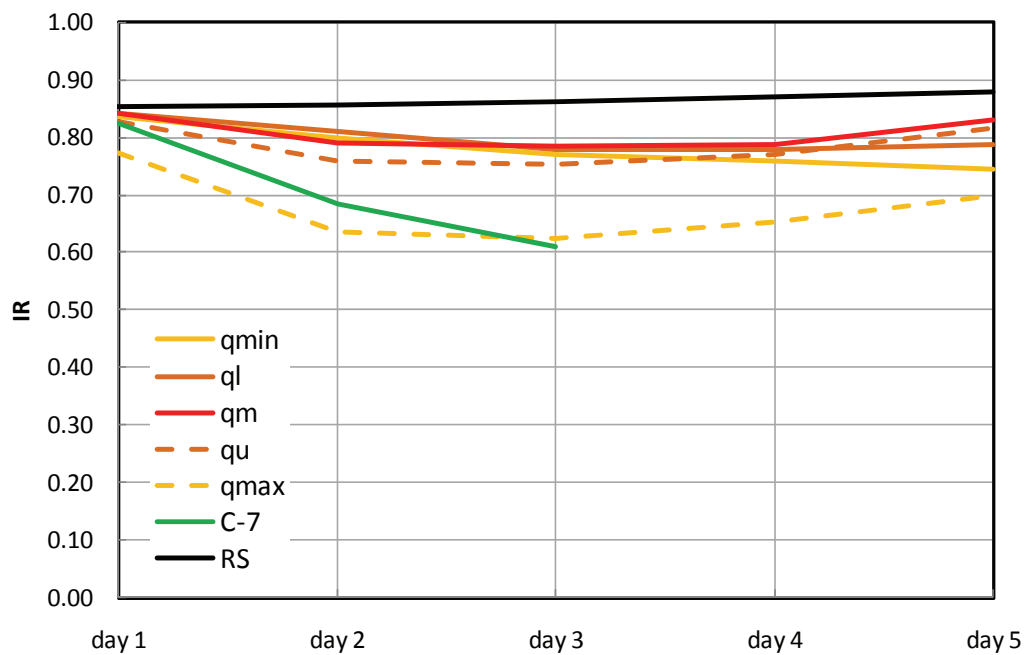


Figure 5.16 Results at Porte du Scex for the studied events for the Index of resemblance (IR) for COSMO-7 (C-7) and for COSMO-LEPS which is represented by the median  $q_m$ , the upper  $q_u$  and lower quartile  $q_l$  as well as by the minimum  $q_{min}$  and maximum volume  $q_{max}$ . RS represents the results of the simulation with a perfect forecast (meteorological observations).

The *Normalized Peak Error* for all forecasts versus the *Peak Time Error* is represented in Figure 5.17. The hydrograph  $q_m$  of COSMO-LEPS provides forecasts with a peak time error between -7 and +12 h and a Normalized Peak Error between 49% lower and 37% higher than the observed peak. COSMO-7 provides forecasts with a peak time error between -18 and +12 h and a normalized peak error between 32% under and 63% over the observed peak. The variability range is, in both cases, higher for the COSMO-7 forecasts.

The hydrographs  $q_l$  and  $q_u$  of the ensemble forecast increase the range of the PTE to -8 and +18 h, as well as the NPE from 57% under to 53% over the observed peak. This performance is still similar that the one obtained by COSMO-7.

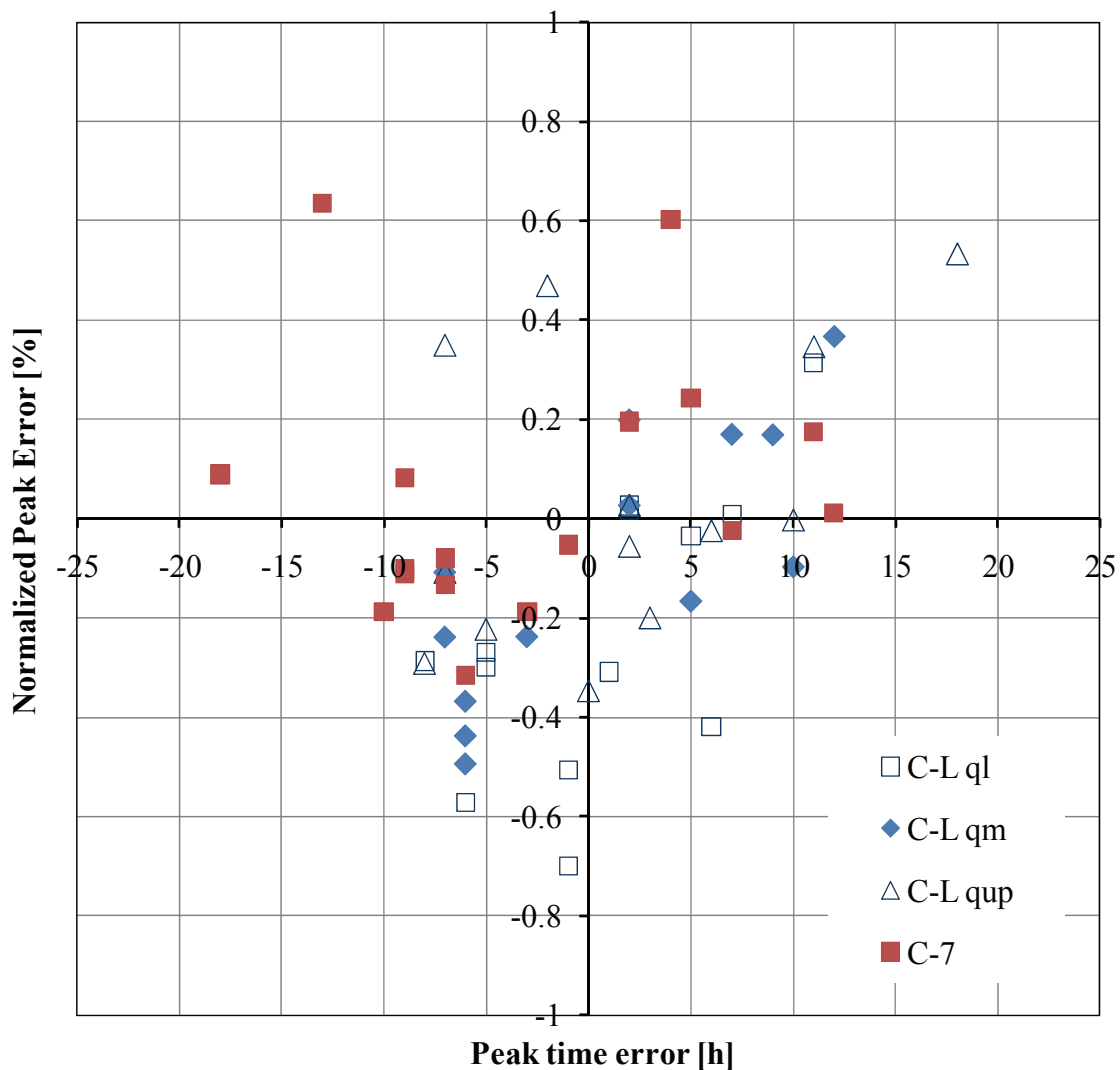


Figure 5.17 Normalized Peak Error as a function of Peak Time Error for all the forecasts

It has to be mentioned that the hydrograph  $q_m$  of COSMO-LEPS does not provide forecasts which overestimates the peak flow in advance (upper-left quadrant in Figure 5.17). Furthermore, COSMO-7 does not provide forecasts which underestimates and delays peak

flows (lower-right quadrant). Therefore, for preventive operations, the first option obtained from COSMO-LEPS is preferable because COSMO-7 seems to lead to excessive preventive reservoir emptying in hydropower plants and, consequently, to increased energy losses.

Finally, the representative hydrographs of the ensemble forecasts are also compared with COSMO-7 in Table 5.8. Only the hydrograph  $q_{max}$  has systematically displayed worse results than COSMO-7, which, again, means that even  $q_l$  and  $q_u$  performed better than COSMO-7.

Table 5.8 Deterministic indexes results of the three events as well as the average for the representative hydrograph  $q_m$  of COSMO-LEPS (C-L) and for COSMO-7 (C-7). NPE represents the Normalized Peak Error, PTE the Peak Time Error,  $r_{CVol}$  the Cumulated volume ratio,  $R_{bVol}$  the relative volume bias, RMSE the Root Mean Square Error, Nash the Nash Index, IA the Index of Agreement and IR the index of Resemblance.

Flood	1993		2000		2008		Average	
	C-7	C-L ( $q_m$ )	C-7	C-L ( $q_m$ )	C-7	C-L ( $q_m$ )	C-7	C-L ( $q_m$ )
<b>NPE</b>	0.11	0.32	0.12	0.18	0.32	0.22	0.19	0.24
<b>PTE</b>	6.8	5.50	9.83	6	6.67	7.5	7.77	6.33
<b><math>r_{CVol}</math></b>	1.20	0.88	1.09	0.95	0.94	1.01	1.08	0.95
<b><math>R_{bVol}</math></b>	0.55	0.18	0.69	0.16	0.23	0.23	0.49	0.19
<b>RMSE</b>	0.68	0.27	0.80	0.22	0.28	0.28	0.59	0.26
<b>Nash</b>	-7.38	-1.73	-15.77	-0.99	-14.29	-14.50	-12.48	-5.74
<b>IA</b>	0.50	0.54	0.52	0.70	0.50	0.40	0.51	0.54
<b>IR</b>	0.62	0.79	0.64	0.83	0.80	0.79	0.69	0.80

In Table 5.9, individual and averaged results for all the examined floods are shown. The hydrograph  $q_m$  of the ensemble is compared with COSMO-7. NPE analysis lead to slightly better skill for COSMO-7 estimates, even if the range of dispersion is larger than that of COSMO-LEPS (Figure 5.17). PTE was better for COSMO-LEPS forecast but, again, without significant differences. The relative volume bias and RMSE revealed a big difference between forecasts of the 1993 and 2000 floods. The Nash index presents negatives values. Nevertheless, a better performance was obtained by COSMO-LEPS. The IA analyses reflected similar performance with both types of forecasts, although with a little higher performance of COSMO-LEPS.

Table 5.9 Average of the forecasts studied with deterministic indexes average for the representative hydrographs of COSMO-LEPS and for COSMO-7. Index represented are the same than in Table 5.8.

	COSMO-7	COSMO-LEPS				
		$q_{\min}$	$q_l$	$q_m$	$q_u$	$q_{\max}$
<b>NPE</b>	0.19	0.40	0.28	0.24	0.24	0.60
<b>PTE</b>	7.77	11.45	4.75	6.33	6.37	8.80
<b>r<sub>CVol</sub></b>	1.08	0.72	0.83	0.95	1.08	1.46
<b>Rb<sub>Vol</sub></b>	0.49	0.26	0.21	0.19	0.23	0.54
<b>RMSE</b>	0.59	0.31	0.27	0.26	0.30	0.61
<b>Nash</b>	-12.48	-11.67	-6.94	-5.74	-10.65	-71.25
<b>IA</b>	0.51	0.51	0.54	0.54	0.52	0.41
<b>IR</b>	0.69	0.78	0.80	0.80	0.78	0.67

Finally, it should be underlined that computing an average value of indicators over different events sometimes may produce non-significant results. Common sense is always necessary and highly valuable for the evaluation of this type of results. It should also be noticed that COSMO-LEPS results are given for a five days average, while COSMO-7 is evaluated for a three days period. Nevertheless, both results for COSMO-LEPS (three and five-day based) are rather similar.

### Results of probabilistic indexes

Regarding probabilistic indexes, the Brier Score and the Brier Skill Score are shown in Figure 5.18. Hydrographs derived from COSMO-LEPS are better than hydrographs generated from COSMO-7 for both indexes. ROC curves, presented in Figure 5.19, confirm this conclusion.

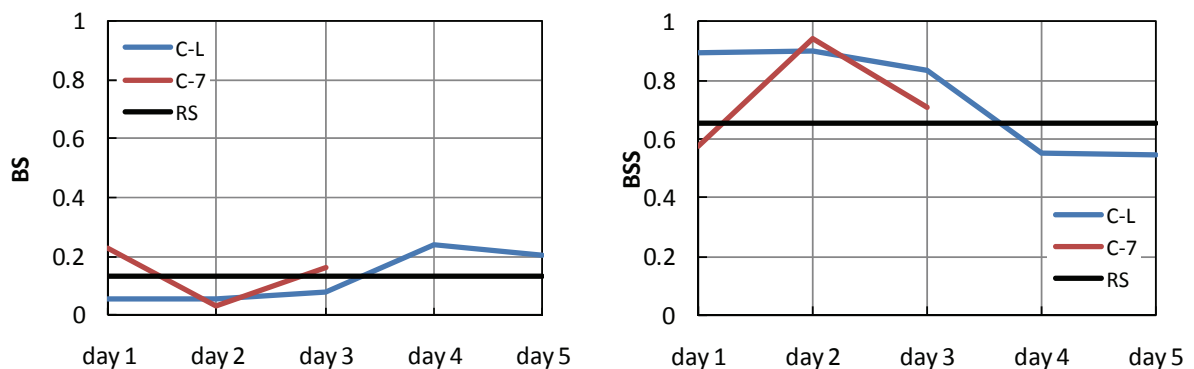


Figure 5.18 Results for the threshold  $Q=700 \text{ m}^3/\text{s}$  in Porte du Scex for COSMO-LEPS (C-L), COSMO-7 (C-L) and for the simulation with perfect forecasts (RS). Left: Brier Score (BS). Right: Brier Skill Score (BSS).

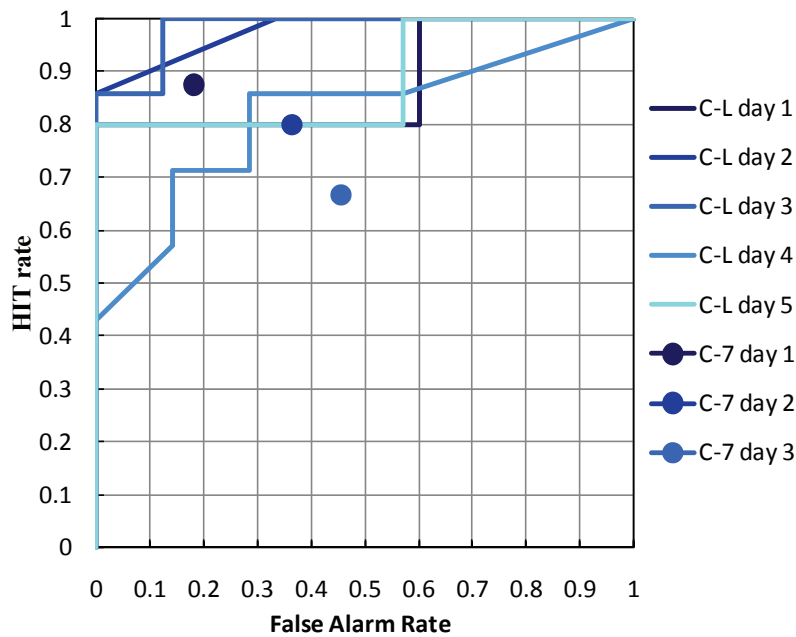


Figure 5.19 Relative Operating Characteristic curves results for COSMO-LEPS (C-L) and COSMO-7 (C-7).

Regarding the economic analysis (Figure 5.20), the uncertainty about cost-loss ratio  $\psi$  values did not allow reaching an unquestionable conclusion. A value for  $\psi$  could give more information for a deeper analysis. Nonetheless, hydrograph  $q_m$  has significantly higher performance in the *REV* assessment.

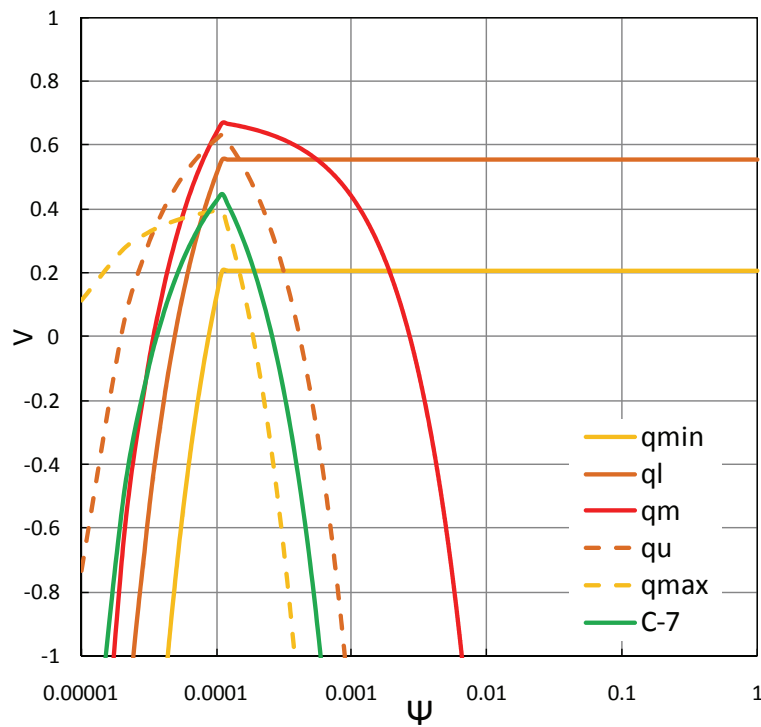


Figure 5.20 Relative Economic Value (*REV*) results for COSMO-7 (C-7) and for COSMO-LEPS which is represented by the median  $q_m$ , the upper  $q_u$  and lower quartile  $q_l$  as well as by the minimum  $q_{min}$  and maximum discharge  $q_{max}$ .

Different probabilistic indexes are also presented in Table 5.10. REV, which depends on an arbitrated  $\Psi$  and has an extra degree of uncertainty, is not shown.

Table 5.10 Probabilistic indexes for the threshold  $Q=700 \text{ m}^3/\text{s}$  for COSMO-LEPS (C-L) and COSMO-7 (C-7). BS represents the Brier Score, BSS the Brier Skill Score and ROC the Relative Operating Characteristic.

Flood	1993		2000		2008		All events	
	C-7	C-L	C-7	C-L	C-7	C-L	C-7	C-L
BS	0.15	0.18	0.00	0.05	0.15	0.13	0.10	0.12
BSS	0.72	0.70	1.00	0.93	0.72	0.79	0.81	0.80
ROC Score	0.45	0.71	0.63	1.00	0.56	1.00	0.70	0.90

An analysis of three warnings levels is also proposed for the available forecasts depending on the different threshold exceedance set, as presented in Table 5.3. Figure 5.21 illustrates the results obtained for the hydrographs  $q_m$  and  $q_u$  from the probabilistic COSMO-LEPS and for those derived from COSMO-7. The pie charts reveal that the hydrograph  $q_m$  of COSMO-LEPS is more conservative than the hydrograph from COSMO-7, resulting in less false alarms but more missed events for every threshold. Comparing the probabilistic upper quartile  $q_u$  with the deterministic forecast, the number of missed events and false alarms is similar. However,  $q_u$  obtains more hits.

The Correct Alarm Ratio (CAR) has the best results for the second threshold,  $T_2$ . For the threshold  $T_3$  of  $1200 \text{ m}^3/\text{s}$  at Porte-du-Scex, the CAR values are worse because the event frequency decreases. The Miss Rate is similar for all cases. The worst result is obtained for the hydrograph  $q_m$  and the first threshold. However,  $q_m$  had better CAR than the other forecasts for this threshold  $T_1$ .



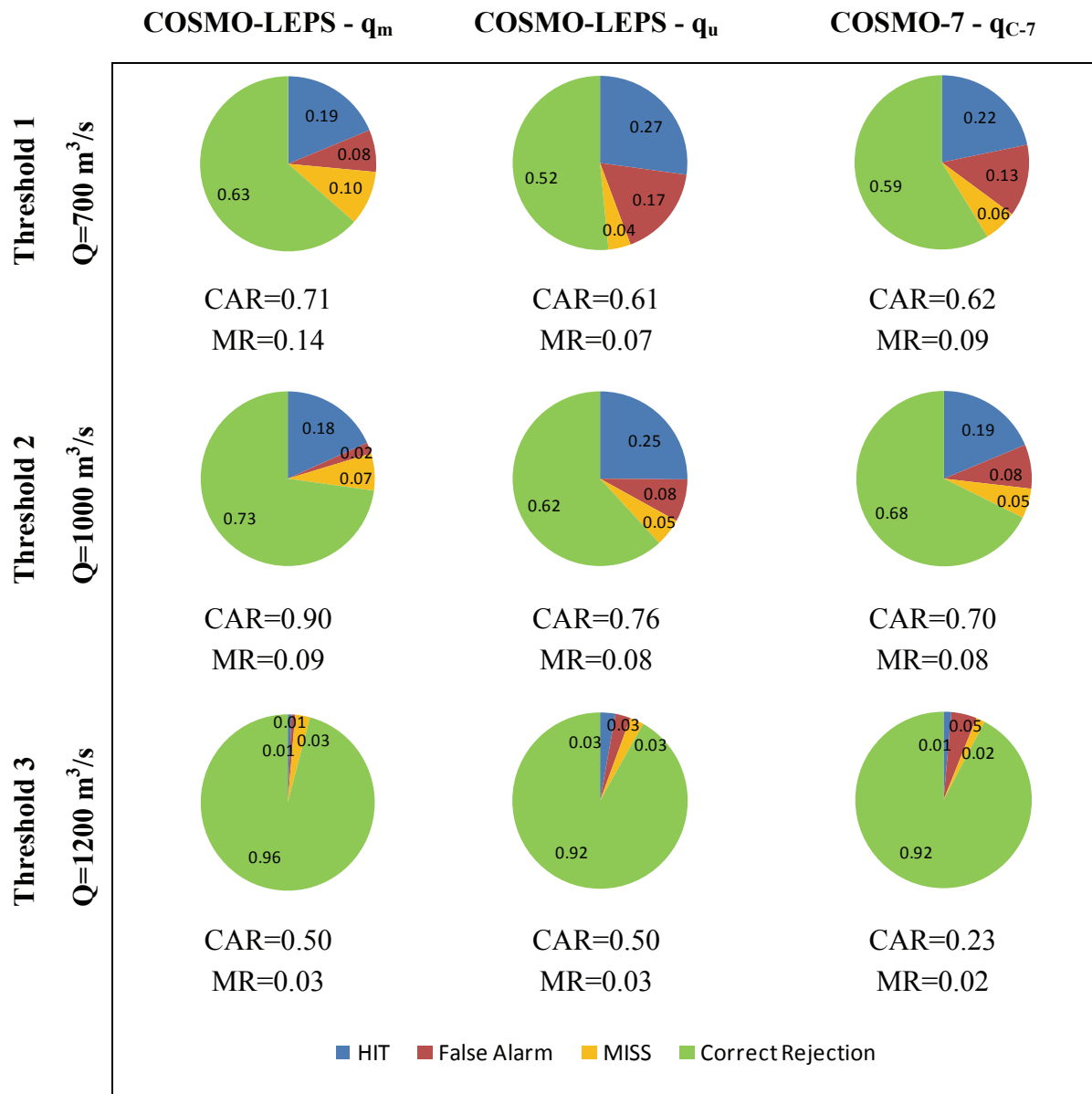


Figure 5.21 Forecasts performance and CAR (Correct Alarm Ratio) and MR (Miss Ratio) indexes

### 5.3.3 Hydrological performance of studied events

The performance of the COSMO-LEPS is generally better than the performance of COSMO-7, as proven in this chapter. COSMO-7 has a higher variability between two successive forecasts that leads to more uncertainty during a real-time utilisation. In addition, the third day of COSMO-7 provides poor results, with an overestimation of the volumes. COSMO-LEPS usually predicts correct discharge volumes but its interquartile range (difference between the upper and lower quartiles) increases with the time horizon. BS, BSS and ROC indexes confirm the skill of both forecasts through the hydro-meteorological simulations.

The added value of forecast systems for providing early warnings in case of floods could be shown. Even if forecast systems can never have perfect performances, they provide advantageous estimation of floods and have a high ability for providing warnings. As an example, hydrographs  $q_m$  and  $q_u$  of the ensemble forecast, according to the *Correct Alarm Ratio* in Figure 5.21, are correct in over 75% of the cases when a warning is given for the threshold  $T_2$ , corresponding to  $Q=1000 \text{ m}^3/\text{s}$ . At the same time, false and miss alarms, according to the *False Alarm Rate* and the *Miss Rate*, are considered acceptable (less than 10% in both cases).

When considering the three forecasts and being able to take advantage of their information, the system can be really helpful for establishing a sound warning system. In a similar way, the system is also valuable concerning the hydropower plants management, when information on the correct initial levels in the reservoirs is available.

Even if a result is given for a representative hydrograph such as the median, the knowledge of the variability range is an important data that should not be forgotten. Moreover, the selection of a different characteristic hydrographs could be carried out depending on the specific aims of each system and on the *ROC* analysis results. For example, one quartile could be chosen for the purpose of predicting a notice level warning (first threshold  $T_1$ ) and other different for the alert or alarm level warnings ( $T_2$  and  $T_3$ ).

Extending such considerations, the *Relative Economic Value*, and not only the hydrographs themselves, could be also taken into account. The *Relative Economic Value* of a forecast could be then a good basis for decision-making. However, this option is not practical for the Upper Rhone River basin due to the limited number of historical flood events available. For the moment, there is no option other than to evaluate the skill of the EPS and the deterministic driven flood forecasts on a case by case basis.

## 5.4 Warning reports

The warning report is presented in the following for the resimulation of the October 2000 flood. All presented forecasts were not available at that time and the warning reports presented were done after the event. It has to be noticed that different forecasts are missing due to short resimulations periods (only during the event). In an operational case, all lines of the forecasts should be filled with the corresponding warnings.

For the activation of a warning from COSMO-LEPS, the hydrograph corresponding to the median,  $q_m = 50\%$ , has been selected. This threshold of COSMO-LEPS could be differentiated according to forecast performance results for each level of warning. Nevertheless, the available data is not currently representative.

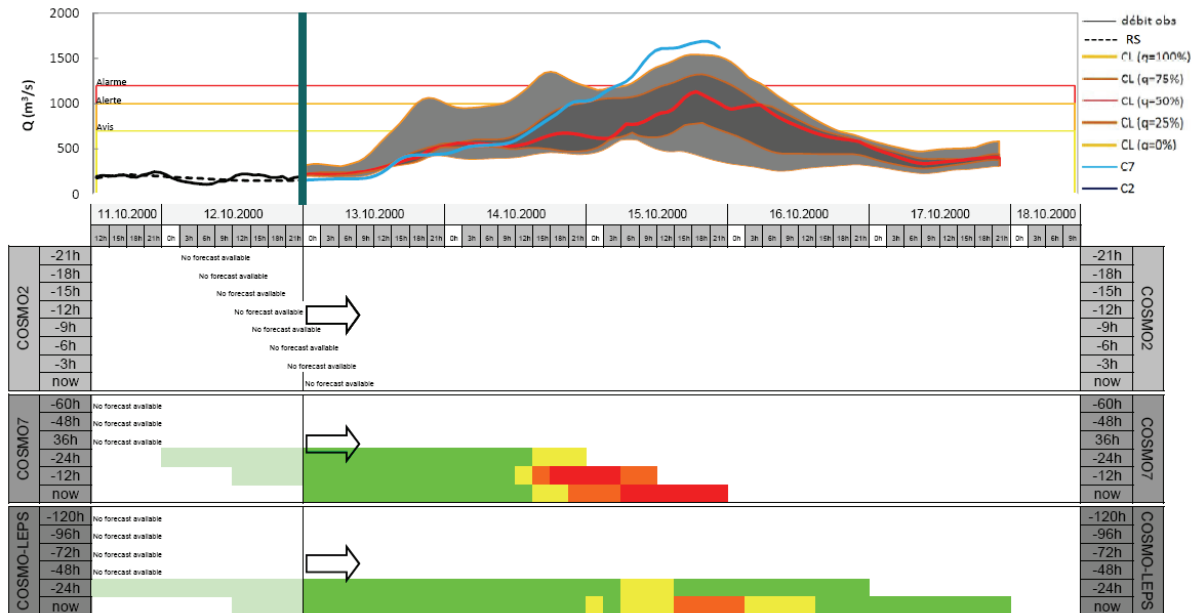


Figure 5.22 Warning report *Porte-du-Scex* on October 13, 2000 at 00h

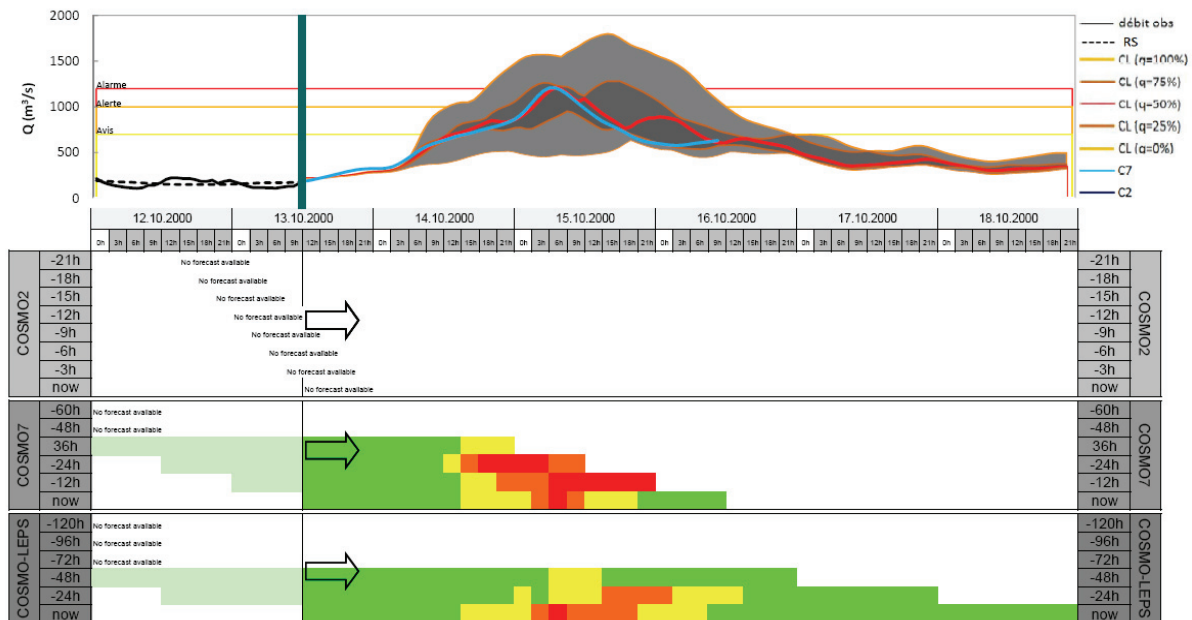


Figure 5.23 Warning report at *Porte-du-Scex* on October 13, 2000 at 12h

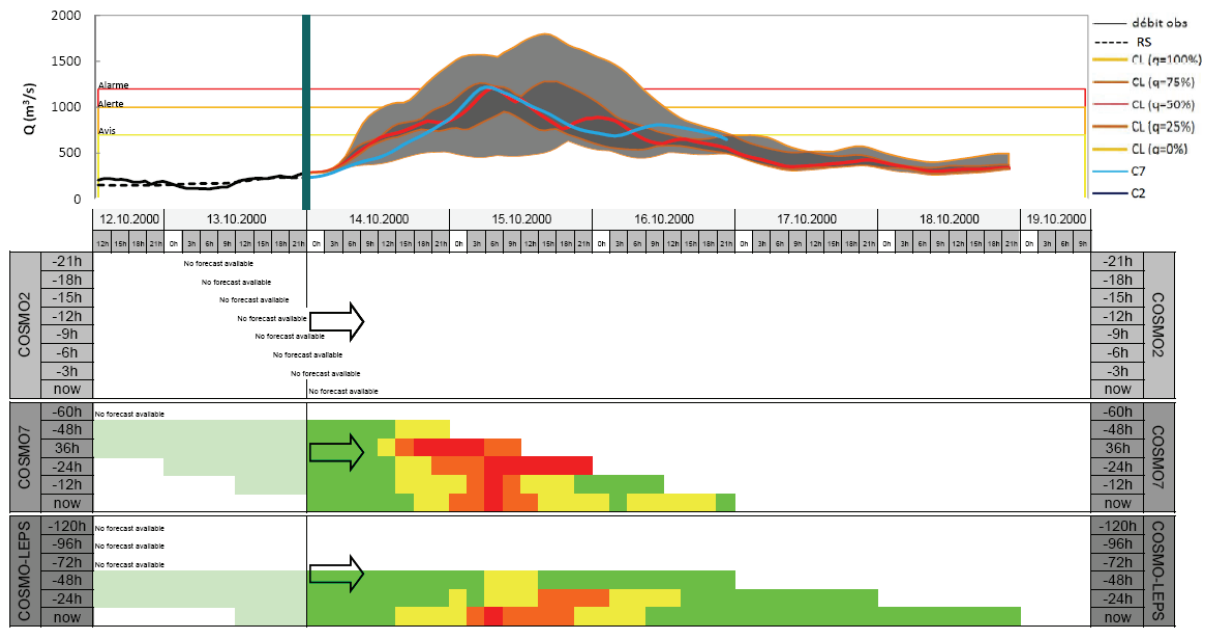


Figure 5.24 Warning report at Porte-du-Scex on October 14, 2000 at 00h

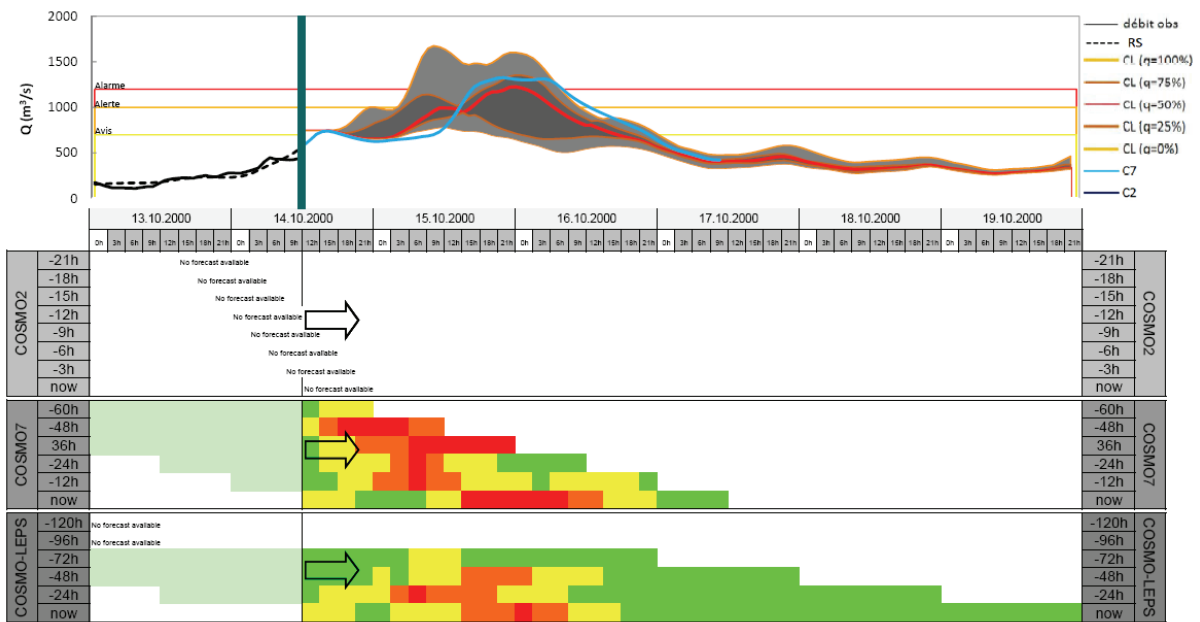


Figure 5.25 Warning report at Porte-du-Scex on October 14, 2000 at 12h

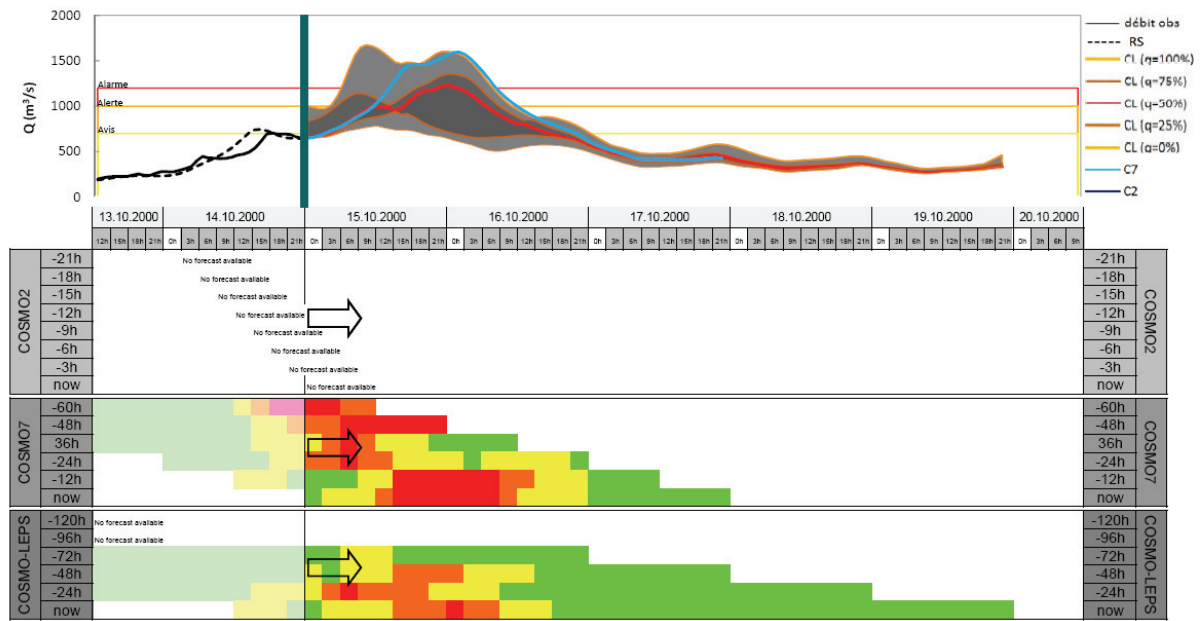


Figure 5.26 Warning report at Porte-du-Scex on October 15, 2000 at 00h

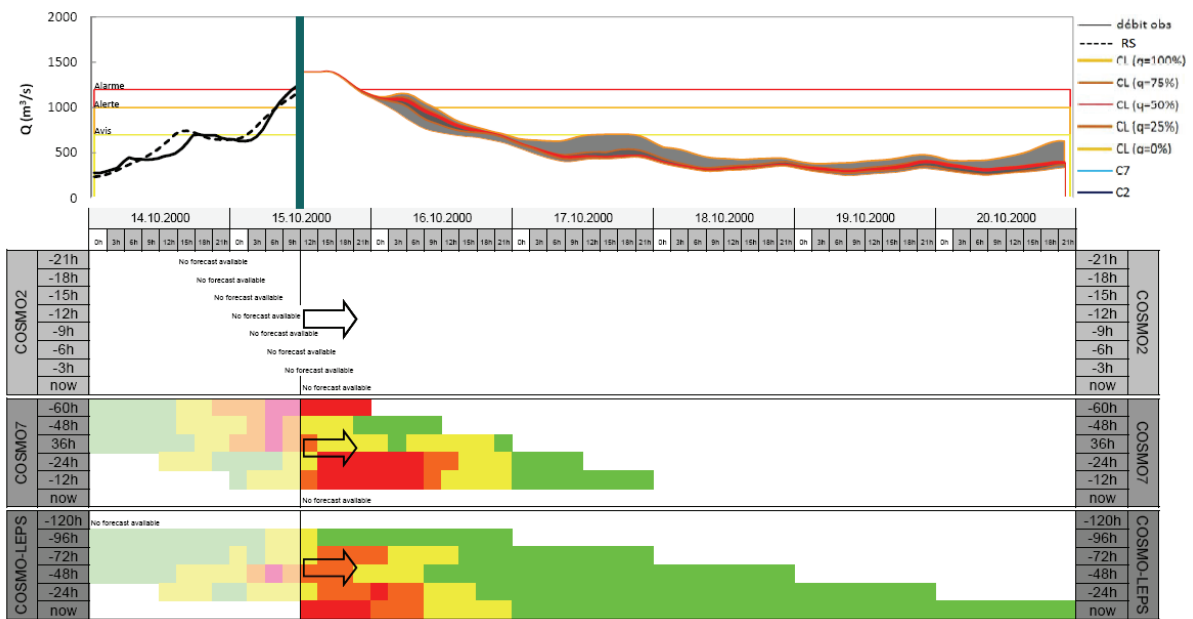


Figure 5.27 Warning report at Porte-du-Scex on October 15, 2000 at 12h

## 5.5 Hydro-meteorological conclusions

### 5.5.1 Hydrological forecast system

The MINERVE model developed for the Upper Rhone River has been operational with deterministic forecast inputs since 2006 (first stage of the MINERVE project) and with

ensemble forecasts since 2008. This flood forecast system is the basis for the decision-making tool used for limiting flood damages during flood events.

COSMO-LEPS has been implemented in the system during this research project in order to improve uncertainties related to meteorological forecasts. COSMO-7 and COSMO-2 are complementary for the short range forecast. Forecasts could be even modified by assuming, for example, more or less rain than forecasted, different temperatures in certain valleys or other changes depending on expert advice. Also, additional forecasts could be used in order to improve the consistency of the hydro-meteorological results.

The use of all available forecast models (three in this case) appears as a reasonable way for controlling the quality of the forecasts. Similar results obtained from all different forecasts models within a small variation range could be expected to comfort decisions (issuing a warning advertisement in case of expected floods). Nevertheless, it must be kept in mind that the hydro-meteorological task cannot be considered as a mathematic product providing an outcome with an exact performance or error. The trained point of view of the meteorologist and the engineer is necessary for understanding and correctly interpreting forecast results.

### ***5.5.2 Outlook of the hydrological forecasts***

Analysing the performance of hydrological forecasts is convenient to communicate better the forecasted values and transmit their uncertainty to end users. Nevertheless flood forecasting based on Numerical Weather Predictions (NWP) remains a relatively new field. Using probabilistic forecasts is an even younger discipline where the forecast inconsistencies have still to be evaluated (Pappenberger et al., 2011).

The aim of the presented analysis was not to achieve a final measure on the performance of the hydro-meteorological forecasts, but mostly to understand the behaviour of the system and to be able to deal with its results in future situations. The assessment of the past events is necessary for understanding new forecasts, increasing the knowledge of meteorologists and engineers and contributing for ever-evolving flood forecasts systems.

Furthermore, the performances of future flood events in the basin will not remain the same due to expected variation in meteorological forecasts performance as well as to the atmosphere situation itself. At the same time, NWPs may not represent the full uncertainty of the model atmosphere state. Nonetheless, flood warning systems are currently considered as useful and valuable tools for decision making.

“Objectivity in sciences is a myth, in life an impossibility and in decision making an  
irrelevance”

(Anderson et al., 1977)

## **6. MINERVE Interactive Decision Support System**

## 6.1 Interactive decision support system for flood management

The hydrological forecast for MINERVE is based on the meteorological forecasts provided by MeteoSwiss and on a semi-distributed conceptual model of the catchment area, including all significant hydraulic schemes. The hydrological simulation tool Routing System MINERVE provides useful information regarding decision-making tasks. It allows the coordination of intervention measures or hydropower plant management regarding flood protection if a catastrophic event is expected.

MINDS (MINERVE Interactive Decision Support System) has been developed for this purpose, as an improvement of the previous deterministic management tool (Jordan, 2007; Jordan et al., 2010). MINDS suggests preventive turbine and bottom outlet releases to the hydropower plants' operators depending on river flow observations, hydrological forecasts and reservoir levels. The goal is to retain floods in reservoirs and to reduce their outflow during the flood peak. Appropriate operation rules should diminish the peak discharges in the Rhone River and its tributaries, reducing or avoiding damages.

### 6.1.1 Hydraulic simulations

The hydraulic simulation model, implemented in MINDS, includes 21 reservoirs and 24 hydropower plants. They are regrouped into 10 independent hydropower groups (i.e. without any interconnections), which can be independently managed.

The inputs of the model are computed hydrographs at check points as well as the inflow and current water levels of the reservoirs. The constraints are installed capacity of turbines and pumps at the hydropower plants, the volume in the reservoirs, the capacity of the bottom outlets, the reservoir spillway characteristics and the emergency rules.

The hydraulic simulations take into account economical losses including the expected damages caused by the flood and the potential costs for the hydropower plants preventive operations. The suggested measures to the hydropower plants' operators are defined by the starting and ending time of the turbines, pumps and bottom outlet operations, respecting constraints of the system.

Different objective functions are defined by multi-attribute decision making (MADM) approaches and can be chosen by the decision maker. The MADM methods calculate the loss function based on damages and costs of preventive operations taking into account the probabilistic forecast and the weight of each one of its members (i.e. particular forecast).



### **6.1.2 Optimisation approach**

Once a check point CP at the outlet of a considered catchment area is selected by the decision maker, the objective function of the system is defined in order to minimize the combination of expected damages and energy losses upstream. The selected CP is usually identical with the check point located at the outlet of the entire Rhone River catchment area, Porte-du-Scex. The optimisation of the objective function gives then the optimal sequences of turbines, bottom outlets and pumps operations in the considered hydropower plants which minimize the global losses. Both, the expected damages and the energy losses are expressed as monetary values for comparison reasons. If no damage is expected in the catchment area, the system logically does not propose any preventive operation.

Considering the energy production costs related to the preventive operations, they simultaneously result in a maximization of the use of the reservoir capacity over the optimisation period. The reason is that preventive operations are only suggested if they reduce the expected damages.

The preventive operations (i.e. the resolution of the objective function) are either optimised in a global way (all hydropower groups at the same time) by using the SCE-UA (Shuffled Complex evolution – University of Arizona) algorithm or independently group by group by using the Greedy algorithm.

The purpose is to deal with the concept of risk and to transmit it to the end users. The methodology avoids deterministic evaluations when using COSMO-LEPS and compares the set of expected damages before and after the optimisation. The decision-maker has to be involved in operating and understanding this new probabilistic concept currently used in applied sciences.

Before describing the optimisation computation description (section 6.4 to 6.8), the hydraulic simulation model is presented in section 6.2. The expected damages in the catchment area due to flooding as well as the potential energy production costs of the hydropower plants resulting from preventive operations are investigated in section 6.3.

## 6.2 Hydraulic simulation model

### 6.2.1 Model description

A hydraulic simulation model of the Upper Rhone River basin (Figure 6.1) has been developed for the hydropower operation simulations in the optimisation tool MINDS (MINERVE Interactive Decision Support System). It is a simplified model of the complex catchment area (LCH, 2005) which aims to be used for real-time calculations.

Reservoir management and real-time calculations have been performed with this model. It includes the most important reservoirs (RES) with their bottom outlets and spillways, the hydropower plants (HPP) as well as the main river network with the check points (CP). It is based on the concept that every simulation keeps the correct balance of water volume in each element of the whole system (reservoirs, check points, turbines,...) at each time step.

The hydropower schemes have been divided into hydropower groups (GR) which are independently managed and have no physical connexions between each other. A list of the groups with their reservoirs is presented in Table 6.1.

Reservoirs have storage and distribution functions and can be linked between each other. Turbines, pumps, bottom outlets and spillways direct the water discharge from a reservoir to another one or to a check point in the downstream river network, taking into account a fixed transit time between the elements which have been previously estimated.

Even if reservoirs are generally used to store water, several of them operate without this function, just as compensation basins for short time storage. Thus, 12 of the 21 reservoirs allow seasonal water storage and are modelled with their level-volume relationship. The other 9 reservoirs have small storage volumes and have no significant effect on flood retention. Therefore, they have been represented as punctual reservoirs and modelled as elements with exclusively distribution functions (turbine, pump or derivation of flows) according to their physical characteristics.

The hydropower plants included in the model connect either two reservoirs or a reservoir with the river network. If preventive operations are decided, hydropower plants work at maximum installed capacity to limit operation time as much as possible. Therefore no additional parameters are required. In fact, forecast horizon is normally short and preventive operations are generally restricted in time, requiring this maximum installed capacity. Nevertheless, decision maker could test other scenarios and check their results in the DSS before applying

them. The description of the hydropower plants (turbines, pumps and bottom outlet) are presented in detail in Appendix 1. The main characteristics for turbines, pumps and bottom outlets include:

- Turbine: name, maximum discharge capacity, hydraulic head, plant efficiency, operability and current rate of discharge capacity (e.g. 0.8 if one of five equivalent turbine units is temporarily out of service), upstream reservoir as well as the river reach located downstream with its name and the transit time to it.
- Pump: name, maximum discharge capacity, operability, lower reservoir and upper reservoir.
- Bottom Outlet: reservoir where it is located, discharge capacity, operability, discharge rate capacity as well as the river reach located downstream with its name and the transit time to it.

Table 6.1 Hydropower groups and reservoirs implemented in the MINDS hydraulic model (P for punctual reservoirs).

Group (GR)	Reservoir (RES)		Group (GR)	Reservoir (RES)	
	Name	Vol (m <sup>3</sup> )		Name	Vol (m <sup>3</sup> )
<b>GD (Grande Dixence)</b>	Grande Dixence	422 · 10 <sup>6</sup>	<b>EL (Lienne)</b>	Zeuzier	61 · 10 <sup>6</sup>
	Cleuson	28 · 10 <sup>6</sup>		Croix	P
		Emosson	255 · 10 <sup>6</sup>	<b>SAL (Salanfe)</b>	Salanfe
<b>ESA (Emosson)</b>	Esserts	P	<b>GSB (Pallazuit)</b>	Toules	27.3 · 10 <sup>6</sup>
	Châtelard CFF	P		Pallazuit	P
	Châtelard ESA	P	<b>EM (Bitsch)</b>	Gebidem	9.6 · 10 <sup>6</sup>
<b>FMM (Mauvoisin)</b>	Mauvoisin	215 · 10 <sup>6</sup>	<b>KWL (Lötschen)</b>	Ferden	2.12 · 10 <sup>6</sup>
	Fionnay	P			
<b>KWM (Mattmark)</b>	Mattmark	188 · 10 <sup>6</sup>			
	Zermeiggern	P			
	Moiry	83.3 · 10 <sup>6</sup>			
<b>FMG (Gougra)</b>	Turtmann	0.844 · 10 <sup>6</sup>			
	Mottec	P			
	Vissoie	P			

Moreover, twelve check points (CP) are defined along the river network in the Upper Rhone River basin. Each CP is linked to its downstream neighbour until reaching the system outlet of the entire basin at Porte-du-Scex. Their characteristics concerning the river location, the immediately downstream CP and the transit time to it are shown in Appendix 1.

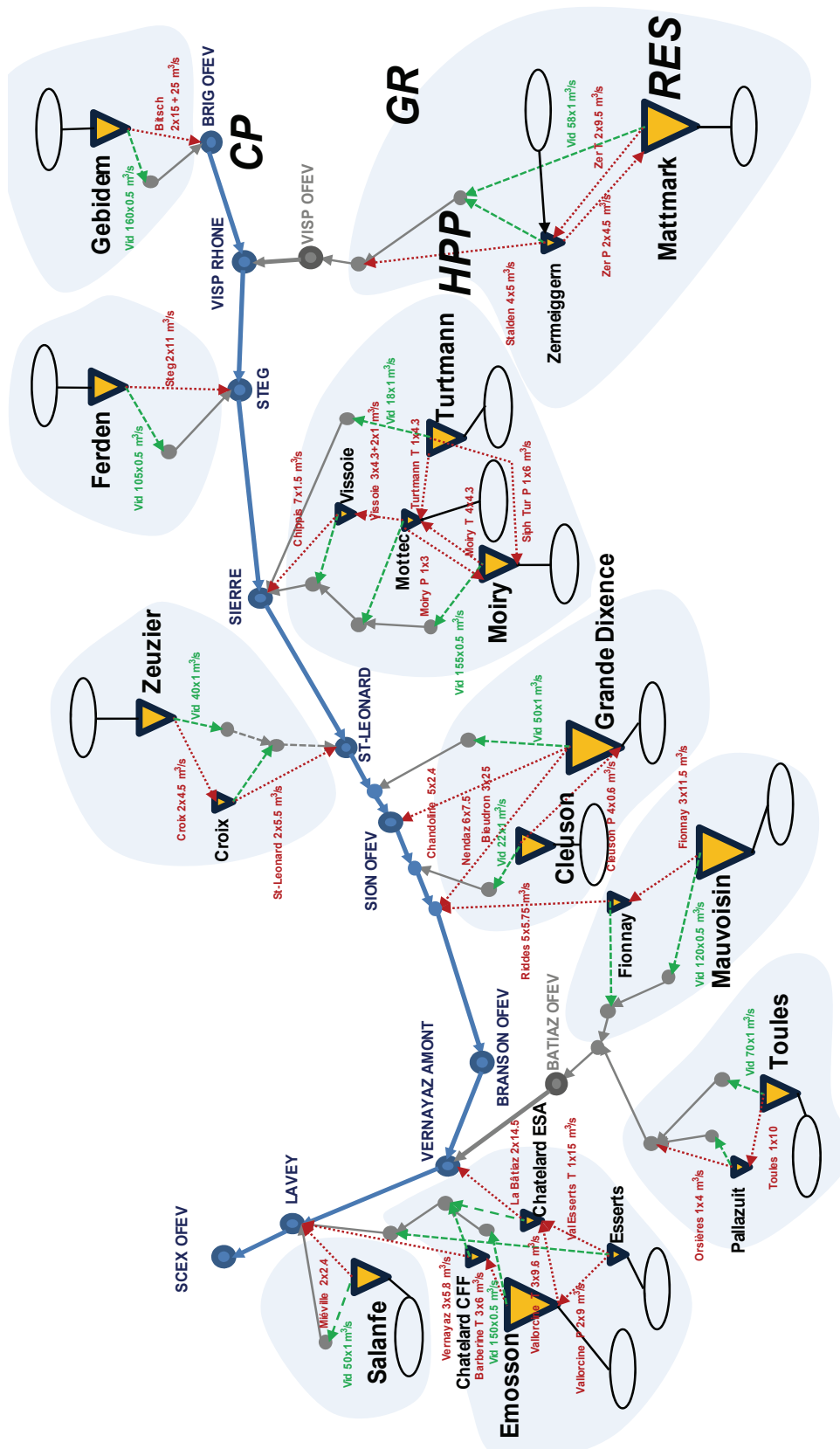


Figure 6.1 Functionality scheme of the complex hydraulic model with: inflows (ovals); reservoirs, RES (triangles); bottom outlets and spillways (square dotted lines); hydropower plants, HPP (round dotted lines); main river network (solid lines); groups, GR (shading zones); and check points, CP (big circles). More details are shown in Appendix 2.

The critical discharge producing inundations ( $Q_{fl}$ ) is individually defined for every CP based on 1D flow simulation. In addition, an extreme discharge ( $Q_{ex}$ ), corresponding to the flood with 1000-year return period, was also defined. The extreme discharge is assumed as the flow provoking maximum damage in the CP sector. These threshold values have been defined as presented in Table 6.2.

Table 6.2 Check points (CP) with the overflow discharge  $Q_{fl}$  of the levees and the extreme discharge  $Q_{ex}$

Check Point (CP)	$Q_{fl}$ (m <sup>3</sup> /s)	$Q_{ex}$ (m <sup>3</sup> /s)
<b>Brig OFEV</b>	560	750
<b>Visp OFEV</b>	190	590
<b>Visp Rhone</b>	760	1380
<b>Steg</b>	779	1380
<b>Sierre</b>	826	1480
<b>St-Léonard</b>	859	1520
<b>Sion OFEV</b>	910	1580
<b>Branson OFEV</b>	980	1600
<b>Bâtiaz OFEV</b>	196	204
<b>Vernayaz Am.</b>	1176	1804
<b>St-Maurice</b>	1236	1913
<b>Scex OFEV</b>	1370	2120

### 6.2.2 Model equations

The elements of the system are defined by their hydraulic functions. The whole network is thus described by the help of four functions: water storage, flow regulation, addition of flow and flow transport. Furthermore, the data flux between elements is regulated by defining an upstream-downstream relation and having fixed transit time for the data propagation.

The functions of each element are defined by different equations and constraints explained hereafter.

#### Check Points

The discharge at each Check Point (CP<sub>k</sub>) is calculated according to the continuity constraints as presented in Eq. 6.1 to 6.4. The final discharge at CP<sub>k</sub> of the equipped basin is calculated from the discharge of the natural basin, corrected depending on the inflows and outflows from the upstream reservoirs and taking into account the different propagation times.

$$Q_{eq,k,t} = Q_{nat,k,t} + \sum_{e=1}^{e_f} (Q_{out,ek,t_{ek}^*}) - \sum_{r=1}^{r_f} (Q_{in,rk,t_{rk}^*}) + \sum_{z=1}^{z_f} (Q_{eq,zk,t_{zk}^*} - Q_{nat,zk,t_{zk}^*}) \quad 6.1$$

$$t_{ek}^* = t - t_{transit(e \rightarrow k)} \quad 6.2$$

$$t_{rk}^* = t - t_{transit(r \rightarrow k)} \quad 6.3$$

$$t_{zk}^* = t - t_{transit(z \rightarrow k)} \quad 6.4$$

with  $t$ : step time [h];  $Q_{eq,k,t}$ : discharge on the equipped basin at  $CP_k$  at time  $t$  [ $m^3/s$ ];  $Q_{nat,k,t}$ : discharge coming from the natural basin at  $CP_k$  at time  $t$  [ $m^3/s$ ];  $Q_{out,ek,t^*}$ : outflow from a turbine or bottom outlet  $e$  which is directly guided to  $CP_k$  [ $m^3/s$ ];  $Q_{in,rk,t^*}$ : inflow to reservoir  $r$  which is directly guided to  $CP_k$  in the natural basin [ $m^3/s$ ];  $Q_{eq,zk,t^*}$ : discharge on the equipped basin in  $CP_z$ , located directly upstream of  $CP_k$  [ $m^3/s$ ];  $Q_{nat,zk,t^*}$ : discharge on the natural basin in  $CP_z$ , located directly upstream of  $CP_k$  [ $m^3/s$ ];  $t_{transit}$ : transit time between two elements  $a$  and  $b$  [h];  $e_f$ : total number of elements (turbines or bottom outlets) directing the flow to  $CP_k$  [-];  $r_f$ : total number of reservoirs whose inflow is directed to  $CP_k$  [-];  $z_f$ : total number of check points directing discharge directly to  $CP_k$  [-].

Furthermore, if overflow occurs at a CP, the return flow is considered as equal. No decrease in hydrograph or peak flow downstream is therefore achieved. Even if this assumption does not correspond to reality, it is the worst possible case scenario by assuming that the entire water volume is transported from upstream to downstream.

### Reservoirs

Simulations in reservoirs consider the retention equation, as shown in Eq. 6.5, assuming a general reservoir (without sub-index). Due to continuous update of reservoir levels, possible evaporation and infiltration are not taken into account.

$$V_{t+1} = V_t + Q_{in,t} \cdot \Delta t - Q_{out,t} \cdot \Delta t \quad 6.5$$

with  $V_{t+1}$ : Volume at time  $t+1$  [ $m^3$ ];  $V_t$ : Volume at time  $t$  [ $m^3$ ];  $\Delta t$ : time step [h];  $Q_{in,t}$ : total inflow at time  $t$  [ $m^3/s$ ];  $Q_{out,t}$ : total outflow at time  $t$  [ $m^3/s$ ].

Particular physical constraints are also considered for adequate and physically-based simulations. The volume cannot be lower than  $V_{min}$  in any case, assuming that  $V_{min}$  corresponds to the minimum operational volume for turbines and bottom outlets. When

volume exceeds the maximum capacity of the reservoir ( $V_{max}$ ), spillways automatically release to limit the water level in the reservoir.

Turbines, pumps and bottom outlets have a limited capacity. They also depend on available volume in the reservoir at the current time.

$$\begin{aligned}
 V_{min} &\leq V_t && \forall t \in (0, t_{fin}) \\
 Q_{spillway,t} &> 0 && \text{if } V_t > V_{max} \\
 0 &\leq Q_{turb,t} \leq Q_{turb,max} \\
 0 &\leq Q_{pomp,t} \leq Q_{pomp,max} \\
 0 &\leq Q_{bottomoutlet,t} \leq Q_{bottomoutlet,max} \\
 Q_{turb,t} + Q_{bottomoutlet,t} &\leq \frac{V_t}{\Delta t} + Q_{in,t}
 \end{aligned} \tag{6.6}$$

with  $V_{min}$ : Minimum volume at reservoir [ $m^3$ ];  $V_t$ : Volume at reservoir at time  $t$  [ $m^3$ ];  $t_{fin}$ : final time of the period [h];  $Q_{spillway,t}$ : total discharge by spillways at time  $t$  [ $m^3/s$ ];  $V_{max}$ : Maximum volume at reservoir [ $m^3$ ];  $Q_{turb,t}$ : total discharge by turbines at time  $t$  [ $m^3/s$ ];  $Q_{pomp,t}$ : total discharge by pumps at time  $t$  [ $m^3/s$ ];  $Q_{bottomoutlet,t}$ : total discharge by bottom outlets at time  $t$ ;  $Q_{turb,max}$ : maximum discharge by turbines [ $m^3/s$ ];  $Q_{pomp,max}$ : maximum discharge by pumps at time  $t$  [ $m^3/s$ ];  $Q_{bottomoutlet,max}$ : maximum discharge by bottom outlets [ $m^3/s$ ].

Finally, the last conditions to satisfy are related to reservoir rules. They concern fixed discharges (by turbine or bottom outlet operations) planned when determinate levels or volumes thresholds are exceeded.

$$\begin{aligned}
 Q_{turb,t} &= Q_{threshold1} && \text{if } V_t > V_{threshold1} \\
 Q_{bottomoutlet,t} &= Q_{threshold2} && \text{if } V_t > V_{threshold2}
 \end{aligned} \tag{6.7}$$

with  $Q_{threshold1}$ : Discharge threshold 1 [ $m^3/s$ ];  $Q_{threshold2}$ : Discharge threshold 2 [ $m^3/s$ ];  $V_{threshold1}$ : Volume threshold 1 [ $m^3$ ];  $V_{threshold2}$ : Volume threshold 2 [ $m^3$ ].

### 6.2.3 Turbining cycle with Business as Usual operations

For the usual HPP operations, if the actual state of turbine operation is unknown, theoretical “Business as Usual” (BasU) discharge series are suggested in the model based on experience. This simplified approach deals with two different stages, called “peak” (for the discharge  $Q_{peak}$  and the peak load price  $c_{peak}$ ) and “base” (for the discharge  $Q_{base}$  and the base load price

$c_{low}$ ). Each one of these stages is used depending on the time of day and day of week as presented in Table 6.3.

Table 6.3 Period of peak and base discharge and energy prices for the Business as Usual operations

Type	Period	Time
Peak {	Monday-Friday	$T_{p1} - T_{p2}$
Base {	Monday-Friday	00h - $T_{p1}$ & $T_{p2} - 24h$
	Weekend	00h - 24h

Nevertheless, the Business as Usual discharge series can also be introduced by the end user if known for the different HPPs.

### 6.3 Economical analysis of flood events

#### 6.3.1 Expected damages

Once the discharge corresponding to the overflow threshold  $Q_{fl}$  is exceeded in a check point (CP), a percentage of the total expected damage in the vicinity of the selected CP is considered. The expected damage depends on the flow peak and increases according to a power function. If the discharge reaches  $Q_{ex}$ , the expected damage is equivalent to the maximum damage. Thereafter, the damages are kept constant.

Furthermore, the check points also include the possible breach opening which considers the vulnerability of the levees. Breaches and/or overflows simultaneously generated at all critical points are very unrealistic. Therefore, a scenario is established in advance in collaboration with survey authorities. This scenario provides a breach opening possibility at different locations depending on the hydraulic and geotechnical characteristics of the levees which generate maximum damages at its final stage. Nonetheless, this scenario can be adapted by the survey authorities or the decision makers if new data is available.

The expected damages have been estimated in collaboration with the team of the Third Rhone Correction (Third Rhone Correction, 2008). For every CP, they are associated with the upstream local damages (see Appendix 1). The maximum expected damages associated to a CP, the possible breach opening characteristic and the function parameters of Eq. 6.8 (presented hereafter) for damage calculations are presented in Table 6.4.



Table 6.4 Check points with associated maximum damages and parameters for damages calculation

Check Point (CP)	Maximum expected damages in CP area, $ED_{max}$ ( $10^6$ CHF)	Possibility of breach opening	$\delta$ : initial damage parameter (initial damage in % of $ED_{max}$ )	$\lambda$ : power function parameter
Brig OFEV	207.9	No	0.10	0.25
Visp OFEV	441.0	No	0.20	0.50
Visp Rhone	2835.0	Yes	0.20	0.50
Steg	560.0	No	0.10	0.50
Sierre	1106.8	Yes	0.20	0.50
St-Léonard	50.4	No	0.10	0.25
Sion OFEV	896.7	Yes	0.20	0.50
Branson OFEV	452.3	Yes	0.10	0.50
Bâtiaz OFEV	56.3	No	0.20	0.50
Vernayaz Am.	8.0	No	0.10	0.25
St-Maurice	313.2	No	0.20	0.50
Scex OFEV	1936.4	Yes	0.20	0.25

### Calculation of damages

For the estimation of the expected damages ( $ED$ ), the maximum predicted discharge for a given member of the forecast  $Q_{max}$  is computed over the concerned period at each individual check point  $k$ . It is then compared to the theoretical discharge for flooding ( $Q_{fl,k}$ ) and to the probable maximum flood discharge  $Q_{ex,k}$  at the same CP according to Eq. 6.8. If  $Q_{max,k}$  exceeds  $Q_{fl,k}$ , an initial damage ( $\delta_k \cdot ED_{max,k}$ ,  $\delta_k \leq 1$ ) in the vicinity area of the CP is estimated. The damages grow according to  $Q_{max,k}$  and depending on a power factor ( $1-\lambda_k$ ). The maximum damage  $ED_{max,k}$  occurs if  $Q_{max,k}$  reaches  $Q_{ex,k}$ .

$$ED_k(a_{i,set}|f_j) = \begin{cases} 0 & \text{if } Q_{max_k}(a_{i,set}|f_j) \leq Q_{fl_k} \\ \delta_k \cdot ED_{max_k} + (1-\delta_k) \cdot \left( \frac{Q_{max_k}(a_{i,set}|f_j) - Q_{fl_k}}{Q_{ex_k} - Q_{fl_k}} \right)^{1-\lambda_k} \cdot ED_{max_k} & \text{if } Q_{fl_k} < Q_{max_k}(a_{i,set}|f_j) < Q_{ex_k} \\ ED_{max_k} & \text{if } Q_{max_k}(a_{i,set}|f_j) \geq Q_{ex_k} \end{cases} \quad 6.8$$

with  $a_{i,set}$ : total set  $i$  of preventive operations in all the reservoirs [-];  $f_j$ : forecast scenario  $j$  [-];  $\delta_k$ : initial damage parameter, representing the percentage of initial damages compared to  $ED_{max,k}$  [-];  $\lambda_k$ : damage power function parameter [-];  $Q_{max,k}$ : maximum discharge over the entire period studied [ $m^3/s$ ];  $Q_{fl,k}$ : overflow discharge [ $m^3/s$ ];  $Q_{ex,k}$ : probable maximum discharge [ $m^3/s$ ];  $ED_{max,k}$ : maximum expected damages [CHF].

The total expected damages for a set  $i$  of preventive operations and a forecast  $j$  corresponds to the sum of all expected damages in the basin upstream of the selected objective CP. It is computed according to Eq. 6.9.

$$ED(a_{i,set} | f_j) = \sum_{k=1}^{k=p} ED_k(a_{i,set} | f_j) \quad 6.9$$

with  $p$ : total number of upstream check points.

### 6.3.2 Costs of potential preventive operations

For the potential preventive operation costs (*PPOC*), the installed capacity ( $P$ ) and the energy ( $E$ ) are computed depending on the timely operating discharge sequences proposed as preventive operations (PrevOp) and on the “Business as Usual” (BasU) discharge series, the head  $H$  and the efficiency factor  $\eta$  of the hydropower plant  $h$ , HPP <sub>$h$</sub> . If a reservoir is connected to several hydropower plants, the same preventive operation series is provided for all of them, but with discharges corresponding to each HPP specific installed capacity.

The potential costs per reservoir  $r$  (RES <sub>$r$</sub> ) or group  $g$  (GR <sub>$g$</sub> ) is computed comparing the reference BasU series and the proposed PrevOp series. BasU series considers two theoretical energy price (Table 6.3),  $c_{peak}$  and  $c_{low}$ . It is assumed that energy produced during preventive operations can be sold only at the low price  $c_{low}$ . It is not considered as a usual operation and is therefore economically not recommended (i.e. they are not foreseen in the market and presuming another price could be too optimistic). In addition, a potential price ( $c_{pot}$ ) at which energy could be sold in the future is also introduced. It has been defined for possible economical compensations to hydropower plant’s operators due to losses by preventive operations.

#### Calculation of potential costs

The potential preventive operation costs (PPOC) are related to losses of flexibility in HPPs, losses due to changes at BasU operation as well as to storage volume differences at the end of the concerned period.

It has to be noted that all these losses cannot be summed up since the potential costs would be overestimated. For example, if a PrevOp of 10 h is carried out as well as a 10 h turbines stop (during the BasU period), it would produce one economical indemnity corresponding to the

difference between the benefit not reached during the turbines stop and the profit of the preventive turbinning.

This consideration of equitable indemnities separates the PPOC in three different cases. All of them assume the maximum possible costs due to PrevOp. It means that worst scenario of inflow leading to this PPOC is assumed. Therefore, the releases or the not turbinated volumes due to preventive operations are assumed as lost, without considering the rain compensation (inflow to reservoirs). This assumption allows the decision maker to have an idea of the possible maximum costs in case of bad preventive operations, which is not as complicated as if the costs vary depending on the selected forecast.

The first PPOC occurs when, at the end of the period, the preventive turbine operation leads to a higher volume than the BasU reference series. In this case, the assumption to reach the maximum PPOC is that the rainfall is zero. Thus, the emptied volume difference (the difference between the turbine and bottom outlet operation series and the BasU series) will not be compensated at the end of the period.

The second potential cost appears when, at the end of the period, the proposed PrevOp series (turbinning plus bottom outlet opening) presents a higher volume than the BasU series. In this case, the assumption to reach the maximum PPOC is also that the rainfall is zero and the emptying volume (the difference between the two series) will consequently not be recovered at the end of the period.

These two cases are rather similar, both having PrevOp volumes higher than the reference ones (BasU series). However, the cost calculations will be different as presented hereafter.

The third case occurs when the proposed series (turbinning plus bottom outlet opening) delivers a smaller volume than the BasU reference series. Then, to obtain the maximum PPOC, it is assumed that the rainfall is high enough to fill up the reservoir and produce spillway flows. Consequently, it is assumed that the not turbinated BasU volume will have been lost after the end of the period.

This approach for PPOC has two main advantages for the decision maker. First, the given value is invariable for a proposed preventive action, not depending on the probabilistic inflows. As a result, it is easy to understand and to take into account. Secondly, this value corresponds to the upper limit of the potential costs and is therefore conservative. The lower limit equals to zero in some cases. The real final value, not known until the end of the period, will vary between the lower and the upper values depending on the observed inflow, real

market prices and implemented preventive actions. Moreover, it should be close to zero (low costs) in the case of good predictions and accurate preventive operations.

For achieving this estimate, the differences between the proposed PrevOp series and the BasU series are calculated (Eq. 6.10 to 6.12).  $V_{StopTurb}$  corresponds to the turbine discharge volume that has been retained due to the proposed series (it normally corresponds to the peak flow time).  $V_{PrevTurb}$  indicates the turbined discharge exceeding the BasU discharge, which usually matches the PrevOp before the flood peak.  $V_{PrevEmpt}$  denotes the bottom outlet discharge volume.

$$V_{StopTurb} = \sum_{interval=0}^{s_s} \int_{t=t_i}^{t=t_f} (Q_{BasU,t} - Q_{ProposedTurb,t}) dt \quad \text{with } Q_{BasU,t} \geq Q_{ProposedTurb,t} \quad \forall t \in (t_i, t_f) \quad 6.10$$

$$V_{PrevTurb} = \sum_{interval=0}^{s_p} \int_{t=t_i}^{t=t_f} (Q_{ProposedTurb,t} - Q_{BasU,t}) dt \quad \text{with } Q_{ProposedTurb,t} \geq Q_{BasU,t} \quad \forall t \in (t_i, t_f) \quad 6.11$$

$$V_{PrevEmpt} = \int_{t=0}^{t=t_{leadtime}} Q_{ProposedEmpt,t} dt \quad 6.12$$

with  $Q_{BasU}$ : Discharge series BasU [ $m^3/s$ ];  $Q_{ProposedTurb}$ : proposed turbining series for *PrevOp* [ $m^3/s$ ];  $Q_{ProposedEmpt}$ : proposed bottom outlet release series for *PrevOp* [ $m^3/s$ ];  $s_s$ : number of intervals during the concerned period with  $Q_{BasU} \geq Q_{ProposedTurb}$  [-];  $s_p$ : number of interval during the concerned period with  $Q_{ProposedTurb} \geq Q_{BasU}$  [-];  $t_i$ : starting time of an interval [h];  $t_f$ : ending time of an interval;  $t_{leadtime}$ : ending time of the studied period [h].

These volumes are used to calculate the potential costs due to PrevOp. The equations presented in the following for PPOC assume one power house per reservoir, with the aim of simplifying the definitions. When several power houses are connected to a reservoir, which is quite usual, the discharge volumes are related to their discharge capacity.

### Potential costs: case 1

If the proposed turbined series as PrevOp leads to a higher volume than the BasU series ( $V_{\text{PrevTurb}} \geq V_{\text{StopTurb}}$ ), case 1 appears. The PPOC is defined in Eq. 6.13 to 6.16:

$$E_1 = \rho \cdot g \cdot H_{HPP_h} \cdot V_{\text{StopTurb}} \cdot \eta_{HPP_h} \quad 6.13$$

$$E_2 = \rho \cdot g \cdot H_{HPP_h} \cdot (V_{\text{PrevTurb}} - V_{\text{StopTurb}}) \cdot \eta_{HPP_h} \quad 6.14$$

$$E_3 = \rho \cdot g \cdot H_{HPP_h} \cdot V_{\text{PrevEmpt}} \cdot \eta_{HPP_h} \quad 6.15$$

$$PPOC = E_1 \cdot (c_{\text{peak}} - c_{\text{base}}) + E_2 \cdot (c_{\text{pot}} - c_{\text{base}}) + E_3 \cdot (c_{\text{pot}}) \quad 6.16$$

with  $\rho$ : water density [ $\text{kg/m}^3$ ];  $g$ : gravity, [ $\text{m/s}^2$ ];  $\eta_{HPP_h}$ : plant efficiency [-];  $P_{HPP_h}$ : installed power capacity at  $HPP_h$ , belonging to concerned reservoir [ $\text{kW}$ ];  $E$ : energy production [ $\text{kWh}$ ];  $PPOC$ : potential preventive operation costs [ $\text{CHF}$ ].

Cost  $C_1$  corresponds to the displacement of the BasU series to another interval of the period and is considered as a permanent costs (Figure 6.2).

Costs  $C_2$  and  $C_3$  are potential, assuming no rain, or at least not enough for filling up the reservoir. If the reservoir is full at the end of the period, these two costs would be eliminated.  $C_2$  is due to the additional volume turbined as preventive operation during the period. The cost related to  $E_3$  corresponds to the emptying volume during the period, which is not sold, but just released.

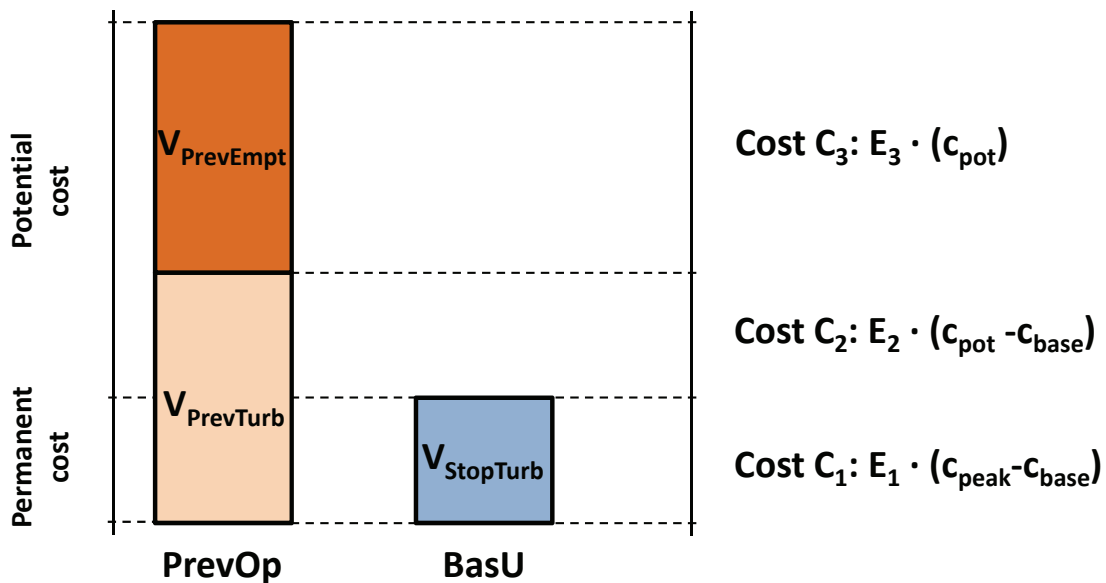


Figure 6.2 Potential costs due to the case 1 of preventive operations (BasU for Business as Usual operations and PrevOp for preventive operations).

**Potential costs: case 2**

Case 2 occurs if the proposed series as preventive operation leads to a higher volume than the BasU series ( $V_{PrevTurb} + V_{PrevEmpt} \geq V_{StopTurb}$ , but  $V_{PrevTurb} \leq V_{StopTurb}$ ). The PPOC is defined as follows:

$$E_1 = \rho \cdot g \cdot H_{HPP_h} \cdot V_{PrevTurb} \cdot \eta_{HPP_h} \tag{6.17}$$

$$E_2 = \rho \cdot g \cdot H_{HPP_h} \cdot (V_{StopTurb} - V_{PrevTurb}) \cdot \eta_{HPP_h} \tag{6.18}$$

$$E_3 = \rho \cdot g \cdot H_{HPP_h} \cdot (V_{PrevEmpt} + V_{PrevTurb} - V_{StopTurb}) \cdot \eta_{HPP_h} \tag{6.19}$$

$$PPOC = E_1 \cdot (c_{peak} - c_{base}) + E_2 \cdot (c_{peak}) + E_3 \cdot (c_{pot}) \tag{6.20}$$

In this case, the cost  $C_1$  presented in Figure 6.3 corresponds to  $E_1$  and concerns, as previously, the cost due to the displacement of the BasU turbinage. The cost related to  $E_2$  corresponds to the volume not turbinage in BasU and released by the bottom outlets.

The cost  $C_3$ , which could be zero at the end of the period if the rainfall fills up the reservoir, corresponds to a decrease of the storage volume due to bottom outlet releases.

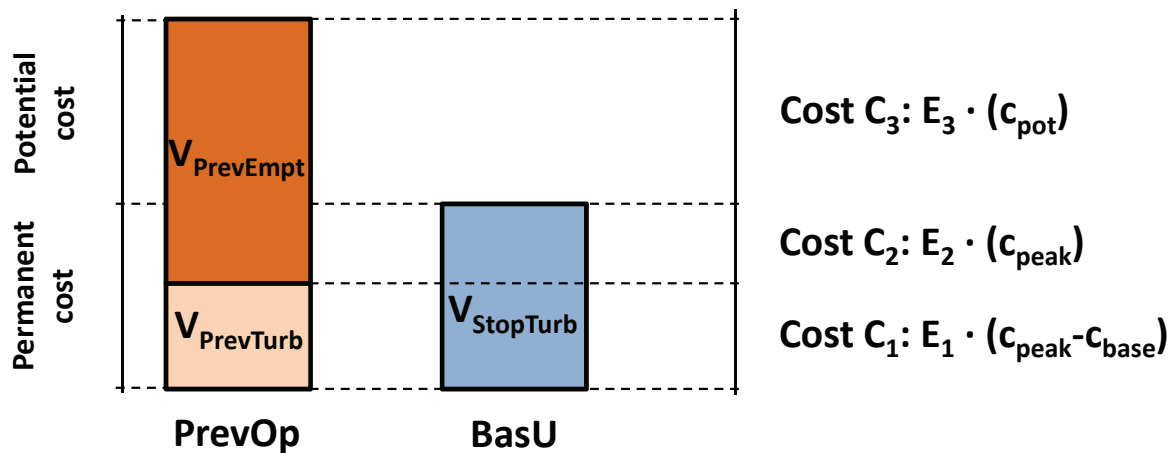


Figure 6.3 Potential costs in case 2 of preventive operations (BasU for Business as Usual operations and PrevOp for preventive operations).

### Potential costs: case 3

If the proposed PrevOp series furnishes a smaller volume than the BasU series ( $V_{StopTurb} > V_{PrevTurb} + V_{PrevEmpt}$ ), the case 3 is considered. The PPOC is then defined as follows:

$$E_1 = \rho \cdot g \cdot H_{HPP_h} \cdot V_{PrevTurb} \cdot \eta_{HPP_h} \quad 6.21$$

$$E_2 = \rho \cdot g \cdot H_{HPP_h} \cdot V_{PrevEmpt} \cdot \eta_{HPP_h} \quad 6.22$$

$$E_3 = \rho \cdot g \cdot H_{HPP_h} \cdot (V_{StopTurb} - V_{PrevTurb} - V_{PrevEmpt}) \cdot \eta_{HPP_h} \quad 6.23$$

$$PPOC = E_1 \cdot (c_{peak} - c_{base}) + E_2 \cdot (c_{peak}) + E_3 \cdot (c_{peak}) \quad 6.24$$

The cost related to  $E_1$  is due to the displacement of the BasU turbinning (Figure 6.4). The cost  $C_2$  corresponds to the released volume by bottom outlet opening and not turbinned as BasU.

The cost  $C_3$  corresponds to the not turbinned BasU volume. It could be removed if the volume could be sold in the future (after the end of the optimisation period).

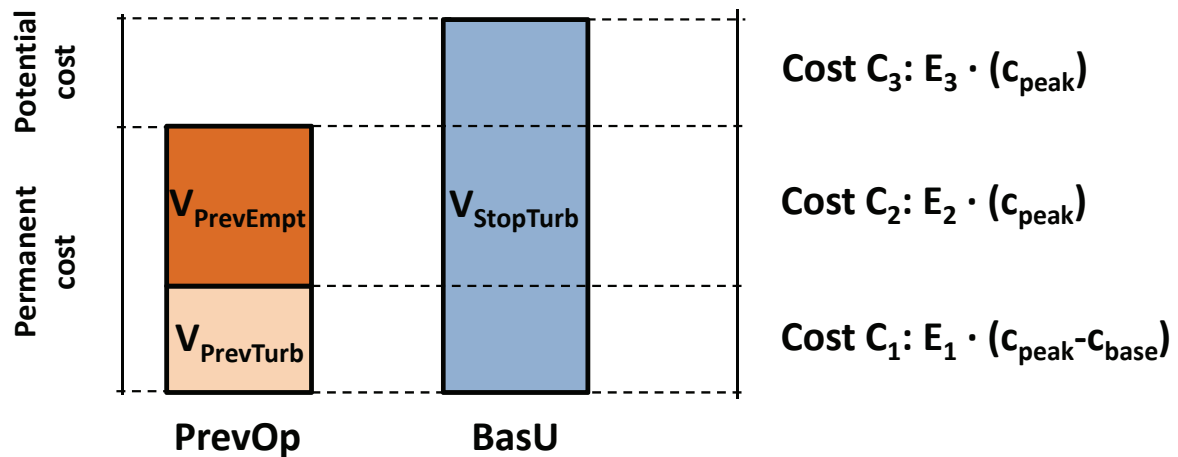


Figure 6.4 Potential costs because the case 3 of preventive operations (BasU for Business as Usual operations and PrevOp for preventive operations).

### Total potential costs

As explained before, it is assumed that the PPOC does not vary for different forecasts. Then, the potential costs for a group of reservoirs  $g$  related to the energy losses due to PrevOp are computed according to Eq. 6.25 and the total costs for all optimised groups are summarized in Eq. 6.26.

$$PPOC_{GR_g}(a_{i,GR_g}) = \sum_{r=1}^{r=v} PPOC_{RES_r, RES_r \in GR_g}(a_{i,RES_r}) \quad 6.25$$

$$PPOC(a_{i,set}) = \sum_{g=1}^{g=s} PPOC_{GR_g}(a_{i,GR_g}) \quad 6.26$$

with  $a_{i,RES_r}$ : preventive operation  $i$  in the reservoir  $r$ ;  $a_{i,GR_g}$ : set  $i$  of PrevOp in the reservoirs of group  $g$ ;  $v$ : total number of reservoirs in group  $g$  [-];  $s$ : total number of groups to be optimised [-].

### 6.3.3 Global loss function

The global loss function, expressed as economical value, is defined as the summation of expected damages and potential preventive operations costs. A weight factor coefficient  $\beta$  ( $\beta \geq 1$ ) for the PPOC has been introduced to provide the possibility of increasing the weight of the PPOC value compared to damages. This coefficient could be used by decision maker with the aim of decreasing the possibility of wrong preventive operations. If  $\beta$  is equal to one, the theoretical final cost is assumed as real. Otherwise, if  $\beta$  is higher than one, a higher weight is given to the PPOC, assuming than the decision maker gives a higher importance to this value than to the real one.

The final function value for a given combination of preventive operations ( $a_{i,set}$ ) depending on a forecast  $j$  is then defined in Eq. 6.27.

$$m(a_{i,set} | f_j) = ED(a_{i,set} | f_j) + \beta \cdot PPOC(a_{i,set} | f_j) \quad 6.27$$

with  $m$ : final function value for the set  $a_{i,set}$  with the forecast  $j$  [CHF];  $\beta$ : preventive operation costs coefficient [-].

The objective function consists in the minimization of the selected global function, explained hereafter in section 6.4, taking into account all forecasts, for obtaining the optimal set of variables  $a_{i,set}$  related to it.



## 6.4 Multi-Criteria Optimisation

### 6.4.1 Perception of the objective function

As explained in section 3.5, the Multi-Attribute Decision Making (MADM) methodology (McCrimmon, 1968, 1973) is chosen for defining the utility function of the system. Before presenting the methods retained for this research project, the general overview of the problem is introduced.

When deterministic forecasts are evaluated, the definition of the utility function and its minimization (objective function) is easily solved. The goal is to decrease the value of the utility function to the minimum loss (as represented by the arrow in Figure 6.5), i.e. to search the optimal parameters which minimise the function value as much as possible. The goal could be also to increase the difference between the value of the function and the maximum possible loss. In the deterministic case, these two options give the same result.

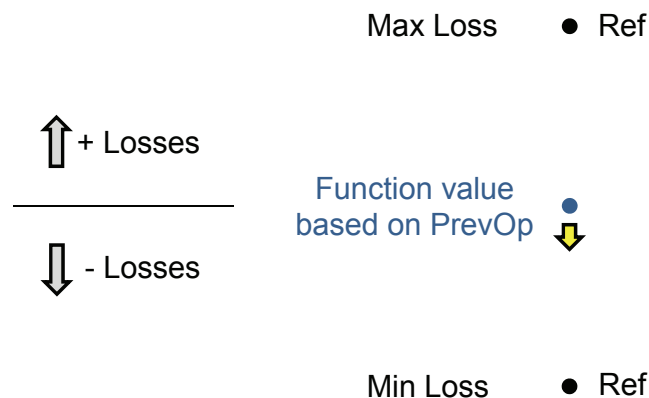


Figure 6.5 Example of a deterministic optimisation with references (Ref) values.

However, the resolution of the problem becomes more complicated when probabilistic values (for forecasts) are used. The best and worst options are not anymore a value but a set of values; and the function value also becomes a set depending on the number probabilistic forecast. Figure 6.6 presents the values of the functions by assuming a box plot graphic representing the distribution of all forecast values. It has to be noticed that the set of minimum (or maximum) theoretical losses give a reference alternative which is not real. In fact, for each forecast of the set, the best decision (or worst) is searched among all alternatives, but it will not be necessarily the same for all forecasts.

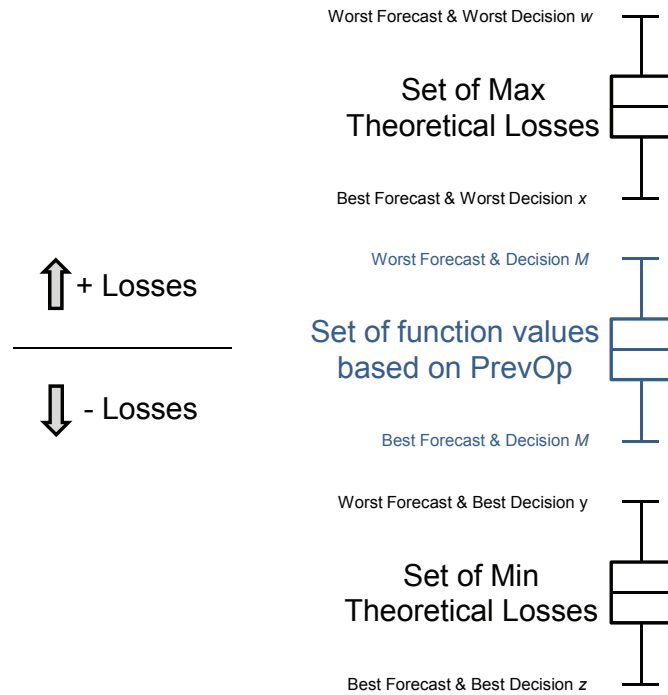


Figure 6.6 Example of a probabilistic optimisation and the possible sets of references taken into account, with the sign + representing a combination of forecasts and decisions.

In reality, limit values could be superimposed as presented in Figure 6.7. For example, the set of function values based on PrevOp could provide a high value for the worst forecast assuming high losses. This value could be higher than one of the set of Maximum Theoretical Losses for a forecast with a low discharge and therefore small potential losses.

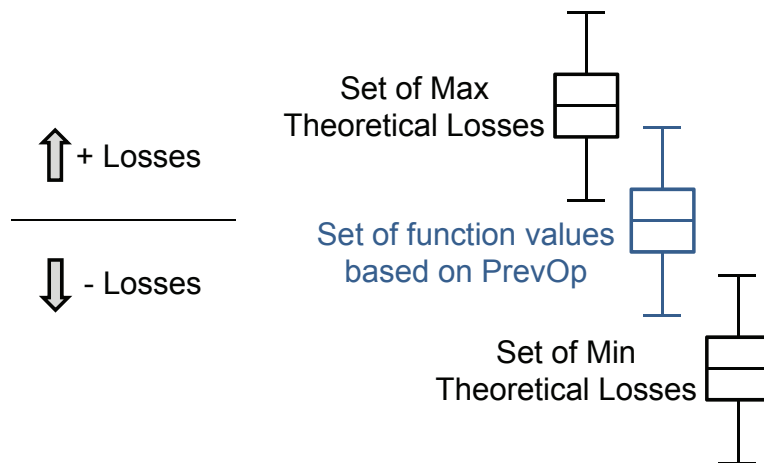


Figure 6.7 Example of a probabilistic optimisation with “crossed” values depending on the forecasts.

### **6.4.2 Review of algorithms for Multi-Attribute Decision Making**

The most commonly used traditional MADM methods are: Bayes risk criterion (also called expected mean value), Laplace criterion, Maximin criterion (or pessimistic criterion), Maximax criterion (or optimistic criterion), decision maker criterion, Hurwicz criterion, Minimax regret criterion (also named Savage principle), ELECTRE, TOPSIS, fuzzy logic, etc. The goal of these methods is to define a final unique utility function taking into account all values of the set or the most representative values weighted by different coefficients.

#### ***Bayes Risk and Laplace's criteria***

The Bayes risk criterion, or expected mean value, calculates the weighted average of all possible values (final loss) that a simulation with a set  $i$  of preventive operations can take for different forecasts. This method has not to be confused with the Bayesian theory which implements conditional probabilities.

The arithmetical mean of all possible values is called Laplace's Criterion, assuming the same probability for each scenario (for each forecast member in the present project).

#### ***Minimax, Maximax and Minimin criteria***

Regarding costs minimization, the pessimistic criterion, trying to maximize the minimum benefit, becomes the Minimax regret Criterion, which minimizes the maximum costs. Weighting is not used in this methodology.

The optimistic criterion is impractical in costs minimization problems, such as flood damage problems. The optimistic criterion (or Maximax), which maximizes the maximum benefit, should be changed to Minimin, which minimizes the minimum costs. However, such optimisation would not be reasonable in flood control.

#### ***Decision Maker Criterion***

The Decision Maker Criterion is based on the acceptable risk defined by the decision maker according to a maximum probability of occurrence of a pre-defined discharge and/or damage (Morss et al., 2005; Mediero et al., 2007). The concept of acceptable risk is becoming more popular than preset levels of protection associated with a specific probability of occurrence, e.g., the 100-year flood (United Nations, 2004).

### ***Hurwicz Criterion***

Hurwicz criterion (Hurwicz, 1951) combines both the Maximax and Maximin criteria. The decision maker is neither optimistic nor pessimistic. With this criterion, the decision attributes are weighted by coefficients  $\tau$  and  $(1-\tau)$  defined by the decision maker, e.g.,  $\tau$  for the Maximax and  $(1-\tau)$  for the Maximin. When  $\tau$  is equal to one, the configuration using the Maximax criterion is selected, assuming an optimistic decision maker. Inversely, when  $\tau$  is equal to zero, a pessimistic decision maker is assumed and the Maximin criterion chosen.

For the present research project, the Hurwicz criterion with this combination is not plausible. Nevertheless, the combination could be obtained by the Minimax regret and the expected mean value criteria, so-called hereafter Hurwicz Derived for Floods (HDF).

### ***ELimination Et Choix Traduisant la REalité - ELECTRE***

The multi-criteria decision making ELECTRE method was developed in the 60's (Roy, 1968). The acronym ELECTRE stands for: ELimination Et Choix Traduisant la REalité (ELimination and Choice Expressing Reality). This method has two main steps. The first is the construction of one or more outranking relations which compares in a comprehensive way each pair of actions. The second step elaborates recommendations obtained during the first one. The nature of the recommendation depends on the problem being addressed: choosing, ranking or sorting. The main goal is then to select those alternatives which are preferred for most of the criteria without violating an acceptable level of discontent for any criterion. This procedure is performed by comparing pair-wise alternatives among members of a set of alternatives, and eliminating a subset of less desirable ones (Ko and al, 1994). This method was compared to the fuzzy approach by Bender and Simonovic (2000), with equal consistency of results for both cases.

### ***Analytic Hierarchy Process - AHP***

The Analytic Hierarchy Process (AHP) was first proposed by Saaty (1977, 1980). The basic idea is to convert subjective assessments of relative importance to a set of overall scores or weights. The methodology is also based on pair-wise comparisons. The evaluation is thus realised between two alternatives rather than evaluating all alternatives simultaneously. The weights are established in order to assess the performance scores for alternatives on the subjective criteria. However, many authors have criticized some fundamental aspects of AHP

(Stewart, 1992), being the axiomatic basis of this method different from that of the utility theory developed in MADM approaches.

### ***Technique for Order Preference by Similarity to Ideal Solution -TOPSIS***

The multi-attribute decision making TOPSIS (Technique for Order Preference by Similarity to Ideal Solution) was developed by Hwang and Yoon (1981). It solves the problem with an intuitively appealing procedure. Its fundamental premise is that the best alternative should have the shortest Euclidean distance  $S_s$  from the ideal solution (made up of the best value for each attribute regardless of alternative) and the farthest distance  $S_f$  from the anti-ideal solution (made up of the worst value for each attribute). The alternative with the highest relative closeness measure  $S_f / (S_f + S_s)$  is chosen (Zanakis et al., 1998). An extension of TOPSIS for group decision making (Shih et al., 2007) was conducted recently with the same criterion. A case of water management in Brazil was also treated using this methodology (Srdjevic et al., 2004).

Zanakis et al. (1998) compared the expected mean value method, AHP, ELECTRE and TOPSIS. They conclude that the distribution of criteria weights affects the performance measures less than the number of alternatives or the number of criteria. However, it differently affects the examined methods, producing a variation in the ranking results. Nevertheless, results of the method's performances cannot be extrapolated since the type of MADM problem can considerably affect the performance and results.

Accordingly to Shih et al. (2007), TOPSIS offers several advantages among other multi-attribute algorithms: a sound logic that represents the rationale of human choice, a scalar value that accounts for both the best and worst alternatives simultaneously and a simple computation process that can be easily programmed. Thus, these advantages make TOPSIS a major MADM technique compared with other related techniques such as AHP and ELECTRE.

### ***Fuzzy Theory***

Fuzzy set theory was first introduced by Zadeh (1965) because the precise quantification of many system performance criteria and parameters was not always possible. When they cannot be precisely specified, they are said to be uncertain or fuzzy.

If the values are uncertain, probability distributions can be used to quantify them. Alternatively, if they are best described by qualitative adjectives, such as dry or wet, hot or

cold and high or low, fuzzy membership functions can be also used to quantify them. Both probability distributions and fuzzy membership functions of these uncertain or qualitative variables can be included in quantitative optimisation models (Loucks and Beek, 2005).

The fuzzy theory has been largely used in projects related to water resources management, such as: the optimal modelling of the flood system of the upper and middle reaches of the Yangtze River (Cheng, 1999); the multi-objective conflict decision for reservoir flood control and its application to the Fengman reservoir located in the Songhua River Basin in China (Cheng and Chau, 2002); the flood management in the Red River Basin in Manitoba, Canada (Akter and Simonovic, 2005); the flood control operations of the Fengman reservoir (Yu et al., 2004); the flood operations in the Sanmenxia reservoir, in the middle reach of the Yellow River in China (Fu, 2008); the spillway gates operation of the Adana Catalan Dam, in Turkey, during floods (Karaboga et al., 2008); the release optimisation in the Jayakwadi reservoir in India (Regulwar and Kamodkar, 2010); or the real-time hydropower reservoir operation in Dez reservoir in Iran (Moeini et al., 2011). In most of these applications, fuzzy logic is operated with a formulation similar to TOPSIS. Thus, the difference between TOPSIS and fuzzy chiefly lies in the rating approaches. The merit of fuzzy is to assign the importance of attributes and the performance of alternatives with respect to various attributes by using fuzzy numbers instead of precise numbers (Chen and Tsao, 2008).

Nevertheless, the Fuzzy Theory generally deals with different objectives and different decision makers' points of view, especially when working with subjective objectives. When having different attributes representing each member of the ensemble forecasts, the weights are usually given and the uncertainty linked to fuzzy logic does not theoretically exist.

The TOPSIS approach could then be used as a "certain" approach to the Fuzzy Theory. In fact, in literature, the same approach is sometimes hidden behind these two names when Fuzzy Theory uses the same formulation as in the TOPSIS case. For example, Cheng (1999) explains that the resolution for the better alternative of the fuzzy logic problem could be achieved "when the weight vector  $w$  is known from experience or in some other manner". Yu et al. (2004) also studied the fuzzy method, developing the optimal decision for a given decision maker which provides the weight vector for the objectives (the paper goes then far away with more than one decision maker). Since in this method the procedure and equations are equivalent, that is exactly TOPSIS! Others papers describe correctly this difference and propose the extension of TOPSIS methodology to TOPSIS fuzzy methodology (Chen, 2000; Yang and Hung, 2007; Fu, 2008; Jadidi et al., 2008).

**Notation simplification of global loss function**

For the explanation hereafter about the MADM criteria, the value  $m$  of the utility function (Eq. 6.27) depending on the studied preventive operation (set  $i$ ) and on forecast  $j$  is simplified as follows:

$$m_{i,j} = m(a_{i,set} | f_j) \quad 6.28$$

$$w_j = P(f_j) \quad 6.29$$

with  $m_{i,j}$ : final function value for the set  $a_{i,set}$  with the forecast  $j$  [CHF];  $w_j$  and  $P(f_j)$ : occurrence probability of forecast  $j$  [-].

**6.4.3 Selected MADM methods for MINDS****Methods selected for the definition of the objective function**

As a result of the review of existing methods found in literature, different approaches have been selected and tested for the definition of the objective function: Bayes Risk Criterion (BRC), MinMax Regret (MMR), Decision Maker Criterion (DMC), Hurwicz Derived for Floods (HDF) and TOPSIS.

The five selected approaches can be graphically explained as presented in Figure 6.8. BRC tries to decrease the expected mean value to obtain a minimum loss. MMR minimizes the loss produced by the worst forecast. DMC minimizes a mean value without taking into account a defined percentage of higher values of the set determined by the decision maker. HDF combines the last two approaches, minimizing both of them depending on a given weight factor. Finally, TOPSIS seeks to minimize distances between the set of losses (for a given ensemble forecast) and the set of theoretical minimum losses as well as to maximize distances to the set of theoretical maximum losses.

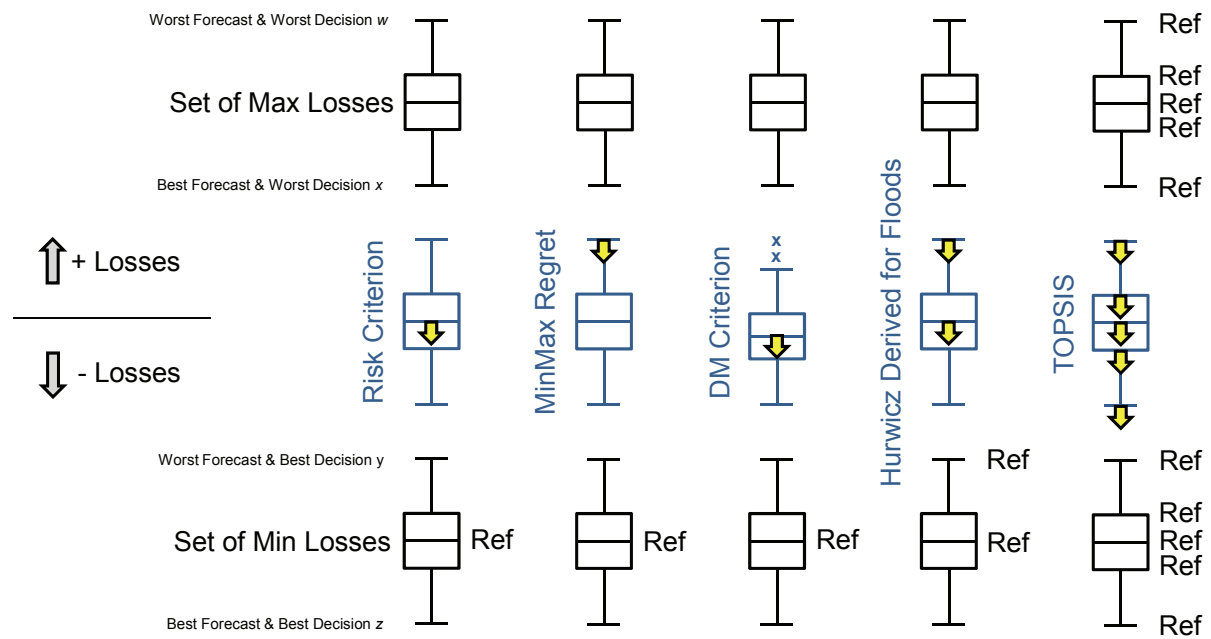


Figure 6.8 Overview of methods of multi-attribute decision making implemented in MINDS. The objective function reduces the set of economical losses in a different way depending of the selected method.

### Bayes Risk Criterion (BRC)

The expected mean value is usually called the Bayes Risk Criterion (BRC), since Thomas Bayes was the first decision theorist to advocate the expectation principle for decision making. This Bayes risk is assumed as the computed mean risk (since all occurrence probabilities are known) and has not to be confused with the Bayesian theory.

The optimal solution is then the one that minimizes the Bayes risk. In the MINERVE system, the risk  $r$  for the expected damages and PPOC in the whole basin upstream of the selected check point for a given decision  $i$  are computed according to Eq. 6.30.

$$r_i = \frac{1}{n_f} \cdot \sum_{j=1}^{j=n} (m_{i,j} \cdot w_j) \quad 6.30$$

with  $r_i$ : risk for the set  $i$  of preventive operations [CHF];  $n_f$ : total number of forecast members [-].

Minimizing  $r_i$  results in the objective function of the system  $R$  defined as:

$$R = \min_i (r_i) \quad 6.31$$

The BRC identifies the ideal preventive operations for the ensemble hydrological forecasts based on a risk assessment which depends on expected damages, potential costs and the occurrence probability of the forecasts taken into account.



When the probability associated with the scenarios is not available or the decision maker decides to not take them into account, the equal probability for each scenario can be assumed. Then, the optimal solution is the one minimizing the arithmetical mean of costs over all forecasts (Laplace's Criterion).

**MinMax Regret (MMR)**

The Savage MinMax Regret criterion, also so-called the Savage Principle (Savage, 1951), is generally used for uncertain decision problems where both the decision states and their likelihoods are unknown. For current utility function minimization, this criterion corresponds to the pessimistic criterion. Thus, the Minimax Regret selects the alternative that contains the best (the minimum) of the worst possible losses (the higher losses).

$$d_i = \max_j (m_{i,j}) \tag{6.32}$$

with  $d_i$ : maximum value given by the set  $i$  of preventive operations for all possible forecasts [CHF].

The objective function becomes here:

$$D = \min_i (d_i) \tag{6.33}$$

**Decision Maker Criterion (DMC)**

This criterion is based on an accepted risk chosen by the decision maker. A loss threshold  $L_t$  preassumed as zero (starting of overflowing) is considered. Then, the decision maker determines an acceptable percentage of occurrence probability exceeding it, according to Eq. 6.34. The worst forecasts (higher losses values) exceeding the occurrence probability threshold are not taken into account in this criterion.

$$z_i = \frac{1}{n_f^*} \cdot \sum_{j=1}^{j=n^*} (m_{i,j} \cdot w_j) \quad \text{with } n_f^* = \min n_f / \sum_{j=1}^{j=n_f^*} w_j \geq 1 - \varphi \tag{6.34}$$

with  $z_i$ : risk associated to the set  $i$  of preventive operations taking into account a certain number of forecasts [CHF] ;  $n_f^*$ : number of forecast members taken into account [-];  $\varphi$ : decision maker accepted coefficient [-].

Minimizing  $b_i$  results in the objective function of the system,  $B$ , defined as:

$$Z = \min_i (z_i) \tag{6.35}$$

**Hurwicz derived for floods criterion (HDF)**

According to this criterion, the best strategy is the one minimizing the linear combination between the expected mean loss and the maximum loss according to the objective function presented in Eq. 6.36.

$$H = \min_i (\tau \cdot (r_i) + (1 - \tau) \cdot (d_i)) \tag{6.36}$$

with  $\tau$ : HDF weight coefficient [-].

When  $\tau$  is equal to one, the BRC criterion is used. With this criterion, the decision maker selects the design representing the expected mean value criteria. When the Hurwitz weight  $\tau$  is equal to zero, the MinMax Regret Criterion is chosen.

**TOPSIS**

For MINERVE, a new utilisation of TOPSIS with hydrological ensemble forecasts for decision making under probabilistic forecasts is proposed. Thus, it is assumed that the forecasts correspond to the attributes of the problem.

The multi-attribute decision making problem can be expressed in a matrix, combining all the attributes (or forecasts) of the system as well as all the possible alternatives to minimize the costs, as follows:

$$\begin{array}{c}
 \text{Alternatives} \\
 \mathbf{A}_T =
 \end{array}
 \begin{array}{c}
 \text{Forecasts (attributes)} \\
 \mathbf{f}_1 \quad \mathbf{f}_2 \quad \dots \quad \mathbf{f}_j \quad \dots \quad \mathbf{f}_n \\
 \left[ \begin{array}{cccccc}
 \mathbf{a}_1 & m_{1,1} & m_{1,2} & \dots & m_{1,j} & \dots & m_{1,n} \\
 \mathbf{a}_2 & m_{2,1} & m_{2,2} & \dots & m_{2,j} & \dots & m_{2,n} \\
 \cdot & \cdot & \cdot & \cdot & \cdot & \cdot & \cdot \\
 \cdot & \cdot & \cdot & \cdot & \cdot & \cdot & \cdot \\
 \mathbf{a}_i & m_{i,1} & m_{i,2} & \dots & m_{i,j} & \dots & m_{i,n} \\
 \cdot & \cdot & \cdot & \cdot & \cdot & \cdot & \cdot \\
 \cdot & \cdot & \cdot & \cdot & \cdot & \cdot & \cdot \\
 \mathbf{a}_m & m_{m,1} & m_{m,2} & \dots & m_{m,j} & \dots & m_{m,n}
 \end{array} \right]
 \end{array}
 \tag{6.37}$$

with  $A_T$ : matrix of function values depending on alternatives and forecasts [CHF];  $a_1, a_2, \dots$ : alternatives (preventive operation sets) [-];  $f_1, f_2, \dots$ : forecasts [-];  $m_{i,j}$ : function value depending on the preventive operation studied (set or alternative  $i$ ) and on a forecast  $j$  [CHF].

Furthermore, the weights related to each forecast are generally given by the forecast provider, as it is the case for the MeteoSwiss forecast, even if they can be changed by the decision maker in any case.

$$\mathbf{W} = \begin{matrix} & \text{Forecasts (attributes)} \\ & \mathbf{f}_1 & \mathbf{f}_2 & \dots & \mathbf{f}_j & \dots & \mathbf{f}_n \\ \begin{bmatrix} \\ \\ \\ \end{bmatrix} & w_1 & w_2 & \dots & w_j & \dots & w_n \end{matrix} \quad 6.38$$

with  $W$ : vector of forecast weights [-].

Then, it is necessary to normalize the decision making matrix. This operation generally calculates the higher and smaller values for a given attribute (for a forecast in the presented case) among all alternatives. However, in the present research project, it would produce inaccurate results because the normalisation of different forecasts would induce the same performance for an alternative decreasing a flood peak from 1000 to 500 m<sup>3</sup>/s, than for decreasing it from 100 to 50 m<sup>3</sup>/s. For that reason, the normalisation is completed with the next minimum and maximum values (Eqs. 6.39 and 6.40), calculated by taking into account the whole matrix.

$$x_{\max} = \max(m_{i,j}) \quad 6.39$$

$$x_{\min} = \min(m_{i,j}) \quad 6.40$$

with  $x_{\max}$  and  $x_{\min}$ : calculated values for the normalisation of the matrix [CHF].

The normalised values of the matrix elements will thus be as presented in Eq. 6.41:

$$s_{i,j} = 1 - \frac{m_{i,j} - x_{\min}}{x_{\max} - x_{\min}} \quad 6.41$$

The theoretical ideal alternative  $G$  ( $g_1, g_2, \dots, g_n$ ) is defined in Eq. 6.42, where each of its values represents the maximum normalised value of a forecast among all the alternatives. The anti-ideal alternative  $B$  ( $b_1, b_2, \dots, b_n$ ) is defined in Eq. 6. 43 in the same way. It is evident that the closer the alternative  $a_i$  is to  $G$ , the better the alternative  $a_i$ , and *vice versa* for  $B$ .

$$g_j = \max_i (s_{i,j}) \quad 6.42$$

$$b_j = \min_i (s_{i,j}) \quad 6.43$$

The normalised matrix and vectors  $G$  and  $B$  can be presented as follows:

$$\begin{array}{c} \text{Alternatives} \\ \mathbf{N}_T = \end{array} \begin{array}{c} \text{Forecasts (attributes)} \\ \mathbf{f}_1 \quad \mathbf{f}_2 \quad \dots \quad \mathbf{f}_j \quad \dots \quad \mathbf{f}_n \\ \left[ \begin{array}{cccccc} \mathbf{a}_1 & s_{1,1} & s_{1,2} & \dots & s_{1,j} & \dots & s_{1,n} \\ \mathbf{a}_2 & s_{2,1} & s_{2,2} & \dots & s_{2,j} & \dots & s_{2,n} \\ \cdot & \cdot & \cdot & \cdot & \cdot & \cdot & \cdot \\ \cdot & \cdot & \cdot & \cdot & \cdot & \cdot & \cdot \\ \mathbf{a}_i & s_{i,1} & s_{i,2} & \dots & s_{i,j} & \dots & s_{i,n} \\ \cdot & \cdot & \cdot & \cdot & \cdot & \cdot & \cdot \\ \cdot & \cdot & \cdot & \cdot & \cdot & \cdot & \cdot \\ \mathbf{a}_m & s_{m,1} & s_{m,2} & \dots & s_{m,j} & \dots & s_{m,n} \end{array} \right] \end{array} \quad 6.44$$

$$\mathbf{G} = \left[ \begin{array}{cccccc} g_1 & g_2 & \dots & g_j & \dots & g_n \end{array} \right] \quad 6.45$$

$$\mathbf{B} = \left[ \begin{array}{cccccc} b_1 & b_2 & \dots & b_j & \dots & b_n \end{array} \right] \quad 6.46$$

with  $N_T$ : Normalised matrix [-];  $G$ : theoretical ideal alternative [-];  $B$ : theoretical anti-ideal alternative [-].

The difference between the vector of alternative  $a_i$  and the vector  $G$  can be then expressed as a general Euclidean weighted distance as presented in Eq. 6.47, which denotes the distance from optimum to alternative  $a_i$  with  $n$  attributes (forecasts in this research project).

$$dG_i = \left[ \sum_{j=1}^n [w_j \cdot (g_j - s_{i,j})]^2 \right]^{1/2} \quad 6.47$$

Similarly, the difference between alternative  $a_i$  and  $B$  is defined in Eq.6.48:

$$dB_i = \left[ \sum_{j=1}^n [w_j \cdot (s_{i,j} - b_j)]^2 \right]^{1/2} \quad 6.48$$

Then, in order to solve the optimal alternative, the calculation procedure can be completed as presented by Cheng (1999) or Yu et al. (2004), being the final membership degree for the alternative  $a_i$  presented in Eq. 6.49 or equivalently in Eq. 6.50:

$$u_i = \frac{1}{1 + \frac{\sum_{j=1}^n [w_j \cdot (g_j - s_{i,j})]^2}{\sum_{j=1}^n [w_j \cdot (s_{i,j} - b_j)]^2}} \quad 6.49$$

$$u_i = \frac{1}{1 + \frac{dG_i}{dB_i}} \quad 6.50$$

with  $u_i$ : membership degree for the alternative  $a_i$  [-].

or, if the expression is presented in the classical way of TOPSIS (Zanakis et al., 1998; Chen, 2000; Shih et al., 2007):

$$u_i = \frac{dB_i}{dG_i + dB_i} \quad 6.51$$

According to the definition,  $u_i$  varies between zero and one. The larger the index value, the better the performance of the alternative is. Thus, the objective function becomes:

$$U = \max_i (u_i) \quad 6.52$$

For having a minimization objective function, as performed in all the selected MADM methods of the system, equation 6.52 can be changed to:

$$U^* = \min_i (1 - u_i) \quad 6.53$$

## 6.5 Optimisation process of MINDS

### 6.5.1 System optimisation

Independently from the selected optimisation algorithm (Greedy or SCE-UA) and the MADM method chosen (BRC, MMR, DMC, HDF or TOPSIS), the aim of the system is to find the optimal set of variables  $a_{i,set}$  which produces the lowest flood damage with the lowest potential preventive operation costs.

Once a check point (CP) is selected, the objective is to optimise the whole upstream basin. Only the upstream CPs are taken into account for damage calculation as well as the upstream hydropower groups.

The simulation is performed in the whole basin even if not all the CPs are taken into account for damage calculation. The hydropower groups located downstream the selected CP are simulated with Business as Usual operations.

Furthermore, the decision maker can also deselect any hydropower group considered as not necessary/possible to manage. As a last option, the decision maker can also use an external proposition for turbine operation for one or several groups.

### 6.5.2 Reference simulations of natural basin and equipped basin

As explained in section 6.2.2, the discharge at CPs in the natural basin (from Routing System MINERVE with the natural basin) is taken into account as initial condition for the discharge calculation in the equipped basin. The Routing System MINERVE software with the equipped basin provides the inflows into the reservoirs. These two inputs are fixed for the whole optimisation due to their independency to reservoir operations.

The reservoir operations by BasU or PrevOp are the basis for the simulations to achieve an optimisation.

The BasU operation for hydropower plants is assumed as follows. The peak discharge is operated as a percentage of the maximum discharge of the turbines, according to a coefficient  $\gamma$ , and becomes then  $\gamma \cdot Q_{max}$  [m<sup>3</sup>/s]. This coefficient has been pre-defined as a value of 0.5. The base discharge is assumed as zero.

Based on the Swiss market (Office Fédéral de l'Economie Hydraulique, 1996), the periods of BasU operations are simplified and assumed as proposed in Table 6.5.

Table 6.5 Periods of peak and base turbine discharge for the Business as Usual operations

Type	Period	Time
Peak	{ Monday-Friday	08h – 18h
Base	{ Monday-Friday	00h – 08h & 18h - 24h
	{ Weekend	00h - 24h

Finally, the proposed PrevOp series are built according to the optimised parameters. These simulations, in contrast to the BasU simulation which is realized just once, are iteratively performed for the optimisation of the required parameters for flood minimization.

### **6.5.3 Description of main model parameters**

For the optimisation, some general parameters have to be selected before the calculation.

#### ***Selected CP***

First, the decision maker has to select the downstream CP, which defines the basin to be optimised. As default value, it is defined Porte-du-Scex, which is the most downstream check point at the outlet of the Upper Rhone River basin.

#### ***Duration for the optimisation***

The duration is pre-established to three days, but can be changed from one to ten days. The usual optimisation duration corresponds to three or five days, which are the lead times for the deterministic and the probabilistic forecasts respectively.

#### ***Type of forecast***

If all forecasts are available, the decision maker can use all or only selected scenarios. The system accepts one deterministic and one probabilistic forecast, but more forecasts could be included if required. Then, the decision maker can run all forecasts or just one.

If the probabilistic forecast is selected, the number of members of the forecast has to be mentioned. It is pre-defined as 16, which is the number of COSMO-LEPS members. Furthermore, the weights for the probabilistic forecasts have to be provided. The decision maker can also choose equal probability for all members of the forecast.

Finally, if both forecasts are selected, the decision maker has to provide a weight factor for each one. A pre-defined values of 1/17 for deterministic and 16/17 for probabilistic are set as default, but they can be changed at any moment.

#### ***PPOC coefficient***

The PPOC weight factor  $\beta$  can also be modified by the decision maker. The pre-defined value is fixed to one.

#### ***Safety coefficient of overflowing***

The safety coefficient for overflowing,  $s_{fl}$ , can be modified by the decision maker and defines the final critical discharge of flooding,  $s_{fl}Q_{fl}$ . The pre-defined value is fixed to one.

**Market prices**

The time periods for energy prices have been defined previously for BasU operations (Table 6.4). The values for the prices corresponding to approximate Swiss market prices are presented in Table 6.6.

Table 6.6 Theoretical values of electricity prices

Type	Price
Potential price ( $c_{pot}$ )	0.10 CHF / kWh
Peak price ( $c_{peak}$ )	0.10 CHF / kWh
Base price ( $c_{base}$ )	0.02 CHF / kWh

**6.5.4 Preventive operation parameters**

Regarding operation of turbines, the initial state is assumed as the BasU series. PrevOp can start from any time of the studied period. Then, they have a variable duration, from where a turbines stop period can be proposed. From this moment until the end of the concerned period, the initially defined BasU series is maintained.

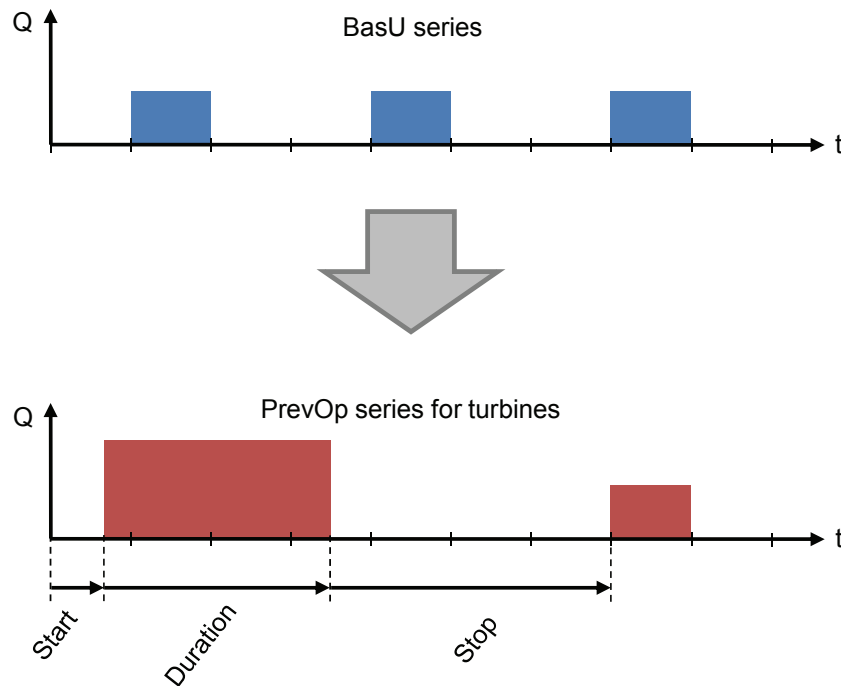


Figure 6.9 BasU turbine operation series becomes the proposed PrevOp turbine operation series

Concerning the bottom outlet operations, the initial state is assumed as inactive (null series). PrevOp of bottom outlets can start at any time of the interval with an adaptable duration.



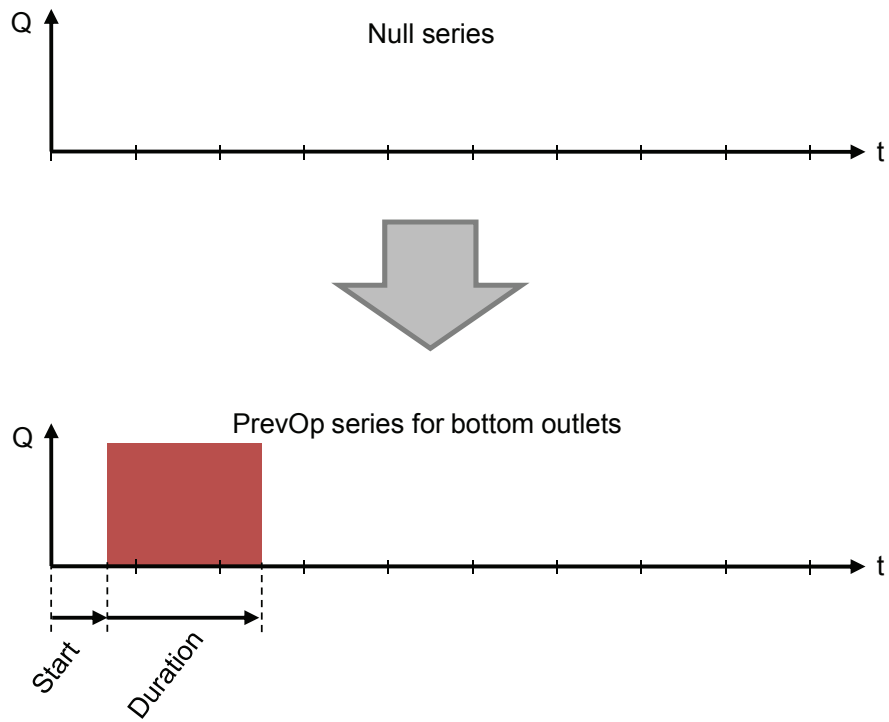


Figure 6.10 Final PrevOp of bottom outlets from an initial null series

Concerning the pump operation, the initial state is also assumed as a null series. PrevOp pump operation starts at the ending time of the preventive turbine operation with a flexible duration.

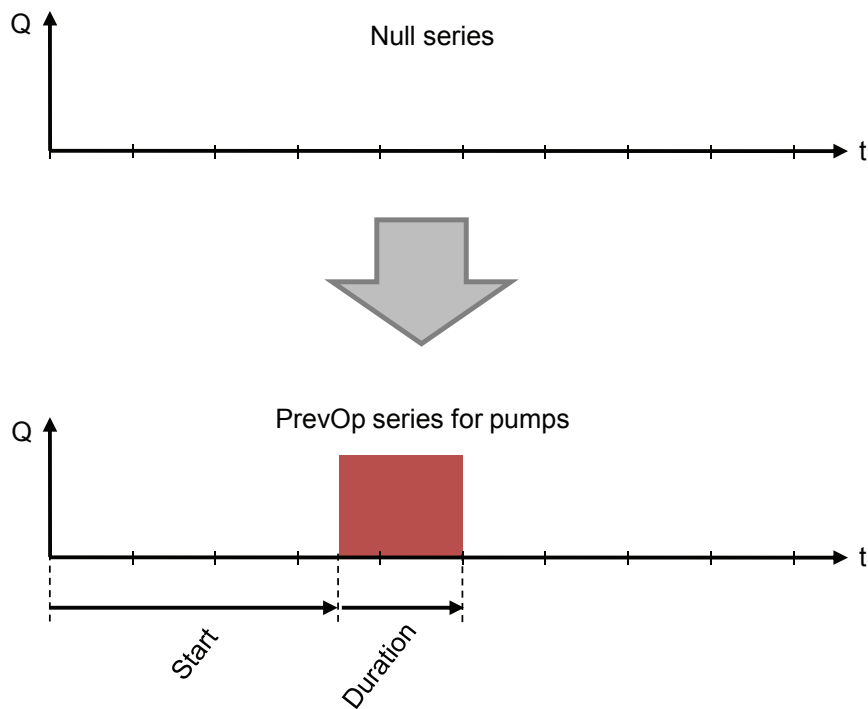


Figure 6.11 Final PrevOp of pumping from an initial null series

These three sequences are optimised in series, starting from the turbines operations, next the bottom outlet operations (re-evaluating the stop turbine period) and finally the pumping operations.

### ***Solution space of feasible parameters***

In order to produce only feasible solutions and reduce the possible solution space of parameters as much as possible for decreasing the calculation time, the following assumptions are made:

- Starting time of turbine and bottom outlet operation: from zero to a defined value (pre-defined as 24 h). The space solution with a higher starting time is not considered as logical because the update of the optimisation is produced before and no PrevOp would be produced until this update time.
- Duration of turbine and bottom outlet operation: from zero to a defined value, pre-defined as 48 h. Due to continuous update optimisation orders and the capacity of reservoirs, the time necessary for optimisation is generally not more than 48 h.
- Periods of turbines stop: from the end time of the PrevOp of turbinning, an interval of turbines stop can be defined for the turbines. It assumes the stop any turbine activities. Three periods of the BasU series are set as default.
- Duration of pumping: from zero to a defined value, pre-defined as 24 h. Pumping is generally carried out during the flood peak, and durations higher than 24 h are usually not necessary.
- Solution space resolution for homogeneous grid discretization: the solution space is discretized depending on a parameter fixed before the optimisation, set as 4 h. Lower discretization considerably increases the calculation time without important improvements of final results.

## **6.6 Iterative Ranking Greedy optimisation algorithm**

### ***6.6.1 Introduction to the Greedy approach***

Assuming that the final loss function is selected from MADM methods (among objective functions  $R$ ,  $D$ ,  $Z$ ,  $H$  and  $U^*$ ), the aim of the Iterative Ranking Greedy Algorithm (IRGA) is to

find the global optimisation of this objective function, i.e. the alternative  $i$  ( $a_{i,set}$ ) that minimizes the overall losses in the basin.

However, since calculation time considerably increases when simultaneously solving all possibilities for the PrevOp sequences, the Greedy algorithm procedure has been implemented in the process to solve them in different stages, reservoir by reservoir. This procedure reduces the calculation time and makes the real-time decision possible. Thus, when solving the optimisation of the objective function, parameters to optimise at each stage are those of the HPPs associated to one reservoir, all the other parameters for the other reservoirs being assumed as constant.

A similar procedure was already implemented for deterministic optimisation in the Upper Rhone River basin. (Jordan, 2007). It was shown that this approach did not affect the results for optimal management in the considered basin.

### **6.6.2 Model architecture of the Greedy approach**

Dechter and Dechter (1989) defined the Greedy method as a controlled search strategy, divided in stages, which selects the next stage to achieve the highest improvement possible in the value of some measures, which may or may not be the objective function.

The Greedy algorithm is a metaheuristic approach making a local optimal choice at each step, expecting to find the global optimum (Vince, 2002; Alidaee et al., 2001). Curtis (2003) also describes it as the algorithm that makes a sequence of choices, each choice being the best available at that time. A large overview of the methodology is given by Dasgupta et al. (2006).

The Greedy algorithm has been largely used in hydrological and hydraulic engineering problems such as: management of temporary storage of drainage water from different polders in a network composed by lakes and canals (Breur et al., 2009); sites prioritization for wetland restoration depending on a combined hydrologic simulation and a landscape design model (Newbold, 2005); as well as for reliability improvement for water distribution networks by increasing pipe size (Fujiwara and Tung, 1991).

In MINDS, the Greedy algorithm allows the mathematical serial solving for all hydropower groups. First of all, the priority management for the chosen groups is defined. Each stage is then related to a group (GR). The hierarchy of the groups is given by different possibilities depending on their efficiency for storing water during a flood, on upstream location or on a random ranking.

Each stage achieves the minimization of expected damages in the considered basin as well as PPOC of preventive operations in the hydropower group. Figure 6.12 summarizes the detailed procedure. Once all the stages achieved, the process can be repeated (iteration) until the convergence is obtained.

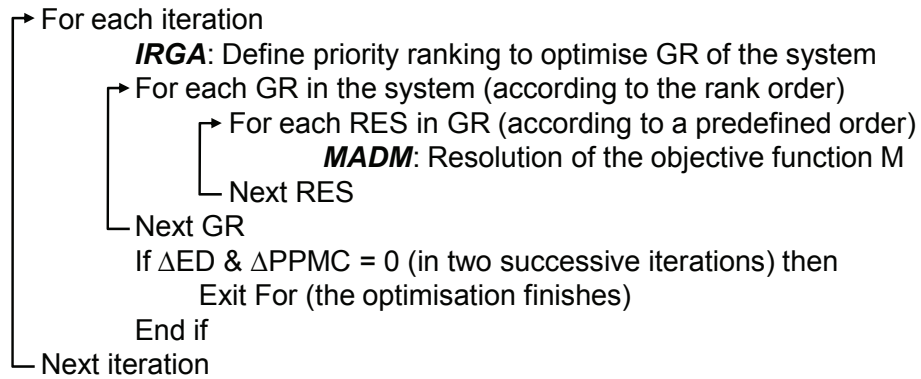


Figure 6.12 Scheme for the Greedy optimisation

The optimisation of a hydropower group (GR) at each stage is obtained by a two-step exploration in the solution space with different density in the solutions exploration, searching by the method of the uniform grid of possible solutions (Andreu, 1993). It looks for the start and end time of the PrevOp for turbine and bottom outlet operations as well as the turbine stop periods and the pump operation duration for the ensemble of the forecasts in the power houses linked to the reservoir to be optimised. The optimisation is successively realised for turbine, bottom outlet and pump operations.

For each one of them, the first step defines the sequence of PrevOp with a smaller density of potential solutions than the second one. The density is defined by the user, but pre-defined as 4 h as seen in section 6.5.4. Once this solution is found, a second step defines the optimal solution around the solution space of the first one. The calculation density is higher in this case, normally corresponding to hydrograph and inflow series time step (1 h in this system).

This optimisation is carried out for each reservoir of the system. When the PrevOp in the HPPs connected to the current reservoir are being optimised, the operations of other HPPs are defined and kept invariable.

The optimisation is iteratively performed until the optimum is found and the expected damages in each sector and PPOC in the hydropower groups do not vary anymore. The calculation stop criterion is thus assumed as the convergence between two successive iterations. In addition, the group ranking is re-computed before the next iteration and the ranking of the groups may be changed.

### 6.6.3 Groups ranking

#### Options to rank the groups

Several possibilities have been implemented in MINDS for ranking the hydropower groups (GR) in order to perform the optimisation with the Greedy algorithm. The decision maker can select the ranking order of the GRs depending on his own experiences.

#### Reservoir Space Ranking (RSR)

The Space rule (Maass et al., 1962; Neelakantan et al., 1999; Lund and Guzman, 1999; Paredes and Lund, 2006) seeks to leave more space (i.e. volume) in reservoirs where big inflows are expected, trying to minimize the total volume of spills. From this concept, a Reservoir Space Index (RSI) has been defined and developed for establishing a ranking of GRs.

It has to be mentioning that the storage volume is calculated from the moment when PrevOp in a HPPs finish or from the start time of the optimisation if there is no PrevOp. Before the end time of the PrevOp, releases are assumed not to influence the flood peak discharge.

Equation 6.54 provides the relative capacity of storage for a reservoir. Equation 6.55 gives the final RSI value per group, corresponding to the sum of the individual values of its reservoirs. Finally, the GRs are ranked from highest relative storage volume to lowest ( $RSI_{\max\text{to}\min}$ ).

$$RSI_{RES_x} = \frac{\int_{t_{RES_x}^*}^{t_f} (Q_{in,t_{RES_x}} - Q_{out,t_{RES_x}}) dt}{\sum_{r=1}^{r=v} \int_{q_{RES_r}}^{t_f} (Q_{in,t_{RES_r}} - Q_{out,t_{RES_r}}) dt} \quad 6.54$$

$$RSI_{GR_w} = \sum_{r=1}^{r=h} RSI_{RES_r, RES_r \in GR_w} \quad 6.55$$

with  $Q_{in}$ : inflow [ $m^3/s$ ];  $Q_{out}$ : outflow [ $m^3/s$ ];  $t_{RES_x}^*$ : time when PrevOp stops in reservoir  $x$  (zero if no operation was executed) [h];  $v$ : total number of reservoirs [-];  $h$ : number of reservoirs in group  $GR_w$  [-].

Additionally, this method is also tested by ranking GRs from lowest to highest relative storage volume ( $RSI_{\min\text{to}\max}$ ).

### ***Upstream to Downstream Ranking (UsToDs)***

This method optimises the system in the same way hydrological models are calibrated, from upstream to downstream. This procedure of optimisation has been also applied in other projects of water resources management (Cuenca and Molina, 2004; Tingsanchali and Boonyasirikul, 2006). Moreover, this approach is also investigated optimising the GRs from downstream to upstream (DsToUs).

### ***Random Ranking (RR)***

In order to check if the GRs ranking for the global optimisation produces an improvement or a deterioration of the results, a random method is also performed. It generates a random order each time a resolution over the basin is achieved.

#### ***6.6.4 Algorithm parameters of the IRGA approach***

The IRGA algorithm has been implemented in MINDS. The method for ranking the GRs is one of the first choices which have to be realised by the decision maker. The maximum number of iterations, initially set at 10, can be also determined by the decision maker. However, the optimisation usually converges after 5 or 6 iterations and this parameter does not influence the calculation.

A first solution space resolution was already defined by the decision maker in the general parameters of the optimisation. Here, a second time resolution of 1 h can be chosen in order to improve the results.

#### ***6.6.5 Objective function of the IRGA approach***

The objective function can be chosen among the loss functions presented in Eq. 6.56, depending on the selected MADM method. It has to be noted that the IRGA method optimises the function at each stage, where the parameters to be optimised are not the global set  $i$  ( $a_{i,set}$ ) but just the parameters associated to a reservoir ( $a_{i,res}$ ). The initial conditions assumed as the starting iteration are the BasU series for each HPPs.

$$\begin{array}{ll}
 R = \min_i (r_i) & \text{if MADM = Bayes Risk Criterion} \\
 D = \min_i (d_i) & \text{if MADM = Min Max Regret} \\
 Z = \min_i (z_i) & \text{if MADM = Decision Maker Criterion} \\
 H = \min_i (\lambda \cdot (r_i) + (1 - \lambda) \cdot (d_i)) & \text{if MADM = Hurwicz derived for floods} \\
 U^* = \min_i (1 - u_i) & \text{if MADM = TOPSIS}
 \end{array} \tag{6.56}$$

## 6.7 SCE-UA optimisation algorithm

### 6.7.1 Introduction to the Shuffled Complex Evolution – University of Arizona approach

The Shuffled Complex Evolution – University of Arizona (SCE-UA) algorithm is a global optimisation method (Duan et al., 1992, 1993) based on a synthesis of the best features from several existing algorithms, including the genetic algorithm, and introduces the concept of complex information exchange, so-called complex shuffling.

The method was designed for solving problems encountered in conceptual watershed model calibration (Muttill and Liong, 2004), but has also been satisfyingly used in water resources management (Zhu et al., 2006; Lin et al., 2008; Wang et al., 2010).

### 6.7.2 Model architecture of the SCE-UA approach

The SCE-UA method was developed to obtain the traditional best parameter set and its underlying posterior distribution within a single optimisation run. The goal is to find a single best parameter set in the feasible space. It starts with a random sample of points distributed throughout the feasible parameter space, and uses an adaptation of the Simplex Downhill search scheme (Nelder and Mead, 1965) to continuously evolve the population toward better solutions in the search space, progressively relinquishing occupation of regions with lower posterior probability (Mariani et al., 2011).

A general description of the steps of the SCE-UA method is given below (Duan et al., 1994) and illustrated in Figure 6.13:

#### *Step 1*

Generate sample: Sample NPT points in the feasible parameter space and compute the criterion value at each point. In the absence of prior information on the location of the global optimum, use a uniform probability distribution to generate a sample.

#### *Step 2*

Rank points: Sort the NPT points to increase criterion value so that the first point represents the point with the lowest criterion value and the last the one with the highest criterion value (assuming that the goal is to minimize the criterion value).

**Step 3**

Partition into complexes: Partition the NPT points into NGS complexes, each containing NPG points. The complexes are partitioned in such a way that the first complex contains every  $NGS \cdot (k-1) + 1$  ranked point, the second complex contains every  $NGS \cdot (k-1) + 2$  ranked point, and so on, where  $k = 1, 2, \dots, NPG$ .

**Step 4**

Evolve each complex: Evolve each complex independently by taking NSPL evolution steps, according to the Competitive Complex Evolution (CCE) algorithm. Figure 6.15 illustrates how each evolution step is taken.

**Step 5**

Shuffle complexes: Combine the points in the evolved complexes into a single sample population; sort the sample population in order of increasing criterion value; re-partition or shuffle the sample population into NGS complexes according to the procedure specified in the third step.

**Step 6**

Check convergence: If the number of trials MAXN has been exceeded, or the criterion value has not been improved by  $PECNTO \cdot 100$  in KSTOP shuffling loops, stop; otherwise, continue.

**Step 7**

Check complex number reduction: If MINGS (the minimum number of complexes)  $<$  NGS, remove the complex with the lowest ranked points; set  $NGS = NGS - 1$  and  $NPT = NGS \cdot NPG$ ; and return to Step 4. If  $MINGS = NGS$ , return to Step 4.



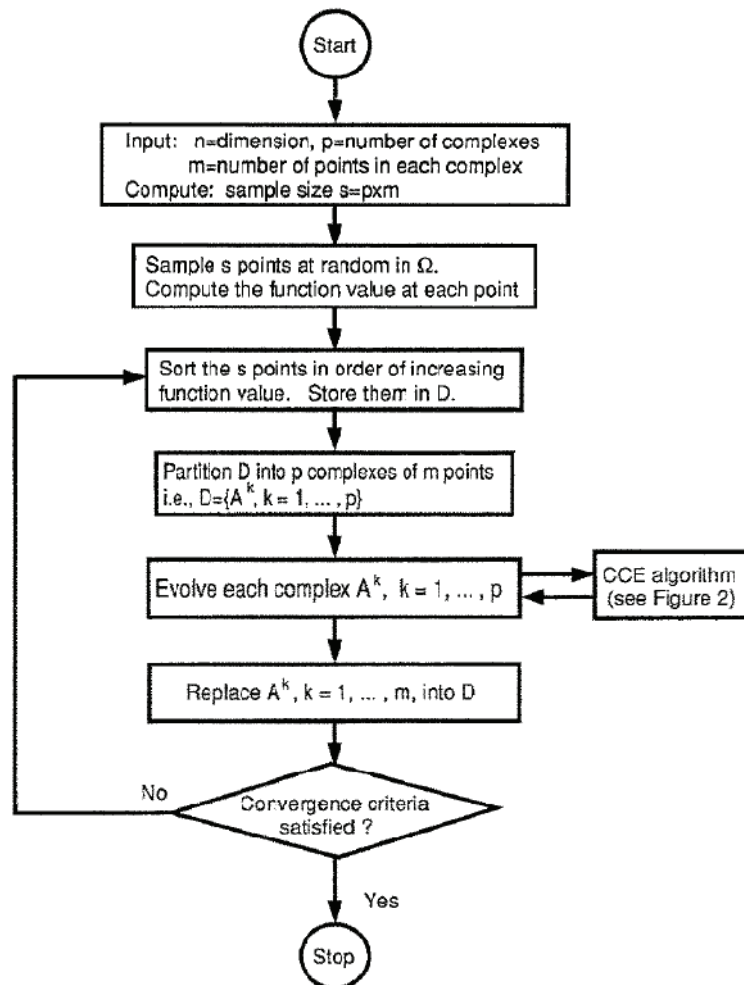


Figure 6.13 Flow chart of the shuffled complex evolution method (from Duan et al., 1993), with  $V=n$ ,  $NGS=p$ ,  $NPG=m$  and  $NPT=s$

The SCE-UA method is explained in Figure 6.14 and Figure 6.15 for a two dimensional case (Duan et al., 1994). The contour lines in Figure 6.14 and Figure 6.15 represent a function surface having a global optimum located at (4,2) and a local optimum located at (1,2). Figure 6.14a shows that a sample population containing  $NPT$  ( $=10$ ) points is divided into  $NGS$  ( $=2$ ) complexes. Each complex contains  $NPG$  ( $=5$ ) points which are marked by  $\bullet$  and  $*$  respectively. Figure 6.14b shows the locations of the points in the two independently evolved complexes at the end of the first cycle of evolution. It can be seen that one complex (marked by  $*$ ) is converging towards the local optimum, while the other (marked by  $\bullet$ ) is converging toward the global optimum. The two evolved complexes are shuffled according to step 5. Figure 6.14c displays the new membership of the two evolved complexes after shuffling.

Figure 6.14d illustrates the two complexes at the end of the second cycle of evolution. It is clear that both complexes are now converging to the global optimum at the end of second cycle.

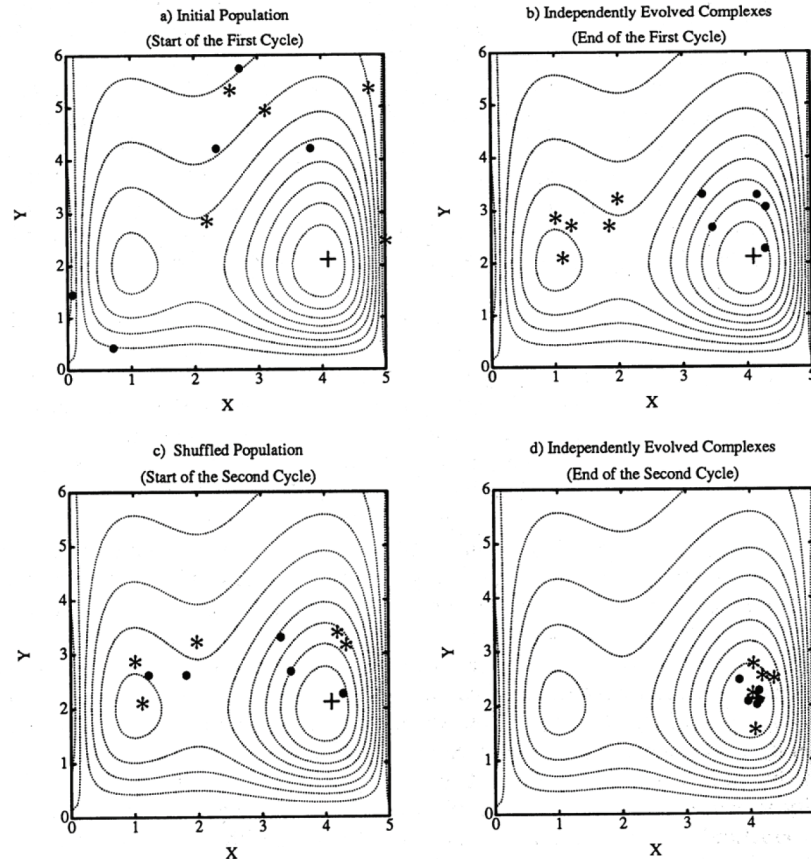


Figure 6.14 Illustration of the shuffled complex evolution (SCE-UA) method (from Duan et al., 1994).

The CCE algorithm is graphically illustrated in Figure 6.15. The black dots ( $\bullet$ ) indicate the locations of the points in a complex before the evolution step is taken. A sub-complex containing NPS ( $=3$ , i.e. forms a triangle in this case) points is selected according to a prespecified probability distribution to initiate an evolution step.

The probability distribution is specified such that the better points have a higher chance of being chosen to form the sub-complex than the worse points. The symbol (\*) represents the new points generated by the evolution steps. There are three types of evolution steps: reflection, contraction and mutation.

Figure 6.15a, Figure 6.15b and Figure 6.15d illustrate the "reflection" step, which is implemented by reflecting the worst point in a sub-complex through the centroid of the other points. Since the reflected point has a lower criterion value than the worst point, the worst point is discarded and replaced by the new point. Thus an evolution step is completed.

In Figure 6.15c, the new point is generated by a "contraction" step (the new point lies halfway between the worst point and the centroid of the other points), after rejecting a reflection step for not improving the criterion value.

In Figure 6.15e, a "mutation" step is taken by random selection of a point in the feasible parameter space to replace the worst point of the sub-complex. This is realized after a reflection step is attempted, but results in a point outside of the feasible parameter space. Another scenario in which a mutation step is taken is when both the reflection step and the contraction step do not improve the criterion value.

Finally, the Figure 6.15f shows the final complex after NSPL (=5) evolution steps.

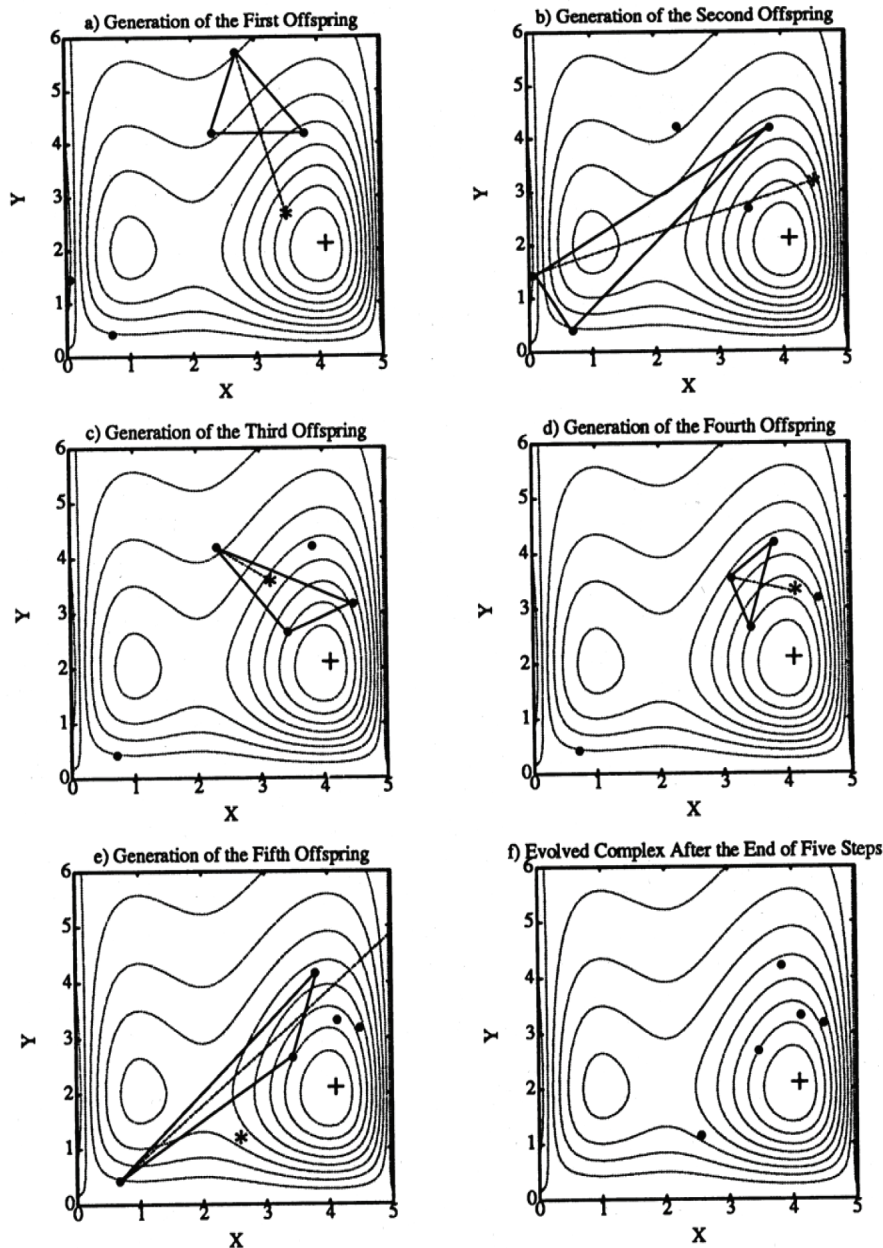


Figure 6.15 Illustration of the evolution steps taken by each complex (from Duan et al., 1994).

### 6.7.3 Algorithm parameters of the SCE-UA approach

The SCE-UA method has been implemented in MINDS. An initial set of variables is given by the user or is assumed as zero (no preventive operations, i.e. BasU operations) for all the variables of the set. The other NPT-1 points (or parameters sets) are randomly created by the algorithm.

The parameters of the SCE-UA algorithm are assumed as follows. The number of variables  $V_{OPT}$  to optimise depends on the number of reservoirs to optimise (five or six values per reservoir). If all GRs are selected,  $V_{OPT}$  corresponds to 64. The number of complexes NGS is:

$$NGS = \begin{cases} 2 & \text{if } V_{OPT} \leq 10 \\ V_{OPT}/5 & \text{if } 10 < V_{OPT} < 30 \\ 6 & \text{if } V_{OPT} \geq 30 \end{cases} \quad 6.57$$

with NGS: number of complexes [-];  $V_{OPT}$ : Number of variables to optimise [-].

The number of points NPG in each complex corresponds to  $2 \cdot V_{OPT} + 1$  and the number of points NPS in each sub-complex to  $V_{OPT} + 1$ . The number of evolution steps allowed for each complex before complex shuffling, NSPL, is equal to NPG. The minimum number of complexes required is defined as NGS. Then, the total number of points NPT in the entire sample population is  $NGS \cdot NPG$ . It has to be noted that each point corresponds to a set of variables ( $a_{i,set}$ ).

The maximum number of function evaluations MAXN is assumed as 200'000, but can be modified by the user. The number of shuffling loops (KSTOP) in which the criterion value must change by a fixed percentage (PCENTO) before optimisation is finished is defined in Eq. 6.58. This percentage PECNTO is established as 0.01

$$KSTOP = \begin{cases} 10 & \text{if } NPT \leq 10 \\ NPT & \text{if } NPT > 10 \end{cases} \quad 6.58$$

### 6.7.4 Objective function of the SCE-UA approach

The objective function corresponds in this case to one of the loss functions presented in Eq. 6.59. All variables of the system ( $a_{i,set}$ ) are here optimised at the same time. The objective function depends on the selected MADM method, which does not include TOPSIS. This method is not incorporated to SCE-UA because TOPSIS solves the problem from a finite number of alternatives, already calculated. However, SCE-UA only proposes and calculates a

subset of alternatives from all the set, and, so, the ideal and anti-ideal solution cannot be calculated, neither the procedure proposed for TOPSIS.

$$\begin{aligned}
 R &= \min_i (r_i) && \text{if MADM = Bayes Risk Criterion} \\
 D &= \min_i (d_i) && \text{if MADM = Min Max Regret} \\
 Z &= \min_i (z_i) && \text{if MADM = Decision Maker Criterion} \\
 H &= \min_i (\lambda \cdot (r_i) + (1 - \lambda) \cdot (d_i)) && \text{if MADM = Hurwicz derived for floods}
 \end{aligned}
 \tag{6.59}$$

## 6.8 Hybrid optimisation algorithm

A hybrid method using the Greedy and the SCE-UA algorithms is also applied. The Greedy solution is used here as the starting point for a more comprehensive search through the decision space (Newbold, 2005). Then, as starting from this solution, the SCE-UA algorithm is conducted.

The proposed coupled approach applies the two optimisation methods, IRGA and SCE-UA, in series (Figure 6.16). The IRGA is used here as explained in section 6.6. The set of variables obtained as results by the IRGA method is introduced as initial conditions in the SCE-UA algorithm, which continues to optimise the system. If SCE-UA improves the results, a new set of variables is provided. Otherwise, the first set proposed by IRGA remains the final optimum set.

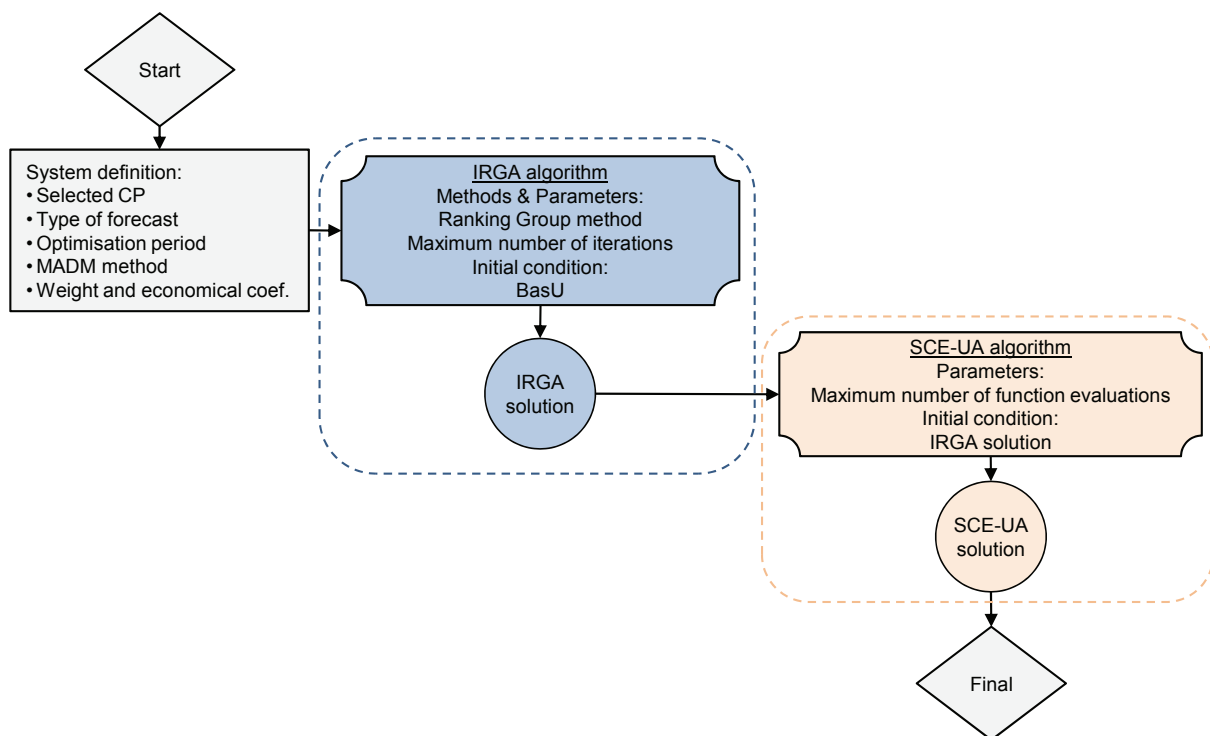


Figure 6.16 Coupled approach of IRGA and SCE-UA algorithms

When the hybrid procedure is selected, the parameters for the two optimisation methods have to be defined. This hybrid procedure leads to a smaller calculation time for the SCE-UA method, related to a faster convergence to optimal solution.

Once again, the objective function can be selected according to Eq. 6.59.

## **6.9 MINDS software**

### **6.9.1 User interface**

Created as a standard executable program, MINDS software offers the convenience of modern system visualization. The interface gives an overview of the studied basin, allows the consideration of key parameters and shows the main results. A special effort has been put on an appealing graphic visualization of all data including flow inputs as well as characteristics of the check points, reservoirs and hydropower plants. The plot of results allows the verification of the model and the mathematical computations as well as the analysis of the preventive operation effects.

The DSS interface is one of the most important tasks to achieve when developing systems for real-time decisions. As explained in previous chapters, the communication of results is a key element of the system and implies a certain degree of maturation. The interface has to reflect the uncertainty of results and to represent them with clarity for providing confidence to decision makers.

The MINDS main interface (Figure 6.17) contains the menu bar, the tool bar, the map of the basin with hydropower groups and check points and the access to the main results of the optimisation. This content is detailed here after.



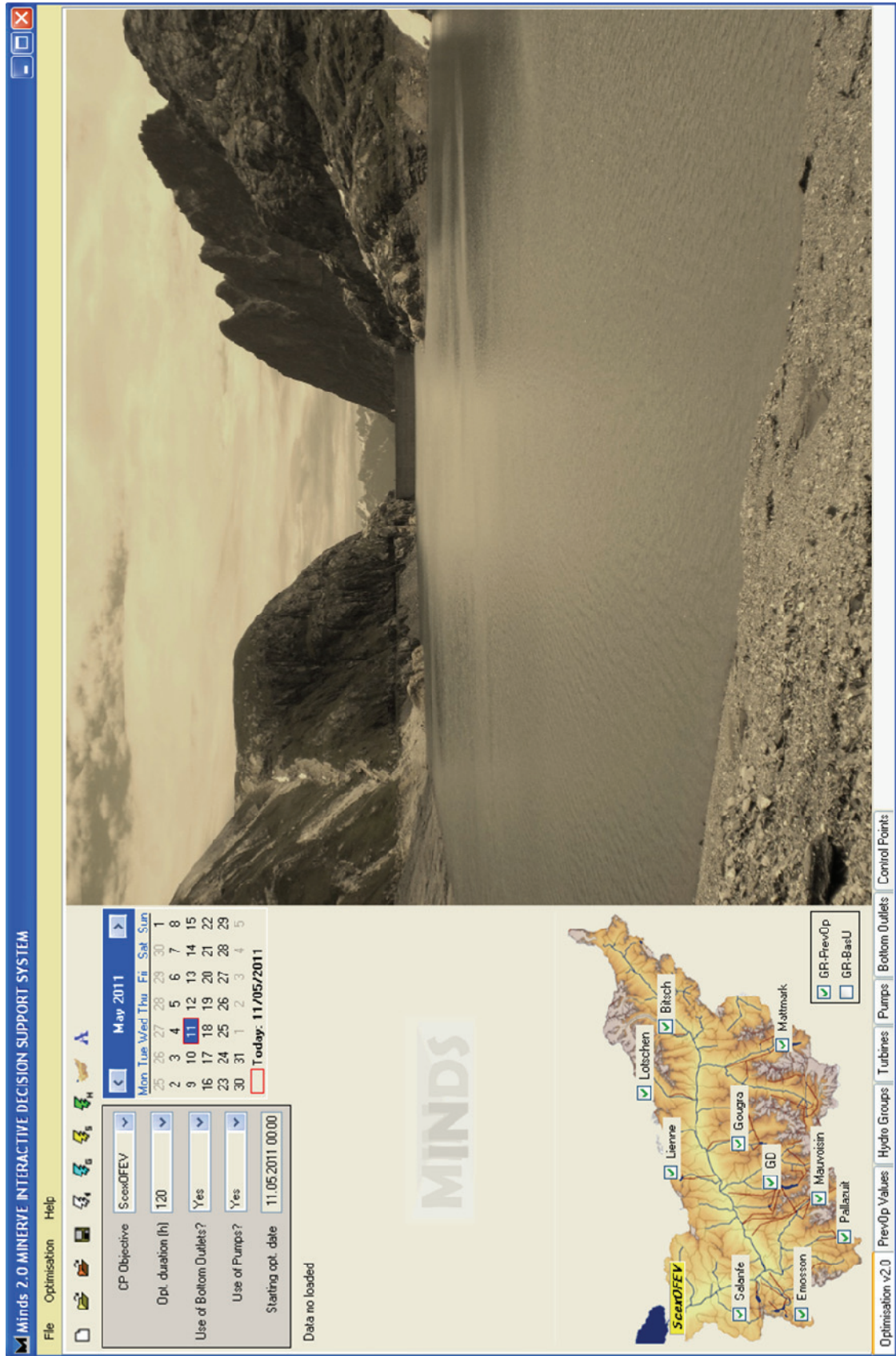


Figure 6.17 Main interface of MINDS

### **Menu bar**

The menu bar contains several commands. They can be accessed by a mouse click for selecting different options or functions of the program such as loading of forecasts and reservoirs levels, optimisation of the system or saving the results after optimisation.

- File:
  - Load a file: loading the data for an optimisation
  - Load a folder: loading a folder where different files can be chosen.
  - Save: saving the results of the performed optimisation.
  - Exit: Exit of the program.
- Optimisation:
  - Run Greedy algorithm: Starting the optimisation with the IRGA algorithm.
  - Run SCE-UA algorithm: Starting the simulation with the SCE-UA algorithm.
  - Run Hybrid algorithm: Starting the simulation with the hybrid algorithm.
  - Run one simulation: Run a simulation with given preventive operations.
  - Advanced parameters: Opening the Advanced parameters window.
- Help:
  - Procedure: Opening a description of the MINDS procedure
  - HPP schema: Opening a functionality schema of the hydraulic simulation balance model used in MINDS.
  - About MINDS: General information about MINDS

### **Tool bar**

The functions of the tool bar are the same as in the menu bar and provide therefore short-cuts to main options of the decision support system.



Clear the interface



Short-cut of *File* → *Load a file*



Short-cut of *File* → *Load a folder with different files*







Short-cut of *Run* → *Run (Greedy optimisation)*



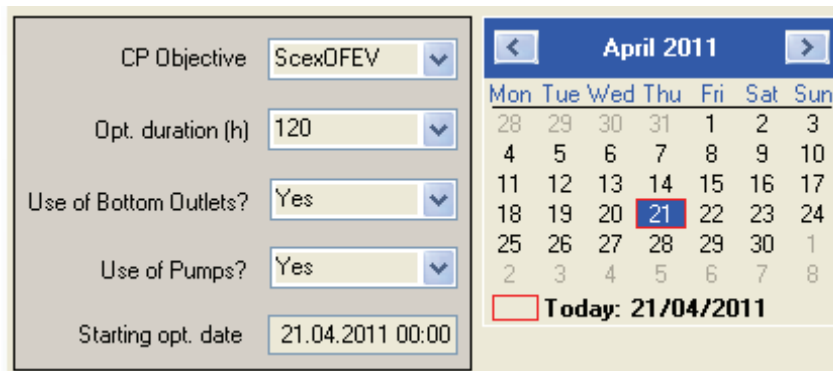
Short-cut of *Run* → *Run (SCE-UA optimisation)*



-  Short-cut of *Run* → *Run (Hybrid optimisation)*
-  Short-cut of *Run* → *Run (Simulation with pre-defined parameters)*
-  Short-cut of *File* → *Load Help* → *HPP functionality schema*
-  Short-cut of *Advanced parameters window*

### **Main parameters area**

The main parameters of the system are accessible in the main window of the interface. The selected check point as objective of the basin, the duration of the optimisation, the use of the bottom outlets and pumps as well as the starting date for the optimisation can be easily changed (Figure 6.18)



CP Objective	ScexDFEV
Opt. duration (h)	120
Use of Bottom Outlets?	Yes
Use of Pumps?	Yes
Starting opt. date	21.04.2011 00:00

April 2011						
Mon	Tue	Wed	Thu	Fri	Sat	Sun
28	29	30	31	1	2	3
4	5	6	7	8	9	10
11	12	13	14	15	16	17
18	19	20	21	22	23	24
25	26	27	28	29	30	1
2	3	4	5	6	7	8

Today: 21/04/2011

Figure 6.18 Main parameters area of MINDS

### **Basin map**

The selection of a check point in the main parameters area of the main MINDS window defines the groups to be optimised (Figure 6.19). Nevertheless, the decision maker can manually change the groups to be optimised checking or unchecking the groups directly over the basin map. The non activated groups will be simulated with Business as Usual operations over the whole period.

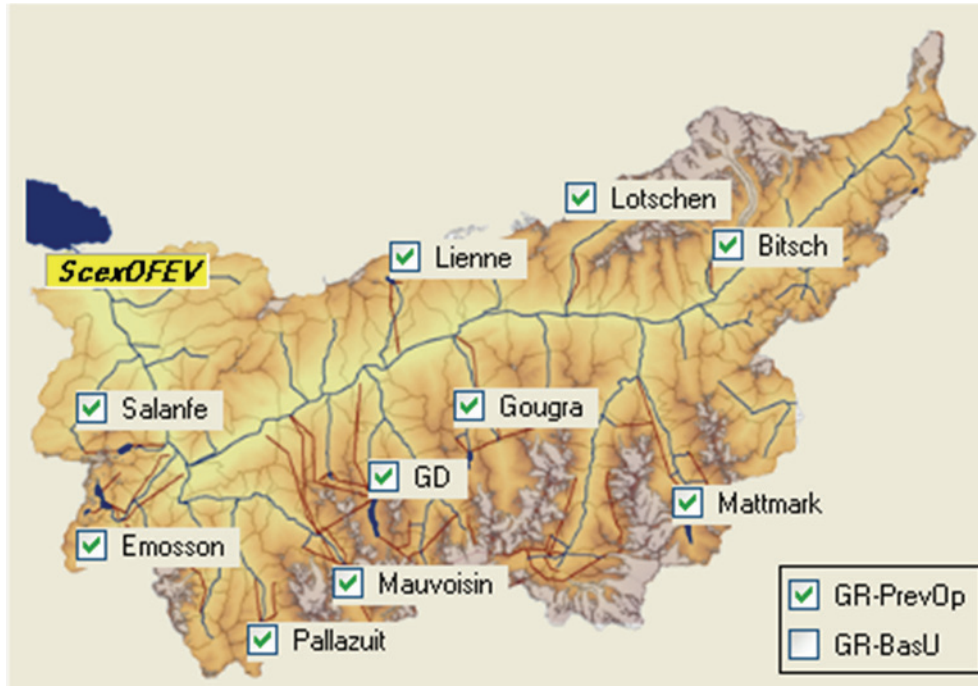


Figure 6.19 Basin map for the selection of the groups to be optimised

### Advanced parameters window

The secondary parameters can be modified in the advanced parameters window (Figure 6.20). They comprise the type of forecast selected for optimising and its characteristics, the type of algorithm used for the optimisation and its parameters, the multi-criteria parameters, the calculation parameters and the energy parameters.

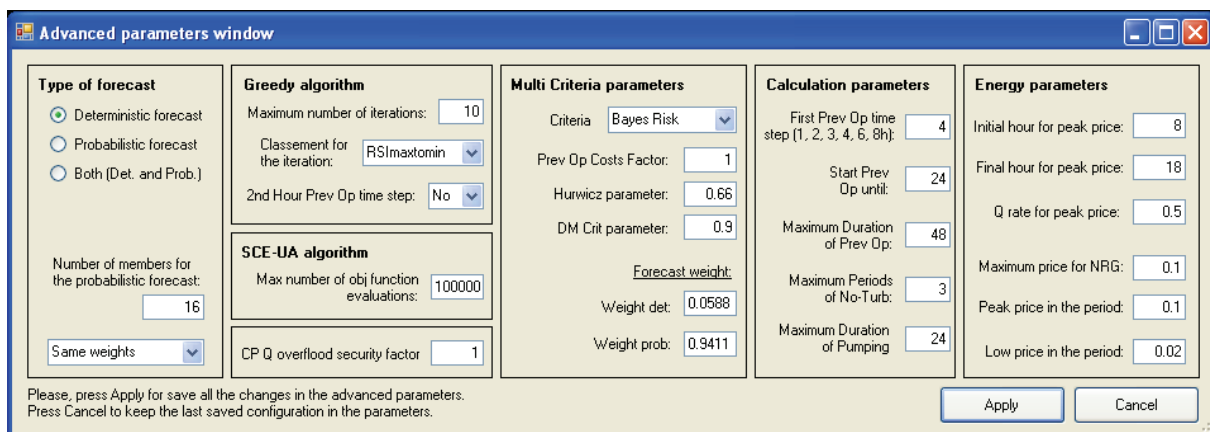


Figure 6.20 MINDS advanced parameters window

### 6.9.2 Results presentation

Once a simulation is completed, most important results are presented in the main window of the MINDS interface. Detailed data and results in others windows can be easily visualised by clicking in their <tab>.

#### *Main window of MINDS*

Key results of the optimisation are displayed as presented in Figure 6.21. Not all results of the optimisation are shown, but just an overview containing the expected damages at check points, the need of decision for the groups and the estimated hydrographs.

This main window of the interface concerns the foremost results of the optimisation (Figure 6.22):

- Part 1 and part 2 show the primary and secondary parameters chosen for the optimisation.
- Part 3 displays an overview of the basin, with the selected check point for the optimisation and the optimised groups.
- In part 4, the flood peaks and the expected damages at each check point are shown for the simulation of the natural basin as well as the simulations BasU and PrevOp. The flood reduction due to BasU and PrevOp is given.
- Part 5 displays plots of the hydrographs at the check points for all simulations. Only relevant hydrographs can be selected for a better presentation.
- Part 6 reveals the PPOC for each group as well as the stored volume during the entire period and during the flood peak.
- Finally, part 7 presents the PrevOp for each reservoir. A distinction is done between turbine, bottom outlet and pump operations.

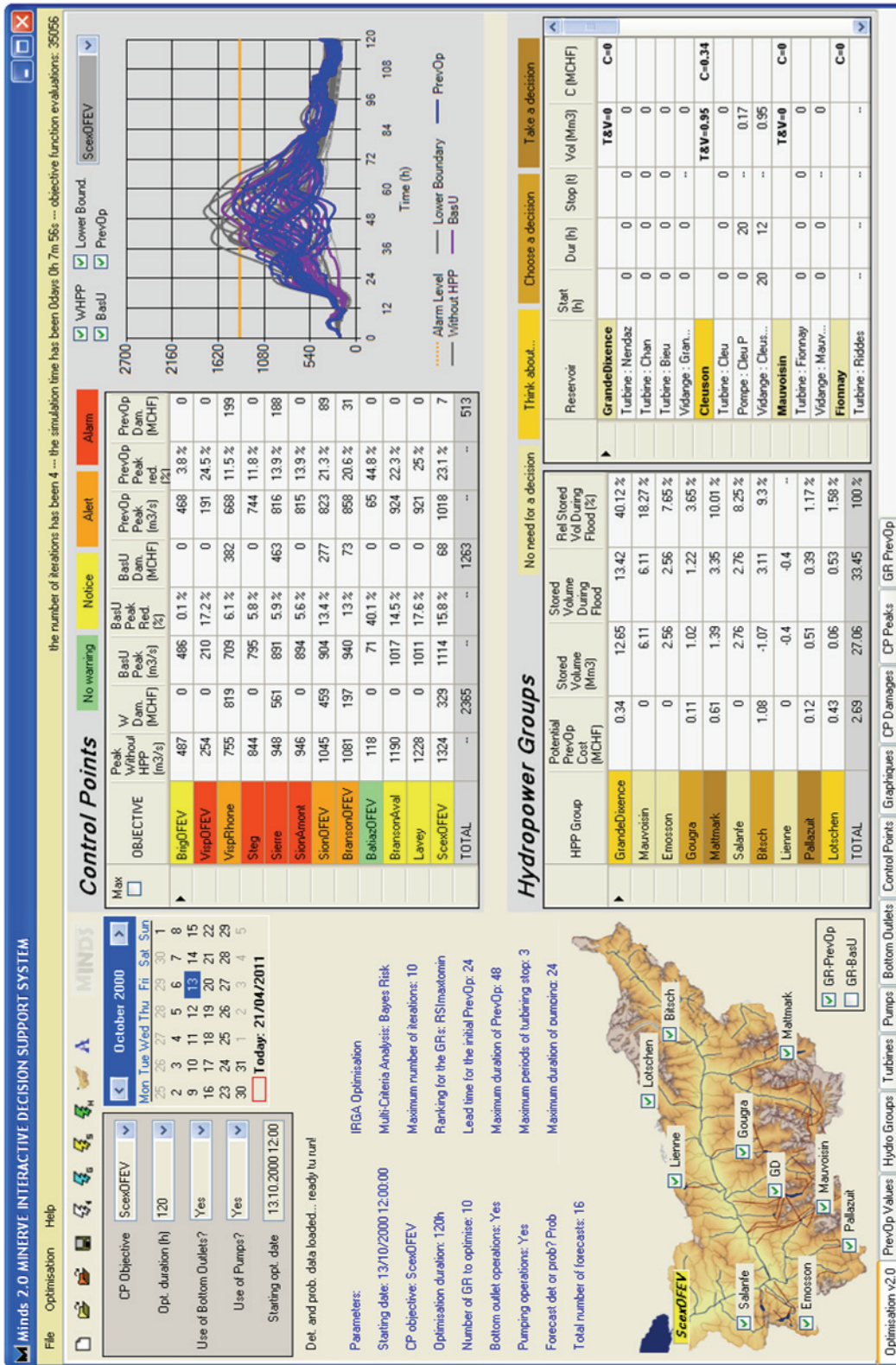


Figure 6.21 Main interface of MINDS after an optimisation.



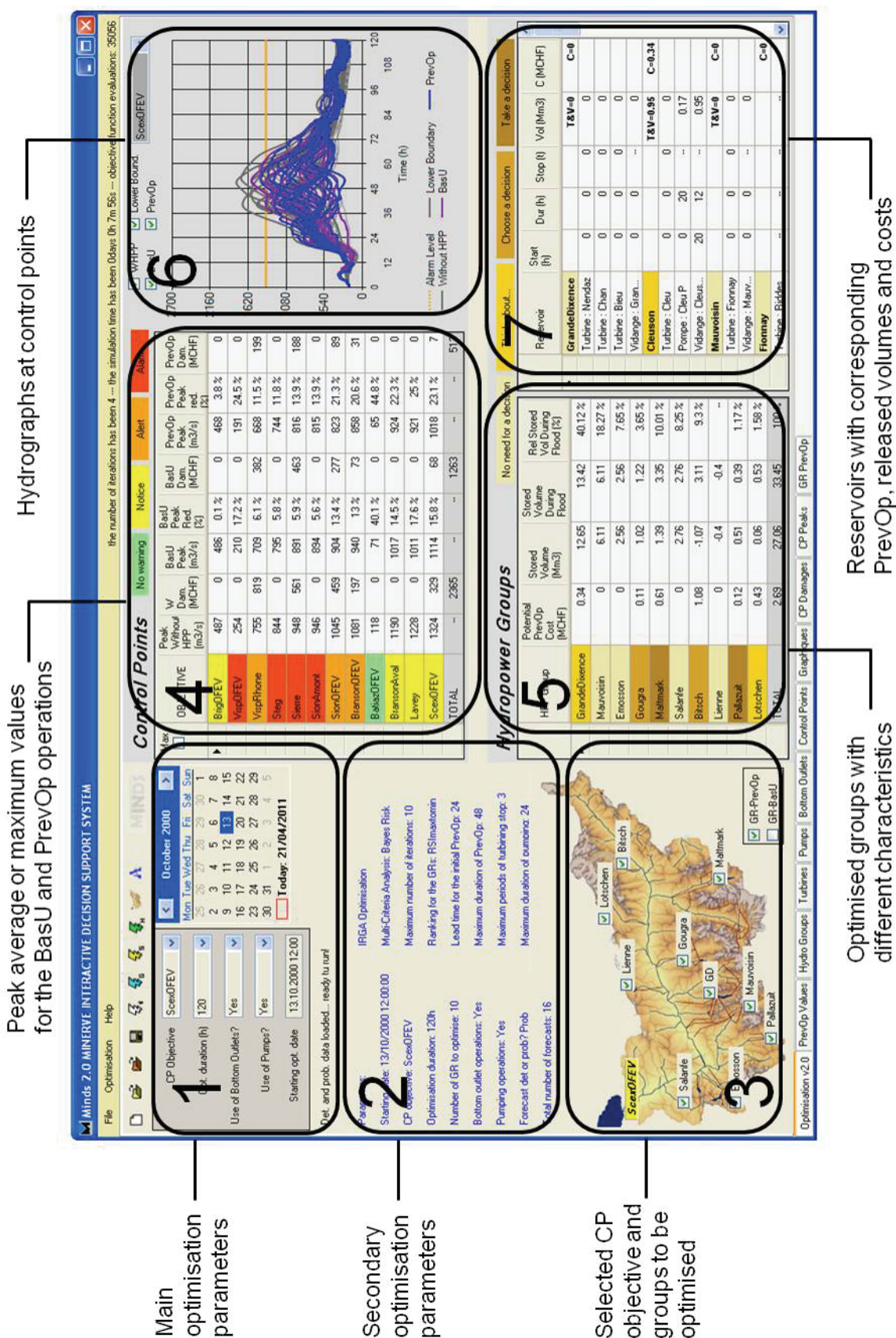


Figure 6.22 Structure of the main interface of MINDS.

### ***Secondary windows of MINDS***

Numerous secondary windows can be opened in the MINDS interface. They generally compare results of the BasU and PrevOp simulations. The hydrographs at the check points with BasU and PrevOp can be individually visualised as well as the inflows and outflows for each reservoir. Turbining, bottom outlet, pumping and spillways releases can be distinguished as presented in Figure 6.23.

Another window of the interface shows the box plots of flood peaks for each check point of the basin, from upstream to downstream. For the whole basin, the differences between BasU and PrevOp simulations are given (Figure 6.24).

Total damages at each check point as well as over the whole basin are also shown in MINDS (Figure 6.25). In addition, total volumes of inflows, outflows, turbine discharges, bottom outlet discharges, pumping discharges, etc. are listed for each reservoir with corresponding potential preventive operation costs (Figure 6.26).

Other windows of the interface show the different reservoirs and the associated hydropower plants, the characteristics of the turbines, pumps and bottom outlets as well as a description of the check points. All parameters of these elements can be modified on the corresponding window if required.

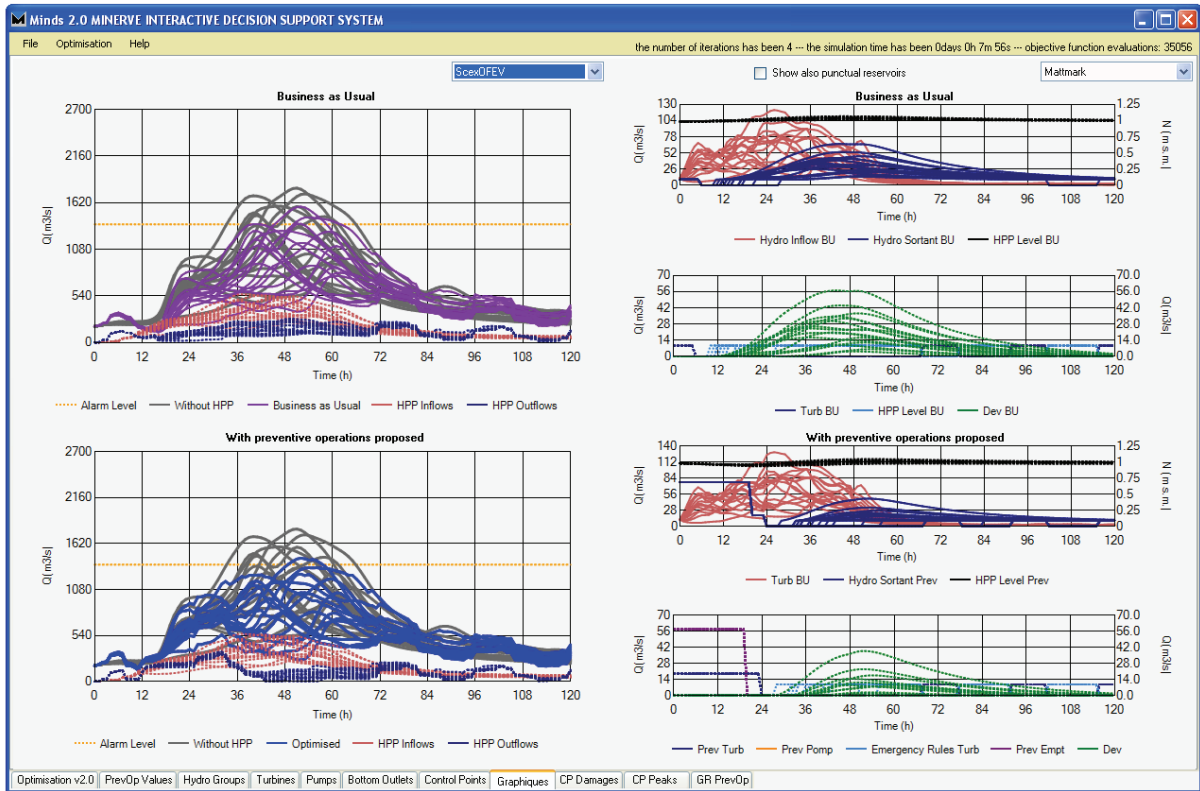


Figure 6.23 Hydrographs at check points and inflows and outflows in the reservoirs with BasU and PrevOp simulations.



Figure 6.24 Box plots of peaks at check points with BasU and PrevOp simulations.

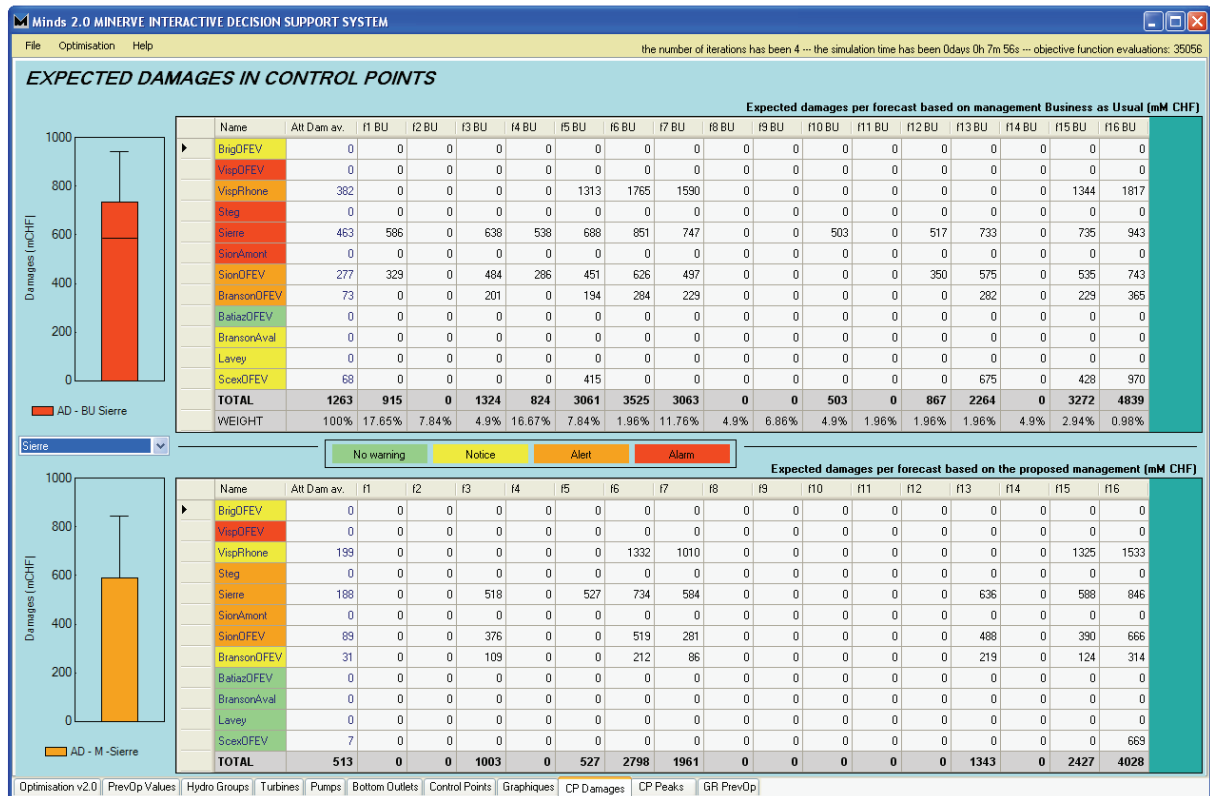


Figure 6.25 Total expected damages at check points with BasU and PrevOp.

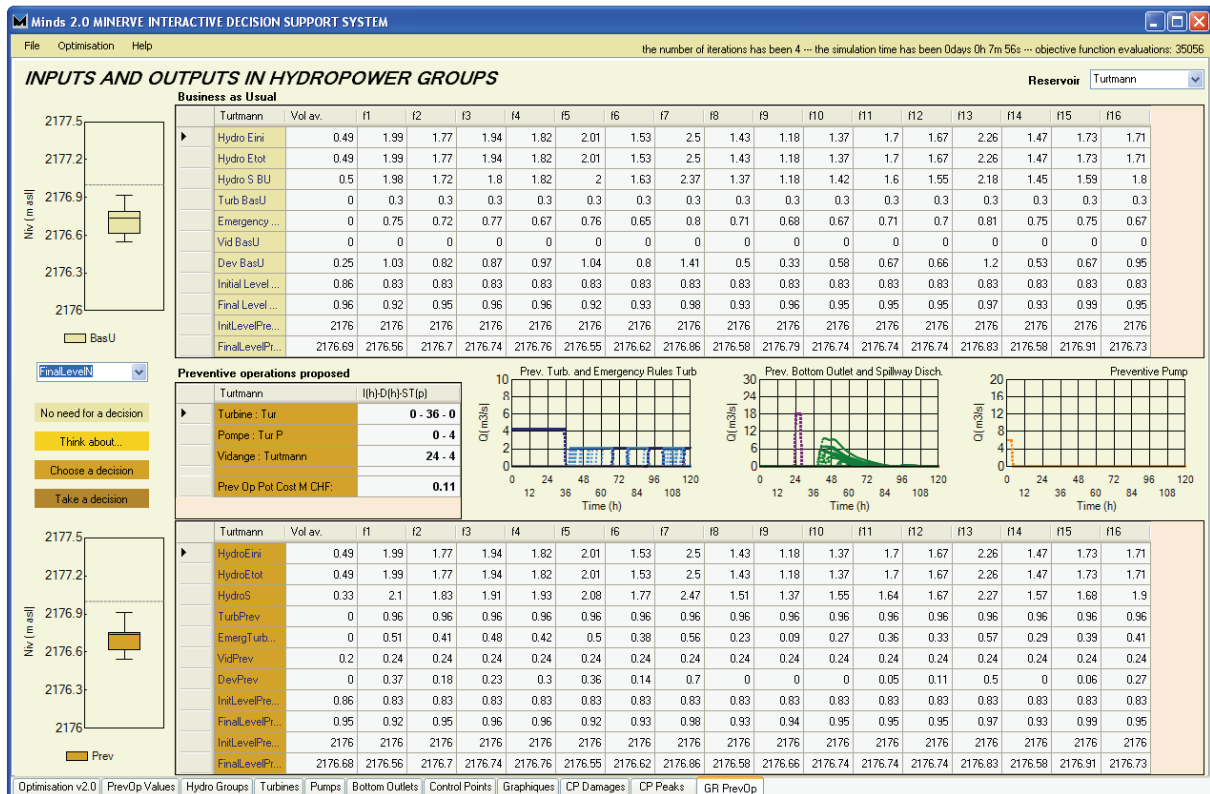


Figure 6.26 Inflows, outflows and volume variations in the reservoirs with BasU and PrevOp.



“In any moment of decision the best thing you can do is the right thing, the next best thing is the wrong thing, and the worst thing you can do is nothing”

Theodore Roosevelt (1858-1919)

## **7. Application of the MINERVE Interactive Decision Support System to the Upper Rhone River basin**

## 7.1 Application to two historical reference flood events

Two historical events have been chosen for studying the performance of MINDS, namely the September 1993 and October 2000 floods (Table 7.1). In these cases, observed discharges at main check points of the system, meteorological data from meteorological stations as well as the forecasts from COSMO-7 and COSMO-LEPS are available during the whole event.

Table 7.1 Reference flood events for COSMO-LEPS (C-L) and COSMO-7 (C-7)

Start	Fin	Peak Flow [m <sup>3</sup> /s]	C-7	C-L
09.23.1993 12h	- 09.26.1993 12h	1081	✓	✓
14.10.2000 00h	- 18.10.2000 00h	1358	✓	✓

First, the methods proposed in Chapter 6 are assessed. The performance of the mathematical algorithms to reduce the damages induced by the flood is studied. Then, the flood peaks at different check points are evaluated taking into account the potential costs generated by the proposed preventive operations at hydropower plants.

The aim of this first task is not to follow a complete event and revising the decisions when forecast is updated, but to evaluate the performance of the algorithms from a mathematical point of view. The knowledge about the performance of the methods and their differences allows the selection of the final approach. Then, it is applied to a complete flood event.

Second, the exercise of a real-time flood management for the two selected events is carried out. The goal is to know the real effect of the management in practical cases. Starting from the first forecast which predicts the flood, the system is iteratively optimised and updated. At the end of the event, the applied operations can be evaluated.

## 7.2 Priority decisions and warnings

### 7.2.1 Introduction to decision making





Results of the decision support system are reservoirs preventive operations and reduction of flood damages. The decisions concern turbinning, bottom outlet and pumping operations, characterized by the start and the end time of each preventive measure.

For decision making, the benefit given by minimisation of flood peaks and damages at check points as well as the potential energy sales costs of preventive operations at hydropower plants and the final levels in the reservoirs have to be considered.

**7.2.2 Priority decisions for reservoir operations**

The first decision is basically whether propose or not preventive operations to the hydropower plant operators. Therefore, various priority decision levels are established and implemented (Table 7.2). They represent the current necessity of taking a decision according to a given reservoir and its associated hydropower plants.

Table 7.2 Priority decision levels for reservoir operations.

Colour	Priority	Type of choice
	ND	No need for a decision
	P3	Think about a possible decision
	P2	Choose a decision soon
	P1	Take a decision

This decision priority has been defined depending on start times and duration of preventive measures according to Figure 7.1. When the start time is below 6 h as well as when start time is below 12 h and durations higher than 12 h, a decision is immediately required (P1 level). Next, for priority P2, a decision has to be taken but is not yet necessary to be proposed to the hydropower plant’ operators. For priority P3, just a discussion about the possible measures should be done. Finally, no decisions (ND) are required for start times above 24h (it is assumed in this case that new forecasts or new discharge observations will be provided within a shorter lag time). A diagram of the decision tree is presented in Figure 7.2.

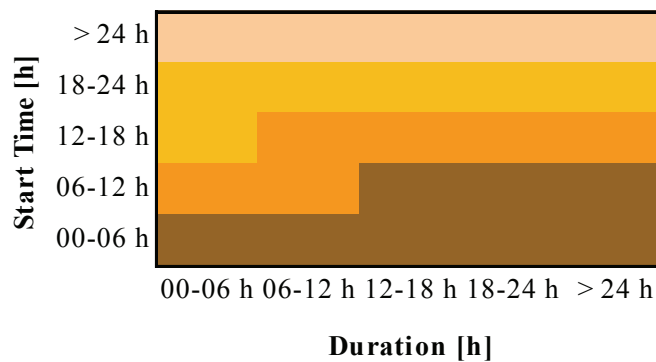


Figure 7.1 Priority decisions for each reservoir depending on its necessary preventive operations

Afterwards, the priority decision for a hydropower group is established by the highest priority level in one of its reservoirs.

This definition of priority decision could be changed in the future but provides a general idea of the need for a decision concerning preventive operations in a reservoir, allowing the distinction between primary and secondary decisions.

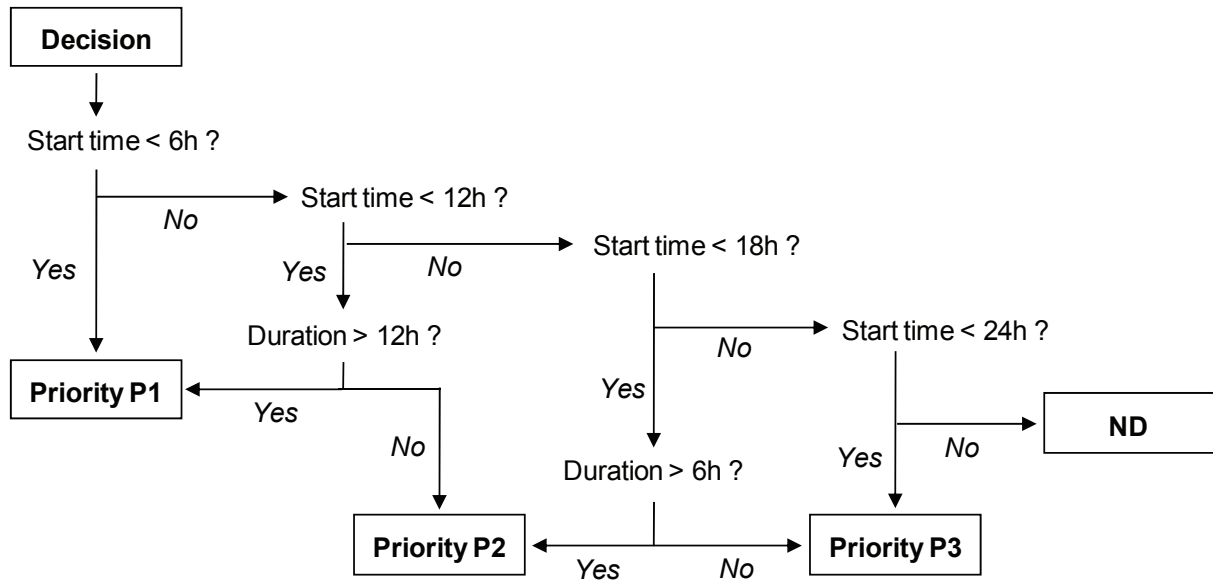






Figure 7.2 Decision tree for priority decision levels in the reservoirs.

### 7.2.3 Check points warnings

The warnings at check points are the same as used for the warning report (Chapter 4). The different warning levels depend on the discharge thresholds defined at each check point and the exceedance threshold defined for the occurrence probability of the probabilistic forecasts. The warnings are used for evaluating the need of preventive operations as shown in Table 7.3.

Table 7.3 Code of colours for the warning levels at check points.

Colour	Warning	Type of choice
	Steady situation	The active monitoring is not necessary at this moment
	Notice warning	Monitoring of the situation becomes required
	Alert warning	Preventive operations could decrease the risk of overflowing
	Alarm warning	Preventive operations should be undertaken when possible

Warnings are given at each check point and so distributed over the basin. It means that in a flood situation, the warning levels will be different at each check point. An assessment of the current circumstances (storage capacity in reservoirs, rain distribution, soil saturation, hydrographs,...) and the potential contribution of the preventive operations to the flood control have to be conducted case by case. General pre-established solutions from an archive of scenarios are not possible due to the complexity of the basin scheme.

### 7.3 Parameters to optimise

The number of parameters to optimise basically depends on the number of hydropower groups taken into account for the optimisation. They directly depend on the check point selected as the outlet of the basin to be optimised. At Porte-du-Scex, all groups (10) are optimised and the number of parameters amounts to 64 (Table 7.4). However, as an example, at Sion, the number of groups to optimise is reduced to 6 and the number of parameters decreases to 43.

Table 7.4 Number of parameters taken into account per group and reservoir, with T representing the turbinning operations, P the pumping operations and V the bottom outlet operations.

Group (GR)		Reservoir (RES)		
Name	Number of parameters	Name	Type of optimisation	Number of parameters
<b>GD (Grande Dixence)</b>	11	Grande Dixence	T, P & V	6
		Cleuson	T & V	5
<b>ESA (Emosson)</b>	6	Emosson	T, P & V	6
		Esserts	-	0
		Châtelard CFF	-	0
		Châtelard ESA	-	0
<b>FMM (Mauvoisin)</b>	5	Mauvoisin	T & V	5
		Fionnay	-	0
<b>KWM (Mattmark)</b>	6	Mattmark	T, P & V	6
		Zermeiggen	-	0
<b>FMG (Gougra)</b>	11	Moiry	T, P & V	6
		Turtmann	T & V	5
		Mottec	-	0
		Vissoie	-	0
<b>EL (Lienne)</b>	5	Zeuzier	T & V	5
		Croix	-	0
<b>SAL (Salanfe)</b>	5	Salanfe	T & V	5
<b>GSB (Pallazuit)</b>	5	Toules	T & V	5
		Pallazuit	-	0
<b>EM (Bitsch)</b>	5	Gebidem	T & V	5
<b>KWL (Lötschen)</b>	5	Ferden	T & V	5

Furthermore, the decision maker can exclude hydropower groups from optimisation. In practise, it means that the number of groups to optimise can vary from 0 to 10 depending on the selected check point and the choice of the end user. Therefore, the number of parameters can effectively vary from 0 to a maximum of 64.

## 7.4 Optimisation performance

### 7.4.1 Presented analysis

#### *Parameters and methods of analysis*

The results can be analysed in different ways depending on the selected check points, the number of groups to optimise, the use of bottom outlet and pumping operations, the type of the objective function, the algorithm use for the optimisation, the type of forecast, etc. The real impossibility of analysing all possibilities and interactions leads to a choice in the optimisations to conduct and the parameters to study in detail.

The check point Porte-du-Scex has been selected as the objective of the system for all optimisations treated in this chapter. This choice is not arbitrary since the usual operation of the system will search to decrease the expected damages over the whole basin.

Results are presented in tables (Table 7.5 to Table 7.13) which contain expected damages, potential preventive operation costs, flow peaks at Porte-du-Scex and flow peaks at Sion. The first two values are used for defining the loss function, but are presented separately for a better understanding of the stakes. Flow peaks are shown as practical useful values for assessing the consequences of the different optimisations.

For comparison reasons, these values are always presented for the natural basin and for the equipped basin with Business as Usual (BasU) operations. They are also shown for the equipped basin with Preventive Operations (PrevOp) using the Iterative Ranking Greedy Algorithm (IRGA) as well as the Shuffled Complex Evolution - University of Arizona (SCE-UA). Moreover, these results have been obtained for all available forecasts of each flood, but only the arithmetic mean values of all forecasts are presented for the October 2000 flood. The results obtained for the September 1993 flood were equivalent and only the case with the real-time flood management is presented.

In addition, two tables are presented when conducting probabilistic forecasts. The first corresponds to the average of the set of values related to probabilistic forecasts, depending on the selected utility function. The second corresponds to the maximum of the set of values. In fact, a box plot graphic could be presented instead of average or maximum values, but the evaluation would become rather complicated. It has to be noted that one single set of preventive operations is proposed when optimising with probabilistic forecasts, as in the deterministic case. Proposing more than one set of preventive operations could cause more

inconvenient than advantage since one only set of operation have to be selected at the end. Nevertheless, the decision maker has the possibility of achieving parallel simulations in order to compare the results of different preventive operations.

The study undertaken comprises one hydropower group optimisation, two groups optimisation and the whole basin network (10 groups) optimization, always with separated deterministic and probabilistic optimisations. The cases of real-time flood events have been finally performed.

#### **7.4.2 Optimisation of one group**

##### ***Characteristics of the optimisation with one hydropower group***

First, one hydropower group is optimised with the IRGA and SCE-UA algorithms. The IRGA algorithm is tested for all five utility functions available (when conducting a probabilistic forecast) and a preventive operation costs coefficient  $\beta$  fixed to one ( $\beta=1$ ). In fact, the variability of results depending on this coefficient is rather insignificant when the IRGA algorithm is used. When a probabilistic forecast is used in the optimisation, the SCE-UA is tested for a preventive operation costs coefficient  $\beta$  of one and two ( $\beta=1$  and  $\beta=2$ ) as well as for the five utility functions available. It has to be remembered than the coefficient  $\beta$  is used for increasing the weight of the PPOC, compared with the expected damages according to Eq. 6.27.

The aim is to check the two methods when the ranking used in the Greedy algorithm for solving in series the groups does not take part in the optimisation. Both algorithms should thus perform rather similarly.

In addition, the system with deterministic forecasts is evaluated with and without using the bottom outlet operations and so varying the number of parameters to be optimised. This option was not explored with probabilistic forecasts due to the large number of cases which make the analysis much too complex and the conclusions less clear.

When optimising one single hydropower group of the system, the number of parameters can vary from 5 to 11 depending on the characteristics of the group. Here, the evaluation of the system is carried out for two groups, Bitsch and Mattmark, which have been selected due to their location upstream of the basin, their high performance in reducing damages over the basin as well as to their simple structure.

The number of parameters to be optimised at Bitsch group is:

- 5 parameters if using turbines and bottom outlet operations and
- 3 parameters if bottom outlet operations are not considered.

The number of parameters to be optimised at Mattmark group is:

- 6 parameters if adjusting turbines, pumps and bottom outlet operations and
- 4 parameters if only turbines and pumps operations are considered.

### ***Optimisation results for one group and deterministic forecasts***

The reduction of damages when optimising one hydropower group directly depends on the group to be optimised, its characteristics, its initial level, the inflow as well as the hydrograph at the check points.

In the present case, PrevOp in Bitsch can reduce expected damages in the whole basin from 35 to 45%, but this reduction is only from 5 to 15% when optimising Mattmark. Main characteristics of the optimisation, presented in Table 7.5, are:

- The results with the SCE-UA algorithm are equals or better than those obtained by IRGA algorithm when optimising one only group. The values of Potential Preventive Operation Costs (PPOC) are similar in both cases. In all presented evaluations, the values of PPOC are equals to zero for the natural basin as well as for the equipped basin with Business as Usual (BasU) operations. This is obvious due to non PrevOp in these simulations.
- In Bitsch, the results are exactly the same using the IRGA or the SCE-UA approaches. However, the optimisation provides better results using the SCE-UA approach in Mattmark, especially when operating the turbines, pumps and bottom outlets at the same time. The reason is that the SCE-UA algorithm searches the better combination of parameters which reduces the damages to a maximum, varying all parameters at the same time. On the contrary, the IRGA algorithm optimises turbines, bottom outlet and pumping sequence operations in series, one sequence after the other, and the global optimum is more difficult to reach.
- The  $\beta$  coefficient does not vary significantly the results of SCE-UA, neither for the expected damages nor for the PPOC. Higher values of  $\beta$  have been also studied and provide identical results.
- Results show that the damage reduction can be higher when using bottom outlets, even if the PPOC can increase up to 50%. In any case, this option seems to be more



interesting than operating only turbines and pumps, especially if the available time for the operations is restraint or the damage reduction is considerable.

- Finally, it has to be noted that even small diminutions in the flood peak at Porte-du-Scex can be associated to high damages reduction. It is mainly due to high damages in the upstream basin, where flow peaks were decreased by higher values.

Table 7.5 Results obtained for Bitsch and Mattmark with deterministic forecasts for one group optimisation, with *T* representing the turbinning operations, *P* the pumping operations, *V* the bottom outlet operations and  $\beta$  the potential preventive operation costs coefficient. Natural basin represents the simulation with the non equipped basin, BasU the simulation with the equipped basin and Business as Usual operations, Greedy the optimisation with the IRGA approach and SCE-UA the optimisation with the Shuffled Complex Evolution – University of Arizona approach.

One group optimisation (Bitsch) with deterministic forecasts						One group optimisation (Mattmark) with deterministic forecasts					
<b>Expected damages [10<sup>6</sup> CHF]</b>						<b>Expected damages [10<sup>6</sup> CHF]</b>					
	<b>Natural basin</b>	<b>BasU</b>	<b>Greedy (<math>\beta=1</math>)</b>	<b>SCE-UA (<math>\beta=1</math>) (<math>\beta=2</math>)</b>			<b>Natural basin</b>	<b>BasU</b>	<b>Greedy (<math>\beta=1</math>)</b>	<b>SCE-UA (<math>\beta=1</math>) (<math>\beta=2</math>)</b>	
<b>T + P + V</b>	2698.0	1294.3	706.1	706.1	706.1	<b>T + P + V</b>	2698.0	1294.3	1156.0	1083.3	1083.4
<b>T + P</b>	2698.0	1294.3	830.3	830.3	830.3	<b>T + P</b>	2698.0	1294.3	1212.7	1208.3	1208.3
<b>Potential Preventive Operations Costs [10<sup>6</sup> CHF]</b>						<b>Potential Preventive Operations Costs [10<sup>6</sup> CHF]</b>					
	<b>Natural basin</b>	<b>BasU</b>	<b>Greedy (<math>\beta=1</math>)</b>	<b>SCE-UA (<math>\beta=1</math>) (<math>\beta=2</math>)</b>			<b>Natural basin</b>	<b>BasU</b>	<b>Greedy (<math>\beta=1</math>)</b>	<b>SCE-UA (<math>\beta=1</math>) (<math>\beta=2</math>)</b>	
<b>T + P + V</b>	0	0	0.541	0.556	0.531	<b>T + P + V</b>	0	0	0.294	0.327	0.329
<b>T + P</b>	0	0	0.371	0.387	0.376	<b>T + P</b>	0	0	0.133	0.144	0.144
<b>Peak Porte-du-Scex [m<sup>3</sup>/s]</b>						<b>Peak Porte-du-Scex [m<sup>3</sup>/s]</b>					
	<b>Natural basin</b>	<b>BasU</b>	<b>Greedy (<math>\beta=1</math>)</b>	<b>SCE-UA (<math>\beta=1</math>) (<math>\beta=2</math>)</b>			<b>Natural basin</b>	<b>BasU</b>	<b>Greedy (<math>\beta=1</math>)</b>	<b>SCE-UA (<math>\beta=1</math>) (<math>\beta=2</math>)</b>	
<b>T + P + V</b>	1298.6	1088.3	1055.6	1055.6	1052.3	<b>T + P + V</b>	1298.6	1088.3	1075.3	1070.4	1074.1
<b>T + P</b>	1298.6	1088.3	1060.7	1060.7	1060.7	<b>T + P</b>	1298.6	1088.3	1080.3	1081.4	1082.9
<b>Peak Sion [m<sup>3</sup>/s]</b>						<b>Peak Sion [m<sup>3</sup>/s]</b>					
	<b>Natural basin</b>	<b>BasU</b>	<b>Greedy (<math>\beta=1</math>)</b>	<b>SCE-UA (<math>\beta=1</math>) (<math>\beta=2</math>)</b>			<b>Natural basin</b>	<b>BasU</b>	<b>Greedy (<math>\beta=1</math>)</b>	<b>SCE-UA (<math>\beta=1</math>) (<math>\beta=2</math>)</b>	
<b>T + P + V</b>	1094.7	937.4	898.0	895.9	890.3	<b>T + P + V</b>	1094.7	937.4	920.7	915.9	915.1
<b>T + P</b>	1094.7	937.4	906.0	906.0	906.0	<b>T + P</b>	1094.7	937.4	924.9	923.6	923.6

### Optimisation results for one group and probabilistic forecasts

When the optimisation is performed with probabilistic forecasts, the results produced by the five proposed utility functions are also tested (each function proposing one different and single set of preventive operations). However, the results with and without bottom outlet operations are not compared in probabilistic forecasts in order to limit the number of evaluations.

Regarding average values of final expected damages, a reduction of 10 to 20% is obtained compared to simulations with BasU operations. Necessary preventive operations to achieve

this reduction have an average potential costs of 0.4 to 1.0·10<sup>6</sup> CHF. Table 7.6 presents the results of this optimisation, which main conclusions are:

- Similar reduction of damages with comparable PPOC is obtained for IRGA and SCE-UA approaches and for both groups.
- The  $\beta$  parameter seems to slightly vary the SCE-UA results and reduces the potential costs (PPOC) when it is equal to 2, but this reduction in PPOC is not systematic.
- If the performance of the five utility functions is studied, several differences are found. BRC and TOPSIS perform better accordingly to the average of the set of values. DHF provides values a little bit higher. MMR obtains the highest average, basically because this methodology does not take into account the average of the set of values but only the maximum. DMC also provides slightly higher values than the first three functions. This is due to the fact that 10% highest damages are not taken into account during the optimisation process and, then, the preventive operations are softer and final damages higher.
- The flood peaks are not significantly reduced at Porte-du-Scex or Sion. Nevertheless, the reduction was sometimes higher in other check points depending on the forecast.

Regarding maximum values of the set of final expected damages (Table 7.7), a reduction of 5 to 10% is obtained, according to the same optimised preventive operations and compared again to the equipped basin simulated with BasU operations. Further conclusions can be drawn from this table:

- Differences between IRGA and SCE-UA approaches are not significantly different.
- Checking the utility functions, the conclusions are congruent with the conclusions of average values. MMR produces the smallest maximum value of the set of expected damages, which is logical since this is the only value taken into account during the optimisation process. DMC produces higher values than those obtained for the other utility functions, which is also reasonable since the highest values are not taken into account during this optimisation. Finally, BRC, DHF and TOPSIS still gives similar results, with a little smaller value for the DHF, as envisaged because this method optimises a combination of the average and the maximum of the set of values.
- The flood peak is slightly reduced at Porte-du-Scex. The reduction is higher at Sion, reaching 14% when optimising Bitsch through the IRGA approach.

Table 7.6 Average of the set of values obtained for Bitsch and Mattmark with probabilistic forecasts and one group optimisation, including Bayes Risk Criterion (BRC), MMR (MinMax Regret), DMC (Decision Maker Criterion), DHF (Derived Hurwicz for Floods) and TOPSIS (Technique for Order Preference by Similarity to Ideal Solution). Natural basin represents the simulation with the non equipped basin, BasU the simulation with the equipped basin with Business as Usual operations, Greedy the optimisation with the IRGA approach and SCE-UA the optimisation with the Shuffled Complex Evolution – University of Arizona approach.  $\beta$  corresponds the potential preventive operation costs coefficient.

One group opt (Bitsch) with prob forecasts (Av. of the set of values)						One group opt (Mattmark) with prob forec (Av. of the set of values)					
Expected damages [ $10^6$ CHF]						Expected damages [ $10^6$ CHF]					
	Natural basin	BasU	Greedy ( $\beta=1$ )	SCE-UA ( $\beta=1$ ) ( $\beta=2$ )			Natural basin	BasU	Greedy ( $\beta=1$ )	SCE-UA ( $\beta=1$ ) ( $\beta=2$ )	
BRC	2005.2	1326.0	1060.0	1060.2	1059.6	BRC	2005.2	1326.0	1189.0	1175.6	1171.0
MMR	2005.2	1326.0	1258.0	1329.0	1189.0	MMR	2005.2	1326.0	1380.0	1423.0	1370.8
DMC	2005.2	1326.0	1123.0	1116.0	1077.8	DMC	2005.2	1326.0	1191.8	1183.4	1176.0
DHF	2005.2	1326.0	1117.6	1087.2	1075.2	DHF	2005.2	1326.0	1172.4	1181.8	1180.8
TOPSIS	2005.2	1326.0	1060.6	--	--	TOPSIS	2005.2	1326.0	1186.0	--	--
Potential Preventive Operations Costs [ $10^6$ CHF]						Potential Preventive Operations Costs [ $10^6$ CHF]					
	Natural basin	BasU	Greedy ( $\beta=1$ )	SCE-UA ( $\beta=1$ ) ( $\beta=2$ )			Natural basin	BasU	Greedy ( $\beta=1$ )	SCE-UA ( $\beta=1$ ) ( $\beta=2$ )	
BRC	0	0	0.948	1.010	0.986	BRC	0	0	0.408	0.426	0.424
MMR	0	0	0.896	0.996	0.924	MMR	0	0	0.496	0.702	0.638
DMC	0	0	0.760	0.772	0.878	DMC	0	0	0.362	0.362	0.338
DHF	0	0	1.004	1.032	0.998	DHF	0	0	0.448	0.416	0.614
TOPSIS	0	0	0.970	--	--	TOPSIS	0	0	0.430	--	--
Peak Porte-du-Scex [ $m^3/s$ ]						Peak Porte-du-Scex [ $m^3/s$ ]					
	Natural basin	BasU	Greedy ( $\beta=1$ )	SCE-UA ( $\beta=1$ ) ( $\beta=2$ )			Natural basin	BasU	Greedy ( $\beta=1$ )	SCE-UA ( $\beta=1$ ) ( $\beta=2$ )	
BRC	1203.8	1068.6	1043.0	1045.0	1041.2	BRC	1203.8	1068.6	1052.6	1050.8	1051.6
MMR	1203.8	1068.6	1056.2	1059.6	1056.8	MMR	1203.8	1068.6	1064.6	1068.6	1064.6
DMC	1203.8	1068.6	1048.6	1047.6	1044.4	DMC	1203.8	1068.6	1052.4	1052.4	1053.0
DHF	1203.8	1068.6	1048.6	1042.6	1043.2	DHF	1203.8	1068.6	1050.6	1054.8	1055.6
TOPSIS	1203.8	1068.6	1042.6	--	--	TOPSIS	1203.8	1068.6	1051.2	--	--
Peak Sion [ $m^3/s$ ]						Peak Sion [ $m^3/s$ ]					
	Natural basin	BasU	Greedy ( $\beta=1$ )	SCE-UA ( $\beta=1$ ) ( $\beta=2$ )			Without HPP	BasU	Greedy ( $\beta=1$ )	SCE-UA ( $\beta=1$ ) ( $\beta=2$ )	
BRC	942.0	847.0	821.0	816.0	817.2	BRC	942.0	847.0	831.4	829.4	829.6
MMR	942.0	847.0	833.8	839.6	829.8	MMR	942.0	847.0	846.2	852.4	844.6
DMC	942.0	847.0	825.6	829.0	822.4	DMC	942.0	847.0	831.4	832.4	831.4
DHF	942.0	847.0	827.2	818.0	816.6	DHF	942.0	847.0	829.4	831.2	834.0
TOPSIS	942.0	847.0	821.4	--	--	TOPSIS	942.0	847.0	830.6	--	--

Table 7.7 Maximum of the set of values obtained for Bitsch and Mattmark with probabilistic forecasts and one group optimisation, including Bayes Risk Criterion (BRC), MMR (MinMax Regret), DMC (Decision Maker Criterion), DHF (Derived Hurwicz for Floods) and TOPSIS (Technique for Order Preference by Similarity to Ideal Solution). Natural basin represents the simulation with the non equipped basin, BasU the simulation with the equipped basin with Business as Usual operations, Greedy the optimisation with the IRGA approach and SCE-UA the optimisation with the Shuffled Complex Evolution – University of Arizona approach.  $\beta$  corresponds the potential preventive operation costs coefficient.

One group opt (Bitsch) with prob forecasts (Max. of the set of values)						One group opt (Mattmark) with prob forec (Max. of the set of values)					
Expected damages [ $10^6$ CHF]						Expected damages [ $10^6$ CHF]					
	Natural basin	BasU	Greedy ( $\beta=1$ )	SCE-UA ( $\beta=1$ ) ( $\beta=2$ )			Natural basin	BasU	Greedy ( $\beta=1$ )	SCE-UA ( $\beta=1$ ) ( $\beta=2$ )	
BRC	4856.6	3798.8	3545.8	3609.2	3602.0	BRC	4856.6	3798.8	3625.6	3617.4	3605.8
MMR	4856.6	3798.8	3469.6	3395.6	3455.2	MMR	4856.6	3798.8	3568.2	3544.4	3546.0
DMC	4856.6	3798.8	3713.0	3649.8	3646.6	DMC	4856.6	3798.8	3642.8	3622.4	3663.8
DHF	4856.6	3798.8	3395.2	3557.0	3452.2	DHF	4856.6	3798.8	3594.0	3589.2	3580.4
TOPSIS	4856.6	3798.8	3487.6	--	--	TOPSIS	4856.6	3798.8	3604.2	--	--
Potential Preventive Operations Costs [ $10^6$ CHF]						Potential Preventive Operations Costs [ $10^6$ CHF]					
	Natural basin	BasU	Greedy ( $\beta=1$ )	SCE-UA ( $\beta=1$ ) ( $\beta=2$ )			Natural basin	BasU	Greedy ( $\beta=1$ )	SCE-UA ( $\beta=1$ ) ( $\beta=2$ )	
BRC	0	0	0.948	1.010	0.986	BRC	0	0	0.408	0.426	0.424
MMR	0	0	0.896	0.996	0.924	MMR	0	0	0.496	0.702	0.638
DMC	0	0	0.760	0.772	0.878	DMC	0	0	0.362	0.362	0.338
DHF	0	0	1.004	1.032	0.998	DHF	0	0	0.448	0.416	0.614
TOPSIS	0	0	0.970	--	--	TOPSIS	0	0	0.430	--	--
Peak Porte-du-Sceux [ $m^3/s$ ]						Peak Porte-du-Sceux [ $m^3/s$ ]					
	Natural basin	BasU	Greedy ( $\beta=1$ )	SCE-UA ( $\beta=1$ ) ( $\beta=2$ )			Natural basin	BasU	Greedy ( $\beta=1$ )	SCE-UA ( $\beta=1$ ) ( $\beta=2$ )	
BRC	1653.0	1446.8	1419.6	1429.0	1428.8	BRC	1653.0	1446.8	1424.6	1423.6	1421.6
MMR	1653.0	1446.8	1410.0	1399.0	1407.6	MMR	1653.0	1446.8	1417.0	1414.2	1411.2
DMC	1653.0	1446.8	1433.2	1420.2	1422.0	DMC	1653.0	1446.8	1425.6	1423.0	1428.0
DHF	1653.0	1446.8	1399.0	1420.4	1409.6	DHF	1653.0	1446.8	1420.0	1419.8	1415.8
TOPSIS	1653.0	1248.8	1411.2	--	--	TOPSIS	1653.0	1446.8	1421.4	--	--
Peak Sion [ $m^3/s$ ]						Peak Sion [ $m^3/s$ ]					
	Natural basin	BasU	Greedy ( $\beta=1$ )	SCE-UA ( $\beta=1$ ) ( $\beta=2$ )			Natural basin	BasU	Greedy ( $\beta=1$ )	SCE-UA ( $\beta=1$ ) ( $\beta=2$ )	
BRC	1326.8	1191.2	1161.6	1168.8	1168.6	BRC	1326.8	1191.2	1169.6	1168.6	1167.0
MMR	1326.8	1191.2	1149.0	1140.8	1148.6	MMR	1326.8	1191.2	1161.4	1159.0	1158.2
DMC	1326.8	1191.2	1174.6	1171.0	1171.2	DMC	1326.8	1191.2	1170.4	1168.2	1173.2
DHF	1326.8	1191.2	1140.8	1161.2	1146.8	DHF	1326.8	1191.2	1164.8	1164.8	1163.0
TOPSIS	1326.8	1191.2	1153.0	--	--	TOPSIS	1326.8	1191.2	1166.4	--	--

**Performances of studied approaches and computation times for one group optimisation**

The main results of one group optimisation are presented in Figure 7.3 and Figure 7.4. IRGA and SCE-UA generally provide rather equivalent results. For deterministic forecasts, they are usually slightly better with the SCE-UA approach (Figure 7.3). For probabilistic forecasts (Figure 7.4), they are similar for average expected values (solids colours), for maximum expected damages (light colours) as well as for potential preventive operation costs.

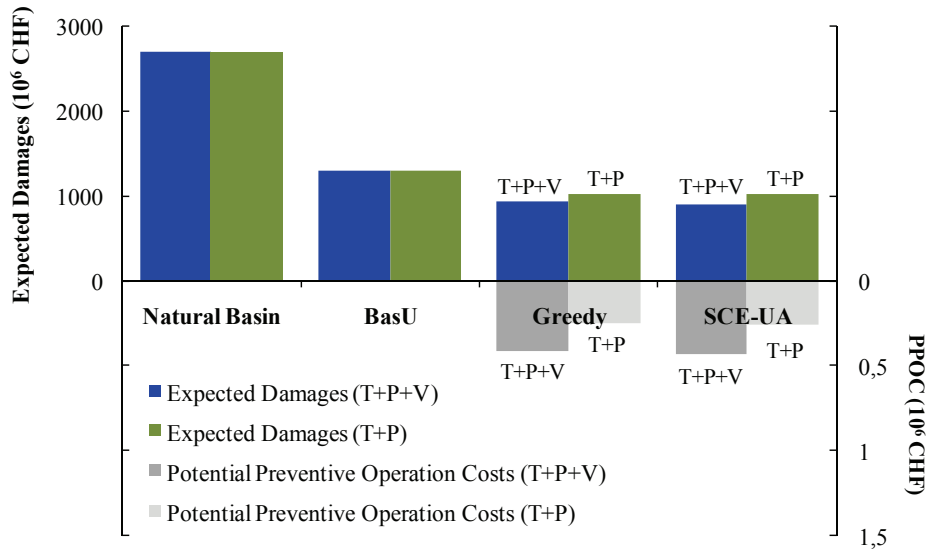


Figure 7.3 Main results obtained for Bitsch and Mattmark with deterministic forecasts for one group optimisation,  $T$  representing the turbinig operations,  $P$  the pumping operations and  $V$  the bottom outlet operations. Natural basin represents the simulation with the non equipped basin, BasU the simulation with the equipped basin and Business as Usual operations, Greedy the optimisation with the IRGA approach and SCE-UA the optimisation with the Shuffled Complex Evolution – University of Arizona approach. PPOC indicates the Potential Preventive Operation Costs.

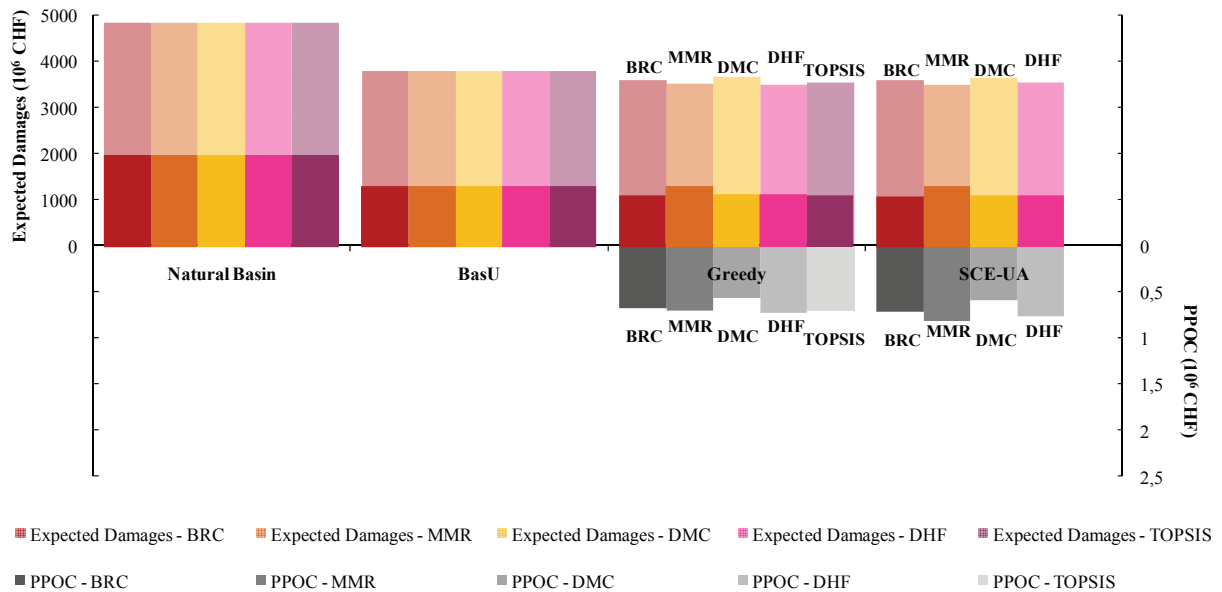


Figure 7.4 Average and maximum of the set of values obtained for Bitsch and Mattmark with probabilistic forecasts and one group optimisation, including Bayes Risk Criterion (BRC), MMR (MinMax Regret), DMC (Decision Maker Criterion), DHF (Derived Hurwicz for Floods) and TOPSIS (Technique for Order Preference by Similarity to Ideal Solution). Natural basin represents the simulation with the non equipped basin, BasU the simulation with the equipped basin and Business as Usual operations, Greedy the optimisation with the IRGA approach and SCE-UA the optimisation with the Shuffled Complex Evolution – University of Arizona approach.  $\beta$  corresponds to the potential preventive operation costs coefficient. PPOC indicate the Potential Preventive Operation Costs. Average expected damages are represented by solid colours and maximum expected damages by lighter colours.

The number of evaluations of the utility function for the IRGA approach related to deterministic forecasts, as presented in Figure 7.5, varies between 2'000 and 3'000, with a total optimisation time of around 2 seconds. The number of evaluations for the SCE-UA approach varies between 400 and 600 with a total optimisation time up to 5 seconds.

If probabilistic forecasts are used, the IRGA approach also evaluates the utility function between 2'000 and 3'000 times but the optimisation time is increased up to 1 minute. The SCE-UA approach evaluates the function up to 1'000 times and the computation time is increased up to 4 minutes.

This computation time difference is due to the SCE-UA procedure, which calculates all group operations for each simulation, even if these operations are already fixed or there are BasU operations. It implies that more hydrographs calculations (additions and subtractions) and mass balance at reservoirs are computed at each evaluation step of the utility function. However, IRGA procedure computes only the group to be optimised, reducing considerably the calculations to complete and the computation time.

Nevertheless, when optimising one or two groups, computation times are not restrictive and this consideration does not become influential. In addition, when optimising all groups at the same time with the SCE-AU algorithm, the preventive operations effectively vary at each evaluation of the utility function and this procedure is accurate because no increase of the computation time is due to the implemented procedure.

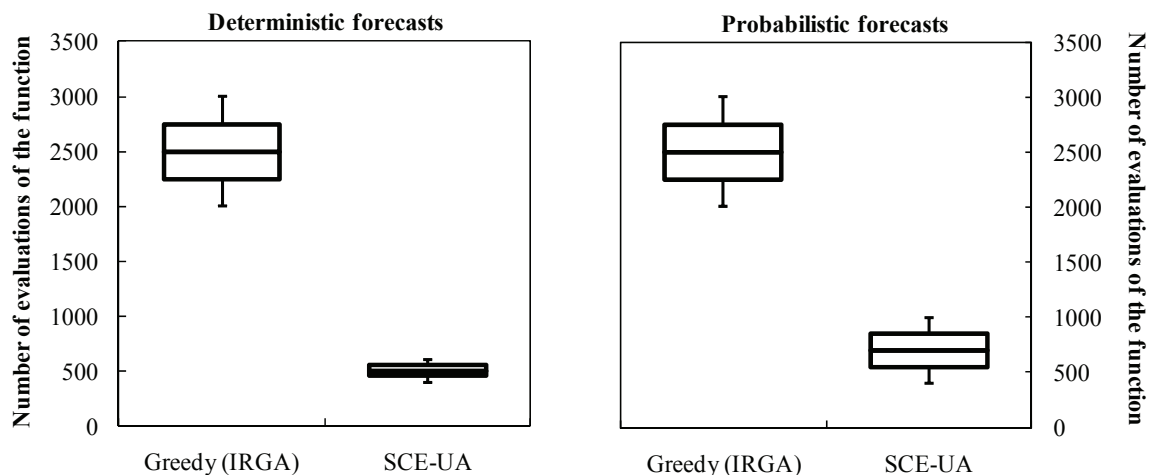


Figure 7.5 Number of evaluations of the objective function with deterministic and probabilistic forecasts and one group optimisation. Greedy (Iterative Ranking Greedy Algorithm) represents the optimisation with this approach and SCE-UA the optimisation with the Shuffled Complex Evolution – University of Arizona algorithm.

### 7.4.3 *Optimisation of two groups*

Second, the simultaneous optimisation of two hydropower groups was analysed in order to study the performance of the methods and algorithms when the number of parameters to optimise increases, but is still around 10 and 15. The selected hydropower groups are again Bitsch and Mattmark, but this time they are simultaneously optimised.

The IRGA algorithm was tested for the five utility functions available (for the probabilistic forecasts) and a preventive operation costs coefficient  $\beta$  fixed to one. Furthermore, since the IRGA approach optimises the groups in series, the results depending on the ranking of the groups offer another new possibility. However, it is only necessary to perform two possible orders here because only two groups are studied. The SCE-UA was tested for a preventive operation costs coefficient  $\beta$  having a value of one and two as well as for the five utility functions available when the probabilistic forecast is conducted during the optimisation.

The purpose was to check the methods for a small number of parameters to optimise, but already differentiating between one method solving the groups in series (Greedy) and the other one solving the groups at the same time (SCE-UA). The solution with and without bottom outlet operations was also tested for the case of deterministic forecasts. The computation time was also examined with the aim of identifying the influence of the number of groups to be optimised.

#### *Optimisation results with two groups and deterministic forecasts*

The reduction of damages when optimising these two groups at the same time can reduce expected damages up to 55% compared with the BasU operations. Main features of the optimisation can be summarized, according to Table 7.8, as follows:

- SCE-UA still provides slight improvements compared to IRGA, especially when taking into account bottom outlet operations.
- The order of the groups to be optimised in the IRGA algorithm does not considerably affect the results. This is also the case when comparing the values of potential preventive operation costs with different coefficient  $\beta$  in the SCE-UA approach, which produce equal optimisation results.
- As explained, the damage reduction when using all possible operations is around 55%, reaching 44% when bottom outlets are not optimised.



- The peak reduction is not considerable at Porte-du-Scex, only 3%, and becomes a little higher at Sion, with an average reduction of around 5%.

Table 7.8 Results obtained for two groups optimisation (Bitsch and Mattmark at the same time) with deterministic forecasts, with *T* representing the turbinning operations, *P* the pumping operations, *V* the bottom outlet operations and  $\beta$  the potential preventive operation costs coefficient. Natural basin represents the simulation with the non equipped basin, BasU the simulation with the equipped basin and Business as Usual operations, Greedy the optimisation with the IRGA approach and SCE-UA the optimisation with the Shuffled Complex Evolution – University of Arizona approach. B→M represents the order of the optimisation for the Greedy approach: first for Bitsch and second for Mattmark. M→B represents the same with the inverse order: first Mattmark, second Bitsch.

Two groups optimisation (Bitsch + Mattmark) with deterministic forecasts						
Expected damages [ $10^6$ CHF]						
	Natural basin	BasU	Greedy ( $\beta=1$ )		SCE-UA	
			B→M	M→B	( $\beta=1$ )	( $\beta=2$ )
T + P + V	2698.0	1294.3	590.9	589.9	574.1	574.1
T + P	2698.0	1294.3	720.7	721.1	717.3	716.4
Potential Preventive Operations Costs [ $10^6$ CHF]						
	Natural basin	BasU	Greedy ( $\beta=1$ )		SCE-UA	
			B→M	M→B	( $\beta=1$ )	( $\beta=2$ )
T + P + V	0	0	0.790	0.763	0.870	0.876
T + P	0	0	0.496	0.493	0.569	0.560
Peak Porte-du-Scex [ $m^3/s$ ]						
	Natural basin	BasU	Greedy ( $\beta=1$ )		SCE-UA	
			B→M	M→B	( $\beta=1$ )	( $\beta=2$ )
T + P + V	1298.6	1088.3	1048.0	1053.3	1049.0	1042.9
T + P	1298.6	1088.3	1057.1	1055.3	1054.3	1057.3
Peak Sion [ $m^3/s$ ]						
	Natural basin	BasU	Greedy ( $\beta=1$ )		SCE-UA	
			B→M	M→B	( $\beta=1$ )	( $\beta=2$ )
T + P + V	1094.7	937.4	881.1	885.6	881.4	874.7
T + P	1094.7	937.4	892.3	891.3	889.1	890.7

### Optimisation results with two groups and probabilistic forecasts

The results with probabilistic forecasts are performed. Each multi-attribute decision making (MADM) method (BRC, MMR, DMC, DHF and TOPSIS) provides an objective function which achieves to an only set of preventive operations. Therefore, the number of results stays the same than the number of forecasts tested for each MADM method.



The reduction due to Preventive Operations (PrevOp) is also clear in this case, and amounts up to 30% for the average of the set of damages compared to the average of the set of damages obtained with Business as Usual (BasU) operations. The characteristics of this optimisation for the average of the set of values are presented in Table 7.9, being the main characteristics:

- IRGA and SCE-UA provide similar results which vary depending on the utility function and therefore, in the preventive operations carried out. Slightly smaller values of expected damages are provided by the SCE-UA approach, also with higher values of Potential Preventive Operation Costs (PPOC).
- The optimisation order of the groups does not significantly change the results of the IRGA approach. The variation of  $\beta$  does not vary the SCE-UA results either.
- Concerning the utility functions, BRC and TOPSIS provides again the better results according to the average of the set of values. Next, DHF and DMC also give good results. MMR does not reduce considerably the expected average damages and does not seem to be an adequate method.
- As in previous cases, the peak is slightly reduced at Porte-du-Scex as well as at Sion due to PrevOp.

When assessing the maximum of the set of values, the damages reduction attains 20% compared to the maximum of the set of values of the BasU operations. Other results proposed in Table 7.10 are:

- MMR and DHF provide similar results, better in both cases than the results provided by the other methods. The worst result is given by the DMC method, which is rational because this method does not take into account the 10% highest hydrographs during the optimisation. Nevertheless, PPOC are not significantly smaller than the PPOC provided by other methods. Thus, the performance of the DMC in this case is questioned.
- Peak reduction at Porte-du-Scex and Sion reaches 5%.

Table 7.9 Average of the set of values obtained with probabilistic forecasts and two groups optimisation (Bitsch and Mattmark at the same time), including Bayes Risk Criterion (BRC), MMR (MinMax Regret), DMC (Decision Maker Criterion), DHF (Derived Hurwicz for Floods) and TOPSIS (Technique for Order Preference by Similarity to Ideal Solution). Natural basin represents the simulation with the non equipped basin, BasU the simulation with the equipped basin and Business as Usual operations, Greedy the optimisation with the IRGA approach and SCE-UA the optimisation with the Shuffled Complex Evolution – University of Arizona approach.  $\beta$  corresponds to the potential preventive operation costs coefficient. B→M represents the order of the optimisation for the Greedy approach: first for Bitsch and second for Mattmark. M→B represents the same with the inverse order: first Mattmark, second Bitsch.

Two groups optimisation with prob. forecasts (Average of the set of values)						
Expected damages [ $10^6$ CHF]						
	Natural basin	BasU	Greedy ( $\beta=1$ )		SCE-UA	
			B→M	M→B	( $\beta=1$ )	( $\beta=2$ )
BRC	2005.2	1326.0	919.0	919.0	984.4	940.0
MMR	2005.2	1326.0	1316.8	1316.8	1229.2	1278.6
DMC	2005.2	1326.0	1048.4	992.0	1004.4	1010.0
DHF	2005.2	1326.0	978.8	978.8	972.4	980.8
TOPSIS	2005.2	1326.0	919.6	931.2	--	--

Potential Preventive Operations Costs [ $10^6$ CHF]						
	Natural basin	BasU	Greedy ( $\beta=1$ )		SCE-UA	
			B→M	M→B	( $\beta=1$ )	( $\beta=2$ )
BRC	0	0	1.342	1.342	1.642	1.412
MMR	0	0	1.360	1.360	1.872	1.864
DMC	0	0	1.214	1.062	1.136	1.188
DHF	0	0	1.374	1.374	1.620	1.568
TOPSIS	0	0	1.358	1.316	--	--

Peak Porte-du-Scex [ $m^3/s$ ]						
	Natural basin	BasU	Greedy ( $\beta=1$ )		SCE-UA	
			B→M	M→B	( $\beta=1$ )	( $\beta=2$ )
BRC	1203.8	1068.6	1026.6	1026.6	1032.4	1031.6
MMR	1203.8	1068.6	1050.4	1050.4	1057.4	1058.4
DMC	1203.8	1068.6	1036.0	1035.2	1036.0	1039.0
DHF	1203.8	1068.6	1033.8	1033.8	1035.4	1044.8
TOPSIS	1203.8	1068.6	1026.6	1028.8	--	--

Peak Sion [ $m^3/s$ ]						
	Natural basin	BasU	Greedy ( $\beta=1$ )		SCE-UA	
			B→M	M→B	( $\beta=1$ )	( $\beta=2$ )
BRC	942.0	847.0	805.0	805.0	808.6	803.6
MMR	942.0	847.0	832.4	832.4	832.6	839.6
DMC	942.0	847.0	814.0	812.0	813.6	815.2
DHF	942.0	847.0	812.0	812.0	807.2	813.0
TOPSIS	942.0	847.0	805.0	806.6	--	--

Table 7.10 Maximum of the set of values obtained with probabilistic forecasts and two groups optimisation (Bitsch and Mattmark at the same time), including Bayes Risk Criterion (BRC), MMR (MinMax Regret), DMC (Decision Maker Criterion), DHF (Derived Hurwicz for Floods) and TOPSIS (Technique for Order Preference by Similarity to Ideal Solution). Natural basin represents the simulation with the non equipped basin, BasU the simulation with the equipped basin and Business as Usual operations, Greedy the optimisation with the IRGA approach and SCE-UA the optimisation with the Shuffled Complex Evolution – University of Arizona approach.  $\beta$  corresponds to the potential preventive operation costs coefficient. B→M represents the order of the optimisation for the Greedy approach: first for Bitsch and second for Mattmark. M→B represents the same with the inverse order: first Mattmark, second Bitsch.

**Two groups optimisation with prob. forecasts (Maximum of the set of values)**

	Expected damages [ $10^6$ CHF]					
	Natural basin	BasU	Greedy ( $\beta=1$ )		SCE-UA	
			B→M	M→B	( $\beta=1$ )	( $\beta=2$ )
<b>BRC</b>	4856.6	3798.8	3148.2	3148.2	3294.6	3258.6
<b>MMR</b>	4856.6	3798.8	3189.4	3189.4	3092.6	3098.0
<b>DMC</b>	4856.6	3798.8	3426.2	3405.6	3503.8	3545.0
<b>DHF</b>	4856.6	3798.8	3109.6	3109.6	3147.2	3205.4
<b>TOPSIS</b>	4856.6	3798.8	3141.0	3161.2	--	--

	Potential Preventive Operations Costs [ $10^6$ CHF]					
	Natural basin	BasU	Greedy ( $\beta=1$ )		SCE-UA	
			B→M	M→B	( $\beta=1$ )	( $\beta=2$ )
<b>BRC</b>	0	0	1.342	1.342	1.642	1.412
<b>MMR</b>	0	0	1.360	1.360	1.872	1.864
<b>DMC</b>	0	0	1.214	1.062	1.136	1.188
<b>DHF</b>	0	0	1.374	1.374	1.620	1.568
<b>TOPSIS</b>	0	0	1.358	1.316	--	--

	Peak Porte-du-Scex [ $m^3/s$ ]					
	Natural basin	BasU	Greedy ( $\beta=1$ )		SCE-UA	
			B→M	M→B	( $\beta=1$ )	( $\beta=2$ )
<b>BRC</b>	1653.0	1446.8	1380.0	1380.0	1396.8	1395.8
<b>MMR</b>	1653.0	1446.8	1386.6	1386.6	1379.4	1381.0
<b>DMC</b>	1653.0	1446.8	1397.8	1556.2	1411.4	1415.4
<b>DHF</b>	1653.0	1446.8	1379.8	1379.8	1387.0	1392.8
<b>TOPSIS</b>	1653.0	1248.8	1379.8	1382.0	--	--

	Peak Sion [ $m^3/s$ ]					
	Natural basin	BasU	Greedy ( $\beta=1$ )		SCE-UA	
			B→M	M→B	( $\beta=1$ )	( $\beta=2$ )
<b>BRC</b>	1326.8	1191.2	1124.4	1124.4	1138.6	1137.8
<b>MMR</b>	1326.8	1191.2	1128.2	1128.2	1121.8	1121.4
<b>DMC</b>	1326.8	1191.2	1148.2	1144.0	1157.4	1161.6
<b>DHF</b>	1326.8	1191.2	1123.8	1123.8	1124.8	1136.0
<b>TOPSIS</b>	1326.8	1191.2	1124.0	1126.4	--	--

**Performances of studied approaches and computation times for two groups optimisation**

When optimising two hydropower groups at the same time, results are rather similar for all approaches. SCE-UA provides slight better results than IRGA for deterministic forecasts (Figure 7.6) but slight worst results for probabilistic ones, as presented in Figure 7.7.

The bottom outlet operations clearly help in decreasing the damages. In addition, the use of BRC or TOPSIS provides the highest damages reduction when operating with probabilistic forecasts. All other parameters do not seem to have a big importance on the results.

The number of evaluations of the utility function for the IRGA approach related to deterministic forecasts, presented in Figure 7.8, varies between 4'000 and 7'500 with a total optimisation time smaller than 5 seconds. The number of evaluations for the SCE-UA approach varies between 1'000 and 1'500 with a total optimisation time up to 15 seconds.

Using probabilistic forecasts, the IRGA approach also evaluates the utility function between 4'000 and 7'500 times but the optimisation time is increased up to 2 minutes. The SCE-UA approach evaluates the function between 1'000 and 3'000 times and the computation time is increased up to 10 minutes.

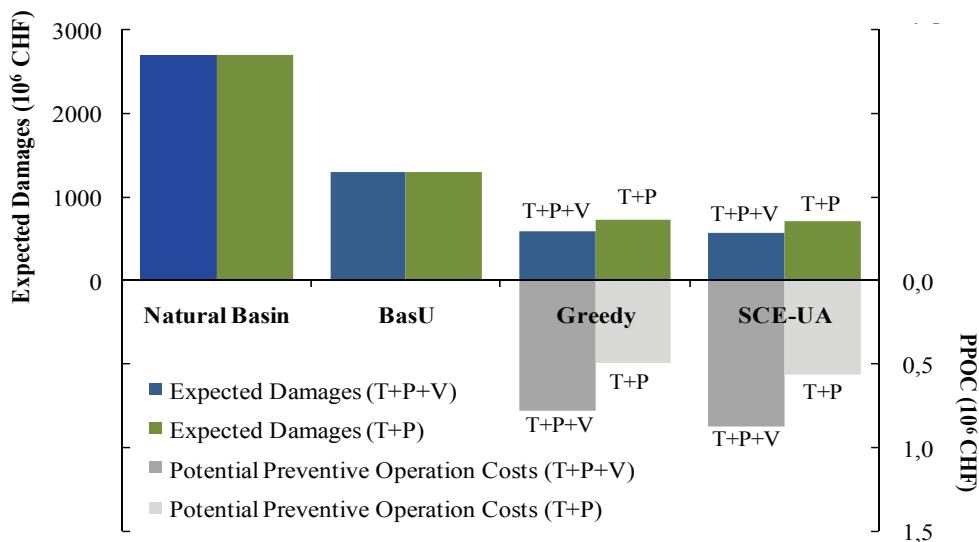


Figure 7.6 Main results obtained with deterministic forecasts for two groups optimisation (Bitsch and Mattmark at the same time), T representing the turbinning operations, P the pumping operations and V the bottom outlet operations. Natural basin represents the simulation with the non equipped basin, BasU the simulation with the equipped basin and Business as Usual operations, Greedy the optimisation with the IRGA approach and SCE-UA the optimisation with the Shuffled Complex Evolution – University of Arizona approach. PPOC indicates the Potential Preventive Operation Costs.

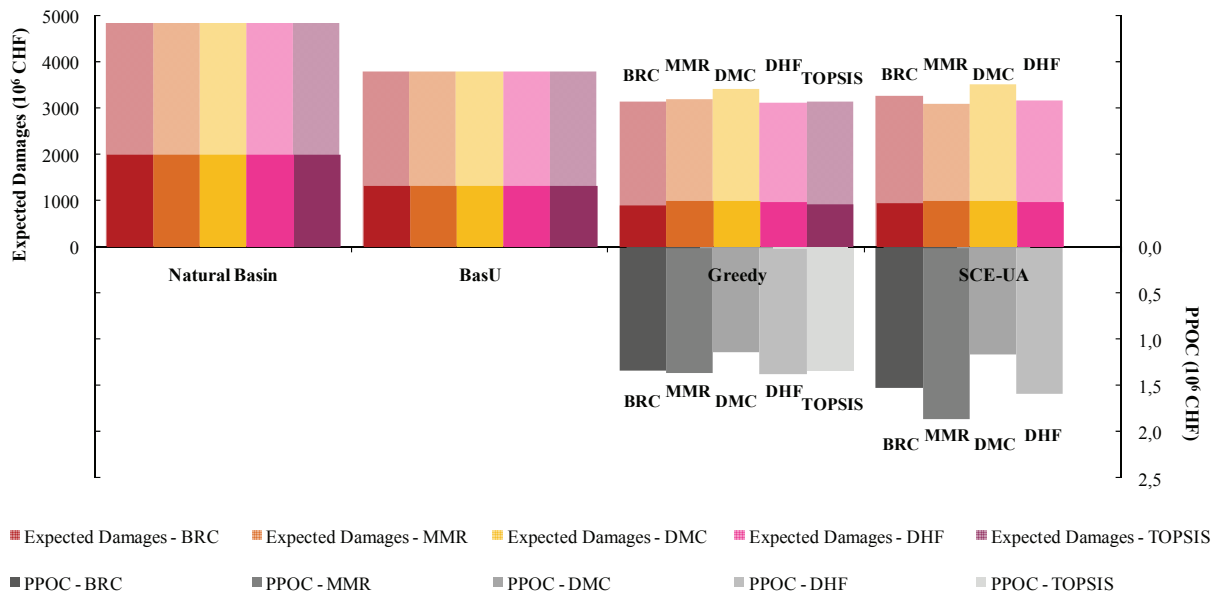


Figure 7.7 Average and maximum of the set of values obtained with probabilistic forecasts and two groups optimisation (Bitsch and Mattmark at the same time), including Bayes Risk Criterion (BRC), MMR (MinMax Regret), DMC (Decision Maker Criterion), DHF (Derived Hurwicz for Floods) and TOPSIS (Technique for Order Preference by Similarity to Ideal Solution). Natural basin represents the simulation with the non equipped basin, BasU the simulation with the equipped basin and Business as Usual operations, Greedy the optimisation with the IRGA approach and SCE-UA the optimisation with the Shuffled Complex Evolution – University of Arizona approach.  $\beta$  corresponds to the potential preventive operation costs coefficient. PPOC indicates the Potential Preventive Operation Costs. Average expected damages are represented by solid colours and maximum expected damages by lighter colours.

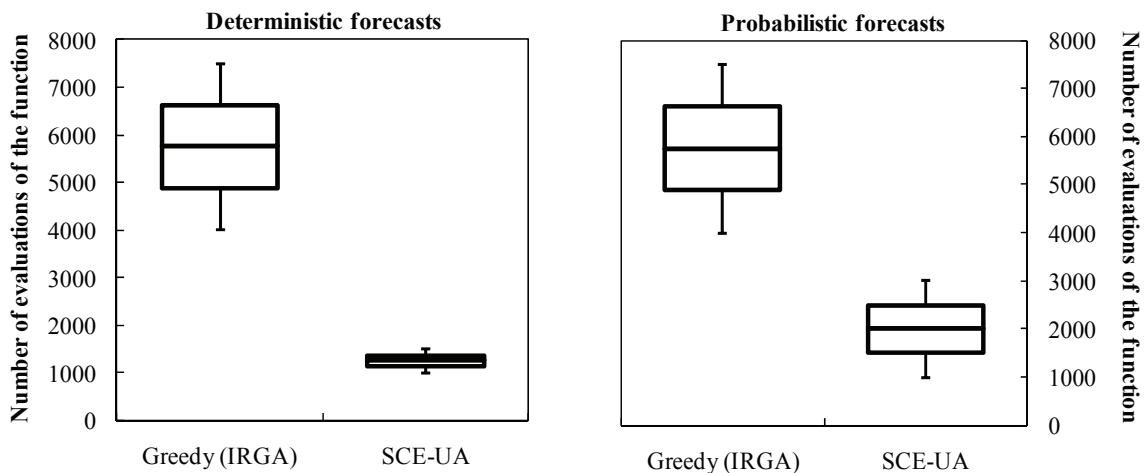


Figure 7.8 Number of evaluations of the objective function with deterministic and probabilistic forecasts and two groups optimisation. Greedy (Iterative Ranking Greedy Algorithm) represents the optimisation with this approach and SCE-UA the optimisation with the Shuffled Complex Evolution – University of Arizona algorithm

#### **7.4.4 Optimisation of the entire basin with all groups**

Finally, the entire basin with all groups is also optimised, testing the performance in the same way than before for IRGA and SCE-UA algorithms. The goal is to evaluate the performance of the methods when a big number of parameters has to be optimised. This evaluation clearly corresponds to the case of a real flood event.

It should be kept in mind that the main difference between IRGA and SCE-UA approaches is that IRGA solves the optimisation group by group, not optimising all parameters at the same time. However, SCE-UA effectively varies and optimises all parameters for all groups simultaneously.

The ranking of the groups for the IRGA approach is used in this case. The considered rankings are the Reservoir Space Index from the highest to the smallest group values ( $RSI_{\max\text{to}\min}$ ) or from the smallest to the highest values ( $RSI_{\min\text{to}\max}$ ), the order of the groups from upstream to downstream (UsToDs) or from downstream to upstream (DsToUs) as well as a random order (RR).

#### **Optimisation results with all groups and deterministic forecasts**

Thanks to the contribution of PrevOp of all groups over the basin, the reduction of expected damages is increased up to 65%. The following conclusions can be given based on the results presented in Table 7.11:

- Regarding the expected damages, the SCE-UA optimisation provides poorer results than the Greedy methodology for an optimisation with bottom outlet operations and similar results for an optimisation with only turbine and pump operations. Regarding PPOC, SCE-UA proposes higher PrevOp compared to IRGA, with values approximately 4 times higher.
- The ranking of the groups of IRGA does not considerably influence the results according to the expected damages, but it does according to PPOC. Minimum PPOC is given by the ranking  $RSI_{\max\text{to}\min}$  and the highest by the UsToDs. The  $\beta$  parameter slightly improves the results with the SCE-UA approach, decreasing a little bit the PPOC. However, these results are not systematic and changing the value of  $\beta$  does not directly reduce the PPOC.
- The use of bottom outlet operations obviously provides a higher reduction of damages. The reduction is around 28% with IRGA and 17% with SCE-UA compared to PrevOp without bottom outlet operations. In this way, PPOC increases of around 50% for the

IRGA approach and more than 200% with the SCE-UA approach. This last result is probably due to the high number of parameters which affects the performance of the optimisation.

- The peak reduction is especially significant at Sion but a little bit less at Porte-du-Scex. As expected, major peak reductions are obtained with the IRGA approach, especially at Porte-du-Scex.

Table 7.11 Results obtained with deterministic forecasts for all groups optimisation, with  $T$  representing the turbines operations,  $P$  the pumps operations,  $V$  the bottom outlet operations and  $\beta$  the potential preventive operation costs coefficient. Natural basin represents the simulation with the non equipped basin, BasU the simulation with the equipped basin and Business as Usual operations, Greedy the optimisation with the IRGA approach and SCE-UA the optimisation with the Shuffled Complex Evolution – University of Arizona approach.  $RSI_{max\ to\ min}$  represents the Reservoir Space Index from the highest to the smallest values in the groups order with the Greedy approach,  $RSI_{min\ to\ max}$  the Reservoir Space Index from the smallest to the highest values, UsToDs, the order from upstream to downstream, DsToUs from downstream to upstream and Random an order with this characteristic.

All groups optimisation with deterministic forecasts									
Expected damages [ $10^6$ CHF]									
	Natural basin	BasU	Greedy ( $\beta=1$ )					SCE-UA	
			$RSI_{max\ to\ min}$	$RSI_{min\ to\ max}$	UsToDs	DsToUs	Random	( $\beta=1$ )	( $\beta=2$ )
T+P+V	2698.0	1294.3	454.6	454.6	454.6	454.6	454.6	519.3	517.4
T+P	2698.0	1294.3	629.3	629.3	629.3	629.3	629.3	625.3	625.7
Potential Preventive Operations Costs [ $10^6$ CHF]									
	Natural basin	BasU	Greedy ( $\beta=1$ )					SCE-UA	
			$RSI_{max\ to\ min}$	$RSI_{min\ to\ max}$	UsToDs	DsToUs	Random	( $\beta=1$ )	( $\beta=2$ )
T+P+V	0	0	0.896	0.961	1.023	0.946	0.951	4.507	4.257
T+P	0	0	0.607	0.617	0.633	0.629	0.626	1.659	1.227
Peak Porte-du-Scex [ $m^3/s$ ]									
	Natural basin	BasU	Greedy ( $\beta=1$ )					SCE-UA	
			$RSI_{max\ to\ min}$	$RSI_{min\ to\ max}$	UsToDs	DsToUs	Random	( $\beta=1$ )	( $\beta=2$ )
T+P+V	1298.6	1088.3	1034.6	1035.0	1032.4	1041.4	1036.0	1089.0	1066.7
T+P	1298.6	1088.3	1041.9	1044.7	1043.9	1046.4	1043.6	1037.7	1039.0
Peak Sion [ $m^3/s$ ]									
	Natural basin	BasU	Greedy ( $\beta=1$ )					SCE-UA	
			$RSI_{max\ to\ min}$	$RSI_{min\ to\ max}$	UsToDs	DsToUs	Random	( $\beta=1$ )	( $\beta=2$ )
T+P+V	1094.7	937.4	873.3	873.0	870.0	872.1	869.7	881.9	879.3
T+P	1094.7	937.4	881.1	884.1	882.9	881.4	881.9	877.6	879.7

### **Optimisation results for all groups and probabilistic forecasts**

For the optimisation with probabilistic forecasts, the average reduction of final expected damages with PrevOp reaches 35% compared to BasU operations, with a PPOC of around 1.5 to  $2.0 \cdot 10^6$  CHF for the IRGA approach. The PPOC are still higher for the SCE-UA approach. The other characteristics of the average of the set of values, presented in Table 7.12, are:

- The IRGA approach clearly provides better results than the SCE-UA approach for the expected damages as well as for the PPOC. In addition, SCE-UA computation times can be prohibitive, usually exceeding 5 hours. The excessive number of parameters as well as the complex solution space could be two explanations for the poor performance of the SCE-UA approach.
- The ranking of groups of the IRGA method slightly influences the results for both expected damages and PPOC. Nevertheless, any pattern cannot be given and the optimal ranking should be based on a case by case study due to the high complexity of the system.
- The  $\beta$  parameter with values equal to 1 and 2 provides similar expected damages for the SCE-UA approach, but it reduces the potential costs when  $\beta=2$ . However, this improvement is not systematic and depends on the selected forecast.
- Some differences can be observed when studying the performance of the system depending on the five utility functions. BRC, DHF and TOPSIS methods again provide the best results according to the average of the set of values. MMR provides the highest average value. DMC results are in the middle of the MMR and the others. It should be noticed that DMC does not take into account the 10% highest damages during the optimisation. It finally increases the average of the set of expected damages between 10 and 15%, but also decreases the average of the set of PPOC by 20%.
- The peak discharge in Porte-du-Scex is reduced by 5% in average, but is reduced up to 10% in some forecasts. The same results are given for the peak discharge in Sion.

Regarding the maximum of the set of the function values, the reductions reach 20% compared with BasU operations. The most important characteristics are (Table 7.13):

- Minimum values of expected damages are given by MMR and DHF and the worst value is provided by DMC. These results confirm those provided in the previous case of this optimisation with the average of the set of values.
- Flow peaks are reduced by around 5% in both Porte-du-Scex and Sion.



Table 7.12 Average of the set of values obtained with probabilistic forecasts and all groups optimisation, including Bayes Risk Criterion (BRC), MMR (MinMax Regret), DMC (Decision Maker Criterion), DHF (Derived Hurwicz for Floods) and TOPSIS (Technique for Order Preference by Similarity to Ideal Solution). Natural basin represents the simulation with the non equipped basin, BasU the simulation with the equipped basin and Business as Usual operations, Greedy the optimisation with the IRGA approach and SCE-UA the optimisation with the Shuffled Complex Evolution – University of Arizona approach.  $\beta$  corresponds to the potential preventive operation costs coefficient.  $RSI_{\max\text{to}\min}$  represents the Reservoir Space Index from the highest to the smallest values in the order of the optimisation for the Greedy approach,  $RSI_{\min\text{to}\max}$  the Reservoir Space Index from the smallest to the highest values, UsToDs, the order from upstream to downstream, DsToUs from downstream to upstream and Random an order with this characteristic.

All groups optimisation with probabilistic forecasts (Maximum of the set of values)									
Expected damages [ $10^6$ CHF]									
	Natural basin	BasU	Greedy ( $\beta=1$ )					SCE-UA	
			$RSI_{\max\text{to}\min}$	$RSI_{\min\text{to}\max}$	UsToDs	DsToUs	Random	( $\beta=1$ )	( $\beta=2$ )
BRC	4856.6	3798.8	3188.2	3094.0	3094.0	3174.8	3173.8	3412.4	3259.0
MMR	4856.6	3798.8	2965.4	2964.8	2965.4	2965.4	2965.4	3182.6	3144.6
DMC	4856.6	3798.8	3418.4	3436.4	3374.4	3377.2	3358.8	3612.6	3616.4
DHF	4856.6	3798.8	3089.6	3041.4	3024.6	3064.2	3089.6	3195.6	3140.8
TOPSIS	4856.6	3798.8	3169.0	3172.0	3158.2	3175.2	3191.8	--	--

Potential Preventive Operations Costs [ $10^6$ CHF]									
	Natural basin	BasU	Greedy ( $\beta=1$ )					SCE-UA	
			$RSI_{\max\text{to}\min}$	$RSI_{\min\text{to}\max}$	UsToDs	DsToUs	Random	( $\beta=1$ )	( $\beta=2$ )
BRC	0	0	1.938	1.854	1.854	1.884	1.926	7.762	4.168
MMR	0	0	1.846	1.878	1.846	1.846	1.846	3.858	3.910
DMC	0	0	1.492	1.488	1.492	1.600	1.382	2.506	2.390
DHF	0	0	1.906	2.006	1.888	1.900	1.906	4.764	4.330
TOPSIS	0	0	1.942	1.960	1.926	1.846	2.012	--	--

Peak Porte-du-Scex [ $m^3/s$ ]									
	Natural basin	BasU	Greedy ( $\beta=1$ )					SCE-UA	
			$RSI_{\max\text{to}\min}$	$RSI_{\min\text{to}\max}$	UsToDs	DsToUs	Random	( $\beta=1$ )	( $\beta=2$ )
BRC	1653.0	1446.6	1367.4	1359.8	1359.8	1368.4	1368.2	1446.0	1427.6
MMR	1653.0	1446.6	1346.8	1346.2	1346.8	1346.8	1346.8	1379.6	1380.6
DMC	1653.0	1446.6	1389.4	1395.2	1386.8	1387.6	1384.4	1431.8	1416.4
DHF	1653.0	1446.6	1360.0	1354.8	1358.4	1360.6	1360.0	1380.2	1376.0
TOPSIS	1653.0	1446.6	1366.4	1370.8	1368.2	1372.4	1375.0	--	--

Peak Sion [ $m^3/s$ ]									
	Natural basin	BasU	Greedy ( $\beta=1$ )					SCE-UA	
			$RSI_{\max\text{to}\min}$	$RSI_{\min\text{to}\max}$	UsToDs	DsToUs	Random	( $\beta=1$ )	( $\beta=2$ )
BRC	1326.8	1191.2	1136.8	1121.6	1121.6	1134.2	1134.2	1154.0	1138.8
MMR	1326.8	1191.2	1112.6	1112.6	1112.6	1112.6	1112.6	1129.4	1127.2
DMC	1326.8	1191.2	1149.4	1151.6	1143.2	1144.4	1141.2	1161.4	1169.8
DHF	1326.8	1191.2	1125.6	1119.2	1118.0	1124.0	1125.6	1131.4	1126.0
TOPSIS	1326.8	1191.2	1131.8	1132.8	1130.2	1132.8	1135.2	--	--

Table 7.13 Maximum of the set of values obtained with probabilistic forecasts and all groups optimisation, including Bayes Risk Criterion (BRC), MMR (MinMax Regret), DMC (Decision Maker Criterion), DHF (Derived Hurwicz for Floods) and TOPSIS (Technique for Order Preference by Similarity to Ideal Solution). Natural basin represents the simulation with the non equipped basin, BasU the simulation with the equipped basin and Business as Usual operations, Greedy the optimisation with the IRGA approach and SCE-UA the optimisation with the Shuffled Complex Evolution – University of Arizona approach.  $\beta$  corresponds to the potential preventive operation costs coefficient.  $RSI_{max\ to\ min}$  represents the Reservoir Space Index from the highest to the smallest values in the order of the optimisation for the Greedy approach,  $RSI_{min\ to\ max}$  the Reservoir Space Index from the smallest to the highest values, UsToDs, the order from upstream to downstream, DsToUs from downstream to upstream and Random an order with this characteristic.

All groups optimisation with probabilistic forecasts (Average of the set of values)									
Expected damages [ $10^6$ CHF]									
	Natural basin	BasU	Greedy ( $\beta=1$ )					SCE-UA	
			$RSI_{max\ to\ min}$	$RSI_{min\ to\ max}$	UsToDs	DsToUs	Random	( $\beta=1$ )	( $\beta=2$ )
BRC	2005.2	1326.0	875.4	872.8	872.8	869.8	869.8	1073.2	1068.8
MMR	2005.2	1326.0	1163.8	1154.0	1163.8	1163.8	1163.8	1309.6	1318.4
DMC	2005.2	1326.0	963.2	997.0	991.8	1002.6	999.0	1083.4	1090.2
DHF	2005.2	1326.0	873.0	855.8	885.2	881.2	873.0	1112.3	1284.5
TOPSIS	2005.2	1326.0	877.6	860.0	871.6	852.0	869.0	--	--

Potential Preventive Operations Costs [ $10^6$ CHF]									
	Natural basin	BasU	Greedy ( $\beta=1$ )					SCE-UA	
			$RSI_{max\ to\ min}$	$RSI_{min\ to\ max}$	UsToDs	DsToUs	Random	( $\beta=1$ )	( $\beta=2$ )
BRC	0	0	1.938	1.854	1.854	1.884	1.926	7.762	4.168
MMR	0	0	1.846	1.878	1.846	1.846	1.846	3.858	3.910
DMC	0	0	1.492	1.488	1.558	1.600	1.382	2.506	2.390
DHF	0	0	1.906	2.006	1.888	1.900	1.906	3.428	3.135
TOPSIS	0	0	1.942	1.960	1.926	1.846	2.010	--	--

Peak Porte-du-Scex [ $m^3/s$ ]									
	Natural basin	BasU	Greedy ( $\beta=1$ )					SCE-UA	
			$RSI_{max\ to\ min}$	$RSI_{min\ to\ max}$	UsToDs	DsToUs	Random	( $\beta=1$ )	( $\beta=2$ )
BRC	1203.8	1077.0	1012.4	1012.8	1012.8	1012.6	1012.6	1106.8	1088.2
MMR	1203.8	1077.0	1032.2	1031.6	1032.2	1032.2	1032.2	1082.4	1079.6
DMC	1203.8	1077.0	1021.0	1027.8	1024.4	1026.8	1025.4	1046.4	1040.2
DHF	1203.8	1077.0	1014.6	1013.6	1015.4	1016.2	1014.6	1094.5	1098.5
TOPSIS	1203.8	1077.0	1018.0	1016.2	1017.8	1020.2	1017.8	--	--

Peak Sion [ $m^3/s$ ]									
	Natural basin	BasU	Greedy ( $\beta=1$ )					SCE-UA	
			$RSI_{max\ to\ min}$	$RSI_{min\ to\ max}$	UsToDs	DsToUs	Random	( $\beta=1$ )	( $\beta=2$ )
BRC	942.0	847.0	800.0	797.6	797.6	799.2	799.6	825.2	812.4
MMR	942.0	847.0	819.8	819.2	819.8	819.8	819.8	829.6	831.6
DMC	942.0	847.0	807.4	808.8	806.8	812.4	811.4	812.0	811.8
DHF	942.0	847.0	800.4	799.4	800.2	800.8	800.4	830.0	831.0
TOPSIS	942.0	847.0	801.6	803.2	801.4	803.4	804.4	--	--

**Performances of studied approaches and computation times for all groups optimisation**

The optimisation of all groups at the same time is the best framework for using the IRGA approach (Figure 7.9 for deterministic forecasts and Figure 7.10 for probabilistic forecasts). The results are robust and very similar for all different factors taken into account for the optimisation.

The SCE-UA is not optimal when the number of parameters to optimise is important and the PPOC is particularly high for expected damages similar (or even higher) to the ones calculated with IRGA. Even increasing the  $\beta$  value to 10 does not systematically decrease the PPOC value.

When optimising the system with deterministic forecasts, the number of evaluations of the utility function with the IRGA approach varies between 25'000 and 45'000, with a computation time smaller than 45 seconds. For the SCE-UA approach, the number of evaluations varies between 65'000 and 110'000 with a total computation time up to 15 minutes.

Regarding probabilistic forecasts, the IRGA approach also evaluates the utility function between 25'000 and 45'000 times and the time needed fluctuates up to 12 minutes. The SCE-UA approach evaluates the function between 65'000 and 140'000 times and the computation time increases up to 10 hours. These values are shown in Figure 7.11.

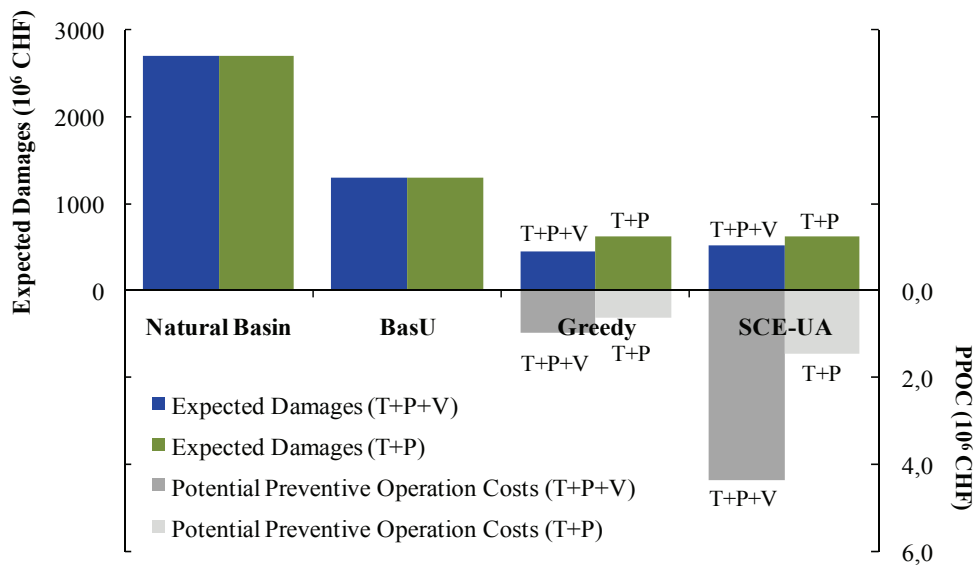


Figure 7.9 Main results obtained with deterministic forecasts for all groups optimisation, T representing the turbines operations, P the pumping operations and V the bottom outlet operations. Natural basin represents the simulation with the non equipped basin, BasU the simulation with the equipped basin and Business as Usual operations, Greedy the optimisation with the IRGA approach and SCE-UA the optimisation with the Shuffled Complex Evolution – University of Arizona approach. PPOC indicates the Potential Preventive Operation Costs.

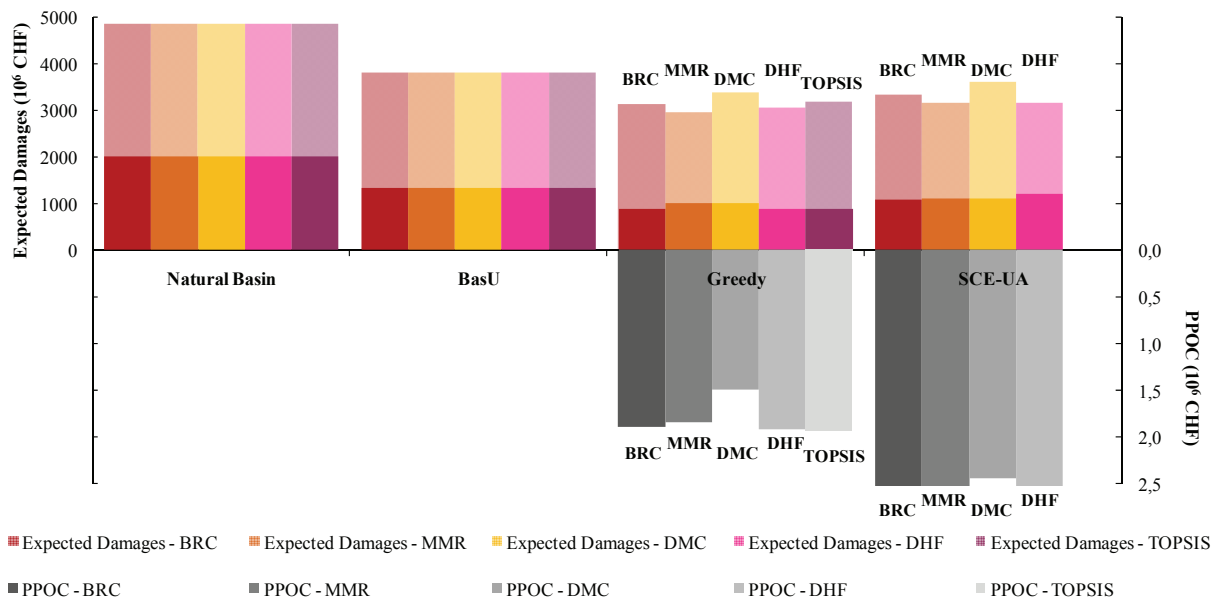


Figure 7.10 Average and maximum of the set of values obtained with probabilistic forecasts and all groups optimisation, including Bayes Risk Criterion (BRC), MMR (MinMax Regret), DMC (Decision Maker Criterion), DHF (Derived Hurwicz for Floods) and TOPSIS (Technique for Order Preference by Similarity to Ideal Solution). Natural basin represents the simulation with the non equipped basin, BasU the simulation with the equipped basin and Business as Usual operations, Greedy the optimisation with the IRGA approach and SCE-UA the optimisation with the Shuffled Complex Evolution – University of Arizona approach.  $\beta$  corresponds to the potential preventive operation costs coefficient. PPOC indicates the Potential Preventive Operation Costs. Average expected damages are represented by solid colours and maximum expected damages by lighter colours.

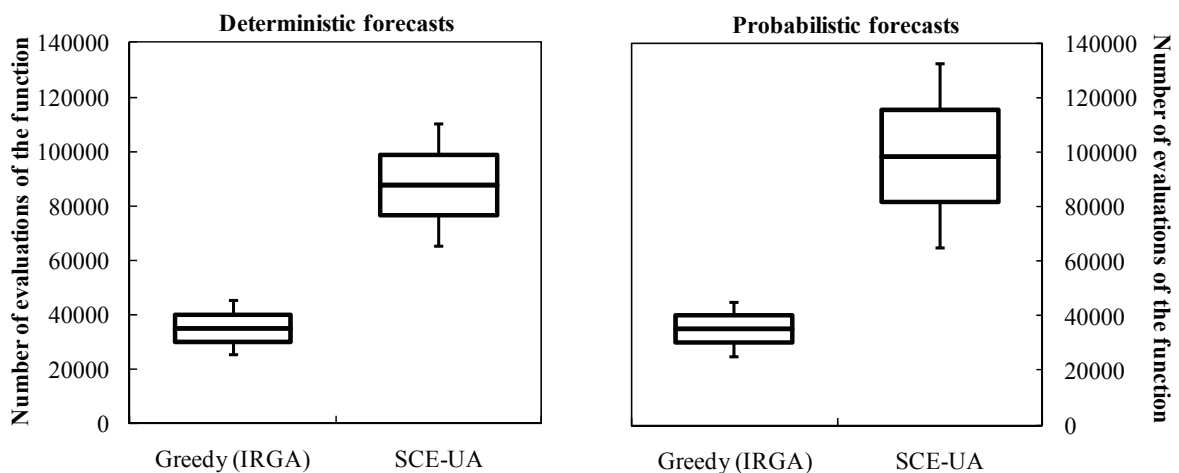


Figure 7.11 Number of evaluations of the objective function with deterministic and probabilistic forecasts and all groups optimisation. Greedy (Iterative Ranking Greedy Algorithm) represents the optimisation with this approach and SCE-UA the optimisation with the Shuffled Complex Evolution – University of Arizona algorithm.

#### **7.4.5 Conclusions from the optimisation results**

Since in a real-case all groups have to be usually optimised, the IRGA approach reveals as the best choice, especially when optimising with probabilistic forecasts due to the real-time constraints.

The performance of IRGA and SCE-UA methods is validated by similar results with both of them, especially when one and two groups have been optimised. The results provided by the SCE-UA algorithm have a decreasing quality when the number of parameters increases. However, the simplicity of the IRGA approach gives satisfactory results whatever the number of parameters is.

Then, once the IRGA approach is chosen, the selected ranking of the groups will be the  $RSI_{\max\text{to}\min}$  (which orders the groups according to the Reservoir Space Index from the highest to the smallest values obtained for each group), since this method generally offer a high performance with reasonable PPOC. Nevertheless, the decision maker could test other rankings during an operational case for validating the choice and verifying the best performance in a particular case.

Regarding the utility function selected as the objective of the system, TOPSIS provides robust results for all set of values since it is the only method which takes into account the whole set for the definition of the utility function. Even if BRF or DHF supply similar results, they are sometimes more inconsistent and have not been selected as a first option.

Finally, the optimisation with and without the bottom outlet operations was examined. Operating with turbines, pumps and bottom outlets presents a great advantage for the system because more efficient preventive operations can be achieved, but higher PPOC are also attained. Even if the option with bottom outlet operations is preferred, it could be re-evaluated after an optimisation, once preventive operations analysed. An optimisation without bottom outlet operations could be then achieved for comparing the results, especially the differences between expected damages and PPOC.

## 7.5 Real-time procedure and results

### 7.5.1 Real-time approach

#### *Introduction to the real-time flood management*

The exercise of a pre-assumed real-time flood management is realised with the forecast resimulations provided by MeteoSwiss (these forecasts were not available at that time). Proposed preventive operations are carried out for each forecast and updating of the model is done before each new optimisation. The process is iteratively repeated till the end of the flood and an assessment of the PrevOp performance is then achieved.

The results are also compared with an optimisation completed with meteorological observations. The aim is to know the optimisation differences due to hydro-meteorological forecasts uncertainty.

The proposed optimisation procedure of previous chapter (section 7.4.5) includes the utility function proposed by TOPSIS and the Iterative Ranking Greedy Algorithm (IRGA) using a ranking of the groups based on the Reservoir Space Ranking ( $RSI_{\max\text{to}\min}$ ). This procedure is applied during the whole period of the flood for testing the performance of the system in a real-case with re-evaluation of decisions.

In this subchapter, the advantages and consequences of reservoir management in a practical case are analysed for deterministic and probabilistic forecasts being continuously updated. However, the decision support system MINDS has been developed with a parameter which could weight each of these forecasts when using them simultaneously. If applied, this parameter would change the final result of the optimisation. Its influence should be studied in detail with a trade-off evaluation between weighted values and expected damages as well as PPOC. This analysis has not been carried out in this research project due to the need of more flood events for providing significant results in the combination of deterministic and probabilistic forecasts.

#### *Operational diagram*

Starting from the first forecast generating preventive operations, a tree operational procedure is applied (Figure 7.12). If preventive operations are carried out, the model (reservoir levels and discharge at check points) is updated following these operations and observed measurements. Then, the next provided forecast is optimised and preventive operations

previously undertaken are re-evaluated. New operations are proposed when necessary. The process is repeated in loops (each time a new forecast is provided) until the end of the flood. Then, the global performance of the preventive operations can be evaluated.

The schema of Figure 7.12 does not have to be followed in a systematic way. It only provides a general overview of the main steps when dealing with a real-time optimisation. In more complex cases, the common sense of decision makers provides the best framework for adequately using this decision support system.

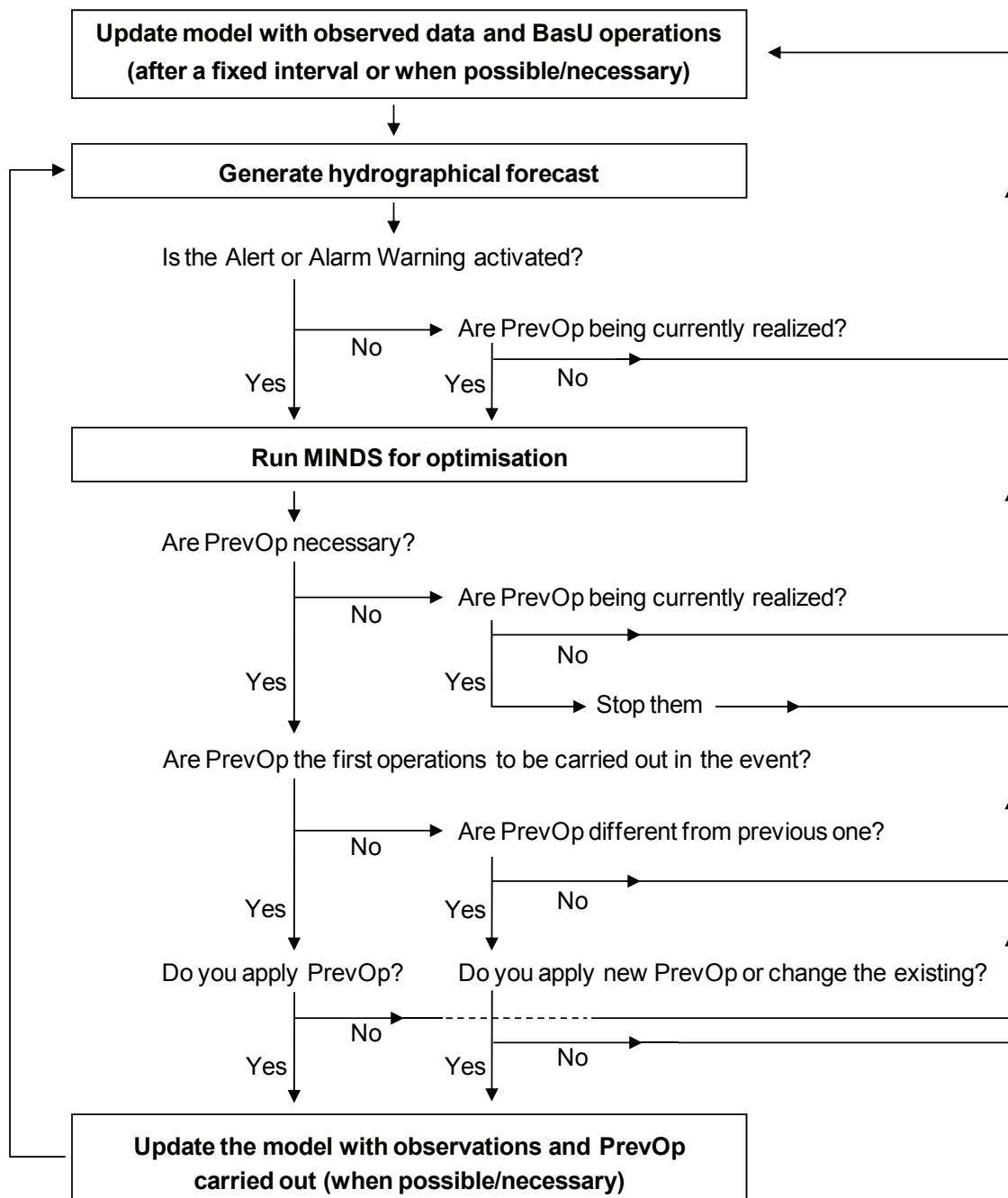


Figure 7.12 Real-time procedure for the reservoir management during floods from the first forecast predicting the flood and with an update of forecasts and preventive operations during the whole flood event.

### 7.5.2 Flood event of October 2000

The procedure is first tested for a perfect forecast computed with meteorological observations. Then, the procedure is also independently tested for deterministic and probabilistic forecasts as follows:

- The perfect forecast corresponds to meteorological observations which are taken as input for the hydrological simulations and the related optimisation. The start of this optimisation is fixed on October 11, 2000 at 12 h.
- The optimisation with COSMO-7 is then performed. The first deterministic forecast which predicted the flood was generated on October 12, 2000 at 00 h. The optimisation therefore starts at that moment. Forecasts are given in 12 h intervals until the last one, on October 15, 2000 at 00 h. Then, the total number of forecasts used for the optimisation is 7.
- The optimisation carried out with probabilistic forecasts COSMO-LEPS can be started on October 11, 2000 at 12 h. The update interval for these forecasts is 24 h. The last forecast used in the optimisation was on October 15, 2000 at 12 h. Therefore, the total number of forecasts used is 5.

#### *Optimisation from meteorological observations for the October 2000 flood*

This optimisation has been performed over the whole period of the flood event. The classical space solution for the parameters proposed in Chapter 6 has been enlarged because the period of optimisation is increased up to 156 h, from October 11, 2000 at 12 h to October 18, 2000 at 00 h. The beginning of preventive operations is varied up to 96 h and the duration of the operations also up to 96 h. Furthermore, the safety coefficient for overflowing,  $s_{fl}$ , is fixed to one ( $s_{fl}=1$ ).

The optimisation is performed only once since all data are available from the first moment and one single optimisation is sufficient. The hydrograph from the natural basin, the observed hydrograph, the hydrograph simulated as Business as Usual as well as the optimised hydrograph are presented at Porte-du-Scex in Figure 7.13.

In addition, inflows to the reservoirs (which are the same for the simulation BasU and for the simulation with optimised values), and releases from reservoirs for the three types of simulations are also shown.



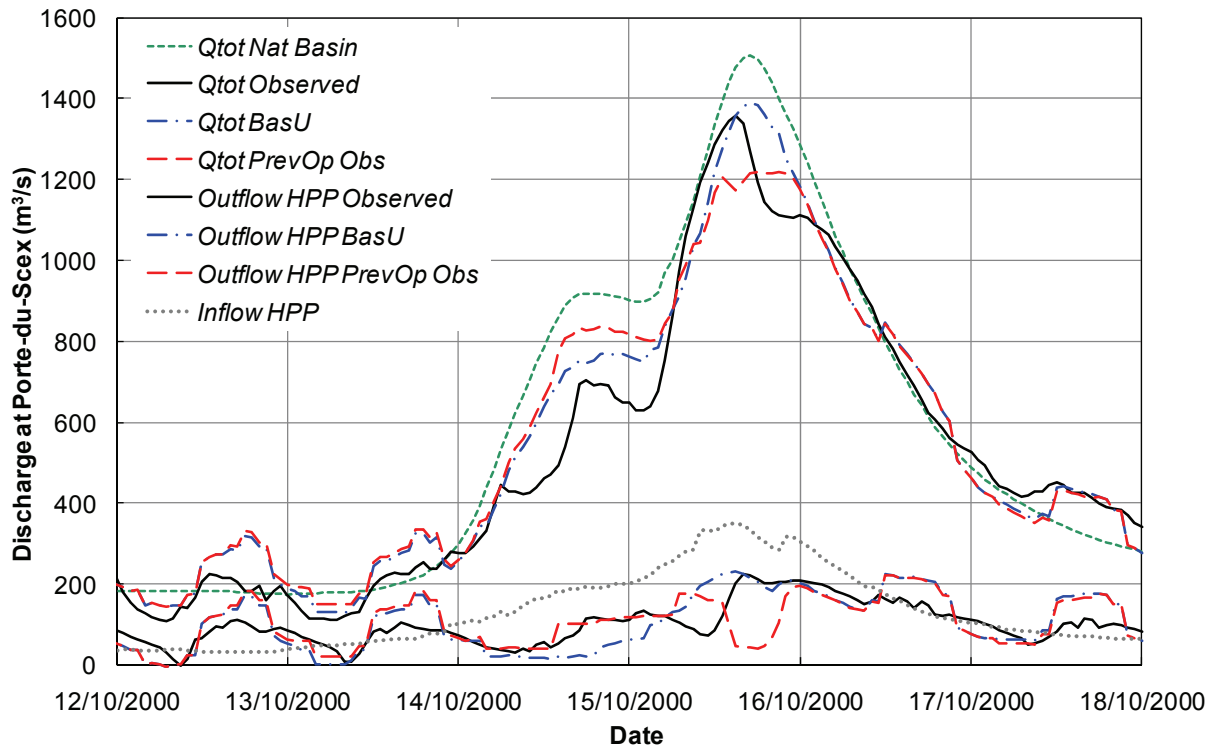


Figure 7.13 Hydrographs with optimisation of the October 2000 flood at the outlet of the basin, Porte-du-Scex, starting on October 11, 2000. “Qtot Nat Basin” corresponds to the hydrograph from the natural basin, “Qtot Observed” to the hydrograph from observed measurements, “Qtot BasU” to the hydrograph of the equipped basin simulated with Business as Usual operations, “Qtot PrevOp Obs” to the hydrograph resulting from the optimisation with a perfect forecast. “Outflow HPP Observed” represents the summation of the outflows from all hydropower plants, “Outflow HPP BasU” the summation of the outflows calculated with Business as Usual operations, “Outflow HPP PrevOp Obs” the summation of the outflows calculated from the optimisation with a perfect forecast. “Inflow HPP” represents the total inflows to the reservoirs of the system.

The number of function evaluations for this optimisation was 222’832, distributed in four iterations, with a total computation time of 3’52’’. The main values of the optimisation are given in Table 7.14. Furthermore, the proposed preventive operations are shown in Table 7.15. These measures concern four different hydropower groups.

Table 7.14 Main results from the optimisation for the October 2000 flood. “Natural basin” represents the results from the simulation of the natural basin without hydropower schemes, “BasU” the results from the equipped basin with Business as Usual operations and “OPT OBS” the results from the optimisation with the equipped basin and perfect forecasts (from meteorological observations)

	Natural basin	BasU	OPT OBS
<b>Expected Damages (10<sup>6</sup> CHF)</b>	3071	2551	111
<b>Potential Prev. Op. Costs (10<sup>6</sup> CHF)</b>	0.00	0.00	1.71
<b>Peak -Porte du Scex (m<sup>3</sup>/s)</b>	1505	1389	1220
<b>Peak - Branson Aval (m<sup>3</sup>/s)</b>	1376	1314	1153
<b>Peak - Sion OFEV (m<sup>3</sup>/s)</b>	1135	1071	908
<b>Peak - Steg (m<sup>3</sup>/s)</b>	866	859	709

Table 7.15 Optimisation results with meteorological observations as input for hydrological simulations (from October 11, 2000 at 12h). “Start T” represents the start time for turbine operations, “Dur T” the duration of the turbine operations, “Per NT” the periods of turbines stop, “Start V” the starting time for the bottom outlet operations, “Dur V” the duration of the bottom outlet operations, “Dur P” the duration of the pumping operations and “to” the start time of the optimisation period.

Group (GR)	Reservoir (RES)							
	Name	Name	Start T [h]	Dur T [h]	Per NT [period]	Start V [h]	Dur V [h]	Dur P [h]
<b>GD (Grande Dixence)</b>	Grande Dixence		t <sub>0</sub> +0	0	0	t <sub>0</sub> +0	0	-
	Cleuson		t <sub>0</sub> +0	0	0	t <sub>0</sub> +0	0	0
<b>ESA (Emosson)</b>	Emosson		t <sub>0</sub> +0	0	0	t <sub>0</sub> +0	0	-
	Esserts		-	-	-	-	-	0
	Châtelard CFF		-	-	-	-	-	-
	Châtelard ESA		-	-	-	-	-	-
<b>FMM (Mauvoisin)</b>	Mauvoisin		t <sub>0</sub> +0	0	0	t <sub>0</sub> +0	0	0
	Fionnay		-	-	-	-	-	-
<b>KWM (Mattmark)</b>	Mattmark		t <sub>0</sub> +52	32	0	t <sub>0</sub> +0	0	0
	Zermeiggern		-	-	-	-	-	0
<b>FMG (Gouggra)</b>	Moiry		0	0	0	t <sub>0</sub> +0	0	-
	Turtmann		t <sub>0</sub> +80	12	0	t <sub>0</sub> +0	0	0
	Mottec		-	-	-	-	-	0
	Vissoie		-	-	-	-	-	-
<b>EL (Lienne)</b>	Zeuzier		t <sub>0</sub> +0	0	0	t <sub>0</sub> +0	0	-
	Croix		-	-	-	-	-	-
<b>SAL (Salanfe)</b>	Salanfe		t <sub>0</sub> +0	0	0	t <sub>0</sub> +0	0	-
<b>GSB (Pallazuit)</b>	Toules		t <sub>0</sub> +0	0	0	t <sub>0</sub> +0	0	-
	Pallazuit		-	-	-	-	-	-
<b>EM (Bitsch)</b>	Gebidem		t <sub>0</sub> +64	24	0	t <sub>0</sub> +0	0	-
<b>KWL (Lôtschen)</b>	Ferden		t <sub>0</sub> +20	76	0	t <sub>0</sub> +80	8	-

It has to be noted that the two most important operations occur at Mattmark and Bitsch (Table 7.16). Since Turtmann, from Gougra group, is a small reservoir, its preventive operations present more risk and the benefits are smaller. Regarding Ferden, from Löttschen group, the high preventive operations correspond to a period before the flood with high inflows. The preventive operations try to keep a low level in the reservoir before the flood peak. Nevertheless, this reservoir only has a total volume of  $2.12 \cdot 10^6 \text{ m}^3$ . This is the reason why this operation would be the most risky one due to its high PPOC.

Table 7.16 Levels and volumes for the optimisation with meteorological observations as input of hydrological simulations (from October 11, 2000 at 12h)

Group (GR)		Reservoir (RES)				
Name	Name	Initial Level [m a.s.l.]	PrevOp Volume [ $10^6 \text{ m}^3$ ]	Stored volume during flood peak [ $10^6 \text{ m}^3$ ]	Final Level [m a.s.l.]	Maximum Level [m a.s.l.]
<b>KWM (Mattmark)</b>	Mattmark	2193.97	2.19	0.04	2195.66	2196.00
	Zermeiggern	-	-	-	-	-
	Moiry	2247.43	0.00	-0.38	2247.14	2249.00
<b>FMG (Gougra)</b>	Turtmann	2176.00	0.19	0.00	2176.40	2177.00
	Mottec	-	-	-	-	-
	Vissoie	-	-	-	-	-
<b>EM (Bitsch)</b>	Gebidem	1434.04	4.75	2.52	1435.90	1436.50
<b>KWL (Löttschen)</b>	Ferden	1310.00	7.36	0.07	1311.06	1311.00

#### *Optimisation from COSMO-LEPS and COSMO-7 forecasts for the October 2000 flood*

When optimising the flood with meteorological forecasts (COSMO-LEPS and COSMO-7), the preventive operations can be updated (with last available meteorological measurement and real reservoir levels) every time a new forecast is provided. The final results achieved are presented in Figure 7.14. This Figure does not present the hydro-meteorological forecasts from COSMO-LEPS and COSMO-7, but only the preventive operations achieved with them at the end of the period, with the aim of knowing the real consequences of the preventive operations proposed by COSMO-LEPS and COSMO-7. Therefore three simulations with PrevOp are presented in the graphic:

- First, a simulation with a perfect forecast and PrevOp also obtained from the perfect forecast,

- Second, a simulation with a perfect forecast and PrevOp obtained from optimisation with COSMO-LEPS during the entire event.
- Third, a simulation with a perfect forecast and PrevOp obtained from optimisation with COSMO-7 during the entire event.

Regarding COSMO-LEPS, it is worth to mention that the flood peak reduction at Porte-du-Scex is quite similar to the optimisation with a perfect forecast, also with comparable outflows from reservoirs during the flood peak.

For COSMO-7, preventive operations are less important and flood peak is higher than in the other cases, but the goal of damages reduction is attained. Furthermore, outflows from reservoirs are also higher during the flood peak.

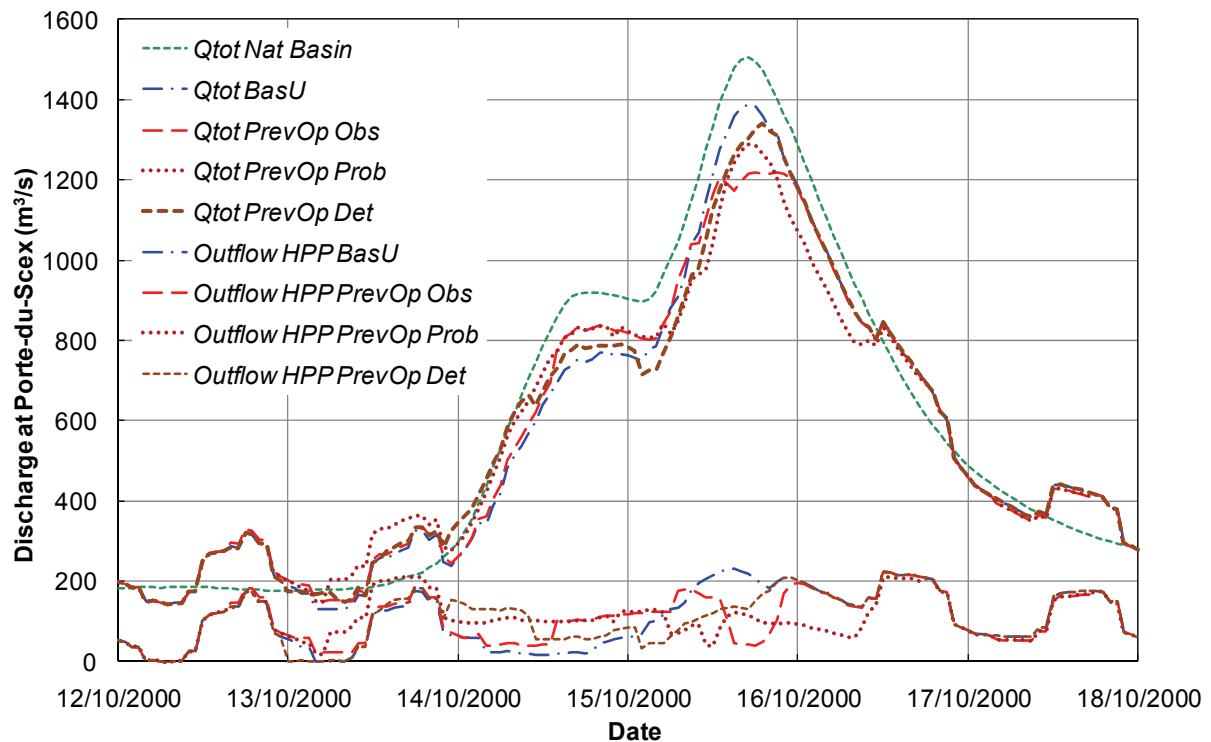


Figure 7.14 Hydrographs with optimisation using hydrological forecasts of the October 2000 flood (starting on October 11, 2000 at 12 h with COSMO-LEPS and on October 12, 2000 at 00 h with COSMO-7). at the outlet of the basin, Porte-du-Scex. “Qtot Nat Basin” corresponds to the hydrograph from the natural basin, “Qtot BasU” to the hydrograph of the equipped basin simulated with Business as Usual operations, “Qtot PrevOp Obs” to the hydrograph from the optimisation with a perfect forecast, “Qtot PrevOp Prob” to the hydrograph from the optimisation with COSMO-LEPS and “Qtot PrevOp Det” to the hydrograph from the optimisation with COSMO-7. “Outflow HPP BasU” represents the summation of the outflows from all hydropower plants calculated with Business as Usual operations, “Outflow HPP PrevOp Obs” the outflows from the optimisation with a perfect forecast, “Outflow HPP PrevOp Prob” the outflows from the optimisation with COSMO-LEPS and “Outflow HPP PrevOp Det” the outflows from the optimisation with COSMO-7. “Inflow HPP” represents the total inflows to the reservoirs of the system.

The final preventive operations after continuous updating of the decisions are presented in Table 7.17. The optimisation with meteorological observations can almost avoid the expected damages in the whole basin.

The optimisation with probabilistic forecasts leads to similar PPOC, but the expected damages are higher than those obtained from a perfect forecast. Nevertheless, the reduction reaches 60% of the damages calculated with the BasU operations. The optimisation with deterministic forecasts provides smaller PPOC. However, the damages are reduced only by 50% compared with the BasU operations.

Table 7.17 Main results from the optimisation with hydrological forecasts for the 2000 flood. “BasU” represents the results from the equipped basin with Business as Usual operations, “OPT OBS” the results from the optimisation with the equipped basin and perfect forecasts (from meteorological observations), “OPT C-L” the results of the optimisation with COSMO-LEPS and “OPT C-7” the results of the optimisation with COSMO-7.

	<b>BasU</b>	<b>OPT OBS</b>	<b>OPT C-L</b>	<b>OPT C-7</b>
<b>Expected damages (10<sup>6</sup> CHF)</b>	2551	111	1045	1269
<b>Potential Prev. Op. Costs (10<sup>6</sup> CHF)</b>	0.00	1.71	1.87	1.13
<b>Peak -Porte du Scex (m<sup>3</sup>/s)</b>	1389	1220	1287	1339
<b>Peak - Branson Aval (m<sup>3</sup>/s)</b>	1314	1153	1207	1248
<b>Peak - Sion OFEV (m<sup>3</sup>/s)</b>	1071	908	972	1030
<b>Peak - Steg (m<sup>3</sup>/s)</b>	859	709	764	827

The preventive operations resulting from COSMO-LEPS forecasts are presented in Table 7.18 and Table 7.19. The most important PrevOp are obtained for Mattmark and Bitsch, followed by PrevOp in reservoirs of other groups: Turtmann from Gouggra, Toules from Pallazuit and Ferden from Löttschen.

As mentioned, most important preventive emptyings occur in Mattmark and Bitsch. Preventive emptying in Turtmann and Ferden is more risky, but also contributes to the reduction of expected damages. The pre-emptying of Toules reservoir may be not required (as shown in the optimisation with perfect forecasts) and therefore produce unnecessary PPOC.

The preventive operations resulting from COSMO-7 forecast are presented in Table 7.20 and Table 7.21. The most important preventive operations are again proposed for Mattmark and Bitsch, followed by Turtmann (Gouggra group) and Ferden (Löttschen group). As for the probabilistic forecasts, PrevOp are mainly focused on Mattmark and Bitsch and secondarily on Turtmann and Ferden. These PrevOp are smaller than in the case of probabilistic forecasts and lead to a smaller reduction of the expected damages. However, final reservoirs levels are similar to the case with COSMO-LEPS due to spillway operations.

Table 7.18 Optimisation results with hydrological forecasts from COSMO-LEPS (presented from October 11, 2000 at 12 h for an easy comparison with the optimisation with perfect forecasts). Non presented groups had non preventive operations. “Start T” represents the start time for turbine operations, “Dur T” the duration of the turbine operations, “Per NT” the periods of turbines stop, “Start V” the start time for the bottom outlet operations, “Dur V” the duration of the bottom outlet operations, “Dur P” the duration of the pumps operations and “ $t_o$ ” the start time of the optimisation period.

Group (GR)		Reservoir (RES)					
Name	Name	Start T [h]	Dur T [h]	Per NT [period]	Start V [h]	Dur V [h]	Dur P [h]
<b>KWM (Mattmark)</b>	Mattmark	$t_o+24$	48	0	$t_o+0$	0	0
	Zermeiggern	-	-	-	-	-	0
<b>FMG (Gougra)</b>	Moiry	$t_o+0$	0	0	$t_o+0$	0	-
	Turtmann	$t_o+72$	16	0	$t_o+0$	0	0
	Mottec	-	-	-	-	-	0
<b>GSB (Pallazuit)</b>	Vissoie	-	-	-	-	-	-
	Toules	$t_o+60$	24	0	$t_o+0$	0	-
<b>EM (Bitsch)</b>	Pallazuit	-	-	-	-	-	-
	Gebidem	$t_o+32$	48	0	$t_o+0$	0	-
<b>KWL (Lötschen)</b>	Ferden	$t_o+0$	0	0	$t_o+72$	12	-

Table 7.19 Levels and volumes for the optimisation with COSMO-LEPS as input of hydrological simulations (presented from October 11, 2000 at 12 h).

Group (GR)		Reservoir (RES)				
Name	Name	Initial Level [m a.s.l.]	PrevOp Volume [ $10^6$ m <sup>3</sup> ]	Stored volume during flood peak [ $10^6$ m <sup>3</sup> ]	Final Level [ $10^6$ m <sup>3</sup> ]	Maximum Level [ $10^6$ m <sup>3</sup> ]
<b>KWM (Mattmark)</b>	Mattmark	2193.97	3.28	1.99	2195.70	2196.00
	Zermeiggern	-	-	-	-	-
<b>FMG (Gougra)</b>	Moiry	2247.43	0.00	-0.38	2247.14	2249.00
	Turtmann	2176.00	0.25	0.03	2176.40	2177.00
	Mottec	-	-	-	-	-
<b>GSB (Pallazuit)</b>	Vissoie	-	-	-	-	-
	Toules	1808.89	0.86	-0.04	1810.04	1810.00
<b>EM (Bitsch)</b>	Pallazuit	-	-	-	-	-
	Gebidem	1434.04	9.50	8.16	1435.89	1436.50
<b>KWL (Lötschen)</b>	Ferden	1310.00	2.29	0.71	1311.06	1311.00

Table 7.20 Optimisation results with hydrological forecasts from COSMO-7 (presented from October 11, 2000 at 12 h for an easy comparison between the optimisation with perfect forecasts). Non presented groups had non preventive operations. “Start T” represents the start time for turbine operations, “Dur T” the duration of the turbine operations, “Per NT” the periods of turbines stop, “Start V” the start time for the bottom outlet operations, “Dur V” the duration of the bottom outlet operations, “Dur P” the duration of the pumps operations and “ $t_0$ ” the start time of the optimisation period.

Group (GR)		Reservoir (RES)					
Name	Name	Start T [h]	Dur T [h]	Per NT [period]	Start V [h]	Dur V [h]	Dur P [h]
<b>KWM (Mattmark)</b>	Mattmark	$t_0+40$	20	0	$t_0+0$	0	0
	Zermeiggern	-	-	-	-	-	0
<b>FMG (Gouggra)</b>	Moiry	$t_0+0$	0	0	$t_0+0$	0	-
	Turtmann	$t_0+52$	8	0	$t_0+0$	0	0
	Mottec	-	-	-	-	-	0
	Vissoie	-	-	-	-	-	-
<b>EM (Bitsch)</b>	Gebidem	$t_0+48$	28	0	$t_0+0$	0	-
<b>KWL (Lötschen)</b>	Ferden	$t_0+0$	0	0	$t_0+48$	12	-

Table 7.21 Levels and volumes for the optimisation with COSMO-7 as input of hydrological simulations (presented from October 12, 2000 at 00 h)

GR		Reservoir (RES)				
Name	Name	Initial Level [m a.s.l.]	PrevOp Volume [ $10^6$ m <sup>3</sup> ]	Stored volume during flood peak [ $10^6$ m <sup>3</sup> ]	Final Level [m a.s.l.]	Maximum Level [m a.s.l.]
<b>KWM (Mattmark)</b>	Mattmark	2193.97	1.37	2.96	2195.88	2196.00
	Zermeiggern	-	-	-	-	-
<b>FMG (Gouggra)</b>	Moiry	2247.43	0.00	-0.38	2247.14	2249.00
	Turtmann	2176.00	0.12	0.11	2176.40	2177.00
	Mottec	-	-	-	-	-
	Vissoie	-	-	-	-	-
<b>EM (Bitsch)</b>	Gebidem	1434.04	5.54	5.30	1435.90	1810.00
<b>KWL (Lötschen)</b>	Ferden	1310.00	2.29	1.70	1311.06	1311.00

It should be notice that the reason why Mattmark and Bitsch are influential reservoirs during this flood event is their high initial level and high inflow volume. The preventive operations allowed the storage of this inflow volume during the flood peak and considerably reduced the expected damages.

### 7.5.3 Flood event of September 1993

The same procedure as applied again for the October 2000 flood event is again tested for a perfect forecast calculated with meteorological observations as well as for deterministic and probabilistic forecasts:

- The perfect forecast with meteorological observations starts on September 21, 1993 at 12 h.
- The optimisation with COSMO-7 starts with the first forecast which predicted the flood on September 22, 1993 at 00 h. Forecasts are optimised in 12 h intervals until the last one, on September 24, 1993 at 00 h. The total number of forecasts used for the optimisation is 5.
- The optimisation with COSMO-LEPS starts on September 21, 1993 at 12 h. The update interval is 24 h. The last forecast is provided on September 24, 1993 at 12 h. The total number of forecasts used is therefore 5.

#### ***Optimisation from meteorological observations for the September 1993 flood***

This optimisation has again been performed over the whole period of the flood event which was fixed to 156 h. The space solution for the parameters has been enlarged as for the first flood event tested (96 h for the beginning of preventive operations and 96 h for the duration of the operations). Furthermore, the safety coefficient for overflowing,  $s_{fl}$ , is this time fixed to 0.9 ( $s_{fl}=0.9$ ) in order to produce a more interesting case. When this coefficient is fixed to one for this event, the preventive operations are limited. The comparison between the optimisation with a perfect forecast, with COSMO-LEPS and with COSMO-7 is therefore more difficult. This is the reason why  $s_{fl}$  was finally fixed to 0.9.

The optimised hydrograph at Porte-du-Scex is presented in Figure 7.15.



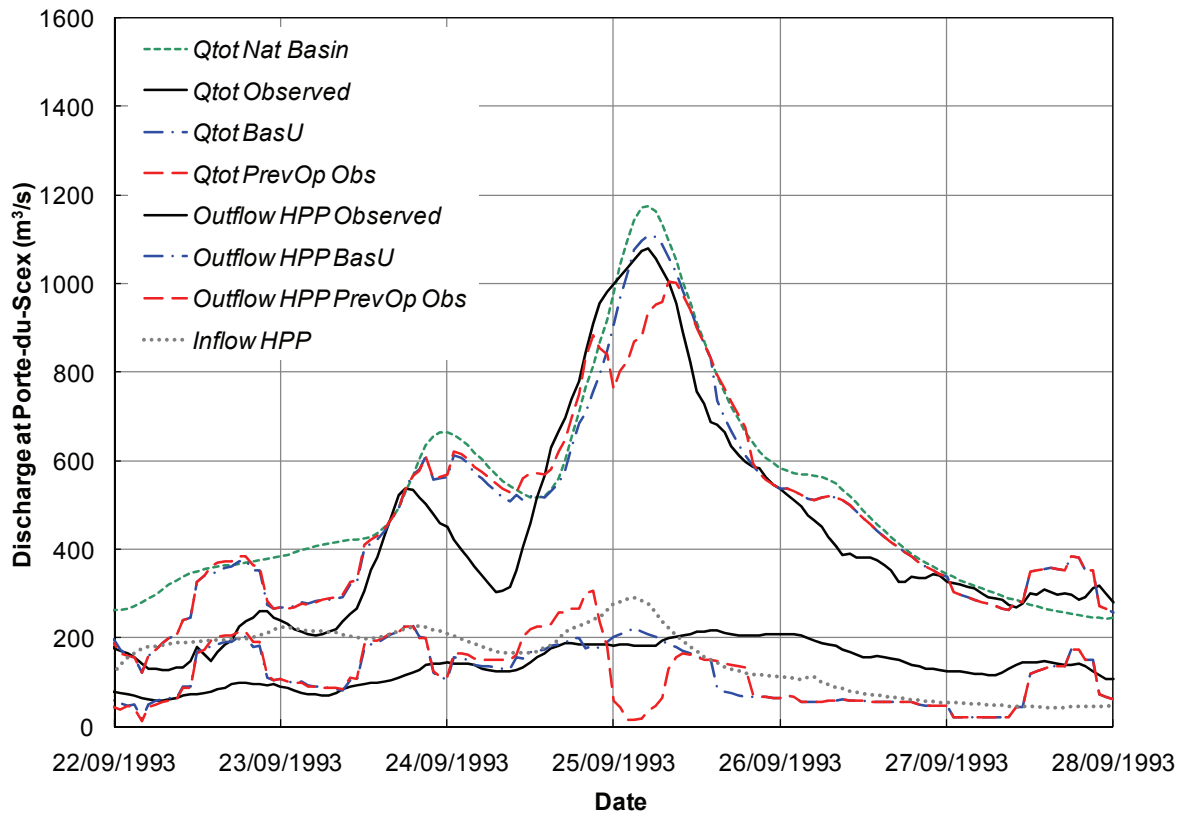


Figure 7.15 Hydrographs with optimisation of the September 1993 flood at the outlet of the basin, Porte-du-Scex, starting on September 21, 1993 at 12 h. “*Qtot Nat Basin*” corresponds to the hydrograph from the natural basin, “*Qtot Observed*” to the hydrograph from observed measurements, “*Qtot BasU*” to the hydrograph of the equipped basin simulated with Business as Usual operations, “*Qtot PrevOp Obs*” to the hydrograph resulting from the optimisation with a perfect forecast. “*Outflow HPP Observed*” represents the summation of the outflows from all hydropower plants, “*Outflow HPP BasU*” the summation of the outflows calculated with Business as Usual operations, “*Outflow HPP PrevOp Obs*” the summation of the outflows calculated from the optimisation with a perfect forecast. “*Inflow HPP*” represents the total inflows to the reservoirs of the system.

The number of function evaluations for this optimisation was 167'124 distributed in three iterations, with a total computation time of 2'44'. The main values of the optimisation are given in Table 7.22 and the proposed preventive operations in Table 7.23.

Table 7.22 Main optimisation results for the September 1993 flood. “Natural basin” represents the results from the simulation of the natural basin without hydropower schemes, “BasU” the results from the equipped basin with Business as Usual operations and “OPT OBS” the results from the optimisation with the equipped basin and perfect forecasts (from meteorological observations)

	Natural basin	B as U	OPT OBS
<b>Expected Damages (10<sup>6</sup> CHF)</b>	2579	2255	289
<b>Potential Prev. Op. Costs (10<sup>6</sup> CHF)</b>	0	0	2.08
<b>Peak -Porte du Scex (m<sup>3</sup>/s)</b>	1176	1109	1004
<b>Peak - Branson Aval (m<sup>3</sup>/s)</b>	1131	1090	938
<b>Peak - Sion OFEV (m<sup>3</sup>/s)</b>	998	921	798
<b>Peak - Steg (m<sup>3</sup>/s)</b>	831	809	680

Table 7.23 Optimisation results with meteorological observations as input of hydrological simulations (from September 21, 1993 at 12h). “Start T” represents the start time for turbine operations, “Dur T” the duration of the turbine operations, “Per NT” the periods of turbines stop, “Start V” the starting time for the bottom outlet operations, “Dur V” the duration of the bottom outlet operations, “Dur P” the duration of the pumping operations and “to” the start time of the optimisation period.

Group (GR)	Reservoir (RES)							
	Name	Name	Start T [h]	Dur T [h]	Per NT [period]	Start V [h]	Dur V [h]	Dur P [h]
<b>GD (Grande Dixence)</b>	Grande Dixence		t <sub>0</sub> +76	4	0	t <sub>0</sub> +0	0	-
	Cleuson		t <sub>0</sub> +0	0	0	t <sub>0</sub> +0	0	0
<b>ESA (Emosson)</b>	Emosson		t <sub>0</sub> +0	0	0	t <sub>0</sub> +0	0	-
	Esserts		-	-	-	-	-	0
	Châtelard CFF		-	-	-	-	-	-
	Châtelard ESA		-	-	-	-	-	-
<b>FMM (Mauvoisin)</b>	Mauvoisin		t <sub>0</sub> +0	0	0	t <sub>0</sub> +0	0	0
	Fionnay		-	-	-	-	-	-
<b>KWM (Mattmark)</b>	Mattmark		t <sub>0</sub> +76	0	1	t <sub>0</sub> +0	0	0
	Zermeiggern		-	-	-	-	-	4
<b>FMG (Gougra)</b>	Moiry		t <sub>0</sub> +0	0	0	t <sub>0</sub> +0	0	-
	Turtmann		t <sub>0</sub> +52	28	0	t <sub>0</sub> +0	0	0
	Mottec		-	-	-	-	-	0
	Vissoie		-	-	-	-	-	-
<b>EL (Lienne)</b>	Zeuzier		t <sub>0</sub> +0	0	0	t <sub>0</sub> +0	0	-
	Croix		-	-	-	-	-	-
<b>SAL (Salanfe)</b>	Salanfe		t <sub>0</sub> +0	0	0	t <sub>0</sub> +0	0	-
<b>GSB (Pallazuit)</b>	Toules		t <sub>0</sub> +0	0	0	t <sub>0</sub> +0	0	-
	Pallazuit		-	-	-	-	-	-
<b>EM (Bitsch)</b>	Gebidem		t <sub>0</sub> +16	56	1	t <sub>0</sub> +0	0	-
<b>KWL (Lötschen)</b>	Ferden		t <sub>0</sub> +68	12	60	t <sub>0</sub> +12	0	-

The most important preventive operations are proposed to Mattmark, Grande Dixence and Bitsch (Table 7.24). The other operations are more risky but still provide some benefits to the system.

Table 7.24 Levels and volumes for the optimisation with meteorological observations as input of hydrological simulations (from September 21, 1993 at 12h)

Group (GR)		Reservoir (RES)				
Name	Name	Initial Level [m a.s.l.]	PrevOp Volume [ $10^6$ m <sup>3</sup> ]	Stored volume during flood peak [ $10^6$ m <sup>3</sup> ]	Final Level [m a.s.l.]	Maximum Level [m a.s.l.]
<b>GD (Grande Dixence)</b>	Grande Dixence	2362.06	1.88	-0.41	2363.46	2364.00
	Cleuson	2185.22	0.00	0.62	2186.57	2186.50
<b>KWM (Mattmark)</b>	Mattmark	2193.32	0.00	1.24	2195.39	2196.00
	Zermeiggern	-	-	-	-	-
<b>FMG (Gougra)</b>	Moiry	2248.82	0.00	-0.08	2248.76	2249.00
	Turtmann	2176.00	0.43	-0.03	2176.31	2177.00
	Mottec	-	-	-	-	-
	Vissoie	-	-	-	-	-
<b>EM (Bitsch)</b>	Gebidem	1435.20	11.09	0.93	1431.75	1436.50
<b>KWL (Lötschen)</b>	Ferden	1310.00	3.21	0.30	1308.27	1311.00

### ***Optimisation from COSMO-LEPS and COSMO-7 forecasts for the September 1993 flood***

When optimising the flood with meteorological forecasts COSMO-LEPS and COSMO-7, the preventive operations are updated every time a new forecast is provided. The final results achieved are presented in Figure 7. 16. Certain hydrographs represents a simulation with a perfect forecast, but the preventive operations of each one have been obtained from the optimisations with hydro-meteorological forecasts (COSMO-LEPS and COSMO-7). The aim was to be able of comparing all preventive operations and its real consequences.

Regarding both COSMO-LEPS and COSMO-7, the flood peak reduction at Porte-du-Scex is equivalent to the optimisation with a perfect forecast. Nevertheless, it is not the case for the flood peaks located at check points upstream.

It has to be noted that different preventive operations with COSMO-LEPS and COSMO-7 produce a rather similar effect in the whole basin, with even similar expected damages.

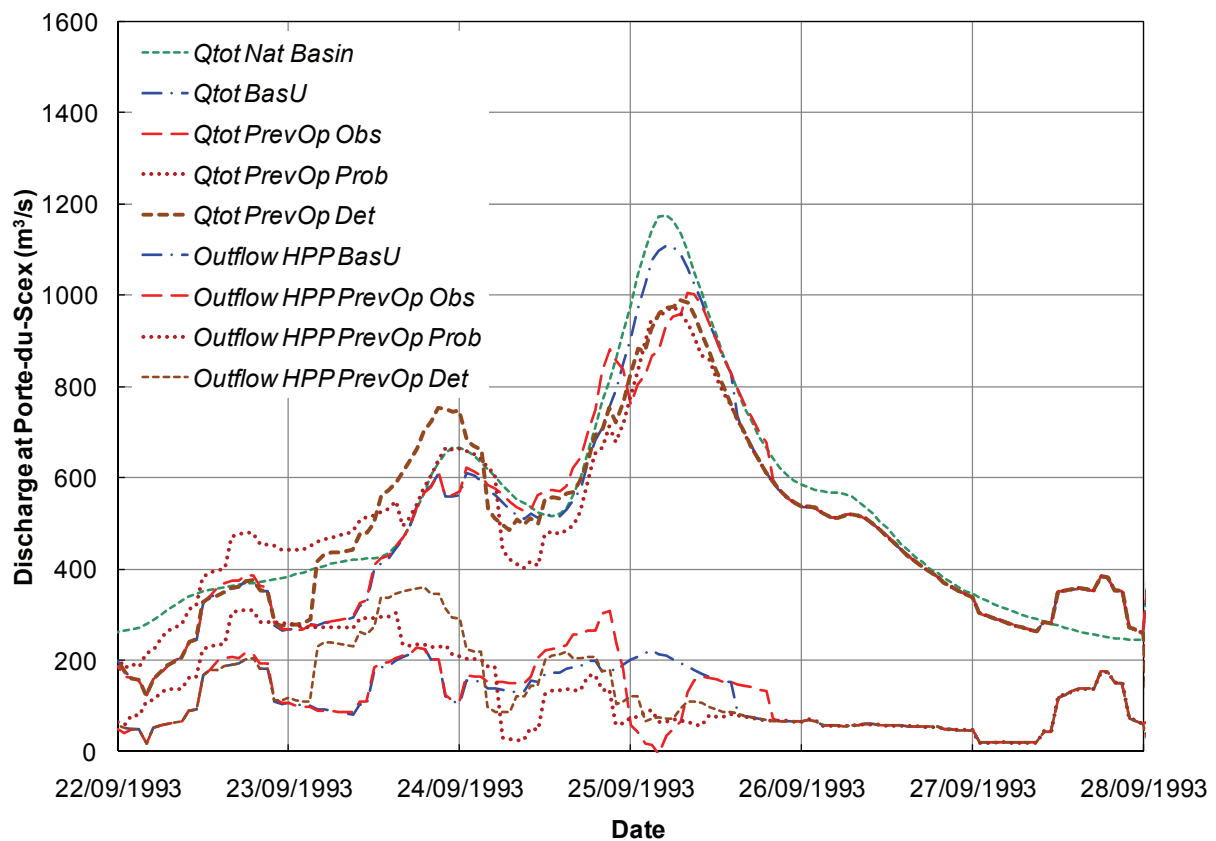


Figure 7. 16 Hydrographs with optimisation using hydrological forecasts of the September 1993 flood (starting on September 21, 1993 at 12 h with COSMO-LEPS and on September 22, 1993 at 00 h with COSMO-7). at the outlet of the basin, Porte-du-Scex. “Qtot Nat Basin” corresponds to the hydrograph from the natural basin, “Qtot BasU” to the hydrograph of the equipped basin simulated with Business as Usual operations, “Qtot PrevOp Obs” to the hydrograph from the optimisation with a perfect forecast, “Qtot PrevOp Prob” to the hydrograph from the optimisation with COSMO-LEPS and “Qtot PrevOp Det” to the hydrograph from the optimisation with COSMO-7. “Outflow HPP BasU” represents the summation of the outflows from all hydropower plants calculated with Business as Usual operations, “Outflow HPP PrevOp Obs” the outflows from the optimisation with a perfect forecast, “Outflow HPP PrevOp Prob” the outflows from the optimisation with COSMO-LEPS and “Outflow HPP PrevOp Det” the outflows from the optimisation with COSMO-7. “Inflow HPP” represents the total inflows to the reservoirs of the system.

The final preventive operations are presented in Table 7.25. The optimisation with meteorological observations almost avoids the expected damages in the whole basin. The damages reduction with COSMO-LEPS and COSMO-7, compared with the BasU operations, is also accomplished (around 65% in both cases). However, these damages are higher than those produced with the optimisation using a perfect forecast. In addition, several pessimistic predictions in both COSMO-LEPS and COSMO-7 produce high Potential Preventive Operation Costs (PPOC), twice higher than the PPOC of the optimisation with a perfect forecast

Table 7.25 Main optimisation results with hydrological forecasts for the 1993 flood. “BasU” represents the results from the equipped basin with Business as Usual operations, “OPT OBS” the results from the optimisation with the equipped basin and perfect forecasts (from meteorological observations), “OPT C-L” the results of the optimisation with COSMO-LEPS and “OPT C-7” the results of the optimisation with COSMO-7.

	<b>BasU</b>	<b>OPT OBS</b>	<b>OPT C-L</b>	<b>OPT C-7</b>
<b>Expected damages (10<sup>6</sup> CHF)</b>	2255	289	809	782
<b>Potential Prev. Op. Costs (10<sup>6</sup> CHF)</b>	0	2.08	5.03	4.12
<b>Peak -Porte du Scex (m<sup>3</sup>/s)</b>	1109	1004	975	990
<b>Peak - Branson Aval (m<sup>3</sup>/s)</b>	1090	938	944	950
<b>Peak - Sion OFEV (m<sup>3</sup>/s)</b>	921	798	845	842
<b>Peak - Steg (m<sup>3</sup>/s)</b>	809	680	746	732

The preventive operations resulting from COSMO-LEPS forecasts are presented in Table 7.26 and Table 7.27. The most important PrevOp are obtained for Grande Dixence, Mauvoisin, Mattmark and Bitsch, followed by PrevOp in reservoir of other groups: Moiry and Turtmann from Gouggra and Ferden from Löttschen.

As in the case of the October 2000 flood, preventive emptying in Turtmann and Ferden is risky. The pre-emptying of Mauvoisin reservoir may be not required (as shown in the optimisation with perfect forecasts) and therefore produce unnecessary PPOC.

The preventive operations resulting from COSMO-7 forecast are presented in Table 7.28 and Table 7.29. The most important preventive operations are again proposed for the same four hydropower groups as with COSMO-LEPS, followed by Moiry and Turtmann (Gouggra group) and Ferden (Löttschen group). These PrevOp are smaller than in the case of probabilistic forecasts and lead to a smaller PPOC. However, the reduction of the expected damages is equivalent, even slight better, in the case of deterministic forecasts.

It has to be noted that the hydropower groups where preventive operations are proposed are the same with both COSMO-LEPS and COSMO-7 forecasts. It is an interesting result which indicates that the reservoir level is as important as the inflow to the reservoir and the hydrographs at check points.

The final level at Gebidem reservoir in Bitsch is lower than at the beginning of the event, but it is only due to the operations realised last day after the flood peak, since a usual operation of turbine decreases the level from 1435 to 1431 m a.s.l.

Table 7.26 Optimisation results with hydrological forecasts from COSMO-LEPS (presented from September 21, 1993 at 12 h for an easy comparison between the optimisation with perfect forecasts). Non presented groups had non preventive operations. “Start T” represents the start time for turbine operations, “Dur T” the duration of the turbine operations, “Per NT” the periods of turbines stop, “Start V” the start time for the bottom outlet operations, “Dur V” the duration of the bottom outlet operations, “Dur P” the duration of the pumps operations and “to” the start time of the optimisation period.

Group (GR)		Reservoir (RES)					
Name	Name	Start T [h]	Dur T [h]	Per NT [period]	Start V [h]	Dur V [h]	Dur P [h]
<b>GD (Grande Dixence)</b>	Grande Dixence	t <sub>0</sub> +24	24	0	t <sub>0</sub> +0	0	-
	Cleuson	t <sub>0</sub> +0	0	0	t <sub>0</sub> +0	0	0
<b>FMM (Mauvoisin)</b>	Mauvoisin	t <sub>0</sub> +12	36	0	t <sub>0</sub> +0	0	0
	Fionnay	-	-	-	-	-	-
<b>KWM (Mattmark)</b>	Mattmark	t <sub>0</sub> +8	48	1	t <sub>0</sub> +0	0	0
	Zermeiggern	-	-	-	-	-	24
<b>FMG (Gougra)</b>	Moiry	t <sub>0</sub> +48	8	1	t <sub>0</sub> +0	0	-
	Turtmann	t <sub>0</sub> +4	72	1	t <sub>0</sub> +0	0	0
	Mottec	-	-	-	-	-	0
	Vissoie	-	-	-	-	-	-
<b>EM (Bitsch)</b>	Gebidem	t <sub>0</sub> +4	52	0	t <sub>0</sub> +48	8	-
<b>KWL (Lötschen)</b>	Ferden	t <sub>0</sub> +48	24	0	t <sub>0</sub> +0	0	-

Table 7.27 Levels and volumes for the optimisation with COSMO-LEPS as input of hydrological simulations (presented from September 21, 1993 at 12 h).

Group (GR)		Reservoir (RES)				
Name	Name	Initial Level [m a.s.l.]	PrevOp Volume [10 <sup>6</sup> m <sup>3</sup> ]	Stored volume during flood peak [10 <sup>6</sup> m <sup>3</sup> ]	Final Level [m a.s.l.]	Maximum Level [m a.s.l.]
<b>GD (Grande Dixence)</b>	Grande Dixence	2362.06	11.25	5.78	2362.93	2364.00
	Cleuson	2185.22	0.00	0.62	2186.57	2186.50
<b>FMM (Mauvoisin)</b>	Mauvoisin	1971.10	4.47	2.95	1971.82	1975.00
	Fionnay	-	-	-	-	-
<b>KWM (Mattmark)</b>	Mattmark	2193.32	3.28	2.83	2194.33	2196.00
	Zermeiggern	-	-	-	-	-
<b>FMG (Gougra)</b>	Moiry	2248.82	0.37	0.28	2248.76	2249.00
	Turtmann	2176.00	1.11	0.05	2176.31	2177.00
	Mottec	-	-	-	-	-
	Vissoie	-	-	-	-	-
<b>EM (Bitsch)</b>	Gebidem	1435.20	12.60	3.19	1431.75	1436.50
<b>KWL (Lötschen)</b>	Ferden	1310.00	1.84	-0.21	1308.27	1311.00

Table 7.28 Optimisation results with hydrological forecasts from COSMO-7 (presented from September 21, 1993 at 12 h for an easy comparison between the optimisation with perfect forecasts). Non presented groups had non preventive operations. “Start T” represents the start time for turbine operations, “Dur T” the duration of the turbine operations, “Per NT” the periods of turbines stop, “Start V” the start time for the bottom outlet operations, “Dur V” the duration of the bottom outlet operations, “Dur P” the duration of the pumps operations and “to” the start time of the optimisation period.

Group (GR)		Reservoir (RES)					
Name	Name	Start T [h]	Dur T [h]	Per NT [period]	Start V [h]	Dur V [h]	Dur P [h]
<b>GD (Grande Dixence)</b>	Grande Dixence	$t_0+36$	24	0	$t_0+0$	0	-
	Cleuson	$t_0+0$	0	0	$t_0+0$	0	0
<b>FMM (Mauvoisin)</b>	Mauvoisin	$t_0+64$	8	0	$t_0+0$	0	0
	Fionnay	-	-	-	-	-	-
<b>KWM (Mattmark)</b>	Mattmark	$t_0+24$	24	2	$t_0+36$	12	0
	Zermeiggern	-	-	-	-	-	0
<b>FMG (Gougra)</b>	Moiry	$t_0+0$	0	0	$t_0+0$	0	-
	Turtmann	$t_0+60$	20	0	$t_0+0$	0	0
	Mottec	-	-	-	-	-	0
	Vissoie	-	-	-	-	-	-
<b>EM (Bitsch)</b>	Gebidem	$t_0+36$	40	1	$t_0+0$	0	-
<b>KWL (Lötschen)</b>	Ferden	$t_0+48$	24	0	$t_0+0$	0	-

Table 7.29 Levels and volumes for the optimisation with COSMO-7 as input of hydrological simulations (presented from September 21, 1993 at 12 h).

Group (GR)		Reservoir (RES)				
Name	Name	Initial Level [m a.s.l.]	PrevOp Volume [10 <sup>6</sup> m <sup>3</sup> ]	Stored volume during flood peak [10 <sup>6</sup> m <sup>3</sup> ]	Final Level [m a.s.l.]	Maximum Level [m a.s.l.]
<b>GD (Grande Dixence)</b>	Grande Dixence	2362.06	11.25	4.35	2362.93	2364.00
	Cleuson	2185.22	0.00	0.62	2186.57	2186.50
<b>FMM (Mauvoisin)</b>	Mauvoisin	1971.10	0.99	2.29	1973.15	1975.00
	Fionnay	-	-	-	-	-
<b>KWM (Mattmark)</b>	Mattmark	2193.32	4.15	2.57	2193.39	2196.00
	Zermeiggern	-	-	-	-	-
<b>FMG (Gougra)</b>	Moiry	2248.82	0.00	-0.08	2248.76	2249.00
	Turtmann	2176.00	0.31	-0.04	2176.31	2177.00
	Mottec	-	-	-	-	-
	Vissoie	-	-	-	-	-
<b>EM (Bitsch)</b>	Gebidem	1435.20	7.92	0.48	1431.75	1436.50
<b>KWL (Lötschen)</b>	Ferden	1310.00	1.84	-0.21	1308.27	1311.00

## 7.6 Optimisation methods and results conclusions

### 7.6.1 Performance of the different methods

The methods implemented in MINDS offers high quality results and are robust enough for being used in real-time situations.

#### *Iterative Ranking Greedy Algorithm - IRGA*

The IRGA heuristic approach performed well in all studied cases and is accurate for all tested forecasts. The possible factors which can be varied within the IRGA approach, such as  $\beta$  or the groups ranking, do not significantly modify the results. This proves its strength and does that the decision maker is not confronted to difficult decisions regarding the factors to choose for the optimisation.

The pre-defined methodology for real-time operations is carried out with the IRGA approach and uses the attributes which slightly improve the results as follows:

- The utility function provided by TOPSIS (Technique for Order Preference by Similarity to Ideal Solution) with a high robustness,
- the ranking obtained by the  $RSI_{\max\text{to}\min}$ , classifying the hydropower groups depending on the Reservoir Space Index from higher to smaller values,
- all possible preventive operations (turbines, pumps and bottom outlets) and
- 4 h of time space resolution. This resolution reveals a good choice, offering high quality results as well as relative small computation times. Several optimisations were also tested with a time space resolution of 2 h, but computation time increases more than 4 times without improving the results significantly.

#### *Shuffled Complex Evolution - University of Arizona – SCE-UA*

The SCE-UA approach offers a good framework of comparison for the IRGA methodology. It allows the validation of the heuristic IRGA approach and confirms that the complexity of this kind of systems does not usually allow obtaining the global optimum solution. Furthermore, the results with the SCE-UA are quite good when the number of hydropower groups to optimise is not excessive.

The parameters of the SCE-UA approach were also varied for improving the performance of this methodology as follows:



- The number of complexes (NGS) provides poorer results for values smaller than 3 and a number of parameters to optimise higher than 30. Values of NGS higher than 6 does not improve the results but increases the computation time. Finally, a NGS depending on the number of parameters to optimise was implemented (Eq. 6.57),
- the maximum number of evaluations (MAXN) was fixed at a high value (200'000 evaluations of the objective function) in order of to allow the optimum calculation of the methodology,
- the number of loops (KSTOP) in which the criterion value has to change by a given percentage (PCENTO) before optimisation is finished was also tested. A value of KSTOP depending on the complexity of the problem (i.e. the number of parameters to optimise), as presented in Eq. 6.58, and a value of PCENTO equals to 0.01 were finally selected. Nevertheless, the obtained results did not significantly vary with other similar values of KSTOP and PCENTO.

#### ***Hybrid method IRGA – SCE-UA***

A hybrid method using the IRGA and the SCE-UA algorithms was also proposed in Chapter 6. The IRGA solution is used as the starting point for a more comprehensive search through the decision space. Then, the SCE-UA algorithm is conducted from this point.

Even if the expectation of this method was high, the results do not produce the expected results. In fact, once a set of preventive operations is provided by the IRGA approach, the SCE-UA does not improve these preventive operations and the first set proposed by IRGA remains the final optimum set. This is the reason why the results of this hybrid method were not presented.

#### ***Mathematical optimisation and real management***

Finally, it has to be noted that even if expected damages and *PPOC* are only approximate values, the expected damages are generally 1'000 times higher than the *PPOC*. Therefore, even if false alarms and preventive operations could sometimes lead to unexpected energy loss compensations, these operations are clearly optimal from a mathematical point of view.

#### ***7.6.2 Computation time***

According to Figure 7.17, SCE-UA requires a smaller number of evaluations of the objective function in order to achieve the optimal result when one or two hydropower groups have to be

optimised. However, if the number of groups is higher than 3, and therefore more than 15 parameters are optimised, the number of evaluations increases considerably with the SCE-UA approach. Furthermore, this method sometimes converges towards a local optimum and includes high *PPOC* which are not feasible or realistic.

The number of evaluations is similar with the IRGA approach for both deterministic and probabilistic forecasts. Nevertheless, the number of evaluations increases with probabilistic forecasts when using the SCE-UA approach, as shown in Figure 7.17.

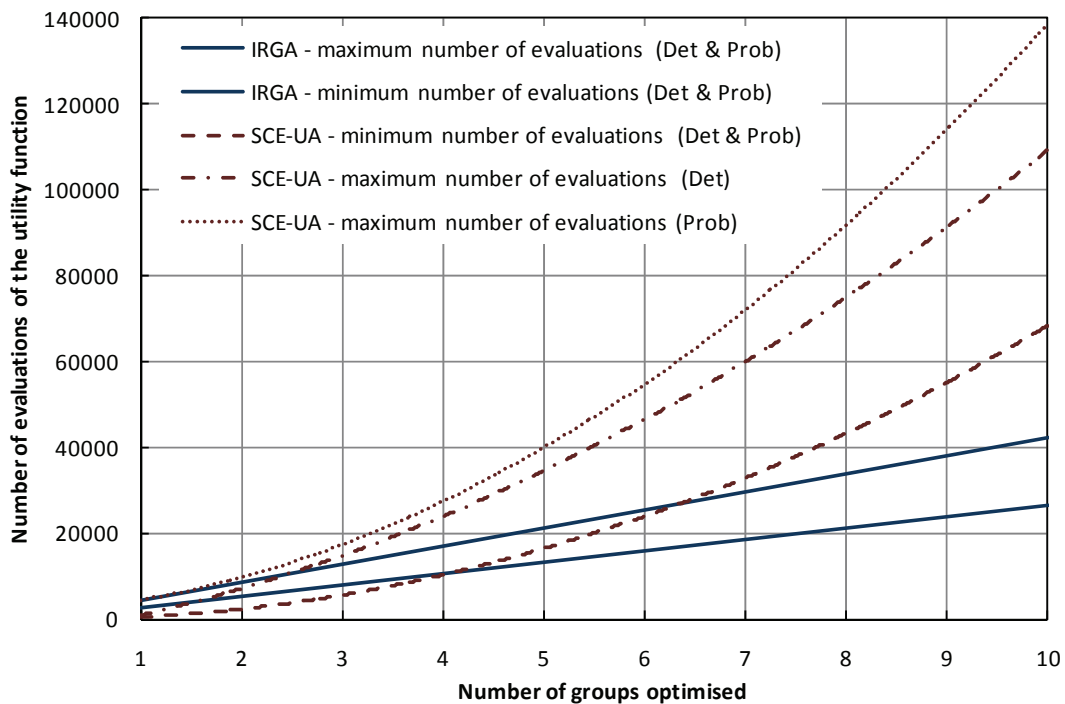


Figure 7.17 Approximate number of evaluations of the objective function with IRGA and SCE-UA approaches when optimising deterministic and probabilistic forecasts.

### 7.6.3 Selected methods for real-time optimisations

From the developed methods, IRGA correspond to the optimal method to use in real-time optimisations for the whole basin, optimising the hydropower groups in series.

The sensitive of the results does not significantly vary depending on the ranking of the hydropower groups. The Reservoir Space Index ordering the hydropower groups from the highest to the smallest value ( $RSI_{\max\text{to}\min}$ ) is selected because this method offer a slightly better performance regarding expected damages and PPOC.

Regarding the objective function, TOPSIS is selected as the best developed method since the provided results are robust for any situation. This method tries to reduce the total economical losses for the whole set of values.

“Make things as simple as possible, but not simpler”

Albert Einstein (1879 - 1955)

## **8. Conclusions and outlook**

## 8.1 General overview

During the last decades a number of floods caused severe inundations in the Upper Rhone River basin (Vaud and Valais Cantons) in Switzerland. As a response to such disasters, the MINERVE flood forecast system has been implemented with the purpose to reduce flood peaks by taking advantage of the multi-reservoir system of existing hydropower schemes.

COSMO-7 meteorological forecast has been operational for the MINERVE project since 2006, COSMO-LEPS forecast since 2008 and COSMO-2 forecast since 2009. Furthermore, resimulation of meteorological forecasts was provided by MeteoSwiss with COSMO-LEPS and COSMO-7 for historical floods in order to analyse their performance in practical cases.

The efforts of this research project comprise different fields: meteorology, hydrology, flood warning, Decision Support Systems (DSS) and real-time decision making processes. Accordingly, the aims were plentiful. Examples of such aims are processing meteorological forecasts, achieving multiple hydrological simulations, conceiving a flood warning report for end users and, finally, developing a DSS within the framework of real-time decision making for reservoir management.

Flood management is not an easy task. A certain practice and familiarity with the system is therefore required to understand the results and take adequate decisions based on uncertain data. A learning period is thus necessary before operating the whole system optimally.

The reservoir management during floods is based on information about potential damages for scenarios corresponding to certain forecast members and on pre-defined discharge thresholds as well as on potential costs according to preventive operation strategies. The large scope of this information requires a DSS able to identify and solve the problem globally.

The present research project focused on the development of a DSS, called MINDS, for flood control taking profit of the existing hydropower schemes. MINDS was specifically adapted for the Upper Rhone River basin in the Vaud and Valais Cantons. Having in mind this final goal, the relevant past developments on deterministic and probabilistic meteorological forecasts, hydrological models and systems, optimisation techniques, multi-criteria decision making methods and decision support systems were reviewed. A conceptual system and a DSS ready to be implemented were then designed and developed. In the following, the main conclusions are presented and the strengths and limitations of the developed system are discussed. Finally, an outlook for future research opportunities and improvements of the system is given.

## 8.2 Hydro-meteorological forecasts and flood warnings

### 8.2.1 Meteorological forecasts

Three types of forecasts provided by MeteoSwiss are implemented in the MINERVE system but, due to their availability, only COSMO-LEPS and COSMO-7 results were tested during the research project. According to the analysis, no substantial differences were observed between them when assessing precipitation and temperature.

Currently, COSMO-7 is the only forecast automatically implemented in the operational system of the Valais Canton. Therefore, this forecast is actually vital for hydrological automatic flood warning simulations. COSMO-2 and COSMO-LEPS will be shortly added to the MINERVE flood forecast system in order to make the model more robust. Once implemented, automatic hydrological simulations will be available for all forecasts.

The daily performance of each forecast has been systematically evaluated in the present research project. Evaluation results of precipitation showed a slightly better performance for the ensemble forecast COSMO-LEPS by comparison with COSMO-7, as well as less overestimation of precipitation volumes. Concerning the temperature, the performance was similar for both forecasts.

### 8.2.2 Hydrological model

The hydrological concept used to simulate runoff and base flows at each sub-catchment is based on the GSM-Socont model, developed during the first stage of the MINERVE project, and takes into account all hydraulic structures of the storage hydropower plants.

The semi-distributed hydrological model includes 239 sub-catchments. Each one is divided in non-glacier elevation bands as well as in glacier bands if a glacier is presented. Every band is associated with a virtual meteorological station which provides precipitation and temperature series. A model of snow composed of a double reservoir (snow and liquid water content in the snow layer) finally produces an equivalent precipitation.

In the case of a non-glacier band, the equivalent precipitation feeds the infiltration and run-off models, respectively producing the slow and fast discharge components at the outlet of the sub-catchment. In case of a glacier band, the equivalent precipitation is transferred to the outlet by means of a linear reservoir. When no more snow exists on the glacier band, a degree-day glacier melt model produces a discharge which is also transferred to the outlet

through a linear reservoir. The total discharge of the sub-catchment is the sum of all mentioned contributions.

This hydrological model has proven its effectiveness in the previous stage of the MINERVE project and was already implemented. It reveals different performance degrees depending on the region, but provides good results when considering the forecasts at the main check points of the Rhone River.

### **8.2.3 Hydrological forecasts**

This semi-distributed hydrological model has been built in the simulation tool Routing System. This software simulates the formation and the propagation of free surface flows in a complex system and conducts hydrological simulations with deterministic or probabilistic meteorological forecasts.

The user-friendly Routing System software has been successfully used since the beginning of the previous stage of the MINERVE project. It has been effectively improved for the present research. It is currently able of simulating multiple hydro-meteorological forecasts and storing all information in databases easily accessible if necessary.

The hydrological forecasts obtained with this tool have proven their usefulness in the Upper Rhone River basin. Regarding the discharges at main check points and indicators such as the relative volume bias, the root mean square error or the cumulated volume ratio, COSMO-LEPS provides a better performance than COSMO-7, which slightly decreases based on the lead time for both of them. Moreover, COSMO-LEPS median provides less reactive forecasts, especially when comparing consecutive forecasts.

### **8.2.4 MINERVE warning system**

The MINERVE warning report, developed during this research project, provides the warning levels at main check points of the river network according to time, being an asset to the decision-making for preventive actions. A Notice, Alert or Alarm level is activated depending on discharge thresholds in the Rhone River, defined by the authorities of Valais Canton.

The results provided during this research project by the studied historical events confirm the added value of the forecast system for early flood warnings. Even with less than perfect performances, the forecast system generally provides flood warnings with rates of correct alarms higher than 0.5 and small rates of false or misses alarms.

Moreover, the appropriate assessment and interpretation of the warning report is as important as high-quality forecasts. A regular communication between developers and end users is therefore essential. A good hydro-meteorological forecast is not useful without a clear visualisation and presentation of results, either without a correct interpretation. Consequently, the developers have to be sensitive to the end users' needs and the end users have to know and understand the results they are dealing with and their potential implications. This premise was carried out over the whole research project. The end users were periodically consulted and their opinion taken into account for continuous improvements of the system.

The MINERVE flood forecast system makes easier the understanding of application of ensemble forecasts for the purposes of flood warning as well as reservoir management with the view of an active participation of the authorities in the decision process.

### **8.3 MINERVE Interactive Decision Support System - MINDS**

#### ***8.3.1 Main goal of the MINERVE Interactive Decision Support System***

Beyond the contribution mentioned above for flood warnings, the forecasts can also be used for defining the priority of decisions regarding the operation of hydropower plants during flood events. Considering the hydrographs at check points as well as the future inflows and levels in reservoirs over the basin, the developed MINDS system suggests optimum preventive turbine and bottom outlet operations. The main purpose is to stop turbines during flood peaks and to store water inflows in the reservoirs as much as possible at this critical moment. Appropriate operations can thus reduce the peak discharges in the Rhone River and its tributaries, avoiding or reducing flood damages.

#### ***8.3.2 Hydraulic simulation model***

The hydraulic balance model of the Upper Rhone River basin was developed for hydraulic simulations in the optimisation tool MINDS. This simplified model of the complex catchment area was especially created for reservoirs management and flood control under real-time conditions.

In spite of the simplification of the complete hydrological model implemented in Routing System, the hydraulic balance model performs accurately and provides a substantial flexibility to MINDS. A more detailed model could be tested, including variable transit times between

the check points and compensation reservoirs. Nevertheless, due to real-time computation requirements, it could be prohibitive even if large improvements in computer capabilities are incorporated.

### ***8.3.3 Optimisation methods for reservoir management***

#### ***Definition of the objective function***

First, a function is defined for the estimation of monetary losses depending on a preventive operation and a forecast member. Then, different multi-attribute decision making methodologies are implemented for defining the utility function to optimise, which depends on preventive operations and a set of forecast members. The operational method can be selected by the decision makers depending on their expertise or on the optimisation results. The five implemented methods provide traditional, innovative and conservative functions which correspond with any future target of the decision maker.

It has to be noted that, if using only the deterministic forecast, all multi-attribute decision making methods provide the same result because the set of function values becomes a unique value. When several forecasts are taken into account (probabilistic forecast), a set of values is obtained and the optimisation results vary depending on the selected method, i.e. on the purpose pointed by the decision maker (e.g. minimizing the maximum damage, the average value, etc). In such case, the TOPSIS method is proposed as default. It provides robust results during the optimisation for the entire range of forecasts.

#### ***Resolution of the objective function***

Concerning the resolution of the system, the Iterative Ranking Greedy Algorithm (IRGA) is finally proposed for solving the objective function in real-time calculations. The resolution in series for the hydropower groups, as performed with the IRGA approach, provides high quality results. Furthermore, it requires small computation times which allow re-calculations of different scenarios if necessary.

The SCE-UA behaves similarly to IRGA when optimising one or two hydropower groups, but its performance substantially decreases when treating all hydropower groups at the same time. Then, SCE-UA tends to recommend excessive preventive operations which result in high potential energy losses.



### ***Conclusions about optimisation***

The developed system MINDS performs adequately in all tested cases, clearly reducing the damages over the basin during a flood event. Furthermore, the simplicity of the system does not affect its performance, making the system valuable for real-time tasks.

The expected damages due to floods are reduced by MINDS through the optimisation of preventive operations of hydropower plants. Moreover, the calculation of potential costs of energy losses due to preventive measures are also useful. They indicate the amount involved by the decision makers if the forecasts are false.

The level of priority decisions in the hydropower groups for making preventive operations also helps decision makers. The main reservoirs able to reduce the flood can be directly visualised, including the available time to order the preventive measures to the hydropower plants' operators.

#### ***8.3.4 Decision Support System interface***

A clear and understandable interpretation of results is one of the main concerns of the decision support tool. Preventive operation measures can lead to energy sale losses at the hydropower plants. In such cases, these losses have to be adequately compensated by the local authorities which have ordered them. Hence, to accurately understand and cope with potential flood events, the crisis task force has to know precisely the exceedance probability of a certain discharge threshold as well as the location and time of its occurrence. The task force should also know the expected reduction of the foreseen damages due to preventive operation measures.

These issues are addressed by MINDS and enable the decision maker to be easily and directly involved in the decision making process. The most important parameters can be found in the main window of the DSS and the secondary parameters are located in the advanced parameters window, as presented in section 6.9. The decision maker can edit the key parameters before starting the optimisation process. Some of them can be varied in order to improve results or assessing their sensitivity. Despite this option, the system remains robust and minor variations in parameter values do not significantly change the results.

The interface was designed to present the relevant decision and its benefits for the considered flood. The results are displayed in different tables and graphics, for each check point or reservoir in order to clearly explain the flood management decisions.

### 8.3.5 *Strengths of MINDS*

In this research project, some new contributions to the theory and application of DSS in water resources management have been developed, particularly in the domain of reservoir regulation and flood control. The strengths of MINDS are in the system conceptual design as well as in the optimisation theory and application. These particularities are presented in the following.

The developed methodology uses deterministic and probabilistic forecasts for flood management. It combines various processes, techniques and theoretical procedures, presented in Chapter 6, for applying them within real cases with a real-time decision support system. The computation method proves its effectiveness and the robustness of the model is confirmed. The possibility of selecting the utility function to optimise depending on various criteria (Expected Mean Risk, MinMax Regret,...) as well as the possibility of selecting the sub-basin and the hydropower groups allows a substantial degree of flexibility to decision makers, providing more confidence in the results.

The main goal of MINDS, which has been noticeably achieved, is the reduction of flood damages. The proposed preventive operations can minimize the damages over the basin as much as possible. The performance of the results is highly satisfying and the required computation time is small enough for real-time applications.

Furthermore, the user-friendly interface for preventive operations at hydropower plants allows the decision makers to understand the proposed measures as well as their consequences, facilitating a clear overview of the incoming flood event.

Additionally, diverse strategies or alternative solutions regarding the potential flood reduction by preventive reservoir operations can be effectively analysed by MINDS through different scenarios proposed by the decision maker. Furthermore, the concluding information of the selected scenario allows the user to validate and to justify the chosen decision.

Although MINDS was specifically developed for the Upper Rhone River basin, the architecture of the system and its conceptual methodology can be applied to other cases in the field of water resources, flood warnings or reservoir management. Only slight modifications of MINDS would be necessary to adapt it to other applications. MINDS has been developed in a structured way, with a well-organized network of groups (system of one or several reservoirs and hydropower plants physically interconnected) and check points, allowing an easy adaptation to other river basins with their own systems of hydropower schemes.

## 8.4 Outlook

### 8.4.1 *General perspectives of the MINERVE flood forecast and management system*

Hydrological forecasting is a complex task, especially when working with ensemble prediction systems. Neither the developers, nor the end users can achieve alone a good hydrological system. The only sound strategy comprises communication, interaction and feedback. Furthermore, training is also necessary for managing the computer tools under extreme situations. These premises were fundamental for achieving the goal of the research project. Nevertheless, the constant improvement of such tools cannot be reduced only to research or programming, but implies the continuous formation of decision makers and end users in order to guarantee the success of the forecasts system.

Only two historical flood events could be tested in the scope of this research project. Even if the implemented procedures and methods are robust enough to obtain good results when applying to other extreme events, the generation of theoretical scenarios (i.e. synthetic floods) could enhance the experience in all aspects, from meteorology to decision making. Furthermore, the behaviour of the basin and the influence of each reservoir could be evaluated depending on the type of flood. Pre-defined scenarios could therefore be useful and a source of knowledge for decision makers.

New meteorological forecasts, the improvement of the current hydrological model and the addition of new hydrological models could be attractive solutions to be tested in the existing system. New optimisation methods in MINDS and improvements on the simplified hydraulic balance model could also be applied having in mind the enhancement of the system regarding flood control.

### 8.4.2 *Outlook for hydro-meteorological forecast systems*

#### *Outlook for meteorology*

The MINDS tool can be used with all existing forecasts. However, because the lead time of COSMO-2 does not leave much manoeuvre margin to make use of preventive operations, it may be difficult to operate it for reservoir management. Instead, using COSMO-2 in combination with another forecast at higher lead time could be a possibility to develop and test in the future.

The implementation of additional forecasts such as the analogue technique, which is currently being developed in a parallel research project, could be very interesting as it may lead to a potential improvement of the system. Nonetheless, these tasks are not of easy or quick understanding, implementation or operation. There is undoubtedly scope for the development of a new procedure to address this issue.

Exploring other types of forecasts (from ECMWF, NCEP,...) could also prove to be interesting, but would require a previous study of aptitude and a performance analysis for the concerned basin. However, the possibility of new meteorological inputs stays open and the flexibility of the system allows new implementations in the hydrological simulation tool as well as in the decision support system without changing the structure of the tools.

### ***Outlook for hydrology***

In spite of the good performance of the hydrological model GSM-Socont, developed during the first stage of the MINERVE project, it was basically created and calibrated for providing high flood forecasts and not for current situations or low flows. Therefore, a new re-calibration would be of interest, even more knowing that a larger database including data from recent years is available and could improve the robustness of the results. This development would however require more precise information about the power schemes operations.

Furthermore, the implementation of advanced interpolation methods for temperature and precipitation is presently studied in another parallel research project at the ECHO laboratory. The hydrological model is also being improved at the same laboratory by a new soil reservoir model, which will provide a more complete output with surface runoff flow, interflow and base flow. New parameters will then be added. Nevertheless, since a model re-calibration would be required, the calibration of new parameters could be achieved at the same time.

The implementation of an alternative hydrological model, for example HBV or PREVAH, could also provide more information about the performance and uncertainty of the hydrological models. In the future, both models could be included in the system for hydrological forecasts, using them with a fixed or variable weight depending on the situation.

Finally, the glacier model was created with a fixed surface. Due to the non-variability of its surface, the glacier does not modify its hydrological effect over the time, which might not be valid on the long term, especially when considering climate changes. Preliminary models including variable glacier mass have been developed and their implementation could also lead to an improvement in the results, especially on a medium term. Alternatively to the

development of such model, a review of the glaciers cover should be regularly undertaken and new surface relations adopted.

### ***Outlook for hydro-meteorological forecasts and flood warnings***

At the present, warning reports are performed manually. A high progress could therefore be attained when coupling the creation of the report to the hydrological tool, directly providing automatic reports for end users, similarly to the Flood Early Warning System (FEWS) implemented in the Swiss Federal Office for the Environment (FOEN).

Furthermore, the incorporation of the uncertainty in the hydrological forecasts could offer an added value to decision makers. The continuous analysis of the warnings performance for each level (Notice, Alert and Alarm) would also provide interesting results regarding the activation. Additionally, it could be completed with the evaluation of the Relative Economic Value (REV) of the forecasts, which would supply a final answer to the real value of the hydro-meteorological flood warning system.

### ***8.4.3 Outlook for the MINERVE Interactive Decision Support System - MINDS***

The improvement of the “Business as Usual” simulation could be one of the first tasks to carry out. Even if results demonstrate its quality concerning the mass balance, a closer reproduction of real operations at hydropower plants could improve the simulation compared to real observations. Furthermore, spot market prices for energy sale as well as hourly time series depending on daily and seasonal periods could be introduced. This could ameliorate the simulation carried out for the usual operations at hydropower plants.

Another point would be to study the expected damages calculation in more detail. The sensitivity of damages estimation at check points should be evaluated as well. Various scenarios could also be produced in order to have a better perspective of the problem.

In the same way, the potential costs of preventive operations could be transformed into a set of likely costs depending on the forecasts, also showing their lower and upper limits for a theoretical best and worst case scenarios. This set of costs would provide a more realistic point of view concerning the costs generated by preventive operations. Consequently, the decision maker could better recognise the risk taken.

In preventive operations, the initial time for pump operations could be added. The system performance in minimizing the damages could then be evaluated. The variation of the used capacity for turbines and bottom outlet operations could also improve the results. However,

this would probably significantly increase computation times and should therefore be carefully addressed.

Turbine, bottom outlet and pump operations for each reservoir are currently optimised in series (successively one after the other). The simultaneous optimisation of all parameters for a reservoir, or even for a hydropower group, could probably improve the results, as proven by the SCE-UA when optimising only one group. The main issue would be to know how relevant and robust this improvement is. Thus, to use the IRGA approach in a general way, but solving preventive operations for each hydropower group by the SCE-UA algorithm could be tested in future developments and could provide an improvement of the results.

Other approaches such as Genetic Algorithms (GA) could be implemented and tested, but an improvement is not expected for real-time calculations. Nevertheless, if GA would provide accurate results, it could offer a framework for comparison with the IRGA approach.

At present, the computation time is one of the most important constraints of the system. For this reason, parallel calculation with a computer network should be studied when implementing higher quality iterations in the process.

Finally, the increase of the forecast period (or the implementation of additional forecasts, e.g. with 10 days prediction as it is the case for various forecasts from the ECMWF) could be also of worthwhile interest. In fact, hydrological forecasts including the whole flood event can provide optimal results. In contrast, hydrological forecasts ending with increasing discharges could produce sub-optimal results. Since in such cases the flood event is not fully taken into account, the proposed solutions can underestimate preventive operations due to aggregated potential high volumes produced in the following part of the flood and still not exploited as input of the system.

## **9. References**

- Abbott, M. B., Bathurst, J. C., Cunge, J. A., O'Connell, P. E. and Rasmussen, J. (1986a). *An introduction to the European Hydrological System - Système Hydrologique Européen, "SHE", 1: History and philosophy of a physically-based, distributed modelling system.* Journal of Hydrology, Vol. 87, 45-59.
- Abbott, M. B., Bathurst, J. C., Cunge, J. A., O'Connell, P. E. and Rasmussen, J. (1986b). *An introduction to the European Hydrological System - Système Hydrologique Européen, "SHE", 2: Structure of a physically-based, distributed modelling system.* Journal of Hydrology, Vol. 87, 61-77.
- Abbott, M. B. and Refsgaard, J. C. (1996). *Distributed Hydrological Modelling.* Kluwer Academic Publishers, Water Science and Technology Library, Vol. 22, 336 p., ISBN 10: 0792340426.
- Abebe, N. A., Ogden, F. L. and Pradhan, N. W. (2010). *Sensitivity and uncertainty analysis of the conceptual HBV rainfall-runoff model: Implications for parameter estimation.* Journal of Hydrology, Vol. 389, 301-310.
- Abrahart, R. J. (2003). *Neural network rainfall-runoff forecasting based on continuous resampling.* Journal of Hydroinformatics, Vol. 5, 51-61.
- Ahmad, S. and Simonovic, S. P. (2000). *System dynamics modelling of reservoir operations for flood management.* Journal of Computing in Civil Engineering, Vol. 14, 190-198.
- Ahmad, S. and Simonovic, S. P. (2001). *Integration of heuristic knowledge with analytical tools for the selection of flood damage reduction measures.* Canadian Journal of Civil Engineering, Vol. 28, 208-221.
- Ahmad, S. and Simonovic, S. P. (2006). *An Intelligent Decision Support System for Management of Floods.* Water Resources Management, Vol. 20, 391-410.
- Ajami, N. K., Gupta, H., Wagener, T. and Sorooshian, S. (2004). *Calibration of a semi-distributed hydrologic model for streamflow estimation along a river system.* Journal of Hydrology, Vol. 298, 112-135.
- Akter, T. and Simonovic, S. P. (2005). *Aggregation of fuzzy views of a large number of stakeholders for multi-objective flood management decision-making.* Journal of Environmental Management, Vol. 77, 133-143.
- ALADIN international team (1997). *The ALADIN project: Mesoscale modelling seen as a basic tool for weather forecasting and atmospheric research.* WMO Bulletin, Vol. 46, No. 4, 317-324
- Alessi Celegon, E., Nicotina, L., Botter, G., Rinaldo, A. and Marani, M. (2007). *A coupled hydrometeorological modelling approach: a case study.* Proceedings of the 32nd Congress of IAHR, Venezia, Special session 10.
- Ali, Md. H., Shui, L. T. and Walker, W. R. (2003). *Optimal Water Resources Management for Reservoir Based Irrigation Projects Using Geographic Information System.* Journal of Irrigation and drainage engineering, Vol. 129, 1-10.
- Alidaee, B., Kochenberger, G. A. and Amini, M. M. (2000). *Greedy solutions of selection and ordering problems.* European Journal Operational Research, Vol. 134, 203- 215.
- Ambrosino, G., Fronza, G., Guariso, G. and Karlin, A. (1979). *Multi-goal analysis of a short-run reservoir operation.* Applied Mathematical Modelling, Vol. 3, Issue 3, 221-227.



- Amorocho, J. and Hart, W. E. (1964). *A critique of current methods in hydrologic systems investigation*. Transactions of the American Geophysical Union, Vol. 45, 307-321.
- Anderson, J. R., Dillon, J. L. and Hardaker, J. B. (1977). *Agricultural Decision Analysis*. Iowa State University Press, 344 p., ISBN: 0813804000.
- Andrade, M. G., Fragoso, M. D. and Carneiro, A. A. F. M. (2001). *A stochastic approach to the flood control problem*. Applied Mathematical Modelling, Vol. 25, 499-511.
- Andreu, J. (1993). *Conceptos y métodos para la planificación hidrológica*. Centro Internacional de Métodos Numéricos en Ingeniería, Barcelona, ISBN 84-87867-19-7.
- Anthes, R.A. and Warner, T. T. (1978). Development of hydrodynamic models suitable for air pollution and other mesometeorological studies. Monthly Weather Review, Vol. 106, 1045-1078.
- Apel, H., Merz, B. and Thielen, A. H. (2008). *Quantification of uncertainties in flood risk assessments*. International Journal of River Basin Management, Vol. 6, 149-162.
- Arduino, G., Reggiani, P. and Todini, E. (2005). *Recent advances in flood forecasting and flood risk assessment*. Hydrology and Earth System Sciences, Vol. 9 (4), 280-284.
- Arheimer, B., Lindström, G. and Olsson J. (2010). *A systematic review of sensitivities in the Swedish flood-forecasting system*. Atmospheric Research, doi:10.1016/j.atmosres.2010.09.013.
- Aristotle (around 350 B.C.E.). *Meteorologica*. Loeb Classical Library, published in 1952, 480 p., ISBN-10: 0674994361.
- Arnott, D. and Pervan, G. (2008). *Eight key issues for the decision support systems discipline*. Decision Support Systems, Vol. 44, 657-672.
- Atger, F. (1999). *The Skill of Ensemble Prediction Systems*. Monthly Weather Review, Vol. 127 (9), 1941-1953.
- Austin, G. L. and Bellon, A. (1974). *The use of digital weather radar records for short term precipitation forecasting*. Quarterly Journal of the Royal Meteorological Society, Vol. 100, 658-664.
- Aven, T. and Pörn, K. (1998). *Expressing and interpreting the results of quantitative risk analyses*. Review and discussion. Reliability Engineering and System Safety, Vol. 61, 3-10.
- Awwad, H. M. and Valdés, J. B. (1992). *Adaptive Parameter Estimation for Multisite Hydrologic Forecasting*. Journal of Hydraulic Engineering, Vol. 118, 1201-1221.
- Bagis, A. and Karaboga, D. (2007). *Evolutionary algorithm-based fuzzy PD control of spillway gates of dams*. Journal of The Franklin Institute, Vol. 344, 1039-1055.
- Bakis, R. (2007). *Electricity production opportunities from multipurpose dams (case study)*. Renewable Energy, Vol. 32, 1723-1738.
- Bárdossy, A. (2000). *Stochastic downscaling methods to assess the hydrological impacts of climate change on river basin hydrology*. Climate Scenarios for Water-Related and Coastal Impacts, Proceedings of the EU Concerted Action Initiative ECLAT-2 Workshop 3, KNMI, Netherlands, May 10-12th 2000, Climatic Research Unit, Norwich, 18-34.

- Barredo, J. I. (2007). *Major flood disasters in Europe: 1950-2005*. Natural Hazards, Vol. 42, 125-148.
- Bartholmes, J. C., Thielen, J., Ramos, M. H. and Gentilini, S. (2009). *The European flood alert system (EFAS) – Part 2: Statistical skill assessment of probabilistic and deterministic operational forecasts*. Hydrology and Earth System Sciences, Vol. 13, 141-153.
- Bellon, A. and Austin, G. L. (1984). *The accuracy of short-term radar rainfall forecasts*. Journal of Hydrology, Vol. 70, 35-49.
- Ben Daoud, A., Sauquet, E. Lang, M., Obled, C. and Bontron, G. (2009). *La prévision des précipitations par recherche d'analogues : état de l'art et perspectives*. La Houille Blanche, No. 6, 60-65.
- Bender, M. J. and Simonovic, S. P. (2000). *A fuzzy compromise approach to water resource systems planning under uncertainty*. Fuzzy Sets and Systems, Vol. 115, 35-44.
- Benkaci A. T. and Dechemi, N. (2004). *Modélisation pluie-débit journalière par des modèles conceptuels et "boîte noire"; test d'un modèle neuroflou*. Hydrological Sciences Journal, Vol. 49 (5), 919-930.
- Bergström, S. (1976) *Development and application of a conceptual runoff model for Scandinavian catchments*. SMHI Reports RHO, No. 7, Norrköping.
- Bergström, S., Carlsson, B. and Graham, L. P. (1996). *Modelling the water balance of the Baltic basin—preliminary results*. Nordic Hydrological Conference, Akureyri, NHP-Report No. 40, pp. 449-455.
- Bérod, D. (1994). *Contribution à l'estimation des crues rares à l'aide de méthodes déterministes. Apport de la description géomorphologique pour la simulation des processus d'écoulement*. PhD Thesis N° 1319, Ecole Polytechnique Fédérale de Lausanne.
- Beven, K. J. and Kirkby, M. J. (1979). *A physically based, variable contributing area model of basin hydrology*. Hydrological Sciences Bulletin, Vol. 24, 43-69.
- Beven, K. J., Kirkby, M. J. Schofield, N. and Tagg, A. F. (1984). *Testing a physically-based flood forecasting model (TOPMODEL) for three U.K. catchments*. Journal of Hydrology, Vol. 69, 119-143.
- Beven, K. (1989). *Changing ideas in hydrology - the case of physically-based models*. Journal of Hydrology, Vol. 105, 157-172.
- Beven, K. J. (1997). *TOPMODEL: a critique*. Hydrological Processes, Vol. 11, 1069-1085.
- Bieri, M., Schleiss, A. J. and Fankhauser, A. (2010). *Modelling and simulation of floods in alpine catchments equipped with complex hydropower schemes*. River Flow, Ed. Dittrich, Koll, Aeberle & Geisenhainer, Braunschweig, 1421-1428.
- Blazkova, S. and Beven, K. (1997). *Flood frequency prediction for data limited catchments in the Czech Republic using a stochastic rainfall model and TOPMODEL*. Journal of Hydrology, Vol. 195, 256-278.
- Blöschl, G., Reszler, C. and Komma, J. (2008). *A spatially distributed flash flood forecasting model*. Modelling & Software, Vol. 23, Issue 4, 464-478.
- Boillat J.-L. and Schleiss A. (2002). *Détermination de la crue extrême pour les retenues alpines par une approche PMP-PMF*. Wasser Energie Luft, Vol. 94, No. 3/4, 107-116.

- Boillat, J.-L. (2005). *L'influence des retenues valaisannes sur les crues Le projet MINERVE*. Communication 21 du Laboratoire de Constructions Hydrauliques, Conférence sur la recherche appliquée en relation avec la 3e Correction du Rhône - Nouveaux développements dans la gestion des crues, Martigny, Ed. A. Schleiss, EPFL, 87-101.
- Boillat, J.-L. (2009). *Prévision hydrologique et aide à la décision*. Swiss Engineering, Vol. 7/8, p.10.
- Bontron, G. (2004). *Prévision quantitative des précipitations: Adaptation probabiliste par recherche d'analogues. Utilisation des Réanalyses NCEP/NCAR et application aux précipitations du Sud-Est de la France*. PhD thesis, Institut National Polytechnique de Grenoble.
- Box, G. and Jenkins, G. (1970) *Time series analysis: forecasting and control*. Holden-Day, San Francisco, 575 p.
- Box, G. E. P. and Draper, N. R. (1987). *Empirical Model-Building and Response Surfaces*. Wiley. 688 p., ISBN 0471810339.
- Brakensiek, D. L. (1967). *A technique for analysis of runoff hydrographs*. Journal of Hydrology, Vol. 5, 21-32.
- Breur, K. J., van Nooyen, R.R.P. and van Leeuwen P.E.R.M. (2009). *Computerized generation of operational strategies for the management of temporary storage of drainage water from several polders in a network of small lakes and canals*. Applied Mathematical Modelling, Vol. 33, Issue 8, 3330-3342.
- Brier, G. W. (1950). *Verification of forecasts expressed in terms of probability*. Monthly Weather Review, Vol. 78 (1), 1-3.
- Bruen, M. (2006). *Decision Support Systems*. in Knight, D.W. & Shamseldin, A.Y. (2006). *River Basin Modelling for flood risk mitigation*. Taylor & Francis, 616 p., ISBN: 978-0-415-38344-8.
- Buizza, R., Hollingsworth, A., Lalauette, F. and Ghelli, A. (1999). Probabilistic predictions of precipitation using the ECMWF Ensemble Prediction System. Weather and Forecasting, Vol. 14, No. 2, 168-189.
- Buizza, R., Houtekamer, P.L., Toth, Z., Pellerin, G., Wei, M. and Zhu, Y. (2005). *A comparison of the ECMWF, MSC and NCEP global ensemble prediction systems*. Monthly Weather Review, Vol. 133, 1076-1097.
- Buizza, R. (2008). *The value of probabilistic prediction*. Atmospheric Science Letters, Vol. 9, 36-42.
- Burlando, P., Montanari, A. and Ranzi, R. (1996). *Forecasting of storm rainfall by combined use of radar, rain gages and linear models*. Atmospheric Research, Vol. 42, 199-216.
- Carpenter, T. and Georgakakos, K. P. (2006). *Intercomparison of lumped versus distributed hydrologic model ensemble simulations on operational forecast scales*. Journal of Hydrology, Vol. 329, 174-185.
- Casati, B., Ross, G. and Stephenson, D. B. (2004). *A new intensity scale approach for the verification of spatial precipitation forecasts*. Meteorological Applications, Vol. 11, 141-154.

- Castelletti, A., De Rigo, D., Rizzoli, A. E. Soncini-Sessa, R. and Weber, E. (2007). *Neuro-dynamic programming for designing water reservoir network management policies*. Control Engineering Practice, Vol. 15, 1031-1038.
- Castelletti, A., Pianosi, F. and Soncini-Sessa, R. (2008). *Water reservoir control under economic, social and environmental constraints*. Automatica, Vol. 44, 1595-1607.
- Celeste, A. B., Suzuki, K. and Kadota, A. (2004). *Genetic algorithms for real-time operation of multipurpose water resource systems*. Journal of Hydroinformatics, Vol. 6, 19-38.
- Cervellera, C., Chen, V. C. P. and Wen, A. (2006). *Optimization of a large-scale water reservoir network by stochastic dynamic programming with efficient state space discretization*. European Journal of Operational Research, Vol. 171, 1139-1151.
- Chandramouli, V. and Deka, P. (2005). *Neural Network Based Decision Support Model for Optimal Reservoir Operation*. Water Resources Management, Vol. 19, 447-464.
- Chandrasekar, A., Philbrick, C. R., Doddridge, B. G., Clark, R. D. and Georgopoulos P. G. (2004). *A comparative study of prognostic MM5 meteorological modeling with aircraft, wind profiler, LIDAR, tethered balloon and RASS data over Philadelphia during a 1999 summer episode*. Environmental Fluid Mechanics, Vol. 4, 339-365.
- Chang L.-C. (2008). *Guiding rational reservoir flood operation using penalty-type genetic algorithm*. Journal of Hydrology, Vol. 354. 54-74.
- Chang, T. J. and Moore, D. (1997). *An expert system approach for water management in case of drought*. Proceedings of the IASTED International Conference on Intelligent Information Systems (IIS '97), 332-339.
- Charney J. G., Fj'rtoft, R., and von Neumann, J. (1950). *Numerical integrations of the barotropic vorticity equations*. Tellus, Vol. 2, 237-254.
- Chen, C.-T. (2000). *Extensions of the TOPSIS for group decision-making under fuzzy environment*. Fuzzy Sets and Systems, Vol. 114, 1-9.
- Chen, S.-T. and Yu, P.-S. (2007). *Real-time probabilistic forecasting of flood stages*. Journal of Hydrology, Vol. 340, 63-77.
- Chen, T.-Y. and Tsao, C.-Y. (2008). *The interval-valued fuzzy TOPSIS method and experimental analysis*. Fuzzy Sets and Systems, Vol. 159, 1410-1428.
- Cheng, C.-T. (1999). *Fuzzy optimal model for the flood control system of the upper and middle reaches of the Yangtze River*. Hydrological Sciences Journal, Vol. 44 (4), 573-582.
- Cheng, C.-T. and Chau, K. W. (2002). *Three-person multi-objective conflict decision in reservoir flood control*. European Journal of Operational Research, Vol. 142, 625-631.
- Cheng, C.-T., Wang, W.-C. and Xu, D.-M. (2007). *Optimizing Hydropower Reservoir Operation Using Hybrid Genetic Algorithm and Chaos*. Water Resources Management, Vol. 22, 895-909.
- Chibanga, R. Berlamont, J. and Vandewalle, J. (2003). *Modelling and forecasting of hydrological variables using artificial neural networks: the Kafue River sub-basin*. Hydrological Sciences Journal, Vol. 48 (3), 363-379.
- Christensen, J. H. and Christensen, O.B. (2003) *Climate modelling: severe summertime flooding in Europe*. Nature, Vol. 421, 805-806.

- Chua, L. H. C. and Wong, T S. W. (2010). *Improving event-based rainfall-runoff modeling using a combined artificial neural network-kinematic wave approach*. Journal of Hydrology, Vol. 390, 92-107.
- Claude, A., Zin, I., Obled, C., Gautheron, A. and Perret C. (2010). *Towards an Operational Flood Forecasting System Taking into Account Hydro-Power Plants Operations*. Mathematical Modelling in Civil Engineering, Technical University of Civil Engineering from Bucharest, Number 4, Vol. 6, 26-42.
- Cloke, H. L. and Pappenberger, F. (2009). *Ensemble flood forecasting: A review*. Journal of Hydrology, Vol. 375, 613-626.
- Cohen, T., García Hernández, J., Dubois, J. and Boillat, J.-L. (2009). *Influence of hydrological model complexity on the estimation of floods in an alpine catchment for PMP conditions*. Proceedings of the 33rd Congress of IAHR Water engineering for a sustainable environment, Vancouver, Canada, 1763-1770. ISBN: 978-94-90365-01-1.
- Consuegra D., Niggli M. and Musy A. (1998). *Concepts méthodologiques pour le calcul des crues. Application au bassin versant supérieur du Rhône*. Wasser Energie Luft, Vol. 9/10, 223-231.
- Côté, J. S., Gravel, S., Methot, A., Patoine, A., Roch, M., and Staniforth, A. (1998). *The operational CMC/MRB Global Environmental Multiscale (GEM) model. Part I: Design considerations and formulation*. Monthly Weather Review, Vol. 126, 1373-1395.
- Cuena, J. and Molina, M. (2004). *A Multiagent System for Emergency Management in Flood*. Lecture Notes in Computer Science, Vol. 1611, 460-469.
- Cunge, J. A., (1969). *Au sujet d'une méthode de calcul de propagation des crues (Méthode Muskingum)*. Journal of Hydraulic Research, Vol. 7(2), 205-230.
- Curtis, S. A. (2003). *The classification of greedy algorithms*. Science of Computer Programming, Vol. 49, 125-157.
- Dasgupta, S., Papadimitriou, C. H. and Vazirani, U. V. (2006). *Algorithms*. McGraw-Hill, 336 p., ISBN/ASIN: 0073523402.
- Dechter, A. and Dechter, R. (1989). *On the Greedy Solution of Ordering Problems*. ORSA Journal on Computing, Vol. 1, No. 3, 181-189.
- Deidda, R. (1999). *Multifractal analysis and simulation of rainfall fields in space*. Physics and Chemistry of the Earth, Part B: Hydrology. Oceans and Atmosphere, Vol. 24 (1-2), 73-78.
- Demeritt, D., Cloke, H., Pappenberger, F., Thielen, J., Bartholmes, J. and Ramos, M. H. (2007). *Ensemble predictions and perceptions of risk, uncertainty and error in flood forecasting*. Environmental Hazards, Vol. 7, 115-127.
- De Roo, A., Gouweleeuw, B., Thielen, J., Bartholmes, J., Bongioannini-Cerlini, P., Todini, E., Bates, P., Horritt, M., Hunter, N., Beven, K., Pappenberger, F., Heise, E., Rivin, G., Hils, M., Hollingsworth, A., Holst, B., Kwadijk, J., Reggiani, P., van Dijk, M., Sattler, K. and Sprokkereef, E., (2003). *Development of a European flood forecasting system*. International Journal River of River Basin Management, Vol. 1, 49-59.
- Descamps L. and Talagrand, O. (2006). *On Some Aspects of the Definition of Initial Conditions for Ensemble Prediction*. Monthly Weather Review, Vol. 135, 3260-3272.



- Devi, K., Yadav, S. P. and Kumar, S. (2009). *Extension of Fuzzy TOPSIS Method Based on Vague Sets*. International Journal of Computational Cognition, Vol. 7, 58-62.
- Di Baldassarre, G., Schumann, G. Bates, P. D., Freer, P. D. and Beven, K. J. (2010). *Floodplain mapping: a critical discussion of deterministic and probabilistic approaches*. Hydrological Sciences Journal, Vol. 55, 364-376.
- Duan, Q., Sorooshian, S. and Gupta, V. (1992). *Effective and Efficient Global Optimization for Conceptual Rainfall-Runoff Models*. Water Resources Management, Vol. 28, No. 4, 1015-1031.
- Duan, Q., Gupta, V. K. and Sorooshian, S. (1993). *A shuffled complex evolution approach for effective and efficient global minimization*. Journal of Optimization Theory and Applications, Vol. 76, No. 3, 501-521.
- Duan, Q., Sorooshian, S. and Gupta, V. K. (1994). *Optimal use of SCE-UA global optimization method for calibrating watershed models*. Journal of Hydrology, Vol. 158, 265-284.
- Dubois, J. and Boillat, J.-L. (2000). *Routing System - Modélisation du routage des crues dans des systèmes hydrauliques à surface libre*. Communication 9 du Laboratoire de Constructions Hydrauliques, Ed. A. Schleiss, Lausanne. ISSN 1661-1179.
- Ebert, E. E. (2008). *Fuzzy verification of high-resolution gridded forecasts: a review and proposed framework*. Meteorological Applications, Vol. 15, 51-64.
- Ebert, E. E. and Manton, M. J. (1998). *Performance of Satellite Rainfall Estimation Algorithms during TOGA COARE*. Journal of Atmospheric Sciences, Vol. 55, 1537-1557.
- Edijatno and Michel, C. (1989). *Un modèle pluie-débit à trois paramètres*. La Houille Blanche, No. 2, 113-121.
- Egorova, R., van Noordwijk J. M. and Holterman, S. R. (2008). *Uncertainty in flood damage estimation*. Intl. J. River Basin Management, Vol. 6, 139-148.
- El-Nasr, A. A., Arnold, J. G., Feyen, J. and Berlamont, J. (2005). *Modelling the hydrology of a catchment using a distributed and a semi-distributed model*. Hydrological Processes, Vol. 19 (3), 573-587.
- Epstein, E. S. (1969). *Stochastic Dynamic Prediction*. Tellus, Vol. 21, 739-759.
- Faber, B. A. and Stedinger, J. R. (2001). *Reservoir optimization using sampling SDP with ensemble streamflow prediction (ESP) forecasts*. Journal of Hydrology, Vol. 249, 113-133.
- Faber M. H. and Stewart, M. G. (2003). *Risk assessment for civil engineering facilities: critical overview and discussion*. Reliability Engineering and System Safety, Vol. 80, 173-184.
- Farinha, F., Portela, E., Domingues, C. and Sousa, L. (2005). *Knowledge-based systems in civil engineering: Three case studies*. Advances in Engineering Software, Vol. 36, 729-739.
- Fedra, K. and Jamieson, D. G. (1996). *The 'WaterWare' decision-support system for river-basin planning. 2. Planning Capability*. Journal of Hydrology, Vol. 177, 177-198.
- Feyen, L., Vázquez, R., Christiaens, K., Sels, O. and Feyen, J. (2000). *Application of a distributed physically-based hydrological model to a medium size catchment*. Hydrology and Earth System Sciences, Vol. 4 (1), 47-63.

- Fleming, G. (1971). *Comment on "river flow forecasting through conceptual models. Parts I, II and III"*. Journal of Hydrology, Vol. 13, 351-356.
- Freeze, R. A. and Harlan, R. L. (1969). *Blueprint for a physically-based digitally-simulated hydrological response model*. Journal of Hydrology, Vol. 9, 237-258.
- French, S. (1986). *Decision theory: an introduction to the mathematics of rationality*. Halsted Press New York, 448 p., ISBN:0470203080.
- Frind, E. O. (1969). *Rainfall-runoff relationships expressed by distribution parameters*. Journal of Hydrology, Vol. 9, 405-426.
- Fu, G. (2008). *A fuzzy optimization method for multicriteria decision making: An application to reservoir flood control operation*. Expert System with Applications Vol. 34, 145-149.
- Fujiwara, O. and Tung, H. D. (1991). *Reliability Improvement for Water Distribution Networks Through Increasing Pipe Size*. Water Resources Research, Vol. 27, No. 7, 1395-1402.
- Gabellani, S., Boni, G., Ferraris, L., von Hardenberg, J. and Provenzale, A. (2007). *Propagation of uncertainty from rainfall to runoff: A case study with a stochastic rainfall generator*. Advances in Water Resources, Vol. 30, 2061-2071.
- Gandolfi, C. and Salewicz, K. A. (1991). *Water resources management in the Zambezi valley: analysis of the Kariba operation*. Hydrology for the Water Management of Large River Basins (Proceedings of the Vienna Symposium. IAHS Publ. 201.
- Ganji, A., Khalili, D. and Karamouz, M. (2007). *Development of stochastic dynamic Nash game model for reservoir operation. I. The symmetric stochastic model with perfect information*. Advances in Water Resources, Vol. 30, 528-542.
- García Hernández, J., Jordan, F., Dubois, J. and Boillat, J.-L. (2007a). *Routing System II: Modélisation d'écoulements dans des systèmes hydrauliques*. Communication 32 du Laboratoire de Constructions Hydrauliques, Ed. A. Schleiss, EPFL, Lausanne. ISSN 1661-1179.
- García Hernández, J., Jordan, F., Boillat, J.-L. and Schleiss, A. J. (2007b). *Meteorological and hydrological forecast for the Upper Rhone River Basin*. Proceedings of the 32nd Congress of IAHR, Venezia, Special session 10.
- García Hernández, J., Sirvent Gimenez, P., Jordan, F., Boillat, J.-L. and Schleiss, A. J. (2009a). *Ensemble meteorological forecast for the Upper Rhone River basin*. Annalen der Meteorologie 44, 30th International Conference on Alpine Meteorology, Germany, 122-123. ISSN 0072-4122, ISBN 978-3-88148-440-4.
- García Hernández, J., Jordan, F., Sirvent Giménez, P., Boillat, J.-L. and Schleiss, A. J. (2009b). *Ensemble hydrological forecasts for the Upper Rhone River basin*. Proceedings of the 33rd Congress of IAHR Water engineering for a sustainable environment, Vancouver, Canada, 1171-1177. ISBN: 978-94-90365-01-1.
- García Hernández, J., Deval Castillo, J., Boillat, J.-L. and Schleiss, A. J. (2009c). *Effect of climate change on hydrological cycle and evolution of the Rhone glacier*. Proceedings of the 33rd Congress of IAHR Water engineering for a sustainable environment, Vancouver, Canada, 773-780. ISBN: 978-94-90365-01-1.

- García Hernández, J., Boillat, J.-L., Jordan, F. and Hingray, B. (2009d). *La prévision hydrométéorologique sur le bassin versant du Rhône en amont du Léman*. La Houille Blanche, No. 5, 61-70.
- García Hernández, J., Horton, P., Tobin, C. and Boillat, J.-L. (2009e). *MINERVE 2010 : Prévision hydrométéorologique et gestion des crues sur le Rhône alpin*. Wasser Energie Luft, No. 4, 297-302.
- García Hernández, J., Boillat, J.-L. and Schleiss, A. J. (2010). *Flood forecast uncertainty and alert decision. Application to the Alpine Rhone River catchment*. Proceedings of Conference SimHydro “Hydraulic modeling and uncertainties”. 198e session of Comité Scientifique et Technique de la Société Hydrotechnique de France, Nice, France, 2nd day, 3rd session.
- García Hernández, J., Boillat, J.-L. and Schleiss, A. J. (2011a). *Présent et futur des prévisions hydrologiques pour la gestion des crues. Le cas du Rhône alpin*. Proceedings of the 2ème Rencontre sur les Dangers Naturels, UNIL, Lausanne, 9-14.
- García Hernández, J., Brauchli, T., Boillat, J.-L. and Schleiss, A. J. (2011b). *La gestion des crues du Rhône en amont du Léman: de la prévision à la décision*. La Houille Blanche, No. 2, 69-75.
- García Hernández, J., Schleiss, A. J. and Boillat, J.-L. (2011c). *Decision Support System for the hydropower plants management: the MINERVE project*. Proceedings of 79rd conference of International Commission on Large Dams (ICOLD), Luzern, Switzerland. Paper accepted
- García Hernández, J., Schleiss, A. J. and Boillat, J.-L. (2011d). *The Decision Support Tool MINDS for Flood Management in the Upper Rhone River*. Proceedings of the 34rd Congress of IAHR Balance and Uncertainty in a Changing World, Brisbane, Australia. Paper accepted.
- Garçon, R. (1996). *Prévision opérationnelle des apports de la Durance à Serre-Ponçon à l'aide du modèle MORDOR*. La Houille Blanche, No. 5, 71-76.
- Gaume, E., Bain, V., Bernardara, P., Newinger, O., Barbuc, M., Bateman, A., Blaskovicová, L., Blöschl, G., Borga, M., Dumitrescu, A., Daliakopoulos, I., Garcia, J., Irimescu, A., Kohnova, S., Koutroulis, A., Marchi, L., Matreata, S., Medina, V., Preciso, E., Sempere-Torres, D., Stancalie, G., Szolgay, J., Tsanis, I., Velasco, D. and Viglione, A. (2009). *A compilation of data on European flash floods*. Journal of Hydrology, Vol. 367, 70-78.
- Georgakakos, K. P., Seo, D.-J., Gupta, H., Schaake, J. and Butts, M. B. (2004). *Towards the characterization of streamflow simulation uncertainty through multimodel ensembles*. Journal of Hydrology, Vol. 298, 222-241.
- Glahn, H. R. and Lowry, D. A. (1972). *The use of model output statistics (mos) in objective weather forecasting*. Journal of Applied Meteorology, Vol. 11 (8), 1203-1211.
- Gneiting, T. and Raftery, A. E. (2005). *Weather Forecasting with Ensemble Methods*. Science, Vol. 310, No. 5746, 248-249.
- Golding, B. W. (1998). *Nimrod: A system for generating automated very short range forecasts*. Meteorological Applications, Vol. 5, 1-16.
- Gouweleeuw, B., Thielen, J., Franchello, G., de Roo, A. and Buizza, R. (2005). *Flood forecasting using medium-range probabilistic weather prediction*. Hydrology and Earth System Sciences, Vol. 9 (4), 365–380.
- Grayson, R. and Blöschl, G. (2000). *Spatial Patterns in Catchment Hydrology*. Cambridge University Press, 432 p., ISBN 0-521-63316-8.



- Guariso, G., Rinaldi, S. and Zielinski, P. (1984). *The value of information in reservoir management*. Applied Mathematics and Computation, Vol. 15, Issue 2, 165-184.
- Gupta, V. K., Waymire, E., and Wang, C. T. (1980). *A representation of an instantaneous unit hydrograph from geomorphology*. Water Resources Research, Vol. 16, No. 5, 855-862.
- Gurtz, J., Baltensweiler, A. and Lang, H. (1999). *Spatially distributed hydrotope-based modelling of evapotranspiration and runoff in mountainous basins*. Hydrological Processes, Vol. 13, 2751-2768.
- Habets, F., LeMaigne, P. and Noilhan, J. (2004). *On the utility of operational precipitation forecasts to served as input for streamflow forecasting*. Journal of Hydrology, Vol. 293, 270-288.
- Hadi, N. S. (2006). *Time Series Analysis for Hydrological Features: Applications of Box-Jenkins Models to Euphrates River*. Journal of Applied Sciences, Vol. 6 (9), 1929-1934.
- Haimes, Y. Y. (1984). *Integrated risk and uncertainty assessment in water resources within a multiobjective framework*. Journal of Hydrology, Vol. 68, 405-417.
- Haimes, Y. Y. and Li, D. (1991). *A Hierarchical-multiobjective Framework for Risk Management*. Automatica, Vol. 27, No. 3, 579-584.
- Hall, J. and Solomatine, D. (2008). *A framework for uncertainty analysis in flood risk management decisions*. Intl. J. River Basin Management, Vol. 6, 85-98.
- Hamdi, Y., Hingray, B. and Musy, A. (2003). *Projet MINERVE, rapport intermédiaire N°1 volet B : Modélisation hydrologique*. Technical report, EPFL. Unpublished report.
- Hamdi, Y., Hingray, B. and Musy, A. (2005a). *Projet MINERVE, rapport intermédiaire N°3 volet B : Modélisation hydrologique*. Technical report, EPFL. Unpublished report.
- Hamdi, Y., Hingray, B. and Musy, A. (2005b). *Un modèle de prévision hydro-météorologique pour les crues du Rhône supérieur en Suisse*. Wasser Energie Luft, Vol. 11-12, 325-332.
- Hansson, S. O. (2007). *Social decisions about risk and risk-taking*. Social Choice and Welfare, Vol. 29, 649-663.
- Harmel, R. D. and Smith, P. K. (2007). *Consideration of measurement uncertainty in the evaluation of goodness-of-fit in hydrologic and water quality modeling*. Journal of Hydrology, Vol. 337, 326-336.
- Harvey, H., Peppé, R. and Hall, J. (2008). *Reframe: a software system supporting flood risk analysis*. Intl. J. River Basin Management, Vol. 6, 163-174.
- Haupt, L. M. (1908). *The waterways problem*. Journal of the Franklin Institute, Vol. 165, Issue 5, 325-344.
- Hayes, B. (2007). *Calculating the Weather. A review of The Emergence of Numerical Weather Prediction: Richardson's Dream, by Peter Lynch*. American Scientist, Vol. 95, No. 3, 271-273.
- He, Y., Wetterhall, F., Cloke, H. L., Pappenberger, F., Wilson, M., Freer, J. and McGregor, G. (2009). *Tracking the uncertainty in flood alerts driven by grand ensemble weather predictions*. Meteorological Applications, Vol. 16 (1), 91-101.

- Heller, P. (2007). *Méthodologie pour la conception et la gestion des aménagements hydrauliques à buts multiples par une analyse systémique*. Thesis Report N°3781, Ecole Polytechnique Fédérale de Lausanne; and Communication 30 du Laboratoire de Constructions Hydrauliques, Ed. A. Schleiss, EPFL, Lausanne.
- Heppner, C. S., Ran, Q., Vanderkwaak, J. E. and Loague, K. (2006). *Adding sediment transport to the integrated hydrology model (InHM): Development and testing*. *Advances in Water Resources*, Vol. 29 (6), 930-943.
- Herschy, R. W. (2002). *The world's maximum observed floods*. *Flow Measurement and Instrumentation*, Vol. 13, 231-235.
- Hess, J. (2010). *Optimisation de l'alerte et de la transmission de l'alarme OWARNA*. Rapport de suivi avec proposition au Conseil fédéral. Rapport interne à l'administration fédérale.
- Hewitson, B. and Crane, R. (1996). *Climate downscaling: techniques and application*. *Climate Research*, Vol. 7, 85-95.
- Higgins, R. W., Mo, K. C. and Schubert, S. D. (1996). *The moisture budget of the central United States in spring as evaluated from the NCEP/NCAR and NASA/DAO reanalyses*. *Monthly Weather Review*, Vol. 124, 93-963.
- Higgins, R. W., Kousky, V. E., Silva, V. B. S., Becker, E. and Xie, P. (2010). *Intercomparison of Daily Precipitation Statistics over the United States in Observations and in NCEP Reanalysis Products*. *Journal of Climate*, Vol. 23, Issue 17, 4637-4650.
- Hingray, B., Mezghani, A., Schaepli, B., Niggli, M., Faivre, G., Guex, F., Hamdi, Y. and Musy, A. (2006). *Estimation des débits de crue du Rhône à Porte du Scex et autres points amont caractéristiques*. Rapport final du projet CONSECRU 2. Laboratoire Hydrologie et Aménagements. EPFL, Lausanne, 83p. + 86p. Annexes.
- Hipel, K. W., McLeod, A. I. and Lennox, W. C. (1977). *Advances in Box-Jenkins Modeling, I. Model Construction*. *Water Resources Research*, Vol. 13, No. 3, 567-575.
- Holko, L. and Lepistö, A. (1997). *Modelling the hydrological behaviour of a mountain catchment using TOPMODEL*. *Journal of Hydrology*, Vol. 196, 361-377.
- Horton, P., Jaboyedoff, M., Metzger, R., Obled, C. and Marty, R. (2011). *Prévision des précipitations par adaptation statistique sur le bassin alpin du Rhône*. Proceedings of the 2ème Rencontre sur les Dangers Naturels, UNIL, Lausanne, 187-191.
- Hsu, K.-L., Gupta, H. V. and Sorooshian, S. (1995). *Artificial neural network modelling of the rainfall-runoff process*. *Water Resources Research*, Vol. 31, No. 10, 2517-2530.
- Hurwicz, L. (1951). *Optimality criteria for decision making under ignorance*. Cowles Commission Discussion Paper 370S, 16 p.
- Hutter, G. and Schanze, J. (2008). *Learning how to deal with uncertainty of flood risk in long-term planning*. *Intl. J. River Basin Management*, Vol. 6, 175-184.
- Hwang, C.L. and Yoon, K. (1981). *Multiple Attributes Decision Making Methods and Applications*. Springer, Berlin Heidelberg, 259 p., ISBN 0387105581.
- Ito, K., Xu, Z. X., Jinno, K., Kojiri, T. and Kawamura, A. (2001). *Decision Support System for surface water planning in river basins*. *Journal of Water Resources Planning and Management*, Vol. 127 (4), 272-276.

- Jadidi, O., Hong, T. S., Firouzi, F. Yusuff, R. M. and Zulkifli, N. (2008). *TOPSIS and fuzzy multi-objective model integration for supplier selection problem*. Journal of Achievements in Materials and Manufacturing Engineering, Vol. 31, No. 2, 762-769.
- Jal, N., Martin, O. and Perret, D. (2009). *Hydrometeorological forecasts... and afterwards?*. La Houille Blanche, No. 6, 76-78.
- Jamieson, D. G. and Fedra, K. (1996a). *The 'WaterWare' decision-support system for river-basin planning. 1. Conceptual design*. Journal of Hydrology, Vol. 177, 163-175.
- Jamieson, D. G. and Fedra, K. (1996b). *The 'WaterWare' decision-support system for river-basin planning. 3. Example Applications*. Journal of Hydrology, Vol. 177, 199-211.
- Janowiak, J. E. (1992). *Tropical rainfall: A comparison of satellite derived rainfall estimates with model precipitation forecasts, climatologies, and observations*. Monthly Weather Review, Vol. 120, 448-462.
- Jasper, K., Gurtz, J. and Lang, H. (2002). *Advanced flood forecasting in Alpine watersheds by coupling meteorological observations and forecasts with a distributed hydrological model*. Journal of Hydrology, Vol. 267, 40-52.
- Jaun, S., Ahrens, B., Walser, A., Ewen, T. and Schär, C. (2008). *A probabilistic view on the August 2005 floods in the upper Rhine catchment*. Hydrology and Earth System Sciences, Vol. 8, 281-291.
- Jeong, D.-I. and Kim, Y.-O. (2005). *Rainfall-runoff models using artificial neural networks for ensemble streamflow prediction*. Hydrological Processes, Vol. 19, 3819-3835.
- Jeong, J., Kannan, N., Arnold, J., Glick, R., Gosselink, L. and Srinivasan, R. (2010). *Development and Integration of Sub-hourly Rainfall-Runoff Modeling Capability Within a Watershed Model*. Water Resources Management, Vol. 24 (15), 4505-4527.
- Jonkman, S. N., van Gelder, P.H.A.J.M. and Vrijling, J. K. (2003). *An overview of quantitative risk measures for loss of life and economic damage*. Journal of Hazardous Materials, Vol. 99, 1-30.
- Jordan, F., Boillat, J.-L., Dubois, J. and Schleiss, A. J. (2005). *Real-time flood management by preventive operations on multiple alpine hydropower schemes*. Proceedings 31th IAHR Congress, Seoul, 3235-3245.
- Jordan, F., Boillat, J.-L., Dubois, J. and Schleiss, A. J. (2006). *Prévision et gestion des crues par opérations préventives sur les retenues alpines*. Proceedings XXIIe Congrès des Grands Barrages, CIGB/ICOLD, Barcelone, 497-510.
- Jordan, F. (2007). *Modèle de prévision et de gestion des crues - optimisation des opérations des aménagements hydroélectriques à accumulation pour la réduction des débits de crue*. Thesis Report N°3711, Ecole Polytechnique Fédérale de Lausanne ; and Communication 29 du Laboratoire de Constructions Hydrauliques, Ed. A. Schleiss, EPFL, Lausanne.
- Jordan, F., Boillat, J.-L., García Hernández, J., Dubois, J. and Schleiss, A. J. (2007a). *Real-time decision-making during floods: application to the Upper Rhone River in Switzerland*. Proceedings of the 32nd Congress of IAHR, Venezia, Special session 10.
- Jordan, F., Boillat, J.-L. and García Hernández, J. (2007b). *Influence des retenues hydroélectriques pour la protection contre les crues de la Sarine*. Journées de rencontre sur les dangers naturels, IGAR, Lausanne.

- Jordan, F., García Hernández, J., Dubois, J. and Boillat, J.-L. (2008). *MINERVE: Modélisation des intempéries de nature extrême du Rhône valaisan et de leurs effets*. Communication 38 du Laboratoire de Constructions Hydrauliques, Ed. A. Schleiss, EPFL, Lausanne, ISSN 1661-1179.
- Jordan, F., García Hernández, J. and Gal, A. (2009). *Operational performance of discharge prediction in alpine regions*. Annalen der Meteorologie 44, 30th International Conference on Alpine Meteorology, Rastatt, Germany, 156-157, ISSN 0072-4122, ISBN 978-3-88148-440-4.
- Jordan, F., Boillat, J.-L. and Schleiss, A. J. (2010). *Prévision et gestion des crues du Rhône supérieur par l'exploitation optimale des retenues alpines*. La Houille Blanche, No. 5, 91-102.
- Ju, Q., Yu, Z., Hao, Z., Ou, G., Zhao, J. and Liu, D. (2009). *Division-based rainfall-runoff simulations with BP neural networks and Xinanjiang model*. Neurocomputing, Vol. 72, 2873-2883.
- Judd, P. H. (2004). *More Lasting Than Brass: A Thread of Family from Revolutionary New York to Industrial Connecticut*. Northeastern University Press, p. 175.
- Kahraman, C. (2008). *Multi-Criteria Decision Making methods and Fuzzy Sets*. In: Kahraman, C. *Fuzzy Multi-Criteria Decision Making*. Springer Optimization and Its Applications, Vol. 16, 590 p. ISBN: 978-0-387-76812-0.
- Källén, E. (1996). *HIRLAM Documentation Manual, System 2.5, SHMI*. Available from SMHI, S-60176 Norrkiöping, Sweden.
- Kalnay, E., Kanamitsu, M., Kistler, R., Collins, W., Gandin, D. L., Iredell, M., Saha, S., White, G., Woollen, J., Zhu, Y., Leetmaa, A., Reynolds, R., Chelliah, M., Ebisuzaki, W., Higgins, W., Janowiak, J. Mo, K. C., Ropelewski, C., Wang, J., Jenne, R. and Joseph, D. (1996). *The NCEP/NCAR 40-Year Reanalysis project*. Bulletin of the American Meteorological Society, Vol. 77, 437-471.
- Kalnay, E. (2002). *Atmospheric Modeling, Data Assimilation, and Predictability*. Cambridge University Press, 364 p. ISBN 0-521-79629-6.
- Karaboga, D., Bagis, A. and Tefaruk, H. (2008). *Controlling spillway gates of dams by using fuzzy logic controller with optimum rule number*. Applied Soft Computing, Vol. 8, 232-238.
- Karamouz, M., Szidarovszky, F. and Zahraie, B. (2003). *Water Resources Systems Analysis*. Lewis Publishers / CRC Press, 608 p., ISBN-10: 1566706424.
- Karbowsky, A. (1991). *FC-ROS - Decision Support System for reservoir operators during flood*. Environmental Software, Vol. 6, No. 1, 11-15.
- Karbowsky, A., Malinowski, K. and Niewiadomska-Szynkiewicz, E. (2005). *A hybrid analytic/rule-based approach to reservoir system management during flood*. Decision Support Systems, Vol. 38, 599-610.
- Karlsson, M. and Yakowitz, S. (1987). *Rainfall-runoff forecasting, old and new*. Stochastic Hydrology and Hydraulics, Vol. 1, No. 4, 303-318.
- Kavetski, D., Kuczera, G. and Franks, S. W. (2006). *Calibration of conceptual hydrological models revisited: 1. Overcoming numerical artefacts*. Journal of Hydrology, Vol. 320, 173-186.



- Katz, R. W. and Murphy, A. H. (1997). *Economic Value of Weather and Climate Forecasts*. Cambridge University Press, 240 p., ISBN-10: 0521434203.
- Kent, F. R. (1932). *Senator James E. Watson: The Professional Public Servant*. The Atlantic Monthly, Vol 149, No. 2.
- Kim, S., Tachikawa, Y. and Takara, K. (2007). *Applying a Recursive Update Algorithm to a Distributed Hydrologic Model*. Journal of Hydrologic Engineering, Vol. 12, 336-344.
- Kim, Y.-O., Eum, H., Lee, E.-G. and Ko, I. H. (2007). *Optimization Operational Policies of a Korean Multireservoir System Using Sampling Stochastic Dynamic Programming with Ensemble Streamflow Prediction*. Journal of Water Resources Planning and Management Vol. 133, 4-14.
- Kirstetter, P.-E., Delrieu, G. and Andrieu, H. (2009). *Estimation quantitative des précipitations par radar météorologique: inférence de la structure verticale des pluies, modélisation des erreurs radar-pluviomètres*. La Houille Blanche, No. 6, 150-156.
- Klemes, V. (1983). *Conceptualization and scale in hydrology*. Journal of Hydrology, Vol. 65, 1-23.
- Klok, E. J., Jasper, K., Roelofsma, K. P., Badoux, A. and Gurtz, J. (2001). *Distributed hydrological modelling of a glaciated Alpine river basin*. Hydrological Sciences Journal, Vol. 46, No. 4, 553-570.
- Ko, S.-K., Fontane, D. G. and Margeta, J. (1994). *Multiple reservoir system operational planning using multi-criterion decision analysis*. Theory and Methodology, Vol. 76, 428-439.
- Kojima, T. and Takara, K. (2003). *A grid-cell based distributed flood runoff model and its performance*. Proceedings of Symposium. HS03, Weather Radar Information and Distributed Hydrological Modelling, IAHS Publ. No. 282, Sapporo, Japan, 234-240.
- Kort, I. A. T. and Booij, M. J. (2007). *Decision making under uncertainty in a decision support system for the Red River*. Environmental Modelling & Software, Vol. 22, 128-136.
- Krause, P., Boyle, D. P. and Bäse, F. (2005). *Comparison of different efficiency criteria for hydrological model assessment*. Advances in Geosciences, Vol. 5, 89-97.
- Kron, W. (2005). *Flood Risk = Hazard\*Values\*Vulnerability*. Water International, Vol. 30, No. 1, 58-68.
- Krzysztofowicz, R., Kelly, K.S. and Long, D. (1994). *Reliability of Flood Warning Systems*. Journal of Water Resources Planning and Management, Vol. 120 (6), 906-926.
- Krzysztofowicz, R. (2001). *The case for probabilistic forecasting in hydrology*. Journal of Hydrology, Vol. 249, 2-9.
- Kundzewicz Z. W. and Schellnhuber, H.-J. (2004) *Floods in the IPCC TAR perspective*. Natural Hazards, Vol. 31, 111-128.
- LCH (2005). *Modèle de prévision et de gestion de crues*. Rapport intermédiaire N°3, LCH-EPFL, Lausanne. Unpublished report.
- LCH (2006). *Gestion des crues de la Sarine par l'utilisation des retenues d'accumulation*. Final Report No. 24/2006. EPFL, Lausanne, 48 p. Unpublished report.

- LCH (2009). *VOLET 1 : Avancement du projet au Laboratoire de Constructions Hydrauliques, LCH-EPFL. Projet MINERVE. Rapport intermédiaire n°1. Période du 1 mars 2008 au 31 décembre 2008.* EPFL/UNIL, Lausanne, 5-43. Unpublished report.
- LCH (2010a). *VOLET 1 : Avancement du projet au Laboratoire de Constructions Hydrauliques, LCH-EPFL. Projet MINERVE. Rapport intermédiaire n°2. Période du 1 janvier 2009 au 31 décembre 2010.* EPFL/UNIL, Lausanne, 6-45. Unpublished report.
- LCH (2010b). *Modélisation du bassin versant de l'Eo pour la Confédération Hydrographique du Cantabrique (Espagne).* Final Report No. 30/2010. EPFL, Lausanne, 26 p. Unpublished report.
- LCH (2011). *VOLET 1 : Avancement du projet au Laboratoire de Constructions Hydrauliques, LCH-EPFL. Projet MINERVE. Rapport intermédiaire n°3. Période du 1 janvier 2010 au 31 mars 2011.* EPFL/UNIL, Lausanne. In Preparation. Unpublished report.
- Lee, J. and Bray, D. I. (1969). *The estimation of runoff from rainfall for new Brunswick watersheds.* Journal of Hydrology, Vol. 9, 427-437.
- Leedal, D., Neal, J., Beven, K., Young, P. and Bates, P. (2010). *Visualisation approaches for communicating real-time flood forecasting level and inundation information.* Journal of Flood Risk Management, Vol. 3, 140-150.
- Leith, C. E. (1974): *Theoretical skills of Monte Carlo forecasts.* Monthly Weather Review, Vol. 102, 409-418.
- Leutbecher, M. and Palmer, T. N. (2008). *Ensemble forecasting.* Journal of Computational Physics, Vol. 227, 3515-3539.
- Levin, O. (1969). *Optimal control of a storage reservoir during a flood season.* Automatica, Vol. 5, Issue 1, 27-34.
- Li, X.-Y., Chau, K. W. Cheng, C.-T. and Li, Y. S. (2006). *A Web-based flood forecasting system for Shuangpai region.* Advances in Engineering Software, Vol. 37, 146-158.
- Li, Z.-J. and Zhang, K. (2008). *Comparison of Three GIS-Based Hydrological Models.* Journal of Hydrologic Engineering, Vol. 13 (5), 364-370.
- Lin, J.-Y., Cheng, C.-T. and Lin, T. (2008). *A Pareto Strength SCE-UA Algorithm for Reservoir Optimization Operation.* Proceedings of the Fourth International Conference on Natural Computation, 406-412, ISBN: 978-0-7695-3304-9.
- Lindström, G., Johansson, B., Persson, M., Gardelin, M. and Bergström, S. (1997). *Development and test of the distributed HBV-96 model.* Journal of Hydrology, Vol. 201, 272-288.
- Llasat, M. C., Atencia, A., Garrote, L. and Mediero, L. (2009). *The hydrometeorological forecasting in Spain in the framework of the European Project Flash.* La Houille Blanche, No. 6, 66-71.
- Llasat, M. C., Llasat-Botiga, M., Prat, M. A., Porcú, F., Price, C., Mugnai, A., Lagouvardos, K., Kotroni, V., Katsanos, D., Michaelides, S., Yair, Y., Savvidou, K. and Nicolaidis, K. (2010). *High-impact floods and flash floods in Mediterranean countries: the FLASH preliminary database.* Advances in Geosciences, Vol. 23, 47-55.
- Loucks, D. P. (1995). *Developing and Implementing Decision Support Systems: A Critique and a Challenge.* Water Resources Bulletin, Vol. 31, No. 4, 571-582.

- Loucks, D. P. and Beek, E. V. (2005). *Water Resources Systems Planning and Management. An Introduction to Methods, Models and Applications*. UNESCO Publishing, ISBN 92-3-103998-9
- Lorenz, E. (1963). *Deterministic nonperiodic flow*. Journal of Atmospheric Sciences, Vol. 20, 130-141.
- Lorenz, E. (1965). *A study of the predictability of a 28-variable atmospheric model*. Tellus, Vol. 17, 321-333.
- Lorenz, A. C. (1986). *Analysis methods for numerical weather prediction*. Quarterly Journal of the Royal Meteorological Society, Vol. 112 (474), 1177-1194.
- Lynch, P. (2006). *The Emergence of Numerical Weather Prediction: Richardson's Dream*. Cambridge University Press, xii + 279 pp.
- Lund, J. R. and Guzman, J. (1999). *Derived Operating Rules for Reservoirs in Series or in Parallel*. Journal of Water Resources Planning and Management, Vol. 125, No. 3, 143-153.
- Ma, J. Fan, Z.-P. and Huang, L.-H. (1999). *A subjective and objective integrated approach to determine attribute weights*. European Journal of Operational Research, Vol. 112, 397-404.
- Maass, A., Hufschmidt, M. M., Dorfman, R., Thomas, H. A., Marglin, S. A. and Fair, G. M. (1962). *Design of Water Resources Systems*. Cambridge, Mass., Harvard University Press. Mass., U.S.A., 638 p. ISBN-10: 0674199502.
- MacCrimmon, K. R. (1968). *Decision-making among multiple-attribute alternatives: a survey and consolidated approach*. Rand Corp, Memorandum RM-4823-ARPA. 63 p.
- MacCrimmon, K.R. (1973). *An overview of multiple objective decision making*. In: Cochrane, J. L. and Zeleny, M. Editors. *Multiple criteria decision making*. University of South Carolina Press, Columbia, SC, 18-44.
- Makropoulos, C. K., Butler, D. and Maksimovic, C. (2003). *Fuzzy Logic Spatial Decision Support System for Urban Water Management*. Journal of Water Resources Planning and Management, Vol. 129 (1), 69-77.
- Malekmohammadi, B., Zahraie, B. and Kerachian, R. (2011). *Ranking solutions of multi-objective reservoir operation optimization models using multi-criteria decision analysis*. Expert Systems with Applications, Volume 38, Issue 6, 7851-7863.
- Manen, S. E. and Brinkhuis, M. (2005). *Quantitative flood risk assessment for Polders*. Reliability Engineering and System Safety, Vol. 90, 229, 237.
- Manos, B., Bournaris, T., Silleos, N., Antonopoulos, V. and Papathanasiou, J. (2004). *A decision support system approach for rivers monitoring and sustainable management*. Environmental Monitoring and Assessment, Vol. 96, 85-98.
- Mariani, V. C., Justi Luvizotto, L. G., Guerra, F. A. and Coelho, L. d. S. (2011). *A hybrid shuffled complex evolution approach based on differential evolution for unconstrained optimization*. Applied Mathematics and Computation, In Press, Corrected Proof, Available online 21 December 2010, ISSN 0096-3003, DOI: 10.1016/j.amc.2010.12.064.
- Markwart, A. H. (1927). *Power in California*. Journal of the Franklin Institute, Vol. 204, Issue 2, 145-192.

- Marsigli, C., Boccanera, F., Montani, A. and Paccagnella, T. (2005). *The COSMO-LEPS ensemble system: validation of the methodology and verification*. Nonlinear Processes in Geophysics, Vol. 12, 527-536.
- Marsigli, C., Montani, A. and Paccagnella, T. (2007). *Ensemble activities at ARPA-SIM: the COSMO-LEPS and COSMO-SREPS systems*. Proceedings, 29th International Conference on Alpine Meteorology, 4.-8. June 2007, Chambéry.
- Marsigli, C., Montani, A. and Paccagnella, T. (2008). *A spatial verification method applied to the evaluation of high-resolution ensemble forecasts*. Meteorological Applications, Vol. 15 (1), 125-143.
- Martinerie, R., Boillat, J.-L., García Hernández, J. and Jordan, F. (2009). *Numerical modelling of stormwater and wastewater conveyance system of Lausanne City (Switzerland)*. Proceedings of the 33rd Congress of IAHR Water engineering for a sustainable environment, Vancouver, Canada, 6978-6985, ISBN: 978-94-90365-01-1.
- Masmoudi, M. and Habaieb, H. (1993). *The performance of some real-time statistical flood forecasting models seen through multicriteria analysis*. Water Resources Management, Vol. 7 (1), 57-67.
- Mason, S.J. and Graham, N.E. (1999): *Conditional probabilities, relative operating characteristics, and relative operating levels*. Weather and Forecasting, Vol. 14 (5), 713-725.
- Mason, W.P. (1914). *Advantages and disadvantages of reservoir storage*. Journal of the Franklin Institute, Vol. 177, Issue 4, 369-384.
- Mathevet, T. (2005) *Which lumped rainfall-runoff models at the hourly time step? Empirical development and intercomparison of models on a large set of catchments*. PhD Thesis, ENGREF (Paris), Cemagref (Antony), France, 463 pp.
- Mays, L. W. (1996). *Water Resources Handbook*. McGraw-Hill, New York, 1568 p., ISBN-10: 0070411506.
- McDonald, A. (1994). *The HIRLAM two time level, three dimensional semi-Lagrangian, semi-implicit, limited area, grid point model of the primitive equations*. HIRLAM Technical Report No. 17, Available from SMHI, S-60176 Norrköping, Sweden.
- McElroy, S. (1862). *Papers in Hydraulic Engineering*. Journal of the Franklin Institute, Vol. 74, Issue 1, 13-19.
- McLeod, A. I., Hipel, K. W. and Lennox, W. C. (1977). *Advances in Box-Jenkins Modeling. 2. Applications*. Water Resources Research, Vol. 13, No. 3, 577-596.
- Mediero, L., Garrote, L. and Martin-Carrasco, F. (2007). *A probabilistic model to support reservoir operation decisions during flash floods*. Hydrological Sciences Journal, Vol. 52 (3), 523-537.
- Mein, R. and Larson, C. (1973). *Modeling infiltration during a steady rain*. Water Resources Research, Vol. 9 (2), 384-394.
- Metcalf and Eddy, Inc., University of Florida, and Water Resources Engineers, Inc., (1971), *Storm Water Management Model, Vol. I*. Final Report, 11024DOC07/71 (NTIS PB-203289), U.S. EPA, Washington, DC, 20460.
- Miao, J.-F., Chen, D., Wyser, K., Borne, K., Lindgren, J., Svensson, M. K., Thorsson, S., Achberger, C. and Almkvist, E. (2008). *Evaluation of MM5 mesoscale model at local scale*



- for air quality applications over the Swedish west coast: Influence of PBL and LSM parameterizations*. *Meteorology and Atmospheric Physics*, Vol. 99 (1-2), 77-103.
- Minns, A. W. and Hall, J. (1996). *Artificial neural networks as rainfall-runoff models*. *Hydrological Sciences*, Vol. 41, 399-417.
- Mirfenderesk, H. (2009). *Flood emergency management decision support system on the Gold Coast, Australia*. *The Australian Journal of Emergency Management*, Vol. 24 No. 2, 48-58.
- Mo, K. C., Wang, X. L., Kistler, R. Kanamitsu, M. and Kalnay, E. (1995). *Impact of Satellite Data on the CDAS-Reanalysis System*. *Monthly Weather Review*, Vol. 123, 124-139.
- Moeini, R. Afshar, A. and Afshar, M. H. (2011). *Fuzzy rule-based model for hydropower reservoirs operation*. *Electrical Power and Energy Systems*, Vol. 33, 171-178.
- Molteni, F. and Palmer, T.N. (1993). *Predictability and finite-time instability of the northern winter circulation*. *Quarterly Journal of the Royal Meteorological Society*, Vol. 119, 269-298.
- Molteni, F., Buizza, R., Palmer, T. N. and Petroliagis, T. (1996). *The ECMWF Ensemble Prediction System: methodology and validation*. *Quarterly Journal of the Royal Meteorological Society*, Vol. 122, 73-119.
- Montanari, A. and Brath, A. (2004). *A stochastic approach for assessing the uncertainty of rainfall-runoff simulations*. *Water Resources Research*, Vol. 40 (1), W01106.
- Moore, R. J., Bell, V. A. and Jones, D. A. (2005). *Forecasting for flood warning*. *C. R. Geoscience*, Vol. 337, 203-217.
- Morss, R. E., Wilhelmi, O. V. Downton, M. W. and Grunfest, E. (2005). *Flood risk, uncertainty, and scientific information for decision making: Lessons from an Interdisciplinary Project*. *Bulletin of the American Meteorological Society*, Vol. 86, No. 11, 1593-1601.
- Muttill, N. and Liong, S.-Y. (2004). *Superior exploration-exploitation balance in shuffled complex evolution*. *Journal of Hydraulic Engineering*, Vol. 130, No. 12, 1202-1205.
- Narapusetty, B. and Mölders, N. (2005). *Evaluation of snow depth and soil temperature predicted by the Hydro-Thermodynamic Soil Vegetation Scheme (HTSVS) coupled with the PennState/NCAR Mesoscale Meteorological Model (MM5)*. *Journal of Applied Meteorology*, Vol. 44, 1827-1843.
- Ndiritu, J. G. (2005). *Maximizing water supply system yield subject to multiple reliability constraints via simulation-optimisation*. *Water SA*, Vol. 31(4), 423-434, ISSN 0378-4738.
- Neelakantan, T. R. and Pundarikanthan, N. V. (1999). *Hedging Rule Optimisation for Water Supply Reservoirs System*. *Water Resources Management* Vol. 13, 409-426.
- Nelder, J. A. and Mead, R. (1965). *A Simplex Method for function minimization*. *Computer Journal*, Vol. 7, No. 4, 308-313.
- Newbold, S. C. (2005). *A combined hydrologic simulation and landscape design model to prioritize sites for wetlands restoration*. *Environmental Modeling and Assessment*, Vol. 10, 251-263.
- Niggli, M. and Musy, A. (2005). *A Bayesian combination method of flood models: Principles and application results*. *Agricultural Water Management*, Vol. 77, 110-127.

- Nobert, S., Demeritt, D., and Cloke, H. (2010). *Informing operational flood management with ensemble predictions: lessons from Sweden*. Journal of Flood Risk Management, Vol. 3-1, 72-79.
- Norbiato, D., Borga, M., Degli Esposti, S., Gaume, E. and Anquetin, S. (2008). *Flash flood warning based on rainfall thresholds and soil moisture conditions: An assessment for gauged and ungauged basins*. Journal of Hydrology, Vol. 362, 274-290.
- November, V., Penelas, M. and Viot, P. (2009). *When flood risk transforms a territory: the Lully effect*. Geography, Vol. 94, 189-197.
- Obled, C., Bontron, G. and Garçon, R. (2002). *Quantitative precipitation forecasts: a statistical adaptation of model outputs through an analogues sorting approach*. Atmospheric Research, Vol. 63 (3-4), 303-324.
- Office fédérale de l'économie hydraulique (1996). *Gesamtbeurteilung der Pumpspeicherung*. Studienbericht Nr. 6/1996. Confédération Suisse, Berne.
- Ogawara, M (1955). *Efficiency of a Stochastic Prediction*. Papers in Meteorology and Geophysics, Meteorological Research Institute, Tokyo, Vol. 5, Nos. 3-4, 203-211.
- Olsson, J. and Lindström, G. (2008). *Evaluation and calibration of operational hydrological ensemble forecasts in Sweden*. Journal of Hydrology Vol. 350, 14-24.
- Pappenberger, F., Cloke, H. L., Persson, A., and Demeritt, D. (2011). *HESS Opinions "On forecast (in)consistence in a hydro-meteorological chain: curse or blessing?"*. Hydrological Earth System Sciences Discussion, Vol. 8, 1225-1245.
- Paredes, J. and Lund, J. R. (2006). *Refill and Drawdown Rules for Parallel Reservoirs: Quantity and Quality*. Water Resources Management Vol. 20, 359-376.
- Paredes Arquiola J., Solera Solera A. and Andreu Álvarez J. (2008). *Reglas de operación para sistemas multiembalse combinando métodos heurísticos y redes de flujo*. Ingeniería Hidráulica de México. Vol: 23, 1-10, ISSN 0186-4076.
- Pellerin, G., Lefaivre, L., Houtekamer, P., and Girard, C. (2003). *Increasing the horizontal resolution of ensemble forecasts at CMC*. Nonlinear Processes in Geophysics, Vol. 10, 463-468.
- Perrine, F. (1906). *The Value and Design of Water Power Plants as Influenced by Load Factor*. Journal of the Franklin Institute, Vol. 162, Issue 4, 269-278.
- Peters, N. E. Freer, J. and Beven, K. (2003). *Modelling hydrologic responses in a small forested catchment (Panola Mountain, Georgia, USA): a comparison of the original and a new dynamic TOPMODEL*. Hydrological Processes, Vol. 17, 345-362.
- Philbrick, C. R. and Kitanidis, P. K. (1999). *Limitations of deterministic optimization applied to reservoir operations*. Journal of Water Resources Planning and Management, Vol. 125, 135-142.
- Piccardi, C. and Soncini-Sessa, R. (1989). *An interactive program to simulate the management of a multi-purpose water reservoir*. Environmental Software, Vol. 4, 142-149.
- Pistrika, A. and Tsakiris, G. (2007). *Flood Risk Assessment: A Methodology Framework*. Water Resources Management: New Approaches and Technologies, European Water Resources Association, Chania, Greece.

- Poh, K. L. (1998). *A knowledge-based guidance system for multi-attribute decision making*. Artificial intelligence in Engineering, Vol. 12, 315-326.
- Power, D. J. (2002). *Decision Support Systems: Concepts and Resources for Managers*. Quorum Books division Greenwood Publishing, 272 p., ISBN: 156720497X.
- Pujol Reig, L., Ortiz, E., Cifres, E. and García Bartual, R. (2007). *Real-time flow forecasting in the Parana River: a comparison between armax and ANN models*. Proceedings of the 32nd Congress of IAHR, Special session 10 (SS10-22).
- Radnoti, G., Ajjaji, R., Bubnova, R., Caian, M., Cordoneanu, E., Emde, K., Gril, J. D., Hoffman, J., Horanyi, A., Issara, S., Ivanovici, V., Janousek, M., Joly, A., Le Moigne, P. and Malardel, S. (1995). *The spectral limited area model ARPEGE/ALADIN*. PWPR Report Series n°7, WMO-TD n° 699, 111-117.
- Regulwar, D. G. and Kamodkar, R. U. (2010). *Derivation of Multipurpose Single Reservoir Release Policies with Fuzzy Constraints*. Journal of Water Resource and Protection, Vol. 2, No. 12, 1030-1041.
- Reis, L. F. R., Walters, G. A., Savic, D. and Chaudhry, F. H. (2005). *Multi-Reservoir Operation Planning Using Hybrid Genetic Algorithm and Linear Programming (GA-LP): An Alternative Stochastic Approach*. Water Resources Management, Vol. 19, 831-848.
- Renner, M. Werner, M.G.F. Rademacher, S. and Sprokkereef, E. (2009). *Verification of ensemble flow forecasts for the River Rhine*. Journal of Hydrology, Vol. 376, 463-475.
- Ribeiro, J., Lauzon, N., Rousselle, J., Trung, H. T. and Salas, J. D. (1998). *Comparaison de deux modèles pour la prévision journalière en temps réel des apports naturels*. Canadian Journal of Civil Engineering, Vol. 25, 291-304.
- Richard, E., Buzzi, A. and Zängl, G. (2007). *Quantitative precipitation forecasting in the Alps: The advances achieved by the Mesoscale Alpine Programme*. Quarterly Journal of the Royal Meteorological Society, Vol. 133, 831-846.
- Richardson, L. F. (1922). *Weather Prediction by Numerical Process*. Cambridge University Press, xii+236 pp.
- Rinaldo, A. and Rodriguez-Iturbe, I. (1996). *Geomorphological theory of the hydrological response*. Hydrological Processes, Vol. 10, 803-829.
- Rinaldo, A., Botter, G., Bertuzzo, E., Uccelli, A., Settin, T. and Marani, M. (2006). *Transport at basin scales: 1. Theoretical framework*. Hydrology and Earth System Sciences, Vol. 10, 19-29.
- Richardson, D. S. (2000). *Skill and relative economic value of the ECMWF ensemble prediction system*. Quarterly Journal of the Royal Meteorological Society, Vol. 126, 649-667.
- Ritchie, H. and Beaudoin, C. (1994). *Approximations and sensitivity experiments with a baroclinic semi-Lagrangian spectral model*. Monthly Weather Review, Vol. 122, 2391-2399.
- Rizzoli, A. E., Davis, J. R. and Abel, D. J. (1998). *Model and data integration and re-use in environmental decision support systems*. Advances in Engineering Software, Vol. 36, 729-739.
- Roberts, N. M. and Lean, H. W. (2008). *Scale-Selective Verification of Rainfall Accumulations from High-Resolution Forecasts of Convective Events*. Monthly Weather Review, Vol. 136 (1), 78-97.

- Rodríguez-Iturbe, I. and Valdés J. B. (1979). *The geomorphologic structure of hydrologic response*. Water Resources Research, Vol. 15, 1409-1420.
- Roulin, E. (2007). Skill and relative economic value of medium-range hydrological ensemble predictions. Hydrology and Earth System Sciences, Vol. 11, 725-737.
- Roy, B. (1968). *Classement et choix en présence de points de vue multiples (la méthode ELECTRE)*. Revue d'Informatique et de Recherche Opérationnelle (RIRO), No. 8, 57-75.
- Saaty, T.L. (1977). *A scaling method for priorities in hierarchical structures*. Journal of Mathematical Psychology, Vol. 15 (3), 234-281.
- Saaty, T.L. (1980). *The Analytic Hierarchy Process: Planning, Priority Setting, Resources Allocation*. McGraw-Hill, New York, 287 p. ISBN-10: 0070543712.
- Saha, S., Nadiga, S., Thiaw, C., Wang, J., Wang, W., Zhang, Q., Van den Dool, H. M., Pan, H.-L., Moorthi, S., Behringer, D., Stokes, D., Peña, M., Lord, S., White, G., Ebisuzaki, W., Peng, P. and Xie, P. (2006). *The NCEP Climate Forecast System*. Journal of Climate, Vol. 19, Issue 15, 3483-3517
- Sahoo, G. B., Ray, C. and De Carlo, E. H. (2006). *Calibration and validation of a physically distributed hydrological model, MIKE SHE, to predict streamflow at high frequency in a flashy mountainous Hawaii stream*. Journal of Hydrology, Vol. 327, 94-109.
- Salas, J. D., Delleur, J. W., Yevjevich, V. and Lane, W. L., (1980). *Applied Modeling of Hydrologic Time Series*. Water Resources Publications, Littleton, Colorado, 484 p. (4rd Printing, 1988, ISBN-13: 978-0918334374).
- Santhi, C., Srinivasan, R., Arnold, J.G. and Williams, J.R. (2006). *A modeling approach to evaluate the impacts of water quality management plans implemented in a watershed in Texas*. Environmental Modelling & Software, Vol. 21, 1141-1157.
- Savage, L. J. (1951). *The theory of statistical decision*. Journal of the American Statistical Association Vol. 46, 55-67.
- Schaefli, B., Hingray, B., Niggli, M. and Musy, A. (2005). *A conceptual glacio-hydrological model for high mountainous catchments*. Hydrology and Earth System Sciences Discussions, Vol. 2, 73-117.
- Schuol, J., Abbaspour, K. C., Yang, H., Srinivasan, R. and Zehnder, A. J. B. (2008). *Modeling blue and green water availability in Africa*. Water Resources Research, Vol. 44, W07406, doi:10.1029/2007WR006609.
- SCS (1972). National engineering handbook, section 4, hydrology. US Department of Agriculture, SCS, Washington, DC.
- Service de la sécurité civil et militaire (2009). *Procédure lors de crues du Rhône pour les cantons du Valais et de Vaud*. Rapport final accepté, Section organisation, planification et prévention en cas de catastrophes, Département des finances, des institutions et de la sécurité, Grône, Canton du Valais.
- Shamseldin, A. (1997). *Application of a neural network technique to rainfall-runoff modelling*. Journal of Hydrology, Vol. 199, 272-294.
- Sharma, V., Jha, R. and Naresh, R. (2004). *Optimal multi-reservoir network control by two-phase neural network*. Electric Power Systems Research, Vol. 68, 221-228.



- Sherman, L. K. (1932). *Streamflow from rainfall by the unit hydrograph method*. Engineering News Record, Vol. 108, 501-505.
- Shih, H.-S., Shyur, H.-J. and Lee, E. S. (2007). *An extension of TOPSIS for group decision making*. Mathematical and Computer Modelling, Vol. 45, 801-813.
- Simonovic, S. P. and Bender, M. J. (1996). *Collaborative planning-support system: an approach for determining evaluation criteria*. Journal of Hydrology, Vol. 177, 237-251.
- Skalin, R. and Bjorge, D. (1997). *Implementation and performance of a parallel version of the HIRLAM limited area atmospheric model*. Parallel Computing, Vol. 23, 2161-2172.
- Smith, J. and Eli, R. N. (1995). *Neural-Network Models of Rainfall-Runoff Process*. Journal of Water Resources Planning and Management. Vol. 121, 499-508.
- Smith, M B. (2004). *The distributed model intercomparison project (DMIP)*. Journal of Hydrology, Vol. 298, 1-3.
- Stefanova, L. and Krishnamurti, T. N. (2002). *Interpretation of Seasonal Climate Forecast Using Brier Skill Score, The Florida State University Superensemble, and the AMIP-I Dataset*. Journal of Climate, Vol. 15, 537-544.
- Stewart, T. J. (1992). *A critical Survey on the Status of Multiple Criteria Decisin Making Theory and Practice*. OMEGA, Vol. 20, 569-586.
- Srdjevic, B., Medeiros, Y. D. P. and Faria, A. S. (2004). *An Objective Multi-Criteria Evaluation of Water Management Scenarios*. Water Resources Management, Vol. 18, 35-54.
- Sun, X., Mein, R.G., Keenan, T.D. and Elliott, J.F. (2000). *Flood estimation using radar and raingauge data*. Journal of Hydrology Vol. 239, 4-18.
- Tamea, S., Laio, F. and Ridolfi, L. (2005). *Probabilistic nonlinear prediction of river flows*. Water Resources Research, Vol. 41 (9), W09421, ISSN: 0043-1397.
- Taylor, E. R. (1908). *Natural and artificial conservation of water power for electrical purposes*. Journal of the Franklin Institute, Vol. 166, Issue 6, 409-432.
- The European Parliament and the Council of the European Union (2007). *DIRECTIVE 2007/60/EC of the European Parliament and the Council of the European Union of 23 October 2007 on the assessment and management of flood risks*. Official Journal of the European Union, L 288, 27-34.
- Theis, S. E., Hense, A. and Damrath, U. (2005). *Probabilistic precipitation forecasts from a deterministic model: a pragmatic approach*. Meteorological Applications, Vol. 12 (3), 257-268.
- Theophrastus (around 300 B. C. E.). *On Weather Signs*. Brill, published in 2007, 270 p., ISBN-10: 9004155937.
- Thielen, J., Bartholmes J., Ramos. M.-H. and de Roo, A. (2009a). *The European Flood Alert System-Part I: Concept and development*. Hydrology and Earth System Sciences, Vol. 13, 125-140.
- Thielen, J., Bogner, K., Pappenberger, F., Kalas, M, del Medico, M. and de Roo, A. (2009b). *Monthly-, medium-, and short-range flood warning: testing the limits of predictability*. Meteorological Applications, Vol. 16, 77-90.

- Third Rhone Correction (2008). *5.4 Dégâts potentiels après mesures pour les différentes variants*. Elaboration du Plan d'Aménagement Rhône. Rapport. Groupement Rhône 3.
- Thompson, J. C. and Brier, G. W. (1955). *The Economic Utility of Weather Forecasts*. Monthly Weather Review, Vol. 83, No. 11, 249-254.
- Tilmant, A., Faouzi, E. H. and Vanclooster, M. (2002). *Optimal operation of multipurpose reservoirs using flexible stochastic dynamic programming*. Applied Soft Computing, Vol. 2, 61-74.
- Tingsanchali, T. and Boonyasirikul, T. (2006). *Stochastic Dynamic Programming with Risk Consideration for Transbasin Diversion System*. Journal of Water Resources Planning and Management, Vol. 132, No. 2, 111-121.
- Tobin, C., Schaepli, B. and Rinaldo, A. (2011a). *MINERVE and the application of Generalized Likelihood Uncertainty Estimation*. Proceedings of the 2ème Rencontre sur les Dangers Naturels, UNIL, Lausanne, 237-238.
- Tobin, C., Nicotina, L., Parlange, M. B., Berne, A. and Rinaldo, A. (2011b). *Improved Interpolation of Meteorological Forcings for Hydrologic Applications in a Swiss Alpine Region*. Journal of Hydrology, doi: 10.1016/j.jhydrol.2011.02.010.
- Todini, E. (2007). *Hydrological catchment modelling: past, present and future*. Hydrology and Earth System Sciences, Vol. 11, 468-482.
- Toll, D. G. and Barr, R. J. (2001). *A decision support system for geotechnical applications*. Computers and Geotechnics, Vol. 28, 575-590.
- Toth, Z., and Kalnay, E. (1993). *Ensemble forecasting at NMC: The generation of perturbations*. Bulletin of the American Meteorological Society, Vol. 74, 2317-2330.
- Tracton, M. S. and E. Kalnay, (1993). *Ensemble forecasting at NMC: Operational implementation*. Weather and Forecasting, Vol. 8, 379-398.
- United Nations (2004). *Guidelines for Reducing Flood Losses*. Geneva: International Strategy for Disaster Reduction. United Nations, 87 p.
- United States Congress (1928). *An Act to provide for the construction of works for the protection and development of the Colorado River Basin, for the approval of the Colorado River compact, and for other purposes*. December 21; Enrolled Acts and Resolutions of Congress, 1789-1996; General Records of the United States Government; Record Group 11, National Archives.
- Unver, O. I. and Mays, L. W. (1990). *Model for real-time optimal flood control operation of a reservoir system*. Water Resources Management, Vol. 4, 21-46.
- Valadares Tavares, L. (1984). *Theoretical properties of the optimal release for a multi-purpose reservoir with correlated inflows*. Journal of Hydrology, Vol. 58, 237-250.
- Vedula, S. and Mohan, S. (1990). *Real-time multipurpose reservoir operation: a case study*. Hydrological Sciences Journal, Vol. 35, 447-462.
- Verbunt, M., Zappa, M., Gurtz, J. and Kaufmann, P. (2006). *Verification of a coupled hydrometeorological modelling approach for alpine tributaries in the Rhine basin*. Journal of Hydrology, Vol. 324, 224-238.

- Verbunt, M., Walser, A., Gurtz, J., Montani, A. and Schär, C. (2007). *Probabilistic Flood Forecasting with a Limited-Area Ensemble Prediction System: Selected Case Studies*. Journal of Hydrometeorology. Vol. 8, 897-909.
- Vince, A. (2002). *A framework for the greedy algorithm*. Discrete Applied Mathematics, Vol. 121, 247-260.
- Vitvar, T., Gurtz, J. and Lang, H. (1999). *Application of GIS-based distributed hydrological modelling for estimation of water residence times in the small Swiss pre-alpine catchment Rietholzbach*. Integrated methods in catchment hydrology. Proceedings of the International symposium IUGG, Birmingham, HS4, No. 258, 241-248, ISBN 1-901502-01-5.
- Vivoni, E. R., Entekhabi, D., Bras, R. L., Ivanov, V. Y. and van Horne, M. P. (2006). *Extending the Predictability of Hydrometeorological Flood Events Using Radar Rainfall Nowcasting*. Journal of Hydrometeorology, Vol. 7, 660-677.
- Wang, J. (2007). *Development of a Decision Support System for Flood Forecasting and Warning - A case study on The Maribyrnong River*. PhD Thesis, School of Architectural, Civil and Mechanical Engineering, Faculty of Health, Engineering and Science, Victoria University, Melbourne, Australia.
- Wang, L., Nyunt, C. T., Koike, T., Saavedra, O., Nguyen, L. C. and Sap, T. V. (2010). *Development of an integrated modeling system for improved multi-objective reservoir operation*. Frontiers of Architecture and Civil Engineering in China, Vol. 4, No. 1, 47-55.
- Wei, C.-C. and Hsu, N.-S., (2008). *Multireservoir real-time operations for flood control using balanced water level index method*. Journal of Environmental Management, Vol. 88, 1624-1639.
- Wei, C.-C. and Hsu, N.-S. (2009). *Optimal tree-based release rules for real-time flood control operations on a multipurpose multireservoir system*. Journal of Hydrology, Vol. 365, 213-224.
- Werner, M. G. F., Schellekens, J. and Kwadijk, J. C. J. (2006). *Flood early warning systems for hydrological (sub) catchments*. Encyclopedia of Hydrological Sciences, John Wiley & Sons Ltd., UK, DOI: 10.1002/0470848944.hsa022.
- Wernli, H. and Paulat, M. (2008). *SAL - A novel quality measure for the verification of quantitative precipitation forecasts*. Monthly Weather Review, Vol. 136, 4470-4487.
- Wetterhall, F. (2005). *Statistical Downscaling of Precipitation from Large-scale Atmospheric Circulation: Comparison of Methods and Climate Regions*. PhD thesis, Uppsala University.
- Whitaker, J. S., Hamill, T. M., Wei, X., Song, Y. and Toth, Z. (2008). *Ensemble Data Assimilation with the NCEP Global Forecast System*. Monthly Weather Review. Volume 136, Issue 2, 463-482.
- White, G. F. (1942). *Human Adjustment to Floods*. Chicago: University of Chicago Department of Geography, Research Paper No. 29, 1942, published 1945.
- Wilks, D. S. (1995). *Statistical Methods in the Atmospheric Sciences*. International Geophysics Series 59, Academic Press, 464 p.
- Wilks, D. S. (2001). *A skill score based on economic value for probability forecasts*. Meteorological Applications, Vol. 8 (2), 209-219.
- Willmott, C. J. (1981). *On the validation of models*. Physical Geography, Vol. 2, 168-194.

- Windsor, J. S. (1973). *Optimization Model for the Operation of Flood Control Systems*. Water Resources Research, Vol. 9 (5), 1219-1226.
- Wu, C. L., Chau, K. W. and Fan, C. (2010). *Prediction of rainfall time series using modular artificial neural networks coupled with data-preprocessing techniques*. Journal of Hydrology, Vol. 389, 146-167.
- Xu, C.-Y. (1999). *From GCMs to river flow: a review of downscaling methods and hydrologic modelling approaches*. Progress in Physical Geography, Vol. 23(2), 229-249.
- Yang, I-T. (2008). *Utility-based decision support system for schedule optimisation*. Decision Support Systems, Vol. 44, 595-605.
- Yang, T. and Hung, C.-C. (2007). Multiple-attribute decision making methods for plant layout design problem. Robotics and Computer-Integrated Manufacturing, Vol. 23, 126-137.
- Yehia, S., Abudayyeh, O. Fazal, I. and Randolph, D. (2008). *A decision support system for concrete bridge deck maintenance*. Advances in Engineering Software, Vol. 39, 202-210.
- Yu, Y.-B., Wang, B.-D. Wang, G.-L. and Li, W. (2004). *Multi-Person Multiobjective Fuzzy Decision-Making Model for Reservoir Flood Control Operation*. Water Resources Management, Vol. 18, 111-124.
- Zadeh, L A. (1965). *Fuzzy Sets*. Information and Control, Vol. 8, 338-353.
- Zanakis, S. H., Solomon, A. Wishart, N., and Dubliss, S. (1998). *Multi-attribute decision making: a simulation comparison of methods*. European Journal of Operational Research, Vol. 107, 507-529.
- Zappa, M. Pos, F., Strasser, U., Warmerdam, P. and Gurtz, J. (2003). *Seasonal Water Balance of an Alpine Catchment as Evaluated by Different Methods for spatially Distributed. Snowmelt Modelling*. Nordic Hydrology, Vol. 34 (3), 179-202.
- Zealand, C. M., Burn, D. H. and Simonovic, S. P. (1999). *Short term streamflow forecasting using artificial neural networks*. Journal of hydrology, Vol. 214, 32-48.
- Zhang, Z., Wang, S., Sun, G., McNulty, S. G., Zhang, H., Li, J., Zhang, M., Klaghofer, E. and Strauss, P. (2008). *Evaluation of the MIKE SHE model for application in the Loess Plateau, China*. Journal of American Water Resources Association, Vol. 44, No. 5, 1108-1120.
- Zhu, Y., Toth, Z., Wobus, R., Richardson, D. and Mylne, K. (2002). *The economic value of ensemble-based weather forecasts*. Bulletin of the American Meteorological Society, Vol. 83 (1), 73-83.
- Zhu, X., Wu, J. and Wu, J. (2006). *Application of SCE-UA to Optimize the Management Model of Groundwater Resources in Deep Aquifers of the Yangtze Delta*. Proceedings of the First International Multi-Symposiums on Computer and Computational Sciences, Hangzhou, Zhejiang, China, 303-308, ISBN: 0-7695-2581-4.
- Zurada, J. M. (1992). *Introduction to artificial neural systems*. PWS Publishing Company, 785 p., ISBN 0-534-95460-X.



## Acknowledgements

The MINERVE project is developed in partnership by the Swiss Federal Office for Environment (FOEV), Roads and Water courses Service, Energy and Water Power Service of the Valais Canton and Water, land and Sanitation Service of the Vaud Canton. The Swiss Weather Services (MeteoSwiss) provides the weather forecasts and hydroelectric companies communicate information regarding their hydropower plants. Scientific developments are entrusted to two entities of the Ecole Polytechnique Fédérale Lausanne (EPFL), the Hydraulic Constructions Laboratory (LCH) and the Ecohydrology Laboratory (ECHO), as well as to the Institute of Geomatics and Analysis of Risk (IGAR) of the University of Lausanne (UNIL). I would like to thank all of them for the deep collaboration during last years.

My first gratitude goes to my thesis director, Prof. Anton Schleiss, who offered me the opportunity of starting my thesis at the Laboratory of Hydraulic Constructions and who let me all the independence necessary for including new lines and approaches to the project. My thanks also go to Jean-Louis Boillat, my thesis co-director, responsible for the MINERVE project, and who helped me with his support and creative comments, being constant source of inspiration.

This research project would not have been possible without the collaboration of Frédéric Jordan, who helped me developing the multi-simulation tool module for probabilistic forecasts; Jerome Dubois, who proposed me the first example of a tool with an oriented-object approach, from which MINDS grows; Xavier Penya for helping me to improve the interface of the MINDS system; and Javier Paredes, invaluable support for discussion about multi-criteria decision-making methods and optimisation algorithms.

Pascal Horton and Cara Tobin, PhD students taking part in the other research projects gave me the opportunity of discussing methods, results and conclusions along the whole project. Thanks for sharing this project with me. My thanks grows to each one of their laboratories, their directors (Prof. Michel Jaboedoff and Prof. Andrea Rinaldo, respectively), and all the people collaborating on the project, such as Richarg Metzger, Charles Obled and Bettina Schafli.

I cannot forget all the master projects, stages and semester projects carried out within the framework of my research project. Renaud Champredonde and Joan Deval collaborated in the

improvement of this hydrological concept, especially in the glacier part, studying a new balance model for studying the glacier evolution based on climate changes. Jordi Ayats helped with the development of a meteorological analysis tool. Paul Sirvent considerably joins forces with me during his master project for improving the warning report tool as well as for studying the performance of hydro-meteorological forecasts. Tristan Brauchli also collaborated assessing the damages costs in the Alpine Rhone due to flood inundations. Carlos Mas studied the dynamic algorithms for reservoir management. Big thanks to all of them. In addition, a long number of semester projects with a direct relation with this research project were also accomplished by: Matthias, Jonhatan, Claudia, Nicolas, Stéphane, Katrina, Ricardo, Dimitri, Etienne, Sylvain,...

I cannot forget all people who participated to the MINERVE project as a partners or collaborators, such as Dominique Bérod, Jean-Pierre Jordan, Therese Bürgi, Eric Vez, Tomas Schneider, Cédric Roy, Pascal Ornstein, Jean-Yves Deleze, Ion Iorgulescu, Louis Bourguinet, Toni Arborino, Stéphanie André, Didier Ulrich, Constance Jaillet,...

My gratitude also goes to all people who spent these years at the LCH, old generation (Marcelo Leite, Frédéric Jordan, Philippe Heller, Pedro Manso, Martine Tiercy, Caroline Etter, Azin Amini, Tobias Meile, Giovanni De Cesare, Jolanda Jenzer, Burkhardt Rosier, Rafael Duarte, Sameh Kantoush, Selim Sayah, Michel Teuscher, Louis Schneiter and especially Rémi Martinerie and Alexandre Duarte) and new generation (Martin Bieri, Théodora Cohen, Violaine Dugué, Sonia Collaud, Michael Muller, José Pedro Matos, Fadi Hachem, Matteo Federspiel, Tamara Ghilardi, Scarlett Monnin, Milad Daneshvari, Michael Pfister, Ana Margarida, Cédric Bron, Marc-Eric Pantillon, Mike Jaton,...).

All my friends, from Spain and from Switzerland. It would have been impossible to achieve the final without you. Thanks. Really thanks to all of you.

To my parents, who encouraged me to realize the PhD and who had confidence on me during all the studies, especially when studying Civil Engineering at UPV in Valence. It is not possible to thank them as much as they deserve.

My last thanks go to my wife, Angela, who gave me the happiness as well as the strength to work as hard as possible to finish my PhD.

# List of Figures

<i>Figure 1.1 Scheme of the first stage of the project – MINERVE 2007</i>	7
<i>Figure 1.2 Scheme of the current stage of the project MINERVE 2011</i>	9
<i>Figure 1.3 Scheme of the research project with the main objectives developed</i>	11
<i>Figure 2.1 Schematic diagram of the relationship between model complexity, data availability and predictive performance (from Grayson and Blösch, 2000, p. 73).</i>	38
<i>Figure 2.2 The Rhone River basin in Switzerland upstream from the Lake of Geneva</i>	42
<i>Figure 4.1 Inverse air masses trajectories at 500 hPa, corresponding to rain days with more than 100 mm at Binn station (from García Hernández et al., 2009e)</i>	77
<i>Figure 4.2 Illustration of successive stages of the analogue technique (from García Hernández et al., 2009e)</i>	77
<i>Figure 4.3 Model of non glacier altitude band</i>	80
<i>Figure 4.4 Model of glacier altitude band</i>	85
<i>Figure 4.5 Routing System MINERVE main window</i>	87
<i>Figure 4.6 Hydrographs obtained by deterministic and probabilistic hydrographs. C-7 represents COSMO-7 and C-L COSMO-LEPS represented by the median <math>q_m</math>, the upper <math>q_u</math> and lower quartile <math>q_l</math> as well as by the minimum <math>q_{min}</math> and maximum discharge <math>q_{max}</math>. Update symbolises the simulations with meteorological observations and the update of the initial conditions of the hydrological model.</i>	88
<i>Figure 4.7 Operational scheme of flood management in the Upper Rhone valley.</i>	90
<i>Figure 4.8 Operational scheme of the procedure in case of flood in the Vaud and Valais Cantons (from Service de la Sécurité Civil et Militaire, 2009)</i>	92
<i>Figure 4.9 Example of a warning report</i>	96
<i>Figure 5.1 Example of a ROC curve showing the performance of a perfect forecast (solid black line), a forecast with skills (solid grey line with markers), and a forecast with no skills (dotted line).</i>	103

- Figure 5.2 Relative volume bias ( $R_{bVol}$ ) depending on the day for COSMO-7 and for the representative hyetographs of COSMO-LEPS: the median  $i_m$ , the upper  $i_u$  and lower quartile  $i_l$  as well as by the minimum  $i_{min}$  and maximum precipitation  $i_{max}$ . 105
- Figure 5.3 Cumulated volume ratio depending on the day as well as in average for COSMO-7 (diamond point) and for the representative hyetographs of COSMO-LEPS.  $M$  represents the average of the results. 106
- Figure 5.4 Brier Score performance depending on the day for COSMO-7 (C-7) and COSMO-LEPS (C-L). Left: 30 mm/day threshold (C-L 30 and C-7 30). Right: 50 mm/day threshold (C-L 50 and C-7 50). 107
- Figure 5.5 ROC curves for different days of COSMO-7 (C-7) and COSMO-LEPS (C-L). Left: 30 mm/day threshold. Right: 50 mm/day threshold 107
- Figure 5.6 Hydrological forecasts starting the 22.09.1993 12h00 C-7 represents the simulation with COSMO-7 forecast and C-L the simulation with COSMO-LEPS, represented by the median  $q_m$ , the upper  $q_u$  and lower quartile  $q_l$  as well as by the minimum  $q_{min}$  and maximum discharge  $q_{max}$ . Update symbolises the simulations with meteorological observations and the update of the initial conditions of the hydrological model. 115
- Figure 5.7 Hydrological forecasts starting the 23.09.1993 12h00. 115
- Figure 5.8 Hydrological forecasts starting the 13.10.2000 12h00. C-7 represents the simulation with COSMO-7 forecast and C-L the simulation with COSMO-LEPS, represented by the median  $q_m$ , the upper  $q_u$  and lower quartile  $q_l$  as well as by the minimum  $q_{min}$  and maximum discharge  $q_{max}$ . Update symbolises the simulations with meteorological observations and the update of the initial conditions of the hydrological model. 116
- Figure 5.9 Hydrological forecasts starting the 14.10.2000 12h00. 116
- Figure 5.10 Hydrological forecasts starting the 27.05.2008 12h00. C-7 represents the simulation with COSMO-7 forecast and C-L the simulation with COSMO-LEPS, represented by the median  $q_m$ , the upper  $q_u$  and lower quartile  $q_l$  as well as by the minimum  $q_{min}$  and maximum discharge  $q_{max}$ . Update symbolises the simulations with meteorological observations and the update of the initial conditions of the hydrological model. 117
- Figure 5.11 Hydrological forecasts starting the 28.05.2008 12h00. 117
- Figure 5.12 Results at Porte-du-Scex for the studied events depending on the day for Relative volume bias ( $R_{bVol}$ ) for COSMO-7 (C-7) and for the ensemble

- forecasts COSMO-LEPS which is represented by the median  $q_m$ , the upper  $q_u$  and lower quartile  $q_l$  as well as by the minimum  $q_{min}$  and maximum volume  $q_{max}$ . RS represents the results of the simulation with a perfect forecast (meteorological observations) 118
- Figure 5.13 Results at Porte-du-Scex for the studied events depending on the day for Root Mean Square Error (RMSE) for COSMO-7 (C-7) and for the ensemble forecasts COSMO-LEPS which is represented by the median  $q_m$ , the upper  $q_u$  and lower quartile  $q_l$  as well as by the minimum  $q_{min}$  and maximum volume  $q_{max}$ . RS represents the results of the simulation with a perfect forecast (meteorological observations). 119
- Figure 5.14 Cumulated volume ratio ( $r_{CVol}$ ) for COSMO-7 ( $q_{C-7}$ ) and COSMO-LEPS depending on different days or thresholds and in average ( $\bar{a}$ ), Porte-du-Scex. COSMO-LEPS is represented by the weighted value  $q_w$ , the median  $q_m$ , the upper  $q_u$  and lower quartile  $q_l$  as well as by the minimum  $q_{min}$  and maximum volume  $q_{max}$ .  $q_{RS}$  represents the results of the simulation with a perfect forecast (meteorological observations). 119
- Figure 5.15 Results at Porte-du-Scex for the studied events for the Index of agreement (IA) for COSMO-7 (C-7) and for COSMO-LEPS which is represented by the median  $q_m$ , the upper  $q_u$  and lower quartile  $q_l$  as well as by the minimum  $q_{min}$  and maximum volume  $q_{max}$ . RS represents the results of the simulation with a perfect forecast (meteorological observations). 121
- Figure 5.16 Results at Porte du Scex for the studied events for the Index of resemblance (IR) for COSMO-7 (C-7) and for COSMO-LEPS which is represented by the median  $q_m$ , the upper  $q_u$  and lower quartile  $q_l$  as well as by the minimum  $q_{min}$  and maximum volume  $q_{max}$ . RS represents the results of the simulation with a perfect forecast (meteorological observations). 121
- Figure 5.17 Normalized Peak Error as a function of Peak Time Error for all the forecasts 122
- Figure 5.18 Results for the threshold  $Q=700 \text{ m}^3/\text{s}$  in Porte du Scex for COSMO-LEPS (C-L), COSMO-7 (C-L) and for the simulation with perfect forecasts (RS). Left: Brier Score (BS). Right : Brier Skill Score (BSS). 124
- Figure 5.19 Relative Operating Characteristic curves results for COSMO-LEPS (C-L) and COSMO-7 (C-7). 125

<i>Figure 5.20 Relative Economic Value (REV) results for COSMO-7 (C-7) and for COSMO-LEPS which is represented by the median <math>q_m</math>, the upper <math>q_u</math> and lower quartile <math>q_l</math> as well as by the minimum <math>q_{min}</math> and maximum discharge <math>q_{max}</math>.</i>	125
<i>Figure 5.21 Forecasts performance and CAR (Correct Alarm Ratio) and MR (Miss Ratio) indexes</i>	127
<i>Figure 5.22 Warning report Porte-du-Scex on October 13, 2000 at 00h</i>	129
<i>Figure 5.23 Warning report at Porte-du-Scex on October 13, 2000 at 12h</i>	129
<i>Figure 5.24 Warning report at Porte-du-Scex on October 14, 2000 at 00h</i>	130
<i>Figure 5.25 Warning report at Porte-du-Scex on October 14, 2000 at 12h</i>	130
<i>Figure 5.26 Warning report at Porte-du-Scex on October 15, 2000 at 00h</i>	131
<i>Figure 5.27 Warning report at Porte-du-Scex on October 15, 2000 at 12h</i>	131
<i>Figure 6.1 Functionality scheme of the complex hydraulic model with: inflows (ovals); reservoirs, RES (triangles); bottom outlets and spillways (square dotted lines); hydropower plants, HPP (round doted lines); main river network (solid lines); groups, GR (shading zones); and check points, CP (big circles). More details are shown in Appendix 2.</i>	138
<i>Figure 6.2 Potential costs due to the case 1 of preventive operations (BasU for Business as Usual operations and PrevOp for preventive operations).</i>	147
<i>Figure 6.3 Potential costs in case 2 of preventive operations (BasU for Business as Usual operations and PrevOp for preventive operations).</i>	148
<i>Figure 6.4 Potential costs because the case 3 of preventive operations (BasU for Business as Usual operations and PrevOp for preventive operations).</i>	149
<i>Figure 6.5 Example of a deterministic optimisation with references (Ref) values.</i>	151
<i>Figure 6.6 Example of a probabilistic optimisation and the possible sets of references taken into account, with the sign + representing a combination of forecasts and decisions.</i>	152
<i>Figure 6.7 Example of a probabilistic optimisation with “crossed” values depending on the forecasts.</i>	152
<i>Figure 6.8 Overview of methods of multi-attribute decision making implemented in MINDS. The objective function reduces the set of economical losses in a different way depending of the selected method.</i>	158
<i>Figure 6.9 BasU turbine operation series becomes the proposed PrevOp turbine operation series</i>	166

<i>Figure 6.10 Final PrevOp of bottom outlets from an initial null series</i>	167
<i>Figure 6.11 Final PrevOp of pumping from an initial null series</i>	167
<i>Figure 6.12 Scheme for the Greedy optimisation</i>	170
<i>Figure 6.13 Flow chart of the shuffled complex evolution method (from Duan et al., 1993), with <math>V=n</math>, <math>NGS=p</math>, <math>NPG=m</math> and <math>NPT=s</math></i>	175
<i>Figure 6.14 Illustration of the shuffled complex evolution (SCE-UA) method (from Duan et al., 1994).</i>	176
<i>Figure 6.15 Illustration of the evolution steps taken by each complex (from Duan et al., 1994).</i>	177
<i>Figure 6.16 Coupled approach of IRGA and SCE-UA algorithms</i>	179
<i>Figure 6.17 Main interface of MINDS</i>	181
<i>Figure 6.18 Main parameters area of MINDS</i>	183
<i>Figure 6.19 Basin map for the selection of the groups to be optimised</i>	184
<i>Figure 6.20 MINDS advanced parameters window</i>	184
<i>Figure 6.21 Main interface of MINDS after an optimisation</i>	186
<i>Figure 6.22 Structure of the main interface of MINDS.</i>	187
<i>Figure 6.23 Hydrographs at check points and inflows and outflows in the reservoirs with BasU and PrevOp simulations.</i>	189
<i>Figure 6.24 Box plots of peaks at check points with BasU and PrevOp simulations.</i>	189
<i>Figure 6.25 Total expected damages at check points with BasU and PrevOp.</i>	190
<i>Figure 6.26 Inflows, outflows and volume variations in the reservoirs with BasU and PrevOp.</i>	190
<i>Figure 7.1 Priority decisions for each reservoir depending on its necessary preventive operations</i>	193
<i>Figure 7.2 Decision tree for priority decision levels in the reservoirs.</i>	194
<i>Figure 7.3 Main results obtained for Bitsch and Mattmark with deterministic forecasts for one group optimisation, T representing the turbinning operations, P the pumping operations and V the bottom outlet operations. Natural basin represents the simulation with the non equipped basin, BasU the simulation with the equipped basin and Business as Usual operations, Greedy the optimisation with the IRGA approach and SCE-UA the optimisation with the Shuffled Complex Evolution – University of</i>	



- Arizona approach. PPOC indicates the Potential Preventive Operation Costs.* 203
- Figure 7.4 Average and maximum of the set of values obtained for Bitsch and Mattmark with probabilistic forecasts and one group optimisation, including Bayes Risk Criterion (BRC), MMR (MinMax Regret), DMC (Decision Maker Criterion), DHF (Derived Hurwicz for Floods) and TOPSIS (Technique for Order Preference by Similarity to Ideal Solution). Natural basin represents the simulation with the non equipped basin, BasU the simulation with the equipped basin and Business as Usual operations, Greedy the optimisation with the IRGA approach and SCE-UA the optimisation with the Shuffled Complex Evolution – University of Arizona approach.  $\beta$  corresponds to the potential preventive operation costs coefficient. PPOC indicate the Potential Preventive Operation Costs. Average expected damages are represented by solid colours and maximum expected damages by lighter colours.* 203
- Figure 7.5 Number of evaluations of the objective function with deterministic and probabilistic forecasts and one group optimisation. Greedy (Iterative Ranking Greedy Algorithm) represents the optimisation with this approach and SCE-UA the optimisation with the Shuffled Complex Evolution – University of Arizona algorithm.* 204
- Figure 7.6 Main results obtained with deterministic forecasts for two groups optimisation (Bitsch and Mattmark at the same time),  $T$  representing the turbinning operations,  $P$  the pumping operations and  $V$  the bottom outlet operations. Natural basin represents the simulation with the non equipped basin, BasU the simulation with the equipped basin and Business as Usual operations, Greedy the optimisation with the IRGA approach and SCE-UA the optimisation with the Shuffled Complex Evolution – University of Arizona approach. PPOC indicates the Potential Preventive Operation Costs.* 210
- Figure 7.7 Average and maximum of the set of values obtained with probabilistic forecasts and two groups optimisation (Bitsch and Mattmark at the same time), including Bayes Risk Criterion (BRC), MMR (MinMax Regret), DMC (Decision Maker Criterion), DHF (Derived Hurwicz for Floods) and TOPSIS (Technique for Order Preference by Similarity to Ideal Solution). Natural basin represents the simulation with the non equipped basin, BasU the simulation with the equipped basin and Business as*



*Usual operations, Greedy the optimisation with the IRGA approach and SCE-UA the optimisation with the Shuffled Complex Evolution – University of Arizona approach.  $\beta$  corresponds to the potential preventive operation costs coefficient. PPOC indicates the Potential Preventive Operation Costs. Average expected damages are represented by solid colours and maximum expected damages by lighter colours.* 211

*Figure 7.8 Number of evaluations of the objective function with deterministic and probabilistic forecasts and two groups optimisation. Greedy (Iterative Ranking Greedy Algorithm) represents the optimisation with this approach and SCE-UA the optimisation with the Shuffled Complex Evolution – University of Arizona algorithm* 211

*Figure 7.9 Main results obtained with deterministic forecasts for all groups optimisation, T representing the turbines operations, P the pumping operations and V the bottom outlet operations. Natural basin represents the simulation with the non equipped basin, BasU the simulation with the equipped basin and Business as Usual operations, Greedy the optimisation with the IRGA approach and SCE-UA the optimisation with the Shuffled Complex Evolution – University of Arizona approach. PPOC indicates the Potential Preventive Operation Costs.* 217

*Figure 7.10 Average and maximum of the set of values obtained with probabilistic forecasts and all groups optimisation, including Bayes Risk Criterion (BRC), MMR (MinMax Regret), DMC (Decision Maker Criterion), DHF (Derived Hurwicz for Floods) and TOPSIS (Technique for Order Preference by Similarity to Ideal Solution). Natural basin represents the simulation with the non equipped basin, BasU the simulation with the equipped basin and Business as Usual operations, Greedy the optimisation with the IRGA approach and SCE-UA the optimisation with the Shuffled Complex Evolution – University of Arizona approach.  $\beta$  corresponds to the potential preventive operation costs coefficient. PPOC indicates the Potential Preventive Operation Costs. Average expected damages are represented by solid colours and maximum expected damages by lighter colours.* 218

*Figure 7.11 Number of evaluations of the objective function with deterministic and probabilistic forecasts and all groups optimisation. Greedy (Iterative Ranking Greedy Algorithm) represents the optimisation with this*

- approach and SCE-UA the optimisation with the Shuffled Complex Evolution – University of Arizona algorithm.* 218
- Figure 7.12 Real-time procedure for the reservoir management during floods from the first forecast predicting the flood and with an update of forecasts and preventive operations during the whole flood event.* 221
- Figure 7.13 Hydrographs with optimisation of the October 2000 flood at the outlet of the basin, Porte-du-Scex, starting on October 11, 2000 . “Qtot Nat Basin” corresponds to the hydrograph from the natural basin, “Qtot Observed” to the hydrograph from observed measurements, “Qtot BasU” to the hydrograph of the equipped basin simulated with Business as Usual operations, “Qtot PrevOp Obs” to the hydrograph resulting from the optimisation with a perfect forecast. “Outflow HPP Observed” represents the summation of the outflows from all hydropower plants, “Outflow HPP BasU” the summation of the outflows calculated with Business as Usual operations, “Outflow HPP PrevOp Obs” the summation of the outflows calculated from the optimisation with a perfect forecast. “Inflow HPP” represents the total inflows to the reservoirs of the system.* 223
- Figure 7.14 Hydrographs with optimisation using hydrological forecasts of the October 2000 flood (starting on October 11, 2000 at 12 h with COSMO-LEPS and on October 12, 2000 at 00 h with COSMO-7). at the outlet of the basin, Porte-du-Scex. “Qtot Nat Basin” corresponds to the hydrograph from the natural basin, “Qtot BasU” to the hydrograph of the equipped basin simulated with Business as Usual operations, “Qtot PrevOp Obs” to the hydrograph from the optimisation with a perfect forecast, “Qtot PrevOp Prob” to the hydrograph from the optimisation with COSMO-LEPS and “Qtot PrevOp Det” to the hydrograph from the optimisation with COSMO-7. “Outflow HPP BasU” represents the summation of the outflows from all hydropower plants calculated with Business as Usual operations, “Outflow HPP PrevOp Obs” the outflows from the optimisation with a perfect forecast, “Outflow HPP PrevOp Prob” the outflows from the optimisation with COSMO-LEPS and “Outflow HPP PrevOp Det” the outflows from the optimisation with COSMO-7. “Inflow HPP” represents the total inflows to the reservoirs of the system.* 226

Figure 7.15 Hydrographs with optimisation of the September 1993 flood at the outlet of the basin, Porte-du-Scex, starting on September 21, 1993 at 12 h . “Qtot Nat Basin” corresponds to the hydrograph from the natural basin, “Qtot Observed” to the hydrograph from observed measurements, “Qtot BasU” to the hydrograph of the equipped basin simulated with Business as Usual operations, “Qtot PrevOp Obs” to the hydrograph resulting from the optimisation with a perfect forecast. “Outflow HPP Observed” represents the summation of the outflows from all hydropower plants, “Outflow HPP BasU” the summation of the outflows calculated with Business as Usual operations, “Outflow HPP PrevOp Obs” the summation of the outflows calculated from the optimisation with a perfect forecast. “Inflow HPP” represents the total inflows to the reservoirs of the system.

231

Figure 7. 16 Hydrographs with optimisation using hydrological forecasts of the September 1993 flood (starting on September 21, 1993 at 12 h with COSMO-LEPS and on September 22, 1993 at 00 h with COSMO-7). at the outlet of the basin, Porte-du-Scex. “Qtot Nat Basin” corresponds to the hydrograph from the natural basin, “Qtot BasU” to the hydrograph of the equipped basin simulated with Business as Usual operations, “Qtot PrevOp Obs” to the hydrograph from the optimisation with a perfect forecast, “Qtot PrevOp Prob” to the hydrograph from the optimisation with COSMO-LEPS and “Qtot PrevOp Det” to the hydrograph from the optimisation with COSMO-7. “Outflow HPP BasU” represents the summation of the outflows from all hydropower plants calculated with Business as Usual operations, “Outflow HPP PrevOp Obs” the outflows from the optimisation with a perfect forecast, “Outflow HPP PrevOp Prob” the outflows from the optimisation with COSMO-LEPS and “Outflow HPP PrevOp Det” the outflows from the optimisation with COSMO-7. “Inflow HPP” represents the total inflows to the reservoirs of the system.

234

Figure 7.17 Approximate number of evaluations of the objective function with IRGA and SCE-UA approaches when optimising deterministic and probabilistic forecasts.

240



# List of Tables

<i>Table 1.1 High costs floods from 1990 to 2005 with original values, not adjusted for inflation (from Kron, 2005)</i>	4
<i>Table 4.1 Characteristics of the different COSMO models of MeteoSwiss</i>	75
<i>Table 4.2 Recent events in the Upper Rhone River basin and available forecasts COSMO-LEPS (C-L), COSMO-7 (C-7) and COSMO-2 (C-2). Start and end time are only proposed for guidance.</i>	76
<i>Table 4.3 Critical discharge (<math>m^3/s</math>) for different threshold warnings at check points (indicative, under validation by the Valais Canton).</i>	90
<i>Table 4.4 Code of colours, threshold and associated warning</i>	94
<i>Table 4.5 Code of colours for the different warnings and associated forecasts to</i>	95
<i>Table 5.1 Evaluated flood events</i>	98
<i>Table 5.2 Meteorological stations located in the Upper Rhone River basin</i>	99
<i>Table 5.3 Set matrix for the creation of the ROC index</i>	102
<i>Table 5.4 Precipitation performance for COSMO-7 (C-7) and for the ensemble forecasts COSMO-LEPS which is represented by the median <math>i_m</math>, the upper <math>i_u</math> and lower quartile <math>i_l</math> as well as by the minimum <math>i_{min}</math> and maximum precipitation <math>i_{max}</math>. Left: relative volume bias (<math>R_{bVol}</math>). Right: cumulated volume ratio (<math>R_{cVol}</math>).</i>	105
<i>Table 5.5 Average temperature bias (<math>b_{at}</math>) for COSMO-7 (C-7) and for the ensemble forecasts COSMO-LEPS which is represented by the median <math>i_m</math>, the upper <math>i_u</math> and lower quartile <math>i_l</math> as well as by the minimum <math>i_{min}</math> and maximum precipitation <math>i_{max}</math>.</i>	106
<i>Table 5.6 Probabilistic indexes BS (Brier Score) and ROC (Relative Operating Characteristic) for COSMO-LEPS (C-L) and COSMO-7 (C-7) for the threshold <math>i=30</math> mm/day.</i>	107
<i>Table 5.7 Set matrix for the Relative Economic Value (REV)</i>	113
<i>Table 5.8 Deterministic indexes results of the three events as well as the average for the representative hydrograph <math>q_m</math> of COSMO-LEPS (C-L) and for COSMO-7 (C-7). NPE represents the Normalized Peak Error, PTE the Peak Time Error, <math>r_{cVol}</math> the Cumulated volume ratio, <math>R_{bVol}</math> the relative</i>	

<i>volume bias, RMSE the Root Mean Square Error, Nash the Nash Index, IA the Index of Agreement and IR the index of Resemblance.</i>	123
<i>Table 5.9 Average of the forecasts studied with deterministic indexes average for the representative hydrographs of COSMO-LEPS and for COSMO-7. Index represented are the same than in Table 5.8.</i>	124
<i>Table 5.10 Probabilistic indexes for the threshold <math>Q=700 \text{ m}^3/\text{s}</math> for COSMO-LEPS (C-L) and COSMO-7 (C-7). BS represents the Brier Score, BSS the Brier Skill Score and ROC the Relative Operating Characteristic.</i>	126
<i>Table 6.1 Hydropower groups and reservoirs implemented in the MINDS hydraulic model (P for punctual reservoirs).</i>	137
<i>Table 6.2 Check points (CP) with the overflow discharge <math>Q_{fl}</math> of the levees and the extreme discharge <math>Q_{ex}</math></i>	139
<i>Table 6.3 Period of peak and base discharge and energy prices for the Business as Usual operations</i>	142
<i>Table 6.4 Check points with associated maximum damages and parameters for damages calculation</i>	143
<i>Table 6.5 Periods of peak and base turbine discharge for the Business as Usual operations</i>	164
<i>Table 6.6 Theoretical values of electricity prices</i>	166
<i>Table 7.1 Reference flood events for COSMO-LEPS (C-L) and COSMO-7 (C-7)</i>	192
<i>Table 7.2 Priority decision levels for reservoir operations.</i>	193
<i>Table 7.3 Code of colours for the warning levels at check points.</i>	194
<i>Table 7.4 Number of parameters taken into account per group and reservoir, with T representing the turbining operations, P the pumping operations and V the bottom outlet operations.</i>	195
<i>Table 7.5 Results obtained for Bitsch and Mattmark with deterministic forecasts for one group optimisation, with T representing the turbining operations, P the pumping operations, V the bottom outlet operations and <math>\beta</math> the potential preventive operation costs coefficient. Natural basin represents the simulation with the non equipped basin, BasU the simulation with the equipped basin and Business as Usual operations, Greedy the optimisation with the IRGA approach and SCE-UA the optimisation with the Shuffled Complex Evolution – University of Arizona approach.</i>	199

*Table 7.6 Average of the set of values obtained for Bitsch and Mattmark with probabilistic forecasts and one group optimisation, including Bayes Risk Criterion (BRC), MMR (MinMax Regret), DMC (Decision Maker Criterion), DHF (Derived Hurwicz for Floods) and TOPSIS (Technique for Order Preference by Similarity to Ideal Solution). Natural basin represents the simulation with the non equipped basin, BasU the simulation with the equipped basin with Business as Usual operations, Greedy the optimisation with the IRGA approach and SCE-UA the optimisation with the Shuffled Complex Evolution – University of Arizona approach.  $\beta$  corresponds the potential preventive operation costs coefficient.*

201

*Table 7.7 Maximum of the set of values obtained for Bitsch and Mattmark with probabilistic forecasts and one group optimisation, including Bayes Risk Criterion (BRC), MMR (MinMax Regret), DMC (Decision Maker Criterion), DHF (Derived Hurwicz for Floods) and TOPSIS (Technique for Order Preference by Similarity to Ideal Solution). Natural basin represents the simulation with the non equipped basin, BasU the simulation with the equipped basin with Business as Usual operations, Greedy the optimisation with the IRGA approach and SCE-UA the optimisation with the Shuffled Complex Evolution – University of Arizona approach.  $\beta$  corresponds the potential preventive operation costs coefficient.*

202

*Table 7.8 Results obtained for two groups optimisation (Bitsch and Mattmark at the same time) with deterministic forecasts, with  $T$  representing the turbinning operations,  $P$  the pumping operations,  $V$  the bottom outlet operations and  $\beta$  the potential preventive operation costs coefficient. Natural basin represents the simulation with the non equipped basin, BasU the simulation with the equipped basin and Business as Usual operations, Greedy the optimisation with the IRGA approach and SCE-UA the optimisation with the Shuffled Complex Evolution – University of Arizona approach.  $B \rightarrow M$  represents the order of the optimisation for the Greedy approach: first for Bitsch and second for Mattmark.  $M \rightarrow B$  represents the same with the inverse order: first Mattmark, second Bitsch.*

206

*Table 7.9 Average of the set of values obtained with probabilistic forecasts and two groups optimisation (Bitsch and Mattmark at the same time), including*

293



*Bayes Risk Criterion (BRC), MMR (MinMax Regret), DMC (Decision Maker Criterion), DHF (Derived Hurwicz for Floods) and TOPSIS (Technique for Order Preference by Similarity to Ideal Solution). Natural basin represents the simulation with the non equipped basin, BasU the simulation with the equipped basin and Business as Usual operations, Greedy the optimisation with the IRGA approach and SCE-UA the optimisation with the Shuffled Complex Evolution – University of Arizona approach.  $\beta$  corresponds to the potential preventive operation costs coefficient.  $B \rightarrow M$  represents the order of the optimisation for the Greedy approach: first for Bitsch and second for Mattmark.  $M \rightarrow B$  represents the same with the inverse order: first Mattmark, second Bitsch.*

208

*Table 7.10 Maximum of the set of values obtained with probabilistic forecasts and two groups optimisation (Bitsch and Mattmark at the same time), including Bayes Risk Criterion (BRC), MMR (MinMax Regret), DMC (Decision Maker Criterion), DHF (Derived Hurwicz for Floods) and TOPSIS (Technique for Order Preference by Similarity to Ideal Solution). Natural basin represents the simulation with the non equipped basin, BasU the simulation with the equipped basin and Business as Usual operations, Greedy the optimisation with the IRGA approach and SCE-UA the optimisation with the Shuffled Complex Evolution – University of Arizona approach.  $\beta$  corresponds to the potential preventive operation costs coefficient.  $B \rightarrow M$  represents the order of the optimisation for the Greedy approach: first for Bitsch and second for Mattmark.  $M \rightarrow B$  represents the same with the inverse order: first Mattmark, second Bitsch.*

209

*Table 7.11 Results obtained with deterministic forecasts for all groups optimisation, with  $T$  representing the turbines operations,  $P$  the pumps operations,  $V$  the bottom outlet operations and  $\beta$  the potential preventive operation costs coefficient. Natural basin represents the simulation with the non equipped basin, BasU the simulation with the equipped basin and Business as Usual operations, Greedy the optimisation with the IRGA approach and SCE-UA the optimisation with the Shuffled Complex Evolution – University of Arizona approach.  $RSI_{max \rightarrow min}$  represents the Reservoir Space Index from the highest to the smallest values in the groups order with the Greedy approach,  $RSI_{min \rightarrow max}$  the Reservoir Space Index from the smallest to the highest values, UsToDs, the order from*



upstream to downstream, DsToUs from downstream to upstream and Random an order with this characteristic. 213

Table 7.12 Average of the set of values obtained with probabilistic forecasts and all groups optimisation, including Bayes Risk Criterion (BRC), MMR (MinMax Regret), DMC (Decision Maker Criterion), DHF (Derived Hurwicz for Floods) and TOPSIS (Technique for Order Preference by Similarity to Ideal Solution). Natural basin represents the simulation with the non equipped basin, BasU the simulation with the equipped basin and Business as Usual operations, Greedy the optimisation with the IRGA approach and SCE-UA the optimisation with the Shuffled Complex Evolution – University of Arizona approach.  $\beta$  corresponds to the potential preventive operation costs coefficient.  $RSI_{max\ to\ min}$  represents the Reservoir Space Index from the highest to the smallest values in the order of the optimisation for the Greedy approach,  $RSI_{min\ to\ max}$  the Reservoir Space Index from the smallest to the highest values, UsToDs, the order from upstream to downstream, DsToUs from downstream to upstream and Random an order with this characteristic. 215

Table 7.13 Maximum of the set of values obtained with probabilistic forecasts and all groups optimisation, including Bayes Risk Criterion (BRC), MMR (MinMax Regret), DMC (Decision Maker Criterion), DHF (Derived Hurwicz for Floods) and TOPSIS (Technique for Order Preference by Similarity to Ideal Solution). Natural basin represents the simulation with the non equipped basin, BasU the simulation with the equipped basin and Business as Usual operations, Greedy the optimisation with the IRGA approach and SCE-UA the optimisation with the Shuffled Complex Evolution – University of Arizona approach.  $\beta$  corresponds to the potential preventive operation costs coefficient.  $RSI_{max\ to\ min}$  represents the Reservoir Space Index from the highest to the smallest values in the order of the optimisation for the Greedy approach,  $RSI_{min\ to\ max}$  the Reservoir Space Index from the smallest to the highest values, UsToDs, the order from upstream to downstream, DsToUs from downstream to upstream and Random an order with this characteristic. 216

Table 7.14 Main results from the optimisation for the October 2000 flood. “Natural basin” represents the results from the simulation of the natural basin without hydropower schemes, “BasU” the results from the equipped basin with Business as Usual operations and “OPT OBS” the

- 
- results from the optimisation with the equipped basin and perfect forecasts (from meteorological observations) 224
- Table 7.15 Optimisation results with meteorological observations as input for hydrological simulations (from October 11, 2000 at 12h). “Start T” represents the start time for turbine operations, “Dur T” the duration of the turbine operations, “Per NT” the periods of turbines stop, “Start V” the starting time for the bottom outlet operations, “Dur V” the duration of the bottom outlet operations, “Dur P” the duration of the pumping operations and “to” the start time of the optimisation period. 224
- Table 7.16 Levels and volumes for the optimisation with meteorological observations as input of hydrological simulations (from October 11, 2000 at 12h) 225
- Table 7.17 Main results from the optimisation with hydrological forecasts for the 2000 flood. “BasU” represents the results from the equipped basin with Business as Usual operations, “OPT OBS” the results from the optimisation with the equipped basin and perfect forecasts (from meteorological observations), “OPT C-L” the results of the optimisation with COSMO-LEPS and “OPT C-7” the results of the optimisation with COSMO-7. 227
- Table 7.18 Optimisation results with hydrological forecasts from COSMO-LEPS (presented from October 11, 2000 at 12 h for an easy comparison with the optimisation with perfect forecasts). Non presented groups had non preventive operations. “Start T” represents the start time for turbine operations, “Dur T” the duration of the turbine operations, “Per NT” the periods of turbines stop, “Start V” the start time for the bottom outlet operations, “Dur V” the duration of the bottom outlet operations, “Dur P” the duration of the pumps operations and “t<sub>o</sub>” the start time of the optimisation period. 228
- Table 7.19 Levels and volumes for the optimisation with COSMO-LEPS as input of hydrological simulations (presented from October 11, 2000 at 12 h). 228
- Table 7.20 Optimisation results with hydrological forecasts from COSMO-7 (presented from October 11, 2000 at 12 h for an easy comparison between the optimisation with perfect forecasts). Non presented groups had non preventive operations. “Start T” represents the start time for turbine operations, “Dur T” the duration of the turbine operations, “Per

---

<i>NT</i> the periods of turbines stop, <i>Start V</i> the start time for the bottom outlet operations, <i>Dur V</i> the duration of the bottom outlet operations, <i>Dur P</i> the duration of the pumps operations and <i>t<sub>o</sub></i> the start time of the optimisation period.	229
Table 7.21 Levels and volumes for the optimisation with COSMO-7 as input of hydrological simulations (presented from October 12, 2000 at 00 h)	229
Table 7.22 Main optimisation results for the September 1993 flood. <i>Natural basin</i> represents the results from the simulation of the natural basin without hydropower schemes, <i>BasU</i> the results from the equipped basin with Business as Usual operations and <i>OPT OBS</i> the results from the optimisation with the equipped basin and perfect forecasts (from meteorological observations)	232
Table 7.23 Optimisation results with meteorological observations as input of hydrological simulations (from September 21, 1993 at 12h). <i>Start T</i> represents the start time for turbine operations, <i>Dur T</i> the duration of the turbine operations, <i>Per NT</i> the periods of turbines stop, <i>Start V</i> the starting time for the bottom outlet operations, <i>Dur V</i> the duration of the bottom outlet operations, <i>Dur P</i> the duration of the pumping operations and <i>to</i> the start time of the optimisation period.	232
Table 7.24 Levels and volumes for the optimisation with meteorological observations as input of hydrological simulations (from September 21, 1993 at 12h)	233
Table 7.25 Main optimisation results with hydrological forecasts for the 1993 flood. <i>BasU</i> represents the results from the equipped basin with Business as Usual operations, <i>OPT OBS</i> the results from the optimisation with the equipped basin and perfect forecasts (from meteorological observations), <i>OPT C-L</i> the results of the optimisation with COSMO-LEPS and <i>OPT C-7</i> the results of the optimisation with COSMO-7.	235
Table 7.26 Optimisation results with hydrological forecasts from COSMO-LEPS (presented from September 21, 1993 at 12 h for an easy comparison between the optimisation with perfect forecasts). Non presented groups had non preventive operations. <i>Start T</i> represents the start time for turbine operations, <i>Dur T</i> the duration of the turbine operations, <i>Per NT</i> the periods of turbines stop, <i>Start V</i> the start time for the bottom	

<p>outlet operations, “Dur V” the duration of the bottom outlet operations, “Dur P” the duration of the pumps operations and “to” the start time of the optimisation period.</p>	236
<p>Table 7.27 Levels and volumes for the optimisation with COSMO-LEPS as input of hydrological simulations (presented from September 21, 1993 at 12 h).</p>	236
<p>Table 7.28 Optimisation results with hydrological forecasts from COSMO-7 (presented from September 21, 1993 at 12 h for an easy comparison between the optimisation with perfect forecasts). Non presented groups had non preventive operations. “Start T” represents the start time for turbine operations, “Dur T” the duration of the turbine operations, “Per NT” the periods of turbines stop, “Start V” the start time for the bottom outlet operations, “Dur V” the duration of the bottom outlet operations, “Dur P” the duration of the pumps operations and “to” the start time of the optimisation period.</p>	237
<p>Table 7.29 Levels and volumes for the optimisation with COSMO-7 as input of hydrological simulations (presented from September 21, 1993 at 12 h).</p>	237

# Notation

## Roman symbols

$A$	Cross sectional flow area	[m <sup>2</sup> ]
$A_{GL}$	Glacier degree-day glacier melt coefficient	[m/s/°C]
$A_n$	Snow degree-day coefficient	[m/s/°C]
$A_{ROC}$	Surface between the ROC curve and the x-axis	[-]
$A_T$	Matrix of function values depending on alternatives and forecasts	
$a_i$	Alternative $i$ of preventive operations	
$a_{i,GRg}$	Set $i$ of preventive operations in the hydropower group $g$	
$a_{i,set}$	Set $i$ of preventive operations in the whole basin	
$B$	Theoretical anti-ideal alternative	[-]
$B_r$	Width of the plane	[m]
$b$	Cross sectional variation	[-]
$b_{aT}$	Temperature bias between the average temperature forecasted and observed	[°C]
$b_i$	Average hourly precipitation intensity bias	[mm/h]
$b_j$	Minimum value for a given forecast depending on the sets of preventive operations	[-]
$b_p$	Precipitation coefficient due to melt	[s/m]
$b_T$	Average hourly temperature bias in absolute value	[°C]
$C$	Cost	[CHF]
$C_1$	Cost related to Energy 1	[CHF]
$C_2$	Cost related to Energy 2	[CHF]
$C_3$	Cost related to Energy 3	[CHF]
$c$	Celerity	[m/s]
$c_{base}$	Base load price	[CHF]
$c_{peak}$	Peak load price	[CHF]
$c_{pot}$	Potential load price	[CHF]
$D$	Objective function of the MinMax Regret Criterion	
$D_r$	Discharge rate	[m <sup>3</sup> /s]
$dG_i$	Difference between $a_i$ and $G$ expressed as a general Euclidean weighted distance	[-]
$dB_i$	Difference between $a_i$ and $B$ expressed as a general Euclidean weighted distance	[-]
$d_i$	Maximum value given by the set $i$ of preventive operations for all possible forecasts	[CHF]

$ED_{max}$	Maximum expected damage	[CHF]
$E_i$	Routing efficiency	[-]
$E_{PO}$	Efficiency of preventive operation	[-]
$E_{stock}$	Total retention efficiency	[-]
$E_{sup}$	Supply efficiency	[-]
$E_{sup,max}$	Maximum supply efficiency	[-]
$f$	False alarm	[-]
$f_j$	Forecast $j$	
$f_k$	Occurrence probability of the event $k$ according to the forecast	[-]
$G$	Theoretical ideal alternative	[-]
$g$	Gravity	[m·s <sup>-2</sup> ]
$g_j$	Maximum value for a given forecast depending on the sets of preventive operations	[-]
$H$	Objective function of the Derived Hurwicz for Floods Criterion	
$H_{GL}$	Level of glacier melt reservoir	[m]
$H_N$	Height of snow	[m]
$H_{NGL}$	Level in linear snow reservoir	[m]
$h$	Water level	[m]
$h_{inf}$	Level in the infiltration reservoir	[m]
$h_{max}$	Capacity of infiltration reservoir	[m]
$h_r$	Runoff water level downstream of the surface	[m]
$I_1$	Profile coefficient	[m <sup>3</sup> ]
$I_2$	Coefficient for cross sectional variation	[m <sup>2</sup> ]
$i_{inf}$	Infiltration intensity	[m/s]
$i_l$	Lower quartile of the rain intensity for COSMO-LEPS	[mm/h]
$i_m$	Median of the rain intensity for COSMO-LEPS	[mm/h]
$i_{max}$	Maximum value of the rain intensity for COSMO-LEPS	[mm/h]
$i_{min}$	Minimum value of the rain intensity for COSMO-LEPS	[mm/h]
$i_{net}$	Net intensity	[m/s]
$i_{obs,t}$	Observed intensity at time step $t$	[mm]
$i_r$	Runoff intensity	[m/s]
$i_{sim,t}$	Simulated intensity at time step $t$	[mm]
$i_u$	Upper quartile of the rain intensity for COSMO-LEPS	[mm/h]
$J_f$	Friction slope	[-]
$J_o$	Average slope of the plane	[-]
$K$	Strickler coefficient	
$K_{GL}$	Release coefficient of linear glacier reservoir	[1/s]

---

$K_N$	Release coefficient of linear snow reservoir	[1/s]
$K_s$	Strickler coefficient in SWMM model	[m <sup>1/3</sup> /s]
$KSTOP$	Number of shuffling loops in which the criterion value must change by a fixed percentage (PCENTO) before optimisation is finished (SCE-UA)	[-]
$k$	Release coefficient of infiltration reservoir	[1/s]
$L_a$	Avoidable cost	[CHF]
$L_p$	Wetted perimeter	[m]
$L_u$	Unavoidable cost	[CHF]
$M_N$	Snowmelt of freezing	[m/s]
$MAXN$	Maximum number of function evaluations (SCE-UA)	[-]
$MINGS$	Minimum number of complexes (SCE-UA)	[-]
$m$	Side slope of the bank of the channel	[-]
$m_{i,j}$	Function value for a set $i$ of PrevOp and a forecast $j$	[CHF]
$N$	Solid precipitation	[m/s]
$N_T$	Normalised TOPSIS matrix	[-]
$n$	Total number of observations	[-]
$NGS$	Number of complexes (SCE-UA)	[-]
$NPG$	Number of points in a complex (SCE-UA)	[-]
$NPS$	Number of points in a sub-complex (SCE-UA)	[-]
$NPT$	Total number of points in the entire sample population (SCE-UA)	[-]
$NSPL$	Evolution steps (SCE-UA)	[-]
$n_f$	Total number of forecast members	[-]
$O_{max}$	Maximum observed discharge	[m <sup>3</sup> /s]
$o_k$	Occurrence of the event $k$	[-]
$P$	Precipitation	[m/s]
$P_{eqGL}$	Glacier melt	[m/s]
$P^*$	Liquid precipitation	[m/s]
$PCENTO$	Convergence value for stopping the calculation (SCE-UA)	[-]
$Q$	Discharge	[m <sup>3</sup> /s]
$Q_{fl}$	Flooding discharge	[m <sup>3</sup> /s]
$Q_{base}$	Base discharge	[m <sup>3</sup> /s]
$Q_{baseinf}$	Infiltration base discharge	[m <sup>3</sup> /s]
$Q_{BasU,t}$	Business as Usual discharge at time $t$	[m <sup>3</sup> /s]
$Q_{bottomoutlet,max}$	Maximum discharge by bottom outlets	[m <sup>3</sup> /s]
$Q_{bottomoutlet,t}$	Total discharge by bottom outlets at time $t$	[m <sup>3</sup> /s]
$Q_{ProposedEmpt,t}$	Proposed bottom outlet release series for PrevOp at time $t$	[m <sup>3</sup> /s]
$Q_{eq}$	Equipped discharge	[m <sup>3</sup> /s]

$Q_{ex}$	Extreme discharge	[m <sup>3</sup> /s]
$Q_{fl}$	Critical discharge for overflowing	[m <sup>3</sup> /s]
$Q_{GL}$	Outflow of linear glacier reservoir	[m <sup>3</sup> /s]
$Q_{in}$	Inflow discharge	[m <sup>3</sup> /s]
$Q_{NGL}$	Outflow of linear snow reservoir	[m <sup>3</sup> /s]
$Q_{max}$	Maximum discharge of the period	[m <sup>3</sup> /s]
$Q_{nat}$	Natural discharge	[m <sup>3</sup> /s]
$Q_{obs,t}$	Observed discharge at time $t$	[m <sup>3</sup> /s]
$Q_{out}$	Outflow discharge	[m <sup>3</sup> /s]
$Q_{peak}$	Peak discharge	[m <sup>3</sup> /s]
$Q_{ProposedTurb,t}$	Proposed turbine series for PrevOp at time $t$	[m <sup>3</sup> /s]
$Q_{pump,max}$	Maximum discharge by pumps	[m <sup>3</sup> /s]
$Q_{pump,t}$	Total discharge by pumps at time $t$	[m <sup>3</sup> /s]
$Q_{sim,t}$	Simulated discharge at time $t$	[m <sup>3</sup> /s]
$Q_{spillway,t}$	Total discharge by spillways at time $t$	[m <sup>3</sup> /s]
$Q_{threshold1}$	Discharge threshold 1	[m <sup>3</sup> /s]
$Q_{threshold2}$	Discharge threshold 2	[m <sup>3</sup> /s]
$Q_{turb,max}$	Maximum discharge by turbines	[m <sup>3</sup> /s]
$Q_{turb,t}$	Total discharge by turbines at time $t$	[m <sup>3</sup> /s]
$\overline{Q}_{obs}$	Average observed discharge	[m <sup>3</sup> /s]
$q_u$	Upper quartile of COSMO-LEPS	[m <sup>3</sup> /s]
$q_l$	Lower quartile of COSMO-LEPS	[m <sup>3</sup> /s]
$q_m$	Median of COSMO-LEPS	[m <sup>3</sup> /s]
$q_{max}$	Maximum hydrograph obtained by combination of all members of COSMO-LEPS	[m <sup>3</sup> /s]
$q_{min}$	Minimum hydrograph obtained by combination of all members of COSMO-LEPS	[m <sup>3</sup> /s]
$q_w$	Weighted value of COSMO-LEPS	[m <sup>3</sup> /s]
$R$	Objective function of the Bayes Risk Criterion	
$R_{bVol}$	Relative volume bias between the forecast and the observation	[-]
$R_{GL}$	Linear glacier reservoir	
$R_h$	Hydraulic radius	[m]
$R_{NGL}$	Linear snow reservoir	
$RSI_{GRW}$	Value of Reservoir Space Index for a hydropower group $g$	[-]
$RSI_{RESx}$	Value of Reservoir Space Index for a reservoir $x$	[-]
$r_{CVol}$	Cumulated volume ratio between the forecast and the observation	[-]
$r_i$	Risk for the set $i$ of preventive operations	[CHF]



$S$	Surface	$[\text{m}^2]$
$S_{GL}$	Glacier surface	$[\text{m}^2]$
$S_{max}$	Maximum simulated discharge	$[\text{m}^3/\text{s}]$
$s_{fl}$	Safety coefficient for overflowing	$[-]$
$s_{i,j}$	Normalised element of the TOPSIS matrix $A_T$	$[-]$
$s_s$	Number of intervals during a turbine discharge period	$[-]$
$s_p$	Number of intervals during a bottom outlet release period	$[-]$
$T$	Temperature	$[\text{°C}]$
$T_{cp1}$	Minimum critical temperature for liquid precipitation	$[\text{°C}]$
$T_{cp2}$	Maximum critical temperature for solid precipitation	$[\text{°C}]$
$T_{cr}$	Critical snowmelt temperature	$[\text{°C}]$
$T_{obs,t}$	Observed temperature at time step $t$	$[\text{°C}]$
$T_{p1}$	Initial time of the day for the peak energy price	$[\text{h}]$
$T_{p2}$	Final time of the day for the peak energy price	$[\text{h}]$
$T_{sim,t}$	Simulated temperature at time step $t$	$[\text{°C}]$
$T_1$	Evaluation threshold 1	$[\text{m}^3/\text{s}]$
$T_2$	Evaluation threshold 2	$[\text{m}^3/\text{s}]$
$T_3$	Evaluation threshold 3	$[\text{m}^3/\text{s}]$
$t$	Time	$[\text{h}]$
$t_f$	Final time step	$[\text{h}]$
$t_{leadtime}$	Ending time of the period	$[\text{h}]$
$t_i$	Initial time step	$[\text{h}]$
$t^*_{RESx}$	Time when PrevOp stops in reservoir $x$ (zero if no operations are proposed)	$[\text{h}]$
$t_{transit}$	Transit time between two elements	$[\text{h}]$
$t_{Omax}$	Date with maximum observed discharge	$[\text{date}]$
$t_{Smax}$	Date with maximum simulated discharge	$[\text{date}]$
$U$	Preliminary objective function of the TOPSIS Criterion	
$U^*$	Final objective function of the TOPSIS Criterion	
$u_i$	Membership degree for the alternative $a_i$	$[-]$
$V$	Volume	$[\text{m}^3]$
$V_{OPT}$	Number of variables to optimise	$[-]$
$V_{min}$	Minimum volume	$[\text{m}^3]$
$V_{max}$	Maximum volume	$[\text{m}^3]$
$V_{PrevEmpt}$	PrevOp bottom outlet releases volume	$[\text{m}^3]$
$V_{PrevTurb}$	PrevOp turbined volume	$[\text{m}^3]$
$V_{StopTurb}$	Stopped BasU turbine discharge volume	$[\text{m}^3]$
$V_{threshold1}$	Volume threshold 1	$[\text{m}^3]$
$V_{threshold2}$	Volume threshold 2	$[\text{m}^3]$

$W$	Vector of forecast weights	[-]
$W_N$	Water content	[m]
$W_j$	Occurrence probability of the forecast $j$	[-]
$x_{max}$	Maximum value calculated for the normalisation of the TOPSIS matrix ( $A_T$ )	[CHF]
$x_{min}$	Minimum value calculated for the normalisation of the TOPSIS matrix ( $A_T$ )	[CHF]
$Z$	Objective function of the Decision Maker Criterion	
$z_i$	Risk associated to the set $i$ of preventive operations taking into account a certain number of forecasts	[CHF]

### Greek symbols

$\alpha$	Proportion of liquid precipitation	[-]
$\alpha_c$	Numerical celerity	[-]
$\beta$	PPOC coefficient	[-]
$\gamma$	BasU discharge coefficient	[-]
$\delta$	Initial damage parameter	[-]
$\eta$	Plant efficiency	[-]
$\lambda$	Damage power function parameter	[-]
$\theta$	Relative water content in the snow pack	[-]
$\theta_{cr}$	Critical relative water content in the snow pack	
$\rho$	Water density	[kg·m <sup>-3</sup> ]
$\tau$	HDF weight coefficient	[-]
$\varphi$	Decision maker accepted risk coefficient	[-]
$\psi$	Cost-loss ratio	[-]
$\varsigma$	Diffusion coefficient	[m <sup>2</sup> /s]

## Acronyms

AQUA	Alert threshold
ALADIN	Aire Limitée Adaptation dynamique Développement InterNational
ALTO	Alarm threshold
AHP	Analytical Hierarchy Process
ANN	Artificial Neural Network
AR	AutoRegressive
ARMAX	AutoRegressive Moving Average with exogenous inputs
ARPEGE	Action de Recherche Petite Echelle Grande Echelle
BasU	Business as Usual
BM	Bred Modes
BRC	Bayes Risk Criterion
BS	Brier Score
BSS	Brier Skill Score
CAR	Correct Alarm Ratio
CCE	Competitive Complex Evolution
CERISE	Cellule scientifique de crise du Canton du Valais
CIR	Cellules d'Intervention Renforcées
CP	Control Point
CONSECRU	Concept de sécurité contre les crues
COSMO-LEPS (C-L)	Consortium for Small scale Modeling - limited-area Ensemble Prediction System
COSMO-2 (C-2)	Consortium for Small-scale Modeling (2.2 km de résolution)
COSMO-7 (C-7)	Consortium for Small-scale Modeling (6.6 km de résolution)
CP	Control Point
CRUEX	Modélisation des Crues Extrêmes dans les bassins versants alpins
DMC	Decision Maker Criterion
DsToUs	Downstream to Upstream
DP	Dynamic Programming
DSS	Decision Support System
DomEAU-GE	Domaine de l'eau (département du territoire) du canton de Genève
EA	Evolutionary Algorithm

ECMWF	European Centre for Medium-Range Weather Forecasts
ED	Expected Damages
EFAS	European Flood Alert System
ELECTRE	Elimination et Choice Translation Reality
EnKF	Ensemble Kalman Filter
EP	Evolutionary Programming
EPFL	Ecole Polytechnique Fédérale Lausanne
EPS	Ensemble Prediction System
ES	Expert System
ESP	Ensemble Streamflow Prediction
FAR	False Alarm Rate
FEWS	Flood Early Warning System
FL	Fuzzy Logic
FOEN	Federal Office for the Environment
GA	Genetic Algorithm
GEM	Global Environmental Multiscale
GIUH	Geomorphologic Instantaneous Unit Hydrograph
GR	Hydropower Group
GSM-SOCONT	Glacier Snow Melt – SOil CONTRibution model
HBV	Hydrologiska Byråns Vattenbalansavdelning
HDF	Hurwicz Derived for Floods
HIRLAM	High Resolution Limited Area Model
HPP	HydroPower Plant
HR	Hit Rate
IA	Index of Agreement
ICARO	Information Catastrophe Alarme Radio Organisation
IR	Index of Resemblance
IRGA	Iterative Ranking Greedy Algorithm
IUH	Instantaneous Unit Hydrograph
KF	Kalman Filter
LCH	Laboratory of Hydraulic Constructions at EPFL
LP	Linear Programming
MADM	Multi-Attribute Decision Making
MCDM	Multi-Criteria Decision Making
MINERVE	Modélisation des Intempéries de Nature Extrême dans le Rhône valaisan et de leurs effets (Flood events modelling in Valais reservoirs and their effects)
MINDS	MINERVE Interactive Decision Support System
MMR	MinMax Regret

---

MM5	Mesoscale Model, Generation 5
MODM	Multi-Objective Decision-Making
MORDOR	Modèle à Réservoirs de Détermination Optimale du Ruissellement
MR	Miss Ratio
MSC	Meteorological Service of Canada
NCEP	National Centers for Environmental Prediction
NDP	Neuro Dynamic Programming
NLP	NonLinear Programming
NPE	Normalised Peak Error
NSGA	Non-Dominated Sorting Genetic Algorithm
NWP	Numerical Weather Prediction
OFEV	Office Fédéral de l'Environnement
OI	Optimal Interpolation
OWARNA	Optimierung von Warnung und Alarmierung bei Naturgefahren - Optimization of Early Warning and Alerting
PPOC	Potential Preventive Operation Cost
PREVAH	Precipitation Runoff Evapotranspiration Hydrotope
PrevOp	Preventive Operations
PSU/NCAR	Pennsylvania State University / National Center for Atmospheric Research
PTE	Peak Timing Error
QPF	Quantitative Precipitation Forecasting
RES	Reservoir
REV	Relative Economical Value
RMSE	Root Mean Square Error
ROC	Relative Operating Characteristic
RR	Random Ranking
RRMSE	Relative Root Mean Square Error
RSII	Routing System II
RSM	Routing System MINERVE
$RSI_{\text{maxto min}}$	Reservoir Space Index from higher to smaller values
$RSI_{\text{mintomax}}$	Reservoir Space Index from smaller to higher values
RSR	Reservoir Space Ranking
SAC-SMA	SACramento Soil Moisture Accounting
SCE-UA	Shuffled Complex Evolution – University of Arizona
SCM	Successive Corrections Method

SDP	Stochastic Dynamic Programming
SESA	Service des Eaux, Sols et Assainissement du Canton de Vaud
SHE	European Hydrological System
SRCE	Service des Routes et des Cours d'Eau du Canton du Valais
SSCM	Service de la sécurité civile et militaire du Canton de Vaud
SSDP	Sampling Stochastic Dynamic Programming
SV	Singular vectors
SWAT	Soil and Water Assessment Tool
SWURVE	Etude de l'influence des changements climatiques sur les bassins versants alpins
TOPMODEL	TOPography based hydrological MODEL
TOPSIS	Technique for Order Preference by Similarity to Ideal Solution
TS	Tabu Search
UH	Unit Hydrograph
UsToDs	Upstream to Downstream
UTC	Coordinated Universal Time
VD	Canton de Vaud
VS	Canton du Valais
WaSiM	Water balance Simulation Model
3D-Var	Three dimensional variational assimilation
4D-Var	Four-dimensional variational assimilation

## Appendix 1

### Characteristics of the MINDS hydraulic balance simulation model

Table A1. 1 Characteristics of the turbines of the system

<b>Turbine Name</b>	<b>Installed Capacity [m<sup>3</sup>/s]</b>	<b>Head [m]</b>	<b>Plant efficiency</b>	<b>Operational</b>	<b>Active rate</b>	<b>Group</b>	<b>Name of the reservoir source</b>
<b>Nendaz</b>	45	1007	0.85	Yes	1	GD	GrandeDixence
<b>Chan</b>	10.2	1869	0.85	Yes	1	GD	GrandeDixence
<b>Bieu</b>	75	1883	0.85	Yes	1	GD	GrandeDixence
<b>Cleu</b>	0	0	0	Non	0	GD	Cleuson
<b>Fionnay</b>	34.5	481	0.85	Yes	1	FMM	Mauvoisin
<b>Riddes</b>	27.5	1014	0.85	Yes	1	FMM	Fionnay
<b>Val Ess</b>	15	805	0.85	Yes	1	ESA	Esserts
<b>Val ESA</b>	27	805	0.85	Yes	1	ESA	Emosson
<b>Batiaz</b>	29	660	0.85	Yes	1	ESA	Chatelard ESA
<b>Chat</b>	18	811	0.85	Yes	1	ESA	Emosson
<b>Ver CFF</b>	17.4	646	0.85	Yes	1	ESA	Chatelard CFF
<b>Moiry</b>	12.9	685	0.85	Yes	1	FMG	Moiry
<b>Tur</b>	4.3	685	0.85	Yes	1	FMG	Turtmann
<b>Vissoie</b>	12.9	438	0.85	Yes	1	FMG	Mottec
<b>Chippis</b>	10.5	564	0.85	Yes	1	FMG	Vissoie
<b>Stalden</b>	20	1022	0.85	Yes	1	KWM	Zermeiggern
<b>Zer</b>	19	468	0.85	Yes	1	KWM	Mattmark
<b>Mieville</b>	4.8	1472	0.85	Yes	1	SAL	Salanfe
<b>Bitsch</b>	55	743	0.85	Yes	1	EM	Gebidem
<b>Croix</b>	9	855	0.85	Yes	1	EL	Zeuzier
<b>St-Leonard</b>	11	420	0.85	Yes	1	EL	Croix
<b>Pallazuit</b>	10	479	0.85	Yes	1	GSB	Toules
<b>Orsieres</b>	8	387	0.85	Yes	1	GSB	Pallazuit
<b>Steg</b>	21.3	664	0.85	Yes	1	KWL	Ferden



Table A1. 2 Elements downstream of the turbines

<b>Turbine Name</b>	<b>Elements downstream</b>	<b>Name of the element</b>	<b>Transit time [h]</b>
<b>Nendaz</b>	CP	BransonOFEV	0
<b>Chan</b>	CP	SionOFEV	0
<b>Bieu</b>	CP	BransonOFEV	0
<b>Cleu</b>	CP	BransonOFEV	0
<b>Fionnay</b>	RES	Fionnay	0
<b>Riddes</b>	CP	BransonOFEV	0
<b>Val Ess</b>	RES	ChatelardESA	0
<b>Val ESA</b>	RES	ChatelardESA	0
<b>Batiaz</b>	CP	BransonAval	0
<b>Chat</b>	RES	ChatelardCFF	0
<b>Ver CFF</b>	CP	Lavey	0
<b>Moiry</b>	RES	Mottec	0
<b>Tur</b>	RES	Mottec	0
<b>Vissoie</b>	RES	Vissoie	0
<b>Chippis</b>	CP	Sierre	0
<b>Stalden</b>	CP	VispOFEV	0
<b>Zer</b>	RES	Zermeiggern	0
<b>Mieville</b>	CP	Lavey	0
<b>Bitsch</b>	CP	BrigOFEV	0
<b>Croix</b>	RES	Croix	1.1
<b>St-Leonard</b>	CP	SionAmont	0
<b>Pallazuit</b>	RES	Pallazuit	0
<b>Orsieres</b>	CP	BatiazOFEV	1.9
<b>Steg</b>	CP	Steg	0.5

Table A1. 3 Characteristics of the bottom outlets

<b>Reservoir</b>	<b>Bottom outlet capacity [m<sup>3</sup>/s]</b>	<b>Operational</b>	<b>Active rate</b>	<b>Group</b>	<b>Element downstream</b>	<b>Name of the element</b>	<b>Transit time [h]</b>
<b>GrandeDixence</b>	50	1	1	GD	CP	SionOFEV	2.2
<b>Cleuson</b>	22	1	1	GD	CP	BransonOFEV	1
<b>Mauvoisin</b>	120	0.5	0.5	FMM	CP	BatiazOFEV	3.1
<b>Fionnay</b>	P	1	1	FMM	CP	BatiazOFEV	1.6
<b>Emosson</b>	150	1	0.5	ESA	CP	Lavey	2.1
<b>Esserts</b>	P	1	1	ESA	CP	Lavey	1.1
<b>ChatelardESA</b>	P	1	1	ESA	CP	Lavey	1.6
<b>ChatelardCFF</b>	P	1	1	ESA	CP	Lavey	1.6
<b>Moiry</b>	155	1	0.5	FMG	CP	Sierre	2.8
<b>Turtmann</b>	18	1	1	FMG	CP	Sierre	2.6
<b>Mottec</b>	P	1	1	FMG	CP	Sierre	1.6
<b>Vissoie</b>	P	1	1	FMG	CP	Sierre	0.6
<b>Mattmark</b>	58	1	1	KWM	CP	VispOFEV	3.9
<b>Zermeiggern</b>	P	1	1	KWM	CP	VispOFEV	1.8
<b>Salanfe</b>	50	1	1	SAL	CP	Lavey	0.6
<b>Gebidem</b>	160	1	0.5	EM	CP	BrigOFEV	0.2
<b>Zeuzier</b>	40	1	1	EL	CP	SionAmont	3.1
<b>Croix</b>	P	1	1	EL	CP	SionAmont	1.2
<b>Toules</b>	70	1	1	GSB	CP	BatiazOFEV	4.9
<b>Pallazuit</b>	P	1	1	GSB	CP	BatiazOFEV	2.9
<b>Ferden</b>	106	1	0.5	KWL	CP	Steg	3.2

Table A1. 4 Characteristics of the pumps

<b>Pump Name</b>	<b>Installed capacity [m<sup>3</sup>/s]</b>	<b>Operational</b>	<b>Plant efficiency</b>	<b>Group</b>	<b>Reservoir source</b>	<b>Reservoir destination</b>
<b>Cleu P</b>	2.4	1	1	GD	Cleuson	GrandeDixence
<b>Val P</b>	18	1	1	ESA	Esserts	Emosson
<b>Moiry P</b>	3	1	1	FMG	Mottec	Moiry
<b>Tur P</b>	6	1	1	FMG	Turtmann	Moiry
<b>Zer P</b>	9	1	1	KWM	Zermeiggern	Mattmark

Table A1. 5 Control points with the river location, the control point located downstream and the transit time to it

<b>Check Point (CP)</b>	<b>River</b>	<b>CP downstream</b>	<b>Transit time to the next CP [minutes]</b>
Brig OFEV	Rhone	Visp Rhone	60
Visp OFEV	Vispa	Visp Rhone	15
Visp Rhone	Rhone	Steg	55
Steg	Rhone	Sierre	92
Sierre	Rhone	St-Léonard	51
St-Léonard	Rhone	Sion OFEV	36
Sion OFEV	Rhone	Branson OFEV	131
Branson OFEV	Rhone	Vernayaz Am.	19
Batiaz OFEV	Dranses	Vernayaz Am.	15
Vernayaz Am.	Rhone	Lavey	44
St-Maurice	Rhone	Scex OFEV	105
Scex OFEV	Rhone	Geneva Lake	0

Table A1. 6 Control points with the zones associated with each one

<b>Check Point (CP)</b>	<b>Damages coming from...</b>
Brig OFEV	Brig + Brig P+ Naters
Visp OFEV	Visp
Visp Rhone	Visp + Visp P + Lalden + Lalden P + Baltschieder
Steg	Steg + Steg P + Hohtenn + Niedergesteln
Sierre	Sierre + Chippis + Chippis P
St-Léonard	St-Léonard + Grône
Sion OFEV	Sion + Sion P
Branson OFEV	Martigny VC+ martigny VC P + Saxon + Charrat + Saillon + Fully
Batiaz OFEV	Martigny (VC) + Martigny P
Vernayaz Am.	Martigny BV
St-Maurice	Vernayaz + Vernayaz P + Dorénaz + Collonges + Evionnaz + Evionnaz P + St-Maurice
Scex OFEV	Collombey + Collombey P + Monthey + Massongex + Aigle + Aigle P + Ollon + Bex + Lavey-Morcles + Vouvry + Yverne

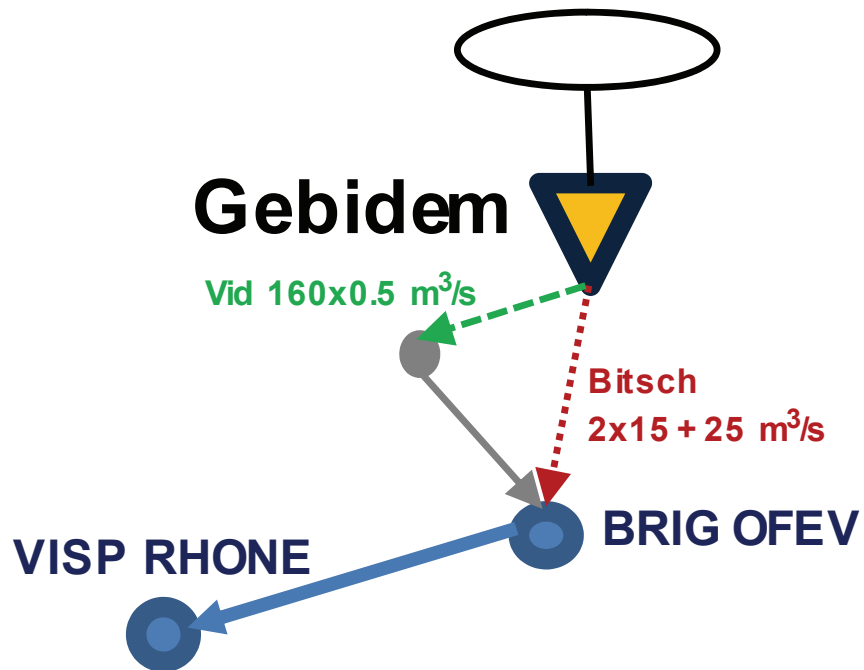


## Appendix 2

### Simplification of the MINDS groups

- **Bitsch according to MINDS:**

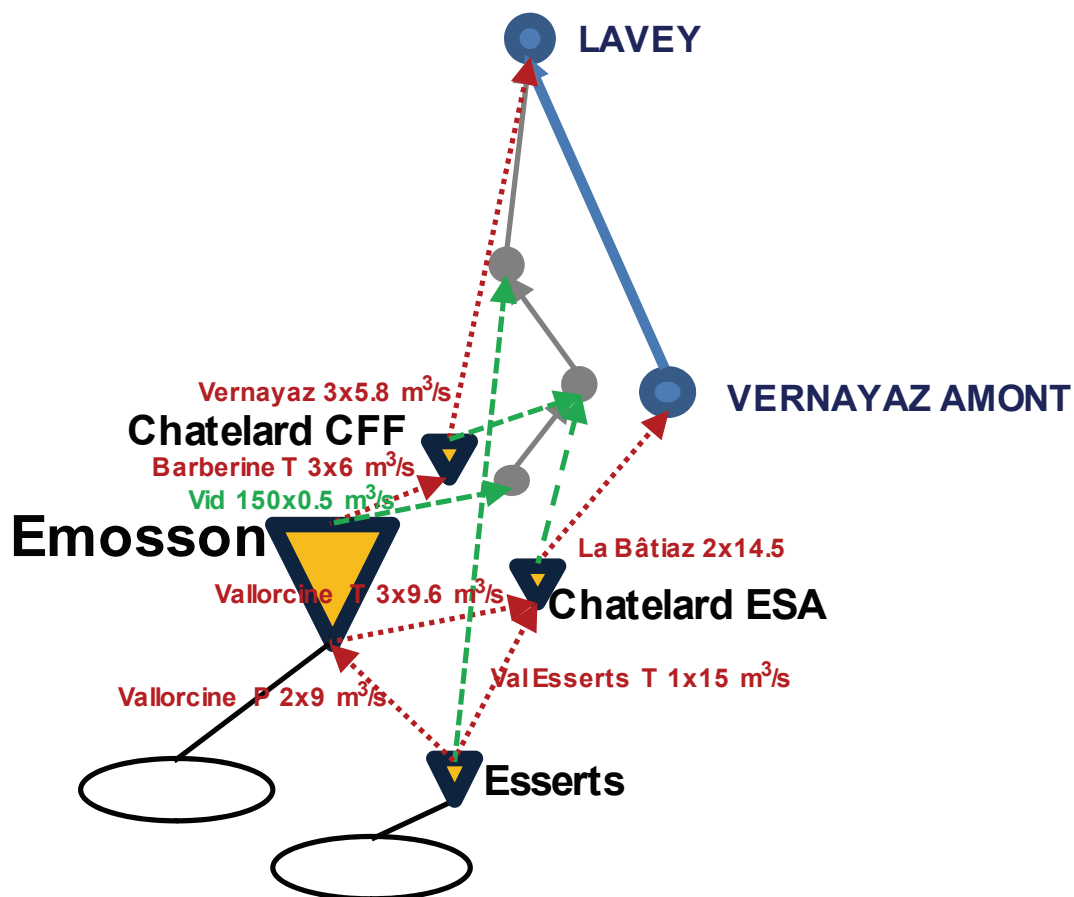
- Simplification in Gebidem:
  - Residual flow ( $2 \text{ m}^3/\text{s}$ ) not taken into account
- Optimisation:
  - Preventive operations in turbines: Bitsch
  - Preventive operations in bottom outlets: Gebidem





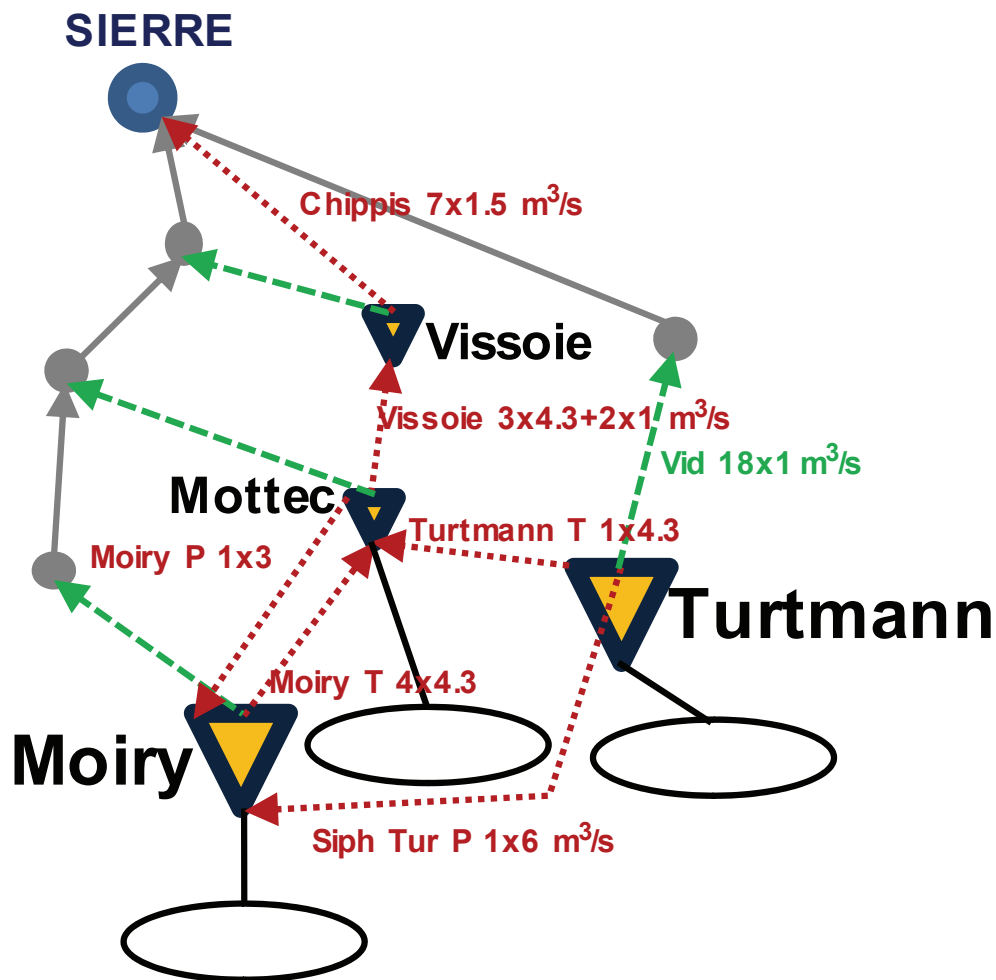
- **Emosson according to MINDS:**

- Simplification in Esserts:
  - Turbining is favoured over pumping
- Simplification in Châtelard CFF:
  - Punctual volume (inflow=outflow)
  - Turbining is favoured before bottom outlets releases
  - Intake from Tri 2 neglected
- Simplification in Châtelard ESA:
  - Punctual volume (inflow=outflow)
  - Turbining is favoured before bottom outlets releases
  
- Optimisation:
  - Preventive operations in turbines: Barberine T and Vallorcine T
  - Preventive operations in bottom outlets: Emosson
  - Preventive operations in pumps: Vallorcine P



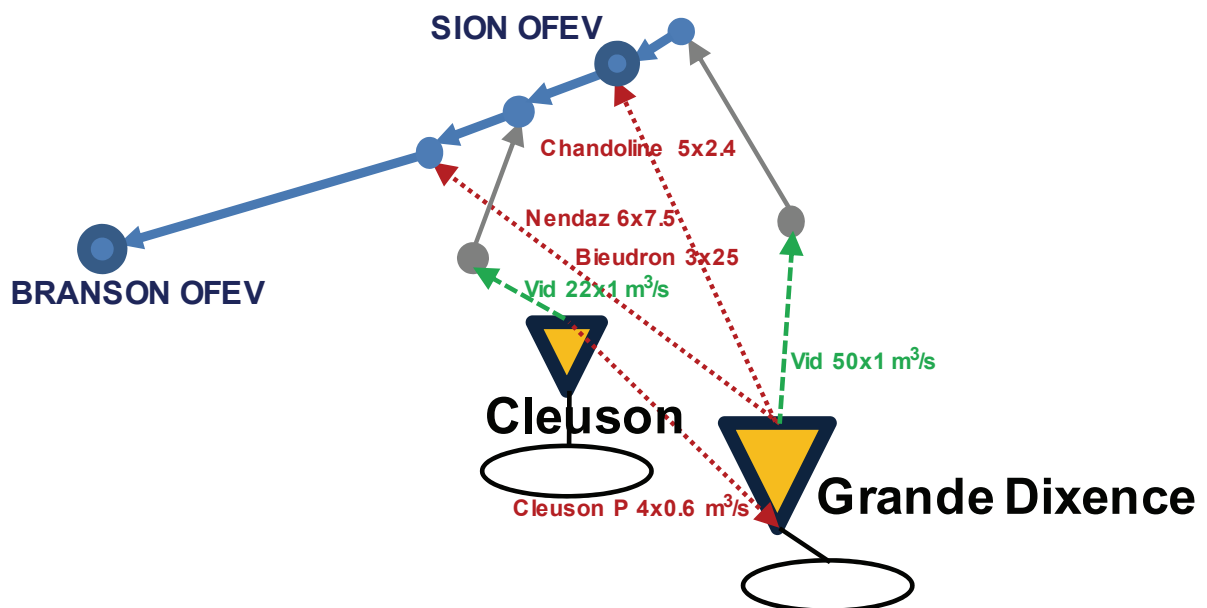
▪ **Grougra according to MINDS:**

- Simplification in Mottec:
  - Punctual volume (inflow=outflow)
  - Turbining is favoured before bottom outlets releases
- Simplification Vissoie:
  - Punctual volume (inflow=outflow)
  - Turbining is favoured before bottom outlets releases
  - Intakes from Nav 5 and Nav 6 neglected
- Optimisation:
  - Preventive operations in turbines: Moiry T and Turtmann T
  - Preventive operations in bottom outlets: Moiry and Turtmann
  - Preventive operations in siphons: Siph Tur P (si  $N_{Moiry} < N_{Turtmann}$ )
  - Preventive operations in pumps: Moiry P



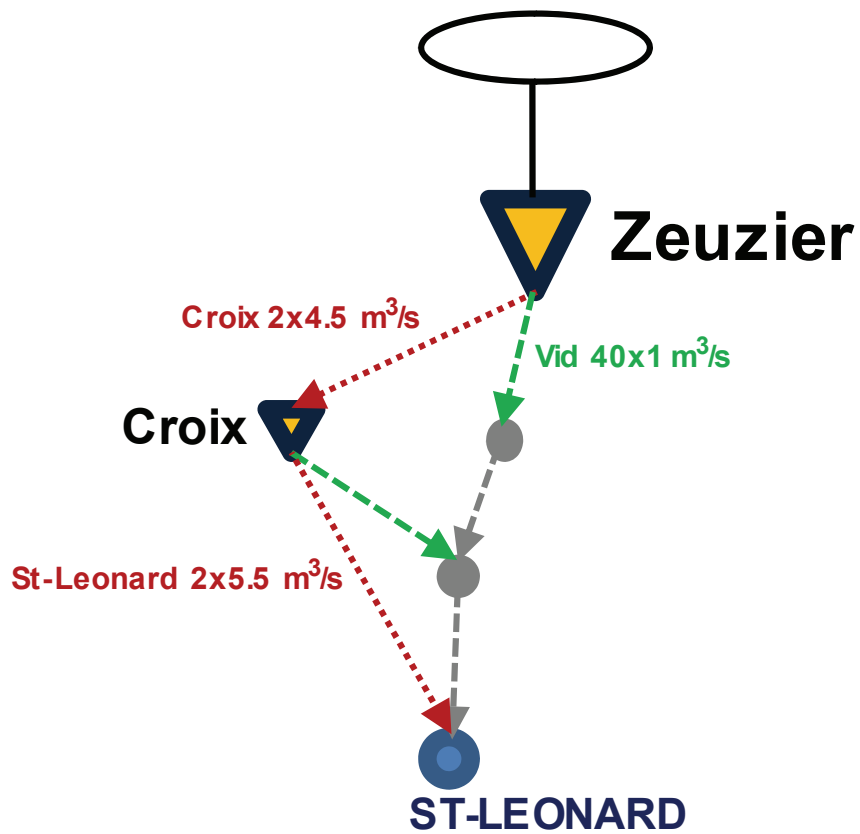
▪ **Grande Dixence according to MINDS:**

- Simplification Stafel: Not taken into account
- Simplification Zmutt: Not taken into account
- Simplification Arolla: Not taken into account
- Simplification Ferpèche: Not taken into account
- Simplification Fionnay GD: Not taken into account
  
- Optimisation:
  - Preventive operations in turbines: Nendaz, Bieudron and Chandoline
  - Preventive operations in bottom outlets: Grande Dixence and Cleuson
  - Preventive operations in pumps: Cleuson P

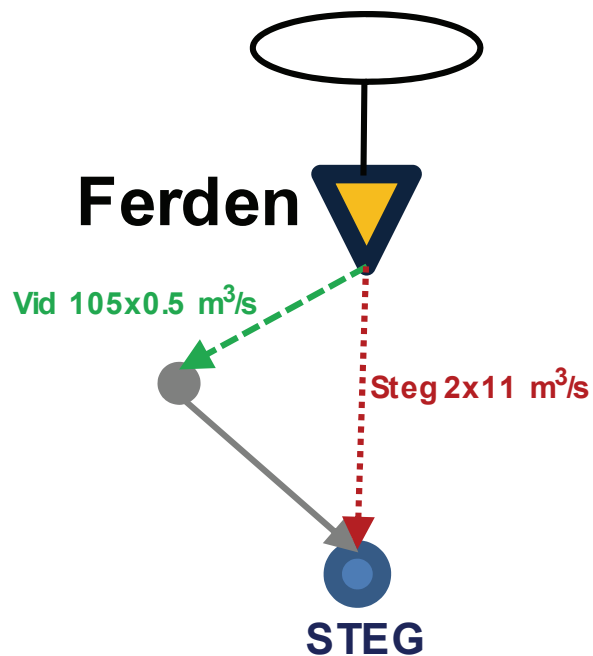


▪ **Lienne according to MINDS:**

- Simplification Croix:
  - Punctual volume (inflow=outflow)
  - Turbining is favoured before bottom outlets releases
  - Intake from Lie 2 neglected
  
- Optimisation:
  - Preventive operations in turbines: Croix
  - Preventive operations in bottom outlets: Zeuzier

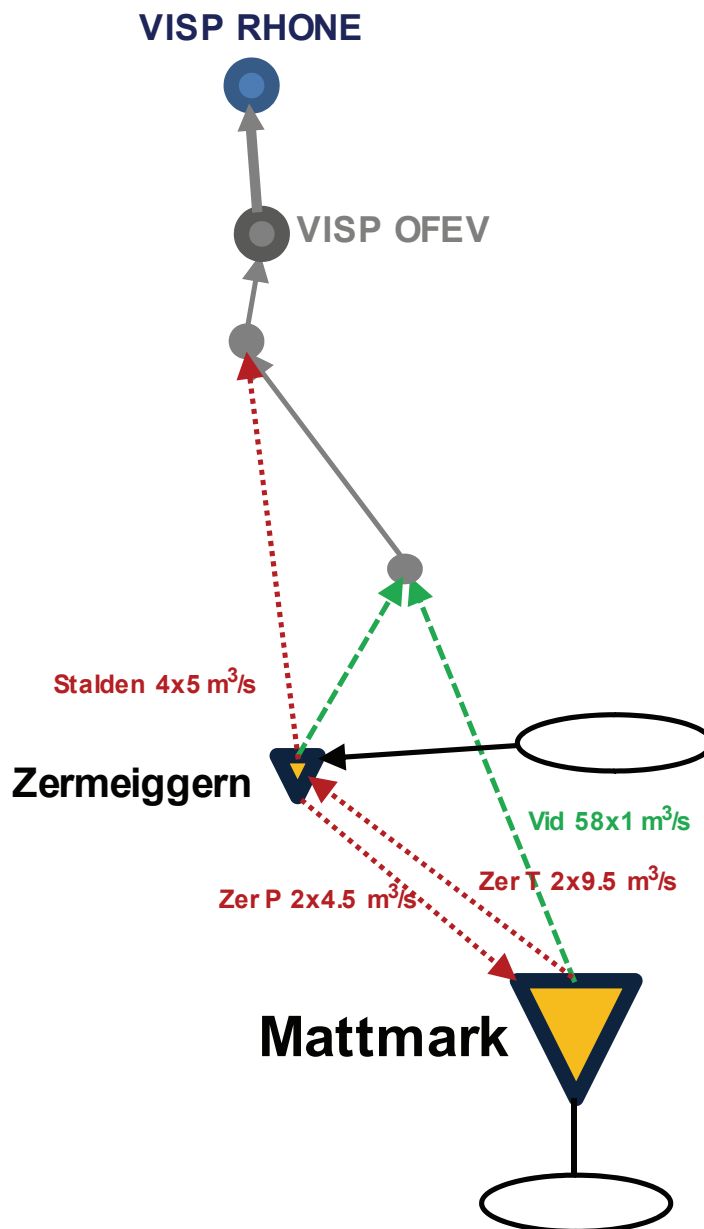


- **Lôtschen according to MINDS:**
  - Without simplifications!
  - Optimisation:
    - Preventive operations in turbines: Steg
    - Preventive operations in bottom outlets: Ferden



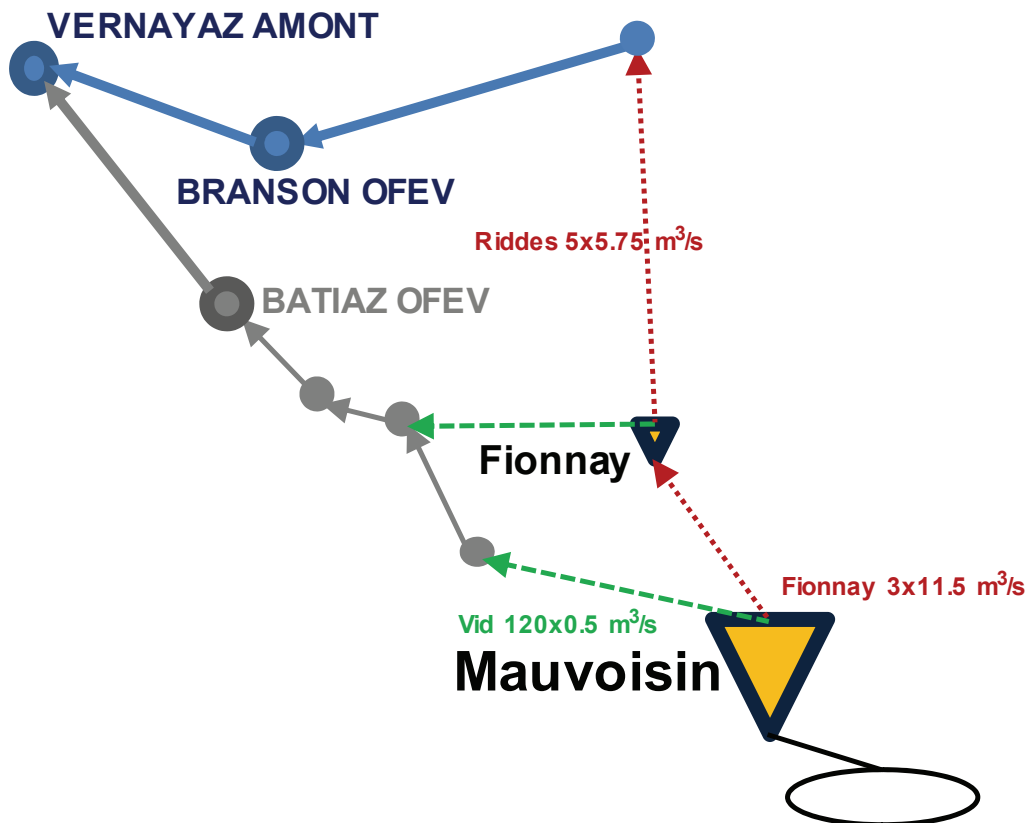
▪ **Mattmark according to MINDS:**

- Simplification Zermeiggern:
  - Punctual volume (inflow=outflow)
  - Turbining is favoured before bottom outlets releases
  - Bottom outlets from Mattmark directly upstream of Zermeiggern
  
- Optimisation:
  - Preventive operations in turbines: Zer T
  - Preventive operations in bottom outlets: Mattmark
  - Preventive operations in pumps: Zer P



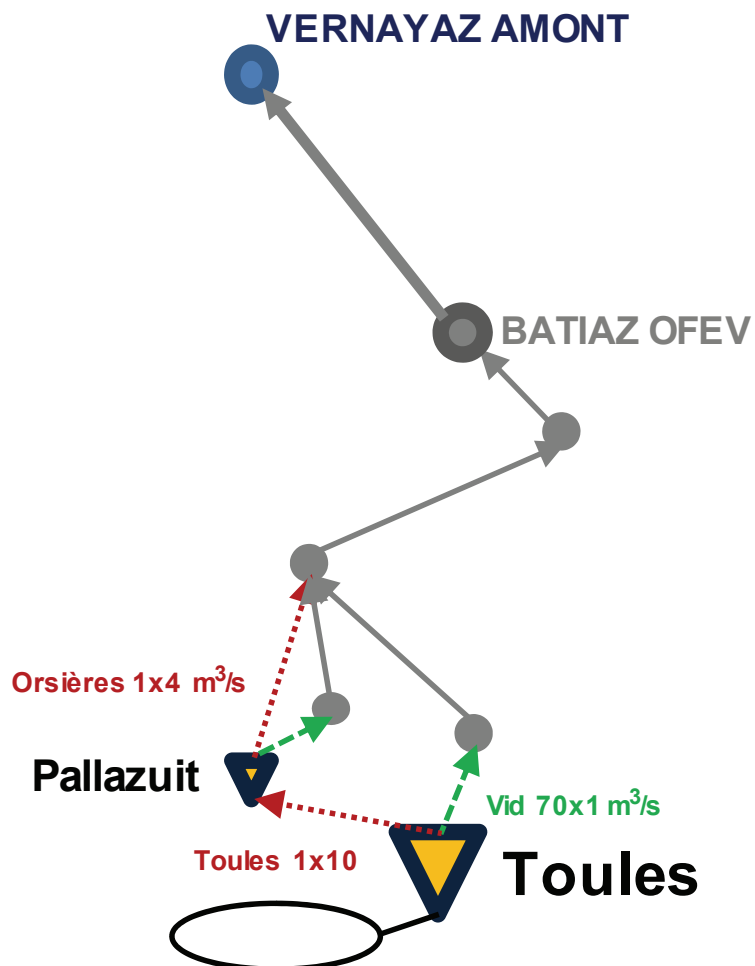
- **Mauvoisin according to MINDS:**

- Simplification Fionnay:
  - Punctual volume (inflow=outflow)
  - Turbining is favoured before bottom outlets releases
  - Intake from Dra 3 neglected
- Optimisation:
  - Preventive operations in turbines: Fionnay
  - Preventive operations in bottom outlets: Mauvoisin



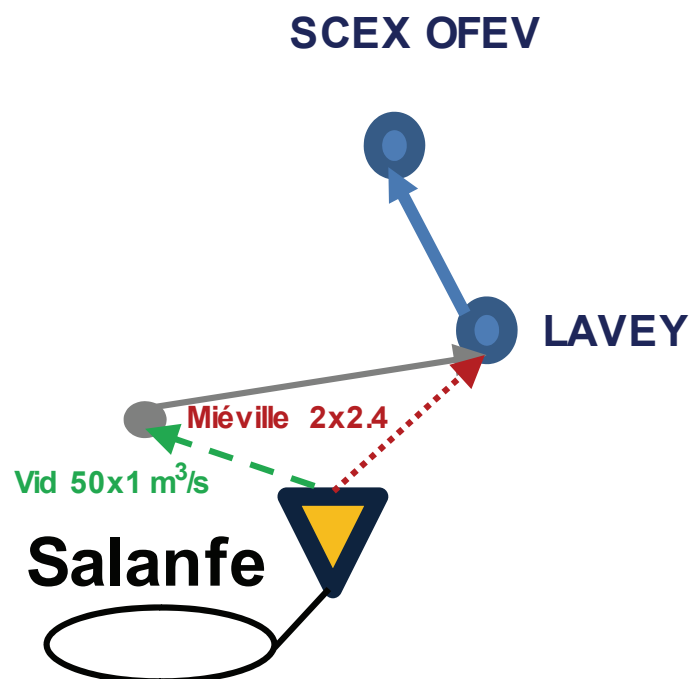
▪ **Pallazuit according to MINDS:**

- Simplification Pallazuit:
  - Punctual volume (inflow=outflow)
  - Turbining is favoured before bottom outlets releases
  - Intake from Dra 10 neglected
- Optimisation:
  - Preventive operations in turbines: Toules
  - Preventive operations in bottom outlets: Toules





- **Salanfe according to MINDS:**
  - Without simplifications!
  - Optimisation:
    - Preventive operations in turbines: Mièville
    - Preventive operations in bottom outlets: Salanfe





## Appendix 3

### Channel routing approaches

**St. Venant**

St. Venant solves the complete equations of a 1D unsteady flow as follows (Eq. A3.1 and A3.2):

$$\frac{\partial A}{\partial t} + \frac{\partial Q}{\partial x} = 0 \quad \text{A3.1}$$

$$\frac{\partial Q}{\partial t} + \frac{\partial}{\partial x} \cdot \left( \frac{Q^2}{A} + g \cdot I_1 \right) = g \cdot A \cdot (J_0 - J_f) + g \cdot I_2 \quad \text{A3.2}$$

with  $A$ : cross sectional flow area [ $\text{m}^2$ ];  $Q$ : discharge [ $\text{m}^3/\text{s}$ ];  $J_0$ : bottom slope;  $J_f$ : friction slope;  $I_1$ : profile coefficient [ $\text{m}^3$ ];  $I_2$ : coefficient for cross sectional variation [ $\text{m}^2$ ].

Equation A3.1 expresses the mass conservation while equation A3.2 ensures the conservation of momentum. The term  $I_1$  takes into account the shape of the transversal profile and is calculated as follows (Eq. A3.3):

$$I_1 = \int_0^h (h - \eta) \cdot b(\eta) d\eta \quad \text{A3.3}$$

The term  $b$  represents the cross sectional variation for the level  $\eta$  and constitutes an integration variable according to Figure A3.1.

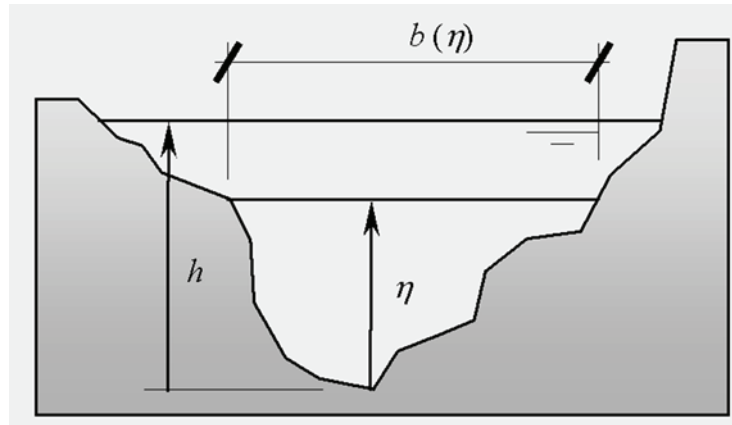


Figure A3.1 Descriptive sketch for parameters used in the calculation of  $I_1$

At present, Routing System II is able to solve the St. Venant equations for a simplified trapezoidal transversal as shown in Figure A3.2.

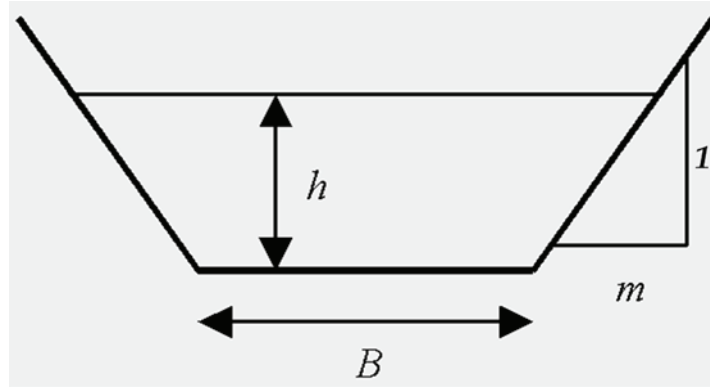


Figure A3.2 Transversal trapezoidal profile available in Routing System for the computation of channel routing

For a trapezoidal section the equation defining  $I_1$  is reduced to (Eq. A3.4):

$$I_1 = \frac{B \cdot h^2}{2} + \frac{m \cdot h^3}{3} \quad \text{A3.4}$$

with B: width of the base of the transversal profile [m]; h: water level [m]; m: side slope of the bank of the channel (1 vertical / m horizontal).

The friction slope  $J_f$  is calculated according to Manning-Strickler (Eq. A3.5 and A3.6):

$$J_f = \frac{Q |Q|}{A^2 \cdot K^2 \cdot R_h^{4/3}} \quad \text{A3.5}$$

$$R_h = \frac{A}{L_p} \quad \text{A3.6}$$

with K: Strickler coefficient;  $R_h$ : hydraulic radius [m]; A: flow area [m<sup>2</sup>];  $L_p$ : wetted perimeter [m].

The term  $I_2$  takes into account the variation of the section along the channel. In the case of a prismatic channel  $I_2$  is equal to zero. In general  $I_2$  is:

$$I_2 = \int_0^h (h - \eta) \frac{\partial b}{\partial x} \Big|_{h=\eta} \quad \text{A3.7}$$

For a prismatic channel, equations A3.1 and A3.2 are solved by the Euler method (first order) as follows:

$$A_{j+1,t+1} = A_{j+1,t} - \frac{\Delta t}{\Delta x} \cdot (Q_{j+1,t} - Q_{j,t}) \quad \text{A3.8}$$

$$\begin{aligned}
 Q_{j+1,t+1} = & Q_{j+1,t} - \frac{\Delta t}{\Delta x} \cdot \left( \frac{(Q_{j+1,t})^2}{A_{j+1,t}} - \frac{(Q_{j,t})^2}{A_{j,t}} + g \cdot I_{1,j+1,t} - g \cdot I_{1,j,t} \right) + \\
 & + \Delta t \cdot g \cdot \frac{(A_{j,t} + A_{j+1,t})}{2} \cdot J_0 - \Delta t \cdot g \cdot A_{j+1,t} \cdot J_{f,j+1,t}
 \end{aligned}
 \tag{A3.9}$$

with index  $j$  and  $j+1$  representing the spatial position;  $t$  and  $t+1$  representing the time increment;  $g$ : 9.81 [m<sup>2</sup>/s];  $\Delta x$ : longitudinal increment [m].

The downstream boundary condition used by Routing System II is the normal flow depth.

In practice, according to the physical situation to be simulated, some terms of the complete dynamic equations can be eliminated in order to get simplified expressions without losing precision. Applicable solutions are the diffusive and kinematic waves which are presented in the following.

### ***Muskingum-Cunge***

Ruling out the first two terms of Eq. A3.2 yields to Eq. A3.10:

$$\frac{\partial I_1}{\partial x} = A \cdot (J_0 - J_f) + I_2
 \tag{A3.10}$$

This new equation is the approximation of a diffusive wave. With the supplementary hypothesis of a prismatic channel, it is possible to express Eq. A3.2 as follows (Eq. A3.11):

$$\frac{\partial Q}{\partial t} + \left( \frac{Q}{BD} \cdot \frac{dD}{dh} \right) \cdot \frac{\partial Q}{\partial x} - \frac{D_r^2}{2 \cdot B \cdot |Q|} \cdot \frac{\partial^2 Q}{\partial x^2} = 0
 \tag{A3.11}$$

with  $B$ : width of the bottom of the transversal profile [m];  $D_r$ : discharge rate [m<sup>3</sup>/s].

The discharge rate is the capacity of a cross section of a channel to transport a certain flow as defined in Eq. A3.12:

$$Q = D \cdot J_0^{1/2}
 \tag{A3.12}$$

Equation A3.11 is an equation with partial derivatives of parabolic type which represents the convection and the diffusion of the variable  $Q$ . Hence, the flow transported with a velocity  $c$  (equation A3.13) and diffused with a diffusion coefficient  $\zeta$  (equation A3.14):

$$c = \frac{Q}{B \cdot D} \cdot \frac{dD}{dh}
 \tag{A3.13}$$

$$\zeta = \frac{D^2}{2B \cdot |Q|} \quad \text{A3.14}$$

Based on the hypothesis of a clearly defined relation between the flow  $Q$  and the water level  $h$ , equation A3.13 is reduced to:

$$\frac{\partial Q}{\partial t} + \left( \frac{dQ}{dA} \right)_{x_0} \frac{\partial Q}{\partial x} = 0 \quad \text{A3.15}$$

This equation is called «equation of the kinematic wave» and describes the simple convection of the flow with a velocity  $c$  according to equation A3.13. It can be solved by the following numerical finite difference scheme (Eq. A3.16 and A3.17):

$$\frac{\partial Q}{\partial t} \approx \frac{X \cdot (Q_{j,t+1} - Q_{j,t}) + (1+X) \cdot (Q_{j+1,t+1} - Q_{j+1,t})}{\Delta t} \quad \text{A3.16}$$

$$\frac{\partial Q}{\partial x} \approx \frac{\frac{1}{2} \cdot (Q_{j+1,t+1} - Q_{j,t+1}) + \frac{1}{2} \cdot (Q_{j+1,t} - Q_{j,t})}{\Delta x} \quad \text{A3.17}$$

Applying this scheme to equation A3.15 yields to equation A3.18:

$$\frac{X \cdot (Q_{j,t+1} - Q_{j,t}) + (1+X) \cdot (Q_{j+1,t+1} - Q_{j+1,t})}{c \cdot \Delta t} + \frac{\frac{1}{2} \cdot (Q_{j+1,t+1} - Q_{j,t+1}) + \frac{1}{2} \cdot (Q_{j+1,t} - Q_{j,t})}{\Delta x} = 0 \quad \text{A3.18}$$

The solution of this equation as a function of the unknown variable  $Q_{j+1,t+1}$  leads to Eq. A3.19:

$$Q_{j+1,t+1} = C_1 \cdot Q_{j,t+1} + C_2 \cdot Q_{j,t} + C_3 \cdot Q_{j+1,t} \quad \text{A3.19}$$

with:

$$C_1 = - \frac{K \cdot X - \frac{\Delta t}{2}}{K \cdot (1-X) + \frac{\Delta t}{2}}$$

$$C_2 = \frac{K \cdot X + \frac{\Delta t}{2}}{K \cdot (1-X) + \frac{\Delta t}{2}} \quad \text{A3.20}$$

$$C_3 = \frac{K \cdot (1-X) - \frac{\Delta t}{2}}{K \cdot (1-X) + \frac{\Delta t}{2}}$$

$$K = \frac{\Delta x}{c} \quad \text{A3.21}$$

$$c = \frac{Q_{j+1,t} - Q_{j,t}}{A_{j+1,t} - A_{j,t}} \quad \text{A3.22}$$

Muskingum is the name of the river localized in the United States where the method was employed for the first time. The Muskingum method represents an approximation by finite differences of the equation for the kinematic wave. Developing the terms of equation A3.18 in terms of a Taylor series around the point (j, t) assuming  $\Delta x/\Delta t = c$  and neglecting the quadratic terms ( $\Delta x^2$ ), the equation can be written as follows (Cunge, 1969):

$$\frac{\partial Q}{\partial t} + c \cdot \frac{\partial Q}{\partial x} - c \cdot B \cdot \frac{\partial^2 Q}{\partial x^2} = 0 \quad \text{A3.23}$$

$$B = \Delta x \cdot \left( \frac{1}{2} - X \right) \quad \text{A3.24}$$

It can be noted that the Muskingum equation is a solution in terms of finite differences of the equation of the diffusive wave (A3.11) under the condition of correctly introducing the value of the parameters K ( $K = \Delta x/c$ ) and X, which corresponds to:

$$X = \frac{1}{2} - \frac{D^3}{2 \cdot \Delta x \cdot |Q| \cdot Q \cdot \frac{dD}{dh}} \quad \text{A3.25}$$

This function of the diffusive wave implemented in Routing System II can solving the Muskingum-Cunge equation for a trapezoidal geometry of a transversal profile according to Figure A3.2.

### ***Kinematic Wave***

The kinematic wave is the most simplified routing model. The terms of inertia and pressure of the St. Venant equations are neglected. As a consequence, the kinematic hypothesis assumes that the gravity forces are identical, though with an opposite sign, to the friction forces. This implies that there is an explicit relationship between the flow and the water level (measured normal water depth).

The equation of the cinematic wave as presented in the previous chapter becomes:



$$\frac{\partial Q}{\partial t} + \left( \frac{dQ}{dA} \right)_{x_0} \cdot \frac{\partial Q}{\partial x} = 0 \quad \text{A3.26}$$

This is a simple convection equation which indicates that the flow  $Q$  is transported downstream with a celerity  $c$  which is defined by:

$$c = \frac{\partial Q}{\partial A} \quad \text{A3.27}$$

This simplified model transports each point of the hydrograph from upstream to downstream with a velocity  $c$ . Since no diffusive term appears in the equation the peak discharge remains constant and is not reduced. On the contrary, the general behaviour of a flood is modified, since high discharges are transferred downstream more rapidly than small ones.

The initial parameters are the same than those of the diffusive wave model. The geometry of the transversal profiles also are the same than of the Muskingum-Cunge method (trapezoidal channels, Figure A3.2). Contrary to the model of the diffusive wave, no reduction of the flood is produced as mentioned before. Kinematic wave is solved according to the following equations A3.28 to A3.30:

$$c = \frac{Q_{j+1,t} - Q_{j,t}}{A_{j+1,t} - A_{j,t}} \quad \text{A3.28}$$

$$\alpha_c = c \cdot \frac{\Delta t}{\Delta L} \quad \text{A3.29}$$

$$\begin{aligned} Q_{j+1,t+1} &= \alpha_c \cdot Q_{j,t} + (1 - \alpha_c) \cdot Q_{j+1,t} & \text{if } \alpha_c \leq 1 \\ Q_{j+1,t+1} &= \frac{1}{\alpha_c} \cdot Q_{j,t} + \left(1 - \frac{1}{\alpha_c}\right) \cdot Q_{j,t+1} & \text{if } \alpha_c > 1 \end{aligned} \quad \text{A3.30}$$

## Javier García Hernández

Nationality: Spanish

Date of birth: 25.04.1978

Place of birth: Valence - Spain

Telephone: +34 676 334 335 / +41 76 242 3355

e-mail: [javier.garcia@a3.epfl.ch](mailto:javier.garcia@a3.epfl.ch)



### EDUCATION

---

- 2007 - 2011**     **Dr ès Sciences.** Laboratory of Hydraulic Constructions (LCH), Ecole Polytechnique Fédérale de Lausanne (EPFL), Switzerland.
- Research Project: Flood management in a complex river basin with a real-time decision support system based on hydrological forecasts.
- 1997 – 2006**     **MSc in Civil Engineering.** Polytechnic University of Valence (UPV), Valence, Spain.
- Specialization in hydraulic and environmental engineering.

### CONTINUOUS TRAINING

---

- 2010**             **Conference:**
- SymHydro, Hydraulic Modelling and uncertainties. Société Hydrotechnique de France. Nice, France.
  - Risk of Overflowing. Société Hydrotechnique de France. Paris, France.
- 2009**             **Conference:**
- International Conference on Alpine Meteorology, ICAM. Rastatt, Germany.
- 2008**             **Course:**
- Fundamentals and applications of Probabilistic Forecasts and Ensemble Prediction Systems. Agenzia regionale per la protezione dell'ambiente della Sardegna (ARPAS). Alghero, Italy.
- Symposium:**
- Hydrometeorological forecasts. Société Hydrotechnique de France. Lyon, France.
- 2007**             **Conferences:**
- International Association of Hydraulic Engineering and Research, IAHR. Venice, Italy.
  - International Conference on Alpine Meteorology, ICAM. Chambéry, France.
- 2002**             **Seminar:**
- Formation of student-tutors for team work, time management and help to new university students. Education Sciences Institute, UPV, Valence, Spain.
- 2001**             **Course:**
- Planning and Control of projects works: Strategies for resources assignation, project costs, performance calculation. Centre of Postgrade Formation, UPV, Valence, Spain.

## EXPERIENCE AT LABORATORY OF HYDRAULIC CONSTRUCTIONS

---

- 2007-2011**     **System implementation for hydropower plants management for real-time flood control**
- Meteorological and hydrological forecasting, warning systems and decision support systems. Client: Swiss Confederation and Valais and Vaud Cantons.
- 2010**            **Numerical modelling of the Eo basin for the Hydrographical Confederation of Cantabria in Spain**
- Numerical modelling for the development of an operational flood warning system. Client: OFITECO.
- 2009**            **Rainwater modelling in Capelard basin, Lausanne wastewater system**
- Determination of the hydraulic behaviour and optimal location of a grid for wastewater filtering. Client: Water Service of Lausanne City.
- 2008**            **Effects of retention on the Project of the 3rd Rhone River Correction**
- Study of the influence of reservoirs, hydropower plants, and retention zones on the Rhone river flood events. Client: Group R3 (3rd Rhone Correction).
- 2007**            **Numerical modelling of the sewerage system of Lausanne city**
- Development and optimisation of a numerical model for urban flow computations. Client: Water Services of Lausanne city.
- Physical modelling study regarding the sedimentation in the Clusanfe reservoir**
- Optimisation of a gallery for reservoir sedimentation management. Client: HydroExploitation S.A.
- 2006**            **Analysis of the hydropower schemes influence on the Sarine flood events**
- Study of the potential flood control with the storage reservoirs and the hydropower plants located on the Sarine River. Client: Fribourg Canton.
- Hydrological forecasting in the Rhone River with meteorological forecasts**
- Application of the MeteoSwiss meteorological forecasts to the hydrological model of the Rhone River basin. Client: Valais Canton.

## LIST OF PUBLICATIONS

---

- 2011**            García Hernández, J., Schleiss, A. J. and Boillat, J.-L. (2011). *The Decision Support Tool MINDS for Flood Management in the Upper Rhone River*. Proceedings of the 34rd Congress of IAHR Balance and Uncertainty in a Changing World, Brisbane, Australia.
- García Hernández, J., Schleiss, A. J. and Boillat, J.-L. (2011). *Decision Support System for the hydropower plants management: the MINERVE project*. Proceedings of 79rd conference of International Commission on Large Dams (ICOLD), Lucerne, Switzerland.
- García Hernández, J., Brauchli, T., Boillat, J.-L. and Schleiss, A. J. (2011). *La gestion des crues du Rhône en amont du Léman: de la prévision à la décision*. La Houille Blanche, No. 2, 69-75.
- García Hernández, J., Boillat, J.-L. and Schleiss, A. J. (2011). *Présent et futur des prévisions hydrologiques pour la gestion des crues. Le cas du Rhône alpin*. Proceedings of the 2ème Rencontre sur les Dangers Naturels, UNIL, Lausanne, 9-14.
- 2010**            García Hernández, J., Boillat, J.-L. and Schleiss, A. J. (2010). *Flood forecast uncertainty and alert decision. Application to the Alpine Rhone River catchment*. Proceedings of Conference SimHydro “Hydraulic modeling and uncertainties”. 198e session of Comité Scientifique et Technique de la Société Hydrotechnique de France, Nice, France, 2nd day, 3rd session.
- Haldimann, S., Cohen, T., García Hernández, J. and Boillat, J.-L. *Modélisation des rejets lausannois dans le Léman*. Gas, Wasser, Abwasser, N°3, 209-220.

- 2009** García Hernández, J, Horton, P., Tobin, C. and Boillat, J.-L. (2009). *MINERVE 2010: Prévission hydrométéorologique et gestion des crues sur le Rhône alpin*. Wasser Energie Luft N°4, 297-302.
- García Hernández, J., Boillat, J.-L., Jordan, F. and Hingray, B. (2009). *La prévission hydrométéorologique sur le bassin versant du Rhône en amont du Léman*. La Houille Blanche, Vol. 5, 61-70.
- García Hernández, J., Jordan, F., Sirvent, P., Boillat, J.-L. and Schleiss, A. (2009). *Ensemble hydrological forecasts for the Upper Rhone River basin*. Proceedings of the 33rd Congress International Association of Hydraulic Engineering and Research IAHR, Vancouver, Canada, 1171-1177.
- García Hernández, J., Deval Castillo, J., Boillat, J.-L. and Schleiss, A. (2009). *Effect of climate change on hydrological cycle and evolution of the Rhone glacier*. Proceedings of the 33rd Congress IAHR, Vancouver, Canada, 773-780.
- García Hernández, J., Sirvent, P., Jordan, F., Boillat, J.-L. and Schleiss, A. (2009). *Ensemble meteorological forecast for the Upper Rhone River basin*. Annalen der Meteorologie 44, 30th International Conference on Alpine Meteorology ICAM Conference, Rastatt, Germany.
- Cohen, T., García Hernández, J., Dubois, J. and Boillat, J.-L. (2009). *Influence of hydrological model complexity on the estimation of floods in an alpine catchment for PMP conditions*. Proceedings of the 33<sup>rd</sup> Congress of IAHR Water engineering for a sustainable environment, Vancouver, Canada, 1763-1770.
- Jordan, F., García Hernández, J. and Gal, A. (2009). *Operational performance of discharge prediction in alpine regions*. Annalen der Meteorologie 44, 30th International Conference on Alpine Meteorology, 11 – 15 May, Rastatt, Germany.
- Martinerie, R., Boillat, J.-L., García Hernández, J. and Jordan, F. (2009). *Numerical modelling of stormwater and wastewater conveyance system of Lausanne City, Switzerland*. Proceedings of the 33<sup>rd</sup> Congress of IAHR Water engineering for a sustainable environment, Vancouver, Canada, 6978-6985.
- 2008** Boillat J.-L., Martinerie R., García Hernández J. and De Cesare G. (2008). *La gestion sédimentaire en milieu alpin*. La Houille Blanche, N°4, 122-129.
- Jordan, F., García Hernández, J., Dubois, J. and Boillat, J.-L., (2008). *MINERVE: Modélisation des intempéries de nature extrême du Rhône valaisan et de leurs effets*. Communication du Laboratoire de Constructions Hydrauliques 38, Ed. A. Schleiss, EPFL, Lausanne, ISSN 1661-1179.
- Jordan F., García Hernández J., Boillat J.-L. and Schleiss A. J. (2008). *Flood forecast and flood management model – Optimization of the operation of storage power plants for flood routing*. Interpraevent, Dornbirn, Vorarlberg, Austria, Conference Proceedings, Vol. 1, 141-151.
- 2007** García Hernández, J., Jordan, F., Boillat, J.-L. and Schleiss, A. (2007). *Meteorological and hydrological forecast for the Upper Rhone River basin*. Proceedings of the 32nd Congress of International Association of Hydraulic Engineering and Research IAHR, SS10, Venice, Italy.
- García Hernández, J., Jordan, F., Dubois, J. and Boillat, J.-L. (2007). *Routing System II: Modélisation d'écoulements dans des systèmes hydrauliques*. Communication 32 du Laboratoire de Constructions Hydrauliques, Ed. A. Schleiss, EPFL, Lausanne.
- Jordan, F., Boillat, J.-L., García Hernández, J., Dubois, J. and Schleiss, A. J. (2007). *Real-time decision-making during floods: application to the Upper Rhone River in Switzerland*. Proceedings of the 32nd Congress of International Association of Hydraulic Engineering and Research IAHR, SS10, Venice, Italy.
- Jordan, F., Boillat, J.-L., García Hernández, J. and Schleiss, A. (2007). *Flood forecasting in the Upper Rhone River for the management of multireservoir systems*. Proceedings of the 29nd International Conference on Alpine Meteorology, Session M, Mountain Hydrology, Chambéry, France.
- Jordan, F., Boillat, J.-L. Boillat and García Hernández, J. (2007). *Influence des retenues hydroélectriques pour la protection contre les crues de la Sarine*. Journées de rencontre sur les dangers naturels 2007, IGAR, Lausanne, Switzerland.
- Jordan, F., Boillat, J.-L., García Hernández, J., Dubois, J. and Schleiss, A. J. (2007). *Aide à la décision en situation de crue: le cas du Rhône en Valais*. Forum für Wissen, Zurich, Switzerland, 79-83.

## **LANGUAGE SKILLS**

---

Spanish and Catalan	Mother tongues
French	Good
English	Good
German	Basic

## **COMPUTER SKILLS**

---

Daily user	<i>Microsoft Windows, Office applications, Adobe, AutoCAD</i>
Hydraulic software	<i>Routing System, SWMM, Epanet, Hec-Ras, ArcGIS</i>
Programming	<i>Visual Basic.Net, Matlab</i>

## **PERSONAL INTERESTS**

---

Hobbies	Winter sports, hiking, motorcycling, travelling
Football	Player in "Regional Preferente" and Coach in young leagues